Electric Technology U.S.S.R.

960

ЭЛЕКТРИЧЕСТВО

Volume 5, December, 1960

Selected papers from
Elektrichestvo Nos. 1, 2 and 3, 1960

Published by

PERGAMON PRESS NEW YORK LONDON OXFORD PARIS LOS ANGELES

for Pergamon Institute, Washington and Oxford

ELECTRIC TECHNOLOGY, U.S.S.R.

EDITORIAL BOARD

H. M. Barlow, *London;* F. W. Bowden, *San Luis Obispo;* F. Brailsford, *London;* G. S. Brown, *Cambridge, Mass.;* F. M. Bruce, *Glasgow;* C. C. Carr, *Brooklyn;* G. W. Carter, *Leeds;* A. G. Conrad, *New Haven, Conn.;* G. F. Corcoran, *College Park, Md.;* J. D. Craggs, *Liverpool;* A. L. Cullen, *Sheffield;* G. E. Dreifke, *St. Louis;* V. Easton, *Birmingham;* A. R. Eckels, *Vermont;* W. Fishwick, *Swansea;* C. Froehlich, *New York;* C. G. Garton, *Leatherhead;* J. Greig, *London;* L. D. Harris, *Salt Lake City;* J. D. Horgan, *Milwaukee;* E. C. Jones, *Morgantown;* E. C. Jordan, *Urbana;* I. H. Lovett, *Rolla, Missouri;* J. M. Meek, *Liverpool;* J. H. Mulligan, Jnr., *N.Y.;* W. A. Murray, *Blacksburg, Virginia;* J. E. Parton, *Nottingham;* H. A. Peterson, *Madison;* A. Porter, *London;* J. C. Read, *Rugby;* W. G. Shepherd, *Minneapolis;* W. P. Smith, *Lawrence, Kansas;* Philip Sporn (Chairman), *New York;* J. A. Strelzoff, *East Lansing;* F. W. Tatum, *Dallas, Texas;* C. V. O. Terwilliger, *Monterey;* D. H. Tompsett, *Stafford;* A. Tustin, *London;* S. Reid Warren Jnr., *Philadelphia;* A. R. van C. Warrington, *Stafford;* A. H. Waynick, *Pa.;* E. M. Williams, *Pittsburgh;* F. C. Williams, *Manchester;* H. I. Wood, *Manchester;* C. M. Zieman, *Ohio.*

1960

PERGAMON INSTITUTE

A DIVISION OF PERGAMON INTERNATIONAL CORPORATION, OPERATED IN THE PUBLIC SERVICE FOR THE FURTHERANCE AND DISSEMINATION OF SCIENTIFIC KNOWLEDGE

President of the Scientific Advisory Council:
Sir Robert Robinson, O.M., F.R.S.

Executive Director: Captain I. R. Maxwell, M.C.

122 *East 55th Street, New York 22, N.Y.* (*Telephone No. Plaza* 39651).

Headington Hill Hall, OXFORD. (*Telephone No. Oxford* 64881)

Pergamon Institute can occasionally use additional translators for science and engineering material to assist with this programme of translation from Russian and other Slavonic languages.

Scientists and engineers who have a knowledge of Russian, and who are willing to assist with this work, should apply to the Administrative Secretary of the Institute. They should write to New York or Oxford for rates of payment and other details.

Four volumes per annum. Approximately 700 pages per annum.
Annual Subscription Rate £20 ($56).
Single volumes may be purchased for £6 ($14).

Orders should be sent to the distributors at either of the following addresses

Headington Hill Hall, Oxford
122 East 55th Street, New York 22, N.Y.

PUBLISHED BY

PERGAMON PRESS LTD.

NEW YORK · LONDON · OXFORD · PARIS · LOS ANGELES

December 1960

ELECTRIC TECHNOLOGY U.S.S.R.

VOLUMES 5—8, 1960

Selected papers from Elektrichestvo, Nos. 1—12, 1960

EDITORIAL BOARD

H. M. Barlow (London)
F. W. Bowden (San Luis Obispo)
F. Brailsford (London)
G. S. Brown (Cambridge, Mass.)
F. M. Bruce (Glasgow)
C. C. Carr (Brooklyn)
G. W. Carter (Leeds)
A. G. Conrad (New Haven, Conn.)
G. F. Corcoran (College Park, Md.)
J. D. Craggs (Liverpool)
A. L. Cullen (Sheffield)
G. E. Dreifke (St. Louis)
V. Easton (Birmingham)
A. R. Eckels (Vermont)
W. Fishwick (Swansea)
C. Froehlich (New York)
C. G. Garton (Leatherhead)
J. Greig (London)
L. D. Harris (Salt Lake City)
J. D. Horgan (Milwaukee)
E. C. Jones (Morgantown)
E. C. Jordan (Urbana)
I. H. Lovett *Rolla*, (Missouri)
J. M. Meek (Liverpool)
J. H. Mulligan Jnr. (N.Y.)
W. A. Murray (Blacksburg, Virginia)
J. E. Parton (Nottingham)
H. A. Peterson (Madison)
A. Porter (London)
J. C. Read (Rugby)
W. G. Shepherd (Minneapolis)
W. P. Smith (Lawrence, Kansas)
Philip Sporn (Chairman) (New York)
J. A. Strelzoff (East Lansing)
F. W. Tatum (Dallas, Texas)
C. V. O. Terwilliger (Monterey)
D. H. Tompsett (Stafford)
A. Tustin (London)
S. Reid Warren Jnr. (Philadelphia)
A. R. van C. Warrington (Stafford)
A. H. Waynick (Pa.)
E. M. Williams (Pittsburg)
F. C. Williams (Manchester)
H. I. Wood (Manchester)
C. M. Zieman (Ohio)

PERGAMON PRESS LTD.

OXFORD . LONDON . NEW YORK . PARIS

ELECTRIC TECHNOLOGY, U.S.S.R.

CONTENT OF VOLUMES 5—8, 1960

Vol. 5

	PAGE
N. I. Borisenko: The tasks of the electrical engineering industry	1
S. M. Domanitskii: Optimum control systems for the flying shears drive in a rolling mill	13
B. P. Petrov: Transient processes in automatic step chronometric control of electric rolling stock	28
A. I. Balakin: A new method of testing the rupturing capacity of high voltage circuit breakers	41
Abstracts from papers published in Elektrichestvo No. 1, 1960	52
I. L. Shapiro, E. M. Grossman, Iv. A. Raisov and Iu. V. Tikhvinskii: A digital programme control system for a large lathe	57
A. B. Chebiustkin and V. A. Ivanov: Self-aligning system for automatic control of welding conditions on electrical tube welding machines	66
L. D. Razumov: Location and efficiency of insulating couplings and flanges for the protection of underground metal structures against electrical corrosion	80
N. M. Chernyshev and V. D. Liashenko: Synchronizing device for synthetic rupturing capacity tests on circuit breakers	96
Abstracts from papers published in Elektrichestvo No 2, 1960	106
D. V. Vilesov and I. A. Riabinin: How to select the basic parameters of excitation systems for self-excited synchronous generators	110
N. A. Panfilov: How the rating of d.c. machines varies with ambient temperature and altitude	122
N. M. Okhremenko: Electro-magnetic phenomena in flat induction pumps for molten metals	132
G. I. Poliak and V. C. Goliatin: A scheme for testing large high voltage valves	152
Abstracts from papers published in Elektrichestvo No. 3, 1960	157
Abstracts from papers published in Elektrichestvo No. 4, 1960	161
Abstracts from papers published in Elektrichestvo No. 5, 1960	165

Vol. 6

	PAGE
T. A. Glazenko: A reversing scheme for automatic speed control using electromagnetic powder clutches	171
S. V. Usov, G. M. Pavlov, V. A. Slazikov and I. A. Budkin: Automatic device for load distribution in power systems	185
I. S. Taev: Investigation of the extinction processes in a free a.c. arc	196
N. S. Kochanov: Calculating transient processes in linear circuits by recurrence formulæ	212
Abstracts from papers published in Elektrichestvo No. 4, 1960	221
V. M. Mantrov: An improved system of arc excitation in mercury arc rectifiers	225
A. T. Golovan and I. M. Kruglyanskii: Excitation systems for variable frequency induction machines	231
K. A. Vodop'ianov, B. I. Vorozhtsov, G. L. Potakhova and N. I. Ol'shanskaia: The electrical and physical properties of electrical insulating materials	244
S. I. Fedorov: Designing cooling systems for semiconductor triodes	260
Abstracts from papers published in Elektrichestvo No. 5, 1960	269
M. P. Kostenko, E. Ia. Kazovskii and Ia. B. Danilevich: An experimental study of new methods of determining the parameters of a.c. machines	273
M. P. Chesov: A study of out-of-step conditions and the resynchronization of a generator after losing transient stability	281
S. B. Losev and A. B. Chernin: The performance of three-phase directional impedance relays in the presence of faults and under unbalanced conditions (compensator distance relaying)	290
Dan Teodorescu: A hyrotron with controlled grids (a new type of high frequency ionic converter 0.5 to 50 kc/s for induction heating)	314
Abstracts from papers published in Elektrichestvo No. 6, 1960	322
Abstracts from papers published in Elektrichestvo No. 7, 1960	328

1960

Vol. 7

	PAGE
F. F. Olefir: New electrical drives for continuous cold rolling mills	333
A. A. Sirotin and V. A. Eliseev: An automatic motor drive for grinding machines with follow-up feed	334
I. R. Freidzon: An electronic computer study of an automatic helmsman	355
L. D. Gustov, M. I. Levin, A. M. Marinov, L. M. Myzin and A. P. Petrov: The 500 kV substation at Sverdlovsk	369
Abstracts from papers published in Elektrichestvo No. 7, 1960	379
V. S. Popov, M. N. Solov'ena and Yu. A. Mal'tsev: An electric current stabilizer	384
G. G. Rekus: Conditions for the symmetrical performance of a capacitor motor	394
B. A. Ivobótenko: Step motors	401
L. N. Fitsner: Automatic electrical optimizers	417
Abstracts from papers published in Elektrichestvo No. 8, 1960	432
L. L. Ivanov: First fundamentals of an analytical theory for discontinuous functions in the design of non-linear electrical circuits	436
N. V. Boriv: Modelling the leakage losses of a large power transformer	454
V. M. Kolesnikov: Full wave rectification with "zero" anodes and its use for exciting excitrons	463
V. A. Liul'ko: The impulse characteristics of turbine generators	473
Abstracts from papers published in Elektrichestvo No. 9, 1960	481

Vol. 8

	PAGE
A. G. Moskalev: Self-adjusting decentralized system automatically controlling power system frequency and real power flow	485
Khu Tszia Iao and V. A. Shubenko: Transients in magnetic amplifiers with an RL (active inductive) load in the rectified current circuit	500
S. A. Sokolovskii and P. P. Snovgenov: A new instrument for investigating surge phenomena in windings	517
O. G. Vegner: A novel excitation system for the compoles of d.c. machines	524
Abstracts from papers published in Elektrichestvo No. 10, 1960	531
G. G. Kostanian: Calculating complicated faults using the results of computations of simpler system conditions	534
L. V. Leites: A coreless toroidal reactor for power systems	555
L. M. Tverdin and Iu. M. Kurzanov: The use of transistors for controlling mercury arc rectifiers	569
Ia. S. Shvartsbart: The screening of railway communication cables—a new application for 3% silicon steel	576
Abstracts from papers published in Elektrichestvo No. 11, 1960	580
I. M. Markovich, V. A. Taft, S. A. Sovalov, V. A. Venikov and L. V. Tsukernik: The application of computer techniques in power system operation and design	585
K. Ia. Kafieva: A study of radio interference from corona on transmission lines	598
A. T. Golovan and Iui-Ian: The effect of transient starting currents in induction motors on the starting losses	613
I. Z. Agfev: The commutation of wide-range variable-speed machines	623
Abstracts from papers published in Elektrichestvo No. 12, 1960	641

PERGAMON INSTITUTE

A DIVISION OF PERGAMON INTERNATIONAL CORPORATION, OPERATED IN THE PUBLIC SERVICE FOR THE FURTHERANCE AND DISSEMINATION OF SCIENTIFIC KNOWLEDGE

President of the Scientific Advisory Council:
Sir Robert Robinson, O.M., F.R.S.

Executive Director: Captain I. R. Maxwell, M.C.

122 *East 55th Street, New York 22, N.Y.* (*Telephone No. PLAZA* 39651).
Headington Hill Hall, OXFORD. (*Telephone No. Oxford* 64881).

1960

Elektrichestvo

Editor-in-Chief: N. G. DROZDOV

EDITORIAL BOARD

L. A. BESSONOV, N. I. BORISENKO, G. V. BUTKEVICH, T. P. GUBENKO, N. G. DROZDOV, A. D. DROZDOV, L. A. DUBINSKII, L. A. ZHEKULIN, A. M. ZALESKII, M. P. KOSTENKO, V. S. KULEBAKIN, B. YU. LOMONOSOV, L. G. MAMIKONYANTS, L. R. NEIMAN, I. I. PETROV, I. M. POSTINKOV, S. I. RABINOVICH, B S. SOTSKOV, I. A. SYROMYATNIKOV, YU. G. TOLSTOV, A. M. FEDOSEEV, M. G. CHINKIN

1960

THE TASKS OF THE ELECTRICAL ENGINEERING INDUSTRY

N.I. BORISENKO

(Received 14 November 1959)

During the years of Soviet power the electrical engineering industry has grown into a many-sided branch of the national economy. A resolution moved by the 21st congress of the Communist Party of the U.S.S.R. on the control figures for the development of the national economy in the years 1959-65 specifies the generation of 500-520,000, million kWh of electrical energy in 1965, the extensive development of complex mechanization and automation of production methods and the continuous electrification of the country, which determines the leading tempo of development of the electrical engineering industry. Thus, for example, in 1965 the gross output of electrical engineering plant will increase by almost three times in comparison with 1958, whereas gross engineering production will only rise by 1.8 times over the same period.

This increase of production is mainly due to the reconstruction of existing undertakings and their specialization. The complex mechanization and automation of the manufacture of electrical engineering products will be of substantial importance to the growth of operating efficiency and output.

Mechanization and automation of industrial processes in all branches of the national economy are demanded from the electrical engineering industry, apart from an increase in output and the expansion of all types of electrical engineering production. There is an urgent need to reduce considerably the time required to bring into production new kinds of products which can be manufactured on assembly lines.

The technical level of the electrical engineering industry must be substantially raised. In the first place it is essential to revise existing types and ranges of electrical engineering products, to ascertain their technical level and conformity to modern requirements for automated electric drives and to plan their optimum diversity on

---

* *Elektrichestvo*, No.1, 1-5, 1960.

the basis of the requirements of every branch of the national economy.

Modern engineering demands the manufacture of new kinds of electrical engineering products: semiconductor power rectifiers, magnetic amplifiers, steel tank arc rectifiers, and so on.

New ranges of different types of electrical engineering products must be created on the basis of previous scientific and technical progress and in so doing special attention must be given to durability and reliability in operation. Technical parameters must be selected taking into consideration the economic effect within the framework of the entire national economy. Unfortunately, there is no acknowledged unique method of appraising economic questions. It is therefore very necessary to discuss this problem extensively and to evolve a single system of determining an alternative structure within the framework of the total national economy.

The design of electrical engineering products must be based on wide unification and standardization of units and components. Only in this way will one be able to create the proper conditions for the organization of mass production and at the same time satisfy the extremely diverse requirements of modern automatic electric drives in every branch of the national economy and fruitfully take advantage of the known remarkable properties of electrical energy.

A good example of most complete unification and standardization is the range of automatic machine tools of 25 to 600 A. It consists of five basic standard sizes of casings and has more than 16,000 uses according to the type and magnitude of the current and the number of terminals, etc.

The basic technical trends in the current seven years in the production of new modern equipment are given below for each class of equipment.

Turbo- and hydro-generation construction

It is essential to build new ranges of turbo-alternators from the small to the very large ones with the best cooling facilities for each series (air, hydrogen, liquid), with an efficiency factor and other technical parameters which are the most economical within the framework of the national economy.

Performances must be accomplished with a reduction of the thickness of electrical insulation and at the same time with increased dielectric strength and without using bitumin-mica insulation.

It is necessary to use ionic excitation in cases, where it is econ-

omically justified. Turbo- and hydro-generators with a capacity of 300-500MW have to be built being, in particular, of suitable construction to allow them to be installed and operated in the open air.

Unification of the couplings of the steam turbines and generators is also essential.

Electrical machine construction

At present work is being carried out on the construction and introduction into industry of unit ranges of d.c. and a.c. electric motors and generators covering all capacity and running speed ranges.

Particular regard must be given to the development of specialized groups of electric motors: submerged electrical motors for the oil industry, miniature motors for automation and domestic purposes, coal-cutting and explosion-proof motors for the coal, chemical and gas industries, direct current electric motors for controlling electric drives in various branches of the national economy and so forth.

The new unit ranges of electric motors are being based on new kinds of synthetic insulation. Winding conductor and slot insulation thicknesses are being considerably reduced and at the same time mechanical and dielectric strength and reliability are being increased in operation. Furthermore the dimensions and weight of machines are beihg considerably reduced.

Designers and technologists must extensively introduce plastics into the electrical industry. Units, such as commutators, terminal assemblies, blowers, outlet boxes and so forth can and must be manufactured from plastic materials, for instance, from an AG4 type of substance.

It is necessary to introduce into production excitation systems for synchronous machines using semiconductor and magnetic amplifiers with automatic voltage control.

In the current seven years plan, the development of completely enclosed electric motors with water-cooling for the ancillary drives of power stations is imminent.

It is also necessary to extend the range of electric motors, built for a voltage of 10kV, to the smaller capacity size, for example, up to 600-700 kW, and to eliminate the use of two voltages, 10 and 6 kV, by some consumers. It is necessary to fix a minimum output limit according to economic expediency within the framework of the national economy, taking into account, of course, the reliability of such electric motors in operation.

Furthermore, the economic expediency of using a voltage of 600 V and of building suitable electrical equipment for this voltage should be considered.

Transformer construction

Electrical industrial concerns must manufacture single ranges of transformers (oil and dry) using steel with small electromagnetic losses, large magnetic permeability and an increased number of applications on load tap-changing.

The optimum efficiency of transformers must be determined according to economic conditions within the framework of the national economy.

Transformers must have facilities for cable terminations and must be standardized to fit into a complete transformer substation. Power transformers must be developed for a voltage of more than 500kV and for a capacity of 360 MVA and over.

The national economy will be acquiring from electrical industrial factories packaged transformer substations in a heavy unit-type form with capacities up to 30 MVA and for voltages of up to 220 kV.

The inclusion of a range of mobile transformer substations with a capacity of up to 320 kVA and a voltage of up to 10 kV has also been planned for mines. Suitable ranges of transformers, reactors and anode dividers must be developed and mastered for electrothermal equipment, electric locomotives, local electric trains, static converter substations, etc. In the first place after the cable products it is essential to introduce aluminium as a conductor material into transformer construction.

The problems of building unit ranges of high-voltage insulator lead-ins, detachable insulator lead-ins for a voltage of up to 35 kV, standardized cooling apparatus, built into the oil of motor-pumps, etc., must be solved in connexion with the development of transformer construction.

High voltage apparatus

In accordance with the far-reaching electric transmission line construction programme and the programme of continuous electrification of the country it is essential to build unit ranges of high-voltage circuit-breakers. It is necessary to establish the field of application of bulk-oil, low oil volume and air-blast circuit breakers. The wide applications of simplified circuits in high-voltage networks requires the construction of a series of load disconnecting switches, short-circuiting devices, high-speed isolators and other apparatus. New

ranges of lightning arresters, reactors, fuses, instrument transformers and similar high-voltage apparatus have to be built.

A large growth in the production of complete distributing equipment in large-scale unit-type form is planned, for which it is necessary to manufacture a series of high-voltage switchgear in unit form with plug-in contacts. At the same time reflection of the tendency to increase the voltage of distribution networks to 35kV must be found in the electrical engineering industry.

It is also expedient to build a series of insulated high-voltage conductors of small dimensions.

Static converters

The tendency to use electronic, mechanical and semi-conductor rectifiers in place of rotating current and frequency converters has given rise to the necessity of developing transforming apparatus with mercury-arc or semiconductor valves and mechanical rectifiers. These rectifiers are essential to ferrous and non-ferrous metallurgy and the chemical industry, electric traction and a number of other branches of the national economy.

Electric traction and electrical equipment for steam and electric locomotives

The task of the electrical engineering industry in this field is to construct main line a.c. electric locomotives with a capacity of up to 4,200 and 5,600 kW, using semiconductor rectifiers, commercial a.c. electric locomotives and electric locomotives with independent traction apparatus (diesel-generator or accumulator).

It is also necessary to develop new electrical equipment for electric mining locomotives, main line locomotives of 3,000 h.p. capacity, shunting locomotives and multiple unit stock for local traffic using a.c. with static semiconductor rectifier apparatus.

Electrothermal and arc welding equipment

The expanding application of electrical energy for thermal and welding processes requires an extensive development of the diversity of electrical equipment for these purposes.

Electrothermal processes are often incorporated in the normal technological pattern of any industry and are an indispensable part of it.

It is essential to develop a range of electric furnaces taking the technology and location of their use into consideration, and with

mechanization and automation of all production methods. All the familiar electrothermal methods (arc, resistance, induction, high frequency) will obtain very extensive application.

Electric welding equipment will be supplemented by new forms of different sources of supply for welding processes, welding transformers, automatic and semi-automatic welding machines, welding apparatus for contact welding, etc.

Furthermore, complete units with a specific degree of automation for welding operations on the automatic lines of any industrial process are being built.

Electric drive and low-voltage apparatus

In the current seven years it is planned to introduce, on a wide scale, heavy-duty low voltage equipment for distributing electrical energy to consumers. For this purpose ranges of varied forms of low-voltage apparatus must be developed into complete equipment suitable for easy installation, for instance by means of plug-in contacts.

It is proposed to build ranges of apparatus in casings, which enable it to be assembled into complete low-voltage distributing equipment for the various consumers of the national economy.

The production of switching apparatus with increased disconnecting capacity, a great number of connexion and small dimensions is also planned.

In the field of automatic electric drives the evolution of standard solutions for controlling and regulating industrial processes in every branch of the national economy is urgently needed on a new technical basis which rests on scientific and technical achievements.

Wide use of non-contact systems must be formed for the operation and control of electric drives using semiconductors, magnetic amplifiers and other apparatus. Radio electronics and computer techniques must become an integral part of electric drives.

In modern electric drives the work of "transmitters", transducers, amplifiers, recording apparatus, servo-mechanisms and the final "power component" is so integrated that it represents a single entity.

Consequently the development of standard solutions of electric drives using the minimum number of instruments and apparatus is very important and promises to have an immense impact on the national economy.

Just as in the field of electric drives a great amount of work is

required in unifying and standardizing plans and ways of solving problems of operation and control, since very many organisations are and will be concerned with these questions.

The development of new ranges of low-voltage control apparatus is closely connected with the solution of the problems mentioned. It is essential that the existing diversity of apparatus (contractors, controllers, relays, etc), which is identical as far as its use is concerned, is reduced to the maximum necessary quantity, which satisfies the modern technical standard and trends of electric drive development. New ranges of magnetic amplifiers, semi-conductor triodes, miniature relays, isolating switches, contactors and so forth have to be built.

Extensive use in low-voltage apparatus must be found for plastics, cermets, special magnetic materials, insulating compounds for windings, and heat-resisting materials for arc-extinguishing chambers.

Special attention should be paid to the capacity of the apparatus to sustain a great number of operations while it is in service.

In a very short space of time electrical industrial factories need to organize the manufacture of high capacity equipment and appropriate control systems. A planned electric drive system must be produced in the form of a properly unitized arrangement (switchboard) or arrangement of blocks with a complete commutation system, so that at the point of installation it is only necessary to connect to the blocks the conductors from the transmitters and signal instruments and the power cables to the main electric motors. This would enable the commissioning of expensive items to be accelerated considerably and the national economy to be saved thousands of millions of rubles.

Cable products

The main problems of the cable industry are the use of aluminium and bimetal (steel-aluminium, copper-aluminium) as conductor material, the use of enamel insulation for winding conductors instead of textiles; the introduction of protective cable sheathing made of aluminium and plastic instead of lead; conversion to plastic insulation of cable cores instead of paper-oil and partial rubber insulation and the construction of high voltage power cables easy to operate at a voltage of up to 500 kV.

It is also necessary to guarantee the production of armoured cables for the coal industry, and the construction of flexible cables with long service for excavators and other mechanisms.

Furthermore, it is necessary to create continuous industrial proces-

ses in the cable industry using complex mechanization and automation and, in particular, continuous transport.

Electric insulating materials and electro-porcelain

As is well-known, electrical insulation to a considerable degree determines progress in electrical machine and apparatus construction. The creation of a complexity of insulating materials and varnishes in a synthetic base, reducing the use of vegetable oils in varnishes and in insulation to a minimum and producing the essential minimum diversity of insulating materials for the F class of insulation are the basic problems in the field of electric insulation. A rapid discontinuation of the use of micanite for the insulation of electrical machines and the introduction of s-mica into industry are needed. It is essential to work on substitutes for mica, for example, to obtain insulation of the "escapon" type to the standard of the B and F classes. Extensive use of varnishes and enamels in epoxide, polybutadiene and polyucethane bases must be produced.

The seven year plan provides for the development of new heat-resistant polymers of a silicone organic type. Solutions must be found for the reliable and durable performance of insulation in electric machines in conditions of thermal shocks, vibrations and other forms of stress.

The technology of electrical machine impregnation and compounding must be improved, the length of processes shortened and the use of solvents reduced to a minimum, and at the same time, the quality and "monolithicity" of coil sections must be increased.

In the current seven years, operations are planned for reducing the thickness of body insulation and at the same time increasing mechanical and dielectric strength and thermal conductivity.

It is essential to produce improved laminated insulating materials and also to introduce into industry in large quantities grain orientated magnetic steel, which should be of great interest to electrical machine designers, as it enables the efficiency and cos ϕ of machines to be increased.

The development and inception of heat-resistant coverings on a ceramic base for sheet steel are also required to enable it to be annealed without damaging the insulation sheathing.

The problems of electro-porcelain production lie in the development and introduction into industry of porcelain with increased stability and the creation of small-dimensional insulators on this base.

Another task of the electrical industry is to introduce stealite widely in electrical equipment construction. Planned measures must be be taken for the drastic extension of the use of glass in insulator production.

Chemical sources of current and electro-carbon products

The main problem in this field of the electrical engineering industry lies in the introduction into industry and the national economy of nickel-iron accumulators with an increased period of service and reduced weight per unit capacity.

The commutating capacity and quality of electric brushes are of immense significance for electrical machine construction. This most important problem has to be solved by the appropriate organizations. Furthermore it is planned to perform operations to obtain nearer absolute carbons with increased luminous flux for cine-projectors. There will be a great development in the use not only of metallo-ceramic switches and magnets but also metallo-ceramic construction components for products of the electrical industry.

Problems in adjacent industries

The chemical industry must bring into the industry and produce in adequate quantities masticated rubbers, plastics, coatings, varnishes and enamels on bases of synthetic polymers.

The wood and paper industry must tune up production of glass, asbestos and cellulose papers and pressed paper. The improvement of the quality of large-size electrical engineering unshrinkable pressed paper used in transformer construction is of special importance.

Ferrous metallurgy must ensure production of electrical engineering steel with a cubic texture, rolled steel with an insulated heat-resistant covering, and steel with specific losses amounting to about 0.5 W/kg with an induction (flux density) equal to 10,000 G.

At the same time it is necessary to tool up production for a series of special magnetic sheet steels for use in magnetic amplifiers, chokes, instrument transformers and other instruments and machines, required for automatic electric drives.

The enumerated basic, but far from complete technical trends and problems confronting the electrical engineering industry, require organised measures for their solution. Therefore, for purposes for accelerating utilization and introduction into industry of perfected designs of electrical engineering products, it is planned primarily to

rely on the realization of experimental construction operations for the development of these products in the laboratory and design offices of the leading concerns (organizations) of the electrical engineering industry. This measure will increase their responsibility for the introduction of new techniques and will be a stimulus towards the rapid growth of design offices, laboratories and experimental bases in factories.

Moreover the scientific research institutes, on which the co-ordination of the experimental construction and scientific research operations in the various branches of production rests will be more intensively occupied with scientific research into the general problems which direct the development of engineering.

Responsibility for the technical development and the technical level of the branches of the electrical engineering industry rests on the leading scientific research institutes.

Scientific research institutes are founded and organized for purposes of relating scientific research to production needs in the largest factories of the electrical industry.

Scientific technical councils, whose membership includes representatives of large factories and factory scientific research institutes, are being set up in the leading scientific research institutes. These councils will realize the co-ordination of the tasks involved in a new technique in a given branch of the electrical engineering industry.

It is foreseen that the staff of design and technological departments, laboratories and experimental sections in factories will increase by many times in order to solve the problems in the field of a new technique. The problem of the Councils of the National Economy and organizations of the electrical engineering industry, it to produce the material resources required by the government rapidly and relentlessly.

The hitherto existing practice in which there are no laboratory or experimental bases in factories has led to the production of obsolete equipment and must no longer take place.

For instance, the Ural electrical apparatus factory has been running for 30 years, but still has no laboratory, as a result of which the oil disconnecting switches of this factory are heavy and have little disconnecting capacity.

The Kharkov factory "Elektrotiazhmash" (Electric traction machines) also has not was yet constructed a laboratory building and in consequence is slow to solve the problems of the new techniques of locomotive and

turbo-generator construction.

The Novosibisk turbo-generator factory and a series of other factories are in exactly the same position. The Ministry of Power Station Construction must take every available measure and by 1960 complete the building of a range of breaking capacities, which enables progress in high-voltage electrical equipment to be accelerated and our power stations to be supplied with modern and reliable equipment.

Coincident with the expansion of factory experimental bases, the development of the leading scientific research institutes, as specified by the seven-year plan, must be realized. The accomplishment of this task rests on the State Committee of the Council of Ministers of the U. S. S. R. for Automation and Engineering.

Apart from the expansion of factory experimental and construction bases for the realization of the development of the electrical engineering industry it is essential for every organization and Council of National Economy to reinforce preparatory production facilities in the factories, since, frequently, finished designs are not being introduced into industry because of lack of tools and technological equipment.

Only a considerable extension of the tool rooms in factories will enable new types of products to be introduced quickly into industry.

It seems to us that the expansion reserve of the tool room lies first, in increasing inter-changeability in tool rooms (up to two complete changes) and, secondly, the extension of these workshops at the expense of areas vacated, once complex mechanization and automation and centralized production of fastening components, plastic products, etc. are accomplished.

A great number of assembly lines and assembly machines have been selected by the Government for purposes of increasing rapidly the technological level of industry and of improving operating efficiency. This measure must be realized within the shortest time possible.

The large reserves of the electrical engineering industry must be utilized by working on the unification and standardization of creative designs. The leading institutes plan to develop their standardization and nationalization departments in order to ensure the maximum economically justifiable unification of new workable designs. The direction and co-ordination of work to establish optimum dimensional ranges (series) and types of electrical engineering products is the responsibility of these departments.

The responsibility for the co-ordination of the plans of all sections

of the electrical engineering industry, their functional control and organization rests with the State Committee of the Council of Ministers of the U.S.S.R. for Automation and Machine Construction.

In order to fulfil the tasks confronting the electrical engineering industry, cohesion of every force and an iron discipline in accomplishing the approved plans is needed.

One can rest assured, that the workers of the electrical engineering industry will honourable fulfil the tasks set them by the Party and the Government.

Translated by J.F. Boyland

1960

OPTIMUM CONTROL SYSTEMS FOR THE FLYING SHEARS DRIVE IN A ROLLING MILL*

S.M. DOMANITSKII

Automation and Telemechanics Institute of the
Academy of Sciences of the U.S.S.R.

(Received 12 September 1959)

By optimum systems are meant nonlinear automatic control systems ensuring maximum rapidity in operation under the definite limitations placed on the co-ordinates of the controlled object. In recent years the theory of optimum systems has developed extensively. In the main works on this problem [1-3] the questions of the analysis and synthesis of expremely important classes of systems are posed and resolved. In [4] a method is presented for the design of the controlling part of optimum systems, the object of which can be presented as two integrating links and a link with pure delay. The ideas given in these works have been used for designing optimum control systems with d.c. motors, in particular, drive systems for the flying shears of a rolling mill.

The main principles of the theory

Let us examine the main principles of the theory of optimum transient processes in respect of the controlled object – a d.c. motor. In actual drives the values of the current and speed of the motor are usually limited. The limitation to the current of the motor is specified by commutation, and the limitation to the speed by the maximum voltage supplied to the armature of the motor. In order that the current and voltage of the motor should not exceed the admissible quantity, appropriate feed-backs are usually introduced in the control system for the drive, which limit these quantities.

In the majority of cases, apart from the limitations with respect to the current and voltage, there is also a limitation to the temperature rise of the motor. The theory of systems intended for working through a path in the presence of a limitation on temperature rise has

---

* *Elektrichestvo*, No.1, 27-33, 1960.

been described in detail in [5 and 6]. For drives where the static load torque is small and adjustment of a misalignment in the path takes a relatively short time, there is no limitation to the temperature rise of the motor. In the present work this simpler, but practically important class of systems is examined in the case of only one limitation – namely with respect to the current of the motor.

We will first consider the simplest case – a drive intended for working through a path with inertia-less control of the motor, e.g. a controlled mercury-arc rectifier/motor system (Fig. 1, a). We assume that only one limitation is imposed on the system – a limitation to the motor current. Before adjustment and after adjustment of an misalignment in the path, the motor is stationary.

1960

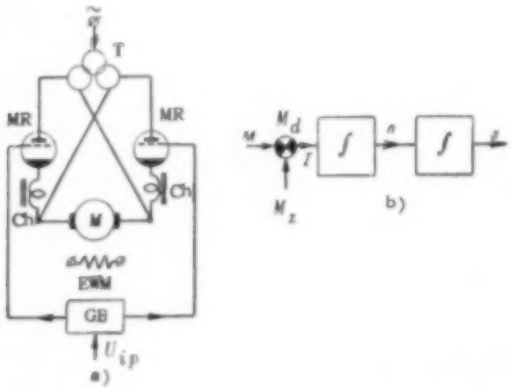

Fig. 1. Controlled mercury-arc rectifier/motor (a) and its basic circuit (b).
T – transformer; MR – mercury-arc rectifiers; M – motor; EWM – motor field winding; Ch – choke coil; GB – grid control system; U_{ip} – control action.

The differential equations describing the movement of the drive when working through the given path in this system are written as follows:

$$\frac{dn}{dt} = \frac{375}{GD^2}(M - M_z) = \frac{375}{GD^2} M_d \tag{1}$$

$$\frac{ds}{dt} = n, \tag{2}$$

where M is the torque developed by the motor;

M_z is the load torque;
M_d is the dynamic torque;
n is the speed of rotation of the motor;
s is the path completed by its shaft;
GD^2 is the flywheel moment of the drive with respect to the shaft of the motor.

Since $M = cI\Phi$, where Φ = const. and $M_z = 0$, the drive can be presented in the form of two series-connected elements (Fig. 1, *b*). The input quantity of the first element is the current I and of the second the speed n of the motor. In the general case in the presence of a load, a quantity proportional to the acceleration A of the motor is passed to the input of the first integrating element. The motor adjusts some given misalignment in the path s_0 within a minimum time, if the average speed during the transient process is the maximum. For this it is necessary for the speed to vary with the maximum possible acceleration, which is limited by the admissible current I_{max} of the motor. As is shown in [1], for systems described by second-order differential equations, the optimum transient process always consists of two intervals. In each of these intervals the motor current must be kept constant and equal to the maximum admissible value (positive or negative). Fig. 2 shows graphs of the variation of the current, acceleration, speed and adjustment path with M_z = const., and the steady-state speed n_0 of the motor, equal to zero. Similar graphs of the speed and other quantities can only be obtained in nonlinear control systems. As can be seen from the graphs, in Fig. 2 the acceleration time t_a and braking time t_b are not equal to one another.

If we write

$$\frac{t_a}{t_b} = \frac{A_b}{A_a} = k \tag{3}$$

then the acceleration or braking times (first and second intervals) can be calculated from the formulae

$$t_a = k\sqrt{\frac{s_0}{\frac{A_b}{2}(1+k)}} \quad \text{and} \quad t_b = \sqrt{\frac{s_0}{\frac{A_b}{2}(1+k)}}, \tag{4}$$

where s_0 is the misalignment in the path which the optimum system must adjust.

Depending on the sign of the misalignment in the path, the first

pulse of the control action must be given for acceleration of the motor in one direction or the other. This can be done with a simple logical system. After working through the acceleration path

$$s_a = \frac{k}{1+k} s_0 \tag{5}$$

the control unit of the optimum system must alter the sign of the control action. The motor will decelerate and when it has stopped the control action must be switched off.

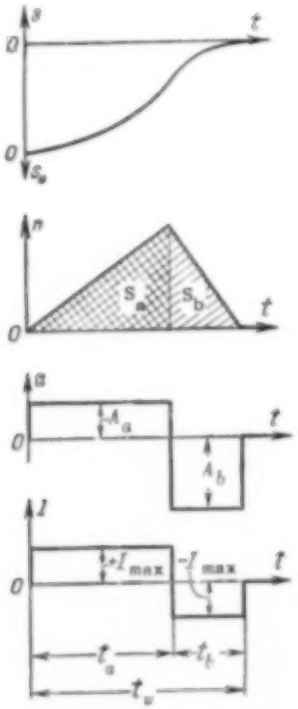

Fig. 2. Graphs of the variation of the current, acceleration, speed and displacement in the optimum control systems where M_z = const and $n = 0$.

In the absence of a load $A_a = A_b = A$, and therefore the acceleration and deceleration times can be determined from the formulae

$$t_a = t_b = \sqrt{\frac{s_a}{a}}. \tag{6}$$

In this case switching of the control action must take place after working through the path $s_0/2$. The over-all times for the transient process for the cases $M_z = 0$ and $M_z = \text{const.}$, are $t_w = t_a + t_b$, where t_a and t_b are determined from equations (6) or (4) and (5).

Thus, to obtain an optimum transient process, the control unit of the system must ensure variation of the sign of the control action at a definite moment of time in relation to the path value s_0. In particular, to determine the moment of switch-over it is possible to use a computer for determining the amount of the misalignment path covered during the first interval of the transient process.

Control of flying shears drive

The flying shears must cut a strip of metal coming from the last stand of a continuous mill into pieces of a given length. The required accuracy in the measured cut is achieved by synchronizing the speed of the shears and the speed of the strip, in such a way that, during the period between two meetings of the blades, a strip of metal of the specified length passes between the shears. The linear speed of the strip v_s should here be close to the linear speed v_c of the blades. Where this is not the case, the metal may damage the blades or a poor cut may be obtained. The relations between the speed of the shears and the strip must be preserved when the rolling speed changes. This is ensured by the tachometric system (Fig. 3) by comparison of the voltages of two tachogenerators. The tachogenerator *TGS* is on the shaft of one of the stands of the mill and its voltage is proportional to the speed of the metal strip, and the tachogenerator *TGC* is installed on the shaft of the shears. The difference between the voltages of the tachogenerators is amplified and controls the voltage of a mercury-arc rectifier or generator supplying the motor *MC* of the shears. As a result, the drums of the shears rotate continuously in synchronizm with the shaft of the stand, both during cuts and between them. The relation between the speeds of the mill stand motor and the shears motor and, consequently, the length of the measured cut also l_s, are established by means of a potentiometer P (Fig. 3 and 4). The supply of the next billet into the rolling mill occurs at random moments and therefore, unless special measures are taken, the length of the first cut piece Δl will be any length from zero to the measured length l_s.

The use of a new system of controlling the cut of the front end, designed on the basis of the theory of optimum processes, will make it possible to obtain a first piece which is always of one and the same given length, regardless of the time of delivery of the billet from the mill. The control apparatus of the system carries out automatically the following operations: determines and memorizes the misalignment

between the position of the blades of the shears and the forward end of the rolled strip, transmits the control action to the shears drive system, which causes braking of the motor, determines the moment for changing the sign of the control action, ensures acceleration of the motor to the steady-state speed n_0, switches off the control action. The process of adjustment of the misalignment between the position of the blades and the front end of the strip is always carried out in the system within the minimum period in accordance with the triangular tachogram. After the front end is cut, the drive operates in accordance with the tachometric system and the shears cut the metal into the measured lengths.

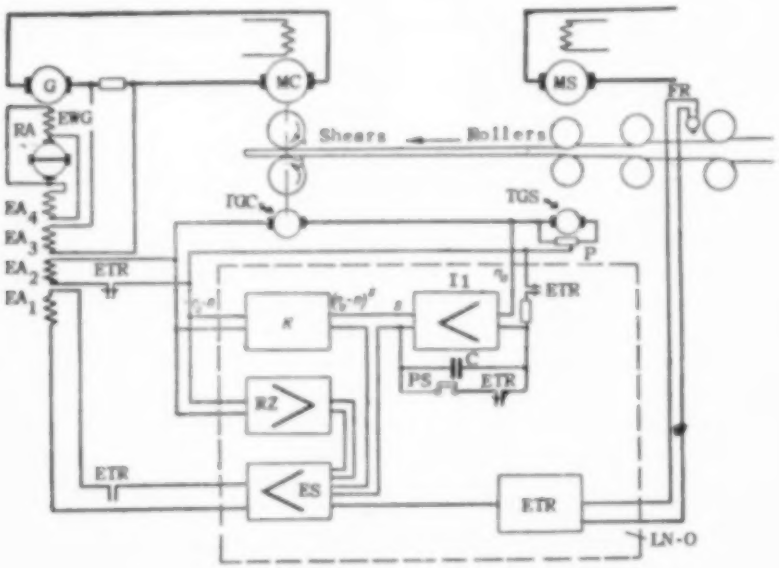

Fig. 3. Block diagram of optimum system with *LN-O* control apparatus.

In designing optimum control systems for the flying shears drive, the following must be taken into account:

1. In steady-state conditions the speed of the motor for the shears is not zero, and therefore the misalignment adjustment path must be defined as $\int_0^t (n_0 - n)\,dt$.

2. The load of the drive is zero.

3. In the system the generator voltage is limited.

4. The flying shears drive can be designed both according to the controlled mercury-arc rectifier/motor system (*CMR-M*), and according to the *G - M* system, where it is necessary to allow for the inertness of the generator and the rotary amplifier.

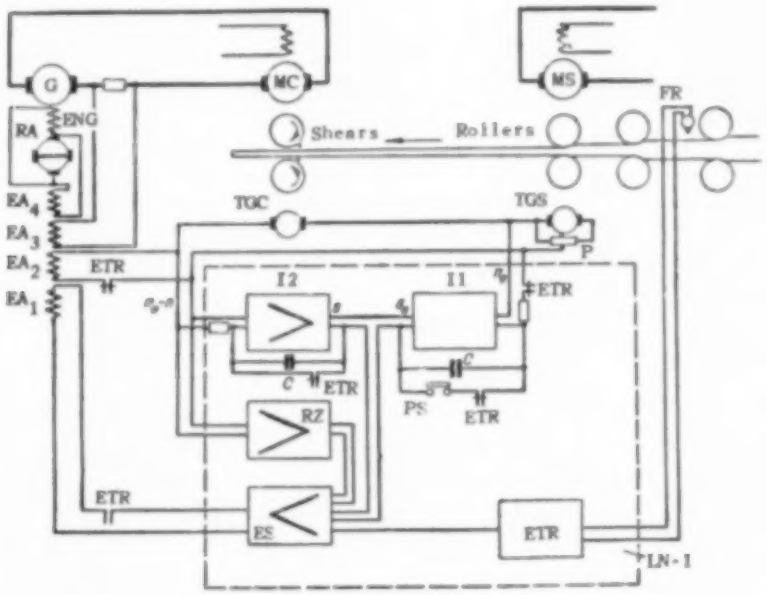

Fig. 4. Block diagram of optimum system with *LN-1* control apparatus.

The first and second conditions are allowed for very simply. With no limitation of the generator voltage, the optimum control system for the flying shears can be designed in such a way that adjustment of the misalignment s_0 is achieved where $0 < s_0 < \frac{l_M}{2}$ by a reduction, and where $\frac{l_M}{2} < s_0 < l_M$ by an increase in the speed of the motor. However, where there is a limitation on the generator voltage, this is inexpedient, since the shears motor and the mercury-arc supply rectifier (generator) must be designed for a voltage 2-2.5 times greater than the voltage corresponding to the steady-state speed of the shears. With adjustment of a misalignment merely by means of a reduction in the speed of the motor simultaneously with a reduction in the output of the generator and the motor, the control unit is simplified since the first control action pulse is always for braking of the motor. In this case

the limitation on the generator voltage is of no importance since operation in accordance with the triangular speed graph is possible up to the final speed of $n = -n_0$.

Therefore, for the flying shears drive, in any misalignments it is expedient to carry out adjustment by reducing the speed of the motor.

To ensure a rapid increase in the current of the motor in a *G - M* system with a rotary amplifier (Fig.3 and 4), the latter is embraced by a rigid voltage feedback. In this case it is possible to achieve a current increase time of 0.15-0.2 sec and in practice the *G - M* system can be presented in the same way as the *CMR - M* system - in the form of two integrating elements. Good filling of the current diagram in the circuits is obtained by means of a negative feedback for the motor current. During adjustment of the misalignment s_0, the circuit of the winding EA_2, of the rotary amplifier, connected to the difference between the voltages of the tachogenerators, is broken, and action of the appropriate sign is transmitted from the control apparatus to the winding EA_1.

Block diagrams of optimum systems

In the Institute of Automation and Remote Control of the Academy of Sciences of the U.S.S.R., two circuits have been developed for the systems ensuring adjustment of the misalignment in accordance with an optimum law. The first of them with an *LN-0* device, which has a computing section based on an integrator and a quadrator, and the second with an *LN-1* control apparatus, where the quadrator is replaced by another integrator.

The block diagram of the system with the *LN-0* control device is shown in Fig.3. The position of the blades of the shears and the misalignment in the path between the blades and the forward end of the strip is determined in the system at the moment when the photo-electric relay *FR* lights up. For this purpose, a voltage taken from the potentiometer *P* to which the tachogenerator *TGS* is connected is passed to the integrator *II*. This voltage is proportional to the speed of the strip and with a high amplification factor in the tachometric circuit it corresponds to the speed of the blades. The capacitor *C* of the integrator *II* is periodically short-circuited by the path switch *PS* each time the blades of the flying shears meet. If the measured cut is made at each revolution of the shears drum, the path switch will close in a time t^*. Then, at the output of the integrator *II* the saw-tooth voltage shown in Fig.5a by the continuous lines is obtained. If the cut is made with a system of omissions, e.g. every fourth revolution of the drum, the maximum voltage at the integrator input will be 4 times

greater, since the path switch will short-circuit the capacitor for intervals equal to $4t^*$. The corresponding curve is shown in Fig.5, *a* by the dotted line.

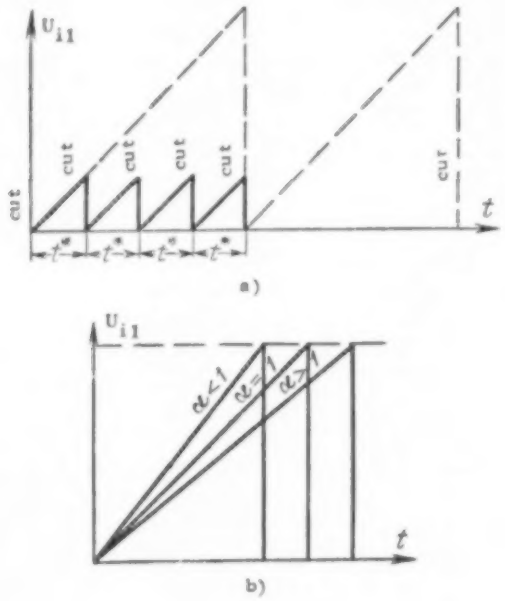

Fig. 5. Voltage at the output of the memory integrator *Il*.
a) with different numbers of revolutions of the drum per cut;
b) with different values of the quantity

If the operator alters the measured length $l_м$, the voltage taken from the potentiometer *P* and passed to the input of the integrator *Il* alters. Hereupon the speed of the shears motor changes and also the time between cuts t^*. If the speed of the shears motor decreases $\left(\alpha = \frac{v_м}{v_c} > 1\right)$, then the time t^* increases and vice-versa. As a result of a simultaneous variation in the slope of the straight-line voltage curve at the input of the integrator $U_{il} = f(t)$ and in the time t^* at different values of α the quantity U_{il} corresponding to one revolution of the drum remains constant. Thus, the voltage at the input of the integrator *Il* always characterizes the position of the blades at a given moment of time.

Determination of the misalignment s_0 is achieved in the system in Fig. 3 in the following way. After the photo-electric relay *FR* lights up, the electronic time relay *ETR* operates and opens its normally-closed contacts in the circuits of the integrator *Il*. Hereupon the input of the integrator *Il* is disconnected and at the capacitor *C* of the integrator a definite voltage U_{il} is stored. The time lag of the relay *ETR* is chosen so that, when the forward end is cut off at the given length Δl, a voltage equal to zero is stored at the integrator. This case corresponds to the absence of a misalignment in the system. Then, with any misalignments, a voltage will be stored at the integrator proportional to the path which must be covered (Fig. 5*b*). The length of the forward end Δl can be regulated by varying the time lag of the relay *ETR*.

In the circuit in Fig. 3, simultaneously with the memorizing of the misalignment, the winding EA_2 of the rotary amplifier *RA* is disconnected from the tachometric circuit, and a control action pulse is passed to the winding EA_1 causing braking of the motor. To determine the moment of alteration of the sign of the control action, the misalignment path covered by the shears motor during braking is evaluated. For this, the voltage difference between the tachogenerators *TGS* and *TGC* is passed to the input of the quadrator *K*. In the case of a constant acceleration, the path covered by the motor is proportional to the quantity $(n_0 - n)^2$. Therefore it is possible to determine the moment when the control action sign changes if the voltages taken from the integrator *Il* and the quadrator *K* are selected in such a way that when the path $s_0/2$ is covered, $U_k = U_{il}$. At this moment of time the difference between the voltages passed to the input of the electronic switch *ES* changes sign and the latter changes over the control action. At this the motor will begin to accelerate. When the former steady-state speed n_0 is reached, the control action is switched off by means of the electronic zero-relay *RZ*, and the winding EA_2 of the *RA* is again connected to the tachometric circuit.

As quadrator in the *LN*-0 apparatus we used thyrites with a non-linear characteristic. With compensation of the variation in the characteristics of the thyrite in relation to the temperature by means of thermistors, we obtained a squaring accuracy of about 0.5 per cent.

The circuit with a quadrator examined above has an essential disadvantage. With a non-stabilized control action source (control voltage passed to the winding of the *RA*) the currents and acceleration of the motor may vary. The system in Fig. 3 carries out switching-over of the control action as a function of the voltage proportional to $(n_0 - n)^2$. Therefore, with identical values of s_0 but different accelerations, the switching processes will take place at the same motor speed.

1960

As a result, the path actually covered will be smaller when acceleration is increased, and greater when it is reduced than the given path s_0. Thus, an error develops in the system when the acceleration is varied. This defect is eliminated in the system with the *LN-1* apparatus.

The block diagram of the optimum system with the *LN-1* device is given in Fig. 4. The apparatus carries out the same functions as the *LN-O* apparatus. The integrator *I1*, in the same way as in the *LN-O* system, serves to determine the size of the misalignment in the path. When the time relay *ETR* operates, after the photo-electric relay *FR* lights up, at the integrator *I1* a voltage U_{i1} is stored which is proportional to the misalignment which must be adjusted. At the same time a pulse is passed into the system, causing braking of the motor. The integrator *I2* serves to determine the moment for the control action to change sign. It has the same circuit as the integrator *I1* and is connected to the difference between the voltages taken from the tacho-generators *TGS* and *TGC*. The capacitor of the integrator *I2* is normally short-circuited by the contacts of the relay *ETR* and is disconnected when the pulse is transmitted for braking of the motor. The voltage at the integrator output will be proportional to the quantity

$$\int_0^t (n_0 - n)\,dt.$$

at any acceleration of the motor.

Therefore, the use of the integrator *I2* in place of the quadrator *K* increases the accuracy of adjustment. The time constant of the integrator *I2* is half that of the integrator *I1*, and therefore the output voltage U_{i2} of the integrator *I2* becomes equal to the voltage U_{i1} at the moment when the drive has worked through half the misalignment angle in the braking period.

When the quantities U_{i1} and U_{i2} are equal, the difference between these voltages which is passed to the input of the relay *ES* will be zero. The relay *ES* operates and changes the sign of the control action. Where $n = n_0$, the zero relay *RZ* switches off the action and the necessary misalignment will be adjusted.

In the presence of a constant load, the change-over of the control action must take place after working through the braking path $s_b = \frac{s_0}{1+k}$. This can be achieved if a corresponding change is made in the amplification factor of the integrator *I2*. In the system with the *LN-O* control element, the influence of the load can be allowed for if a voltage divider is installed between the tacho-generator *TGS* and the

input of the quadrator *K*.

Experimental investigation of optimum control systems

The experimental investigation of the optimum systems was carried out on the continuous electronic modelling installation *EMU-6* and on a physical model of flying shears.

On the electronic modelling installation we investigated a flying shears drive system based on a *G - M* system with a rotary amplifier. As control apparatus we used a *LN-0* apparatus with a quadrator based on a thyrite. In the investigation we ignored the time constant of the armature circuit of the *G - M* system and the time constants of the control windings of the amplifier.

The differential equations written for the closed electric drive system in deviations of quantities take the form:

$$(T_{RA}\,p + 1)\,E_{RA} = k_1 F_y; \tag{7}$$

$$(T_g\,p + 1)\,E_g = k_2 E_{RA}; \tag{8}$$

$$(\theta p + 1)\,n = k_3 E_g; \tag{9}$$

$$s = k_4 \frac{n}{p}. \tag{10}$$

where E_{RA} and F_y are the e.m.f. of the longitudinal circuit and the resultant magnetizing force of the *RA*;

E_g is the generator e.m.f.;

n and s are the speed and the path covered by the shaft of the motor;

T_{RA} is the time constant of the transverse circuit of the *RA*;

T_g is the time constant of the generator excitation circuit;

θ is the electro-mechanical constant of the motor;

$k_1 - k_4$ are amplification factors.

From the block diagrams in Fig. 3 and 4 it follows that in the regulation systems there are feedbacks for the speed and current of the motor. On the modelling installation we set up a drive circuit corresponding to these block diagrams. In order, on the model (Fig. 6), to separate directly the quantity proportional to the current of the motor, we used an additional differential equation

$$(\theta p + 1) I = k_5 E_{RA} - k_6 E_g. \tag{11}$$

To model the drive we used seven decision amplifiers *DA-1* to *DA-7*, one of which was necessary merely for changing the sign. In the investigation we selected circuit parameters corresponding to the drive of 100-ton planetary flying shears. For this circuit $T_{RA} = 0.15$ sec, $T_g = 2.8$ sec, $= 0.335$ sec, $k_1 = 1$, $k_2 = 3.38$, $k_3 = 1.05$, $k_4 = 1$, $k_5 = 2.12$, $k_6 = 0.625$.

In the system with current and speed feedbacks, the expression for the resultant magnetizing force of the rotary amplifier can be written in the following way:

$$F = F_y - k_7 I - k_8 n. \tag{12}$$

The amount of the speed and current feedback was controlled by variation of the coefficients k_7 and k_8 by varying the resistances R_1, R_2 and R_3 at the input of the decision amplifier *DA-1*.

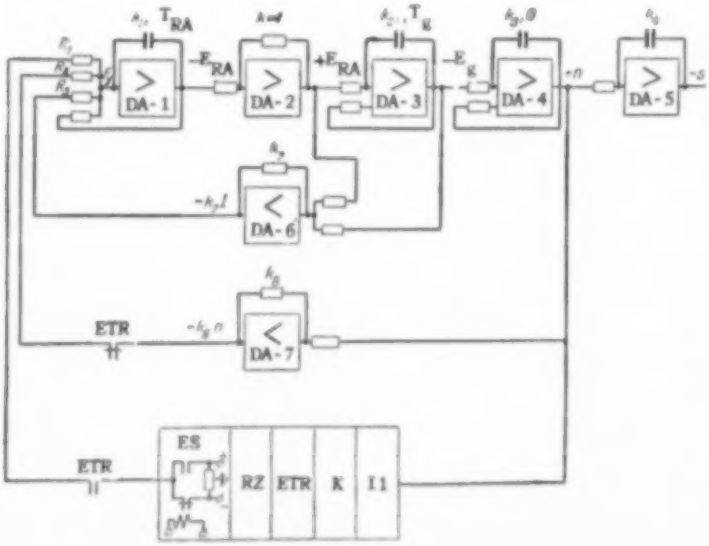

Fig. 6. Block diagram of the model of the optimum control system for the flying shears drive with an actual control apparatus.

The investigations carried out on the electronic modelling installation showed that where $T_{RA} < 0.1$ sec, the transient processes are

close to the optimum. For the purpose of increasing the steepness in the rise and improving the form of the current curve in the system with the rotary amplifier, it is desirable to encompass the latter by a negative feedback of the amplifier voltage.

Fig.7 shows oscillograms of the variation of the control action U_{ip} (the voltage passed to the input of the *RA*), the current *I*, the speed *n* and the path *s* where $0 < s_0 < s_{0max}$. As the investigations showed, the adjustment of the misalignment path is carried out in the system with an accuracy of up to 1 per cent of the maximum misalignment corresponding to the measured cut l_m. As can be seen from the oscillograms, the transient processes are close to the optimum.

On the physical model, a circuit was assembled* with a PN-85 motor fed from a PN-290 generator, in accordance with Fig.4. The excitation of the generator was carried out from a *EMU*-50 rotary amplifier. All the time constants of the electrical machines were fixed in accordance with the data given above for the electronic model. The motor *MC* turned the contact apparatus via a reduction gear. When the contacts of the *PS* closed, the meeting of the blades in a cut was simulated and the capacitor of the memory integrator *II* was connected. The control apparatus *LN-1* with two integrators, at a motor speed correspon-

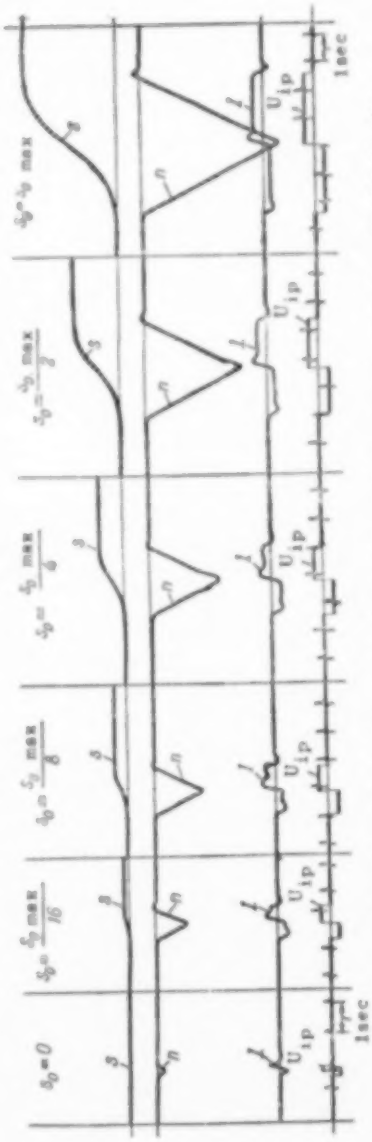

Fig. 7. Oscillograms of the control action, motor current, speed and path in the optimum system shown in Fig.6.

* The investigation on the physical model was carried out by engineers L.N. Zagal'skii and B.B. Bulanov.

1960

ding to the speed of the strip of 5.3 m/sec, ensured a mean cutting accuracy of 1 per cent of the maximum measured length of 12 m. Oscillograms recorded on the physical model are similar to the oscillograms on Fig.7. In all misalignments the transient processes took place in accordance with the optimum law.

Translated by D.R.H. Phillips

REFERENCES

1. A.Ia. Lerner, *"Avtomatika i telemekhanika"*, Nos.2 and 4 (1952).
2. A.A. Fel'dbaum, *K voprosu o sinteze optimal'nykh sistem avtomaticheskogo regulirovaniia (On the problem of the synthesis of optimum automatic control systems)* Transactions of the 2nd All-Union Conference on the Theory of Automatic Control, Vol.II, (1955).
3. A.Ia. Lerner, *Postroeniy bystrodeistvuyushchikh sistem avtomaticheskogo regulirovaniia pri ogranichenii znachenii koordinat reguliruemogo ob'ektra (Design of high-speed automatic control systems with limitation to the values of the co-ordinates of the controlled object)*, Transactions of the 2nd All-Union Conference on the Theory of Automatic Control, Vol.II (1955).
4. A.G. Butkovskii and S.M. Domanitskii, *O sinteze upravliaiushchei chasti optimal'nykh sistem dlia nekotorykh ob'ektov s zapazdyvaniem (On the synthesis of the control element of optimum systems for certain objects with delay)*. Report to the conference on the theory and application of discrete automatic systems (1958).
5. E.A. Rozenman, *"Avtomatika i telemekhanika"*, No.6 (1957).
6. E.A. Rozenman, *"Avtomatika i telemekhanika"*, No.7 (1958).

TRANSIENT PROCESSES IN AUTOMATIC STEP CHRONOMETRIC CONTROL OF ELECTRIC ROLLING STOCK*

B.P. PETROV Cand. tech. sci., docent.

Moscow Power Institute

(Received 1 September 1959)

In addition to control as a function of current (with acceleration relay), use is in many cases made of control as a function of time (chronometric control), now employed universally in smooth (continuous) electric control device installations, in order to automate step (intermittent) starting and braking of electric rolling stock traction motors.

The control parameter (the starting or braking resistance r, the voltage of the rectifier installation U etc.) is varied in jumps in these systems by means of group switches in given time intervals Δt by a finite, usually constant quantity (Δr, ΔU_{rec}).

In chronometric control systems not dependent on current, the time interval Δt remains constant, but in chronometric systems dependent on current Δt increases as the motor current I rises. Systems of the second type are the most promising and are being more and more widely used.

With some approximation, step chronometric systems in the steady-state and transient conditions may be regarded as equivalent to continuous control systems in which the rate of change of the control parameter, for example the resistance r, is equal to:

$$\frac{dr}{dt} = \frac{\Delta r}{\Delta t}. \qquad (1)$$

Therefore the methods used to investigate continuous control systems [1] are applicable for a preliminary evaluation of the properties of step chronometric control systems.

---

* *Elektrichestvo*, No.1, 33-37, 1960.

A complete evaluation of the properties of chronometric step systems is given only by an investigation which allows for the intermittent alteration of the circuit parameters. Possible methods for such an investigation are set forth below. In this connexion, chronometric control systems of two basic types are examined – with and without fixation of the group switch positions.

The system without position fixation (with continuous rotation of the armature shaft) is used during fairly large accelerations and retardations of the train, during which the minimum possible shaft rotation speed of the group switching device with contacts of the usual type and the corresponding making and breaking speed of the contacts are such that risk of interference with the arc quenching does not arise. A very simple arrangement of a current-dependent, chronometric, starting system of this type, which contains, however, all the main elements of the regulator, is presented in Fig. 1 (*a*).

In contrast to continuous control circuits, a rectifier *P* is provided in addition to preclude automatic reversal of the servomotor *SM* during excessive current peaks. Approximate curves of the time alteration of motor current *I*, angular velocity of rotation ω of the *SM* shaft and its angular displacement α after successive making of the contacts are presented in Fig. 1(*b*). The curves $\omega(t)$ and $\alpha(t)$ are presented for two cases. The continuous curves relate to the case where *SM* stops and the dotted curves to the case where *SM* does not stop.

The calculation consists of the successive determination of the shape of these curves for each successive starting position so as to establish the nature of the starting or braking diagrams $v(I)$ or $v(F)$. From the shape of these diagrams it is not difficult to give an evaluation of the properties of the control system.

To calculate the curve $I(t)$ after an intermittent change in r or U the equations for e.m.f.s and voltages in the traction motor circuit and the equation of motion of the train are used.

For rheostatic or non-rheostatic starting

$$U = L\frac{dI}{dt} + Ir + c_1 v\Phi; \tag{2}$$

$$m\frac{dv}{dt} = ma = F - w = c_2\Phi I - w, \tag{3}$$

where U is the supply voltage;
L and r are the inductance and resistance of the entire traction motor circuit;

m, w and v are the mass, resistance to motion and velocity of the train

c_1, c_2, I, Φ and F are constants,: the current, magnetic flux and tractic force of the motor.

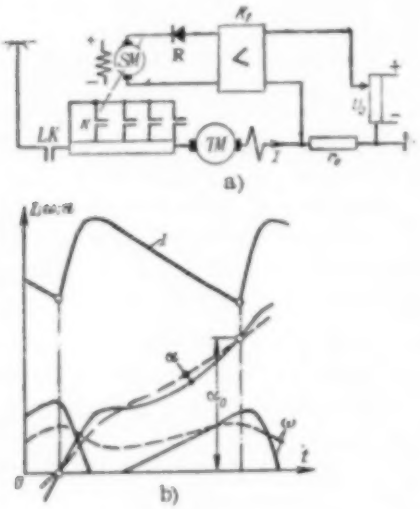

Fig. 1. Arrangement of current-dependent chronometric starting without position fixation (a) and curves of transient processes peculiar to it (b).
K-- group switch contacts; α_0 – angle of rotation of shaft of servomotor SM in the limits between the making of adjacent contacts K.

$\Phi(I)$ and $L(I)$ occur in equations (2) and (3) and also products of the variables depending on current and time $v\Phi$ and $I\Phi$. The solution is simplified if we adopt a number of usual assumptions. Firstly, linearize the magnetization curve $\Phi(I)$ in the calculation intervals ΔI, i.e. take

$$\Phi = \Phi_0 + kI. \tag{4}$$

Secondly, the inductance L and the accleration a in each calculation interval may be considered constant and equal to their mean values. Then equations (2) and (3) will be reduced to one equation:

$$U = L\frac{dI}{dt} + Ir + c_1(v_0 + at)(\Phi_0 + kI). \tag{5}$$

where v_0 is the velocity of the train at the commencement of the calculation interval.

Equations (2) and (3) take no account of eddy currents in the motor magnetic circuit as starting and also rheostatic braking (after self-excitation has been achieved) usually occur during current oscillations within the range of values where the magnetic circuit of the motor is saturated, and therefore the effect of eddy currents is insignificant.

In cases where the effect of eddy currents is substantial, for example, in the initial phase of rheostatic braking (before self-excitation has been achieved), approximate methods may be used to calculate the curve $I(t)$ (for example, [2]), taking the speed as constant for each mathematical interval and equal to its mean value (within the limits of the interval).

Solution of equation (5) in a general form is impossible as a probability integral occurs in it. For its numerical solution, a table of probability integrals should be used, or a graphical-analytical method, that of Bashkirov [3] for example.

In the latter case, equation (5) may be written in the form:

$$T(t)\frac{dI}{dt}+I=f(t), \tag{6}$$

where

$$T(t)=\frac{L}{r+c_1k(v_0+at)};$$

$$f(t)=\frac{U-c_1(v_0+at)\Phi_0}{r+c_1k(v_0+at)}.$$

Equation (6) may be solved, using the formula

$$\frac{\Delta I}{\Delta t}=\frac{f(t+\Delta t/2)-I(t)}{T(t+\Delta t/2)+\Delta t/2}. \tag{7}$$

The corresponding initial conditions are introduced during the construction.

For illustration, curves of $I(t)$ for a number of cases of starting and braking are presented in Fig. 2. It follows from Fig. 2 that smoothing of current peaks occurs more intensively the greater the acceleration or retardation and the equivalent time constant of the motor circuit

$$T_e = \frac{L}{r + c_1 k v}. \tag{8}$$

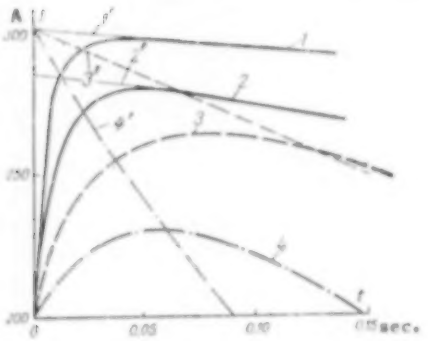

Fig. 2. Curves of motor current change after a step change of controlling parameter.
1 - second step of rheostatic starting;
2 - last step of rheostatic starting;
3 - second step of non-rheostatic starting; 4 - last step of non-rheostatic braking.
1, 2 and 3 - at $a \approx 2$ m/sec^2; 4 - at $a = -1$ m/sec^2.

The degree of current peak smoothing may be conveniently judged by comparing curves 1, 2, 3 and 4 with curves 1′, 2′, 3′ and 4′ constructed for similar conditions but with $L = 0$.

The initial values for the latter are the same as in the case of starting and braking with $L \neq 0$, but during acceleration (retardation), near to zero.

The results obtained agree with the data presented in [4] and [5].

For the calculation of the curves of $\omega(t)$ and $\alpha(t)$ on Fig.1 (б), equations are used which were constructed to apply to the arrangement in Fig.1 (а) for the circuit of the motor SM:

$$k_1 |U_a - I(t) r_a| = I_{SM} r_{SM} + L_{SM} \frac{dI_{SM}}{dt} + c_{1SM} \Phi_{SM} \omega \tag{9}$$

and the equation of motion of SM with the group switch

(9)

and the equation of motion of *SM* with the group switch

$$J\frac{d\omega}{dt}=M-M_c=c_{2SM}\Phi_{SM}I_{SM}-M_S, \tag{10}$$

where J and M_s are the moments of inertia and of resistance for the shaft of *SM*.

Due to the constructional features of group cam switches, the moments J and M_S usually alter as the shaft rotates. Therefore the calculation should be made for angular intervals $\triangle\alpha$ within the limits of which J and M_S are taken as constant and equal to their mean values.

The function $I(t)$ in equation (9) is given for the system of the motor *SM* according to equation (5).

Therefore it is possible to linearize it in intervals of time $\triangle t$, i.e. take

$$I(t)=I_0+k_2t. \tag{11}$$

No difficulties are then encountered in the analytical solution of equations (9) and (10).

On solving, the shape of the $\omega(t)$ curve is determined, and then that of the $\alpha(t)$ curve. Successive switching in the circuit occurs after the rotation of the shaft through an angle α_0. Later the calculation is repeated for new initial conditions determined by the terminal values of the variables in the preceding interval and correspondingly of the step-changed values of r or U.

Chronometric control with position fixation of the group switch is stationary until the expiry of the given time-lag, after which it switches rapidly from one position to another, changing the controlling parameter.

These systems are usually used at very small accelerations and retardations of the train, for example when starting (braking) electric locomotives with very heavy rolling stock. The time-lag t_l is effected by a time relay. Fig.3 *(a)* presents a very simple arrangement for a current-dependent, chronometric start with electric motor time relays, whereby stable time-lags of various magnitudes are obtained.

The relay motor *TRM* is connected similarly to *SM* in Fig. 1 (a). The

time of rotation of the contact disk between the making of contacts a_1 - a_2 and b_1-b_2 lengthens as the current increases. The contacts *BZ* and *BO* of the group switch are closed corresponding to its even and odd positions. The contact *BP* is closed in the intervals between the positions and serves to bring the switch to the fixed position.

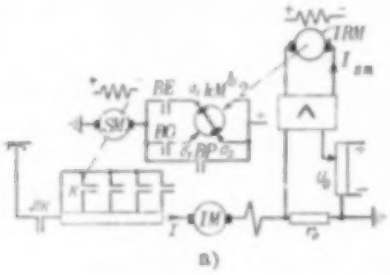

a)

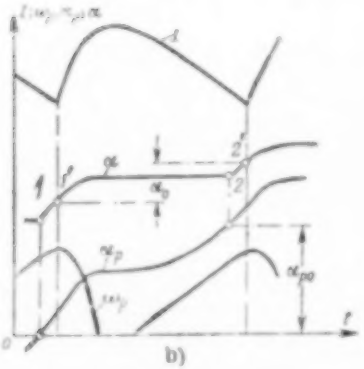

b)

Fig. 3. Simplest arrangement of current-dependent chronometric starting with position fixation (*a*) and curves of transient processes peculiar to it (*b*).

The remaining blocking contacts (terminal, return and others) are not shown on Fig. 3 (*a*).

Fig. 3 (*b*) shows approximate curves of the change with respect to time of the current of the motors $I(t)$, the angular velocity of *TRM* $\omega_r(t)$, its angle of rotation $\alpha_r(t)$, and the angle of rotation of the group switch shaft $\alpha(t)$. The points *1* and *2* correspond to the moments of closing of the time relay contacts a_1-a_2 or b_1-b_2 by the strip on the contact disk, and the points *1'* and *2'* to the moments of closing of contacts *K* of the group switch. Here α_{r0} and α_0 are the angles of

rotation of the armatures of *TRM* and *SM* in the interval between the closures of the contacts.

The sequence of construction of the curves $I(t)$, $\omega_r(t)$, $\alpha_r(t)$ is the same as for the curves $I(t)$, $\omega(t)$ and $\alpha(t)$ in Fig. 1 (*b*).

Construction of the curve of $\alpha(t)$ for *SM* is done allowing for the change in J and M_s as the shaft of *SM* rotates.

In many cases of chronometric control there is no necessity to carry out such cumbersome calculations, as the shape of some transient processes is quite obvious.

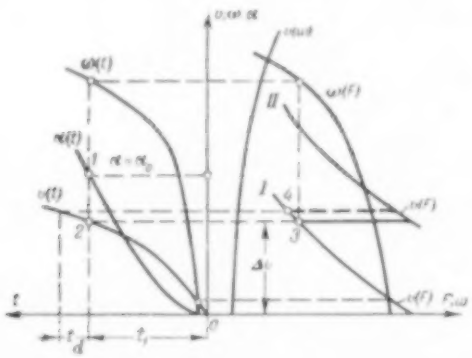

Fig. 4. Curves for determining the moment of switching of the group switch from one position to another when acceleration is low and the control system has a current-dependent characteristic.

For example, at the very small accelerations inherent in the starting of heavy trains the current peaks from one position to another are completely determined by the intercepts of the abscissae between the characteristics $v(I)$ (initial and successive) at constant velocity. With further change in velocity, the change in current proceeds in accordance with these characteristics. Therefore the construction of the starting diagrams $v(F)$ is considerably simplified, especially for current-independent, chronometric systems, and also for current-dependent control systems with little inertia, when the change in the speed of rotation of the motor *SM* (or of the time relay *TRM*) proceeds fairly exactly in accordance with the static curve (I) of the control system.

In this case, at the start of the calculation curves of $v(F)$ and ω

(F) are constructed on the basis of the curves of $v(I)$, $\omega(I)$ and $F(I)$ (Fig.4). Then the following curves are constructed for the original characteristic $v(F)$: motion of the train $v(t)$, $\omega(F)$, $\omega(t)$ and $\alpha(t) = \int \omega dt$. If α_0 is the angle of rotation of *SM* in the interval between the closures of the contacts (in the arrangement in Fig.1 (a)), then the point *1* determines the instant of time t_1 when the next contact of the group switch will be closed and the transition to the next $v(F)$ characteristic accomplished. (point *3*).

The curves $\omega(F)$ and $\omega(t)$ also relate to the relay *TRM* in the arrangement in Fig.3 (a). Here the switching time of the group switch t_2 should be added to t_1. Then switching to the next position will occur at point *4*.

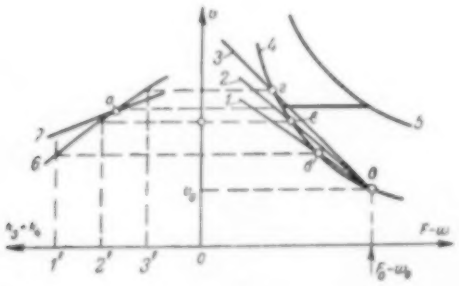

Fig. 5. More precise method for determining the moment of transition from one position to another during current-independent chronometric control.

The graphical methods familiar from the theory of tractive calculations are adequate for the construction of the curve of motion $v(t)$. It is simpler to use analytical methods of calculation when the characteristics $v(F)$ are linearized [6].

The equation for each section of the tractive characteristic linearization is

$$F = F_0 - k_1 v. \tag{12}$$

The curve of resistance to motion $v(w)$ also may be linearized:

$$w = w_0 + k_2 v. \tag{13}$$

Substituting (12) and (13) in the equation of motion and integrating

it, we obtain:

$$\Delta v = \frac{F_0 - w_0}{k_3 + k_4}\left(1 - e^{-\frac{k_3 + k_4}{m} t}\right), \tag{14}$$

where for F_0 and w_0 values are taken corresponding to the beginning of the mathematical interval on the selected tractive characteristic $F(v)$;

Δv is the velocity increment in the mathemtical interval.

In the case where the control system is a chronometric one, not dependent on current, i.e. the position time-lag t_l is invariable, the velocity increment Δv from its original value v_0 is determined directly from equation (14) at the moment of transition from the preceeding characteristic for which the calculation is being made (for example, 4 on Fig. 5) to another one, 5. However, in such a calculation a difficulty arises in connexion with the determination of coefficients k_3 and k_4 as it is not known in advance what part of the characteristics $v(F)$ and $v(w)$ should be linearized.

This difficulty is avoided by means of a simple supplementary construction.

From the starting point 0, strainght lines 0-1, 0-2, 0-3 are drawn (Fig. 5), which intersect the curve $v(F - w)$ at the points b, c and d respectively. The velocity increments corresponding to the latter points are Δv_{k1}, Δv_{k2} and Δv_{k3}. According to the angular coefficients $k_3 + k_4$ of the straight lines 0-1, 0-2 and 0-3 the velocity increments Δv_{r1}, Δv_{r2} and Δv_{r3} are determined from equation (14) and the curves $\Delta v_k(k_3 + k_4)$ (curve 6) and $\Delta v_r\ (k_3 + k_4)$ (curve 7) are constructed.

Their point of intersection a determines the desired value of Δv and the corresponding value of $k_3 + k_4$. A similar calculation is repeated for each of the tractive characteristics.

Using the methods discussed for example, starting diagrams were calculated for an NO rectifier electric locomotive with current-independent (Fig. 6) and current-dependent (Fig. 7) control systems.

The calculation shows that with a step control system independent of current, as with continuous control, the mean starting current rises essentially as the increase in resistance to motion (intercepts 2 and 3, Fig. 6).

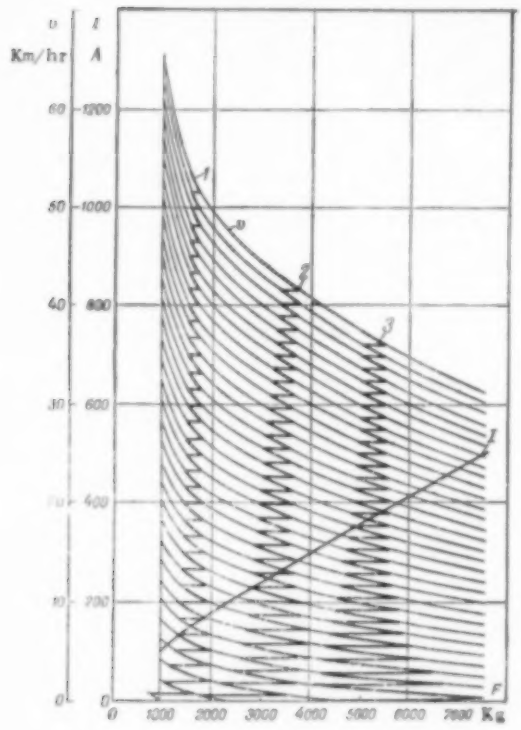

Fig. 6. Calculated starting diagram of MO electric locomotive with current-independent chronometric control.

1 – electric locomotive by itself on the flat (time of switching to one position $\Delta t \approx 0.9$ sec; *2* – electric locomotive with 3000 tons of rolling stock on the flat; *3* – MO electric locomotive with 3000 tons of rolling stock on a 1 in 250 gradient. For the last two cases the time of switching to one position $\Delta t \approx 9$ sec.

On the other hand, if current-dependent, chronometric control is used with a characteristic of the form of curve *3* in Fig. 7, the starting current remains almost constant at various resistances to motion (intercepts *1* and *2*, Fig. 7). This is of great significance in the case of a start at the coupling limit. Moreover, there is a substantial decrease in the time for the current to increase from its initial value, corresponding to the first position, to the mean starting (or braking) current.

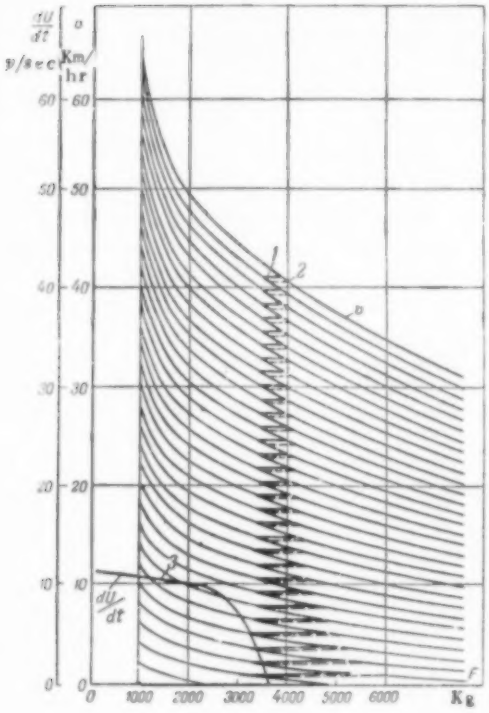

Fig. 7. Calculated starting diagrams for MO electric locomotive with current-dependent chronometric control.

1 - electric locomotive with 3000 tons of rolling stock on the flat; *2* - electric locomotive with 3000 tons of rolling stock on a 1 in 250 gradient (in both starts the time-lag at positions $\Delta t \approx$ 9 sec); *3* - control system characteristic.

All these characteristic relationships, presented in Fig. 6 and 7, are confirmed by the results of testing the chronometric control systems of NO and N60 electric locomotives.

Translated by R.D.M. Hegarty

REFERENCES

1. B.P. Petrov and A.D. Stepanov, *Upravleniye elektricheskim podvizhnym sostavom (Control of electric rolling stock)*, Gosenergoizdat (1956).
2. A.B. Ioffe, *Tyagovyye elekricheskiye mashiny (Electric traction machines)*,

Gosenergoizdat (1957).

3. D.A. Bashkirov, *Grafoanaliticheskiye metody postroyeniia perekhodnykh protsessov v sistemakh avtomaticheskogo regulirovaniia (Graphoanalytical methods of plotting transient responses in automatic regulating systems)*, symposium *"Osnovy avtomaticheskogo regulirovaniia" ("Automatic regulating fundamentals")*, Mashgiz (1954).
4. V. Bader, *El. Bahnen*, p. 247 (1931).
5. V.E. Skobelev, *Zaklyuchitel'naia faza reostatnogo tormozheniia (The final phase of rheostatic braking)*, *"Elektrichestvo"*, No. 9 (1956).
6. N.N. Sidorov *Rasch't kharakteristik puska i tormozheniia pri zamedlennom khode kontrolle ra (Calculation of starting and braking characteristics with a delayed-action controller)*, *Tekh. shel. dor.*, No. 1 (1953).

1960

A NEW METHOD OF TESTING THE RUPTURING CAPACITY OF HIGH VOLTAGE CIRCUIT BREAKERS*

Ing. A.I. BALAKIN

All-Union Lenin Institute of Electrical Engineering
Leningrad Branch

(Received 3 June 1959)

Construction of new more powerful high voltage circuit breakers is possible only when test installations are available in which these circuit breakers can be tested with regard to their ability to trip the given power of a short circuit.

The limited possibilities of the grid test benches and the high cost of test installations with shock generators are the main reasons for designing artificial circuits for testing high-voltage circuit-breakers.

Despite a great variety of methods developed for testing the rupturing capacity of circuit breakers under artificial conditions, they all have a common characteristic property; namely the presence of two circuits: a circuit of the current to be broken and a circuit of the recovery voltage.

In these installations the current circuit is separated from the recovery voltage circuit by an air gap of a sphere discharger or by a resistance of a few thousand ohms.

Consequently, in these networks the source of energy of the recovery voltage circuit (capacitor banks previously charged or the transformer winding) does not take part in producing short-circuit currents, and is destined only for generating the recovery voltage.

The combination of operation of these two circuits in a desired order to ensure their equivalence with direct tests presents certain difficulties. Moreover, in certain networks it is necessary to perform

* *Elektrichestvo*, No.1, 1960, 43-47.

a considerable number of preliminary tests with the breaking of currents of limiting values to obtain the necessary synchronization of the current circuit with the circuit of the recovery voltage.

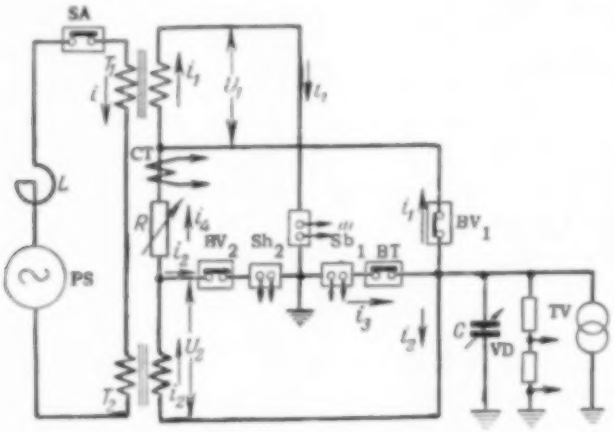

Fig. 1. Diagram of the network of the testing installation.

CT – current transformer; *TV* – voltage transformer; *VD* – voltage divider; Sh_1, Sh_2, Sh_3 – shunts; *C* – capacitance controlling the frequency of the recovery voltage; *L* – coefficient of self-inductance of the power supply circuit.

Since synchronization occurs when the current is approaching its zero value, it should be carried out with great accuracy, and for this purpose special synchronizing circuits are used. Because of the conditions of equivalence to real tests, in an artificial system, in which a voltage is applied at the moment when the current to be broken is equal to zero, the time lag should not exceed 10 μsec, moreover, there should be at least one test with time lag not greater than 1-2 μsec.

In a two-frequency network the variation of the derivative of current with respect to time in the circuit breaker on test at the moment of the arc quenching in the auxiliary circuit breaker should not exceed $\pm$ 20 per cent.

These difficulties are considerably increased in tests with apparatus with a time of arcing of 0.03-0.04 sec., since the preliminary tests prematurely wear out the circuit breaker on test.

In the new method of testing the rupturing capacity of high voltage

circuit breakers under artificial conditions, the source of energy of the recovery voltage circuit is built up from the sources of energy of the current circuits [1].

Consequently, all sources of energy in the network contribute in building up both the total short-circuit current and the total recovery voltage.

The formation of the recovery voltage circuit occurs automatically when the current approaches its zero value, therefore there is no need for synchronizing these two circuits. For testing circuit breakers by this method the existing installation which is designed for direct tests may be used.

Fig. 1 shows a diagram of the network for testing the installation discussed.

Description of the operation of the installation

Before the beginning of a test and circuit breaker to be tested *BT* and the auxiliary breaker *BV* are closed and the switching apparatus *SA* is open. Then the power supply *PS*, which may be a shock generator or a power system (grid), are connected by means of the switching apparatus with the testing transformers T_1 and T_2. In this case the primary windings of transformers are connected in series and the secondary in parallel thus forming two current circuits. One circuit consists of the secondary winding of the transformer T_1, the breaker on test *BT* and the auxiliary breaker BV_1. The second circuit includes the secondary winding of the transformer T_2, the auxiliary breaker BV_2 and the breaker on test *BT*.

Instead of two transformers we may use one transformer with a secondary tapped winding. In this case an equal number of sections of the transformer secondary winding is connected in each current circuit.

The current of the secondary winding of the transformer T_1 flows in the auxiliary breaker BV_2 and in the auxiliary breaker *BV* there flows the current of the secondary winding of the transformer T_2.

A current equal to the sum of the transformer currents T_1 and T_2 flows in the breaker on test.

After that, the breaker on test and the auxiliary breaker are switched off. Have the arc in the auxiliary breaker should be quenched at the end of the current half-period, during which it should have been quenched by the breaker on test. If the auxiliary breaker has already quenched the arc, but in the breaker on test, conditions for quenching

do not yet exist, and there is a sufficient conductivity, then a current will flow through the breaker, and this current is capable of sustaining the conductivity of the arc gap. In the case considered an artificial increase of the time of arcing in the auxiliary breakers is foreseen, and this also increases the duration of the flow of the total current in the breaker on test.

Synchronous operation of the auxiliary breakers is ensured by the fact that the currents flowing through the auxiliary breakers are practically in phase. Moreover, if in one of the auxiliary breakers the arc is extinguished earlier than in the others, then on this breaker a voltage builds up exceeding its rated value. In the case of series connexion of the primary transformer windings, the voltage applied to them is so redistributed that practically the total voltage of the power supply will be applied to this transformer, in which the secondary winding is open (by the auxiliary breaker). Consequently, twice the rated voltage will be recovered on this breaker, and this will result in repeated arc ignition.

In this way the autosyncrhonization of operation of the auxiliary circuit breakers takes place.

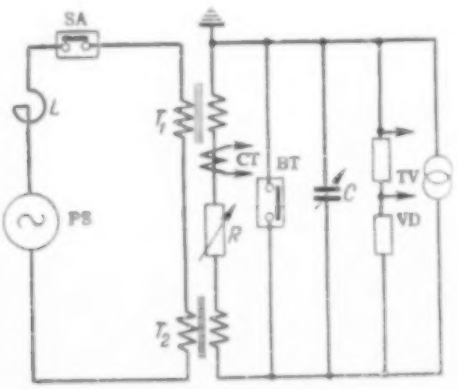

Fig. 2. Diagram of the network characterizing the process of the voltage recovery on the contacts of the circuit breaker on test.

The ability of the network to synchronize ensures the simultaneous quenching of arcs in all auxiliary circuit breakers, and, moreover, the greater is the factor of the power increase, the greater is the number

of auxiliary breakers and the better becomes the autosynchronization.

The auxiliary circuit breakers are all of the same construction. A special device in the auxiliary breakers permits a simultaneous opening of their contacts. The moment of opening of contacts in the circuit breaker on test and in the auxiliary breakers is fixed before the experiment with the limiting short circuit current, and this prevents the premature wear of the breaker tested.

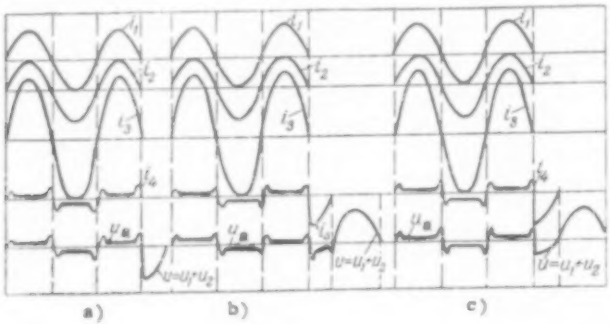

Fig. 3. Current and voltage graphs characterising operation of the network.

i_1, i_2 – currents in the auxiliary breakers; i_3 – current in the breaker on test; i_4 – current in the connecting resistance; U_A – voltage drop across the arc in the breaker on test; U_1, U_2 – voltages of the secondary windings of transformers T_1, T_2; u – recovery voltage on the contacts of the breaker on test. *a* – the breaker on test successfully cut off the short-circuit; *b* – the breaker on test did not cut the short-circuit current; *c* – the breaker on test cut off the current earlier than did the auxiliary breakers/signal for disconnecting the auxiliary breakers was delayed.

After the extinction of the electric arc on the contacts of the auxiliary breakers and of that on test, a voltage is recovered equal to the sum of the voltages of the two secondary windings of the transformer (Fig.2), whereas in the ordinary test installation on the breaker on test a voltage would be recovered equal only to the voltage of one transformer.

In this way during the process of the arc quenching the circuit breaker tested is subjected to the total short circuit current and the total recovery voltage.

Hence, the power of a short circuit broken by the circuit breaker tested is over twice the basic power of the power supply.

If in the breaker on test, restriking of the arc were to occur (failure to trip the short-circuit current) then a current would flow through it, whose magnitude is determined mainly by the magnitude of the connecting resistance R. This current is broken at the first transition through zero of the breaker on test.

Fig. 3 shows curves characterizing the operation of the network.

A network for a three-fold or fourfold increase in the short circuit power to be cut-off is assembled in a way similar to that shown in Fig. 1, where a network for a twofold increase of the short-circuit power to be cut-off is represented; in the former cases three or four current circuits are needed respectively.

1960

The equivalence of the network to the direct tests

To determine the equivalence of the network to direct tests it is necessary first to consider the operation of a network in testing an ideal circuit-breaker, i.e. such a breaker in which the resistance of the arc gap would be equal to zero during the time of arcing and equal to infinity after the extinction of the arc. Such an investigation is necessary for evaluation of the influence of the differences in the parameters of the transformers T_1 and T_2.

The shape of the current flowing through the breaker on the auxiliary breakers had zero values simultaneously, i.e. when the currents of the secondary windings of the transformers T_1 and T_2 were in phase.

As is known [2] the current of the primary transformer winding compensating the demagnetizing action of the short circuited secondary winding. The magnetizing current of the test transformers of the installation discussed is only 6 A (for a short-circuit current in the primary winding equal to 50,000 A), and this is explained by the small value of the voltage drop in the primary winding. We may therefore safely assume that the current of the transformer secondary winding is shifted in phase by 180° with respect to the primary current.

Since the primary windings of the transformers are series connected, then the angle of the phase shift between the secondary currents of the transformers T_1 and T_2 is equal to the difference in the angles of the phase shifts of the secondary currents of the transformers with respect to the primary current.

Consequently, we may assume that the secondary currents of the transformers are in phase.

We may tolerate certain difference in values of ϕ_K and in the transformation ratios since this only affects the magnitude of the recovery voltage, but not the angle shift of the currents. However, it is better to use, whenever possible, transformers with equal parameters.

In the case of direct tests, the resultant current of the real *BT* is characterized by the following equations:

$$i = \frac{U_m}{\omega L} \sin \omega t_A - \frac{U_A}{L} t_A, \tag{1}$$

where U_m - the amplitude of the applied voltage;
L - coefficient of self-inductance;
t_A - duration of arcing in the last half-period before quenching
U_A - voltage drop across the arc.

In our case the current in question is given by the formula:

$$i = \left(\frac{U_{m1}}{\omega L_1} + \frac{U_{m2}}{\omega L_2}\right) \sin \omega t_A - \frac{U_{A1} + U_A}{L_1} t_A - \frac{U_{A2} + U_A}{L_2} t_A - \frac{U_{A1} + U_{A2} + U_A}{R}, \tag{2}$$

where U_{m1}, U_{m2} - voltage amplitudes of the secondary windings of the transformers T_1 and T_2;
U_{A1}, U_{A2} - voltage drop across the arcs of the auxiliary breakers,
R - ohmic resistance of the connexion;
L_1, L_2 - coefficients of self-inductance of the network with respect of the transformers T_1 and T_2.

Since the auxiliary breakers used are all of the same type with the same rated voltage, several times smaller than the rated voltage of the circuit breaker on test, then

$$U_{m1} \approx U_{m2} = kU_m,$$

where $k = \frac{U_{A1}}{U_A} < 1$.

In the network considered $L_1 = L_2 = L$ and

$$U_{m1} = U_{m2} = U_{m\,tr} = 0{,}5U_m.$$

Moreover, we can neglect the last term of the expression (2) since

$\frac{R}{L} \approx 10^4$. Hence

$$i = \frac{U_{m\,tr}}{\omega \frac{L}{2}} \sin \omega t_A - \frac{(k+1)U_A}{\frac{L}{2}} t_A. \qquad (3)$$

It is seen from equality (3) that the rate of change of current when the value of the current is near to zero, will be a somewhat greater in our case than for direct tests, and this makes the conditions of the test more difficult.

We choose the ohmic resistance R in such a way as to ensure both the value of the current necessary to sustain the arc after its restriking in the breaker on test and a sufficient rate of increase of the current immediately after the discharge in the arc gap.

Moreover, it is necessary to bear in mind that in direct tests the current varies sinusoidally, and in our case it varies according to the following law:

$$i = \frac{U_m}{R}\left(1 - e^{-\frac{R}{2L}t}\right).$$

To ensure the oscillatory character of the recovery voltage the following conditions should be fulfilled $R \leqslant 2\sqrt{\frac{2L}{C}}$.

The average rate of change of the recovery voltage, on the contacts of the breaker tested, during the half-period of the natural frequency in the installation discussed, is determined by the formula:

$$\left|\frac{du_c}{dt}\right|_{av} = 2\alpha f_0' U_m \cdot 10^{-6} \ [\text{v}/\mu\text{sec}],$$

where α - the factor of increase of the amplitude of the recovery voltage

$f_0' = \frac{1}{2\pi\sqrt{2LC}}\sqrt{1 - \frac{R^2C}{8L}}$ - frequency of the recovery voltage.

To obtain the desired value of the factor α, the value of R should be equal to:

$$R = 8Lf_0 \ln\frac{1}{\alpha - 1},$$

where $f_0 = \frac{1}{2\pi\sqrt{2LC}}$.

The resistance R will probably affect the magnitude of the residual

current only to a small degree, since its magnitude is of the order of a few tens of ohms.

Illustration of the operation of the new testing network

The operation of the new network was verified by testing various types of high-voltage switchgear. Examples of certain tests are given below.

Test of a tubuler aischarger type RTV-35. A shock generator type TI-75 with a rated voltage of 10 kV was used as the power supply. Four sections of the secondary winding of a step-up transformer were used as the source of energy for the current and recovery voltage circuits. A rated voltage of each section of the secondary winding was 35 kV. The rated voltage of the primary winding was 7 kV. In every current circuit there were two parallel connected sections of the secondary winding of the transformer. Two tubular dischargers type RTV-35 were used as auxiliary breakers.

The breaker on test tripped the short-circuit power of 240 MVA for a recovery voltage of line frequency equal to 30 kV. In this case the power of the short-circuit of the power supply (generator) was 120 MVA at a voltage of 3 kV.

In this way a doubling of the short-circuit power of the power supply was achieved. Fig. 4 shows the oscillograms of this experiment.

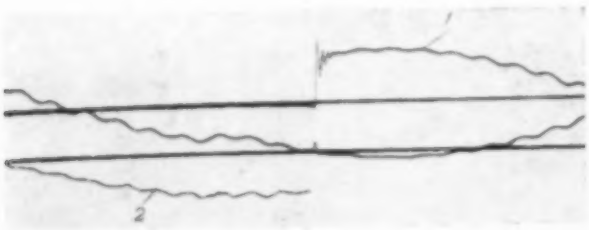

Fig. 4. Oscillogram of the breaking of the current by a discharger RTV-35
1 – recovery voltage; 2 – the derivative of the current in the discharger in test.

Test of an oil-tank circuit breaker type MKP-35. A shock generator type TI-75 and two step-up transformers were connected to the testing network; the parameters of the individual components differed from one

another only slightly. The secondary winding of the transformer was connected in each circuit. Two poles of an air breaker type VVN-35 were used as auxiliary breakers.

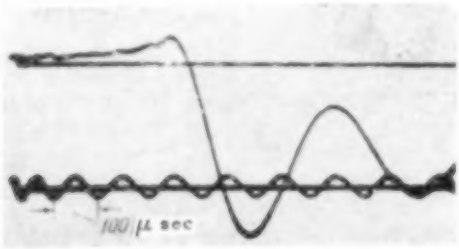

Fig. 5. Oscillogram of the recovery voltage for the breaking of the current by a breaker MKP-35.

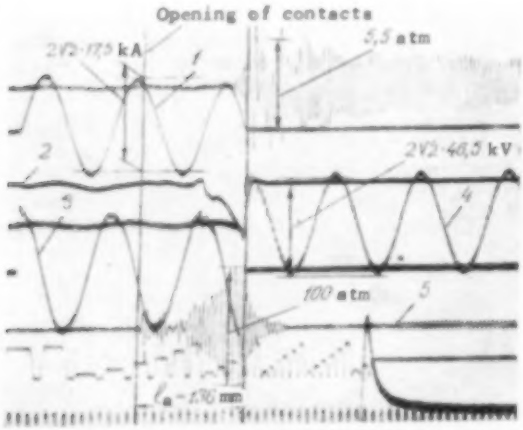

Fig. 6. Oscillogram of an experiment of the breaking of the current by a breaker VMK-110.
1 – current to be broken; *2* – current through the connecting resistance; *3* – derivative of this current to be broken; 4 – recovering voltage; 5 – pressure in the body of the breaker.

The breaker on test type MKP-35 switched off a short circuit power of 200 MVA, for a recovery voltage of line frequency of 25 kV (Fig.5). The short-circuit power of the power supply was 100 MVA, for a recovery voltage of line frequency equal to 5 kV.

A small VMK-110 oil breaker was tested in the same kind of network, it cut off a short-circuit power of 822.5 MVA for a recovery voltage of line frequency equal to 47 kV (Fig.6). The power of the short-circuit of the power supply was 411.25 MVA for a recovery voltage of 9.4 kV.

The oscillograms given in Figs.4 to 6 show that the new method of testing satisfies the conditions required for artificial methods of testing and confirm the equivalence of this method to direct tests.

Conclusion

The method of testing devised makes it possible to increase several times the power of the short-circuit which can be tripped by the test installation; it permits the testing of high voltage switchgear of different types with the necessary equivalence to direct tests; it also makes an increase possible in the number of tests since there is no need to perform a considerable number of preliminary tests with limiting currents.

Moreover, with the method discussed for testing high-voltage switchgear, use is made of the same equipment as devices for direct tests, and no additional equipment is needed.

Translated by S. Szymanski

REFERENCES

1. *Avtorskoye svidetelstvo No. 110926 ot 30 ianvaria 1958 g. (Authors certificate No. 110926 dates 30 January 1958).*
2. G.N. Petrov. *Transformatory (Transformers)* vol. 1. Energoizdat. (1934).

ABSTRACTS FROM PAPERS PUBLISHED IN ELEKTRICHESTVO No. 1, 1960

The supply system of the synchrophasotron electro-magnet at the consolidated nuclear research institute: M.A. Gashev, E.G. Korrar, N.A. Monoszon, F.M. Spevakova and A.M. Stolov. (pp 6-10)

The synchrophasotron in question claims to be the largest existing accelerator of charged particles. Protons are accelerated to 10 million eV. The supply system for the magnet is intended to create a periodically varying magnetic field with a repeat frequency of 5/min. Characteristics of the supply system: maximum output 140 MW, maximum current 12,8kA, maximum voltage 11kV, reserve energy in the magnetic field of the magnet 148×10^6 J, losses in magnet winding 4 MW. A description is given of the power circuits.

Some problems of the dynamics of automated induction motor drives: V.A. Shubenko. (pp 10-18)

The results are given of certain investigations made by the author into the effect of electromagnetic transient phenomena caused by commutation in the stator on the dynamics and reliability of modern automated asynchronous drives within intensified operating conditions. Starting, reversing and braking conditions are considered.

Equations for a.c. machines using physical quantities, and in per unit form: N.I. Aliab'ev. (pp 18-26)

Owing to inconsistency in the use of different systems of physical and relative units in mathematical calculations, the author introduces the results of the elaboration of 10 systems of units, and analysis and compares them in order to discover the best systems and make it easier to understand and compare the work of different authors using different systems. Use is made of relationships and equations true for 'ideal' electrical machines on groups of machines. Synchronous machines with a large number of rotor circuits are a special case.

On obtaining high voltages across small converter transformers: P.V. Tanofeev and In.A. Simchenks. (pp 38-42)

Light is thrown on the design and construction of transformers for obtaining impulses of high transient voltages. A general study is made of the problem of obtaining high transient voltage pulses in the transformer with linear and non-linear core magnetization curves, in the presence of powerful magnetic connexion. Attention is paid to the conditions for optimum tuning of the transformer, the maximum secondary voltage and the effect of non-linearing in the core magnetization curve. The use of transformers with a powerful magnetic connexion and a closed steel core with low magnetic resistance is advocated.

On using semi-conductor Rectifiers in Electrified urban transport; I.S. Efrenov, N.Q. Zagainov and S.S. Tikhomirov. (pp 47-51)

To increase the output of tram and trolley-bus substations decentralize the power supply, introduce automatic control into the substations, reduce eddy and parasitic currents and improve traction networks, the author's consider a changeover of Urban transport to a.c. and the installation of silicon rectifiers directly on the vehicles and advocate the use of the 100 A and 300 V silicon rectifiers now in production in the U.S.S.R.

Asynchronous torque components of a synchronous machine, with compensation of the field circuit resistance: B.K. Karpenko. (pp 51-55)

A mathematical study is made of one of the methods of increasing the asynchronous torque of synchronous machines created by the excitation winding. It is claimed that compensation of the resistance of the excitation circuit can produce asynchronous torques created by the excitation winding equal to (1.2 to 1.5) M_N.

The achievement of P. S. Zhdanov in the field of power system stability. V.A. Venikov. (pp 56-58)

The late P.S. Zhdanov, former professor at the Moscow Power Institute, was a specialist in static and dynamic stability, but his interests ran much wider, he was for instance consultant to the Moscow-Volga hydroelectric power station project. The article is in memory of his death 10 years ago.

Generating undamaged high-frequency oscillations by means of controlled electronic discharge gaps: A.D. Artyn and A.V. Donskoi. (pp 59-63)

A study is made of the principle underlying the production of fading oscillations in discharge schemes using ionic controlled valves (dischargers), the de-ionization time of which is considerably longer than the period of the oscillations to be generated. The character of fading high frequency oscillations in certain cases, for instance in induction heating, makes it possible to use them as well as non-fading oscillations. Generator schemes are considered together with the optimum relationships of their parameters ensuring maximum output for a given current impulse and a discharge of given electrical strength.

Fundamental laws on the impulse strength of the insulation in air-filled switching apparatus: M.I. Syscov. (pp 63-68)

The article supplements previously published work of the transformer laboratory of the Lenin All-Union Electrical Engineering Institute on the use of compressed air as insulation for switchgear. The test gear was filled with air from an industrial-type compressor as used at substations with air-blast circuit breakers. A standard pulse wave of 1.5/40 μ sec. was used. The distribution of the probable values of the impulse puncture voltages are plotted and discussed in considerable detail.

Designing full-wave rectifier schemes: L.A. Sinitskii. (pp 68-72)

The author suggests a way of designing a circuit with several rectifiers by similar equations to those used for designing a circuit with one rectifier. An example is given of a two half-period rectifier of single phase current (bridge scheme and a scheme with a neutral conductor).

On pulling synchronous generators into step: M.G. Portnoi. (pp 73-78)

A method is proposed for calculating the conditions for the restoration of synchronism and determining the duration of asynchronous operation. An example is given of a turbo-generator feeding power into a system of infinite power. Conditions for the resynchronization of one and two generators are considered separately. Two appendices deal with the method involved and the comparison of experimental and theoretical findings.

Some ways of improving the characteristics of reactors with d.c. magnetizations: I.S. Pinchuk and F.A. Zykin. (pp 78-80)

The results are given of experimental investigation of the effect of certain factors on the shape of the characteristics of reactors with d.c. magnetization and consequently on the constructional dimensions and the power of d.c. sources and reactors with magnetization such as can be used to control the speed of induction motors. Certain proportions in the article also apply to the construction of magnetic amplifiers and reactors for a different purpose.

A composite a.c. auto-compensator: L.Ia. Miziuk and V.I. Gol'dgefter. (pp 80-85)

In view of the difficulty of measuring small alternating voltages against a background of intensive interference, a method is proposed of introducing a negative feedback into the selective device to stabilize the parameter and reduce errors in measurement. For this purpose the negative feedback is fed through synchro-phase filter which works on the double conversion of the frequency spectrum. The auto compensator, tested with different resonance and quasi-resonance amplifiers (with T-shaped RC-filters), has considerable advantages as regards stability for selective devices of the metering type.

Taking oscillograms with voltage dividers connected in an H-circuit: A.M. Ryvkin. (pp 86-88)

A study is made of the effect of the loss on distortion, the character of distortion, the possibility of using dissimilar dividers and the participation of a divider is several h-shaped schemes at the same time.

Automatic voltage regulation using the electrostatic capacitance of the p.n. junction as the non-linear element of the measuring device: L.S. Bermon (pp. 88-89)

The electrostatic (barrier) capacitance of the p-n junction has a number of advantages over variable condensers which make it suitable as a non-linear element in metering devices for automatic control purposes, especially for low direct voltages of several V or a fraction of I V. A description is given of a scheme for voltage regulation using a p-n

junction with a stabilization factor of 120. Temperature compensation is however necessary.

A DIGITAL PROGRAMME CONTROL SYSTEM FOR A LARGE LATHE*

I.L. SHAPIRO, S.M. GROSSMAN, IU.A. RAISOV and IU.V. TIKHVINSKII

Kharkov

(Received 20 July 1959)

Components of comparatively complex shape requiring a great deal of machining time and labour are often machined on large general-purpose and special lathes.

The use of programme control on lathes makes it possible to achieve a considerable increase in output. When introducing programme control systems for heavy lathes, a number of difficulties have to be overcome in connexion with the large amount of information required for machining large workpieces which can be disturbed if for example the cutter wears out.

A study is made below of a digital programme control system designed for heavy lathes** with centres about 500 mm high and a distance of up to 4000 mm between them. Components weighing up to 10 tons with complex curvilinear surfaces can be machined on the lathe. Components can be machined to an accuracy of up to 0.1 mm. The machine table is driven by a 40 kW induction motor via a multistage gearbox, several electromagnetic couplings being provided for changing gear. The total range of control over the machine's speed is 1:50 with a control "leap" not exceeding $\phi = 1.35$.

The machine has one saddle driven by two variable motors: one effects longitudinal feed and the other transverse feed, (there is no kinematic link between the saddle and gear box). Feed should be regulated electrically within the limits of 5 to 200 mm/min.

---

* *Elektrichestvo*, No.2, 9-12, 1960.

** The system was developed jointly by the TsKB for electric drives and automatics KhEMZ and the automatics laboratory of the KhPI.

Provision is also made on the machine for three auxiliary motors intended for "setting up" adjustment of the saddle and rear mandrel and rotating the oil pump.

A digital system of programme control was adopted for the machine using "executive step-by-step" motors and interval recording of the programme on magnetic tape. The choice of this system of programme control (SPC) was based on the following points:

1. The comparatively low degree of accuracy required for machining components on the machine and the small feed (up to 200 mm/min) enables use to be made of powerful step by step motors* for the feed of the saddle, which considerably simplifies the system of programme control (feedback circuits etc are excluded).

2. The use of intermediate recording of the machine operating programme on magnetic tape enables the control system of the saddle to be effected by relatively simple and reliable means. In this case, the device for recording the programme on magnetic tape (DRM) (comparatively complex and expensive), can serve several similar programme-controlled machines.

3. The use of the selected SPC makes it possible to machine components on the lathe in any of three operating conditions: (a) programme control of the lathe, (b) electro-copying and (c) manual control. Here the same elements of electrical equipment can generally be used for the machine.

The machine's electrical drive system

Fig.1. shows the block-scheme and Fig.2 the main circuit of the basic electrical drives of the lathe. Use is made of the selector *S* to adjust the lathe (Fig.2) to any of the operating conditions stated above.

If the machine is controlled in accordance with a pre-determined programme, the programme is recorded on magnetic tape. The work programme of the motor for the longtitudinal feed of the saddle is applied on one track. The work programme of the motor for the transverse feed of the saddle is recorded on the second and third tracks, (a separate track is provided for each direction of rotation of this motor). The work programme for the main motor and gear box, the signal that the machining of the component is finished and auxiliary commands (commands to the operator for manual change of the tools, inspection measurement

* The prototypes of the step-by-step motors were made by KhEMZ from the technical documentation of the Electrical Engineering Institute of the Academy of Science, U.S.S.R.

of the workpiece and so forth) are recorded on the fourth track. After toolsetting (to be carried out in the "set up" condition) the latter can be started by pressing the button "start" in order to operate in accordance with the predetermined programme. In this case, the signals to be counted with the magnetic heads 1*GM*-3*GM* which move the tape, are fed to the input to the appropriate amplifiers 1*A*-3*A* and control the step by step motors 1*SSM* and 2*SSM* by means of thyratron units 1*TV* and 2*TV*. The count of each step by the motors for the saddle, corresponding to one impulse of the magnetic tape, equals 0.02 mm. Fig. 3 shows a step-by-step motor in disassembled form. Its weight is about 23 kg.

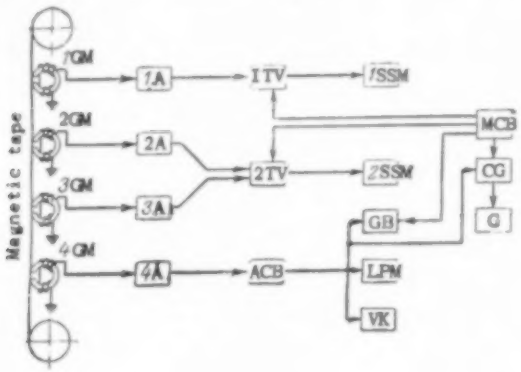

Fig. 1. Block-scheme of machine drive

The signals to be counted by head 4*GM* on the fourth track of the magnetic tape enter the automatic control block of apparatus ACB. The latter comprises a seven-discharge tube binary electronic counter (1*EC*-7*EC*), Kipp relay *T*, intermediate relays connected to individual tubes of the counter and certain additional elements. Depending on the number of pulses arriving at the input to the counter with the fourth track, some of the tubes of the counter and the relays connected to them operate. The closure of relays 1*RC*-4*RC*, which are fed from the first four trigger tubes of the counter, produces the appropriate change in the gear box *GB*, which brings about definite speeds of the machine spindle.

The process of machining large workpieces on the lathe under investigation can take a comparatively long period of time, one traverse of the cutter sometimes taking 2 to 3 hr. Therefore the work programme recorded on the tape usually has to include a certain number of intermediate stops for the saddle at pre-determined positions for each traverse of the cutter (the cutter being taken off the workpiece). At these positions the operator should verify the state of the cutter and

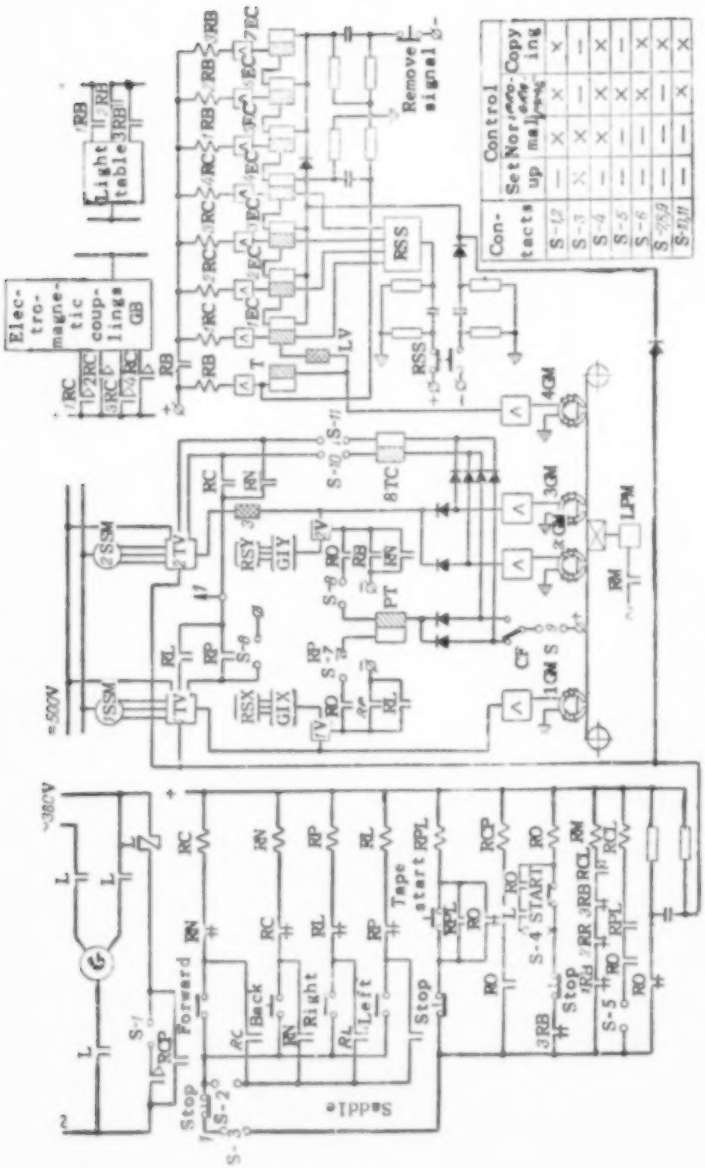
Control
Contacts
Set up
Normal machining
Copying
Remove signal
Electromagnetic couplings GB
Light table
Tape start
Forward
Back
Right
Left
Stop
Saddle
START
Stop
~380V
=500V
RSS
LV
PT
CF
LPM
RM
RC
RN
RP
RL
RO
RB
RCP
RPL
RCL
RPR
RRB
RRL
RRP
RRC
RRN
RRO
RRCP
RRPL
RRCL
RRPR
RRRB
RRRL
RRRP
RRRC
RRRN
RRRO
RRRCP
RRRPL
RRRCL
RRRPR
RRRRB
RRRRL
RRRRP
RRRRC
RRRRN
RRRRO
RRRRCP
RRRRPL
RRRRCL
RRRRPR
RRRRRB
RRRRRL
RRRRRP
RRRRRC
RRRRRN
RRRRRO
RRRRRCP
RRRRRPL
RRRRRCL
RRRRRPR
RRRRRRB
RRRRRRL
RRRRRRP
RRRRRRC
RRRRRRN
RRRRRRO
RRRRRRCP
RRRRRRPL
RRRRRRCL
RRRRRRPR
RRRRRRRB
RRRRRRRL
RRRRRRRP
RRRRRRRC
RRRRRRRN
RRRRRRRO
RRRRRRRCP
RRRRRRRPL
RRRRRRRCL
RRRRRRRPR
RRRRRRRRB
RRRRRRRRL
RRRRRRRRP
RRRRRRRRC
RRRRRRRRN
RRRRRRRRO
RRRRRRRRCP
RRRRRRRRPL
RRRRRRRRCL
RRRRRRRRPR
RRRRRRRRRB
RRRRRRRRRL
RRRRRRRRRP
RRRRRRRRRC
RRRRRRRRRN
RRRRRRRRRO
RRRRRRRRRCP
RRRRRRRRRPL
RRRRRRRRRCL
RRRRRRRRRPR
RRRRRRRRRRB
RRRRRRRRRRL
RRRRRRRRRRP
RRRRRRRRRRC
RRRRRRRRRRN
RRRRRRRRRRO
RRRRRRRRRRCP
RRRRRRRRRRPL
RRRRRRRRRRCL
RRRRRRRRRRPR
RRRRRRRRRRRB
RRRRRRRRRRRL
RRRRRRRRRRRP
RRRRRRRRRRRC
RRRRRRRRRRRN
RRRRRRRRRRRO
RRRRRRRRRRRCP
RRRRRRRRRRRPL
RRRRRRRRRRRCL
RRRRRRRRRRRPR
RRRRRRRRRRRRB
RRRRRRRRRRRRL
RRRRRRRRRRRRP
RRRRRRRRRRRRC
RRRRRRRRRRRRN
RRRRRRRRRRRRO
RRRRRRRRRRRRCP
RRRRRRRRRRRRPL
RRRRRRRRRRRRCL
RRRRRRRRRRRRPR
RRRRRRRRRRRRRB
RRRRRRRRRRRRRL
RRRRRRRRRRRRRP
RRRRRRRRRRRRRC
RRRRRRRRRRRRRN
RRRRRRRRRRRRRO
RRRRRRRRRRRRRCP
RRRRRRRRRRRRRPL
RRRRRRRRRRRRRCL
RRRRRRRRRRRRRPR
RRRRRRRRRRRRRRB
RRRRRRRRRRRRRRL
RRRRRRRRRRRRRRP
RRRRRRRRRRRRRRC
RRRRRRRRRRRRRRN
RRRRRRRRRRRRRRO
RRRRRRRRRRRRRRCP
RRRRRRRRRRRRRRPL
RRRRRRRRRRRRRRCL
RRRRRRRRRRRRRRPR
RRRRRRRRRRRRRRRB
RRRRRRRRRRRRRRRL
RRRRRRRRRRRRRRRP
RRRRRRRRRRRRRRRC
RRRRRRRRRRRRRRRN
RRRRRRRRRRRRRRRO
RRRRRRRRRRRRRRRCP
RRRRRRRRRRRRRRRPL
RRRRRRRRRRRRRRRCL
RRRRRRRRRRRRRRRPR
RRRRRRRRRRRRRRRRB
RRRRRRRRRRRRRRRRL
RRRRRRRRRRRRRRRRP
RRRRRRRRRRRRRRRRC
RRRRRRRRRRRRRRRRN
RRRRRRRRRRRRRRRRO
RRRRRRRRRRRRRRRRCP
RRRRRRRRRRRRRRRRPL
RRRRRRRRRRRRRRRRCL
RRRRRRRRRRRRRRRRPR
RRRRRRRRRRRRRRRRRB
RRRRRRRRRRRRRRRRRL
RRRRRRRRRRRRRRRRRP
RRRRRRRRRRRRRRRRRC
RRRRRRRRRRRRRRRRRN
RRRRRRRRRRRRRRRRRO
RRRRRRRRRRRRRRRRRCP
RRRRRRRRRRRRRRRRRPL
RRRRRRRRRRRRRRRRRCL
RRRRRRRRRRRRRRRRRPR
RRRRRRRRRRRRRRRRRRB
RRRRRRRRRRRRRRRRRRL
RRRRRRRRRRRRRRRRRRP
RRRRRRRRRRRRRRRRRRC
RRRRRRRRRRRRRRRRRRN
RRRRRRRRRRRRRRRRRRO
RRRRRRRRRRRRRRRRRRCP
RRRRRRRRRRRRRRRRRRPL
RRRRRRRRRRRRRRRRRRCL
RRRRRRRRRRRRRRRRRRPR
RRRRRRRRRRRRRRRRRRRB
RRRRRRRRRRRRRRRRRRRL
RRRRRRRRRRRRRRRRRRRP
RRRRRRRRRRRRRRRRRRRC
RRRRRRRRRRRRRRRRRRRN
RRRRRRRRRRRRRRRRRRRO
RRRRRRRRRRRRRRRRRRRCP
RRRRRRRRRRRRRRRRRRRPL
RRRRRRRRRRRRRRRRRRRCL
RRRRRRRRRRRRRRRRRRRPR
RRRRRRRRRRRRRRRRRRRRB
RRRRRRRRRRRRRRRRRRRRL
RRRRRRRRRRRRRRRRRRRRP
RRRRRRRRRRRRRRRRRRRRC
RRRRRRRRRRRRRRRRRRRRN
RRRRRRRRRRRRRRRRRRRRO
RRRRRRRRRRRRRRRRRRRRCP
RRRRRRRRRRRRRRRRRRRRPL
RRRRRRRRRRRRRRRRRRRRCL
RRRRRRRRRRRRRRRRRRRRPR
RRRRRRRRRRRRRRRRRRRRRB
RRRRRRRRRRRRRRRRRRRRRL
RRRRRRRRRRRRRRRRRRRRRP
RRRRRRRRRRRRRRRRRRRRRC
RRRRRRRRRRRRRRRRRRRRRN
RRRRRRRRRRRRRRRRRRRRRO
RRRRRRRRRRRRRRRRRRRRRCP
RRRRRRRRRRRRRRRRRRRRRPL
RRRRRRRRRRRRRRRRRRRRRCL
RRRRRRRRRRRRRRRRRRRRRPR
RRRRRRRRRRRRRRRRRRRRRRB
RRRRRRRRRRRRRRRRRRRRRRL
RRRRRRRRRRRRRRRRRRRRRRP
RRRRRRRRRRRRRRRRRRRRRRC
RRRRRRRRRRRRRRRRRRRRRRN
RRRRRRRRRRRRRRRRRRRRRRO
RRRRRRRRRRRRRRRRRRRRRRCP
RRRRRRRRRRRRRRRRRRRRRRPL
RRRRRRRRRRRRRRRRRRRRRRCL
RRRRRRRRRRRRRRRRRRRRRRPR
RRRRRRRRRRRRRRRRRRRRRRRB
RRRRRRRRRRRRRRRRRRRRRRRL
RRRRRRRRRRRRRRRRRRRRRRRP
RRRRRRRRRRRRRRRRRRRRRRRC
RRRRRRRRRRRRRRRRRRRRRRRN
RRRRRRRRRRRRRRRRRRRRRRRO
RRRRRRRRRRRRRRRRRRRRRRRCP
RRRRRRRRRRRRRRRRRRRRRRRPL
RRRRRRRRRRRRRRRRRRRRRRRCL
RRRRRRRRRRRRRRRRRRRRRRRPR
RRRRRRRRRRRRRRRRRRRRRRRRB
RRRRRRRRRRRRRRRRRRRRRRRRL
RRRRRRRRRRRRRRRRRRRRRRRRP
RRRRRRRRRRRRRRRRRRRRRRRRC
RRRRRRRRRRRRRRRRRRRRRRRRN
RRRRRRRRRRRRRRRRRRRRRRRRO
RRRRRRRRRRRRRRRRRRRRRRRRCP
RRRRRRRRRRRRRRRRRRRRRRRRPL
RRRRRRRRRRRRRRRRRRRRRRRRCL
RRRRRRRRRRRRRRRRRRRRRRRRPR
RRRRRRRRRRRRRRRRRRRRRRRRRB
RRRRRRRRRRRRRRRRRRRRRRRRRL
RRRRRRRRRRRRRRRRRRRRRRRRRP
RRRRRRRRRRRRRRRRRRRRRRRRRC
RRRRRRRRRRRRRRRRRRRRRRRRRN
RRRRRRRRRRRRRRRRRRRRRRRRRO
RRRRRRRRRRRRRRRRRRRRRRRRRCP
RRRRRRRRRRRRRRRRRRRRRRRRRPL
RRRRRRRRRRRRRRRRRRRRRRRRRCL
RRRRRRRRRRRRRRRRRRRRRRRRRPR
RRRRRRRRRRRRRRRRRRRRRRRRRRB
RRRRRRRRRRRRRRRRRRRRRRRRRRL
RRRRRRRRRRRRRRRRRRRRRRRRRRP
RRRRRRRRRRRRRRRRRRRRRRRRRRC
RRRRRRRRRRRRRRRRRRRRRRRRRRN
RRRRRRRRRRRRRRRRRRRRRRRRRRO
RRRRRRRRRRRRRRRRRRRRRRRRRRCP
RRRRRRRRRRRRRRRRRRRRRRRRRRPL
RRRRRRRRRRRRRRRRRRRRRRRRRRCL
RRRRRRRRRRRRRRRRRRRRRRRRRRPR
RRRRRRRRRRRRRRRRRRRRRRRRRRRB
RRRRRRRRRRRRRRRRRRRRRRRRRRRL
RRRRRRRRRRRRRRRRRRRRRRRRRRRP
RRRRRRRRRRRRRRRRRRRRRRRRRRRC
RRRRRRRRRRRRRRRRRRRRRRRRRRRN
RRRRRRRRRRRRRRRRRRRRRRRRRRRO
RRRRRRRRRRRRRRRRRRRRRRRRRRRCP
RRRRRRRRRRRRRRRRRRRRRRRRRRRPL
RRRRRRRRRRRRRRRRRRRRRRRRRRRCL
RRRRRRRRRRRRRRRRRRRRRRRRRRRPR
RRRRRRRRRRRRRRRRRRRRRRRRRRRRB
RRRRRRRRRRRRRRRRRRRRRRRRRRRRL
RRRRRRRRRRRRRRRRRRRRRRRRRRRRP
RRRRRRRRRRRRRRRRRRRRRRRRRRRRC
RRRRRRRRRRRRRRRRRRRRRRRRRRRRN
RRRRRRRRRRRRRRRRRRRRRRRRRRRRO
RRRRRRRRRRRRRRRRRRRRRRRRRRRRCP
RRRRRRRRRRRRRRRRRRRRRRRRRRRRPL
RRRRRRRRRRRRRRRRRRRRRRRRRRRRCL
RRRRRRRRRRRRRRRRRRRRRRRRRRRRPR
RRRRRRRRRRRRRRRRRRRRRRRRRRRRRB
RRRRRRRRRRRRRRRRRRRRRRRRRRRRRL
RRRRRRRRRRRRRRRRRRRRRRRRRRRRRP
RRRRRRRRRRRRRRRRRRRRRRRRRRRRRC
RRRRRRRRRRRRRRRRRRRRRRRRRRRRRN
RRRRRRRRRRRRRRRRRRRRRRRRRRRRRO
RRRRRRRRRRRRRRRRRRRRRRRRRRRRRCP
RRRRRRRRRRRRRRRRRRRRRRRRRRRRRPL
RRRRRRRRRRRRRRRRRRRRRRRRRRRRRCL
RRRRRRRRRRRRRRRRRRRRRRRRRRRRRPR
RRRRRRRRRRRRRRRRRRRRRRRRRRRRRRB
RRRRRRRRRRRRRRRRRRRRRRRRRRRRRRL
RRRRRRRRRRRRRRRRRRRRRRRRRRRRRRP
RRRRRRRRRRRRRRRRRRRRRRRRRRRRRRC
RRRRRRRRRRRRRRRRRRRRRRRRRRRRRRN
RRRRRRRRRRRRRRRRRRRRRRRRRRRRRRO
RRRRRRRRRRRRRRRRRRRRRRRRRRRRRRCP
RRRRRRRRRRRRRRRRRRRRRRRRRRRRRRPL
RRRRRRRRRRRRRRRRRRRRRRRRRRRRRRCL
RRRRRRRRRRRRRRRRRRRRRRRRRRRRRRPR
RRRRRRRRRRRRRRRRRRRRRRRRRRRRRRRB
RRRRRRRRRRRRRRRRRRRRRRRRRRRRRRRL
RRRRRRRRRRRRRRRRRRRRRRRRRRRRRRRP
RRRRRRRRRRRRRRRRRRRRRRRRRRRRRRRC
RRRRRRRRRRRRRRRRRRRRRRRRRRRRRRRN
RRRRRRRRRRRRRRRRRRRRRRRRRRRRRRRO
RRRRRRRRRRRRRRRRRRRRRRRRRRRRRRRCP
RRRRRRRRRRRRRRRRRRRRRRRRRRRRRRRPL
RRRRRRRRRRRRRRRRRRRRRRRRRRRRRRRCL
RRRRRRRRRRRRRRRRRRRRRRRRRRRRRRRPR
RRRRRRRRRRRRRRRRRRRRRRRRRRRRRRRRB
RRRRRRRRRRRRRRRRRRRRRRRRRRRRRRRRL
RRRRRRRRRRRRRRRRRRRRRRRRRRRRRRRRP
RRRRRRRRRRRRRRRRRRRRRRRRRRRRRRRRC
RRRRRRRRRRRRRRRRRRRRRRRRRRRRRRRRN
RRRRRRRRRRRRRRRRRRRRRRRRRRRRRRRRO
RRRRRRRRRRRRRRRRRRRRRRRRRRRRRRRRCP
RRRRRRRRRRRRRRRRRRRRRRRRRRRRRRRRPL
RRRRRRRRRRRRRRRRRRRRRRRRRRRRRRRRCL
RRRRRRRRRRRRRRRRRRRRRRRRRRRRRRRRPR
RRRRRRRRRRRRRRRRRRRRRRRRRRRRRRRRRB
RRRRRRRRRRRRRRRRRRRRRRRRRRRRRRRRRL
RRRRRRRRRRRRRRRRRRRRRRRRRRRRRRRRRP
RRRRRRRRRRRRRRRRRRRRRRRRRRRRRRRRRC
RRRRRRRRRRRRRRRRRRRRRRRRRRRRRRRRRN
RRRRRRRRRRRRRRRRRRRRRRRRRRRRRRRRRO
RRRRRRRRRRRRRRRRRRRRRRRRRRRRRRRRRCP
RRRRRRRRRRRRRRRRRRRRRRRRRRRRRRRRRPL
RRRRRRRRRRRRRRRRRRRRRRRRRRRRRRRRRCL
RRRRRRRRRRRRRRRRRRRRRRRRRRRRRRRRRPR
RRRRRRRRRRRRRRRRRRRRRRRRRRRRRRRRRRB
RRRRRRRRRRRRRRRRRRRRRRRRRRRRRRRRRRL
RRRRRRRRRRRRRRRRRRRRRRRRRRRRRRRRRRP
RRRRRRRRRRRRRRRRRRRRRRRRRRRRRRRRRRC
RRRRRRRRRRRRRRRRRRRRRRRRRRRRRRRRRRN
RRRRRRRRRRRRRRRRRRRRRRRRRRRRRRRRRRO
RRRRRRRRRRRRRRRRRRRRRRRRRRRRRRRRRRCP
RRRRRRRRRRRRRRRRRRRRRRRRRRRRRRRRRRPL
RRRRRRRRRRRRRRRRRRRRRRRRRRRRRRRRRRCL
RRRRRRRRRRRRRRRRRRRRRRRRRRRRRRRRRRPR
RRRRRRRRRRRRRRRRRRRRRRRRRRRRRRRRRRRB
RRRRRRRRRRRRRRRRRRRRRRRRRRRRRRRRRRRL
RRRRRRRRRRRRRRRRRRRRRRRRRRRRRRRRRRRP
RRRRRRRRRRRRRRRRRRRRRRRRRRRRRRRRRRRC
RRRRRRRRRRRRRRRRRRRRRRRRRRRRRRRRRRRN
RRRRRRRRRRRRRRRRRRRRRRRRRRRRRRRRRRRO
RRRRRRRRRRRRRRRRRRRRRRRRRRRRRRRRRRRCP
RRRRRRRRRRRRRRRRRRRRRRRRRRRRRRRRRRRPL
RRRRRRRRRRRRRRRRRRRRRRRRRRRRRRRRRRRCL
RRRRRRRRRRRRRRRRRRRRRRRRRRRRRRRRRRRPR
RRRRRRRRRRRRRRRRRRRRRRRRRRRRRRRRRRRRB
RRRRRRRRRRRRRRRRRRRRRRRRRRRRRRRRRRRRL
RRRRRRRRRRRRRRRRRRRRRRRRRRRRRRRRRRRRP
RRRRRRRRRRRRRRRRRRRRRRRRRRRRRRRRRRRRC
RRRRRRRRRRRRRRRRRRRRRRRRRRRRRRRRRRRRN
RRRRRRRRRRRRRRRRRRRRRRRRRRRRRRRRRRRRO
RRRRRRRRRRRRRRRRRRRRRRRRRRRRRRRRRRRRCP
RRRRRRRRRRRRRRRRRRRRRRRRRRRRRRRRRRRRPL
RRRRRRRRRRRRRRRRRRRRRRRRRRRRRRRRRRRRCL
RRRRRRRRRRRRRRRRRRRRRRRRRRRRRRRRRRRRPR
RRRRRRRRRRRRRRRRRRRRRRRRRRRRRRRRRRRRRB
RRRRRRRRRRRRRRRRRRRRRRRRRRRRRRRRRRRRRL
RRRRRRRRRRRRRRRRRRRRRRRRRRRRRRRRRRRRRP
RRRRRRRRRRRRRRRRRRRRRRRRRRRRRRRRRRRRRC
RRRRRRRRRRRRRRRRRRRRRRRRRRRRRRRRRRRRRN
RRRRRRRRRRRRRRRRRRRRRRRRRRRRRRRRRRRRRO
RRRRRRRRRRRRRRRRRRRRRRRRRRRRRRRRRRRRRCP
RRRRRRRRRRRRRRRRRRRRRRRRRRRRRRRRRRRRRPL
RRRRRRRRRRRRRRRRRRRRRRRRRRRRRRRRRRRRRCL
RRRRRRRRRRRRRRRRRRRRRRRRRRRRRRRRRRRRRPR
RRRRRRRRRRRRRRRRRRRRRRRRRRRRRRRRRRRRRRB
RRRRRRRRRRRRRRRRRRRRRRRRRRRRRRRRRRRRRRL
RRRRRRRRRRRRRRRRRRRRRRRRRRRRRRRRRRRRRRP
RRRRRRRRRRRRRRRRRRRRRRRRRRRRRRRRRRRRRRC
RRRRRRRRRRRRRRRRRRRRRRRRRRRRRRRRRRRRRRN
RRRRRRRRRRRRRRRRRRRRRRRRRRRRRRRRRRRRRRO
RRRRRRRRRRRRRRRRRRRRRRRRRRRRRRRRRRRRRRCP
RRRRRRRRRRRRRRRRRRRRRRRRRRRRRRRRRRRRRRPL
RRRRRRRRRRRRRRRRRRRRRRRRRRRRRRRRRRRRRRCL
RRRRRRRRRRRRRRRRRRRRRRRRRRRRRRRRRRRRRRPR
RRRRRRRRRRRRRRRRRRRRRRRRRRRRRRRRRRRRRRRB
RRRRRRRRRRRRRRRRRRRRRRRRRRRRRRRRRRRRRRRL
RRRRRRRRRRRRRRRRRRRRRRRRRRRRRRRRRRRRRRRP
RRRRRRRRRRRRRRRRRRRRRRRRRRRRRRRRRRRRRRRC
RRRRRRRRRRRRRRRRRRRRRRRRRRRRRRRRRRRRRRRN
RRRRRRRRRRRRRRRRRRRRRRRRRRRRRRRRRRRRRRRO
RRRRRRRRRRRRRRRRRRRRRRRRRRRRRRRRRRRRRRRCP
RRRRRRRRRRRRRRRRRRRRRRRRRRRRRRRRRRRRRRRPL
RRRRRRRRRRRRRRRRRRRRRRRRRRRRRRRRRRRRRRRCL
RRRRRRRRRRRRRRRRRRRRRRRRRRRRRRRRRRRRRRRPR
RRRRRRRRRRRRRRRRRRRRRRRRRRRRRRRRRRRRRRRRB
RRRRRRRRRRRRRRRRRRRRRRRRRRRRRRRRRRRRRRRRL
RRRRRRRRRRRRRRRRRRRRRRRRRRRRRRRRRRRRRRRRP
RRRRRRRRRRRRRRRRRRRRRRRRRRRRRRRRRRRRRRRRC
RRRRRRRRRRRRRRRRRRRRRRRRRRRRRRRRRRRRRRRRN
RRRRRRRRRRRRRRRRRRRRRRRRRRRRRRRRRRRRRRRRO
RRRRRRRRRRRRRRRRRRRRRRRRRRRRRRRRRRRRRRRRCP
RRRRRRRRRRRRRRRRRRRRRRRRRRRRRRRRRRRRRRRRPL
RRRRRRRRRRRRRRRRRRRRRRRRRRRRRRRRRRRRRRRRCL
RRRRRRRRRRRRRRRRRRRRRRRRRRRRRRRRRRRRRRRRPR
RRRRRRRRRRRRRRRRRRRRRRRRRRRRRRRRRRRRRRRRRB
RRRRRRRRRRRRRRRRRRRRRRRRRRRRRRRRRRRRRRRRRL
RRRRRRRRRRRRRRRRRRRRRRRRRRRRRRRRRRRRRRRRRP
RRRRRRRRRRRRRRRRRRRRRRRRRRRRRRRRRRRRRRRRRC
RRRRRRRRRRRRRRRRRRRRRRRRRRRRRRRRRRRRRRRRRN
RRRRRRRRRRRRRRRRRRRRRRRRRRRRRRRRRRRRRRRRRO
RRRRRRRRRRRRRRRRRRRRRRRRRRRRRRRRRRRRRRRRRCP
RRRRRRRRRRRRRRRRRRRRRRRRRRRRRRRRRRRRRRRRRPL
RRRRRRRRRRRRRRRRRRRRRRRRRRRRRRRRRRRRRRRRRCL
RRRRRRRRRRRRRRRRRRRRRRRRRRRRRRRRRRRRRRRRRPR
RRRRRRRRRRRRRRRRRRRRRRRRRRRRRRRRRRRRRRRRRRB
RRRRRRRRRRRRRRRRRRRRRRRRRRRRRRRRRRRRRRRRRRL
RRRRRRRRRRRRRRRRRRRRRRRRRRRRRRRRRRRRRRRRRRP
RRRRRRRRRRRRRRRRRRRRRRRRRRRRRRRRRRRRRRRRRRC
RRRRRRRRRRRRRRRRRRRRRRRRRRRRRRRRRRRRRRRRRRN
RRRRRRRRRRRRRRRRRRRRRRRRRRRRRRRRRRRRRRRRRRO
RRRRRRRRRRRRRRRRRRRRRRRRRRRRRRRRRRRRRRRRRRCP
RRRRRRRRRRRRRRRRRRRRRRRRRRRRRRRRRRRRRRRRRRPL
RRRRRRRRRRRRRRRRRRRRRRRRRRRRRRRRRRRRRRRRRRCL
RRRRRRRRRRRRRRRRRRRRRRRRRRRRRRRRRRRRRRRRRRPR
RRRRRRRRRRRRRRRRRRRRRRRRRRRRRRRRRRRRRRRRRRRB
RRRRRRRRRRRRRRRRRRRRRRRRRRRRRRRRRRRRRRRRRRRL
RRRRRRRRRRRRRRRRRRRRRRRRRRRRRRRRRRRRRRRRRRRP
RRRRRRRRRRRRRRRRRRRRRRRRRRRRRRRRRRRRRRRRRRRC
RRRRRRRRRRRRRRRRRRRRRRRRRRRRRRRRRRRRRRRRRRRN
RRRRRRRRRRRRRRRRRRRRRRRRRRRRRRRRRRRRRRRRRRRO
RRRRRRRRRRRRRRRRRRRRRRRRRRRRRRRRRRRRRRRRRRRCP
RRRRRRRRRRRRRRRRRRRRRRRRRRRRRRRRRRRRRRRRRRRPL
RRRRRRRRRRRRRRRRRRRRRRRRRRRRRRRRRRRRRRRRRRRCL
RRRRRRRRRRRRRRRRRRRRRRRRRRRRRRRRRRRRRRRRRRRPR
RRRRRRRRRRRRRRRRRRRRRRRRRRRRRRRRRRRRRRRRRRRRB
RRRRRRRRRRRRRRRRRRRRRRRRRRRRRRRRRRRRRRRRRRRRL
RRRRRRRRRRRRRRRRRRRRRRRRRRRRRRRRRRRRRRRRRRRRP
RRRRRRRRRRRRRRRRRRRRRRRRRRRRRRRRRRRRRRRRRRRRC
RRRRRRRRRRRRRRRRRRRRRRRRRRRRRRRRRRRRRRRRRRRRN
RRRRRRRRRRRRRRRRRRRRRRRRRRRRRRRRRRRRRRRRRRRRO
RRRRRRRRRRRRRRRRRRRRRRRRRRRRRRRRRRRRRRRRRRRRCP
RRRRRRRRRRRRRRRRRRRRRRRRRRRRRRRRRRRRRRRRRRRRPL
RRRRRRRRRRRRRRRRRRRRRRRRRRRRRRRRRRRRRRRRRRRRCL
RRRRRRRRRRRRRRRRRRRRRRRRRRRRRRRRRRRRRRRRRRRRPR
RRRRRRRRRRRRRRRRRRRRRRRRRRRRRRRRRRRRRRRRRRRRRB
RRRRRRRRRRRRRRRRRRRRRRRRRRRRRRRRRRRRRRRRRRRRRL
RRRRRRRRRRRRRRRRRRRRRRRRRRRRRRRRRRRRRRRRRRRRRP
RRRRRRRRRRRRRRRRRRRRRRRRRRRRRRRRRRRRRRRRRRRRRC
RRRRRRRRRRRRRRRRRRRRRRRRRRRRRRRRRRRRRRRRRRRRRN
RRRRRRRRRRRRRRRRRRRRRRRRRRRRRRRRRRRRRRRRRRRRRO
RRRRRRRRRRRRRRRRRRRRRRRRRRRRRRRRRRRRRRRRRRRRRCP
RRRRRRRRRRRRRRRRRRRRRRRRRRRRRRRRRRRRRRRRRRRRRPL
RRRRRRRRRRRRRRRRRRRRRRRRRRRRRRRRRRRRRRRRRRRRRCL
RRRRRRRRRRRRRRRRRRRRRRRRRRRRRRRRRRRRRRRRRRRRRPR
RRRRRRRRRRRRRRRRRRRRRRRRRRRRRRRRRRRRRRRRRRRRRRB
RRRRRRRRRRRRRRRRRRRRRRRRRRRRRRRRRRRRRRRRRRRRRRL
RRRRRRRRRRRRRRRRRRRRRRRRRRRRRRRRRRRRRRRRRRRRRRP
RRRRRRRRRRRRRRRRRRRRRRRRRRRRRRRRRRRRRRRRRRRRRRC
RRRRRRRRRRRRRRRRRRRRRRRRRRRRRRRRRRRRRRRRRRRRRRN
RRRRRRRRRRRRRRRRRRRRRRRRRRRRRRRRRRRRRRRRRRRRRRO
RRRRRRRRRRRRRRRRRRRRRRRRRRRRRRRRRRRRRRRRRRRRRRCP
RRRRRRRRRRRRRRRRRRRRRRRRRRRRRRRRRRRRRRRRRRRRRRPL
RRRRRRRRRRRRRRRRRRRRRRRRRRRRRRRRRRRRRRRRRRRRRRCL
RRRRRRRRRRRRRRRRRRRRRRRRRRRRRRRRRRRRRRRRRRRRRRPR
RRRRRRRRRRRRRRRRRRRRRRRRRRRRRRRRRRRRRRRRRRRRRRRB
RRRRRRRRRRRRRRRRRRRRRRRRRRRRRRRRRRRRRRRRRRRRRRRL
RRRRRRRRRRRRRRRRRRRRRRRRRRRRRRRRRRRRRRRRRRRRRRRP
RRRRRRRRRRRRRRRRRRRRRRRRRRRRRRRRRRRRRRRRRRRRRRRC
RRRRRRRRRRRRRRRRRRRRRRRRRRRRRRRRRRRRRRRRRRRRRRRN
RRRRRRRRRRRRRRRRRRRRRRRRRRRRRRRRRRRRRRRRRRRRRRRO
RRRRRRRRRRRRRRRRRRRRRRRRRRRRRRRRRRRRRRRRRRRRRRRCP
RRRRRRRRRRRRRRRRRRRRRRRRRRRRRRRRRRRRRRRRRRRRRRRPL
RRRRRRRRRRRRRRRRRRRRRRRRRRRRRRRRRRRRRRRRRRRRRRRCL
RRRRRRRRRRRRRRRRRRRRRRRRRRRRRRRRRRRRRRRRRRRRRRRPR
RRRRRRRRRRRRRRRRRRRRRRRRRRRRRRRRRRRRRRRRRRRRRRRRB
RRRRRRRRRRRRRRRRRRRRRRRRRRRRRRRRRRRRRRRRRRRRRRRRL
RRRRRRRRRRRRRRRRRRRRRRRRRRRRRRRRRRRRRRRRRRRRRRRRP
RRRRRRRRRRRRRRRRRRRRRRRRRRRRRRRRRRRRRRRRRRRRRRRRC
RRRRRRRRRRRRRRRRRRRRRRRRRRRRRRRRRRRRRRRRRRRRRRRRN
RRRRRRRRRRRRRRRRRRRRRRRRRRRRRRRRRRRRRRRRRRRRRRRRO
RRRRRRRRRRRRRRRRRRRRRRRRRRRRRRRRRRRRRRRRRRRRRRRRCP
RRRRRRRRRRRRRRRRRRRRRRRRRRRRRRRRRRRRRRRRRRRRRRRRPL
RRRRRRRRRRRRRRRRRRRRRRRRRRRRRRRRRRRRRRRRRRRRRRRRCL
RRRRRRRRRRRRRRRRRRRRRRRRRRRRRRRRRRRRRRRRRRRRRRRRPR
RRRRRRRRRRRRRRRRRRRRRRRRRRRRRRRRRRRRRRRRRRRRRRRRRB
RRRRRRRRRRRRRRRRRRRRRRRRRRRRRRRRRRRRRRRRRRRRRRRRRL
RRRRRRRRRRRRRRRRRRRRRRRRRRRRRRRRRRRRRRRRRRRRRRRRRP
RRRRRRRRRRRRRRRRRRRRRRRRRRRRRRRRRRRRRRRRRRRRRRRRRC
RRRRRRRRRRRRRRRRRRRRRRRRRRRRRRRRRRRRRRRRRRRRRRRRRN
RRRRRRRRRRRRRRRRRRRRRRRRRRRRRRRRRRRRRRRRRRRRRRRRRO
RRRRRRRRRRRRRRRRRRRRRRRRRRRRRRRRRRRRRRRRRRRRRRRRRCP
RRRRRRRRRRRRRRRRRRRRRRRRRRRRRRRRRRRRRRRRRRRRRRRRRPL
RRRRRRRRRRRRRRRRRRRRRRRRRRRRRRRRRRRRRRRRRRRRRRRRRCL
RRRRRRRRRRRRRRRRRRRRRRRRRRRRRRRRRRRRRRRRRRRRRRRRRPR
RRRRRRRRRRRRRRRRRRRRRRRRRRRRRRRRRRRRRRRRRRRRRRRRRRB
RRRRRRRRRRRRRRRRRRRRRRRRRRRRRRRRRRRRRRRRRRRRRRRRRRL
RRRRRRRRRRRRRRRRRRRRRRRRRRRRRRRRRRRRRRRRRRRRRRRRRRP
RRRRRRRRRRRRRRRRRRRRRRRRRRRRRRRRRRRRRRRRRRRRRRRRRRC
RRRRRRRRRRRRRRRRRRRRRRRRRRRRRRRRRRRRRRRRRRRRRRRRRRN
RRRRRRRRRRRRRRRRRRRRRRRRRRRRRRRRRRRRRRRRRRRRRRRRRRO
RRRRRRRRRRRRRRRRRRRRRRRRRRRRRRRRRRRRRRRRRRRRRRRRRRCP
RRRRRRRRRRRRRRRRRRRRRRRRRRRRRRRRRRRRRRRRRRRRRRRRRRPL
RRRRRRRRRRRRRRRRRRRRRRRRRRRRRRRRRRRRRRRRRRRRRRRRRRCL
RRRRRRRRRRRRRRRRRRRRRRRRRRRRRRRRRRRRRRRRRRRRRRRRRRPR
RRRRRRRRRRRRRRRRRRRRRRRRRRRRRRRRRRRRRRRRRRRRRRRRRRRB
RRRRRRRRRRRRRRRRRRRRRRRRRRRRRRRRRRRRRRRRRRRRRRRRRRRL
RRRRRRRRRRRRRRRRRRRRRRRRRRRRRRRRRRRRRRRRRRRRRRRRRRRP
RRRRRRRRRRRRRRRRRRRRRRRRRRRRRRRRRRRRRRRRRRRRRRRRRRRC
RRRRRRRRRRRRRRRRRRRRRRRRRRRRRRRRRRRRRRRRRRRRRRRRRRRN
RRRRRRRRRRRRRRRRRRRRRRRRRRRRRRRRRRRRRRRRRRRRRRRRRRRO
RRRRRRRRRRRRRRRRRRRRRRRRRRRRRRRRRRRRRRRRRRRRRRRRRRRCP
RRRRRRRRRRRRRRRRRRRRRRRRRRRRRRRRRRRRRRRRRRRRRRRRRRRPL
RRRRRRRRRRRRRRRRRRRRRRRRRRRRRRRRRRRRRRRRRRRRRRRRRRRCL
RRRRRRRRRRRRRRRRRRRRRRRRRRRRRRRRRRRRRRRRRRRRRRRRRRRPR
RRRRRRRRRRRRRRRRRRRRRRRRRRRRRRRRRRRRRRRRRRRRRRRRRRRRB
RRRRRRRRRRRRRRRRRRRRRRRRRRRRRRRRRRRRRRRRRRRRRRRRRRRRL
RRRRRRRRRRRRRRRRRRRRRRRRRRRRRRRRRRRRRRRRRRRRRRRRRRRRP
RRRRRRRRRRRRRRRRRRRRRRRRRRRRRRRRRRRRRRRRRRRRRRRRRRRRC
RRRRRRRRRRRRRRRRRRRRRRRRRRRRRRRRRRRRRRRRRRRRRRRRRRRRN
RRRRRRRRRRRRRRRRRRRRRRRRRRRRRRRRRRRRRRRRRRRRRRRRRRRRO
RRRRRRRRRRRRRRRRRRRRRRRRRRRRRRRRRRRRRRRRRRRRRRRRRRRRCP
RRRRRRRRRRRRRRRRRRRRRRRRRRRRRRRRRRRRRRRRRRRRRRRRRRRRPL
RRRRRRRRRRRRRRRRRRRRRRRRRRRRRRRRRRRRRRRRRRRRRRRRRRRRCL
RRRRRRRRRRRRRRRRRRRRRRRRRRRRRRRRRRRRRRRRRRRRRRRRRRRRPR
RRRRRRRRRRRRRRRRRRRRRRRRRRRRRRRRRRRRRRRRRRRRRRRRRRRRRB
RRRRRRRRRRRRRRRRRRRRRRRRRRRRRRRRRRRRRRRRRRRRRRRRRRRRRL
RRRRRRRRRRRRRRRRRRRRRRRRRRRRRRRRRRRRRRRRRRRRRRRRRRRRRP
RRRRRRRRRRRRRRRRRRRRRRRRRRRRRRRRRRRRRRRRRRRRRRRRRRRRRC
RRRRRRRRRRRRRRRRRRRRRRRRRRRRRRRRRRRRRRRRRRRRRRRRRRRRRN
RRRRRRRRRRRRRRRRRRRRRRRRRRRRRRRRRRRRRRRRRRRRRRRRRRRRRO
RRRRRRRRRRRRRRRRRRRRRRRRRRRRRRRRRRRRRRRRRRRRRRRRRRRRRCP
RRRRRRRRRRRRRRRRRRRRRRRRRRRRRRRRRRRRRRRRRRRRRRRRRRRRRPL
RRRRRRRRRRRRRRRRRRRRRRRRRRRRRRRRRRRRRRRRRRRRRRRRRRRRRCL
RRRRRRRRRRRRRRRRRRRRRRRRRRRRRRRRRRRRRRRRRRRRRRRRRRRRRPR
RRRRRRRRRRRRRRRRRRRRRRRRRRRRRRRRRRRRRRRRRRRRRRRRRRRRRRB
RRRRRRRRRRRRRRRRRRRRRRRRRRRRRRRRRRRRRRRRRRRRRRRRRRRRRRL
RRRRRRRRRRRRRRRRRRRRRRRRRRRRRRRRRRRRRRRRRRRRRRRRRRRRRRP
RRRRRRRRRRRRRRRRRRRRRRRRRRRRRRRRRRRRRRRRRRRRRRRRRRRRRRC

if necessary change it or inspect the workpiece for size. When programming the operation of the machine, the appropriate instructions are applied to the fourth track of the magnetic tape in the form of a definite number of pulses. During the process of machining the component they are counted by the head 4*GM* and fed to the input of the control unit counter causing relays 1*RB* to 3*RB* to operate. The latter, acting on the sound signal apparatus and light table, give a definite command to the operator of the machine automatically. By pressing the button "Remove Signal" the operator removes the command previously given from the counter and table and starts the machine again for automatic operation according to the given programme. Here the control unit is prepared to accept the next auxiliary command to be included in the lathe work programme. However, unforeseen failures may arise on the machine, for example, breakage of the cutter. To eliminate such failures, provision is made for bringing the machine slowly to a halt by pressing the button "Stop" The lathe saddle is then set up in the nearest previously passed position provided by the programme for intermediate stoppage. In this position the operator sets up the magnetic tape. Special marks are provided for this. After performing the stated operations, the lathe can then be started again by pressing the appropriate control button.

In order to set up the saddle accurately, necessary for initial synchronization of its position with the programme recorded on the tape, two fixed inductive metering heads are provided on it: one on the slides of the saddle and the other on its carriage. Two cylindrical steel metering scales are mounted along the saddle guides and those of its upper carriage (i.e., across the lathe). Two cylindrical projections on the longitudinal scale. By means of the metering heads it is possible to set up the saddle strictly in accordance with the vertical axis of the projections made on the scales. For this the operator changes the control system into the "Set up" state after an unforeseen stoppage of the machine. Then, pressing the control button for the step by step motors, the saddle is set up in a definite position corresponding to the previously applied mark on the magnetic tape.

In addition, provision is made on the machine for an additional (test) device which makes for simpler starting after being stopped by the "Stop" button. This device has been omitted from Fig. 2. It connects a special magnetic recording-counting head. When the "Stop" button is pressed an electrical pulse is supplied to the stated head at the same time as the switching takes place to stop the electric drives of the lathe. This pulse applies a special synchronizing magnetic mark (command stop) on the fifth track of the magnetic tape. Before the machine is started again the magnetic tape is wound 50 to 100 mm in the

reverse direction (relative to the working direction).

The lathe is then re-started by pressing the button "Start". But the saddle feed only begins when the previously applied "command stop" on the tape engages the counting head on the fifth track of the tape. Synchronization of the saddle feed is thus synchronized with the work programme.

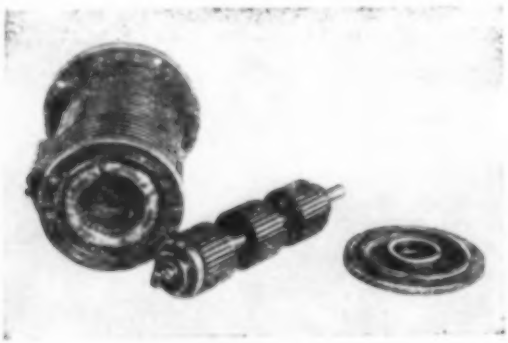

Fig. 3. ESh-1 type step-by-step power motor.

The described device makes it possible for example to effect repeat traverses of the cutter quite simply for machining different parts of the workpiece in accordance with the same programme.

With manual control of the machine starting and stopping, reversing and changing the speed of the step-by-step motors for the saddle and the main motor of the lathe is carried out by a set of apparatus conventionally referred to as the manual control block (*MCB*) in Fig. 1. The step-by-step motors are controlled by buttons "Forward" " Back" " Right" and "Left ". The contacts of the appropriate relays open the cells 1*C* and 2*C* through which the pulses from the generators *G1X* and *G1Y* pass to the units 1*TV* and 2*TV* which supply the step-by-step motors. The speeds of the latter are regulated the regulators *RSX* and *RSY* which adjust the tuning of the generators (the frequency of the pulse sequence).

The main motor is started and stopped by the buttons in the coil circuit of the relay *RO*, whilst its speed is regulated by the regulator *RSS*. The range of speed regulation for the motors 1*SSM*, 2*SSM* and *G* are the same for manual control as for programme control.

As there is no mechanical connexion between the spindle mechanisms and the saddle feed, the latter is regulated independently of the speed

of the spindle (minute feed). The presence of manual electrical regulation for the speed of the step-by-step motors makes it possible to regulate the amount of feed smoothly during the process of turning and impart the necessary direction of travel to the cutter.

In electro-copying conditions, use is made entirely of the elements of electrical equipment provided on the lathe for manual control. The step-by-step motors are controlled in the case in question by a three-position contact feeler (*CF*) which moves along the model together with the saddle, no use being made of buttons.

The closure of any contact of the feeler opens the valve "cell" 2*V* which starts the motor 2*SSM* for transverse feed. The direction of rotation of the motor is determined by the state of the trigger "cell" 8*TC*, controlled by the same feeler. If both contacts of the feeler are open the motor 2*SSM* is tripped and motor 1*SSM* is switched on by potential trigger *PT* and begins to move the saddle along the copying rule (to left or right). The electronic units are semiconductor elements for increased reliability and to save space. All the control gear for the lathe motors is installed at the control "post" and desk, which are relatively small in size.

Experimental verification of the system

The model of the device for recording on the magnetic tape (*DRM*) and also the model of the electric drive for the lathe with programme control were experimentally verified in laboratory conditions.

The model of the *DRM* comprised: (a) a counting device for which use was made of a K45-type controller with a slightly modified control scheme; (b) an electronic code converter.

During the tests punched cards were introduced into the counting device with a programme recorded on them which corresponded to the most strained operating conditions for all the units in the code converter.

During the test a count was made of the number of pulses given by the *DRM* for recording on the magnetic tape and this was compared with the number of pulses recorded on the punched card. The tests showed that the *DRM* was quite capable of working and sufficiently reliable.

The model of the electric drive for the machine was verified by the accuracy with which it reproduced the prescribed programme in order to elicit the quality of its performance and the decision capacity of the step-by-step motors. The tests on the model in the most arduous conditions showed that it works satisfactorily. The test on the step-by-step motors showed that they can operate at a frequency of 0 to 150 c/s

with a static load of about 0.5 kg/m and an additional flywheel torque equal to about 30 kg/cm^2 without loss of pulses. Here a sharp variation in the frequency of the sequence of pulses is permissible from 0 to 150 c/s, which corresponds to a variation in the amount of feed for the lathe saddle of roughtly 0 to 180 mm/min.

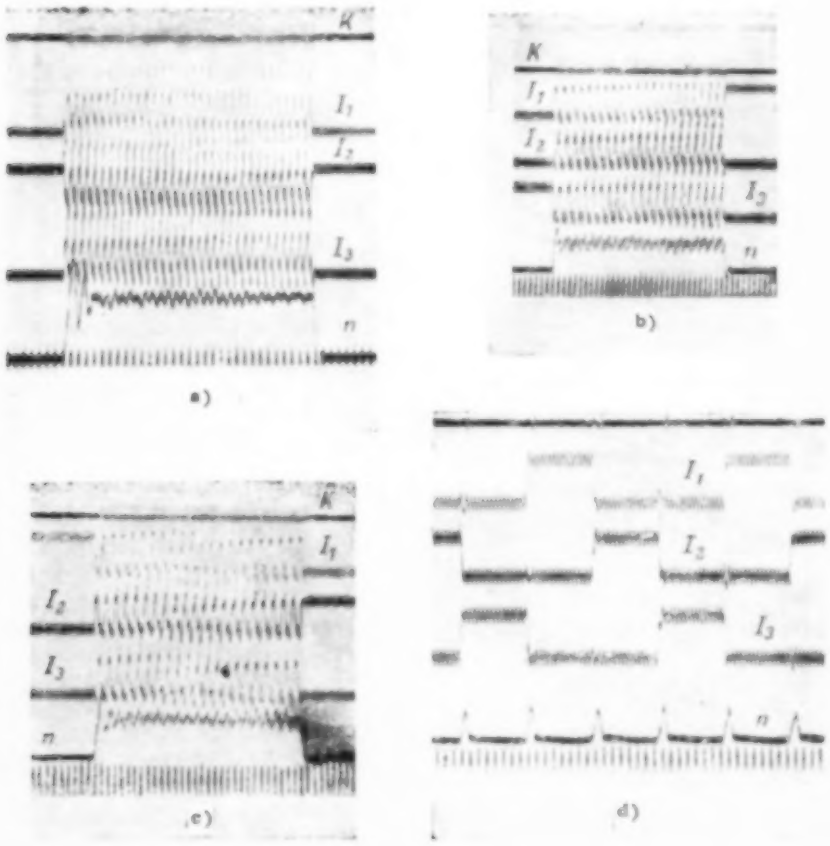

Fig. 4. Oscillograms of ESh-1 type step-by-step motor performance.

a – load torque on motor shaft M_l = 0.5 kg/m, pulse frequency f = 150 ($n \approx 83$ rev/min); b – M_l = 0.5 kg/m, f = 100 ($n \approx 55$ rev/min); c – M_l = 0.65 kg/m, f = 100 ($n \approx 55$ rev/min); d – M_l = 0.65 kg/m, f = 5 ($n \approx 2.8$ rev/min)

Fig.4 shows oscillograms of the performance of an ESh-1 type step-

by-step motor at various pulse frequencies.

Conclusion. The calculations and experimental verification of the above control system has shown the expediency of its application to a heavy lathe. It is however as yet impossible to give a complete evaluation of the system. This requires a trial period of industrial operation lasting several months.

The cost of the lathe in question with programme control should be about 120% of the cost of an anlogous heavy lathe with conventional (manual) control.

An operator can tend several such machines operating with either programme or electro-copying control.

The attachment for recording the programme on the magnetic tape can serve several programme-controlled machines and if there is a computer centre there is generally no need of a *DRM*.

Translated by O.M. Blunn

SELF-ALIGNING SYSTEM FOR AUTOMATIC CONTROL OF WELDING CONDITIONS ON ELECTRICAL TUBE WELDING MACHINES*

A.B. CHELIUSTKIN and V.A. IVANOV

(Institute of Automatics and Telemechanics, Academy of Science U.S.S.R.)

(Received 14 July 1959)

The majority of automatic control systems for production processes at present in use have to maintain pre-determined operating conditions which are not always optimum because of changes in external factors. The use of calculating devices in such systems presents great opportunities for automatic optimization, i.e. the establishment of those operating conditions which ensure that the process has the best technical-economic indices.

The development of optimization systems is now in the initial stage. Current research is mainly connected with the creation of individual types of external regulators (1), intended to maintain the indices of the production process at the maximum high level or minimum low level.

The inclusion of calculating devices in systems of automatic disturbance control which automatically adjust their parameters when the characteristics of the controlled object vary makes it possible to develop self-aligning systems which are capable of ensuring the requisite evaluation of controlled process, so that the field of application is greatly extended for methods which will compensate disturbances affecting the object.

In conventional disturbance control systems (2, 3), the calculator is connected in such a way that its input will receive disturbances received at the input to the system to be controlled (Fig. 1). Using the disturbances received at the input, in accordance with the known transmission function of the system, the compensating action y is then calculated which will neutralize the effect of the disturbance $f(t)$ on the system, and sometimes alter the behaviour of the system as and when the character of the disturbances changes.

---

* *Elektrichestvo*, No.2, 13-18, 1960.

It is obvious that the output quantity can only be held constant i.e. remain independent of the disturbance at the input to the system, if the parameters of the compensation calculator are chosen in accordance with the parameters and characteristics of the automatic control system. In the majority of cases, these characteristics are either not known accurately or else are subject to change. It is therefore necessary to correct the parameters of the compensating calculating device with the variation in the characteristics of the object and regulator. Such correction can be made by means of a second calculating device (CD2) which will analyse the behaviour of the output magnitude x as a result of the effect on the system of the disturbance. Here CD2 will alter the parameters of the compensating calculating device until the output quantity is made independent of the disturbance at the input (Fig.2). It is possible to evaluate the effect of the disturbance on the system by certain criteria of the quality of the automatic control process (4).

$$\int |x|dt;\ \int x^2 dt;\ \int f(t-\tau)|x|dt.$$

Without dwelling on possible principles for realizing methods of minimizing the quantity x from the stated criteria, consider a method (5) where the necessary correction is made to the parameters of the compensating calculating device CD1 by investigating the "pseudo-mutual correcting" function, which has the form:

$$\varphi(t) = \int_0^t x(t)\cdot f(t-\tau)dt,$$

where τ is the lag time, being in fact the time taken for the disturbance to pass through the object.

Consequently, the function $f(t-\tau)$ is a function $f(t)$ combined in time with the function $x(t)$.

It follows from the expression for $\phi(t)$, that if the condition of constancy is satisfied, function $\phi(t)$ will assume a final steady value (since the "sub-integral" expression becomes equal to zero).

Compared with other methods, the method under consideration, characterized by high stability to interference, has a considerable advantage in that no additional disturbances have to be fed into the system when it is used.

The interference resistance of the system is due to the fact that a change in the magnitude of the function $\phi(t)$ will only take place if the variation in $x(t)$ is correlated with the disturbance $f(t)$ affecting

the object. All the remaining possible disturbances, even though they determine the variation of $x(t)$, can be considered as interferences which do not cause a regular variation of the function $\phi(t)$ after a sufficient interval of time.

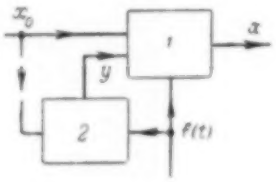

Fig. 1. Block-circuit of automatic control system with disturbance compensation. *1* - automatic control system; *2* - compensating calculating device.

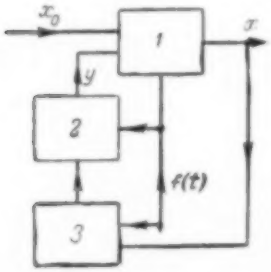

Fig. 2. Block-circuit of self-aligning system using correlated relationships. *1* - automatic control system; *2* - compensating calculating device; *3* - correcting calculating device.

If there are a large number of control objects the transmission coefficient is the only variable parameter of the characteristic and the "transmission" function itself remains almost constant. Such objects include technological processes when material with different characteristics is machined. Thus, metal with different mechanical properties may be rolled on a rolling mill with fixed dynamic drive characteristics. The tube welded on an electrical tube-welding machine with fixed time constants for the welding current control circuit may be made from material with different ohmic and inductive resistance etc.

1960

In the case of these objects the problem of self-alignment is the establishment of the required value of the transmission coefficient in the compensating calculating device CD1 in accordance with the transmission coefficient of the object. It is obvious that if the value of the CD1 transmission coefficient is insufficient, the disturbance $f(t)$ will not be compensated and $x(t)$ will not be zero at the output from the system. Here $x(t)$ will coincide in sign with $f(t)$ so that the function $\phi(t)$ will increase. If the value of the CD1 transmission coefficient is in excess, the signs $f(t)$ and $x(t)$ are different and the value of function $\phi(t)$ will diminish.

Thus, the output value $x(t)$ will only be zero if the transmission coefficient is equal to the required value, which in turn is proportional to the steady state value of the $\phi(t)$ function. Any variation in the transmission coefficient of the object, by disturbing the constancy condition, will cause a variation in the magnitude of the (t) function, and, consequently, an alteration in the CD1 transmission coefficient before it is applied in accordance with the value of the transmission coefficient of the object.

In the following, as an example of the above system of self-alignment, a study is made of a system for automatically, aligning tube welding conditions on an electrical tube welding machine.

Control system for welding conditions

Widespread use is made of resistance welding for tubes owing to a number of advantages compared with other methods of producing tubes. Among these advantages we should mention the following [6]: the possibility of producing a wide range of tubes in diameter and wall thickness, precision production of tubes, high output and low production cost.

When tubes are resistance welded the formed tubular blank enters a welding unit which comprises resistance welding disk electrodes connected to a rotating welding transformer and non-drive pressure rolls. The electrodes and pressure rolls form a closed bore and by combined action create the necessary welding pressure in the welding seat. The transformer is supplied from a generator whose frequency and voltage determine the welding conditions. Part of the current applied to the rotating electrodes passes through the joint between the edges of the blank and heats them to welding temperature. Another part of the current is shunted in the closed circuit of the blank. Under the pressure of the rolls and electrodes the heated edges are pressed together and welded. The process takes place continuously since new

sections of the tube are fed to the welding seat all the time, the tube being shaped from strip on a continuous shaping mill.

The main factor determining the quality of the welded joint when tubes are resistance welded is the temperature of the edges of the tube blank. The temperature is a non-linear function of the magnitude of the welding currents specific resistance, frequency of the welding current, thickness of the tube walls and a number of other factors. In order to stabilize the temperature of the edges of the blank (temperature of the welded joint) it is possible in principle to create a closed automatic control system in which the measured deviation in temperature from the desired value will affect the amount of welding current.

But owing to the design features of the machine the temperature of the welded joint can only be measured at a certain distance from the welding zone. This determines the presence of delay in measurement (up to 1.5 to 3 sec) and stops a closed automatic control system being made sufficiently quick-acting. The disturbances which cause the variations in temperature can also vary contemporaneously at comparatively high frequencies (up to 2 to 3 c/s). These disturbances are mainly the variability of the amount of welding current and the fluctuations in the thickness of the tube walls occasioned by inaccuracies in rolling the strip from which the tube is formed. The welding current is a function of the transient resistance between the contact rings and the workpiece to be welded and therefore varies within wide limits as a function of the finish of the surface of the strip from which the tube workpiece is formed, and the pressure in the welding unit if the voltage on the electrode rings is fixed. Consequently an automatic control circuit must be introduced into the control system to maintain the given quantity of welding current constant. If the wall thickness of the tube to be welded varies, it is necessary to vary the value of the welding current to keep the temperature constant. If this variation is to be performed by a system of automatic temperature control from the deviations, then owing to the presence of delay in the system when temperature varies, such a system cannot conduct the process qualitatively if the thickness of the tube to be welded varies at frequencies of the order of several dozen or unit c/s, and in certain cases may even produce worse results than manual control. In fact, the welding current can in this case for example increase at the moment when an even thinner blank is passing under the welding electrodes, and conversely, a signal to change the welding current may be received when a thinner tube is passing, but the system may in fact operate when a thicker blank is passing under the welding electrodes. Therefore, an additional compensating device must be introduced into the system to enable the

1960

amount of welding current to be varied as a function of the variation in the thickness of the strip so that the welding temperature will remain constant.

Fig.3 shows the principal circuit of such a control system. The welding current regulator, acting via the dynamoelectric amplifier for the excitation of the generator, which supplies the rotary transformer, holds the welding current constant. This can be measured by the current transformer in accordance with the task set by the machine operator. The task of the welding current regulator is changed automatically like additional tasks set by hand, by a certain magnitude proportional to the value of the deviation in the tube wall thickness from nominal. As the existing instruments can only measure the thickness of the tube walls before the strip is shaped into the tube blank, i.e. at the input to the shaping section, the compensating device incorporates a delay unit which makes it possible to memorize the deviation in the thickness of the strip from nominal and reproduce it after a period of time τ_1 equal to the time τ_2 taken for the strip to cover the distance from the point where the thickness "gauge" is installed to the place of welding. Thus the signal reproduced by the delay block is only fed into the system when the section of tube with the irregular wall thickness enters the welding section of the machine.

Thus, the speed of the magnetic tape also varies when the speed of the mill changes so that delay time agrees with the time taken for the workpiece to move through the machine.

In order to make reproduction more accurate, use is made of frequency modulation for the amplitude of the recording voltage, i.e. the recording system enters the demoldulator and a voltage is reproduced at the output of the delay unit equal to that fed in at its input.

Owing to the inertia of the automatic control system, the welding current will follow the alterations in the tasks of the regulator after a certain delay. If the variations in the tasks are harmonic in character, the phase shifts and amplitudes of the welding current depend on the frequency of the variation in the task. In order to ensure full compensation of the effect of thickness on the welding temperature, the compensating device incorporates a dynamic compensating link having such an amplitude-phase characteristic that the phase and amplitude distortions remain constant for the whole working range of frequencies of the variations in thickness.

If these links are present in the compensating device, the constancy of the welded joint temperature is only determined by the system transmission coefficient, i.e. by the coefficient of proportionality between

the amount of deviation in the thickness of the tube wall from nominal and the change in the task of the current regulator. As has been stated above, the temperature of the welded joint is a non-linear function of wall thickness. Also non-linear is the relationship between the amount of welding current and thickness when the welding temperature is fixed. Only when the deviations in wall thickness are small can this relationship be linearized with a sufficient degree of accuracy, its proportionality factor here being dependent on the absolute thickness of the tube wall, the grade of steel from which the tube is made and a number of other parameters. Consequently, this coefficient is generally unknown and should be found every time a new type of tube is welded. The required coefficient is determined and fixed automatically by means of the automatic correction or self-alignment device.

The operating principle of this device is the comparison made between real variations occurring in the thickness of the tube walls and these variations caused by deviations in the temperature of the welded joint. Here it should be borne in mind that the deviations in temperature as well as variations in wall thickness also occur for a number of other reasons which, in relation to variations in thickness, have the character of accidental disturbances or interference, whose distribution is similar to the normal Gauss distribution.

In order to increase the interference resistance of the self-alignment system, use is made of the calculating device CD2 which calculates the "pseudo-mutual correlation" function

$$\varphi(t)=\int_0^t \Delta\vartheta \cdot \Delta\delta \cdot dt, \qquad (1)$$

where $\Delta\vartheta$ is the time function of the variation in temperature at the joint;

$\Delta\delta$ is the time function of the variation in thickness combined with the $\Delta\vartheta$ function by means of the delay unit.

In order to calculate the $\phi(t)$ function, the correcting calculating device should incorporate a multiplier and integrating link as well as the delay unit.

The elucidated deviations in joint temperature and thickness are fed in the form of voltages ΔU_ϑ and ΔU_δ into calculating device CD2. As the deviation in thickness should be measured at the same time as the temperature deviation, the delay unit should accommodate a second reproducing head, which ensures a delay time $\tau_2 + \tau_3$, equal to the time taken for the tube to cover the distance from the thickness gauge to the

contact thermocouple. The calculating CD2 also performs the multiplying and integrating operations. In order to simplify the CD2 scheme, it is electromechanical and comprises a two phase motor as the output element, one of the windings of this motor obtaining a voltage proportional to ΔU_θ whilst the other obtains a voltage proportional to ΔU_δ, but shifted through 90° relative to the first.

Thus the motor' speed and torque are proportional to the product of the two voltages, the angle of turn of the rotor being proportional to the speed integral, i.e. to the integral from the obtained product.

In order to reduce the effect of the moment of friction of the motor on the value of the integral to be calculated, only one of the motor windings is connected via an electronic amplifier to the voltage ΔU_θ. The second winding is always supplied with the full voltage in the form of pulses, the "slottedness" of which is proportional to the magnitude of the second voltage ΔU_δ. Pulsewidth modulation of the voltage to be supplied to the second winding of the motor is achieved by a special electronic scheme consisting of a saw-tooth voltage generator and an element for comparing the value of the voltage amplified by the electronic amplifier ΔU_δ with the "flowing" value of the saw-tooth voltage. From the moment the saw-tooth voltage begins to increase to the moment it is equalized with the amplifier voltage ΔU_δ the scheme feeds the motor winding with an alternating voltage pulse whose phase is determined by the law of the voltage ΔU_θ. Thus the motor's torque, speed and direction of rotation are determined by the magnitude and sign of the product of the voltages ΔU_θ and ΔU_δ.

The shaft of the motor for the calculating device CD2 is coupled via reduction gears to the arm of a reochord at the input to the amplifier in the compensating CD1, whose terminals are supplied with a voltage ΔU_δ, taken from the reproducing head in the delay unit (DU). The required value of the transmission coefficient is thereby established for CD1.

Assume that the value of the function $\phi(t)$ was zero when the system was switched on, i.e. no alteration occurs in the task of the regulator when the thickness of the tube wall varies. Consequently, for example, the increase in thickness will cause a decrease in weld-joint temperature and vice versa. It is obvious that the product of $\Delta\theta \cdot \Delta\delta$ will not be zero here and the calculating device CD2, integrating this product, will move the arm of the reochord to the input of the amplifier for CD1. Here a regulating signal will be produced in CD1 proportional to the measured deviation in the tube wall and producing the corresponding change in welding current. Owing to this the effect of the change in wall thickness on the change in temperature begins to

diminish so that the magnitude of the product $\Delta\vartheta \cdot \Delta\delta$ will decrease and the speed at which the reochord arm is moved to the input of CD1 will be reduced. This movement will cease completely when there is full compensation of the effect of the change in the tube's wall thickness on temperature, i.e. when $\Delta\vartheta \cdot \Delta\delta$ is zero. Here the value of $\phi(t)$ will be determined by the properties of the material from which the workpiece is made and its absolute thickness.

Determination of the parameters of the self-aligning system

The equation which shows the link between the fluctuations in the temperature of the weld joint $\Delta\vartheta$ and the variations in thickness $\Delta\delta$ when a regulating action is present, like a change in the instruction ΔI to the welding current regulator, can be written in the form:

$$\Delta\vartheta = k_2 [-W_\delta(p) \cdot e^{-p\tau_2} \Delta\delta + W_I(p) \cdot \Delta I] e^{-p\tau_2}, \tag{2}$$

where $W_\delta(p)$ and $W_I(p)$ are the transmission functions of the object for the disturbing and regulating actions, the values of which depend on the parameters of the object;

k_2 is a coefficient taking into account the temperature drop between the welding point and the point where temperature is measured.

The variable magnitude of $\Delta\vartheta$ will not depend on the effect of $\Delta\delta$ if the following condition is satisfied:

$$-W_\delta(p) \cdot e^{-p\tau_2} \Delta\delta + W_I(p) \cdot \Delta I = 0, \tag{3}$$

which determines the parameters of the compensating device CD1. The structural scheme of this device has the form presented in Fig. 4. The compensating device CD1, when the thickness of the strip varies, will produce a change in the magnitude of the welding current equal to

$$\Delta I = k_1 W_c(p) \cdot k_n \cdot W_r(p) e^{-p\tau_1} \Delta\delta, \tag{4}$$

where k_1 is the transmission factor of the delay unit;

k_n is the variable amplification factor of the amplifier entering CD1;

$W_c(p)$ is the transmission function of the dynamic compensating link CD1;

$W_r(p)$ is the transmission function of the automatic control system for the welding current.

Making the necessary transformations we find from equations (3) and (4), (if $\tau_1 = \tau_2$, which is always maintained):

$$-W_3(p)+k_1k_nW_1(p)\cdot W_c(p)\cdot W_r(p)=0. \qquad (5)$$

In the general case the transmission function $W(P)$ can be presented in the form $W(p) = \frac{k}{D(p)}$, where k represents the static of the link and the operator $D(p)$ the dynamic.

Consequently, expression (5) can be written in the form of an equation

$$\frac{k_1k_nk_1k_ck_r}{D_1(p)\cdot D_c(p)\cdot D_r(p)}=\frac{k_3}{D_3(p)}. \qquad (6)$$

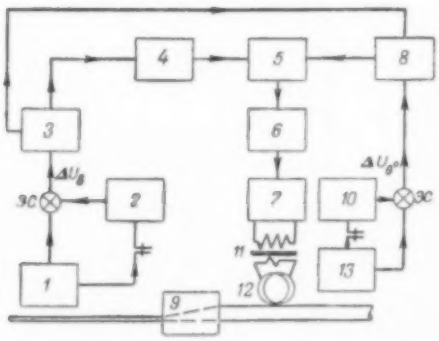

Fig. 3. Structural circuit of self-aligning system for automatic control of welding conditions on an electrical tube welding machine.

1 – thickness transmitter gauge; *2* – memorizing device; *3* – delay unit; *4* – dynamic compensating link; *5* – amplifier with variable amplification factor; *6* – power amplifier; *7* – welding current regulator; *8* – automatic correction device; *9* – shaping stands; *10* – memorizing device; *11* – welding transformer; *12* – welding electrodes; *13* – temperature "transmitter".

which holds when

$$k_n k_1 k_c = \frac{k_\delta}{k_I k_T} \tag{7}$$

and

$$D_c(p) = \frac{D_\delta(p)}{D_I(p) \cdot D_T(p)}. \tag{8}$$

Formulae (7) and (8) make it possible to determine the parameters of the basic links of the compensating calculating device CD1 when the parameters of the object are known.

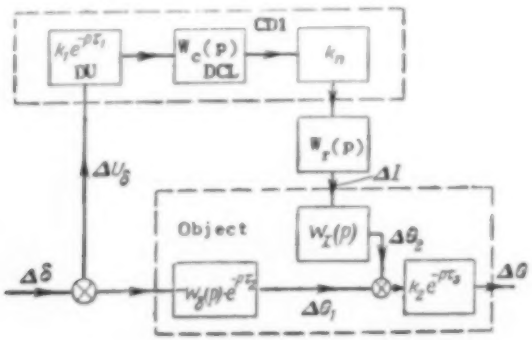

Fig. 4. Structural circuit of compensating calculating device and object.

In view of the variation of coefficients k_δ and k_I and their dependence on the operating conditions of the object, it is also necessary to vary the coefficient k_n appropriately if the effect of thickness on temperature is to be fully compensated. This is effected by means of calculating device CD2.

Transient processes in the self-aligning system

If the effect of changes in the thickness of the strip on temperature is not fully compensated, i.e. if condition (7) does not hold, the value of $\Delta\theta$ will not be zero in the presence of $\Delta\delta$ and the function $\phi(t)$ (1) will vary. The coefficient k_n will also vary in accordance with this function, k_n being proportional to $\phi(t)$:

$$k_n = -m \cdot \varphi(t). \tag{9}$$

Substituting in equation (1) the value of $\Delta\theta$ from equation (2) and bearing in mind that the delay time is maintained accurately by the delay unit, we obtain equation (9) after transformation in the following form:

$$k_n = -m \int k_2 \left[-\frac{k_3}{D_3(p)} + \right.$$
$$\left. + \frac{k_3 k_n k_1 k_c k_r}{D_1(p) \cdot D_c(p) \cdot D_r(p)} \right] \Delta\delta^2 dt. \tag{10}$$

If the frequency of the welding current is 100 to 200 c/s, as occurs on modern machines, heating time amounts to roughly 0.006 sec and, consequently, we can ignore the constant heating time when the effect changes compared with the time constants of the remaining elements in the system. In view of this we can consider $D_3(p) = 1$, and taking equality (8) into consideration, we have:

$$k_n = -m \int k_2 (-k_3 + k_1 k_n k_1 k_c k_r) \Delta\delta^2 dt. \tag{11}$$

On differentiating both parts (11) we obtain an equation which describes the process of self-alignment in a system when welding conditions change

$$\frac{dk_n}{dt} + m k_1 k_2 k_1 k_c k_r \Delta\delta^2 k_n = m k_2 k_3 \cdot \Delta\delta^2. \tag{12}$$

The solution of this equation has the form

$$k_n = \left(\int m k_2 k_3 \Delta\delta^2 e^{\int m k_1 k_2 k_1 k_c k_r \cdot \Delta\delta^2 \cdot dt} dt + C_1 \right) e^{-\int m k_1 k_2 k_1 k_c k_r \cdot \Delta\delta^2 \cdot dt} \tag{13}$$

The necessary value of the coefficient k_n will be established by the automatic correction device in the event of an abrupt jump in the variation of the strip thickness $\Delta\delta$ according to the law:

$$k_n = \frac{k_3}{k_1 k_1 k_c k_r} + \left(k_{n0} - \frac{k_3}{k_1 k_1 k_c k_r} \right) e^{-m k_1 k_2 k_1 k_c k_r \cdot \Delta\delta^2 \cdot t} \tag{14}$$

The process of self-alignment proceeds according to the exponent with a time constant $T_c = \frac{1}{m k_1 k_2 k_1 k_c k_r \Delta\delta^2}$ and is always stable since the quantities which determine the time constant T_{sa} are always positive. The value of the time constant can easily be varied by an appropriate choice of the coefficient m, so that it is possible to ensure the

requisite values of self-alignment speed and time as a function of the parameters of the object. In order to ensure that the system is stable in the presence of interference, the self-alignment time constant T_{sa} should be chosen several times greater than the period of the lowest frequency interferences affecting the system.

In the event of a harmonic change in the deviation of the thickness of the strip $\Delta\delta = \Delta\delta_m \sin \omega t$ the process of self-alignment is described by the equation

$$k_n = \left(\int m k_3 k_\delta \cdot \Delta\delta_m^2 \cdot \sin^2 \omega t \cdot e^{\int m k_1 k_3 k_f k_e k_r \cdot \Delta\delta_m^2 \sin^2 \omega t \cdot dt} dt + C_1\right) e^{-\int m k_1 k_3 k_f k_e k_r \Delta\delta_m^2 \sin^2 \omega t \cdot dt}, \quad (15)$$

the solution of which has the form

$$k_n = \frac{k_\delta}{k_1 k_f k_e k_r} + \left(k_{n0} - \frac{k_\delta}{k_1 k_f k_e k_r}\right) e^{-m k_1 k_3 k_f k_e k_r \cdot \Delta\delta_m^2 \left(\frac{t}{2} - \frac{1}{4\omega} \sin 2\omega t\right)}. \quad (16)$$

The self-alignment proceeds along a continuously rising curve if $k_{n0} < \frac{k_\delta}{k_1 k_f k_e k_r}$ or along a continuously falling curve if $k_{n0} > \frac{k_\delta}{k_1 k_f k_e k_r}$ the curve having the form of an exponent with superposed harmonic variations which diminish in magnitude as time increases. The process is always stable as in the previous case.

The system in question has been installed and experimentally proven for controlling welding conditions or an electrical tube welding machine.

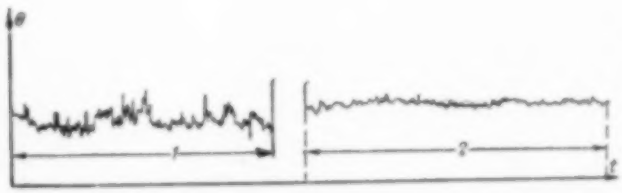

Fig. 5. Welding temperature during (1) manual and (2) automatic control.

The diagram shown in Fig.5 shows the variation in welded joint tem-

perature for manual and automatic control with the same machine operating conditions (identical speed of the sheet, an identical workpiece and so forth). With automatic control the variations in temperature decreased considerably (roughly by a factor of 6 to 8) compared with manual control. This naturally improved the quality of welded joint.

Translated by O.M. Blunn

REFERENCES

1. I.S. Morosanov; *Avtomatika i Telemekhanika*, XVIII, No.11, (1957).
2. V.S. Kulebakin; *O vybore optimal'nykh parametrov avtomaticheskikh regulyatorov i sledyashchukh sistem. (Selection of the optimum parameters for automatic regulators in follow-up systems).* Dokl. Akad. Nauk SSSR, 77, No.2, (1951).
3. A.G. Ivakhnenko; *Electrical automatics. (Elektroavtomatika)*, Gostekhizdat, (1957).
4. A.A. Fel'dbaum; *Avtomatika i Telemekhanika*, XVII, No.11, (1956).
5. A.B. Cheliustin; *Biull. TsIINChM*, Nos.9 and 10, (1958).
6. Ia.E. Zhukovskii and A.B. Chekmarev; *Proizvodstvo trub elektrosvarkoi metodom soprotivleniia. (Tube production by resistance welding)*, Metallurgizdat, (1953).

LOCATION AND EFFICIENCY OF INSULATING COUPLINGS AND FLANGES FOR THE PROTECTION OF UNDERGROUND METAL STRUCTURES AGAINST ELECTRICAL CORROSION*

L. D. RAZUMOV

(Received 2 April 1959)

1960

As is known (1-4), one method of composite protection for underground metal structures from electrical corrosion is electrical sectionalization by means of insulating gaps, i.e. insulating couplings on cables and insulating flanges on conduits. If correct use is made of electrical sectionalization the magnitude of the stray currents in the underground structure is considerably reduced. An approximate scheme of the flow of currents when sectionalization is practised is shown in Fig. 1. As can be seen from this diagram, new anode and cathode zones arise about each such insulating coupling.

The connexion of an insulating coupling denotes a full break in the path of the current along the underground structure. The amount of current at the point where the insulating gap is connected equals zero.

From the electrical point of view this condition can be fulfilled if a fictitious current source is connected in the underground structure instead of the insulating gap Fig. 2.

The current created by this fictitious current source at the point where it is connected should be in the opposite direction to the basic current but equal to it in magnitude.

Having added the basic and fictitious currents algebraically, we obtain the actual current passing in the underground structure when an insulating gap is present.

The remaining magnitudes characterizing the distribution of currents in the underground structures, i.e. the potential in relation to earth and the density of the leakage current, will be equal to the algebraic

* *Elektrichestvo*, No. 2, 19-24, 1960.

sum of the basic quantities and the quantities produced by the fictitious current source.

Consider the distribution of currents in an underground structure when the current source is connected in series (Fig. 2) with an e.m.f. V.

This case is considered in (4).

The magnitude of the current passing in the underground structure:

$$i_M(x) = \frac{V}{2z_c} e^{-\gamma|x|} = i_M(0)\, e^{-\gamma|x|}\ [a]. \tag{1}$$

The potential of the underground structure in relation to the remote earth point

$$u_M(x) = \pm\frac{V}{2} e^{-\gamma|x|} = \pm i_M(0)\, z_c e^{-\gamma|x|}\ [в], \tag{2}$$

where the sign + refers to $x > 0$ and the sign - refers to $x < 0$; the linear density of the leakage current from the underground structure

$$j_M(x) = \mp\frac{V}{2R_{trans}} e^{-\gamma|x|} = \mp i_M(0)\,\gamma e^{-\gamma|x|}\ [\text{А/м}],$$

when the minus sign refers to $x > 0$ and the plus sign to $x < 0$.

The potential of the underground structure relative to the nearby earth points can be determined approximately from the formula

$$u_{(c-э)M} = -j_M(x)\left[R_{trans}\frac{?}{\pi}\ln\frac{1{,}12}{\gamma\sqrt{y^2+h^2}}\right][в]. \tag{4}$$

The following designations are used in formulae (1-4):

$z_c = \sqrt{rR_{trans}}$ - characteristic impedance of the underground structure, ohms;

r - longitudinal impedance of an underground d.c. structure, ohm/m;

R_{trans} - transient impedance between the underground structure and earth, ohm x m;

y - horizontal distance from the underground structure to that point on the surface of the ground relative to which the potential is determined, m;

$R_{trans} = R_{ins} + \frac{P}{\pi} \ln \frac{1,12}{\gamma \sqrt{Dh}}$ (ohm x m);

R_{ins} - impedance of the insulation covering, ohm x m;

$\gamma = \sqrt{\frac{P}{R_{trans}}}$ - constant for the distribution of current along the underground structure, $\frac{1}{m}$;

h - depth of the underground structure, m;

D - outside diameter of the underground (metal) structure, $\frac{1}{m}$;

P - specific earth impedance, ohm m;

x - distance along underground structure, m.

Fig. 1. The passage of stray currents in a sectionalized underground structure (without shunting resistances).
A - anode zone; C - cathode zone.
1 - under structure; 2 - insulating gap.

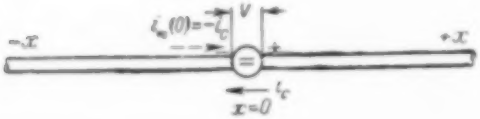

Fig. 2. Inclusion of a fictitious current course instead of an insulating gap.
i_c - current in underground structure before connexion of insulating gap; i_m - current produced by fictitious current source with e.m.f. v.

For the deduction of formulae (1) to (3) it is assumed that the positive direction of the current coincides with the positive direction of the x axis. The signs of all the quantities in formulae (1) to (4) change when the direction of the current is reversed.

It is quite obvious that the magnitude of the fictitious current at the point where the gap is installed should be precisely the same as the basic current taken with the reverse sign if one insulating gap is installed.

If l_1 is the co-ordinate of the connexion of the insulating gap, then the fictitious current i_M at the point where the gap is installed, i.e. at the point with the co-ordinate l_1, equals

$$i_M = -i_c(l_1),$$

where $i_c(l_1)$ is the basic current in the underground structure at the point with the underground structure l_1 if there is no insulating gap.

The quantities which result when an insulating gap is present will then be determined from the formulae

$$i_{res}(x) = i_c(x) + i_M(x) = i_c(x) - i_c(l_1)\, e^{-\gamma |x-l_1|}; \tag{5}$$

$$u_{res}(x) = u_c(x) + u_M(x) = u_c(x) \mp i_c(l_1) z_c e^{-\gamma |x-l_1|}; \tag{6}$$

$$j_{res}(x) = j_c(x) + j_M(x) = j_c(x) \pm i_c(l_1)\gamma e^{-\gamma |x-l_1|}. \tag{7}$$

In expressions (6) and (7) the top signs refer to $x > l_1$ and the lower to $x < l_2$. The signs of the terms in (5) to (7) are assigned for the positive direction of the basic current i_c; if i_c has a negative sign, the signs in the second terms obviously change.

Figs. 3 and 4 show the curves of the current and density of the leakage current from the sheathing of a cable laid along a double track electrified d.c. railway line 100 m away from it with a specific earth resistance of 100 ohms x m for the three co-ordinates for the connexion of the insulating coupling 100, 500 and 2500 m. The load of the traction substation is 1000 A (point $x = 0$ is located opposite the traction substation). As can be seen from these curves, zones with an increased leakage current density arise at the point where the insulating coupling is installed. The magnitude of the leakage current density (on the right hand side of the insulating coupling in the present case) exceeds the maximum leakage current density which arose opposite the traction substation before the insulating coupling was installed. It is quite obvious that the installation of one insulating coupling in the conditions under examination will reduce the amount of current in the cable sheathing, especially when $x = 2500$ m, but from the point of

view of the danger of electrical corrosion it can do nothing but harm.

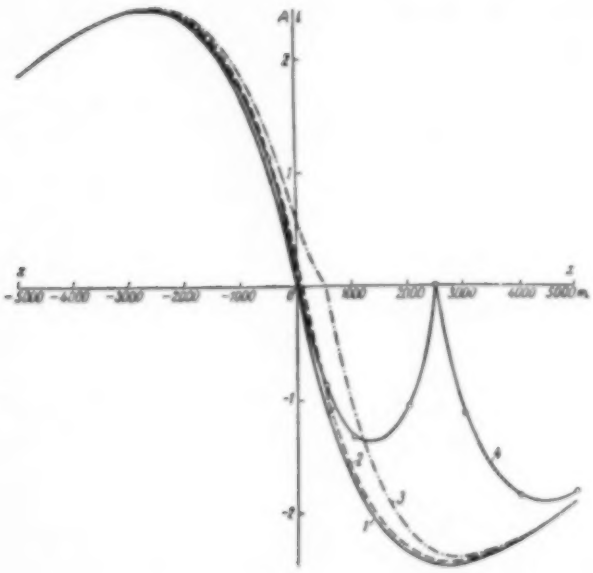

Fig. 3. Currents in cable sheathing with different co-ordinates l for the connexion of insulating gaps.
Values of the current: 1 - without insulating gap; 2 - with l = 100 m; 3 - l = 500 m; 4 - l = 2500 m.

The density of the leakage current on one side of the insulating gap is increased by $\gamma \cdot i_c\,(l_1)$, as can be seen from expression (7).

Thus an insulating gap will always entail increased leakage current density when installed in the zones of the leakage currents from the underground structure.

It follows that the magnitude of the resulting leakage current density will be smaller at points where the values of the basic current are lower. The installation of couplings at points with maximum basic current is more efficient from the point of view of reducing the current, but it leads to the biggest increase in leakage current density.

From the point of view of minimum leakage current density it is advisable to install the insulating gaps in the cathode zones where there is an influx of current into the underground structure. In this case leakage current density rises comparatively less when current is

reduced as a whole.

Consider the case when several insulating gaps are arranged in the underground structure (in the general case, n such gaps).

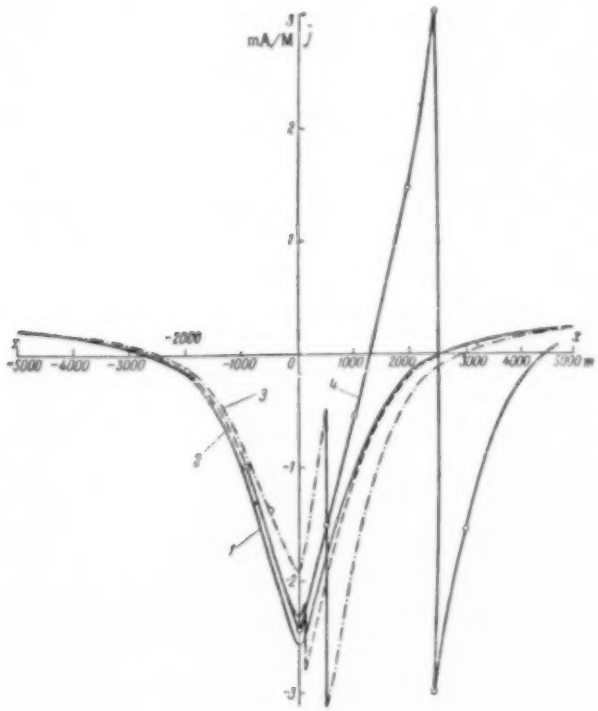

Fig. 4. Linear density of leakage current from cable sheath with different co-ordinates l for the connexion of insulating couplings.

Leakage current density: 1 – without insulating gap; 2 – l = 100 m; 3 – l = 500 m; 4 – l = 2500 m.

Substitute a fictitious current source for each insulation gap. The amount of current produced by the source should be such that the resulting current at the point where the gap is located should be zero. This can be expressed mathematically by the following equations:

$$i_{M1} + i_{M2}\, e^{-\gamma |l_1 - l_2|} + i_{M3} e^{-\gamma |l_1 - l_3|} + \ldots + \\ + i_{Mn} e^{-\gamma |l_1 - l_n|} = -i_{c1}; \qquad (8)$$

$$
\begin{aligned}
&i_{M1}e^{-\gamma|l_2-l_1|}+i_{M2}+i_{M3}e^{-\gamma|l_3-l_2|}+\ldots+\\
&\qquad i_{Mn}e^{-\gamma|l_2-l_n|}=-i_{c2};\\
&\cdots\cdots\cdots\cdots\cdots\cdots\cdots\cdots\cdots\cdots\cdots\cdots\\
&\cdots\cdots\cdots\cdots\cdots\cdots\cdots\cdots\cdots\cdots\cdots\cdots\\
&i_{M1}e^{-\gamma|l_n-l_1|}+i_{M2}e^{-\gamma|l_n-l_2|}+i_{M3}e^{-\gamma|l_n-l_3|}+\\
&\qquad+\ldots+i_{Mn}=-i_{cn}.
\end{aligned}
\tag{8}
$$

cont

In (8):

i_{M1}, i_{M2} ..... i_{Mn} – the currents produced by the fictitious sources connected instead of the first, second and so forth insulating gaps;

l_1, l_2, ... l_n – are the co-ordinates of the location of the insulating gaps;

i_{c1}, i_c, ... i_{cn} – are the basic currents in the underground structure when there are no insulating gaps at points with the co-ordinates l_1, l_2, ... l_n.

Having solved the set of equations (8) we can determine the resulting values of the stated electrical quantities:

$$
i_{res}(x)=i_c(x)+\sum_{k=1}^{n} i_{Mk}e^{-\gamma|x-l_k|};
\tag{9}
$$

$$
\begin{aligned}
u_{res}(x)&=u_c(x)+\\
&+z_c\sum_{k=1}^{n}\frac{x-l_k}{|l_k-x|}\,i_{Mk}e^{-\gamma|x-l_k|};
\end{aligned}
\tag{10}
$$

$$
j_{res}(x)=j_c(x)+\gamma\sum_{k=1}^{n}\frac{l_k-x}{|l_k-x|}\,i_{Mk}e^{-\gamma|x-l_k|}.
\tag{11}
$$

In expressions (10) and (11) when $x=l_k$ the fractions beneath the sign $\Sigma\frac{l_k-x}{|l_k-x|}$ and $\frac{x-l_k}{|l_k-x|}$, as well as when $x\neq l_k$, are equal to unity, but the sign of the term is taken on the right from the insulation gap for $x>l_k$, and on the left for $x<l_k$. These fractions are only introduced so as to take the sign of each term into account correctly.

1960

It is quite obvious that $i_{res} = 0$ when $x = l_k$.

Figs. 5 and 6 show the curves of the current and density of the leakage current from the sheathing of a cable with a different number of insulating couplings.

The parameters of the cables and rails and the cable-laying conditions are the same as those stated above for the examination of one insulating coupling (Fig. 3).

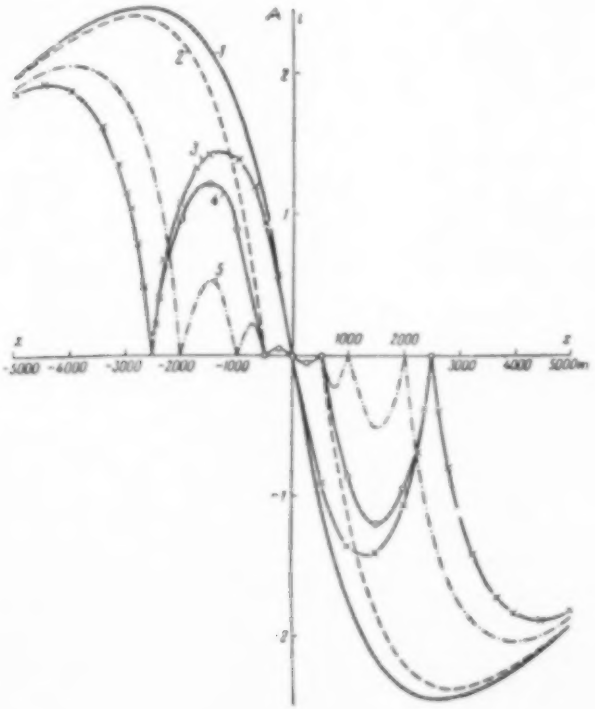

Fig. 5. Currents in cable sheath with different numbers of insulating couplings and different co-ordinates (l_1, l_2, etc.) on installation.

Values of current: 1 – without insulating gaps; 2 – two couplings ($l_1 = -l_2 = -500$ m); 4 – four couplings ($l_1 = -l_4 = -2500$ m, $l_2 = -l_3 = -500$ m); 5 – six couplings ($l_1 = -l_6 = -2000$ m, $l_2 = -l_5 = -1000$ m, $l_3 = -l_4 = 500$ m).

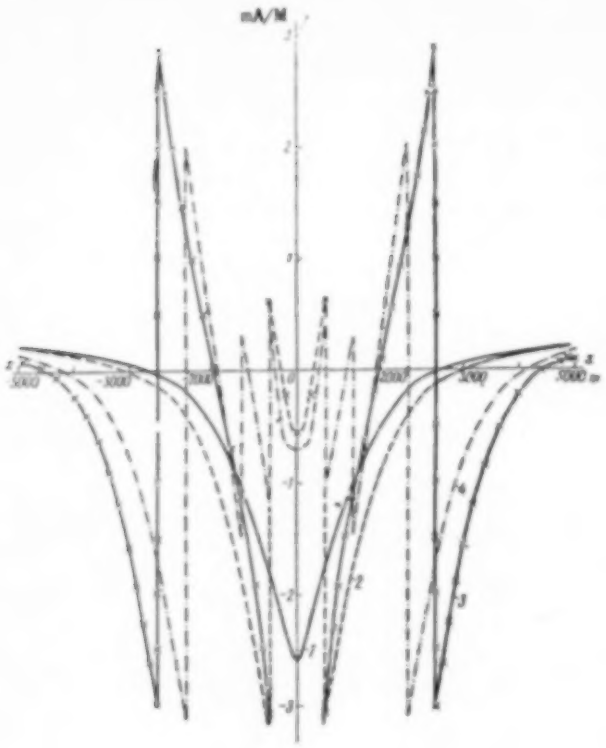

Fig. 6. Linear density of leakage current from cable sheath with different numbers of insulating gaps and different coordinates (l_1, l_2, etc.) on installation.
Leakage current density: 1 – without insulating couplings; 2 – two couplings ($l_1 = -l_2 = 500$ m); 3 – four couplings ($l_2 = -l_4 = -2500$ m); ($l_2 = -l_3 = -500$ m); 4 – six couplings ($l_3 = -l_6 = -2000$ m; $l_2 = -l_5 = 1000$ m; $l_3 = -l_4 = -500$ m).

As can be seen from Fig.5, the total current in the cable sheathing decreases rather sharply when the number of insulating couplings is increased. The maximum effect is produced by installing the couplings at points where the basic current is greatest. Thus, for example, when two couplings are installed at points ± 500 m, the maximum current only decreases by 0.1A, but when couplings are installed at points ± 2500 m, i.e. at points with maximum basic current equal to 2.45A, the highest value of current emerges when x = ± 4500 m and is equal to 1.9A, i.e. 0.55A less.

On the whole, the installation of insulating couplings is instrumental in considerably reducing the amount of current in the cable sheathing. But this cannot possibly be said of the amount of leakage current density. It can be seen from Fig.6 that the leakage current density and consequently, the potential relative to the nearby earth point, is increased when insulating couplings are installed. Thus, for example, when four couplings are installed with co-ordinates ± 500 and ± 2500 m, maximum leakage current density reaches 3.08 ma/m with a maximum basic density of the leakage current of 2.59 ma/m.

It is characteristic that the extreme coupling has maximum leakage current density when couplings are spaced at frequent intervals.

If six couplings are installed, leakage current density is as follows: for couplings with co-ordinates ± 500 m 1.14 ma/m, for couplings with co-ordinates ± 1000 m 1.47 ma/m and for the extreme couplings with co-ordinates ± 2000 m 3.1 ma/m.

It is obvious that the densities of the leakage currents will be less if there are more insulating couplings spaced closer together. The region of maximum leakage current density will shift to the ends of the danger zone when the number of couplings is increased but the values themselves will decrease in view of the reduction in basic current.

But the installation of four to six couplings in the case under consideration will only bring harm.

In order to reduce the positive potential which arises at the insulating gap, as is known (1), it is recommended that the gap be shunted by a resistance, the "balance rheostat" (Fig.7).

The amount of current passing through the resistance of the balance rheostat can be determined from Tevenen's theorem. The current I_b passing through the resistance is equal to the difference between the potentials existing before the connexion of the resistance r_b between points A and B, divided by the sum of the resistances $r_b + 2r_c$. Since the difference between the potentials between points A and B equals $V = i_m 2r_c$, then

$$I_b = \frac{V}{R_b + 2r_c} = \frac{2i_m r_c}{R_b + 2r_c},$$

the direction of the current I_b coincides with the direction of the basic current in the underground structure. This is equivalent to a reduction in the fictitious current and, consequently, on the one hand

leakage current density decreases at the insulating gap, whilst the performance of the gap becomes less efficient on the other, depending on the decrease in basic current.

The equivalent fictitious current will thus be

$$i_{M.eq} = i_M\left(1 - \frac{2z_c}{R_b + 2z_c}\right) \tag{12}$$

and the resulting current in the underground structure when an insulating gap is installed (see formula 5)

$$\begin{aligned} i_{res}(x) &= i_c(x) + i_M\left(1 - \frac{2z_c}{R_b + 2z_c}\right)e^{-\gamma|x-l_1|} = \\ &= i_c(x) - i_c(l_1)\left(1 - \frac{2z_c}{R_b + 2z_c}\right)e^{-\gamma|x-l_1|}. \end{aligned} \tag{13}$$

1960

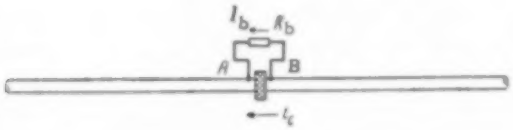

Fig. 7. Inclusion of balanced shunt resistance at insulating gap. i_c = current in underground structure before insulating gap connected; I_b = current in balanced resistance; R_b = = balanced resistance.

As can be seen from (13), when $R_b = 0$, $i_{res}(x) = i_c(x)$, which is what of course it ought to be after shortening the gap.

The resulting leakage current density is

$$j_{res}(x) = j_c(x) \pm i_c(l_1)\gamma\left(1 - \frac{2z_c}{R_b + 2z_c}\right)e^{-\gamma|x-l_1|}. \tag{14}$$

At the point where the insulating gap is installed, i.e. when $x = l_1$

$$\begin{aligned} j_{res}(x) &= j_{res}(l_1) = j_c(l_1) \pm \\ &\pm i_c(l_1)\gamma\left(1 - \frac{2z_c}{R_b + 2z_c}\right). \end{aligned} \tag{15}$$

As can be seen from this formula, if j_c is negative, leakage current density will increase by

$$-i_c(l_1)\gamma\left(1 - \frac{2z_c}{R_b + 2z_c}\right).$$

It is necessary to reduce R_b if this 'negative addition" is to be reduced. Complete absence of any increase in leakage current density will however signify that the insulating gap has been short circuited. On the other hand, if j_c is positive, i.e. if the insulating gap has been installed in the zone where there is an influx of current into the underground structure, then as can be seen from formula (15), the density of the influx current will increase on one side of the gap but decrease on the other. In the later case it may be that the subtrahend is greater than j_c and an anode zone will then arise. In order to eliminate this zone the magnitude of R_b must be so chosen that

$$j_c(l_1) = i_c(l_1)\gamma\left(1 - \frac{2z_c}{R_b + 2z_c}\right). \tag{16}$$

It is found from (16) that to satisfy this condition

$$R_b = \frac{2z_c\, j_c(l_1)}{i_c(l_1)\gamma - j_c(l_1)}.$$

The negative result obtained when using this formula indicates that current density j_c is greater than $i_c\,\gamma$ when l_1 is given and that it is therefore impossible to achieve their equality for any R_b.

Another way of reducing the anode zones arising at the insulating gaps is to provide a current conductor (5).

Consider a scheme of current protection including the insulating gaps. As the insulating gaps are usually installed at comparatively large distances from the point where the cathode station is connected, the effect of the currents in the operative earthing of the cathode station can be ignored.

The basic current in the structure to be protected is then

$$i_c(x) = \mp\frac{I}{2}e^{\mp\gamma x},$$

where, when $x > 0$ the upper signs are taken, and when $x < 0$ the lower signs.

The basic density of the inflowing current is

$$j_c(x) = \frac{I}{2}\gamma e^{\mp\gamma x}.$$

Consider the inclusion of two insulating gaps. Let the insulating gaps be installed at points with co-ordinates $l_1 < 0$ and $l_2 > 0$ (Fig. 8a).

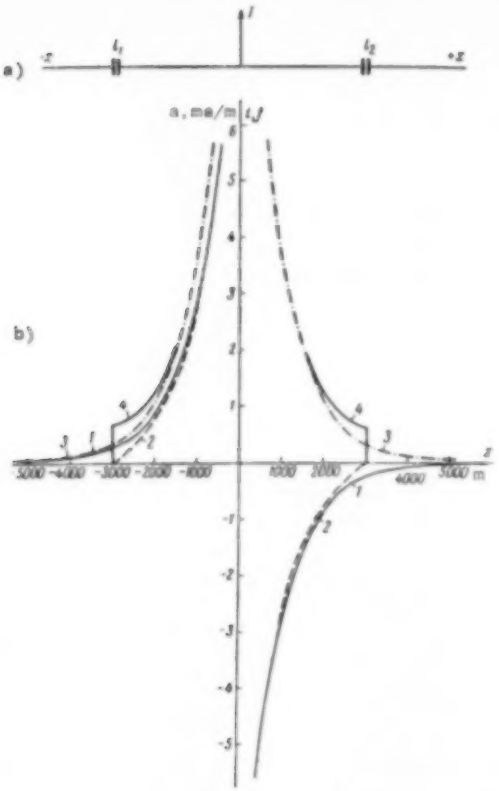

Fig. 8. *A* - installation of insulating couplings on a cable; *b* - curves of current *i* in amperes and density of influx current *j* in ma/m in cable sheath with cathode protection and insulating couplings at points with co-ordinates $l_1 = -3000$ m and $l_2 = 3000$ m.

1 - current without insulating couplings; 2 - the same, with two insulating couplings; 3 - density of influx current without insulating couplings; 4 - the same, with insulating couplings.

The fictitious currents will be

$$i_{M1} = \frac{-\frac{I}{2} e^{\gamma l_1}(1 + e^{-2\gamma l_1})}{1 - e^{-2\gamma (l_2 - l_1)}}; \qquad i_{M2} = \frac{\frac{I}{2} e^{-\gamma l_2}(1 + e^{2\gamma l_1})}{1 - e^{-2\gamma (l_2 - l_1)}}.$$

The resulting current when $x > l_2$

$$i_{res}(x) = -\frac{I}{2} e^{-\gamma x} + i_{M1} e^{-\gamma (x-l_1)} + i_{M2} e^{-\gamma (x-l_2)} = 0.$$

The resulting current when $l_2 > x > 0$

$$i_{res}(x) = i_c(x) \frac{(1 + e^{2\gamma l_1})(1 - e^{-2\gamma (l_2 - x)})}{1 - e^{-2\gamma (l_2 - l_1)}} .$$

when $l_1 = -l_2$

$$i_{res}(x) = i_c(x) \frac{1 - e^{-2\gamma (l_2 - x)}}{1 - e^{-2\gamma l_2}} .$$

Analogously, the resulting linear density of the inflowing current will be

when $x > l_2$

$$j_{res}(x) = \frac{I}{2} \gamma e^{-\gamma x} + \gamma [- i_{M1} e^{-\gamma (x-l_1)} - - i_{M2} e^{-\gamma (x-l_2)}] = 0;$$

when $l_2 > x > 0$

$$j_{res}(x) = j_c(x) \frac{1 + e^{-2\gamma (l_2 - x)}}{1 - e^{-2\gamma l_2}} ;$$

when $l_1 = -l_2$

$$j_{res}(x) = \frac{I}{2} \gamma e^{-\gamma x} + \gamma [- i_{M1} e^{-\gamma (x-l_1)} + + i_{M2} e^{-\gamma (l_2 - x)}] = j_c(x) \frac{(1 + e^{2\gamma l_1})(1 + e^{-2\gamma (l_2 - x)})}{1 - e^{-2\gamma (l_2 - l_1)}} ;$$

when $x = l_2$

$$j_{res}(l_2) = 2 j_c(l_2) \frac{1 + e^{2\gamma l_1}}{1 - e^{-2\gamma (l_2 - l_1)}} .$$

As an example Fig. 8(b) shows curves of the variation in the amount of current and the density of the leakage current when use is made of cathode protection for a cable with the stated parameters and a cathode station current of I = 20 A; when $l_1 = -l_2 = 3000$ m.

Formula (8) to (16) refer to a stable distribution of the cathode and anode zones along the underground structure. Use may also be made of these formulae if a "sign-variable zone" is present on the equipment. Only in this case is it necessary to make a calculation for stray currents in two directions, corresponding to the different signs of the

potentials in the underground structure relative to earth. If there is a "sign-variable zone" on the structure the distribution of the anode and cathode zones will obviously vary with time and likewise with the direction of the current even after insulating gaps have been installed.

No attention has been paid in this article to the effect of the insulating gaps in the underground structure in question on adjacent equipment. The study of this effect should be the object of a separate article. It may however, be mentioned in advance that the insulating gaps should if possible be installed at the same spot on all underground ground structures laid side by side so as to prevent this effect.

Conclusions. 1. The installation of only a few insulating gaps does not stop the danger of electrical corrosion but merely redistributes the dangerous zones. The installation of an insulating gap in the anode zone even increases the density of the leakage current.

Obviously leakage current density will also increase in sign-variable zones whenever a positive potential arises on the underground structure relative to earth so that it is also inadvisable to use insulating gaps in these zones.

2. The installation of insulating gaps may be used in stable cathode zones on underground structures as a means of reducing the stray currents in the gear and thereby reducing the leakage current density in the anode zone. But the connexion of insulating gaps should be accompanied by the installation of additional gear (balance rheostats, current conductors etc.) in order to eliminate the local anode zone arising on one side of the gap.

3. The formulae make it possible to evaluate the effectiveness of installing one or several insulating gaps in actual cable-laying conditions for design purposes and plan additional devices for the elimination of the cathode zones arising about the insulating gaps. First of all it is necessary to evaluate the danger of electrical corrosion on the proposed structure and find the magnitude of the stray currents flowing in them. This can either be done by preliminary calculations or by measurement if the plans relate to structures already in use.

As is known, preliminary calculations are extremely difficult for urban networks owing to the complex configuration of the underground structures and tramlines. In these conditions it is recommended (1) that plans be based on measurements. The above formulae may therefore only be used in urban conditions for the simplest networks of underground structures and tramlines.

Translated by O.M. Blunn

REFERENCES

1. *Guidance for the protection of underground communication cables from corrosion. (Rukovodstvo po zashchite podzemnykh kabelei svitazi ot korrozii).* Syiazizdat, (1956).
2. *Electrical sectionalization of conduits and cables. (Elektricheskoi sektsionirovanie truboprovodov i kabelei).* AKKh im. K.D. Panfilova, Informats. psi'mo No.25-64, (1954).
3. V.A. Pritula; *Electrical protection of underground metal structures from corrosion. (Elektricheskoia zashchita ot korrozii podzemnykh metallicheskikh sooruzhenii).* Gosenergoizdat, (1958).
4. E. Sunde; *Earth conduction effects in transmission systems,* New York, (1949).
5. L.D. Razumov; *Design of conduits in the protection of cables from electrical corrosion. (Rashchet tokootvodov pri zashchite kabelei svyazi ot elektrokorrozii).* Elektrosviaz, No.10, (1958).

SYNCHRONIZING DEVICE FOR SYNTHETIC RUPTURING CAPACITY TESTS ON CIRCUIT BREAKERS*

N.N. CHERNYSHEV and V.D. LIASHENKO

Lenin All Union Electrical Engineering Institute

(Received 29 June 1959)

1960

The synchronization of the operation of the individual elements in the test and metering circuits plays an important part in equipment for testing the rupturing capacity of circuit breakers. If however a synthetic circuit is provided in which the current to be tripped and the recovery voltage are obtained from different sources the problem of synchronizing the operation of these sources is even more complicated.

A description has already been given of an instrument which makes it possible to control the elements of the test plant with precision (1). The present article deals with the principles and design of a synchronizing device for controlling the supply source of a synthetic circuit for testing circuit breakers.

All the various types of synthetic circuit can be divided into three main forms:

(a) circuits in which the increased voltage source is permanently connected to the test object (2, 3);

(b) circuits in which this source is connected precisely at the moment when the current to be tripped passes through zero;

(c) circuits in which the increased voltage source is connected at a strictly pre-determined moment of time before this (5).

The last two circuits require a synchronizing device.

A synchronizing device has already been developed (4) based on the principle that the current curve can be approximated sufficiently

---

* *Elektrichestvo*, No.2, 53-57, 1960.

accurately by a straight line in the interval of time between the moments when this device operates and current attains its zero value, i.e. that the rate of change of the current within this interval

$$\frac{di}{dt} = \text{const.}$$

If this interval equals t_0, then we have the following relationship

$$\frac{i}{-\frac{di}{dt}} = t_0.$$

In other words, the synchronizing device should operate when

$$i + t_0 \frac{di}{dt} = 0.$$

The synchronizing device (SD) incorporates a zero voltage electronic relay. A voltage is applied to the input to this relay proportional to the sum $i + t_0 \frac{di}{dt}$. This voltage is either produced by means of an active and inductive metering shunt or by means of an air-cores current transformer.

Such shunts, as shown by operating experience, can be successfully used at currents up to 20kA. If the current to be tripped is increased it is undesirable to make use of shunts directly in the test circuit owing to the difficulty of ensuring sufficient dynamic and thermal stability of the shunts and the effect of interference from direct connexion of the SD in the circuit of the current to be tripped (because of the differences which appear during the tests between the potentials of the earth points for the SD and test object).

A circuit has therefore been developed which makes it possible to use the secondary windings of a current transformer to supply the input circuits (6).

By regulating the amount of "lead" t_0, it is possible to compensate the proper time of operation of the recovery voltage source and supply a voltage to the test circuit breaker at the moment of time when the current to be tripped is zero. In a two-frequency system of operation the lead should be such that no breaks obtain in the curve for the current to be tripped when the arc is extinguished in the auxiliary arc extinction device.

Principal circuit of the synchronizing device

The synchronizing device consists of two symmetrical parts which

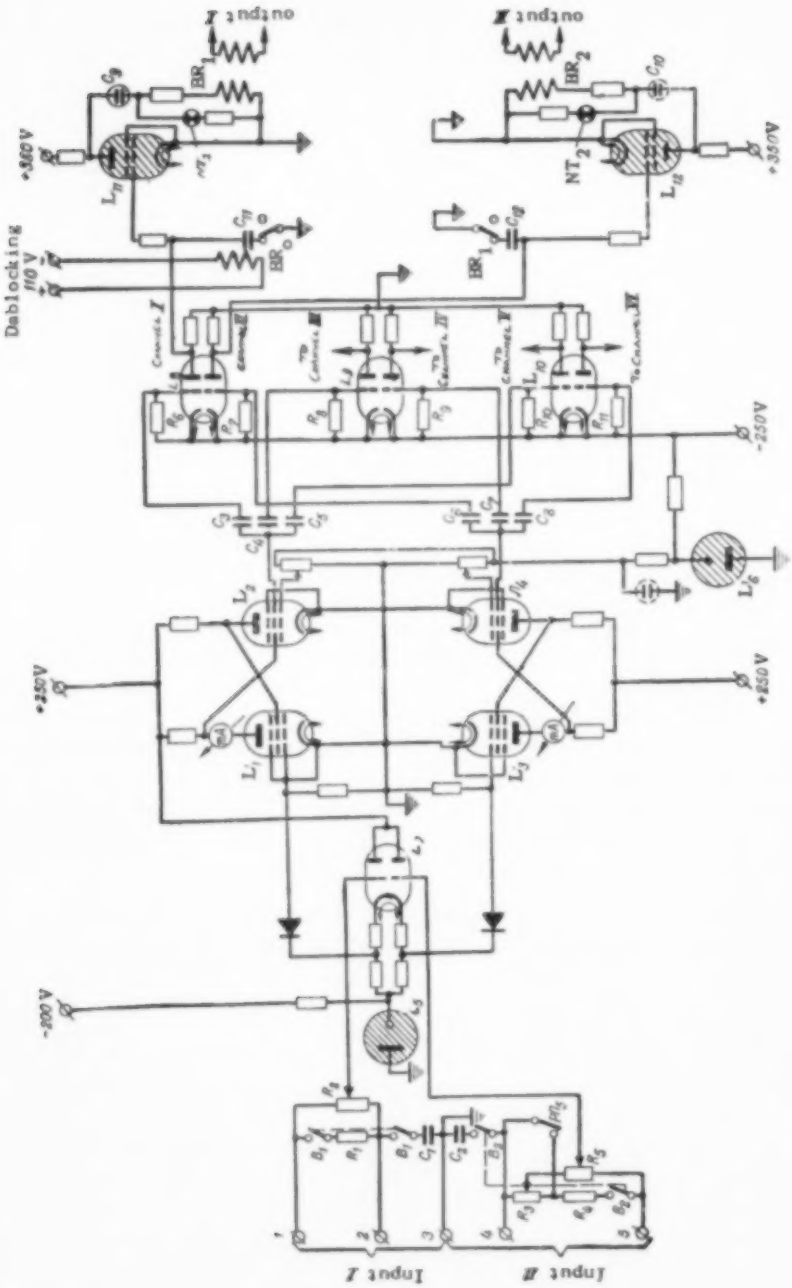

Fig. 1. Main circuit of synchronizing device.

operate alternately in the positive and negative half-periods of the current to be tripped. Each part comprises the following elements (Fig. 1): cathode repeaters L_7, triggers L_1, L_2, L_3 and L_4, differentiating elements C_3 to C_8 and R_6 to R_{11}, and L_{12} and blocking relays BR_0, BR_1 and BR_2.

The SD is supplied with direct current from special units built into the instrument for automatic control of the test.

The scheme operates in the following sequence.

The input voltage of the metering elements (Fig. 2) is supplied via the cathode repeaters to the triggers which perform the function of an electronic zero voltage relay. In the absence of voltage at the input, value L_1 conducts, but when a negative potential is fed to its grid the trigger is "cocked". If the voltage at the input to the scheme drops to zero the trigger operates. The trigger is regulated by varying the negative voltage on the grid of valve L_2.

The second half of the circuit (input *II*, L_3 and L_4) reacts on the other polarity of the current to be tripped).

If the current to be tripped passes through the metering elements then the potentials on the anodes of valves L_1 and L_3 are decreased "in a leap" at the moment of time which precedes the given value of time t_0 for the transition of the curve of the current to be tripped through zero. This change in the potentials by means of differentiating links R_6C_3, R_8C_4 and $R_{10}C_5$ is converted into negative voltage pulses which act on the grids of the triodes L_8 to L_{10}.

In the state of "rest", all the triodes are live and the voltage drops on their anode impedances create negative displacements (biases) on the grids of the output thyratrons L_{11} and L_{12}. When the triggers operate as a function of the polarity of the current to be tripped, the triodes of values L_8 to L_{10} on the left or right cut off.

If the scheme is blocked the voltage on the grids of the thyratrons is practically constant when the triggers operate owing to the shunting of grid-earth circuit by capacitors C_{11} and C_{12}.

In order that the synchronizing device should operate, it is necessary to feed a constant voltage of 110V to the coil of the relay BR_0. This voltage should be applied during that half-period of the current to be tripped, at the end of which the output pulse of the synchronizing device must be produced (for example, in the last period of arc combustion). The contacts of relay BR_0 open and disconnect capacitance C_{11}.

When the trigger first operates (after the contacts of relay BR_0 open) thyratron L_{11} cuts out and capacitance C_9 discharges on one of the windings of relay BR_1. The voltage taken from the second winding of the relay is the output voltage of the synchronizing device.

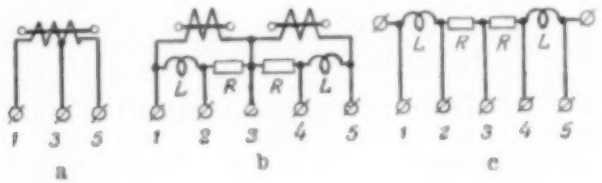

Fig. 2. Connexion of metering elements in synchronizing device. *a* – from air current transformer; *b* – from shunts connected in circuit of the secondary windings of the instrument transformers; *c* – from shunts connected directly in the circuit of the current to be tripped.

The operation of relay BR_1 (disconnexion of capacitor C_{12}) leads to the de-blocking of thyratron L_{12}. At the end of the last half period of the current to be tripped this thyratron opens and a voltage appears on the coils of relay BR_2. The synchronizing device gives a second pulse. The operation of relay BR_2 leads to the de-blocking of the next thyratron.

If the current in the circuit of the breaker continues to flow, the remaining thyratrons will also operate successively in an analogous manner. In all, the synchronizing device under consideration can issue up to six pulses (channels I, II, III, IV, V and VI).

The neon tubes NT_1 and NT_2 indicate each operation of the synchronizing device. Use is made of the second contacts of relay *BR* to mark the moment of operation of the blocking relays on a magnetic oscillograph. In those cases when it is necessary to register the moment of operation of the synchronizing device on the magnetic oscillograph, a high sensitivity loop is connected direct to the appropriate output terminals.

When breakers are tested in automatic reclosure conditions or other cycles, double de-blocking of the circuit is possible (in the first and second cycles). In this case the first pulse is fed to the coil of relay BR_0 and the second to the coil of the relay which de-blocks channel IV. The synchronizing device can issue up to three pulses in both the first and second cycles.

The operation of the synchronizing device is analogous to the above

when fed from an air current transformer supplying a voltage at the output proportional to the product of the current.

In this case the tumblers B_1 and B_2 close and the air transformer is connected to terminals 1-3 and 5-3 (Fig. 1). Capacitors C_1 and C_2 and the internal resistance of the transformer form an integrating link.

The voltage at the input to the cathode repeater equals

$$U_{c.r} = U_C + U_{R_2},$$

where U_c is the voltage at the capacitance;
U_{R2} is the voltage on part of resistance R_2.

But the voltage on the capacitance is proportional to the current to be tripped and the voltage drop on resistance R_2 is proportional to the current product. Consequently,

$$U_{c.r} \equiv i + \tau \frac{di}{dt},$$

where

$$\tau = kR_2C.$$

Coefficient k varies from 0 to 1 and is determined by the position of the "blade" on resistance R_2 or R_5 depending on the polarity of the current to be tripped.

The operation of the synchronizing device is also possible when one limb is fed from the air transformer but the second limb from shunts.

When tests are carried out on a two-frequency system (5), the synchronizing device gives an impulse on the operation of the increased voltage source with a lead which amounts to several thousand μ sec. In certain cases, for example, in the case of an arc of synthetically increased length (7), pulses are formed which are tens or hundreds of μ sec in advance of the moments when the current passes through zero.

Output VI is provided in the synchronizing device in question to control the increased voltage source in a two-frequency scheme. Until output V operates, the synchronizing device works in the way described above. After output V has operated the relay BR_5 (only its contacts are shown in Fig. 1) connects the resistance R_3 in series with resistance R_4. The magnitude of the product of the current supplied to the input increases and this increases the operating lead of the system in the last channel (VI).

Air current transformers may be more conveniently used to produce

large values of t_0.

The metering elements of the synchronizing device

If an aperiodic component is present in the current to be tripped, maximum accuracy of synchronization is produced by the use of one active and one inactive shunt as the metering elements, these shunts being connected directly in the circuit of the current to be tripped. Good results are obtained from air current transformers with an integrating link time constant greater than 1 sec.

If the test is carried out with or without an aperiodic component in the current but the current to be tripped flows for a period of time less than 2 half-periods, the requisite accuracy of synchronization can be ensured if an active shunt and reactive shunt are connected in the secondary winding of the instrument current transformers with steel. In order to reduce the load on the current transformers, the shunts should be set up directly at the outputs to the metering winding, whilst the voltage taken from the shunts is supplied to the synchronizing device.

Let us evaluate the errors which can occur when current transformers are used. Let us use for this purpose equivalent networks of the current transformers as shown in Fig. 3.

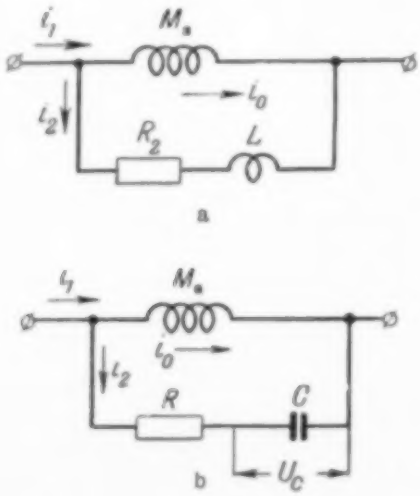

Fig. 3. Equivalent networks of instrument current transformers. a – current transformer with steel core; b – air current transformer.

The main difference between these schemes is the amount of mutual inductance in the secondary winding M. In the case of a current transformer with steel the magnitude of M_S is large, the magnetization current i_0 is insignificant, whilst the secondary current (given value) differs very little from the primary.

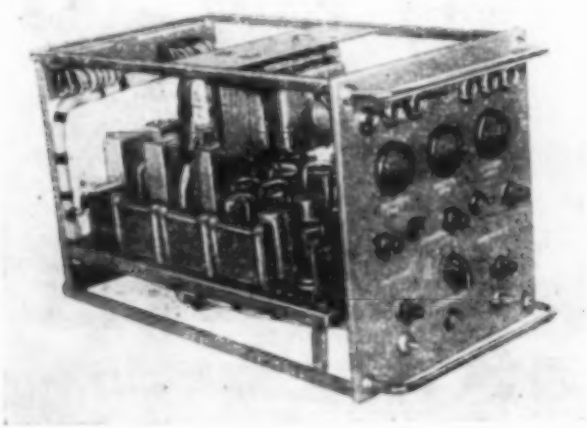

Fig. 4. Synchronizing device.

Conversely, in the case of the air current transformer, the magnitude of M_a is relatively small and the magnetizing current is therefore almost the same as the primary current. The charging current of the capacitance C is proportional to the product of the primary current. The voltage on the capacitance is equal to the integral of the product, i.e. proportional to the primary current.

The differential equations which determine the secondary current or voltage are of the same type and in the case of the schemes shown in Figs.3(a) and (b) are equal respectively to

$$\frac{di_2}{dt}+\frac{1}{T}i_2=\frac{M_a}{M_a+L}\frac{di_1}{dt}; \tag{1}$$

$$\frac{dU_C}{dt}+\frac{1}{T}U_C=\frac{M_a}{T}\frac{di_1}{dt}, \tag{2}$$

where $T=\dfrac{M_S-L}{R_2}$ or $T=RC$, for the scheme in Fig.3(b).

If the current i_2 contains an aperiodic component with a time

constant of attenuation T_a, then

$$i_1 = I_m(\cos \omega t - e^{-\frac{t}{T_a}}).$$

Equations (1) and (2) will also be solved in the same way:

$$i_2 = I_m k\left[-\sin(\omega t - \varphi)\cdot\sin\varphi + \cos^2\varphi e^{-\frac{t}{T}}\right] + \\ + I_m k \frac{T}{T - T_a}\left(e^{-\frac{t}{T_a}} - \frac{T_a}{T}e^{-\frac{t}{T}}\right), \tag{3}$$

where $k = \frac{M_a}{M_a - L}$, for a current transformer with a steel core;

$k = \frac{M_a}{T}$, for the air transformer;

$$\varphi = \arctan \omega T.$$

The angular error of transformation of the symmetrical component of the short circuit current expressed in readians can be calculated from the following formula:

$$\gamma = \frac{1}{\omega T} \pm \sqrt{\left(\frac{1}{\omega T}\right)^2}$$

(the sign "plus" or " minus" depending on the polarity of the current).

When T = 1 sec the angular error in units of time amounts to:

$$\gamma = 10 \pm 0{,}01\,\mu\text{sec}.$$

The maximum error with the aperiodic component taken into account arises at the moment of time equal to

$$t = T_a \frac{\delta}{\delta - 1} \ln \delta,$$

where

$$\delta = \frac{T}{T_a}.$$

Calculations performed for the case when T = 1 sec and T_a = 0.05 sec have shown that the maximum error in transformation of the aperiodic component arises when t is approximately $3T_a$. In consequence of this error, there is a time shift of 160 μ sec between the times when the

primary and secondary currents of the transformer pass through zero.

It is evident from the above that the errors in the current transformers are mainly determined by the presence of an aperiodic component. A decrease in the error can be achieved by increasing the time constant T. If use is made of a current transformer with a steel core this is difficult since the mutual inductance M_s depends on the amount of current and greatly decreases when an aperiodic component is present in it. The synchronizing device operates successfully if the current passes for 1 to 2 half-periods, i.e. when the breaker is tripped before the aperiodic current component fades.

The design of the synchronizing device is shown in Fig. 4. It is made in the form of a portable unit which can be installed in the automatic test control rig (see Fig. 6c, Ref. 1). The front panel accommodates the input switch, arms and instruments for tuning the triggers, arms for regulating the lead of the triggers (timing) relative to the moments when the current to be tripped passes through zero and signal valves (operation indicators).

Operating experience with the described synchronizing device has shown that it ensures precision connexion of the increased voltage source in the synthetic scheme.

Translated by O.M. Blunn

REFERENCES

1. N.M. Chernyshev and A.M. Arzisev; *Elektrichestvo*, No.3, (1959).
2. A.Ia. Builov; *Iskustvennaia skhema dlia ispytaniia vykliuchatelei (Synthetic scheme for circuit breaker tests)*, Trud. VEI, No.37 (1940).
3. Bresson; *Indirect tests on circuit breaker*, CIGRE, Report No. 101 (1948).
4. N.M. Chernyshev; *Elektrichestvo*, No. 4, (1950).
5. A.A. Gorev, V.V. Kaplan and V.M. Nashatyr; *Elektrichestvo*, No.6, (1951).
6. N.M. Chernyshev and V.D. Liashenko; Auth. Cert. No. 122207, (1958).
7. N.M. Chernyshev; *Synthetic circuits for rupturing capacity tests on circuit breakers (Iskusstvennye skhemy dlia ispytaniia vykliuchatelei na otkliuchaiushchuiu sposobnost')*, CIGRE, Report No. 116, (1958).

ABSTRACTS FROM PAPERS PUBLISHED IN ELEKTRICHESTVO No. 2, 1960

Modern concepts of dielectric breakdown: G.I. Skanavi dec'd (pp. 1-8).

The author has discussed the breakdown of gaseous, liquid and solid dielectrics. Test results are analysed and these would appear to justify re-approaching the problem of pre-breakdown processes in the crystals. The electrical breakdown of crystals and highly pure liquids is considered to be influenced materially by a combination of the cold emission of electrons from the cathode and shock ionization. List of 15 references and three diagrams.

Small domain stability of the excitation control system for a synchronous motor: D.P. Petelin (pp. 25-28).

In order to improve the operating conditions and increase the stability of a synchronous motor and the supply system, use may be made of automatic excitation regulation for motors operating on a variable load. It is possible and sometimes expedient to obtain this control by angle θ, as proposed by D.P. Petelin, (Reference given, dated 1959). An equation is formulated characterizing the process of regulating the system (List of four references).

A physical model for the d.c. transmission system Stalingrad hydro-electric station - Donlas: V.V. Voskresenskii, Kh.F. Barakaev and L.V. Travin (pp. 28-35).

In view of the difficulties encountered in the analytical calculation of fault conditions in d.c. transmission, the All-Union Electrical Engineering Institute has produced a physical model for d.c. transmission consisting of six individual converter bridges which can be considered universal' and applicable to the investigation of any multi-bridge conversion schemes. The general characteristic of the model is given and the method of modelling described. The shape of the curves and the amplitude of the voltages are determined for individual points in the scheme in rated conditions.

Some special features of long distance a.c. transmission system performance: I.M. Markovich, S.A. Sovalov and A.A. Kryukov (pp. 35-40).

A study is made of 600 kV transit type transmission over 1500 km with compensating devices and 600 kV transmission with intermediate power systems connected to the line. Special attention is paid to the effect of intermediate synchronous compensators. The installation of compensators at each intermediate substation is advocated, their total output (MVA) being equal to the power to be transmitted along the line (MW). Here it is recommended that the reactance of the compensators be partially compensated by banks of static capacitors. Current density in long distance transmission should be increased to 0.9 to 1.0 A/mm^2 at least. Systems of 'fault discharge' and excitation regulation are also considered.

Glass line suspension insulators: N.A. Nickolaev, T.D. Andryukhima, V.A. Veseliyi and S.I. Dyakivskii (pp. 41-46).

In order to save weight on long distance transmission, the Lvov Polytechnical Institute has envolved two types of glass insulator PS-4.5 and PS-8.5 with an hourly electromechanical test load of 4.5 and 8.5 tons at 50 kV and 50 c/s which are now in use on 35 to 220 kV lines. The oxide content of the glass is given in detail: SiO_2 72.9%, Al_2O_3 1.9%, Fe_2O_3 0.1%, CaO 7.6%, MgO 3.7% and Na_2O 13.4%. Mechanical strength is imparted by a special toughening process whereby the tensions in the glass are uniformly distributed (650°C). The design of the insulators is described and their method of production. Properties and characteristics are described (with photographs).

The electric circuits of a three phase shunted arc: I.T. Zherdav (pp. 46-53).

A theoretical investigation is made by means of equivalent networks into the phenomena in an electric ironmaking furnace. A detailed study is made of the electrical circuit of a three phase shunted arc. Attention is paid to the combustion of one, two and three arcs in the circuit of a three phase shunted arc. The presence of an arc discharge is established together with the presence of charge materials currents. The reduced magnitude of the displacement voltage of the neutral of the furnace compared with the same voltage of a three phase open arc shows that the additional resistance in the circuit of each arc must be taken into account in the equivalent network.

On calculating electromechanical transients in an induction motor synchronous generator set whose machines are of comparable rating: Ta.B. Kadymov and M.M. Rasulov (pp. 57-60).

The author expounds an approximate but practical method of calculating electromechanical transients when starting an induction motor of normal design from a synchronous generator of commensurate power, provided with a device for forcing excitation. Similar assumptions are made to those underlying the usual calculation of starting from a network of infinite power, so that the transient powers can be calculated according to the static characteristics of electrical machines. An example is given.

An asynchronous micro-motor with hollow rotor at an anomalous frequency: L.I. Stolov (pp. 61-63).

A study is made of the relationship between supply voltage and frequency at a fixed electromagnetic starting movement for an asynchronous fractional horse power motor with a hollow non-magnetic rotor which possesses relatively large stator and rotor impedances and a very small inductive resistance of rotor dispersion. It is mathematually established that voltage increases as frequency is considerably reduced. Good agreement has been obtained with experimental data.

The equivalent circuit and exact circle diagram for a reactive synchronous machine; O.B. Pevzner (pp. 64-68).

The author generalizes the equivalent circuit for a reactive synchronous motor and describes an accurate circle diagram constructed by methods widely adopted in design practice for asynchronous machines. The proposed method is claimed to be simpler than that proposed by C.H. Croose and makes it possible to calculate losses in the steel. The equivalent network may be T or L shaped.

A statistical method for basing the voltage accepted in testing the rupturing capacity of circuit breakers: V.V. Kaplan, V.M. Nashatyr and V.L. Ivanov (pp. 69-73).

The results are given of tests carried out in 1958 to 1959 in the Leningrad Polytechnical Institute to verify the possibility of proportionally calculating the tripping capacity of the individual elements of the circuit breakers as a whole independently of the character of the capacitive distribution of the voltage. Objective comparison of the operation of the arc extinction elements was possible when the probability curves of non-extinction of the arc were compared, the

problem then being reduced to the evaluation of the parameters of the normal distribution from the experimentally determined frequencies.

Heating of current conductors in electric apparatus: A.M. Zalesskii, M.B. Moiseev and E.G. Popova (pp. 73-78).

The results are given of an investigation carried out in the Kalinin Polytechnical Institute in Leningrad into the heating of the live parts of electrical gear in order to further the development of high voltage apparatus capable of passing 11 to 12 kA is required by the 7-year plan. At 6 to 12 kA and over, the use of box-section conductors is advocated with flanges turned inwards. Box-section 405 mm square and walls 6 mm thick had considerable heat reserve, at I = 12 kA Silver contacts are recommended. A nomogram is proposed for determining the section sizes in advance.

Accounting for network losses in determining optimum power system operating conditions: N.A. Melnikov (pp. 78-82).

Formulae are proposed for determining the most economic state of power system operation in which attention is paid to the problem of voltage regulation and the distribution of the reactive loads.

How the capacitance of low voltage networks influences safety: G.V. Mindeli (pp. 82-85)

In insulated neutral systems investigations have shown that the effect of the resistance of the network insulation on the current passing through a human being when he comes in contact with a live part decreases sharply if the capacitance in the network is more or less considerable. The use of capacitance compensators is therefore advocated in low voltage networks (eg. pits) and attention is drawn to the fact that an instrument has been invented to effect compensation automatically (see Author Cert. No. 113867, Class 21e, 29).

HOW TO SELECT THE BASIC PARAMETERS OF EXCITATION SYSTEMS FOR SELF-EXCITED SYNCHRONOUS GENERATORS*

D.V. VILESOV and I.A. RIABININ

Leningrad

(Received 1 September 1959)

1960

In recent years a number of papers have been published in connexion with investigations into methods of self-excitation for synchronous generators (SSG). The purpose of these investigations has been to select the optimum excitation system for generators which have to satisfy definite conditions (mainly voltage stability). However, owing to the obscurity of the processes taking place in various excitation systems nobody has as yet taken a good look at the various excitation systems to find which are to be preferred and how their parameters should be calculated, [1 and 2].

The possibility of producing roughly the same SSG voltage regulation characteristics even though the parameters of the excitation system vary within rather wide limits [1] has determined the various approaches to the design of the main elements in the system as compact as possible [3] or else the starting point for the calculation has been the condition that initial self-excitation be assured, or finally the parameters have been based on accumulated design experience [4].

The latter method of choosing the parameters should be discarded in the project stage owing to the obscure position as regards the conditions for producing the recommended relationships and the methods to be used. The aspiration to ensure initial self-excitation in autonomous generator installations by providing additional supply sources for the sake of reliability warrants the conclusion that the first method of determining the parameters is the most rational.

The present article will show how to determine the main parameters

* *Elektrichestvo*, No.3, 20-24, 1960.

of the basic elements in SSG excitation systems theoretically as a function of the generator characteristics in such a way that the generator voltage is stabilized and that the output of the main element is kept at the lowest possible level consonant with high compactness of the system as a whole. In the article a study is only made of one of numerous possible versions of the SSG excitation system (Fig. 1a); namely, a phase compounding scheme with summation of the currents proportional to the voltage and current in the main generator circuit. Use may however be made of the results obtained for any other version of the excitation system.

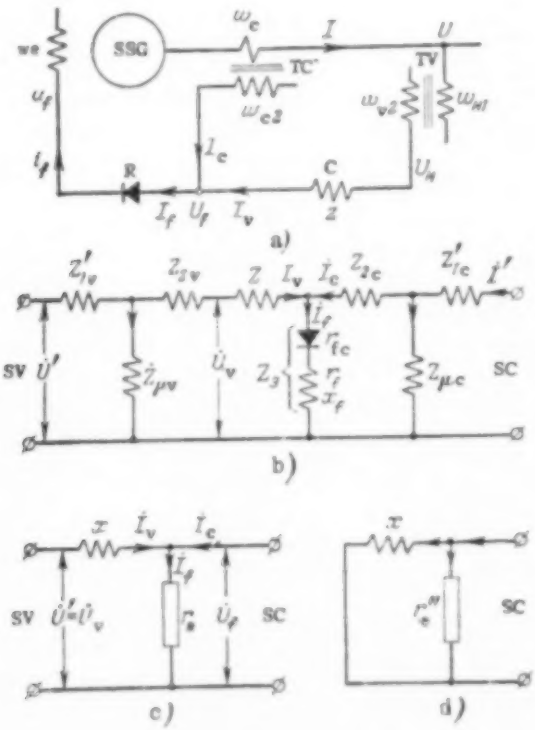

Fig. 1. Principal and equivalent circuits for SSG excitation.

Structure of SSG circuit

The structure and parameters of the converter elements in the excitation system should ensure: (a) matching of the voltages and currents in the stator and rotor circuits; (b) correspondence between

the magnitude of the load regulating signal and the regulation characteristics of the generator.

Use is made of a rectifier (*R*) to match the currents. Provision is made for matching the voltages and currents by voltage and current transformers (*TV* and *TC*). In certain systems the voltage and current transformers are combined in the form of "excitation transformers".

The stated matching elements are essential. However their presence is not enough to ensure that the system is capable of producing the necessary load regulation signal. The system should incorporate an element which will soften the external characteristic at the output of one of the transformers depending on which version of the excitation system is adopted. This element in Fig.1 is the choke (*C*).

In the no load state the excitation winding of the generator (w_e) is supplied along the circuit: generator terminals, voltage transformer *TV*, ballast resistance z, (sometimes called compounding in SSG systems) and rectifier *R*. In the presence of load current I, the excitation winding obtains an additional supply from the stator circuit of the generator via the current transformer *TC*. Thus the supply to the excitation winding of the generator (voltage u_f) is provided by two as it were independent s.c. sources. In steady state conditions one of the sources ensures a voltage of constant magnitude and conditionally constant phase (source with constant voltage *SV*), whilst the other source ensures a current of constant amplitude and phase (source with constant current *SC*). The amplitude and phase of the latter vary as a function of generator operating conditions. No account is taken of the variations in the amplitude of the voltage from the first source (*SV*) which are in practice small.

If no current is present in the stator circuit ($I = 0$) the source *SC* should provide the no load excitation voltage of the generator. The source *SC* should also provide an increase in the excitation current i_f as the load on the generator appears and increases.

The steady state conditions for the supply of the excitation winding from the stator circuit is conventionally examined by means of the equivalent circuit shown in Fig. 1b.

Suppose for purposes of greater simplicity that transformers *TV* and *TC* are ideal, i.e. that there is no leakage and no losses (z_{1v}, z_{2v}, z_{1c} and z_{2c} equal zero; $z_{\mu v} = \infty$; $z_{\mu c} = \infty$). In this the characteristics of both transformers will be "rigid" no matter what the values of I_v and I_c and there will be proportional relationships $U_v = k_v U$ and $I_c = k_c I$, where $k_v = \frac{w_{v2}}{w_{v1}}$ and $k_c = \frac{w_{c1}}{w_{c2}}$; the coefficients of trans-

formation of the voltage and current transformers.

If we ignore the distortions in the shape of the voltage and current curves due to the rectifiers it is easy to produce an expression for the current I_f in the resistance, the equivalent excitation winding we and the rectifier R in the adopted equivalent circuit:

$$I_f = \left| \frac{1}{Z + Z_e} (k_v U + k_c Z I) \right|. \quad (1)$$

The main parameters and conditions for determining them

The design of any version of the SSG system requires that the main parameters be determined; namely, k_v, k_c and z (more precisely, x).

The generator voltage can be kept extremely stable in steady state conditions if its regulation characteristics $i_f = f(I)$ when in excitation current described by (1). An actual system of SSG with a saturated magnetic circuit as the object of load variation can only work in two states in which the deviation of the voltage from the desired (rated) value is zero. Compounded generators are usually so tuned that the voltage deviations in no load and rated conditions are zero. In order that this be observed it is necessary that the curve described by (1) at cos ϕ_{rated} should pass through points A and B (Fig. 2). For the sake of convenience in further calculations, substitute the equivalent requirement that the curve described by (1) at cos $\phi = 0$ should pass through points A and C (Fig. 2), having the ordinates i_{fx} and $i_{fx}(1 - x_d)$.

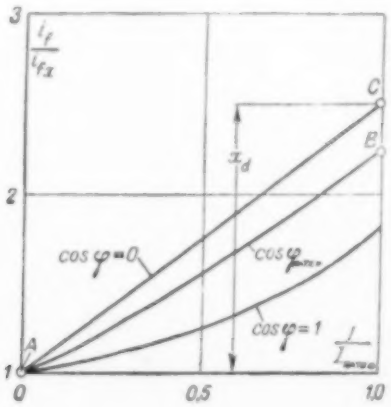

Fig. 2. Regulation characteristics for synchronous generators.

The compactness of the elements in the excitation system for the generator in question is determined by the dimensions of the current and voltage transformers and the choke. The maximum compactness of the first three elements, whose dimensions depend on the magnitudes of k_v, k_c and x, is ensured when the sum of the apparent outputs S is minimum. In the case in question, rectifier R is excluded from our consideration since its dimensions depend on the value of the current $i_{f.rated}$ and voltage $U_{f.con}$ respectively under rated and forced operating conditions.

Thus the optimum values of the main parameters of the system k_v, k_c and x should be chosen in such a way as to ensure that the following conditions are satisfied:

$$i_f = i_{fx} \text{ when } U = 1 \text{ and } I = 0; \tag{2}$$

$$i_f = i_{fx}(1 + x_d) \text{ when } U = 1;\ I = 1 \text{ and } \cos\varphi = 0; \tag{3}$$

$$S(k_v, k_c, x) = \text{minimum}. \tag{4}$$

It should be mentioned that condition (4) does not affect the accuracy with which the voltage is maintained in the presence of phase compounding of non-saturated non-salient-pole generators with loads different from rated load and in no load conditions.

Resistance, equivalent excitation winding connected via the rectifier

In the circuit shown in Fig. 1b and formula (1) use is made of resistance z_e, equivalent to the excitation winding connected via the rectifier. The calculation of the parameters of the SSG excitation system requires that the equivalent resistance z_e be determined by means of quantities which are usually known for the excitation winding (resistance and reactance r_f and x_f) and the rectifier (resistance to forward "direct" current r_{fc}). The difficulty in calculating z_e from the values of the resistance (r_f) and reactance (x_f) in the excitation winding and also from the rectifier's (r_{fc}) to the forward current is connected with the fact that the magnitudes of the rectifier coefficients necessary for the calculation

$$\beta_I = \frac{i_f}{I_f} \text{ and } \beta_u = \frac{u_f}{U_v}$$

are non-linear functions of the relationship between the resistances and reactances of the excitation circuits and, consequently, the para-

meter x which is liable to determination and the shape of current and voltage curves of the supply source.

Set up the expression for the equivalent resistance assuming that coefficients β_i and β_u are known.

First note that the current in the excitation winding is almost constant owing to the inequality* $r_f \ll x_f$ (without pulsation), whilst the power consumed in the excitation winding is purely active. Hence it can be assumed that the total equivalent resistance of the excitation winding and rectifier on the d.c. side r equals

$$r = r_f + r_{fc} = \frac{u_f}{i_f}$$

and that this resistance on the s.c. side is also active, i.e. $z_e = r_e$ (Fig. 1c). The magnitude of r_{fc} can be a first approximation be ascertained from the values of U_f and I_f in conditions when $Im = 1$ and $\cos = 0$. The magnitude of r_{fc} is stated more precisely in the following after the selection of coefficient k_v has been made.

In accordance with the system shown in Fig. 1c, the equation for calculating the equivalent resistance in the no load state r_e has the form:

$$\frac{U_v}{I_v} = z_v = \sqrt{r_e'^2 + x^2},$$

whence

$$r_e' = \sqrt{\left(\frac{\beta_i'}{\beta_u'} r\right)^2 - x^2} = r\sqrt{\left(\frac{\beta_i'}{\beta_u}\right)^2 - \left(\frac{x}{r}\right)^2},$$

since $u_f = \beta_u' U_v$ and $i_f = \beta_i' I_v$.

If the initial condition of the SSG system is assumed to be short circuited (Fig. 1d), there is a different expression for equivalent resistance:

$$r_e'' = \frac{U_f}{I_f} = \frac{\beta_i''}{\beta_u''} \frac{u_f}{i_f} = \frac{\beta_i''}{\beta_u''} r. \qquad (5a)$$

In expressions (5) and (5a) coefficients β_u', β_i' and β_u'', β_i'' are determined at a sinusoidal voltage or current from the supply sources SV and

* For example, x_f = (400 to 700) r_f in the case of MS type generators.

SC respectively.

In conditions other than no load and short circuit conditions there will be an intermediate value of the equivalent resistance r_e.

The authors' calculation of the coefficients β'_u and β'_i for different ratios of $\frac{x}{r}$ (Fig.3), which has been confirmed by $\frac{r'_e}{r} = f\left(\frac{x}{r}\right)$. In the case of actual ratios of $\frac{x}{r}$, the magnitude of r'_e lies within the range

$$r'_e = (0{,}6 - 0{,}9)\, r. \tag{6}$$

When designing SSG in practice, use is made of values of r_e which are close to $r''_e = 0.64r$, since $\beta''_i = 1.42$ and $\beta''_u = 2.22$ in the system in Fig.1*d*.

1960

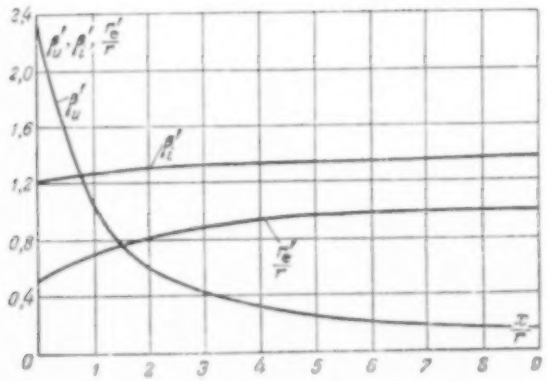

Fig. 3. Dependence of the rectifier coefficients β'_u and β'_i on the relationship between the ballast resistance and the load resistance of the rectifier.

As the normal conditions for the operation of SSG are intermediate, its average value may be used as the theoretical magnitude, roughly equal to

$$r_e = 0.7\ r. \tag{6a}$$

Fundamental theoretical magnitudes

In accordance with (1) and (2) the following expression is true for

the equivalent circuit in Fig. 1c

$$k_v = \frac{\sqrt{r_e^2 + x^2}}{\beta_i'} i_{fx} = \frac{r_e}{\beta_i'} \sqrt{1 + \eta^2}\, i_{fx}, \tag{7}$$

where $x = \eta r_e$, and the magnitude of β_i' is determined by means of Fig. 3.

Equations (1) and (3) for the same circuit enable the condition to be set up

$$k_c = \frac{x_d}{\beta_i x} \sqrt{r_e^2 + x^2}\, i_{fx} = \frac{x_d}{\beta_i} \sqrt{1 + \frac{1}{\eta^2}}\, i_{fx}, \tag{8}$$

in which coefficient β_i satisfies the inequality $\beta_i' < \beta_i < \beta_i''$. Assume $\beta_i = 0{,}5(\beta_i' + \beta_i'') = 0{,}5\beta_i' + 0{,}71$.

It is assumed that the quantities r_e, x, x_d and i_f in formula (7) and (8) and below are expressed in relative units.

The magnitude of the apparent power of the voltage transformer and choke under no load conditions in the SSG system (S_{tv} and S_c), which fundamentally determine the dimensions of these elements, are calculated from the formulae

$$S_{TV} = U_v I_{fx} = P_x \sqrt{1 + \eta^2} \text{ и } S_c = x I_{fx}^2 = P_x \eta, \tag{9}$$

where $P_x = I_{fx}^2 r_e$.

The theoretical magnitude of the apparent power of the current transformer S_{tc} in operating conditions, determined by condition (3), equals

$$SS_{tc} = U_{c.rated}\, I_{c.rated} = k_c r_e (1 - x_d)\, I_{fx},$$

or, paying attention to (8),

$$S_{tc} = P_x (1 + x_d) x_d \sqrt{1 + \frac{1}{\eta^2}}. \tag{10}$$

Knowing S_{tv}, S_c and S_{tc}, set up the expression for the sum of the rated values of the apparent outputs of the elements in the a. c. circuits of the SSG excitation system:

$$S = S_{tv} + \alpha S_c + S_{tc} = P_x \left[\sqrt{1 + \eta^2} + \alpha\eta + x_d (1 + x_d) \sqrt{1 + \frac{1}{\eta^2}} \right], \tag{11}$$

where α is the coefficient taking into account the difference in the specific weights ($\frac{g}{\gamma_a}$) of the transformers and the elements used as the ballast resistances. In the circuit under consideration where the ballast resistance is the choke, $0.7 \leqslant \alpha \leqslant 0.9$.

The minimum of the function $S(\eta)$, determined by (11), gives the optimum value of $\eta = \eta_{opt}$. It is impossible to produce an accurate analytical expression for η_{opt}. The use of an approximate formula may therefore be recommended:

$$\eta_{opt} = \left(\frac{x}{r_e}\right)_{opt} = \sqrt[3]{\frac{(1+x_d)\,x_d}{1+0{,}96x}}. \qquad (12)$$

Fig.4 shows the curves of S, $S_v = S_{tv} + \alpha S_c$ and S_{tc} as a function of η for values of $x_d = 1.8$ and $x = 0.83$.

Expression (12), unlike the methods of calculation in (3) and (4), gives a ratio of $\frac{x}{r_e}$ which as a first approximation ensures that the system is as compact as possible and that it can still be regulated satisfactorily.

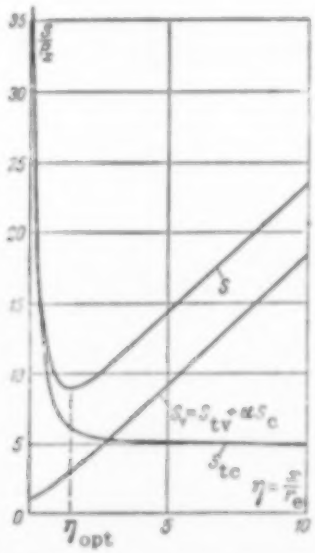

Fig. 4. Dependance of the apparent power of the elements in the excitation system on the parameter

Using expressions (12) or (11), (6a), (7) and (8) and knowing the parameters of the generator, it is easy to determine the main parameters of the SSG excitation system for the initial conditions assumed.

If $k_v \to 1$ or $k_c \to 1$, it is possible to avoid using voltage or current transformers. The results of calculations from (12) should be corrected in this case.

In particular, if k_v is almost unity according to the calculation, it is recommended that a version of the system without *TV* be considered. Here condition (7) degenerates into the equality $k_v = 1$, whilst expression (12) assumes the form

$$\eta_{opt} = \sqrt[3]{\frac{x_d + x_d^2}{0{,}96a}}, \qquad (12a)$$

by virtue of the fact that $S_{tv} = 0$.

The preliminary choice of the rational relationship between the voltages and currents in the rotor and stator circuits can avoid the use of one or another matching element and achieves a considerable reduction in the weight and dimensions of the scheme. This idea has been successfully realized in the ES – 52 – 4 type generator made by Armelektrozavod.

Besides the states corresponding to points *A* and *C* in Fig. 2, a steady short circuit state may also be adopted. This makes it possible to design the current transformer with greater precision with the saturation of its magnetic circuit taken into account.

The proposed method takes no account of elements in the system for regulating deviation. In this case the use of receivers as described in (4) may be recommended.

Example. Using the derived relationships, calculate as an example the fundamental parameters of an SSG phase compounding system based on an SG – 84 – 4 type synchronous generator having the following rated data: 30kVA, 24kW, 400V, 43.2A, 1500 rev/min, $x_d = 1.8$, $r_f = 1.3\ \Omega$, $i_{fx} = 10.5$A.

(1) From formula (12), assuming $a = 0.83$, determine

$$\eta_{opt} = \sqrt[3]{\frac{1{,}8 + 1{,}8^2}{1 + 0{,}96 \cdot 0{,}83}} = 1{,}41$$

(2) To calculate r it is necessary to know the resistance of the rectifier to the forward current r_{fc}. This can be calculated by the method in (5). In the present case $r_{fc} = 0.6\ \Omega$. Then $r = r_f - r_{fc} = 1.3 - 0.6 = 1.9\ \Omega$ (in relative units $r = 0.36$).

(3) From formula (6a) find

$$r_e = 0{,}7 \cdot 0{,}36 = 0{,}252.$$

(4) Calculate the magnitude of the ballast resistance in accordance with (12):

$$x = \gamma_{opt}\, r_e = 1.41 \cdot 0.252 = 0.355 \text{ (or } 1.89\ \Omega \text{).}$$

(5) Using the curve $\beta_i' = f\left(\frac{x}{r}\right)$ on Fig. 3 for $\frac{x}{r} = \frac{0.355}{0.36} = 0{,}985$ determine

$$\beta_i' = 1.26.$$

(6) From expression (7) determine

$$k_v = \frac{r_e}{\frac{\beta_i'}{\gamma_i}} \sqrt{1 + \gamma_i^2}\, i_{fx} = \frac{0.252}{1.26} \sqrt{1 + 1.41^2}\, \frac{10.5}{43.2} = 0.083.$$

(7) Calculate the average value of the coefficient β_i from the formula

$$\beta_i = 0.5\beta_i' + 0.71 = 1.34.$$

(8) From expression (8) determine

$$k_v = \frac{x_d}{\beta_i} \sqrt{1 + \frac{1}{\gamma_i^2}}\, i_{fx} = \frac{1.8}{1.34} \sqrt{1 + \frac{1}{1.41^2}}\, \frac{10.5}{43.2} = 0.4.$$

When the parameters of the scheme have been found, the excitation current under rated load conditions $I_{f.rated}$ in accordance with (1) and when $Z = jx$ is equal to

$$I_{rated} = I_{fx} \left| 1 + \frac{k_c}{k_v} jx \frac{I}{U} \right| =$$

$$= \sqrt{1 + 2\frac{k_c}{k_v} x \sin\varphi_{rated} + \left(\frac{k_c x}{k_v}\right)^2}\, I_{fx} =$$

$$= \sqrt{1 + 2\frac{0.40}{0.083} 0.355 \cdot 0.6 + \left(\frac{0.40 \cdot 0.355}{0.083}\right)^2}\, I_{fx} =$$

$$= 2.45 I_{fx}.$$

The value of this quantity, calculated from the usual relationships for non-salient-pole synchronous generators, is practically the same

$$I_{f\,rated} = i_{fx} \sqrt{1 + 2x_d \sin\varphi_{rated} + x_d^2} =$$

$$= \sqrt{1 + 2 \cdot 1.8 \cdot 0.6 + 1.8^2} \cdot i_{fx} = 2.53 i_{fx}.$$

This demonstrates that condition (3) can be used to ascertain k_c.

Translated by O.M. Blunn

REFERENCES

1. D.V. Vilesov and I.A. Riabinin; *Self-exciting excitation systems for synchronous generators (Sistemy vozbuzhdeniiu samovozbuzhdaiushchikhsia sinkhronnykh generatorov).* Nauchno-tekh. infor. No.16, IMAKV im. Krylova, Leningrad, (1957).
2. G.A. Neleshkin; *Direct voltage synchronous generators for ships (Sudovye sinkhronnye generatory postoiannogo napriazheniia).* Izd. Nopsk. Transport, (1957).
3. K. Gadek; *Investigation into systems of current and voltage summation for compounded synchronous machines (K voprosu ob issledovanii skhem summirovaniia tokov i napriazhenii dlia kompaundirovaniia sinkhronnykh mashin).* E und M, H6, 121-144, Vienna, (1957).
4. H.H. Britten and D.L. Plette; *Application and Industry,* No.38, 271-277 (195 (1958).
5. V.G. Komar; *The performance of semiconductor rectifiers in control circuits (Rabota poluprovodnikovykh vypriamitelei v tsepiakh upravleniia),* Gosenergoizdat, (1952).

HOW THE RATING OF D.C. MACHINES VARIES WITH AMBIENT TEMPERATURE AND ALTITUDE*

N.A. PANFILOV

Moscow

(Received 10 October 1959)

The evaluation of the influence of ambient temperature and altitude on the output of electrical machines is becoming of special importance in view of the widespread use of various modified versions of totally enclosed and tropical machines.

In order to evaluate the extent of the influence of the factors in question, Berger (1) proposed a number of graphical relationships which make it possible to determine the percentage variation in the output of electrical machines as a function of the parameters of the surrounding atmosphere. When plotting these relationships it was demonstrated that the heat losses of the machine in the no load state $\Sigma P_{h.0}$ amount to about 30% of the heat losses appropriate to rated load $\Sigma P_{h.r}$.

In the case of d.c. machines of the totally enclosed and protected type this assumption is quite rudimentary since, depending on the speed of rotation, the permissible temperature rises in the windings, the system of cooling and the electromagnetic parameters, the heat losses in the no load state can vary within wide limits. Thus, for example, according to test data for P-series experimental d.c. machines, it has been established that the following relationship exists between the heat losses in the no load state and on rated load:

(a) for protected type machines:

$$\Sigma P_{h.0} = (0{,}15 \text{ to } 0{,}60)\Sigma P_{h.r}, \tag{1}$$

(b) for totally enclosed machines:

$$\Sigma P_{h.0} = (0{,}25 \text{ to } 0{,}75)\Sigma P_{h.r} \tag{2}$$

---

* *Elektrichestvo*, No.3, 30-33, 1960.

In this connexion, it is expedient to develop a more accurate method of evaluating the influence of ambient temperature and altitude on the output of d.c. machines. An increase in ambient temperature is equivalent to a reduction in the permissible increase in the machine's winding temperature. As a result, the output of the machine should vary.

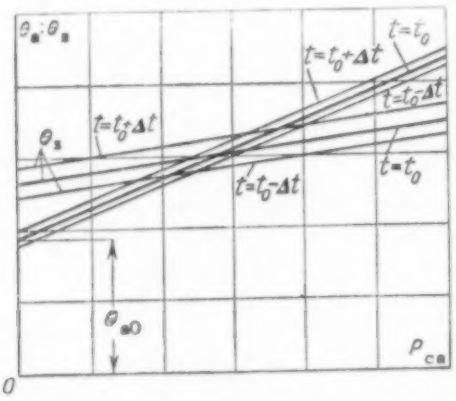

Fig. 1. Temperature rises in the windings of d.c. machines on change of ambient temperature.

In the case of d.c. machines in general, the excitation current corresponding to the rated operating characteristics is held constant, whilst the losses in the copper of parallel excitation windings vary in proportion $(1 - \alpha \theta_s)$, where α is the electrical temperature coefficient and θ_s the overheating of the parallel excitation windings.

With a change in ambient temperature the current in the parallel excitation winding i_s (or m.m.f. F_s) should be held constant since oppositely the speed of the machine will vary when operating in the motor state, whereas it is the voltage at its terminals which varies when operating in the generator state. The analysis of the influence of ambient temperature and altitude can therefore be expediently made on the supposition that:

$$i_s = \text{const} \quad \text{or} \quad F_s = \text{const}. \tag{3}$$

It is thus necessary to consider two aspects of the problem: namely, (a) the effect of the parameters of the surrounding medium on the output of d.c. machines depending on the level to which the armature winding is heated; (b) verification of the temperature rise in the parallel excitation winding when condition (3) is satisfied.

If the temperature of the parallel excitation winding exceeds the permissible limit, then the appropriate measures should be taken to reduce losses or increase the permissible overheating. The overheating of the windings of the additional poles θ_{ad} and the series excitation windings θ_b in the case in question cannot be taken into account since of all the windings in the armature circuit the hottest is usually the armature winding (in correctly designed d.c. machines). For the analysis use is made of the temperature rise characteristics given in Fig. 1.

$$\vartheta_i = f(P_{ca}), \tag{4}$$

where θ_i is the temperature rise in the winding under consideration and P_{ca} the losses in the armature copper.

Assume that the initial ambient temperature increased by Δt. Then the losses in the copper of the parallel excitation winding, corresponding to the given losses in the copper of the armature, can be expressed in the following form:

$$P'_{cs} = P_{cs}\frac{1+\alpha(\vartheta_s+\Delta t)}{1+\alpha\vartheta_s}, \tag{5}$$

where P'_{cs} corresponds to $t = t_o - \Delta t$;

P_{cs} corresponds to $t = t_o$.

Taking (5) into account and the relationships introduced in (Ref. 2), it can be shown that the temperature rise at each point of the parallel excitation winding characteristic, corresponding to the given losses in the armature copper, increases by

$$\Delta\vartheta_s = P_{cs}\frac{\alpha\cdot\Delta t}{1+\alpha\vartheta_s}\left(\frac{1}{A}+\frac{1}{E}\right), \tag{6}$$

where A and E are the thermal conductances of the air inside the machine and the parallel excitation winding (2). Given the same losses in the armature copper the temperature rise of the air inside the machine increases by

$$\Delta\vartheta_{air} = P_{cs}\frac{\alpha\cdot\Delta t}{(1+\alpha\vartheta_s)A}. \tag{7}$$

Taking into account what has been said above, expressions (6) and (7) can be transformed as follows:

$$\Delta\vartheta_s = P_{cs.r}\frac{\alpha\cdot\Delta t}{1+\alpha\vartheta_{sr}}\left(\frac{1}{A}+\frac{1}{E}\right) = \text{const}; \tag{8}$$

1960

$$\Delta\vartheta_{air} = P_{cs.r}\frac{\alpha\cdot\Delta t}{(1+\alpha\vartheta_{ar})A} = \text{const.} \tag{9}$$

-Consequently, when ambient temperature changes by $\pm\Delta t$ the characteristics of the temperature rise in the winding circuit of the armature are displaced parallel to each other in the direction of the axis of the ordinate by $\pm\Delta\theta_{air}$ (equation 9), whilst the analogous characteristic of the parallel excitation winding is shifted by $\pm\Delta\theta_s$ (equation 8), (see Fig. 1).

It follows from 8 and 9 that if use is made of the initial characteristic $\theta_i = f(P_{ca})$, when $t = t_o$, to calculate the output corresponding to ambient temperature $t_o \pm \Delta t$, then the theoretical permissible temperature rise $\theta_{per.r} \pm \Delta t$ should be reduced (when $\Delta t > 0$) or increased (when $\Delta t < 0$) by the magnitude of $\Delta\theta_{air}$, i.e. or,

$$\vartheta'_{per} = \vartheta_{per.r} \mp (\Delta t + \Delta\vartheta_{air}), \tag{10}$$

in other words, the temperature rise in the windings should be increased or decreased by

$$\Delta\vartheta' = \mp(\Delta t + \Delta\vartheta_{air}). \tag{11}$$

When changing from one ambient temperature to another and if there is a corresponding change in the output of the machine, the temperature of the windings in the armature circuit remains constant. It is therefore possible to assume approximately that

$$\frac{\eta}{\eta'}\sqrt{\frac{r_a}{r'_a}} \approx 1, \tag{12}$$

where η and r_a are the efficiency and resistance of the armature winding when $t = t_o$; η' and r'_a are the same, but when $t = t_o + \Delta t$.

Carrying out a number of transformations and taking Fig. 1 and equation (12) into account, it can be shown that the output of the machine P_2 corresponding to the ambient temperature $t_o \pm \Delta t$, can be determined from the formula

$$P_2 = P_{2r}\sqrt{1 - \frac{\Delta t + \Delta\vartheta_{air}}{\vartheta_{per.r} - \vartheta_{a0}}}, \tag{13}$$

when P_{2r} and $\vartheta_{per.r}$ are the output of the machine and the permissible temperature rise in the armature winding in initial conditions;

when θ_{a0} is the increase in temperature in the armature winding in no load conditions.

In order to determine the magnitude of θ_{a0}, use may be made of experimental relationships $\theta_{a0} = f(D_a)$, plotted on the basis of test results for P-series machines (Figs. 2 and 3).

Finally, it is necessary to verify the temperature rise in the parallel excitation windings.

It can be shown [2] that:

$$\theta_a = \theta_{a.r} + \Delta\theta_w - \frac{P_{ca.r}\dfrac{r_{ac}}{r_a}\cdot\dfrac{\pm(\Delta t + \Delta\theta_{air})}{\theta_{perr} - \theta_{a0}}}{A}, \qquad (14)$$

where $P_{ca.r}$ is the losses in the armature copper in initial conditions, and

r_{ca} is the impedance of the armature circuit.

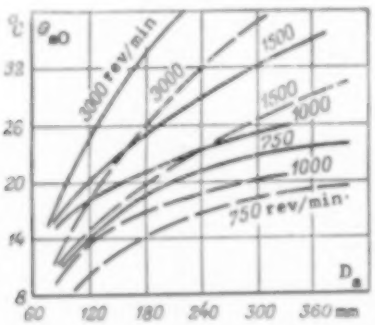

Fig. 2. Average values of θ_{a0} of P-series protected-type machines.

The losses in the copper of the parallel excitation winding (in %), relative to total heat losses, depends mainly on the dimensions of the machine and the speed of rotation, (the greater the speed and larger the size of the machine the smaller this magnitude). In the case of totally enclosed and protected type machines with an output between 0.2 and 150-200 kW in rated conditions

$$\frac{P_{ca}}{\Sigma P_h} 100 \approx (5 \text{ to } 20)\% \qquad (15)$$

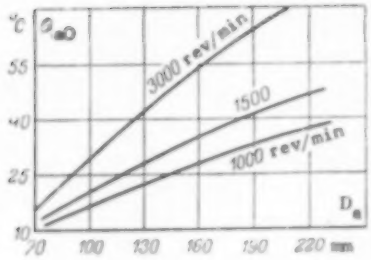

Fig. 3. Average values of θ_{a0} of P-series totally enclosed air-cooled machines.

Taking (15) into account, evaluate the limits of displacement of the $\theta_i = f(P_{ca})$ when ambient temperature changes. Assume that ambient temperature has increased by 40°C (from 15 to 55°) and that the permissible temperature rise of the windings is 80°C. Then, in accordance with (5) the losses in the copper of the parallel excitation winding increase relative to the initial conditions by approximately 12 per cent, whilst the temperature of the air inside the machine (see equation 9) increases by (2.4 to 0.6) per cent.

Since it is always true that

$$\theta_{air} \leq \theta_a;\ \theta_{air} \leq \theta_c;\ \theta_{air} \leq \theta_b$$

the percentage shift of the winding characteristics for the armature circuit will be still less.

Consequently, the shift of the characteristics for the temperature rise in the windings of the armature circuit when ambient temperature changes can be ignored with a sufficient degree of accuracy and then equation (13) maybe written in the form:

$$P_a = P_{2r}\sqrt{1-\frac{\Delta t}{\theta_{per.r}-\theta_{a0}}}. \qquad (16)$$

The amount of displacement of the characteristics for the temperature rise in the parallel excitation winding is more substantial. In fact, according to equations (8) and (9)

$$\frac{\Delta\theta_g}{\Delta\theta_{air}} = \left(1+\frac{A}{E}\right). \qquad (17)$$

Since it is always true that $A \gg E$, then $\Delta\theta_s$ is several times greater than $\Delta\theta_{air}$. It is therefore impossible to ignore the amount of displacement of the $\theta_s = f(P_{ca})$ characteristic relative to the rated condition when $t = t_0$, since the amount of this displacement can in some cases reach about 10 to 15% relative to the initial rated data. Consequently, when calculating the output of a machine in connection with an increase in ambient temperature, it is in many cases impossible to judge the heating of the parallel excitation winding according to the initial $\theta_s = f(P_{ca})$ characteristic without taking its displacement into account in accordance with (8).

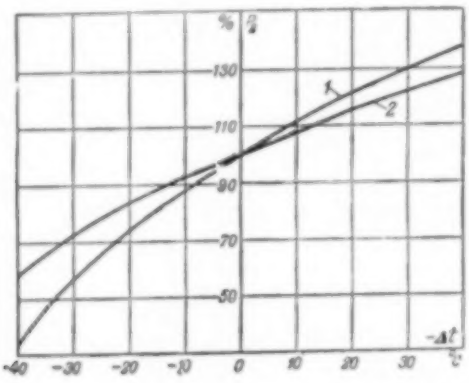

Fig. 4. Relationship $P_2 = f(\Delta t)$ for protected-type machines (2) and totally enclosed machines (1) (both air-cooled).

In order to verify the temperature rise in the parallel excitation winding taking (8) into account, use may be made of the equation

$$\vartheta_s = \vartheta_{s.r} + P_{ca.r}\frac{\alpha\cdot\Delta t}{1+\alpha\vartheta_{s.r}}\left(\frac{1}{A}+\frac{1}{E}\right) - \frac{P_{ca.r}\dfrac{r_{ac}}{r_a}\dfrac{\Delta t}{\vartheta_{per.r}-\vartheta_{a0}}}{A} \leq \vartheta_{per} \qquad (18)$$

obtained from equation (14) with (8) and (16) taken into account.

When calculating the output of a machine in connexion with a reduction in ambient temperature ($\Delta t < 0$), no verification of the temperature rise in a parallel excitation winding can be made since the $\theta_s = f(P_{ca})$ characteristic always slopes more than the characteristic of the hottest winding in the armature circuit, whilst the magnitude of

displacement of the $\Delta\theta_s$ characteristic (8) becomes negative. Therefore, if when $t = t_0$ $\theta_{s;r} < \theta_{per.r}$, then with a reduction in temperature and an increase in output it is always true that

$$\theta_s < \theta_{per}.$$

In the case of totally enclosed machines θ_{a0} is usually considerably greater than in the case of the protected types (see Figs. 2 and 3). Therefore the increase in ambient temperature affects the reduction in output of totally enclosed machines to a greater extent than protected machines. For purposes of illustration Fig. 4 presents the $P_2 = f(\Delta t)$ relationship. One curve applies to enclosed machines and the other to the protected design. The calculation is made in accordance with (16). The temperature rise θ_{a0} corresponds to $D_a \approx 185$ mm; $\eta = 1500$ rev/min in accordance with Figs. 2 and 3.

In order to ascertain the effect of altitude on the output of d.c. machines, use was made of the recommendations of GOST 183-55 and VDE 0530/7. x 55.

If the machine is over 1000 m above sea level the maximum increase in winding temperature independently of the class of insulation, decreases by 0.5° per 100 m above 1000 m provided that ambient temperature does not exceed 35°C in accordance with GOST 183-55 or 40°C in accordance with VDE 0530/7 x 55 and the recommendations of MEK. Then the output of a d.c. machine with an increase in ambient temperature and altitude can be ascertained in the following way:

$$P_2 = P_{2r}\sqrt{1 - \frac{\Delta t + 0{,}5\,\frac{h - 1\,000}{100}}{\theta_{per.r} - \theta_{a0}}}, \tag{19}$$

and the increase in the temperature of the parallel excitation winding from

$$\theta_s = \theta_{s.r} + P_{cs.r}\,\frac{\alpha\left(\Delta t + 0{,}5\,\frac{h - 1\,000}{100}\right)}{1 + \alpha\theta_{s.r}}\left(\frac{1}{A} + \frac{1}{B}\right) - \frac{P_{cs.r}\,\frac{r_{ac}}{r_s}\cdot\frac{\Delta t + 0{,}5\,\frac{h - 1\,000}{100}}{\theta_{per.r} - \theta_{a0}}}{A} < \theta_{per} \tag{20}$$

According to GOST 183-55 the effect of altitude on output is ignored when $h \leqslant 1000$ m. It is shown in GOST 183-55 that the rated data of electrical machines (output, voltage, current etc) apply to machine operating conditions at ambient temperatures up to + 35°C. At ambient temperatures up to 35°C GOST 183-55 specifies that for class A insulating materials the maximum permissible temperature rise in the windings be kept the same as at 35°C, but for more heat resistant insulating materials it should be increased correspondingly to the reduction in temperature, but not by more than 10°C.

In Russian conditions the ambient temperature on site varies on average between +15 to +35°C. Consequently, if the machine operates at the rated output corresponding to 35°C then the windings will in many cases be under-heated by 10 to 20°C. This signifies that the actual output provided by totally enclosed machines may be considerably different from rated output.

1960

If follows from (16) that ambient temperature has a greater effect on the output of a d.c. machine the lower the permissible temperature rise in the windings. Totally enclosed d.c. machines with class A insulation therefore frequently have excess capacity on site (when ambient temperature is low GOST generally provides for no increase in output).

For example, in the case of totally enclosed air-cooled machines running at a speed n = 1500 rev/min, the temperature rise in the armature windings in the no load state θ_{a0} = (10 to 40)°C. If the machine is insulated with class A materials, then at an ambient temperature of t = 15°C, its output from (16) will be

$$P_2 = (1{,}17 - 1{,}34) P_{2r},$$

where P_{2r} corresponds to output at 35°C.

Consequently, at an ambient temperature of t = 15°C the output of the stated machines can on average be increased by 17 to 34% (relative to rated output).

In the case of totally enclosed machines with speeds over 1500 rev/min, the output reserve is still higher at an ambient temperature of t = 15°C and in a number of cases reaches 40 to 50 per cent. Here, as has already been shown, the temperature rise in the parallel excitation winding will be below the permissible level. The rated output of totally enclosed d.c. machines and in the first instance that of high-speed machines with natural cooling can therefore be expediently given as a function of ambient temperature. For purposes of simplifi-

cation, just two or three temperatures can be fixed (15 and 35 or 15, 25 and 35°C), with appropriate rated outputs indicated in the machine certificate.

The proposed recommendations can be expediently extended to all totally enclosed d.c. machines independently of the class of insulation of the windings. The recommendations made in sect. 22 GOST 183-55 in reference to totally enclosed d.c. machines are clearly inadequate.

Conclusions

(1) In order to calculate the output of d.c. machines when ambient temperature and altitude vary it is enough to know the rise in the armature winding in the no load state (see equations 16 and 19). This can be ascertained by tests or from the curves in Figs. 2 and 3.

(2) It follows from equations (16) and (19) and Figs. 2 and 3 that changes in ambient temperature and altitude have a greater effect on permissible output the worse the cooling conditions, the higher the speed of rotation and the larger the dimensions of the machine.

Translated by O.M. Blunn

REFERENCES

1. L. Berger; *Deutsche Elektrotechnik*, No. 11, (1957).
2. N.A. Panfilov; *Thermal calculation of salient-pole d.c. machines (O teplovom raschete yavnopolyusnykh mashin postoyannogo toka). Vest. elektroprom.*, No. 8, (1958).

ELECTRO-MAGNETIC PHENOMENA IN FLAT INDUCTION PUMPS FOR MOLTEN METALS*

N.M. OKHREMENKO

Leningrad

(Received 14 August 1959)

1960

Electromagnetic pumps for molten metals have been employed in nuclear reactors with metallic heat carriers and may also be used in metallurgical and foundry production. Flat linear induction pumps are now very promising because of their simplicity in design, the possibility of supplying them from conventional three phase current sources and other considerations. The design of such pumps is schematically represented in Fig. 1.

The three phase winding 2, disposed on stator core 1, creates a travelling magnetic field which induces currents in the molten metal caught in neck 3. The pressure and movement of the metal in the direction of the x axis causes interaction between the travelling wave and the currents induced in the metal.

Pumps of this type have a number of special features compared with conventional type induction motors:

1. Large air gaps, up to several centimeters in large pumps, determine small inductions in the gap, increased electromagnetic loads for the inductor and large leakage fluxes. If the layer of molten metal is of a considerable thickness it is necessary to consider the demagnetization action of the currents in the metal.

2. The open state of the magnetic circuit and the shunting of the main magnetic flux by fluxes from the side, end and reverse surfaces of the inductor leads to the appearance of a pulsating field besides the travelling magnetic field. Such an effect, ("the longitudinal edge effect") has been studied in reference to electric motors in no load conditions (1). Methods have also been developed for the compensation

* *Elektrichestvo*, No.3, 48-55, 1960.

of the pulsating fields (9 and 10).

3. The end width of the layer of molten metal in the direction of the y axis causes components of current density to appear in the direction of the x axis (Fig. 2). These components are analogous to the currents at the front of electrical machines and take no part in the creation of useful forces. The elongation of the current line leads to a reduction in the useful current component in the direction of the y axis and to a considerable reduction in pressure. This phenomenon is known as the transverse edge effect and is observed in pumps which do not have longitudinal short circuiting bus-bars. Analytical (12) and experimental (5 and 7) investigations have been made into this effect for the case of a flat field in an air gap.

Electromagnetic pumps are still a young branch of engineering and theory has as yet to be developed. A number of investigations into electromagnetic pumps have been made in the U.S.S.R. at the Physics Institute of the Academy of Science in Latvia under the direction of Kirko and Tyutin (2-8). Vol'dek has made a considerable contribution to the theory of this type of machine (9-12). However, a large number of questions remain unexamined including: the calculation of the combined effect of the transverse and longitudinal edge effects and the de-magnetizing action of the currents in the metal on the loss of power and reduction in the pressure developed by the pump; the determination of the equivalent parameters of the secondary circuit etc. These works have not examined such questions in full. Neither were they linked by a single theory. Thus one-dimensional or two-dimensional problems were investigated and not three-dimensional problems. The present article makes an attempt to generalize the examination of electro-magnetic phenomena in flat pumps taking into account the transverse and longitudinal edge effects and the demagnetizing influence of the currents in the metal. The aim is to establish expressions for the pressure developed by the pump, the power loss and the equivalent parameters of the secondary circuit.

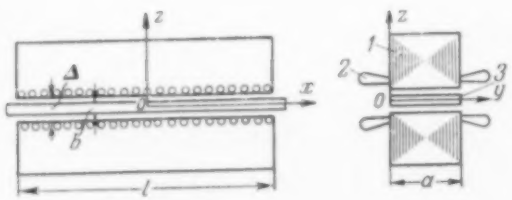

Fig. 1. Induction pump arrangement.

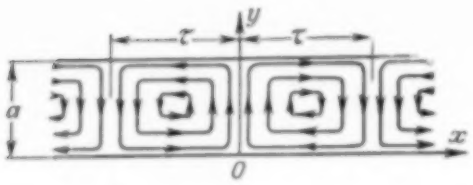

Fig. 2. Distribution of the currents induced in the molten metal.

Fundamental equations and their solution

The solution of the stated problems entails finding the vectors for the intensity of the electrical field $\mathbf{E} = F_1(x, y, z, t)$ and the magnetic induction $\mathbf{B} = F_2(x, y, z, t)$ which characterize the resultant electromagnetic field in the region of the molten metal provided that the normal component of magnetic induction is given on the surface of the inductor.

Make the following assumptions: (1) the magnetic permeability of the inductor steel is infinitely large whilst its surface is slotted; (2) the thickness of the layer of molten metal b equals the size of the air gap Δ; (3) the inductor winding only creates the basic m.m.f. harmonic; (4) the weakening of the magnetic field at the edges of the inductor compared with its value in the mid-part of the inductor can be ignored.

Given the turbulent flow conditions which are fundamental to induction pumps, considerable equalization occurs between the mean velocities across the channel section, whilst the large speed gradients only exist in a thin boundary layer (7 and 8). We can therefore assume for our purpose that the speed of flow is constant across the entire section of the channel. The enumerated assumptions are either close to reality or can be dropped later by introducing appropriate corrections.

The Maxwell system of equations for slowly moving live isotropic media can be written in the following form (8):

$$\mathbf{\delta} = \sigma \mathbf{E} = \sigma(\mathbf{E}^* + [\mathbf{vB}]); \tag{1a}$$

$$\operatorname{rot} \mathbf{B} = \mu_0 \mathbf{\delta}; \tag{1b}$$

$$\operatorname{rot} \mathbf{E}^* = -\frac{d\mathbf{B}}{dt}; \tag{1c}$$

$$\operatorname{div} \mathbf{B} = 0; \tag{1d}$$

$$\operatorname{div} \boldsymbol{\delta} = \sigma \operatorname{div} \mathbf{E} = 0; \tag{1e}$$

$$\mathbf{B} = \mu_0 \mathbf{H}, \tag{1f}$$

where δ, $\mathbf{B}$, $\mathbf{E}^*$ and $\mathbf{H}$ are the respective vectors of current density, magnetic induction and intensity of the electrical and magnetic fields in the region of the molten metal;

$\mathbf{E} = \mathbf{E}^* - (\mathbf{vB})$ is the " effective" intensity of the electrical field creating the conductance current;

v is the rate of flow of the metal;

σ is its electrical conductance;

$\mu_0 = 4\pi \cdot 10^{-7}$ (H/m).

Exclude δ and $\mathbf{E}^*$ from the first three equations in set (1), considering the conductance constant. Here we obtain

$$\nabla^2 \mathbf{B} = \mu_0 \sigma \left(\frac{\partial \mathbf{B}}{\partial t} - \operatorname{rot} [\mathbf{vB}] \right). \tag{2a}$$

In the case of a non-compressible fluid for which div $\mathbf{v}$ = o, considering that $\mathbf{v} = v_x$ = const and div $\mathbf{B}$ = 0, equation (2a) can be transformed into

$$\nabla^2 \mathbf{B} = \mu_0 \sigma \left(\frac{\partial \mathbf{B}}{\partial t} + v \frac{\partial \mathbf{B}}{\partial x} \right). \tag{2b}$$

Analogously, it can be found from (1a) that

$$\operatorname{rot} \mathbf{E} = - \left(\frac{\partial \mathbf{B}}{\partial t} + v \frac{\partial \mathbf{B}}{\partial x} \right). \tag{2c}$$

Equations (2b) and (2c) constitute a solvable system of equations.

The normal component of magnetic induction for the case when the air gap is of the order of several centimeters whilst the magnetic circuit is unsaturated, can be expressed in the following form (10):

$$B_N = B_m \sin (\omega t - ax) - (-1)^p B_{mc} \sin \omega t, \tag{3}$$

where

$$B_{mc} = k_c B_m; \quad \alpha = \frac{\pi}{\tau}; \quad k_c = \frac{\lambda_s}{1+\lambda_s};$$

B_m is the amplitude of induction in the travelling wave on the surface of the inductor;

$\omega = 2\pi f$ is the frequency;

τ is the pole pitch;

p is the number of pairs of poles;

λ_s is the ratio of the magnetic conductance of the shunting sections of the magnetic circuit to the magnetic conductance of the active zone in the air gap.

The quantities k_c and λ_s can easily be determined from test data (10). The first term in equation (3) determines the normal field travelling in the direction of the x axis (Fig. 1), whilst the second term determines the pulsating field caused by the open state of the magnetic circuit. If the rectangular induction wave is disposed along the x axis in a Fourier series according to the cosines with a period equal to twice the length of the inductor $2l$ and only its basic harmonic is considered, then equation (3) can be expressed as follows in complex form:

$$\begin{aligned} B_N = B_0 + B_1 + B_2 = B_m e^{j(\omega t - \alpha x)} - \\ -(-1)^p \frac{2}{\pi} k_c B_m e^{j(\omega t - \nu x)} - \\ -(-1)^p \frac{2}{\pi} k_c B_m e^{j(\omega t + \nu x)}. \end{aligned} \tag{4}$$

In equation (4) the pulsating field is in the form of the sum of two travelling fields: direct B_1 and reverse B_2, whilst ν equals

$$\nu = \frac{\pi}{l} = \frac{\pi}{2p\tau} = \frac{\alpha}{2p}. \tag{5}$$

Note that the synchronous speeds v_c and v_{cl} for adjusting fields B_0 and B_1 are different:

$$v_c = \frac{\omega}{\alpha} = 2f\tau; \quad v_{cl} = \frac{\omega}{\nu} = 2fl = 2pv_c. \tag{6}$$

The distribution of induction B_m in the direction of the y axis can also be described by a harmonic series with a period equal to twice the

width of the inductor 2a:

$$B_m = \frac{4}{\pi} B_m \sum_{n=1}^{\infty} \frac{1}{n} \sin \frac{n\pi}{a} y \quad (n = 1, 3, 5 \ldots). \tag{7}$$

For the time being let us only take the first harmonic in equation (7) into account. In this case the normal induction component on the surface of the inductor is:

$$\dot{B}_N = \dot{B}_0 + \dot{B}_1 + \dot{B}_2, \tag{8}$$

where

$$\dot{B}_0 = \frac{4}{\pi} B_m \sin \frac{\pi}{a} y e^{j(\omega t - \alpha x)}; \tag{9}$$

$$\dot{B}_1 = -(-1)^p \frac{8}{\pi^2} k_c B_m \sin \frac{\pi}{a} y e^{j(\omega t - \nu x)}; \tag{10}$$

$$\dot{B}_2 = -(-1)^p \frac{8}{\pi^2} k_c B_m \sin \frac{\pi}{a} y e^{j(\omega t + \nu x)}. \tag{11}$$

In view of the linearity of equations (2b) and (2c), let us make use of the superposition principle and consider the effect of each of the three induction components (9) to (11) separately. Assuming that all the electrical and magnetic magnitudes vary sinusoidally through time, let us utilize the symbolic method. First find the components of the "effective" intensity of the electrical field E_o and magnetic induction B_o caused by the existence only of a basic field (9). The unknown E_o and B_o will be found in the form

$$\dot{E}_0 = \dot{E}_{m0}(y,z) e^{j(\omega t - \alpha x)}; \tag{12a}$$

$$\dot{B}_0 = \dot{B}_{m0}(y,z) e^{j(\omega t - \alpha x)}. \tag{12b}$$

In complex form, equations (2a) and (2c) are re-written as follows:

$$\nabla^2 \dot{B}_0 = \mu_0 \sigma (j\omega \dot{B}_0 - j\alpha v \dot{B}_0) = j\mu_0 \sigma \omega s \dot{B}_0; \tag{13a}$$

$$\text{rot } \dot{E}_0 = -j\omega s \dot{B}_0. \tag{13b}$$

where

$$s = 1 - \frac{av}{\omega} = \frac{2f\tau - v}{2f\tau}. \tag{13c}$$

When the set of equations (13) has been solved, find the expressions for the components E_0 and B_0 along the x, y and z axes (solution given in appendix 1):

$$\dot{E}_{x0} = -j\frac{4\beta\omega s B_m}{\pi(\alpha^2+\beta^2)\operatorname{ch}\dot{\gamma}\frac{b}{2}}\cos\beta y\cdot\operatorname{ch}\dot{\gamma}z e^{j(\omega t-\alpha x)}; \tag{14}$$

$$\dot{E}_{y0} = \frac{4\alpha\omega s B_m}{\pi(\alpha^2+\beta^2)\operatorname{ch}\dot{\gamma}\frac{b}{2}}\sin\beta y\cdot\operatorname{ch}\dot{\gamma}z e^{j(\omega t-\alpha x)}; \tag{15}$$

$$\dot{E}_{z0} = 0; \tag{16}$$

$$\dot{B}_{x0} = -j\frac{4\alpha\dot{\gamma}B_m}{\pi(\alpha^2+\beta^2)\operatorname{ch}\dot{\gamma}\frac{b}{2}}\sin\beta y\cdot\operatorname{sh}\dot{\gamma}z e^{j(\omega t-\alpha x)}; \tag{17}$$

$$\dot{B}_{y0} = -\frac{4\beta\dot{\gamma}B_m}{\pi(\alpha^2+\beta^2)\operatorname{ch}\dot{\gamma}\frac{b}{2}}\cos\beta y\cdot\operatorname{sh}\dot{\gamma}z e^{j(\omega t-\alpha x)}; \tag{18}$$

$$\dot{B}_{z0} = \frac{4B_m}{\pi\operatorname{ch}\dot{\gamma}\frac{b}{2}}\sin\beta y\cdot\operatorname{ch}\dot{\gamma}z e^{j(\omega t-\alpha x)}. \tag{19}$$

In these equations:

$$\beta = \frac{\pi}{a}; \quad \dot{\gamma} = \varphi + j\psi; \tag{20}$$

$$\varphi = \sqrt{\frac{1}{2}\left[\sqrt{(\alpha^2+\beta^2)^2+(\mu_0\gamma\omega s)^2}+(\alpha^2+\beta^2)\right]}; \tag{21}$$

$$\psi = \sqrt{\frac{1}{2}\left[\sqrt{(\alpha^2+\beta^2)^2+(\mu_0\gamma\omega s)^2}-(\alpha^2+\beta^2)\right]}. \tag{22}$$

The current density components will equal

$$\dot{\delta}_{x0} = \sigma\dot{E}_{x0}; \quad \dot{\delta}_{y0} = \sigma\dot{E}_{y0}. \tag{23}$$

The weakening of the normal induction component in the middle of the layer of metal $B_\Delta = |\dot{B}_{x0}|_{z=0}$ in comparison with its value on the surface of the inductor is characterized by the relationship:

1960

$$\frac{B_{\Delta}}{B_{surf}}=\sqrt{\frac{2}{\operatorname{ch}\varphi b+\cos\psi b}}. \tag{24}$$

The pressure developed by the pump

Average pressure can be defined as

$$p_0=\frac{F_0}{S}, \tag{25}$$

where F_0 is the average value of the e.m.f. along the x axis through time;

S is the cross section of the pump neck.

Force F_0 is determined by the equation

$$F_0=\frac{l}{2}\int_{y=0}^{a}\int_{z=-\frac{b}{2}}^{\frac{b}{2}}\operatorname{Re}[\dot{\delta}_{y0}\dot{B}_{z0}]\,dy\,dz. \tag{26}$$

Thus

$$p_0=\frac{l\sigma}{2ab}\int_{0}^{a}\int_{-\frac{b}{2}}^{\frac{b}{2}}\operatorname{Re}[\dot{E}_{y0}\dot{B}_{z0}]\,dy\,dz, \tag{27}$$

where $\dot{B}_{z0}$ is a complex conjugate with complex $\dot{B}_{z0}$.

Substituting $\dot{E}_{y0}$ and $\dot{B}_{z0}$ into equation (27) and performing integration, the following expression can be produced for the pressure caused by the basic wave of the travelling field:

$$p_0=k_w k_s p_i. \tag{28}$$

In equation (28) P_i is the ideal value of the pressure developed by the pump in the absence of transverse and longitudinal edge effects and the de-magnetizing action of the eddy currents induced in the metal; k_w is the coefficient of weaking taking into account the reduction in pressure due to the transverse edge effect; k_s is the screening factor taking into account the decrease in pressure owing to the de-magnetizing action of the currents in the molten metal (" armature reaction"). In the MKSA system:

$$p_i=B_m^2\sigma f s l\tau\ [n/m^2]. \tag{29}$$

If all the quantities are expressed in the SGS μ_0 system and pressure in kg/cm^2, then

$$p_i = 1{,}02 B_m^2 \tau f s l \tau \cdot 10^{-15} \quad [\text{kg/cm}^2]; \tag{29'}$$

$$k_{oc} \frac{8}{\pi^2 \left[1 + \left(\frac{\tau}{a}\right)^2\right]} = \frac{0{,}81}{1 + \left(\frac{\tau}{a}\right)^2}; \tag{30}$$

$$k_s = \frac{\frac{\operatorname{sh} \gamma b}{\gamma b} + \frac{\sin \psi b}{\psi b}}{\operatorname{ch} \gamma b + \cos \psi b}. \tag{31}$$

If account is taken of spatial harmonics of the series (7), the following expression is produced for pressure:

$$p_0 = (k_w^{(1)} k_s^{(1)} + k_w^{(3)} k_s^{(3)} + k_w^{(5)} k_s^{(5)} + \\ + \ldots + k_{oc}^{(n)} k_s^{(n)} + \ldots) p_i. \tag{32}$$

The weakening factor decreases sharply with an increase in the order of the harmonic in the n series (7). For example:

$$k_w^{(n)} = \frac{8}{\pi^2 n^2 \left[1 + \left(\frac{n\tau}{a}\right)^2\right]}.$$

Therefore, in the case of pumps without short-circuiting bus-bars, a limit can only be set in equation (32) by the first term. If such bus-bars are present or else an infinitely wide channel ($a = \infty$), the screening factors do not depend on the order of the harmonic $k_w^{(n)} = \frac{8}{\pi^2 n^2}$ and instead of series (32) we have

$$p_0 = k_s p_i, \tag{33}$$

that is, without a transverse edge effect the weakening factor is unity, and not 0.81 as follows from formula (30) which determines k_w for the main harmonic in series (7). Note that in the special case of low metal conductance and frequency, when it can be supposed that $k_s^{(n)} = 1$, a formula can be produced by simple transformations from the series standing in brackets in expression (32) for the weakening factor obtained by Vol'dek [12, formula 19].

Ul'manis [5] experimentally produced a relationship for the magnitude

$k\triangle$, inverse to the weakening factor k_w:

$$k_\Delta = 1 + C\left(\frac{\tau}{a}\right)^2, \tag{34}$$

where C is the multiplier depending on frequency.

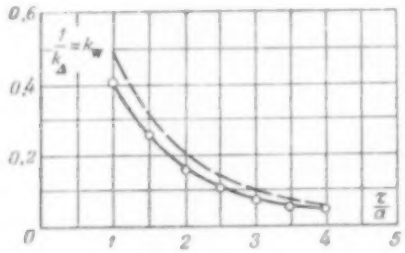

Fig. 3. Relationship $k_w = \frac{1}{k_\Delta} = f\left(\frac{\tau}{a}\right)$.

———— from Ul'manis' tests at 50 c/s;

-------- calculated from formula (34); 0 – points calculated from formula (30).

The values of this multiplier for the various frequencies are not given, but it is assumed to be unity for 50 c/s. The selected formula (34) turned out quite close to formula (30). The curve $k_w = f\left(\frac{\tau}{a}\right)$ (Fig. 3), calculated from formula (30), coincides exactly with the experimental curve produced by Ul'manis. This confirms the validity of the theoretical relationships produced.

The power transmitted to the molten metal

In order to detetmine the apparent power $\widetilde{S}$ transmitted to the metal, it is necessary to calculate the flow of the Poynting vector $\widetilde{P}$ through the closed surface of the pump neck. Since the components of the vector $\widetilde{P}$ are zero on all the planes of the neck except the plane $z = \pm\frac{b}{2}$, it is enough to determine this vector on the surface $z = \frac{b}{2}$:

$$\widetilde{P}_{z0}\Big|_{z=\frac{b}{2}} = \frac{\dot{E}_{x0}\mathring{H}_{y0} - \dot{E}_{y0}\mathring{H}_{x0}}{2}\Bigg|_{z=\frac{b}{2}}, \tag{35}$$

and then calculate the double value of the flow of this vector across

the surface in question:

$$\tilde{S}_0 = -2l \int_0^a [\tilde{H}_{z0}]_{z=\frac{b}{2}} dy = P_0 + jQ_0. \tag{36}$$

Here P_0 and Q_0 are the active and reactive power transmitted to the metal with the existence of the basic wave of the travelling field alone (9). The performance of the operations determined by formulae (35) and (36) will produce the magnitude of active power:

(37)

where k_w and k_s are determined by formulae (30) and (31) whilst P_i in the ideal value of active power transmitted to the metal in the absence of the transverse edge effect and the demagnetizing action of the eddy currents. In the SGSμ_0 system

$$P_i = \frac{v_s^2 B_m^2 gV}{2} \cdot 10^{-16} \quad [w], \tag{38}$$

where $V = abl$ is the volume of the metal;

$v_s = 2f\tau s$ is the rate of slip.

The reactive power can be determined in the same way:

$$Q_0 = k_w k_{sQ} P_i, \tag{39}$$

where

$$k_{sQ} = \frac{2(\varphi \operatorname{sh} \varphi b - \psi \sin \psi b)}{\mu_a g \omega s b (\operatorname{ch} \varphi b + \cos \psi b)}. \tag{40}$$

The active power transmitted to the metal can be presented as a known relationship:

$$P_0 = smE_1 I_2' \cos \psi_2 = mI_2'^2 r_2', \tag{41}$$

where m is the number of phases for the inductor;

E_1 and I_2' are the phase e.m.f. of the inductor and the secondary current applied to the stator;

r_2' is the resistance of the metal on the stator;

ψ_2 is the angle of shift between E_1 and I_2'.

The following expression can be obtained from equality (41):

$$I_2' = \frac{k_w B_m l \tau}{\pi \sqrt{2} m w_1 k_{w1} \mu_0} \sqrt{\frac{(\varphi^2 + \psi^2)(\operatorname{ch} \varphi b - \cos \psi b)}{\operatorname{ch} \varphi b + \cos \psi b}}. \tag{42}$$

When determining I_2' it was supposed that

$$E_1 = 2\sqrt{2} w_1 k_{w1} f B_m \tau a,$$

where w and k_{w1} are the number of successively connected turns in the phase of the stator winding and the winding factor,

and that

$$\cos \psi_2 = \frac{P_0}{\sqrt{P_0^2 + Q_0^2}} = \frac{\psi \operatorname{sh} \varphi b + \varphi \sin \psi b}{\sqrt{(\varphi^2 + \psi^2)(\operatorname{ch}^2 \varphi b - \cos^2 \psi b)}}. \tag{43}$$

Using equations (41) and (42) we obtain:

$$r_2' = \frac{2m (w_1 k_{w1})^2 a \mu_0 \omega s (\psi \operatorname{sh} \varphi b + \varphi \sin \psi b)}{k \omega d (\varphi^2 + \psi^2)(\operatorname{ch} \varphi b - \cos \psi b)}. \tag{44}$$

The inductive resistance of the molten metal is

$$x_2' = r_2' \frac{Q_0}{s P_0} = r_2' \frac{\varphi \operatorname{sh} \varphi b - \psi \sin \psi b}{s(\psi \operatorname{sh} \varphi b + \varphi \sin \psi b)}. \tag{45}$$

The longitudinal edge effect in the secondary circuit

Until the present time the influence of the longitudinal edge effect on the pressure of the pump was only taken into account by empirical coefficients (5 and 6), whilst the power losses caused by this effect were not considered. It is therefore of practical interest to determine the necessary relationships. To do this it is necessary to find the components of the vectors for the intensity of the electrical and magnetic fields in the metal caused by inductances $\dot{B}_1$ and $\dot{B}_2$.

First determine slip s_1 and s_2, caused by the fields $\dot{B}_1$ and $\dot{B}_2$. Substituting $\pm \nu$ in place of a in equality (13c) we find:

$$s_1 = 1 - \frac{1 - s}{2p}; \quad s_2 = 1 + \frac{1 - s}{2p}. \tag{46}$$

The expressions obtained differ from slips

$$S' = S \text{ and } S'' = 2 - S, \tag{47}$$

which obtain in induction motors when a pulsating field appears. This difference is explained by the fact that the pulsating field which arises for example when the phase is broken in an induction motor, has the same number of poles as a rotating field. In the case of machines with an open magnetic circuit the pulsating field under consideration has a different character. As regards it and its components $\dot{B}_1$ and $\dot{B}_2$, the inductor is one pole $l = 2p\tau$ in length. This determines the difference in the synchronous speeds of movement of waves $\dot{B}_0$ and $\dot{B}_1$ and their slips.

The slips which have been defined in accordance with equalities (46) with magnitudes $S = 0.35$ to 0.8 are close to unity in induction pumps and are all practically the same, especially when the number of poles is large. This has a favourable effect on pressure, but considerable power losses occur from the pulsating field. Since the boundary conditions remain as before, the unknown quantities for the intensity of the electrical field and magnetic induction and their arguments can be

1960

produced from equations (14) to (22) by substituting

for $B_m \pm \nu$ for α and S_1 and S_2 for S. For example the component $\dot{E}_{y1}$, caused by induction $\dot{B}_1$, will equal

$$\dot{E}_{y1} = -(-1)^p \frac{8\nu}{\pi^2(\nu^2+\beta^2)} \times$$

$$\times \frac{\omega s k_c B_m}{\operatorname{ch} \dot{\gamma}_1 \frac{b}{2}} \sin \beta y \operatorname{ch} \dot{\gamma}_1 e^{j(\omega t - \nu x)}.$$

Pressure p_1 caused by the direct travelling wave $\dot{B}_1$ is produced by substituting the values $\dot{E}_{y1}$ and $\dot{B}_{z1}$ into equation (27):

$$p_1 = k_c^2 p \frac{s_1}{s} k_{w1} k_{s1} p_i, \tag{48}$$

where

$$k_{w1} = \frac{\left(\frac{8}{\pi^2}\right)^2}{1+\left(\frac{l}{a}\right)^2} = \frac{0{,}656}{1+\left(\frac{2p\tau}{a}\right)^2} \tag{49}$$

is the weakening factor for the pressure caused by the inductance $\dot{B}_1$, whilst k_{s1} is determined from formula (31) with S_1 substituted for S.

ϕ_1 for ϕ and ψ_1 for ψ. The magnitude of p_1 is determined from formula (29). The pressure caused by the reverse travelling wave for induction B_2, will equal:

$$p_2 = -k_c^2 p \frac{s_2}{s} k_{w1} k_{s2} p_i. \tag{50}$$

Since $s_2 > s_1$, the reverse travelling wave will fade to a greater extent with a change in the co-ordinate z than the direct field. Therefore the resulting pressure caused by the pulsating field will be negative. Since s_1 and s_2 are close, then on calculation of the resulting pressure it can be supposed that $k_{s1} \approx k_{s2}$. In this case the counter-pressure caused by the longitudinal edge effect will equal

$$p_{rev} = p_1 + p_2 = -\frac{1-s}{s} k_c^2 k_{w1} k_{s2} p_i. \tag{51}$$

It is deduced from comparison of formulae (30) and (49) that the transverse edge effect will weaken counter-pressure to a considerably greater extent than useful pressure. If there is no transverse edge effect counter-pressure increases and the full pressure which can be developed by the pump becomes equal to

$$p_z = \left(k_{oc} k_y - \frac{1-s}{s} k_c^2 k_{w1} k_{s2}\right) p_i \tag{52}$$

If good conducting bus-bars are present along the faces of the channel it is necessary to put $k_y = k_{w1} = 1$ into equation (52).

The use of equations (35) and (36) make it possible to produce the following expressions for output transmitted to the metal because of the pulsating field $\dot{B}_1 + \dot{B}_2$:

$$P_p = \left(\frac{2pk_c}{s}\right)^2 \left[1 + \left(\frac{1-s}{2p}\right)^2\right] k_{w1} k_{s2} P_i; \tag{53}$$

$$Q_p = \left(\frac{2pk_c}{s}\right)^2 \left[1 + \left(\frac{1-s}{2p}\right)^2\right] k_{w1} k_{sQ2} P_i. \tag{54}$$

In these equations it is supposed that $k_{s1} \approx k_{s2}$ and $k_{sQ1} \approx k_{sQ2}$.

The total outputs transmitted to the secondary circuit by the basic and pulsating fields are determined by the relationships:

$$P = P_0 + P_p; \quad Q = Q_0 + Q_p. \tag{55}$$

The secondary current applied and the resistance with or without the presence of the longitudinal edge effect are found on the basis of equality (41) when P_0 therein is replaced by P.

Conclusion

The proposed problems can be considered solved. The method and results can also be used for solving analogous problems in the field of electrical machines.

Appendix II compares experimental data obtained from (Ref. 7) with pressure and output calculated from formulae (28) to (31) and (37) to (38). The theoretical quantities are in satisfactory agreement (with an accuracy of up to 5 to 15 per cent).

Appendix I. Solution of a system of equations (13). It is required to solve the set of equations:

$$\nabla^2 \dot{B}_0 = j\mu_0 \sigma \omega s \dot{B}_0; \tag{A1}$$

$$\text{rot}\, \dot{E} = -j\omega s \dot{B}. \tag{A2}$$

After transformation we have

$$\nabla^2 \dot{E}_0 = j\mu_0 \sigma \omega s \dot{E}_0. \tag{A3}$$

Substitution of equation (12a) into equation (A3) gives

$$\frac{\partial^2 \dot{E}_{m0}}{\partial y^2} + \frac{\partial^2 \dot{E}_{m0}}{\partial z^2} = \dot{\lambda}^2 \dot{E}_{m0}, \tag{A4}$$

where

$$\dot{\lambda}^2 = \alpha^2 + j\mu_0 \sigma \omega s. \tag{A5}$$

Solving equation (A4) by dividing the variables we find expressions for the E_{m0} components along the x, y and z axes.

$$\dot{E}_{mx0} = (A_1 \cos \beta y + B_1 \sin \beta y)(C_1 \operatorname{ch} \dot{\gamma} z + D_1 \operatorname{sh} \dot{\gamma} z); \tag{A6}$$

$$\dot{E}_{my0} = (A_2 \cos \beta y + B_2 \sin \beta y)(C_2 \operatorname{ch} \dot{\gamma} z + D_2 \operatorname{sh} \dot{\gamma} z); \tag{A7}$$

$$\dot{E}_{mz0} = (A_3 \cos \beta y + B_3 \sin \beta y)(C_3 \operatorname{ch} \dot{\gamma} z + D_3 \operatorname{sh} \dot{\gamma} z). \tag{A8}$$

The parameters β and γ are connected with λ by the relationship

$$-\beta^2 + \dot{\gamma}^2 = \dot{\lambda}^2 \tag{A9}$$

and determined together with the integration constants A, B, C and D.

To do this use is made of the following limiting conditions:

(1). The current density component on the surface of the metal normal to it when $y = 0$, $y = a$ and $z = \pm \frac{b}{2}$ is determined by the expression:

$$\dot{\delta}_N = \sigma \dot{E}_N = 0. \tag{A 10}$$

(2). When $z = 0$, the tangential induction components are zero:

$$\dot{B}_x|_{z=0} = 0; \quad \dot{B}_y|_{z=0} = 0. \tag{A11}$$

(3). On the surface of the metal when $z = \pm \frac{b}{2}$ the normal induction component is continuous and equal to its value on the surface of the inductor, which can be determined by equation (9).

It follows directly from an examination of the limiting conditions (A10) that $\dot{E}_{mz0} = 0$; $A_1 = 0$; $\sin \beta y = 0$ (or $\beta_n = \pm \frac{n\pi}{a}$).

As we are limited by the examination of only the first harmonic inequation (7), we suppose that $n = 1$. From the two values of β (positive and negative), in view of the presence of arbitrary constants in equations (A6) and (A7) it is enough to take the positive alone. Therefore

$$\beta = \frac{\pi}{a}.$$

Supposing in equation (A7) that $A_2 = 0$ and denoting $B_2 C_2 = M_2$ and $B_2 D_2 = N_2$, we obtain

$$\dot{E}_{my0} = (M_2 \operatorname{ch} \dot{\gamma} z + N_2 \operatorname{sh} \dot{\gamma} z) \sin \beta y.$$

In order to determine M_2 and N_2 let us use conditions (A11). First find the induction component of the resulting field along the x axis from equation (A2):

$$\dot{B}_{mx0} = -\frac{j}{\omega s} \cdot \frac{\partial \dot{E}_{my0}}{\partial z} =$$

$$= -\frac{j\dot{\gamma}}{\omega s} (M_2 \operatorname{sh} \dot{\gamma} z + N_2 \operatorname{ch} \dot{\gamma} z) \sin \beta y.$$

Utilizing equations (A11) we find that $N = 0$. Then

$$\dot{E}_{y0} = M_2 \sin \beta y \operatorname{ch} \dot{\gamma} z e^{j(\omega t - \alpha x)}. \tag{A13}$$

$$\dot{B}_{x0} = -\frac{j\dot{\gamma}}{\omega s} M_2 \sin \beta y \operatorname{sh} \dot{\gamma} z e^{j(\omega t - \alpha x)}. \tag{A14}$$

It follows from the law of the continuity of the current div $E = 0$, that

$$\frac{\partial \dot{E}_x}{\partial x} = -\frac{\partial \dot{E}_y}{\partial y}.$$

Thus

$$B_1 = 0; \; D_1 = 0;$$
$$M_1 = A_1 C_1 = -j \frac{\beta}{\alpha} M_2.$$

Therefore

$$\dot{E}_{x0} = -j \frac{\beta}{\alpha} M_2 \cos \beta y \operatorname{ch} \dot{\gamma} z e^{j(\omega t - \alpha x)}. \tag{A15}$$

1960

Determine $\dot{B}_{y0}$ and $\dot{B}_{z0}$:

$$\dot{B}_{y0} = \frac{j}{\omega s} \cdot \frac{\partial \dot{E}_{x0}}{\partial z} = \frac{\beta \dot{\gamma}}{\alpha \omega s} M_2 \cos \beta y \operatorname{sh} \dot{\gamma} z e^{j(\omega t - \alpha x)}, \tag{A16}$$

$$\dot{B}_{z0} = \frac{j}{\omega s} \left(\frac{\partial \dot{E}_{y0}}{\partial x} - \frac{\partial \dot{E}_{x0}}{\partial y} \right) =$$
$$= \frac{\alpha^2 + \beta^2}{\alpha \omega s} M_2 \sin \beta y \operatorname{ch} \dot{\gamma} z e^{j(\omega t - \alpha x)}. \tag{A17}$$

Using the third limiting condition find the constant M_2:

$$M_2 = \frac{4 \alpha \omega s B_m}{\pi (\alpha^2 + \beta^2) \operatorname{ch} \dot{\gamma} \frac{b}{2}}. \tag{A18}$$

The parameter γ is found from relationship (A9):

$$\dot{\gamma} = \sqrt{\alpha^2 + \beta^2 + j \mu_0 \sigma \omega s} = \varphi + j\psi, \tag{A19}$$

where

$$\varphi = \sqrt{\frac{1}{2} \left[\sqrt{(\alpha^2 + \beta^2)^2 + (\mu_0 \sigma \omega s)^2} + (\alpha^2 + \beta^2) \right]}; \tag{A20}$$

$$\psi = \sqrt{\frac{1}{2} \left[\sqrt{(\alpha^2 + \beta^2)^2 + (\mu_0 \sigma \omega s)^2} - (\alpha^2 + \beta^2) \right]}. \tag{A21}$$

Appendix II. Comparison of experimental and theoretical results.

The test data (7) characterize the turbulent flow of mercury under the action of a travelling magnetic field in a model of an infinitely long channel where there is no longitudinal edge effect. Compare test results with theory. From Ref.7, for example, test No.3 gives $a = 8.4$ cm, $b = 0.775$ cm, $\tau = 9.87$ cm, $f = 50$ c/s and $k_\Delta = 2.90$.

Using the relationships in Figs. 3 and 4 in reference to test No.3 we find that the effective value of induction $B = 245$ G ($B^2 = 6 \times 10^4 G^2$) is produced at a pressure of $p = 8.18 \times 10^3$ dyn/cm^2 and average speed $v = 33$ cm/sec.

Calculate slip from equality (13c):

$$s = \frac{2f\tau - v}{2f\tau} = \frac{2 \cdot 50 \cdot 9.87 - 33}{987} = 0.966$$

and the consumption of metal per second

$$Q' = abv = 8.4 \cdot 0.775 \cdot 33 = 215 \text{ cm}^3/\text{sec}.$$

We assume the conductance of the mercury equal to

$$s = 1.015 \cdot 10^4 \text{ 1/ ohm.cm}.$$

The length of the channel

$$l = 2p\tau = 4 \cdot 9.87 = 39.5 \text{ cm}$$

The volume of metal in the channel

$$V = abl = 8.4 \cdot 0.775 \cdot 39.5 = 257 \text{ cm}^2.$$

Dividing equality (37) by equality (28) we have

$$\frac{P_e}{P_0} = 2f\tau sab = Q' \frac{s}{1-s}.$$

Consequently, the power transmitted to the molten metal during the experiment is

$$P_e = p_0 Q' \frac{s}{1-s} \cdot 10^{-7} = 8.18 \cdot 10^3 \times$$

$$\times 215 \frac{0.966}{1-0.966} \cdot 10^{-7} = 5.00 \text{ W}.$$

The weakening factor is found from formula (30):

$$k_w = \frac{0.81}{1 + \left(\frac{\tau}{a}\right)^3} = \frac{0.81}{\left(\frac{9.87}{8.4}\right)^3} = 0.342.$$

Calculate the necessary quantities to determine k_s:

$$a = \frac{\pi}{\tau} = \frac{\pi}{9,87} = 0,3185;$$

$$\beta = \frac{\pi}{a} = \frac{\pi}{8,4} = 0,374;$$

Substituting these quantities into equations (21) and (22) we find

$$\varphi = 0,493 \text{ 1/cm}; \ \psi = 0,0394 \text{ 1/cm};$$
$$\varphi_b = 0,382; \ \psi_b = 0,0305.$$

The screening coefficient is found from formula (31):

$$k_s = \frac{\frac{\sinh \varphi b}{\varphi b} + \frac{\sin \psi b}{\psi b}}{\cosh \varphi b + \cos \psi b} = \frac{\frac{0,389}{0,382} + \frac{0,0305}{0,0305}}{1,074 + 0,999} = 0,977.$$

The theoretical value of the pressure is calculated in accordance with equations (22) and (29):

$$p_t = k_w k_s B_m^2 z f s l \tau \cdot 10^{-9} = 0,342 \cdot 0,977 \cdot 12 \cdot 10^4 \cdot 1,015 \times$$
$$\times 10^4 \cdot 50 \cdot 0,966 \cdot 39,5 \cdot 9,87 \cdot 10^{-9} = 7,63 \cdot 10^5 \text{ dyne/cm}^2$$

The error in the calculation for pressure:

$$\Delta p = \frac{p_e - p_t}{p_e} \cdot 100 = \frac{(8,18 - 7,63) \cdot 10^5}{8,18 \cdot 10^5} \cdot 100 = 6,5\%.$$

The theoretical value of the output transmitted to the metal from equations (37) and (38) will be

$$P_t = k_w k_s \frac{(2f\tau s)^2 B_m^2 z l V \cdot 10^{-16}}{2} =$$
$$= \frac{0,342 \cdot 0,977}{2} (987 \cdot 0,966)^2 \cdot 12 \cdot 10^4 \cdot 1,015 \times$$
$$\times 10^4 \cdot 257 \cdot 10^{-16} = 4,75 \text{ W}.$$

The error in the power calculation is

$$\Delta P = \frac{P_e - P_t}{P_e} \cdot 100 = \frac{5 - 4,75}{5} \cdot 100 = 5,0\%.$$

The error in the determination of pressure and power loss in tests Nos. 2, 4 and 5 lies within the limits of 15 per cent.

1960

Thus, comparison of experimental and theoretical data is satisfactory.

Translated by O.M. Blunn

REFERENCES

1. G.I. Shturman; *Elektrichestvo*, No.10, (1946).
2. I.M. Kirko; *The modelling of magneto-hydrodynamic phenomena in molten metals (O modellirovanie magnitogidrodinamicheskikh iavlenii v zhidkikh metallakh). Prikład. Magnitogidrodinam. Trud. inst. fiz. Akad. Nauk Lat. S.S.R.* No.VIII (1956).
3. I.A. Tiutin; *Introduction to the theory of induction pumps, (Vvedenie v teoriu induktsionnykh nasosov), Priklad. magnitogidrodinam. Trud. inst. fiz. Akad. Nauk Lat. S.S.R.* No.VIII (1956).
4. I.A. Tiutin and E.K. Iankop; *Electromagnetic processes in induction pumps for molten metal, (Elektromagnitnye protsessy v induktsionnykh nasosakh dlia zhidkogo metalla). Priklad. magnitogidrodinam. Trud. inst. fiz. Akad. Nauk Lat. S.S.R.* No.VIII (1956).
5. L.Ia. Ul'manis; *Edge effects in linear induction pumps, (K voprosu o kraevykh e'ffektakh v lineinykh induktsoinnykh nasosakh), Priklad. magnitogidrodinam. Trud. inst. fiz. Akad. Nauk Lat. S.S.R.* No.VIII (1956).
6. Ia.Ia. Lielpeter and I.A. Tiutin; *Method of designing induction pumps for molten metal, (Metodika rascheta induktsoinnykh nasosov dlia zhidkogo metalla). Priklad. magnitogidrodinam. Trud. inst. fiz. Akad. Nauk Lat. S.S.R.* No.VIII (1956).
7. I.M. Kirko, Ia.Ia. Kliavin, I.A. Tiutin and L.Ia. Ul'manis; *Energetika*, No.3, (1958).
8. I.M. Kirko; *Electrichestvo*, No.4, (1959).
9. A.I. Vol'dek, F.Ia. Vil'iamial', Kh.V. Sillamaa and Kh.A. Tiismus; *Experimental investigation into magnetic fields in induction machines and pumps for molten metals with open magnetic circuits, (Eksperimental'noe issledovanie issledovanie magnitnykh polei v induktsionnykh mashinakh i nasosakh dlia zhidkikh metallov s razomknutym magnitoprovodom), Trud. Tallinsk. politekh. inst., seriya A.* No.131, (1958).
10. A.I. Vol'dek; *Elektromekh. i avtomat.*, No.3, (1959).
11. A.I. Vol'dek; *Elektromekhanika*, No.12 (1958).
12. A.I. Vol'dek; *Elektromekhanika*, No.1 (1959).

A SCHEME FOR TESTING LARGE HIGH VOLTAGE VALVES*

G.I. POLIAK and V.G. GOLIATIN

Leningrad

(Received 14 July 1958)

One of the greatest difficulties in the solution of d.c. transmission problems is the development of large high voltage valves. In this connexion it is a matter of prime importance that new valves can only be developed if appropriate test schemes are available. Such schemes can only fulfil their purpose if the actual operating conditions of the valves can be reproduced both as regards the normal and fault states.

The " synthetic" schemes now in use cannot be regarded as the complete answer from this point of view since the power processes taking place in their circuits are very far from actual operating conditions.

The stated schemes comprise two circuits; namely, current and voltage circuits. The purpose of the current circuit consists in reproducing the necessary magnitude and shape of the current curve, whilst the voltage circuit creates the desired rate of increase in the magnitude and shape of the voltage for the valve on test, this voltage here being applied directly after the basic current has passed through zero. The principle underlying the construction of synthetic schemes prevents them from doing this.

The voltage in these schemes can only be applied a little while after the current has passed through zero, determined by the recovery speed of the controlling properties of the divider valve. The current necessary for charging the high voltage capacitor passes through the test valve at this moment. To illustrate this, Fig. 1 shows a syn-

---

* *Elektrichestvo*. No. 3, 73-74, (1960).

synthetic scheme* which operates in the following manner.

A large current of low voltage is passed through two series-connected test valves (1 and 2). The current is switched from valves 1 and 2 to an auxiliary low voltage valve 3 at a definite moment before the current passes through zero in order to produce a steeper drop in current. Valve 5 is opened at the same time. The half-wave of current is passed through valve 1 from the oscillating circuit CL_3 C_1. The parameters of this circuit are so chosen that the duration of the current pulse is sufficient to de-ionize valve 2. When valves 1 and 5 are extinguished the voltage on capacitor C_1 changes sign as a result of overcharging. The entire voltage of capacitor C_1 is therefore applied to valves 1 and 2 via auxiliary valve 6. This voltage is reversed in the case of valve 1 and forward in the case of valve 2; i.e. the first will be tested in the rectifier state and the second in the inverter state.

It is clear from this description that the operating conditions of the valves in the converter installation are considerably different from the state produced in a similar type of synthetic scheme. In view of this it is natural that research has been carried out to improve these schemes. One such scheme is described below.

Fig.2 shows the scheme of a test installation in which unlike synthetic schemes, the voltage which naturally arises in the high voltage converter scheme is supplied to the test valve. Thanks to this test conditions which are sufficiently close to reality can be produced at relatively low outputs in the high voltage circuit.

The installation comprises three circuits: a high voltage circuit *(A)* for which use may be made of an experimental d.c. transmission on a specially constructed high voltage low output converter bridge; a current circuit *(B)* which is the source of the load current for the test valve and an oscillating circuit *(C)*.

Test valve 1 is connected in two circuits: the high voltage circuit and current circuit. Currents caused by the two circuits flow through it successively. Valve 4 is a divider and is intended to separate the high voltage circuit from the current circuit at the time when the voltage in the high voltage circuit is applied to the test valve.

In order that the divider valve should fulfil its purpose its strength characteristic should recover completely at the moment when the test valve is extinguished. This is possible if the divider valve is extinguished before the test valve so that it has the necessary

---

* Proposed by V.G. Goliatin, Auth.Cert. No.103424, dated 6 June 1949.

time to recover its controlling properties. If only two circuits are present (current and voltage) the scheme under consideration is analogous to the test scheme for six-phase valves proposed by I.D. Shkolin*. In this scheme the de-ionization of the divider valve was ensured by the earlier completion of commutation in the current circuit. In this form the scheme with two circuits is unsuitable for testing large high voltage valves, since the steepness of the current drop in the test valve after ignition of the divider valve, determined only by the parameters of the high voltage circuit, is somewhat less than the steepness of the current drop in normal operation.

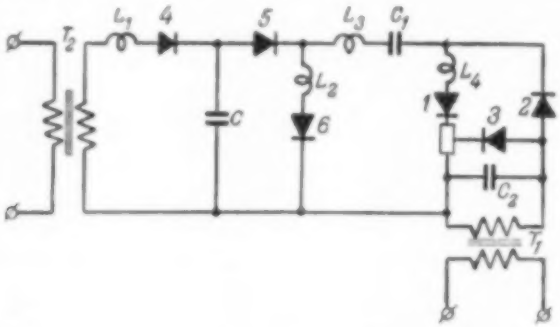

Fig. 1. Synthetic scheme for testing large valves.

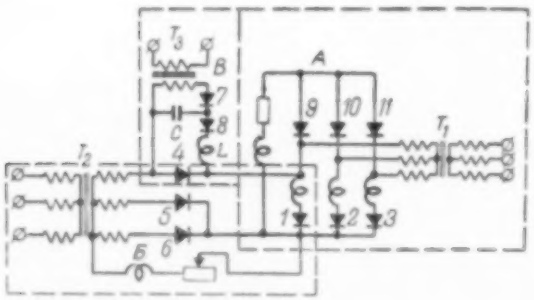

Fig. 2. Test plant with three circuits for large valves.

As regards the parameters of the voltage circuit, they should be such that the high frequency processes taking place on the ignition and extinction of the valves are reproduced. From this point of view even the existing experimental d.c. transmission could produce quite satisfactory results.

*Auth. Cert. No. 34072, dated 22 October 1932.

The addition of an oscillating circuit to the two circuits mentioned above makes it possible to reproduce the operating conditions of the valve both as regards voltage and current. The oscillating circuit, as shown in Fig. 2, consists of charge and discharge parts. The capacitor C is charged for some of the period via the controllable valve 7 from transformer T_3. When valve 8 opens capacitor C begins to discharge through inductance L and valve 4. The discharge is of a periodic nature, and thanks to the presence of valves in the discharge circuit, it lasts one half-period and has the shape of a pulse. The duration and amplitude of the current pulse should be such that the necessary time is allowed for the de-ionization of the divider valve to take place. In normal conditions with all the circuits in operation the scheme works in the following manner.

The operating conditions of the current and high voltage circuits are so set that commutation is completed in them all simultaneously. At this time valve 8 is closed. Valve 8 opens at appropriate moment of time when the current passing through the test valve is switched in the current and high voltage circuits to the next valves in turn. The discharge current of capacitance C which arises here flows counter to the current in the divider valve 4. This is extinguished before commutation is finished in the stated circuits and extinguishes the test valve 1. Thus the necessary time is ensured for de-ionization of the divider valve valve 4. For reliable extinction of valve 8 it is necessary that the voltage on the capacitor after overcharge be equal to or greater than the voltage in the high voltage circuit.

In order to clarify the principle underlying the extinction of divider valve 4, it can be shown by means of the oscillating circuit that in the case in question a new commutation circuit is in effect formed in which the voltage of the charged capacitor C is commutating and there transfers the anode current from the divider valve 4 to the auxiliary valve 8. Owing to the large inductance in the load circuit of the current circuit the magnitude of the anode current remains practically independent of the connexion of the oscillating circuit.

Typical oscillograms of the scheme's performance are given in Figs. 3 to 5 to clarify the principle underlying the operation of the scheme.

Fig. 4 presents curves for the current and voltage at the divider valve. Voltage curve U_p (Fig. 4), immediately after the extinction of the divider valve, reveals a small segment of a curve which represents the reverse voltage for de-ionizing the divider valve. The forward voltage from the high voltage circuit is applied immediately after it.

The rate at which the anode voltage increases and the oscillation processes which take place when the test valve is extinguished may vary slightly if the moment is altered at which the discharge pulse is completed. However, all that has been said above refers in equal measure to tests on valves in the inverter state.

Fig. 3. Current and voltage curves on test valve.

Fig. 4. Current and voltage curves on divider valve.

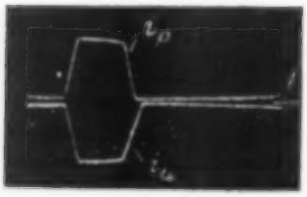

Fig. 5. Currents in test and divider valves.

The scheme under consideration makes it possible to test valves not only in normal conditions but also in the presence of faults provided that grid control is appropriately fulfilled so that a fault in the high voltage circuit would automatically cause a synthetic fault state in the current circuit.

Translated by O.M. Blunn

ABSTRACTS FROM PAPERS PUBLISHED IN ELEKTRICHESTVO NO. 3, 1960

Using electronic analogue computers for studying transients in electric systems: I.A. Gruzdev and M.L. Levinshtein. (pp 1-14).

A study is made of the possibilities of a certain type of mathematical modelling using computers and an attempt is made to elucidate those specific features which arise when solving power system problems. After considering the main elements of the machines and the conditions which they must satisfy the authors quote examples of the use of analogue computers. It is shown that these machines cannot be used for all likely problems. Their most rational field of application is considered to be where there is wide variation in the parameters of the elements of the system and its non-linear characteristics when the scheme itself is not very complex. He stresses the need for improving the elements of these machines and the elaboration of more rational methods of solving equations and, especially equations in partial derivatives. It is held to be equally important to analyse the stability of structural solution schemes containing many linear and non-linear deciding elements. 29 References.

A high-speed differential relay protection using semiconductors: G.T. Grek. (pp 14-20).

A study is made of differential protection on rectified currents with electrical braking from the aperiodic component of the differential current and reacting devices in the form of d.c. relays (polarized or moving coil) which can be connected either to the output from a comparison scheme direct or via a d.c. amplifier. Such protection can be given in such a way that a number of the parameters will be better than the corresponding parameters of differential protection with magnetic braking. Here protection can be given with one reacting device for three phase objects. Selectivity, high speed operation and sensitivity are assured. The use of d.c. sensitive relays as the reacting device connected directly or via an amplifier to the semiconductors makes its possible to reduce protection requirements.

Approximate account of additional hydro-electric generator torque components in appraising transmission system transient stability: G.B. Chernikov. (pp 25-29)

A mathematical study is made of pulsating rotating moments (braking) on the shaft of a synchronous machine and their effect. In the presence of comparatively "close" short circuits it is considered necessary to take this braking action into account in calculations for dynamic stability of transmission with particular reference to the Lenin Volga hydro-electric station.

Magnetic flux distribution and the commutating field in machines having all or half the commutating poles: I.Z. Ageev. (pp 38-43)

In machines operating in a greatly weakened field the main field is strengthened because of the longitudinal component of armature reaction, the asymmetry of the field and the additional poles of the commutating sections and this leads to distortion of the operating characteristics. Besides dealing with the general theory of additional poles, a detailed study is made of the magnetic flux distribution in systems with all or half the number of additional (commutating) poles and a method is given for determining the additional poles and plotting the resulting and commutating fields with an increased number of poles.

Determining the optimum dimensions of a transformer: P. Kyul'ovskii and Kh. Kukushev. (pp 43-48)

A more practical method is proposed for determining the optimum dimensions of a transformer so as to obtain the desired no load current more easily. Given the quality of the steel and the losses in the no load current the specific electromagnetic loads can easily be determined for the calculations. The calculations are based on m-phase transformers with m windings mounted on their cores. The windings are concentric with the same height and number of turns. An example of the method is given.

Natural oscillations in a coil: L. Genov. (pp 55-59)

The author begins by reviewing published works dealing with the theory of over-voltages in transformers and the importance of free oscillations in coils with steel cores. A formula is proposed for calculating the frequency of free oscillations in coils with steel cores, Maxwell equations being used to calculate the mutual inductance between the

1960

turns analytically. The distribution of the current along the length of the coil is taken into account when calculating the magnetic field in the " window" of the core.

A three-wire supply scheme for trolley buses: V.E. Rosenfel'd, V.N. Popelyash and A.G. Smirnov. (pp 60-64)

The author appraises the efficiency of the three-conductor power supply system for trolley buses on the basis of three years research in the Kaluga faculty of " Electrical Transport", the Moscow Power Institute and the " Giprokommundortrans" Institute. Extensive tables are given which show that the three-conductor system is far superior to the two-conductor system.

Calculating rail circuits when accounting for station tracks: D.B. Lomazov. (pp 64-67)

The presence of station tracks on electrified railway lines leads to the reduction of transient resistance from rails to earth, an increase in stray currents and a reduction in the resistance of the whole railway circuit. In order to make the calculations, this heterogeneous rail circuit is replaced by an equivalent circuit-cell scheme and the analytical calculation compared with experimental data. It is recommended that the laying of additional rail " threads" in the inter-track space be abolished as it leads to an increase in stray currents and a waste of material.

Maximum power conditions in a circuit containing a non-linear element: M.E. Syrkin. (pp 68-72)

Certain devices, for example a zero sequence current transformer, have to operate in maximum power conditions when the load, connected in series (parallel) to the device and fed from an e.m.f. (current) source, is such that maximum possible power is generated in it in the circuit with the device in question at the given e.m.f. and variable load. The characteristic of the device is usually non-linear and a study is made of the maximum power conditions in circuits with non-linear elements which are limited by d.c. circuits. Deductions are made which are approximately true for purely reactive (active) circuits containing sinusoidal e.m.f. or current sources (if the harmonics arising due to the non-linearity of the circuit are ignored).

The interdependence of the physical properties of polymers: N.I. Vorob'ev. (pp 75-76)

An attempt is made to establish a relationship between certain physical properties of polymers; namely, the relationships between density and "glassing" temperature, the modulus of elasticity and " glassing" temperature and the coefficient of linear expansion and " glassing" temperature. The majority of physical properties here depend on intermolecular forces which also determine the field of application of the polymers.

Errors of galvonometers in integrating: L.A. Biber. (pp 77-81)

An investigation has been made at the All-Union Electrical power scientific-research Institute into reactions to impulses and the errors of " integrating" galvonometers under the influence of high and low frequency pulses of different shape. An attempt is made to establish the conditions which " integrating" galvonometers must satisfy for the correct reproduction of pulse processes.

Improving the traction characteristics of a.c. electromagnets: P.M. Vaisburd. (pp 82-83)

In order to change the drawing characteristic of an electromagnet without altering the design of the magnet, the author describes three ways of improving the drawing characteristics of a.c. electromagnets: by increasing the supply voltage, rectifying the supply current and the use of ferro-resonance.

ABSTRACTS FROM PAPERS PUBLISHED IN ELEKTRICHESTVO No. 4 1960

Lenin and all-out electrification of the U.S.S.R: I.A. Syromiatnikov. (pp 1-6)

The paper relates Lenin's plans for the electrification of the U.S.S.R. and briefly traces the development of electrification in the U.S.S.R. from 1917 to the present time. The long term plans for the next 20 years are also considered. These do not necessarily exclude the development of atomic power stations. The article is in commemoration of Lenin's birthday 90 years ago.

A method for investigating dynamic stability on analogue computers: V.S. Tarasov, A.I. Vazhnov, IU.V. Rakitskii, V.V. Popop and L.N. Semenova. (pp 7-12).

A method is proposed for using an LPI computer for investigating transient processes in two synchronous machines operating in parallel with a network of infinite power via concentrated resistances. It is assumed that the effect of the active resistance of the stator circuits and the transient processes caused by this resistance can be ignored. The study is made of non-salient pole synchronous machines having a rotor with two symmetrical windings along the *d* and *q* axes, a non-saturated magnetic circuit and variable excitation. The author advocates the design of specialized analogue computers.

Electronic excitation for machines in the main drive of reversing rolling mills: M.Ia. Pistrak and L.M. Balabuev. (pp 13-20).

A study is made of the use of ionic converters instead of dynamoelectric amplifiers for the excitation of d.c. machines in connection with the development of control systems for the drives of blooming and slabbing mills. It is claimed that industrial service has demonstrated the advantages of the ionic converters as described.

A low-inertia motor drive for excavators: M.I. Kraitsberg, D.A. Kaminskaya and V.P. Lomakin. (pp 26-30)

Owing to the frequent shock loads encountered when the bucket strikes an immovable obstacle the authors describe a generator-motor drive system with dynamoelectric control incorporating continuous voltage and current feedbacks with cut-off and a stabilizing transformer. Provision is made for two-stage extinction of the generator magnetic field when the command controller is set in the zero position. A special feature is the additional resistance which is connected in series with the generator excitation winding in order to reduce the electromagnetic time constant of the generator. Stabilization is increased by a ballast resistance connected in parallel with the armature of the amplifier. It is claimed that the proposed scheme prolongs service life, reduces the number of breakdowns, and though costly, is more efficient. A smaller transmission ratio is advocated.

Calculating a.c. machine transients using frequency characteristics: E.Ia. Kazovskii. (pp 30-37)

The mathematical relationships underlying the use of frequency methods for the theory of synchronous machines are given. Frequency characteristics are defined as the experimentally determined dependence of the mean stator current on the slip of the rotor for a non-excited 150 MW turbo-generator of 3000 rev/min connected to a power network as a motor. Such relationships have been produced in the All-Union Electrical Engineering Institute. A study is only made of the case of stator symmetry. Only transient processes are considered at a constant speed, no account being taken of machine saturation. Methods are proposed for determining the frequency characteristics according to transient processes and using the frequency characteristic in the event of a three phase short circuit and for the case when the machine is connected to the network.

The differential equations for a synchronous generator in transient stability studies on analogue computers: B.N. Kagan and E.L. Urman. (pp 37-42)

A study is made of the use of automatic digital computers (ATSVM type). An improvement is required in the mathematical description of transient processes in synchronous machines and other power system elements as well as the development of new methods of investigation. The results are given of an investigation with a digital computer carried out to elucidate the effect on the theoretical limit to dynamic stability in the first cycle of charges in various factors (saturation, damper

system transformer e.m.f.'s induced in the stator windings etc.).

Special performance characteristics of heavily loaded transmission lines: G.M. Sekhniashvili. (pp. 42-46)

A method is proposed for investigating the conditions of heavily loaded transmission lines which can reveal the physical state of the lines and solve problems connected with the establishment of optimum operating conditions, that discovery of cheap methods of improving conditions and the determination of the requirements as regards automatic equipment. The method takes into account the active resistance of the transmission line conductors.

The error and applicability of formulae for specific permeances: B.K. Bul'. (pp. 51-57)

The accuracy with which a magnetic circuit with an air gap can be calculated mainly depends on the accuracy with which the permeance of the field of " swelling" can be determined. This is often impossible as the field is three-dimensional. An investigation has therefore been made into the flux between the side surfaces of the poles with different gaps. The permeance due to field " swelling" is held to be dependent on the ratio of the pole width to the size of the gap. The limits are given within which the Evershed, Roters, Cramp and Colderwood, Finnis and Slivinskii formulae are valid. The "Forb" and Schmidel formulae are not recommended.

The " near-cathode strength" of the a.c. arc is then studied. Extinction of an open arc. A.S. Maikopar. (pp. 64-69)

In order to avoid disconnecting the fault section when an open arc is formed due for instance to mechanical damage to cables, a study is made of the conditions for independent arc extinction. Difficulties arise however due to the tendency for the discharge column to turn into a spiral. After reviewing earlier investigations the author describes the tests carried out and the investigation made into arcs between metallic electrodes corresponding to arcs arising in high voltage equipment.

Theory of current and voltage stabilizers. S.D. Dodik. (pp. 73-77).

Current and voltage stabilizers in the presence of small changes in

current and voltage are represented as a linear multi-pole for which a set of equations can be produced, this set of equations being re-writable in matrix form. This method of analysis is developed and relationships produced suitable for investigation into any type of system of current and voltage stabilizer. Examples of the calculation are given.

A new type of small metal-varnish capacitor; V.T. Renne (pp. 77-81)

The widespread use of semiconductor instruments has reduced the voltage at which capacitors operate to the order of tens of volts and below so that the specific volume of capacitors is reduced because of the thinner dielectric. Earlier attempts to use varnished film failed since weak points could not be eliminated. An account is given of new methods used in Western countries where use is made of a coating in the form of very thin layers of metal (less than 0.1 micron thick) which are applied to the surface of the dielectric by vaporization in vacuum. In the event of puncture the layer of metal about the weak point melts and vaporizes.

ABSTRACTS FROM PAPERS PUBLISHED IN ELEKTRICHESTVO No. 5, 1960

An analytical method for determining the dynamics of d.c. electro-magnets: A.K. Ter-Akopov (pp. 1-5)

A study is made of the method of finding a formula for the movement time of the armature which would not only take into account the basic parameters of the magnet but also make it possible to determine the optimum inductance for the minimum time of movement. Experimental investigation was carried out on an E-shaped magnet made of sheet electrical steel gauge 0.35 mm. The appropriate measures were taken to conform to the theoretical assumptions. Theoretical times were not more than 15 to 18% greater than the test values. The existence of an optimum production force for the minimum time of movement is established.

The effect of corona on voltage surges in transmission lines: G.N. Aleksandrov (pp. 6-13).

Formulae are produced illustrating the relationship between the corona discharge effect on overvoltages on the one hand and the parameter of the line and the transient processes in them on the other. Surges under the influence of corona are lower, the greater the amplitude of the voltage compared with the initial corona voltage and the smaller the radius of the conductors and the equivalent frequency of the transient process.

An improved scheme for exciting the arc in mercury-arc valves: V.M. Mantrov. (pp. 13-15)

In order to reduce the power consumption of the constantly burning excitation arc and simplify the excitation system, the author proposes a modernized arc excitation system for mercury arc rectifiers. This system is diagramatically represented. With positive polarity at the auxiliary anode (1) an arc arises between it and the cathode and a half-wave of current passes through a reactor. When the current in the reactor drops an e.m.f. is induced and anode (2) is ignited. Conse-

quently the second half-period of current in the excitation circuit flows at the expense of the power reserved in the reactor. In subsequent periods the current in anode (1) circuit increases at the expense of the current of the previous half-period, which also increases with the growth of the maximum of current passing through the reactor.

How economic factors affect the parameters of networks with a distributed load: A.A. Derkach and V.M. Sin'kov (pp. 15-22)

An attempt is made to find a method which would be free of all assumptions or technical or economic limitations and could be used to solve equations linking the various forms of expenditure on the equipment and operations of electrical networks in order to ascertain the optimum radii at 1 to 3 degrees of voltage, the voltage losses at each degree of voltage and the economic current density.

Electromagnetic pumps for molten metals: A.I. Voldek (pp. 22-28)

The paper surveys the method and theory of electromagnetic pump design particularly in view of their growing value for nuclear reactors. Distinguishing conduction and induction pumps the author describes and discusses d.c. pumps, single phase a.c. pumps, cylindrical linear induction pumps, spiral induction pumps with rotating inductors and refers to other types of electromagnetic " pressure pumps" and mixers.

Variable-polarity excitation of synchronous condensers for reactive power consumption performance: N.I. Sokolov (pp. 28-31).

The reactive power of a synchronous machine depends on the excitation current or the e.m.f. proportional to it for a synchronous resistance, the voltage at the terminals and angle of rotor shift (δ) relative to voltage. After considering the operating conditions of compensators when $\delta \neq 0$, the author considers the regulation of a synchronous compensator under angles of rotor shift when $\delta \neq 0$ by a simple regulator under the conditions of reactive power consumption. The utilization of synchronous compensators is increased by 30 to 60%.

Excitation systems for variable-frequency induction motors: A.T. Golovan and I.M. Kruglianskii (pp. 31-36).

As no method has as yet been published for selecting the circuit and

calculating the parameters of synchronous self-exciting machines working as variable frequency generators, and the possibility of regulating frequency without switching the capacitor has still to be elucidated, the chair of Electrical Equipment for Industrial Undertakings at the Moscow Power Institute has made a special study of these problems. It is claimed that smooth frequency variation can be produced over a wide range. Generator efficiency is increased at low frequencies by lowering the speed of the drive motor. Capacitors for the excitation of 1.7 kW machines is 450 to 500 μ F with maximum range of regulation. The use of a low frequency machine as generator with a low secondary voltage is not advocated. The generator should have a slightly smaller active resistance in the rotor winding than the usual asynchronous motor.

Calculation of commutating flux rise for suddenly applied loads: V.A. Iakovenko (pp. 36-39).

Simplified methods are proposed for calculating the increases in the commutation flow based on the fact that the load current of a d.c. machine varies very slowly. Good agreement is obtained with experimentally found values.

Grid control of mercury arc rectifiers by means of half-wave magnetic amplifiers: S.S. Roizen (pp. 39-45)

The introduction of such highly productive equipment as reversing rolling mills makes special demands on electrical drives as regards operating speed and control accuracy. The use of a magnetic amplifier with an internal feedback for simultaneously creating a steep front of the networks voltage and displacing this front enables a grid control system to be developed with a delay time which does not exceed several periods of the supplying voltage. There is however a limited range of variations in the ignition angle and the width of the trigger pulse is variable. The single phase scheme is given special attention.

Calculation of the commutation reaction magneto-motive force in d.c. machines for brush overlapping (sparking) greater than unity: V.V. Fetisov (pp. 46-50)

To calculate the transient states in d.c. machines and design dynamolectric amplifiers (amplidynes) it is necessary to calculate the commutation reaction of the armature. This is considered very complicated owing to the complex physical phenomena of the commutation process. After criticizing various other methods the author proposes a method of

calculation for commutation with brush sparking considerably greater than unity which is suitable for usual values of brush sparking in any type of armature winding. Two examples of the method are given.

On electromagnetic calculations on d.c. machines which account for the cooling of their windings: N.A. Panfilov (pp. 50-54)

When the electromagnetic parameters of d.c. machines are selected the magnetic flux usually corresponds to the saturated state of the magnetic system and the permissible temperature rise in the windings does not always ensure that the output of the machine is optimum. Here the author considers the determination of the optimum magnetic flux the deciding factor. Criteria are produced for evaluating the output or temperature rise in the windings of d.c. machines in which the magnetic system is optimum.

Derivation of the integral equations for non-linear circuits using operational calculus: M.M. Glinzburg (pp. 54-58)

The calculation of steady and transient processess in circuits containing non-linear elements is facilitated by relating the mathematical operations involved in calculating both the linear and non-linear elements in the scheme under consideration to the non-linear part of the scheme alone. Two examples of the method are given: one example applies to the steady state of a valve generator and the other to the dynamic stability of a system with three generator stations.

Calculation of the current in an R-L circuit with half-wave rectification: A.I. Glukharev, L.A. Foigel and N.B. Gelman (pp. 58-60).

In view of the practical difficulties involved in analytically calculating the mean value of the rectified current when an active inductive resistance is present in the circuit for the use of single half-period rectification, the authors deduce a simpler analytical dependence of the current on the magnitude and relationship between the active resistance and inductance. The method is directly applicable to long distance transmission systems with an inductive converter when the signal is registered by a magneto-electric (moving coil) meter (logometer).

The electrical and physical properties of electrical insulating materials when subjected to radioactive radiation:

K.A. Vodopianov, B.I. Vorozhtsov, G.I. Potakhova and N.I. Ol' shanskaia (pp. 60-66)

The experimental data are given of a study of the effect of gamma-rays on the electrical and physical characteristics of high polymar dielectrics, silicone-organic and phenoformaldehyde plastics.

Atransistorized d.c. transducer with internal magnetic stabilization: M.E. Poiurovskii (pp. 66-70).

An analysis is made of the performance and design of a converter with magnetic stabilization which ensures effective stabilization of the output voltage and frequency. The power losses in the feedback circuits reduce its efficiency but not significantly.

Thermo-resistor KMT-14: A.L. Burkin, O.N. Filippova and I.T. Sheftel' (pp. 71-73)

An account is given of newly developed Soviet KMT-14 type thermal resistances capable of operating at temperatures up to 300°C.

Designing cooling systems for transistors: S.I. Fedorov (pp. 73-76)

A mathematical study is made of additional heat dissipation in the industrial use of triodes. The use of novel radiator shapes other than plates is duscussed. The anodizing method of producing ferrous plates is advocated in place of varnishes and paints. Lead foil 80 to 100 μ thick is applied to increase the area of contact between radiator and triode.

Non-linear capacitors using Rochelle salt materials: M.M. Nekrasov (pp. 76-79)

A tertiary Rochelle salt non-linear electrical system is discussed which is claimed to combine high dielectric permeability, negative capacitive change with applied voltage and low dielectric losses.

1960

A REVERSING SCHEME FOR AUTOMATIC SPEED CONTROL USING ELECTROMAGNETIC POWDER CLUTCHES*

T. A. GLAZENKO

(Leningrad)

(Received 7 August 1959)

The linearity of the performance characteristics of electromagnetic powder clutches (EPC), low excitation power, the large values of the maximum possible accelerations in the system (with a small flywheel torque on the driven part of the clutch) and the small size and light weight testify to the expediency of using EPC in automatic control systems.

This paper will introduce certain control schemes and study problems connected with the calculation of the static and dynamic characteristics for reversing systems of speed control using EPC.

Operating characteristics and the equation for the torque of the EPC

Powder clutches in follow-up systems and automatic control systems work almost entirely in the state of slip.

The dependence of the torque on the magnetic flux (or induction) in the air gap of the clutch, taken under conditions of relative movement of the working surfaces (operating characteristic) is to a certain extent rather complicated owing to the mechanical hysteresis of the working mixture.

If no excitation current is present in the clutch winding on the shaft of the executive mechanism, a no load torque M_0 is transmitted. In non-reversing systems of speed control, the zone of insensitivity of

* *Elektrichestvo*, No.4, 21-26, 1960.

the drive caused by the static resistance moment M_s on the load shaft can be considerably reduced by the appropriate choice of initial current in the excitation winding of the powder coupling. In EPC reversing systems the choice of clutch, initial current and the appropriate flux (Φ_0) can considerably improve the linearity of the relationship $M = f(\Phi)$.

In this case we can assume that

$$M = C_M \Phi, \tag{1}$$

where $\Phi = \Phi_M - \Phi_0$;

Φ_M is the magnetic flux in the clutch;

Φ_0 the magnetic flux caused by the initial quiescent current in the excitation winding of the coupling.

If the coefficient taking into account the extent to which the cavity of the clutch is filled with iron is greater than 0.35 and no movement of the filler particles takes place between the gaps, the variation in torque will take place simultaneously with the variation in the magnetic flux in the clutch.

The increase in voltage at the terminals of the excitation circuit of the clutch will be

$$U = \frac{r_M}{w_M \lambda}\left[\Phi + T_M \frac{d\Phi}{dt}\right], \tag{2}$$

where w_M is the number of turns in the excitation winding of the clutch;

λ the coefficient of proportionality between the flux and the resulting m.m.f. in the excitation winding of the clutch;

r_M the resistance in the circuit of the excitation winding of the clutch;

The equivalent time constant of the clutch (T_M) can be calculated in accordance with Fridlider (1) or determined experimentally from oscillograms of current variation in the clutch winding.

Taking expressions 1 and 2 into account, we produce an equation for the torque transmitted by the EPC reversing block on the driven shaft:

$$U \frac{\lambda C_M w_M}{r_M} = M + T_M \frac{dM}{dt}.$$

1960

The quantity

$$\frac{\lambda C_M w_M}{r_M} = k_M,$$

measured in kg. cm/V can be called the coefficient of clutch amplification.

If no additional resistance is introduced into the clutch circuit, then

$$r_M = \frac{w_M^2 l_{av}^2}{\gamma V_M},$$

where l_{av} is the average length of a turn in the excitation winding of the clutch;

V_M the volume of copper in the excitation winding;

γ the specific conductance of the winding material.

In this the amplification factor of the powder clutch is

$$k_M = \frac{C_M \lambda V_M \gamma}{w_M l_{av}^2}.$$

Thus, in order to increase the amplification factor, it is worthwhile to design the clutch for a comparatively large control current, a small number of turns, the smallest possible average length of turn in the excitation winding and the maximum possible magnetic conductance in the magnetic circuit.

Block-diagram of EPC reversing system

Fig. 1 shows the main circuit for an EPC reversing system for controlling the speed of rotation of the executive mechanism.

As is known (2 to 5), the torque of powder clutches does not depend on the relative speed of its working surfaces. It is therefore necessary to introduce a speed feedback into the system to ensure that the speed of the executive mechanism is stable when the static resistance moment is constant.

The control voltage U_y is taken from the master potentiometer and compared with the tacho-generator voltage (U_{tg}), which is proportional to the speed of the executive mechanism (ω). The difference between these voltages (U_x) is supplied to the excitation winding of one or

another clutch.

The excitation voltage is switched from the winding of one clutch to the winding of another by a relay, electronic "keys" (switches) on the installation of two divider diodes in the excitation circuits of the EPC. The change in polarity or change in phase of the input voltage (in a.c. systems) can act as the signal for switching.

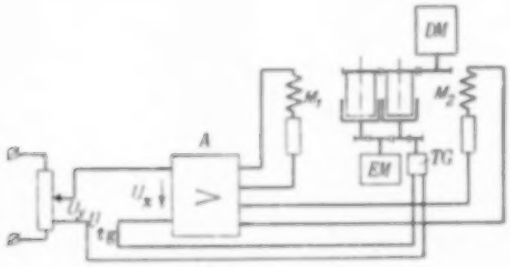

Fig. 1. Main circuit of reversing equipment with EPC for controlling the speed of the executive mechanism: *DM* - drive motor; *EM* - executive mechanism; *TG* - d.c. or a.c. tachometer generator; M_1 and M_2 - excitation windings in the first and second powder clutches; *A* - general amplifier.

The excitation winding of the clutch can be connected in the arm of the output balance cascade of an amplifier, based on electronic valves or semiconductor triodes. In order to reduce losses due to slip in the clutches in the absence of a control signal, the output cascades of such equipment should be so tuned that the minimum quiescent (rest) current is present in the excitation winding of the clutch.

If this requirement is satisfied the sensitivity of the amplifier will often be reduced when the signals are small. It is therefore sometimes expedient to provide an additional winding in the clutch, connected counter to the main winding and neutralizing the magnetic flux created by the quiescent current in the amplifier scheme.

If the system is designed for alternating current (voltages U_y and U_{tg} vary with the same frequency), then the phase sensitive amplification cascade with the differentially connected load can act as the output link.

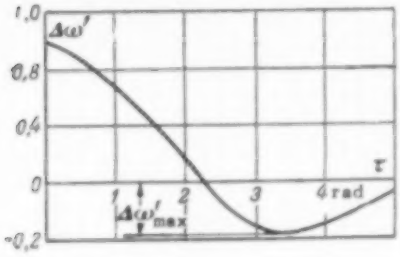

Fig. 2. Variation in the relative deviation in the speed of the output shaft when $\sigma = 0.3$ and $\frac{d\Delta\omega'}{d\tau}(0) = 0$.

Investigation into a system with abrupt changes in the master effect

The equations for the individual links of a system with an electronic amplifier have the form:

$$\left.\begin{aligned} U_{\text{в}} &= U_y - U_{\text{tg}}; \\ U_{\text{tg}} &= C_e\omega; \\ U &= k_{\text{в}}U_{\text{в}}; \\ k_{\text{м}}U &= M + T_{\text{м}}\frac{dM}{dt}; \end{aligned}\right\} \qquad (3)$$

$$M = J\frac{d\omega}{dt} + M_{\text{в}} \text{ when } M > M_{\text{в}}.$$

The steady speed of the output shaft is

$$\omega_y = \frac{U_y}{C_e} - \frac{M_{\text{в}}}{k_{\text{м}}C_e k_{\text{в}}} = \omega_0 - \Delta\omega_{\text{в}}, \qquad (4)$$

where $\omega_0 = \frac{U_y}{C_e}$ is the speed when $M_{\text{в}} = 0$;

$\Delta\omega_{\text{c}}$ the absolute static control error.

The total amplification factor of the system is

$$k = k_{\text{м}}C_e k_{\text{в}} = \frac{\lambda C_{\text{м}}\omega_{\text{м}}C_e k_{\text{в}}}{r_{\text{м}}}. \qquad (5)$$

The moment of the clutch with a speed feedback is

$$M_0 = \frac{\lambda C_M C_e w_M k_a}{r_M} \frac{U_y}{C_e} = k\omega_0.$$

It follows from the set of equations(3) that the variation in the speed of the load shaft appropriate to an increment in the resistance moment of ΔM_s equals, in operator form:

$$\Delta\omega(p) = -\frac{\Delta M_s (1 + pT_M)}{(p^2 T_{eM} T_M + pT_{eM} + 1)k}.$$

The electromechanical constant of the block of the powder clutches load

$$T_{eM} = \frac{Jr_M}{C_M k_a C_e w_M \lambda} = \frac{J}{k} \qquad (6)$$

1960

is determined by the total moment of inertia applied to the shaft of the clutches by the reversible part of the drive, by the parameters of the magnetic and electrical circuits of the clutch, (λ, w_M, r_M), by the properties of the working mixture (C_M), by the coefficient of amplification (k_a) and by the constant of the tachogenerator (C_e).

Introducing relative units:

$$\omega' = \frac{\omega}{\omega_0}, \quad m = \frac{M}{M_0}$$

$$\text{and } m_s = \frac{M_s}{M_0},$$

we obtain an equation for the system in the form:

$$T_M T_{eM} \frac{d^2\omega'}{dt^2} + T_{eM} \frac{d\omega'}{dt} + \omega' = 1 - m_s. \qquad (7)$$

The relative control error in the steady state is

$$\frac{\Delta\omega}{\omega_0} = \frac{\omega_0 - \omega}{\omega_0} = m_s.$$

Passing to relative deviations from the steady speed

$$\Delta\omega' = \omega'_y - \omega',$$

we obtain

$$\frac{d^2\Delta\omega'}{dt^2}+\frac{1}{T_M}\frac{d\Delta\omega'}{dt}+\frac{\Delta\omega'}{T_M T_{eM}}=0, \tag{8}$$

The roots of the characteristic equation of the system

$$p_{1,2}=-\frac{1}{2T_M}\pm\sqrt{\frac{1}{4T_M^2}-\frac{1}{T_{eM}T_M}}= \\ =-\delta\pm\sqrt{\delta^2-\beta_0^2}. \tag{9}$$

The coefficient of attenuation $\delta=-\frac{1}{2T_M}$ is determined by the time constant of the clutch.

The angle frequency of non-fading fluctuation in the system

$$\beta_0=\frac{1}{\sqrt{T_{eM}T_M}}=\sqrt{\frac{C_e C_M k_a w_M \lambda}{Jr_M T_M}}. \tag{10}$$

If the angle $\tau=\beta_0 t$ in radians is introduced into equation 8 in place of time t as an independent variable, the equation of the system will assume the form:

$$\frac{d^2\Delta\omega'}{d\tau^2}+2\sigma\frac{d\Delta\omega'}{d\tau}+\Delta\omega'=0, \tag{11}$$

where $$\sigma=\frac{1}{2}\sqrt{\frac{T_{eM}}{T_M}}=\frac{1}{2}\sqrt{\frac{Jr_M}{C_M k_a C_e w_M \lambda T_M}}$$

is the extent to which the system is made quiescent (damped).

The tuning of a quick-acting system of automatic speed control is usually carried out in conditions of oscillation damping, i.e. when $\sigma<1$.

The law of the variation of the relative deviation of speed from its steady value is determined by the initial values of the speed $\Delta\omega'(0)$ and acceleration $\frac{d\Delta\omega'}{d\tau}(0)$ and depends on the degree of damping (Fig. 2)

$$\Delta\omega'=Ae^{-\sigma\tau}\sin\left[(\sqrt{1-\sigma^2})\tau+\varphi\right], \tag{12}$$

where

$$A=\frac{\Delta\omega'(0)}{\sin\varphi};$$

$$\tan\varphi=\frac{\Delta\omega'(0)\sqrt{1-\sigma^2}}{\frac{d\Delta\omega'}{d\tau}(0)+\sigma\Delta\omega'(0)}.$$

In order to reduce the time of the transient process in the system, the derivative influence from the signal at the input can be introduced

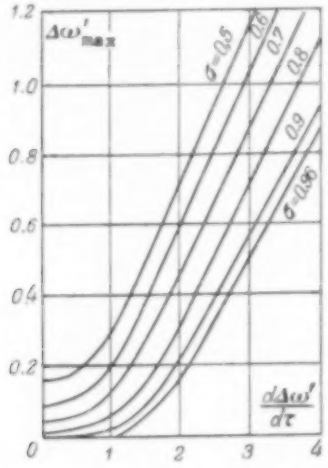

Fig. 3. Maximum over-regulation in a system with EPC

On introducing a differentiating element

$$U_x = U_y - C_e\left(\omega + k_d \frac{d\omega}{dt}\right)$$

and

$$\sigma = \frac{1}{2}\left(1 + \frac{k_d}{T_{em}}\sqrt{\frac{T_{em}}{T_M}}\right). \tag{13}$$

At large initial accelerations in the system (in reverse), the permissible value of the maximum over-regulation $\Delta\omega'_{max}$ (which is usually given) is a factor limiting the decrease in the magnitude of σ.

It can be shown that the angle $\tau_{max} = \beta_0 t_{max}$, corresponding to the maximum over-regulation, equal to

$$\tau_{max} = \frac{\pi + \varphi_0 - \varphi}{\sqrt{1-\sigma^2}},$$

where

$$\varphi_0 = \tan^{-1}\frac{\sqrt{1-\sigma^2}}{\sigma}.$$

Consequently

$$\Delta\omega'_{max} = \Delta\omega'(0)\frac{\sin(\pi-\varphi_0)}{\sin\varphi}\,e^{-\left(\frac{\pi+\varphi_0-\varphi}{\tan\varphi_0}\right)}. \qquad (14)$$

Use may be made of the curves in Fig. 3 for convenience in choosing the optimum values of k_d and σ at given initial accelerations and permissible values of over-regulation.

The operation of the system when a sinusoidal voltage is supplied at the input

$U_y = U_{ym} \cdot \sin qt.$

In this case the drive is influenced by two disturbing forces: the sinusinusoidal voltage of the input signal

$$u'_y = \frac{U_y}{U_{ym}} = \sin qt$$

and the function of the relative static resistance moment $m_s(t)$ which periodically varies in sign as the direction of rotation changes (Fig. 4).

The equation of the system in relative units

$$\sin qt + m_c(t) = T_M T_{eM}\frac{d^2\omega'}{dt^2} + T_{eM}\frac{d\omega'}{dt} + \omega'$$

is true when $\pi n + \psi < qt < \pi n + \psi + \lambda$,
where $n = 0, 1, 2, \ldots$

The solution of this equation when $n \to 0$

$$\omega' = \frac{\sin\left[qt - \tan^{-1}\dfrac{2\sigma\dfrac{q}{\beta_0}}{1-\left(\dfrac{q}{\beta_0}\right)^2}\right]}{\sqrt{\left[1-\left(\dfrac{q}{\beta_0}\right)^2\right]^2 + 4\sigma^2\left(\dfrac{q}{\beta_0}\right)^2}}. \qquad (15)$$

In order to reduce the amplitude and phase of the errors in the drive, it is necessary that the following conditions be observed $q \ll \beta_0$ and $\sigma = 0.5$ to 0.7.

The effect of the resistance moment on to the output shaft consists in that the speed of the output shaft ceases to be a sinusoidal function of time, since the disturbing effect in this case is a complex periodical function (Fig. 4).

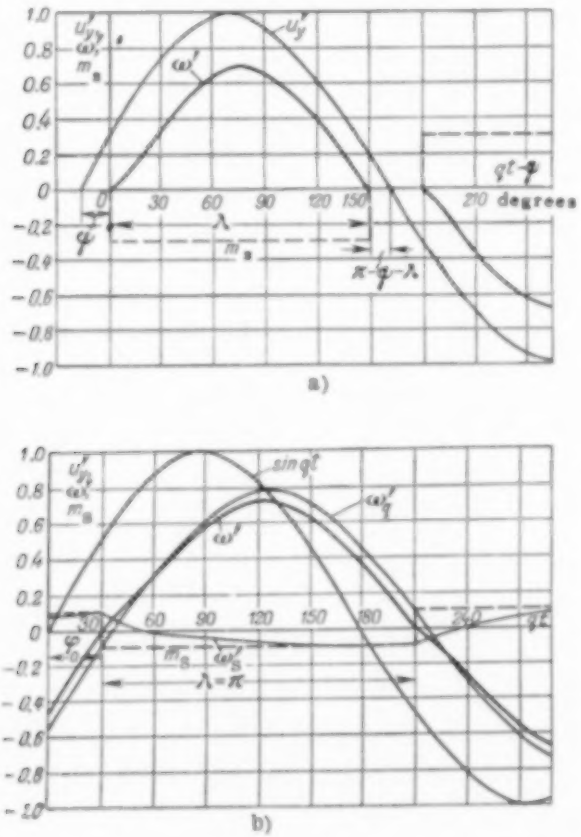

Fig. 4. Variations in speed of the output shaft in the presence of a sinusoidal variation in the signal at the input:
(a) - drive operated with intermittent stops of the output shaft:
$T_{em} = 0.025$ sec; $f = 0.5$ c/s; $a_s = 0.3$;
(b) - drive operated continuously
$T_{em} = 0.025$ sec; $f = 5$ c/s; $a_s = 0.1$.

Linear systems of automatic control can be calculated with friction taken into account by the superposition method. In this case

$$\omega' = \omega'_q + \omega'_s,$$

where ω'_q is the component of the relative speed of the output shaft caused by the action of the controlling voltage and

ω'_s the component of the relative speed of the output shaft due to the moment $m_s(t)$.

The angle between the disturbing influences sin qt and $m_s(t)$ is determined on the basis that when $qt = \phi_0$

$$\omega' = \omega'_q + \omega'_s = 0.$$

The drive can be operated in conditions where the output shaft is intermittently stopped (Fig. 4a) or run continuously (Fig. 4b).

The first state obtains in systems with a small moment of inertia in the reversing part of the drive, a large m_s and when the frequencies of the controlling signals are low. The delay angle in the movement of the output shaft $\psi = \sin^{-1}(m_s)$.

The second state is possible if $\lambda \geqslant \varepsilon$, i.e. at low values of m_s and when the frequencies of the input signals are large. Here the disturbing effect of $m_s(t)$ changes its value instantaneously from $-m_s$ to $+m_s$.

Experimental verification

An investigation was made into two systems of automatic control with EPC, controlled by a.c. and d.c. signals. The reversing unit of the powder clutches (Fig. 5) consists of a motor, tachogenerator and two electromagnetic powder clutches. The total axial length of the unit is 203 mm.

A magneto-electronic amplifier was used in one of the experimental plants. A constant (direct) control voltage is supplied to the input to the scheme, its polarity being determined by the direction in which the shaft of the executive mechanism rotates. In order to make the electronic amplifier more quick-acting, a negative voltage feedback was introduced at the terminals of the excitation winding of the clutches. Divider diodes were connected in the control windings of the magnetic amplifiers.

Powder clutches are made with two working layers and the driven part

with a small moment of inertia in the form of a hollow beaker. The excitation windings of the clutches were sectionalized and drawn out on to three contact rings. Owing to the presence of the auxiliary winding,

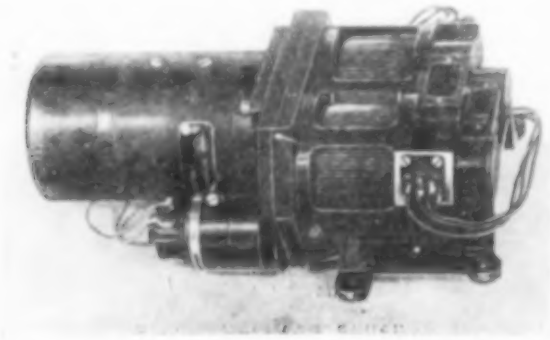

Fig. 5. Powder clutch unit.

which is connected counter to the main winding, use could be made of single cycle magnetic amplifiers with an internal feedback which possess a relatively high no load current. Here the no load slip losses decreased in the clutches, and speed stability was increased with small signals. The connexion of the auxiliary windings, via germanium diodes, was effected in order to exclude the divider transformers and rectifiers, necessary for supplying them from a network at 400 c/s.

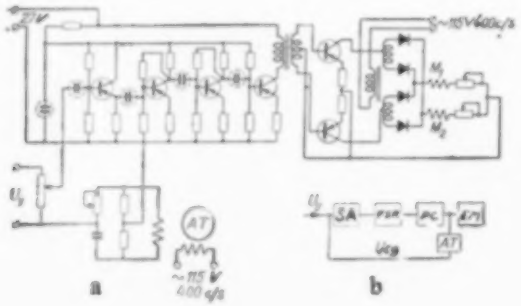

Fig. 6. Electrical (a) and structural (b) schemes of equipment with an amplifier based on semiconductor instruments:
SA - semiconductor amplifier; *FSR* - phase sensitive rectifier; *PC* - powder clutch unit; *EM* - executive mechanism; *AT* - asynchronous tachometer generator; N_1 and N_2 - excitation windings of EPC.

The nominal moment of the clutches was 14 kg. cm. The time constant of the clutch excitation circuit was 0.0075. The moment of inertia of the driven part of the drive applied to the shaft of the clutch was 4 g. cm. sec^2. The moment of static resistance of the load applied to the clutch shaft was 0.5 to 2 kg. cm. The range of speed regulation was 1 : 50.

The investigations showed that intensive forcing of the clutch excitation is ensured as a result of the effect of the speed and voltage feedbacks and the high speed action of the system no matter what the values of the controlling signal.

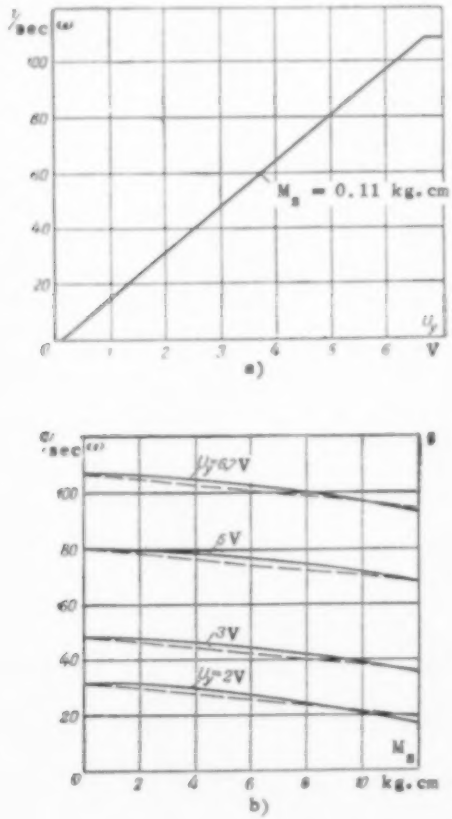

Fig. 7. Control (a) and mechanical (b) characteristics of the system:
- - - - - - - - - theoretical; ——— experimental.

An amplifier based on semiconductor instruments was used in the system controlled by alternating voltage (Fig.6). This made it possible to reduce the weight of the unit by more than 8 times.

The speed feedback was effected by an asynchronous tachogenerator with an AT-3 type hollow rotor.

Depending on the phase of the input voltage, the amplified signal enters the clutch on the right or left of rotation. The signal is divided by a phase sensitive rectifier connected at the output from the amplifier. Owing to saturation, the amplifier has non-linear characteristics. This produces a decrease in the equivalent amplification factor if the signals are large and a reduction in the amount of regulation during reversing.

The control and mechanical characteristics of this system are shown in Fig.7.

Conclusion

Tests on a number of experimental equipments for the purpose of controlling speed have shown that the use of EPC improves the quality of the system, reduces its size and weight, increases operating speed and in certain cases improves the power indices.

Electromagnetic powder clutches may be expediently used in follow-up systems and speed control systems if the load is inert in character. In this case the slip losses in the clutches (7) are negligibly small. The efficiency of the drive is determined by the losses during transient processes. The latter are usually less in plant with electromagnetic clutches than in drives with variable motors.

Translated by O.M. Blunn

REFERENCES

1. G.M. Fridlider; *Avtomat. i telemekh.*, No.1, (1959).
2. T.A. Glazenko; *Elektrichestvo*, No.12, (1954).
3. O.N. Tatur; *Electromagnetic powder clutches, (Elektromagnitnye poroshkovye mufty)*, Iz. ENIMS, (1956).
4. G.M. Petukhin; *Elektrichestvo*, No.3, (1955).
5. W.S. Gerlingen; *Feinwerktechnik*, 2, (1955).
6. L.S. Gol'dfarb; *Avtomat. i telemekh.*, No.5, (1947).
7. T.A. Glazenko; *Elektrichestvo*, No.4, (1958).

AUTOMATIC DEVICE FOR LOAD DISTRIBUTION IN POWER SYSTEMS*

S.V. USOV, G.M. PAVLOV, V.A. SLABIKOV and I.A. BUDKIN

(Kalinin Polytechnical Institute, Leningrad)

(Received 19 October 1959)

The most efficient distribution of active loads between power stations in large power systems should take into account losses in the networks. The operating conditions for such systems are quite complex and the stated distribution of active loads can only be effected by automation of the process. To do this, the Kalinin Polytechnical Institute in Leningrad has developed a very simple counter-resolving device with the abbreviated name ANRAN (automatic device for the most efficient distribution of active loads).

A number of organizations are now developing such devices. However, the special feature of ANRAN is that it solves the problem of load distribution and takes into account the losses no matter what the configuration of the network.

ANRAN is based on the rule in force in Russian powers systems that the partial specific consumptions be equal (1, 2).

$$\delta_1 = \delta_2 = \ldots = \delta_i = \ldots = \delta_n, \tag{1}$$

where $\delta_1 = \frac{dB_i}{dP_i}$ is the partial specific fuel consumption of station i;

B_i the hourly consumption of fuel of station i;

P_i the output of station i.

If rule 1 is fulfilled load distribution is most economic.

The correction for losses in the network is introduced by multiplying the partial specific consumptions by the function $\frac{1}{1-\sigma_i}$, where

---

* *Elektrichestvo*, No.4, 47-51, 1960.

$\sigma_i = \frac{d P_{loss}}{d P_i}$ are the partial specific losses; P_{loss} the total losses in the networks. Rule 1 is then written in the following form:

$$\frac{\delta_1}{1-\sigma_1} = \frac{\delta_2}{1-\sigma_2} = \ldots = \frac{\delta_i}{1-\sigma_i} = \ldots = \frac{\delta_n}{1-\sigma_n}. \qquad (2)$$

Partial specific consumption depends on the characteristics of the basic electrical equipment at the stations and is connected with output by an exclusively non-linear relationship which can be called the economic characteristic of the station and presented in the following form:

$$\begin{aligned} &\delta_1 = f(P_1);\ \delta_2 = f(P_2); \ldots; \\ &\delta_i = f(P_i); \ldots;\ \delta_n = f(P_n). \end{aligned} \qquad (3)$$

Relationships 3 have no adequately full mathematical expression and, on solution of 2, they are given in tabular or graphical form.

In general form, the partial specific losses are not exclusively linear dependencies on the outputs of the stations with the loads of the system and their distribution taken into account. Using the method proposed by Rosenberg (3) for determining partial specific losses we can write:

$$\left.\begin{aligned} \sigma_1 &= \frac{2R_{e1}}{U_{av}^2}\left(P_1 - \sum_{q=1}^{m+n-2} k_{1q} P_{l1q}\right); \\ \sigma_2 &= \frac{2R_{e2}}{U_{av}^2}\left(P_2 - \sum_{q=1}^{m+n-2} k_{2q} P_{l2q}\right); \\ &\ldots\ldots\ldots\ldots\ldots\ldots \\ \sigma_i &= \frac{2R_{ei}}{U_{av}^2}\left(P_i - \sum_{q=1}^{m+n-2} k_{iq} P_{liq}\right); \\ &\ldots\ldots\ldots\ldots\ldots\ldots \\ \sigma_{n-1} &= \frac{2R_{e(n-1)}}{U_{av}^2} \times \\ &\times\left(P_{n-1} - \sum_{q=1}^{m+n-2} k_{(n-1)q} P_{l(n-1)q}\right); \\ \sigma_n &= 0. \end{aligned}\right\} \qquad (4)$$

1960

where R_{e1}; R_{e2} are the pre-determined equivalent impedances of the network;

P_1, P_2 the outputs 1, 2 and so forth of the stations;

U_{av} the average mains voltage;

k_{1q}, k_{2q} the pre-determined coefficients obtained for distributing loads between stations 1, 2 and so on and n stations.

P_{l1q}, P_{l2q} the loads and outputs of those stations between which the loads are not distributed and which are regarded as loads with a negative sign;

m the number of loads;

n the number of power stations.

In order to determine the coefficients of σ from formulae 4 it is necessary to have at hand information about the loads of sub-stations and the volume of telemechanical communications with which it can be reduced (sic). It is for example only possible to take into account loads of large nodal substations. Instead of actual loads use should be made of planned values. If there are consumers with similar load curves it is possible to measure the load of one of them and ascertain the loads of the others from that one. The load of a region may be determined as the difference between the total power put into the network by the power stations in the region and the power transmitted to other regions along the main transmission lines. Thus, if use is made of ANRAN no additional channels are required for telemechanical communications.

The joint solution of equations 1 to 4 gives the most efficient distribution of active loads with losses in the network taken into account. Certain of these equations do not describe sufficiently fully the non-linear characteristic $U_{out} = f(U_{in})$. Solution can be made accurate within 2 to 3 per cent. In order to perform the stated task, it was therefore decided to use an electronic modelling device with an accuracy of 1 to 2%.

ANRAN may come into operation if the actual frequency of the system deviates from its rated value, if the actual output of the driving stations deviates from the desired output or if the actual output of the system deviates from that desired and so forth. The choice of which motivating factor is employed depends on the whole purpose of the device.

For the sake of simplicity in exposition, we shall assume that ANRAN reacts to the difference between the actual and desired outputs of the

power system. The structural scheme is shown in Fig. 1. ANRAN comes into operation when a difference in outputs appears at the output to a differential device:

$$\Sigma P_s - \Sigma P_{ec} = \Delta P \neq 0,$$

where ΣP_s is the actual power in the system;

ΣP_{ec} the sum of the loads of the power stations picked up in ANRAN according to the economic characteristics for the preceding system state on the condition that

$$\frac{\delta_1}{1-\sigma_1} = \ldots = \frac{\delta_i}{1-\sigma_i} = \ldots = \frac{\delta_n}{1-\sigma_n} = \delta_0.$$

A disturbance to the output balance testifies to the fact that δ_0, δ_i and P_i, inter-connected by exclusive relationships $\delta_i = \delta_0 (1-\sigma_i)$ and $P_i = f(\delta_i)$, no longer correspond to the new operating conditions in the system.

1960

The signal $\pm \Delta P$ from the differential device enters the integrating element and $\delta_0 = \pm \int \Delta P dt$ will either increase or decrease. Other values for the outputs of the station correspond to the new value of δ_0 in the $P_i = f(\delta_i)$ element. The magnitude of δ_0 will continue to vary until the difference ΔP becomes zero.

The correction for losses is introduced into the multiplying device $\delta_0 (1-\sigma)$. The value of δ_0 enters here from the integrating element as well as $(1-\sigma)$ from the summing element. Signals are supplied at the input to the summing element from tele-wattmeters at the substations and from $P = f(\delta)$ elements, and the partial specific losses σ_i are found here by adding the loads of the stations and substations in definite scales in accordance with equation 4. The addition operation $1-(-\sigma_i)$ is also performed since it is necessary to supply the difference $(1-\sigma_i)$ and not the partial specific consumptions into the multiplying device.

All the ANRAN units are based on d.c. resolving amplifiers with a negative feedback. The accuracy of the mathematical operations performed by devices made on this bases depends on the amplification factor of the amplifiers. Therefore, in order to obtain accuracy in summation within 0.1 to 0.2%, use has been made of three-cascade amplifiers using 6N2P-type valves with an amplification factor $A = 40{,}000$ and a linearity on load of 50 kΩ and higher within the limits of $\pm$ 100 V.

The structural scheme of the summing unit is shown in Fig. 2. The resolving amplifier is denoted by a square with a letter A. As is

known, the following relationship holds for such schemes

$$X_{out} \approx -R_0 \Sigma \frac{X_{in}}{R_i}.$$

where X_{in} is the input quantities;
X_{out} the output quantity;
R_0 and R_i resistances.

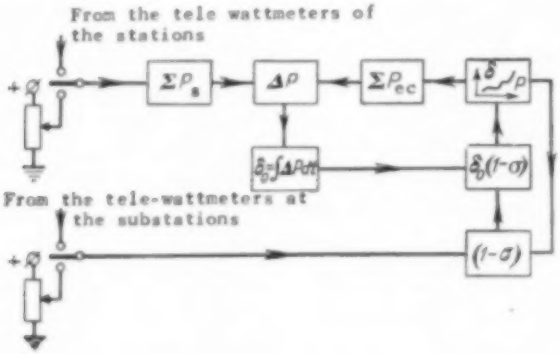

Fig. 1.

The transmission function for one of the signals

$$K_i = \frac{X_{out}}{X_{in}} = -\frac{R_0}{R_i}.$$

Use has been made of these amplifiers to develop resolving units which perform the following additions:

$$\sum_{i=1}^{i=n} P_{si},$$

$$\sum_{i=1}^{i=n} P_{eci},$$

$$\sum_{i=1}^{i=n} P_{si} - \sum_{i=1}^{i=n} P_{eci},$$

$$1 - \sigma_i = 1 - \frac{2R_{ei}}{U_{av}^2}\left(P_i - \sum_{q=1}^{m+n-2} k_{iq} P_{liq}\right).$$

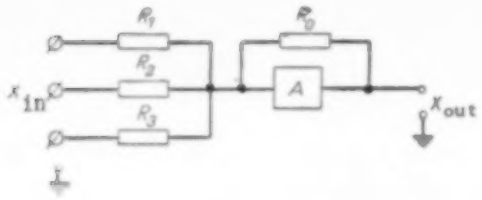

Fig. 2.

The summing unit $\sum_{i=1}^{i=n} P_{si}$ has n output terminals to which signals are fed from the tele-wattmeters of the stations in the system or by manual input of the signals in question taken from potentiometers. Having different transmission functions for each input signal, they can only be added with different scale coefficients. The scale coefficients are determined in advance as a function of the maximum output of the station in question. The ANRAN made in the Kalinin Polytechnical Institute was designed for ten stations with a total maximum established output of 2000 MW. The outputs of the individual stations are between 100 and 400 MW.

The summing unit $\sum_{i=1}^{i=n} P_{ec.i}$ is only different from that described above in that the input signals are fed to it from units at each station reproducing the economic characteristic of each station (Fig. 1).

The differential unit which reacts to the difference in outputs $\Sigma P_{si} - \Sigma P_{ec.i} = \Delta P$, has two elements, viz. detector and executive elements.

For the detector element use is made of a d.c. amplifier with a feedback. The amplifier is based on the 6N3P-type valve. The input to the amplifier receives voltages of different signs which model the outputs ΣP_{si} and $\Sigma P_{ec.i}$ on a definite scale. These outputs are added alegebraically in the amplifier:

$$\Sigma P_{si} + (-\Sigma P_{eci}).$$

The sign of the output signal from the amplifier will depend on their absolute magnitude.

The executive element is a RP-5 type polarized relay which is connected to the output from the amplifier and has $U_{av} = 1$ V. To adjust the model and check the economic characteristics $P_{ec} = f(\delta i)$, provision is made for manual control of the RP-5 relay in the station units.

With a transmission function of the detector element $K = 5$ and an

operating voltage for the RP-5 type polarized relay equal to 1V, the insensitivity of the ANRAN scheme to output differences $\Delta P = \Sigma P_{si} - \Sigma P_{ec}$ is estimated at roughly 20 MW. This is 1.0 to 1.5% of the output fixed for the system.

The summing unit $1 - \sigma_i$, (Fig. 2) is a conventional resolving amplifier. As we have seen, this block, besides calculating the algebraic sum $1 - \sigma_i$, determines the partial specific losses σ in accordance with equations 4, wherefore signals are received at the input to the unit which are proportional to the economic outputs of the power stations. Signals are also received which are proportional to the loads at large nodal substations under the conditions in question. Depending on the established ratio $\frac{R_e}{R_1}$ of the resolving amplifier, each signal is summed with a coefficient equal to $\frac{2R_e}{U_{av}^2} k_{iq}$. The algebraic sum $1 - \sigma_i$ is calculated by supplying a stabilized direct voltage at the input to the unit, this voltage representing unity in a particular scale. The unit for the economic characteristics of the power stations $P_{ec} = f(\delta_i)$ comprises three main elements, namely, a resolving amplifier, a non-linear attachment and an output amplifier.

For the resolving amplifier, which performs the summation, use is made of a typical amplifier with an amplification factor A of 40,000.

The scheme of the non-linear attachment is shown in Fig. 3. It is a specialized functional diode converter in which two types of diode elements are used. The first consists of a potentiometer P_1 diode D_1 and resistances R_4 and R_1, whilst the second consists of potentiometer P_2, diode D_2 and resistances R_4 and R_1. The current characteristics of these elements are shown in Fig. 4.

The two series-connected diode elements reproduce one of the sections of the characteristic which has the form of a broken line and approximately represents the non-linear relationship $P_{ec} = f(\delta)$. The full characteristic is obtained by summation on the amplifier for these sections. The number of sections and consequently the number of pairs of diode elements is only limited by constructional considerations. It is possible to have 5 to 8 of them.

If the output signal of the multiplying device (see below) is to conform in output with the input of the non-linear attachment, a power amplifier has to be installed in between, based on the same 6N3P-type valve. The characteristics of the amplifier are linear between -10 and - 100 V at loads of 5 k Ω and above.

The integrating element is a PD-09 type s.c. capacitor motor

Depending on the position of the contacts of the RP-5 relay in the differential unit, the motor winding is connected to one of the transformer windings so that reverse rotation of the motor is ensured.

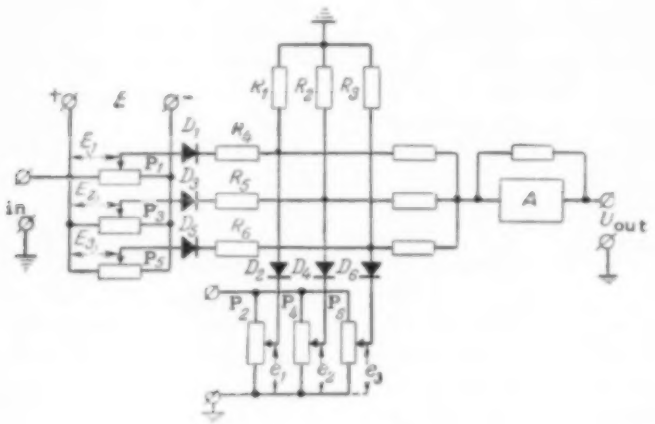

Fig. 3.

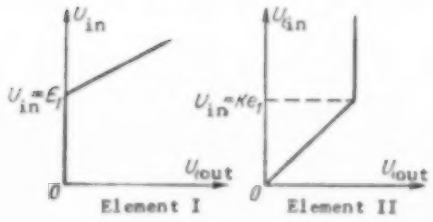

Fig. 4.

In the case of a motor with a constant speed the equation holds

$$\theta = K \int U_{in}\, dt,$$

where θ is the angle of rotation of the motor shaft;

k the scale coefficient;

U_{in} the input signal.

In our case angle θ produces the magnitude of δ_0 (partial specific consumption). The input voltage U_{in}, equal to $-U_{rated}$ of the motor, is supplied if the power difference at the input to the differential unit

is greater than its insensitivity.

The multiplying unit $\delta_0(1 - \sigma_i)$ is based on the dynamoeletric principle. Multiplication is performed by precision potentiometers to which a voltage is applied which represents the multiplicand. Multiplication takes place by the rotation of the potentiometer slide through a certain angle, the voltage taken from the slide being the product of these quantities. In the model use is made of NU-82-98 type precision potentiometers of 30,000 Ω, 1%.

ANRAN can be used both as a control (indicating) device and as a directive device, directly regulating the loads of the power stations in the system. In both cases the results of the solution of the problem of efficient load distribution between the power stations in system can be presented in the form of indications on the appropriate instruments. This purpose is served in ANRAN by high-ohmic voltmeters, graduated in appropriate scales and connected to the output of the resolving units.

The method of introducing the initial data and solving the problem of load distribution is as follows.

The coefficients k_{iq} are determined from the configuration and parameters of the system and established in $(1 - \sigma_i)$ units.

The economic characteristics of the power stations in the units are collected by regulating the source voltages and varying the transmission functions of the amplifier. $P_{ec} = f(\delta_i)$ units enable the characteristic to be obtained with an accuracy of 2 to 2.5%. It takes 3 to 5 min to obtain one characteristic on average. The characteristic can be checked on an oscillograph (Fig. 5) or by instruments. After adjusting the $(1 - \delta_i)$ and $P_{ec} = f(\sigma_i)$ units, the device is ready for operation and can be connected to the network. A signal proportional to the power of the system can be obtained from the power stations along the telemechanical channels or given by potentiometers. The total power of the system can be read from a voltmeter connected at the output from the ΣP_s unit. The load of the substations can also be obtained along the telemechanical channels or established by potentiometers.

ANRAN comes into operation by switching on the executive element of the differential unit. After the necessary time for ANRAN to produce the given power differences (2 to 5 sec), the instruments indicate the economic output and the partial specific consumption of each power station under the conditions in question.

ANRAN, the model of which was produced in the Leningrad Polytechnical

Institute, makes it easily possible to re-organize the economic characteristics of the power stations $\delta_i = f(P_i)$, vary the k_{iq} coefficients (dependent on the configuration and parameters of the network) and introduce the initial data either by hand or automatically; it is easily combined with frequency control devices, it is also possible to distribute the loads in combined power systems in stages. ANRAN consists of identical interchangeable units. This makes it easy to increase the number of power stations taking part in the load distribution system.

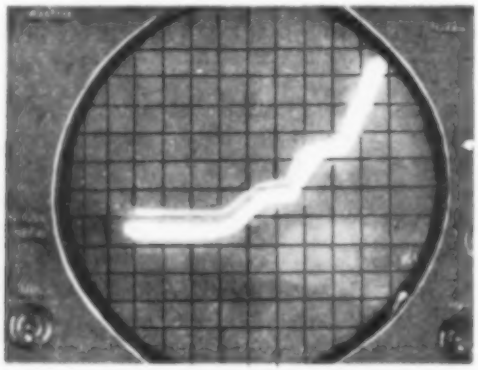

Fig. 5.

ANRAN is designed in the form of a cabinet which is serviced from two sides and houses all the units. The units performing the summation ΣP_g, ΣP_{ec} and $(1 - \sigma_i)$, as well as the station units, are assembled on the same type of chassis. The resolving amplifiers are fixed in the bottom of the chassis. The potentiometers are mounted on side plates. The differential, integrating and multiplying units are assembled on the same chassis. The feedback and zero of the differential unit are regulated by potentiometers on the side. The resistances of the multiplying unit are assembled on the same shaft. This is connected up by plugs and sockets. This means that they can be quickly replaced if necessary.

The inside of the cabinet is divided by an upright well. The external connexions and relays are mounted on the front. There are six horizontal shelves to accommodate the units at the back. The bottom of the cabinet houses the power transformers, supply relays and fuses and the fan at the top is automatically switched on when ANRAN is connected up. All the instruments and control knobs are at the front.

Conclusions

1. The calculation of the most efficient load distribution with the losses in the networks in combined power systems taken into account is a much better practical proposition if use is made of automatic counter-resolving devices for this purpose.

2. Since the calculations must be accurate to within a few per cent, it is advisable to use an electronic modelling installation for this purpose with an accuracy of 1 to 2 per cent.

3. The device developed in the Kalinin Polytechnical Institute in Leningrad can be used either for indicating conditions or for regulating the loads of the power stations in a combined system.

4. With slight modifications, the new device can be used for load distribution with the pre-determined load curves of hydro-electric stations in the system taken into account.

Translated by O.M. Blunn

REFERENCES

1. V.V. Bolotov: *Theoretical bases for the selection of economic conditions in complex electrical power systems, (Teoreticheskie osnovy vybora ekonomichnogo rezhima slozhnoi elektroenergeticheskoi sistemy)*, Iz. Akad. Nauk SSSR, (1947).
2. V.I. Gornshtein: *Most efficient load distribution between power stations operating in parallel, (Naivygodneishee raspredelenie nogruzok mezhdu parallel'no rabotaiushchimi elektrostantsiiami)*, Gosenergoizdat, (1949).
3. B.I. Rosenberg: *Elektrichestvo*, No. 12, (1948).

INVESTIGATION OF THE EXTINCTION PROCESSES IN A FREE A.C. ARC*

I.S. TAEV

(Moscow Power Institute)

(Received 9 July 1959)

The purpose of the present article is to determine the conditions under which a free (open) a.c. arc is extinguished at the contacts of tripping gear at the first transition of the arc current through zero. The data given in the article refer to a range of currents from unity to thousands of amperes, mains voltages from 127 to 660 V and a frequency of 50 c/s. The investigations have been carried out on a contactor with pin copper contacts.

Conditions for the extinction of an a.c. arc

No re-striking of the arc will occur if the recovery strength of the arc gap $U_{r.s}$ exceeds the recovery voltage U_r. It will be seen below that

$$U_{r.s} = U^{\circ}_{r.s} + k l_a \beta t.$$

where $U_{r.s}$ is the initial strength of the gap, V;

l_a the length of the arc column, cm;

t the time after the passage of the current through zero, microsec;

k depends on the current of the test quantity, being the rate of ascent of the curve for the recovery strength per unit length of the arc, V/microsec. cm;

β a coefficient taking into account the effect of the material of the contacts on the process of strength recovery in the arc column (for copper contacts $\beta = 1$).

---

* *Elektrichestvo*, No.4, 57-63, 1960.

The relationship given in (1) is the condition for the extinction of the free electric arc after the current has passed through zero with expression 1 taken into account:

$$n \geqslant \frac{1{,}64 f_0 k_a k_s U_n \sin\varphi}{2U^0_{r.s} f_0 + \frac{5}{\tau} k_a I_a \cdot 10^6}, \qquad (2)$$

where n is the number of breaks on the pole of the gear;

U_n the nominal (rated) linear voltage of the network, V;

ϕ the angle of shift between the current in the circuit and the source voltage at the moment when the current passes through zero;

k_a the amplitude coefficient of the recovery voltage;

k_s the scheme factor;

f_0 the natural frequency of the circuit, c/s.

The coefficient k_a can be calculated approximately from the empirical formula

$$k_a \approx 1 + e^{-0{,}0003 f_0}. \qquad (3)$$

Formula 3 determines the upper limit of the relationship $k_a = f(f_0)$. Within the limit $k_a = 2$. It is necessary to assume that it is such in particularly important cases.

The natural frequency of low voltage networks

In order to determine the limiting values of the natural frequency f_0, appropriate investigations have been made into electrical networks at a Moscow automobile works. The methods and results of the investigations are set out in another paper (2). In the present article we shall therefore only dwell on those relationships and quantities which are necessary for determining the magnitude of f_0 in engineering practice.

In circuits with motors the upper limit of the dependence of f_0 on the nominal (rated) output P_n on the motor is characterized by the empirical formula:

$$f_0 \approx A + BP_n^{1/4} \ [c/s]. \qquad (4)$$

The truth of this formula has been experimentally verified for $P_n = 0.5$ to 50 kW. The coefficients A and B appearing there equal:

For cable networks $A = 8000$ and $B = 2100$;

For overhead networks A = 15,000 and B = 3000.

Tests have shown that the natural frequency falls with a decrease in the load on the motor, the removal of the tripping apparatus from the motor (according to the electrical scheme) and with an increase in the number of motors connected in parallel. These circumstances also arise if the electrical load is in any other form.

In circuits with transformers with low outputs amounting to units of kVA, there are usually two frequencies in the curve for the recovery voltage, namely, high and low. At rated output the high frequency component can be determined from the approximate empirical formula

$$f_0 \approx 30{,}000 + 15{,}000\sqrt{P_n}\ [c/s]. \tag{5}$$

The natural frequency of the circuits of the contactor coils, starters (triggers) and intermediate a.c. relays can be approximately found on the basis of the following expression

$$f_0 \approx \frac{6.5 \cdot 10^6}{w}\sqrt{\frac{l + 100\delta}{s}}\ [c/s], \tag{6}$$

where w is the number of turns in the coil

l the average length of the line for the intensity of the magnetic field, cm;

s the cross section of the magnetic circuit, cm^2;

δ the active air gap, cm.

If the gear is installed on iron panels in the presence of a branched conductor which is electrically connected to the coil in the apparatus, the natural frequency will be 2 to 3 times less than f_0, as calculated from formula 6.

The natural frequency reaches maximum when the short circuited sections of the network are disconnected. In this case the magnitude of f_0 is approximately equal to

$$f_0 \approx 100{,}000\left(0.5 + \frac{5}{l_k + 10}\right)\ [c/s]. \tag{7}$$

where l_k is the distance (in the electrical scheme from the point where the tripping gear is installed to the point of short circuit, m.

The natural frequency of the circuit with a choke at which the

1960

magnetic circuit has the dimensions shown in Fig. 1, can be calculated by the approximate formula:

$$f_0 \approx \frac{1{,}5\cdot 10^8}{w\sqrt{b\left(\frac{a}{\delta}+\frac{h}{\Delta}\right)+0{,}5(a+b+h)}} \quad [c/s]. \tag{8}$$

where w is the number of turns of the choke coil and a, b, h, δ and Δ dimensions in cm.

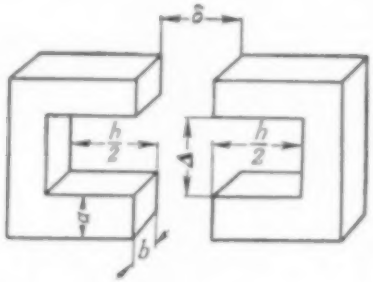

Fig. 1. Determination of the natural frequency of a circuit with chokes.

In formula 8 no account is taken of the effect of the resistance of the steel in the magnetic circuit on the magnitude of f_0. This is permissible if the magnetic circuit is operating under non-saturated conditions when the magnetic resistance of the steel is small and its effect on f_0 insignificant.

The values of the constants in formulae 4 to 8 are so calculated that the theoretical values of f_0 express the upper limits of the test relationships.

The length of the free arc and the speed at which it moves

The trajectory of the free arc has a complex zig-zag shape and it is practically impossible to determine its length accurately. Consequently in order that l_a may be calculated, it is necessary to adopt a comparatively simple model of the propagation of the arc.

The typical shape of the trajectory of a free arc is shown by the dotted line. With the familiar assumptions, the minimum possible

length of the arc may be regarded as equal to the length of the circumference plotted on the chord $a_1 \approx V_d t$ and arrow $h_0 \approx V_a t$.

In these expressions V_d and V_a denote the average speeds at which the contacts diverge in cm/sec and the movement of the upper point of the arc respectively.

The length of the arc will be approximately:

$$l_a \approx \sqrt{(V_d t)^2 + 9(V_a t)^2} \ [\text{cm}]. \tag{9}$$

The value of l_a determined by this formula will be close to that minimum possible length of the arc which must be taken into account in calculations of the process of extinction since there is least probability that the arc will be extinguished at the moment when the current passes through zero if the length of the arc is the minimum possible.

1960

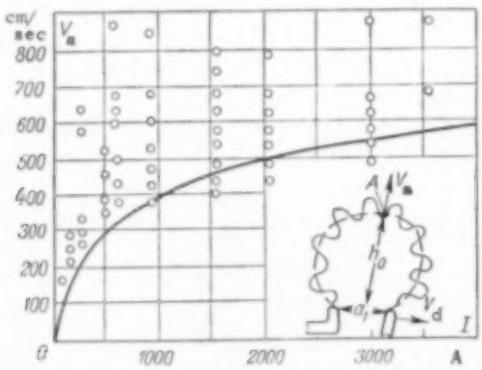

Fig. 2. Rate at which the free arc moves at different currents.

The speed at which a cylindrical arc moves can be calculated theoretically (3) if we suppose that the mass of the moving arc is zero and equate the electrodynamic force acting on the arc to the force of the aerodynamic resistance.

The rate at which a cylindrical arc with a rectlinear axis moves can be calculated from the following formula:

$$V_a \approx \frac{2,12I}{b_k^{1/6}(l_p + \delta_k)^{1/6}} \ [\text{cm/sec}], \tag{10}$$

where b_k is the width of the contact, cm;

l_p the length of the arc in the direction perpendicular to the speed vector of the arc, cm;

δ_k the thickness of the contact, cm.

The actual rates at which the free arc moves in the presence of low currents (several dozen amperes) are governed by this relationship. At currents amounting to hundreds and thousands of amperes however, actual speed is considerably less than the theoretical speed. Its reduction is apparently due to the zig-zag shape of the arc column and the increase in the effective area of the air "piston" which resists the movement of the arc.

It is extremely difficult to take this factor into account theoretically. A series of tests has therefore been carried out in order to determine the dependence of the rate at which the free arc, formed at pin-type contacts, moves on the amount of current. To take the measurements, use was made of probing methods on a magnetic oscillograph.

A thin wire (probe) is set up at a definite distance from the place where the contacts diverge. As the arc only touches the probe when in motion, a voltage emerges between the probe and the contact; this moment is fixed on the loop oscillogram. The distance between the contacts and the probe is known. Having ascertained the time from the oscillogram, it is possible to find the average rate at which the upper point of the arc moves (point A in Fig. 2). At currents equal to hundreds and thousands of amperes, we have yet to be successful in experimentally establishing clearly expressed dependencies of the speed of the arc on the shape and dimensions of the contacts, the distance between them and the moment at which they open. The experimentally obtained magnitudes of V_a are shown in Fig. 2. It can be seen that they are widely scattered. The lower limit of the relationship $V_a = f(I)$ can be expressed by the empirical formula:

$$V_a = 37\sqrt[4]{I} \ [\text{cm/sec}]. \tag{11}$$

The values of V_a determined from this formula are the minimum possible speeds of upper points of the arc corresponding to an arc of minimum length. They therefore correspond to the most unfavourable conditions for arc extinction.

Taking formula 11 into account, the minimum possible length of the arc for pin contacts can be determined in accordance with the following approximate expression:

$$l_a \approx \sqrt{V_d^2 t_b^2 + 12\,300 I^{3/2} t_b^2} \ [\text{cm}]. \tag{12}$$

Tests have shown that conditions are most unfavourable for arc extinction at the moment when the contacts open in the middle of the half-period. In calculations, therefore, arc combustion time t_b may be assumed equal to a quarter of the period of the source frequency.

It would not be possible to calculate the length of the free arc separately for pin-type contacts since the product kl_a appears in the basic relationship 2. The magnitude of kl_a is found experimentally. Separate determination of the value of k and l_a is justified in that it then becomes possible to use the experimental data given in this paper for other kinds of contact.

Use may be made of relationships 11 and 12 within the limits of current variations from 75 to 3600 A, an arc combustion time up to 0.01 sec (for $f = 50$ c/s) and an arc velocity of 1.5 to 6 m/sec.

Growth of recovery strength in the column of a free arc at a source frequency of 50 c/s

The results are given below of an investigation into free arcs, the final purpose of which was to plot curves for the growth of recovery strength $U_{r.s}$ through time. These data refer to "hot electrodes" (pin-type contacts), the electric arc on which it exists during all the time of its combustion.

Two methods may be used to determine the strength of the gap experimentally at different moments of time after the current has passed through zero.

First method. The magnitude of $U_{r.s}$ can be determined from cathode oscillograms of the voltage on the arc gap at different magnitudes of f_0 which itself determines the speed at which the voltage recovers, the oscillograms here having to refer to the same current to be tripped and the length of time the arc burns here having to be greater than one half-period.

After the current has passed through zero the voltage on the gap begins to recover at an average rate roughly equal to

$$\left(\frac{dU}{dt}\right)_{av} \approx 4f_0 \frac{k_a E_f}{2} = 4f_0 \frac{U_{r.s.}}{2},$$

where E_f is the recovery voltage at line frequency, assumed equal to the instantaneous value of the source voltage at the moment the current passes through zero.

The natural frequency of the circuit f_0 and the coefficient k_a can be determined from the above-mentioned cathode oscillogram. The magnitude of E_f is calculated by generally known methods. At the moment of time when the voltage across the gap attained the value of the ignition voltage V_{ig}, the strength of the arc column is equal to U_{ig}. Different values of the ignition voltage should correspond to different rates of voltage recovery. The value of f_0 can be changed by a capacitance shunting the contacts of the tripping apparatus.

Having a number of values for the ignition voltage U'_{ig}, U''_{ig} and so forth and corresponding rates of voltage recovery across the gap $(\frac{dU}{dt})'_{av}$ and $(\frac{dU}{dt})''_{av}$ etc, we can plot a curve for the recovery strength of the gap at the current in question. Fig. 3 illustrates the plotting of the relationship $U_{r.s} = f(t)$ by the method in question. The rate of recovery of the voltage $(\frac{dU}{dt})$ is equal to the tangent of angle α. Producing a number of straight lines 0-1, 0-2, 0-3 and finding their intersection with the corresponding ordinates U'_3, U''_3 and U'''_3, we determine points 1, 2 and 3 for the characteristic $U_{r.s} = f(t)$.

In the final analysis, this method of plotting the curve $U_{r.s} = f(t)$ can be reduced to the determination from the cathode oscillogram (with a large time development) of the magnitude of the ignition voltage U_{ig} and the time from the moment the current passes through zero to the moment when this ignition voltage occurs. At this moment of time $U_{r.s.} = U_{ig}$.

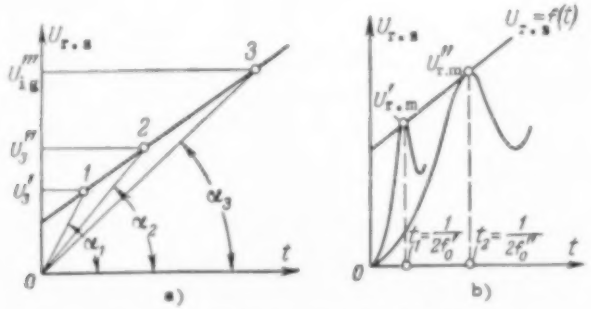

Fig. 3. Plotting the dependence of recovery strength on time.

Second method. In this case it is necessary to create those conditions in the circuit under which the arc will cease re-striking. These conditions, conventionally referred to as " critical ", can be

produced by regulating the natural frequency f_0 and varying the source voltage.

It can be said that under such critical conditions at the moment of time equal to the half-period of the natural frequency of the circuit, the value of the recovery strength across the gap equals the amplitude value of the recovery voltage $U_{r.m}$. By having a number of these data for different values of f_0 we can plot the curve $U_{r.s} = f(t)$ (Fig. 3b).

The amplitude of the recovery voltage can be calculated theoretically or experimentally determined from the oscillogram of the recovery voltage.

To determine arc combustion time, use is made of the cathode oscillograph without taking cathode oscillograms of the voltage. To do this, additional contacts shunted by a small active resistance are connected in the basic current circuit in series with the main contacts.

1960

The voltage drop from this resistance is fed to plates for the oscillograph effect. If the main and additional contacts are both regulated in such a way that they open at the same time then when an arc emerges on the main contacts, an arc current curve will apear on the screen of the oscillograph so that arc combustion time can be determined from this.

The curves for the increase in recovery strength when the currents to be tripped are small (5 to 128 A) are determined by the second method.

Table 1 shows the values of the initial recovery strength $U^0_{r.s}$ and coefficient k, which refers to a unit of length of the arc (1 cm) in the case of copper contacts.

TABLE 1

Current to be tripped, A	5	30	30	43	68	82	128
V/microsec.cm	4.7	2.1	2.0	1.4	0.92	0.7	0.365
$U_{r.s.}$, V ..	340	260	210	190	180	170	142

When tripping currents up to 80 A the arc is weakly stretched by electrodynamic forces and it is the same length as the distance between the contacts. On the other hand, tests have shown that a change in the distance* between the contacts of 1 to 10 mm does not lead to any

* Actual text reads " rastvor": *solution*, and not " rastoianie": *distance*, (Translator).

alteration in the position of the curve $U_{r.s} = f(t)$ at any given current. This means that the reduction in the length of the arc does not lead to a reduced intensity of cooling at currents up to 80 A, since the role of heat dissipation through the contact parts increases in this case. Consequently the effective length of the arc at currents up to 80 A can be more or less regarded as independent of the distance between the contacts and roughly equal to 1 cm. This position has been experimentally verified on contactors with contacts which diverge at rates between 0.75 and 1.25 m/sec.

Let us dwell now on a certain circumstance which must be held in mind when plotting $U_{r.s} = f(t)$ curves by the second method. When determining the amplitude of the recovery voltage at the contacts of the apparatus, it is necessary to reckon with the value of the voltage at the source terminals (generator, transformer), when the current to be tripped passes through the circuit.

The point is that in this case if the voltage is reduced at the output terminals of the supply transformer, two processes will take place simultaneously after the arc has been extinguished: the recovery of the voltage at the contacts of the apparatus and the recovery of the voltage at the transformer. It may well be that the voltage will recover considerably less quickly at the transformer than at the contacts of the apparatus, determined by the high natural frequency of the "transformer-tripping gear" section of the circuit. In this case, when determining the amplitude of the recovery voltage, it is necessary to include the actual value of the voltage at the output terminals of the transformer. By taking this process into account the values of k and $U^{0}_{r.s}$ shown in Table 1 are to a certain extent more accurate than those obtained before (1).

Curves for $U_{r.s} = f(t)$ have been plotted by the first method for currents of 265 to 1000 A. At currents greater than 1000 A it was difficult to make use of this method because the initial strength of the gap in this case was very small and the intersection of the curves for the recovery voltage and the strength of the arc column at the first transition of the current through zero usually took place at the very beginning of the process.

In the case of currents between 1550 and 3600 A, it was necessary to use large capacitances (hundreds of microfarad), which shunt the contacts of the circuit breaker. The rate at which the voltage increases on the gap was small and re-striking of the arc only occurred 100 to 300 μ sec after the current had passed through zero. The ignition voltage U'_{ig} and time t' which elapsed between the moment the current passed through zero and the moment re-striking of the arc occurred was deter-

mined direct from cathode oscillograms.

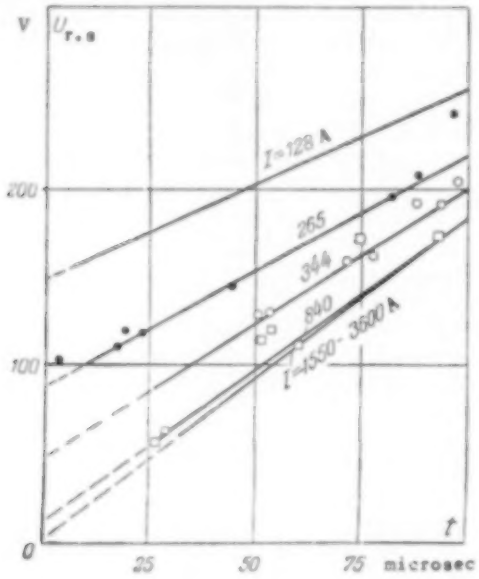

Fig. 4. Increase in recovery strength after first transition of current through zero.

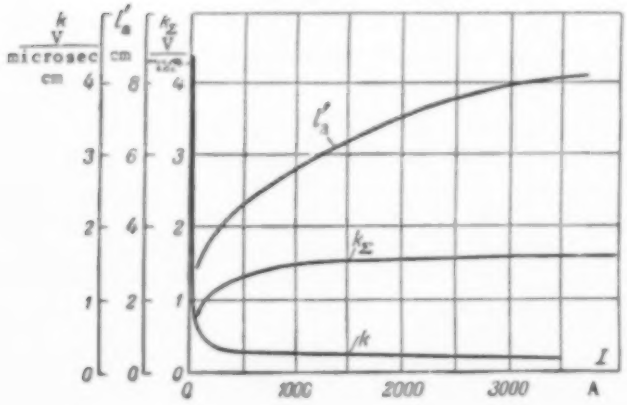

Fig. 5. Dependence of k_Σ, k and l'_a on the current to be tripped.

At the moment of time t' the strength of the gap equalled I'_{ig}. With a

series of such values for U'_{ig} and t' (corresponding to different frequencies f_0) we can plot the curve for $U_{r.s} = f(t)$ for the current in question. It is possible to determine $U_{r.s}$ in this way because the voltage across the gap at different moments of time increases at different speeds; at first it is low and then it rises smoothly.

Fig. 4 shows experimental curves for the growth of recovery strength across the gap after the first passage through zero if high currents are to be tripped. They represent the lower limit of the points obtained in the tests and refer to the full length of the arc. The curves practically coincide with each other at currents of 1550 to 2000 and 2900 to 3600 A.

Let us pay attention to the fact that the initial strength of the gap is fairly small at high currents and that its strength diminishes with increasing current.

The data in Table 1 and the curves presented in Fig. 4 enable us to plot the dependence of the values of k and $U^0_{r.s}$ on the current to be tripped.

Fig. 5 shows the relationship of the magnitude $k_\Sigma = kl'_a = f(I)$, referring to the full length of the arc. This relationship refers to the first passage of current through zero and the opening of the contacts in the middle of the half-period. It was derived theoretically from formula (11) for contacts diverging at an average speed of $V_d \approx 100$ cm/sec.

Having divided to value of k_Σ by l_a, values of k can be obtained for different currents in respect of arcs 1 cm in length. The relationship $k = f(I)$ is introduced in Fig. 5. It can be represented quite accurately in the form of an empirical formula:

$$k = 0{,}17 + \frac{43}{I} \quad \text{(V/microsec . cm)} \tag{13}$$

Having made use of the data of Table 1, we are able to plot the relationship $U^0_{r.s} = f(I)$ shown in Fig. 6. In the case of copper contacts this relationship is characterized by the following empirical expression:

$$U^0_{r.s} = \frac{210}{e^{0{,}0035I}} + \frac{400}{I} \text{ [v]}. \tag{14}$$

It should be noted that the curve shown in Fig. 6 and formula (14) refer to conditions prevailing when the arc is on " hot" contacts along which the bases of the arc move slowly.

Tests have established that in real industrial networks when currents over 1000A are to be tripped the free arc is usually extinguished in the second or subsequent transitions of the current through zero. At this time the arc column is greatly extended and acquires a considerable active resistance, the magnitude of which is commensurate with the remaining resistance of the circuit. The angle of phase shift and the corresponding value of the recovery voltage decreases. The free arc is quenched in one of the transitions of the current through zero (Fig.7).

All the data given in the present article refer to curves for the recovery strength of the gap $U_{r.s}$, only true for the first transition of the current through zero. Coefficient k, as can be seen from the experimental data in Table 2, also has different values for other than the first transition of the current through zero.

TABLE 2

Current to be tripped, A	1st transition k_1	2nd transition k_1	$\frac{k_1}{k_2}$
344	0.295	0.123	2.4
525	0.285	0.122	2.34
840	0.26	0.121	2.15

Strength of the cathode zone in the a.c. arc

As follows from the present article, the experimental values for the initial recovery strength $U^0_{r.s}$ are less than those published in the literature for the " strength of the cathode zone". According to data published by " Slepian" and " Broun," as well as other authors, initial strength is always greater than 160V no matter what currents are to be tripped. In our experiments the value of $U^0_{r.s}$ was only a few tens of volts at currents greater than 1000A.

We have no reason to doubt the correctness of the above method of plotting curves for $U_{r.s} = f(t)$. For example, Fig.8 shows four cathode oscillograms of the voltage at the gap taken on a 2KM-type oscillograph with mechanical scanning (drum cassette) at U = 380V, a trip current of 840A and an average rate of voltage recovery equal to

$$\left(\frac{dU}{dt}\right)_{av} = 2.2 \text{ V/microsec.}$$

It can be seen from the oscillograms that the peaks of the ignition voltage U_{ig} which take place after the first passage of the current

through zero are equal to the strength of the arc column at the appropriate moments of time and that their values are less than those for the "cathode zone strength" published in the literature. These values could not be voltages on a metallic crosspiece since the distance between the contacts was at least 2 to 3 mm and reached 6 mm at the moments when they appeared (Fig. 8b), whereas literary sources declare that the metallic bridges were not above 2 mm in size.

The data given in the article relative to the value of $U^{o}_{r.s}$ are different from the values for initial recovery strength stated by Slepian, since they were obtained in experiments carried out under different conditions. This indicates the need to carry out extensive investigations in order to establish the quantitative dependencies of $U^{o}_{r.s}$ on the material, dimensions and heat-dissipation properties of the electrodes, the intensity of thermo-electronic emission and the vaporization of the metal from the electrodes etc.

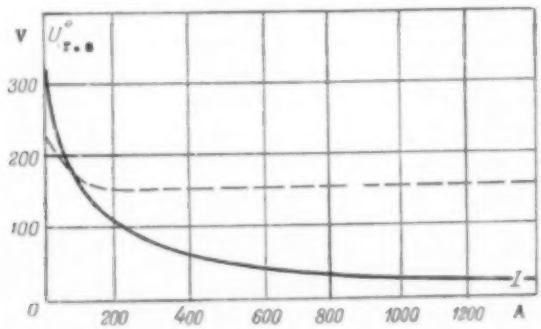

Fig. 6. Dependence of initial recovery strength on the current to be tripped.
——— author's data; - - - - - - Slepian's data.

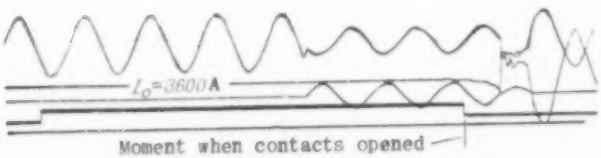

Fig. 7. Oscillogram of the processes of tripping a circuit when I_o = 3600 A

If we admit that the values obtained for $U^{o}_{r.s}$ are not determined

specifically by the processes taking place at the cathode (Slepian effect), but by the parameters proper of the arc column, then the value of $U^0_{r.s}$ can be determined especially approximately from the formula given in another paper (4):

$$U^0_{r.s} = \sqrt{R_a N_0 I_a} = \frac{N_0 I_a}{2\omega\delta I}.$$

But since

$$N_0 \approx EI.$$

then

$$U^0_{r.s} \approx \frac{EI_a}{2\omega\delta}.$$

For a current of 100 A, the time constant of the arc $\delta \approx 100$ microsec, whilst the magnitude of the gradient E = 10 V/cm.

1960

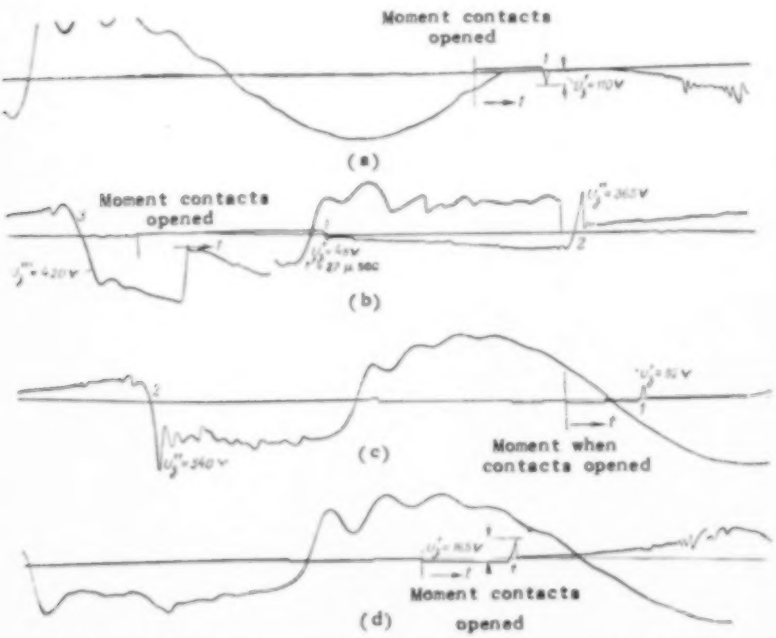

Fig. 8. Oscillograms of the voltage at the contacts of the apparatus when tripping a current of 840-Aand f_0 = 1100 c/s (a); f_0 = 1000 c/s (b); f_0 = 900 c/s (c) and f_0 = 800 c/s (d): 1.2. 3 – ordinal numbers for the transition of current through zero.

In this case, for an arc 1 cm long we have

$$U^0_{r.s} \approx \frac{10 \cdot 1}{2 \cdot 314 \cdot 100 \cdot 10^{-6}} = 159 \text{ v.}$$

which coincides roughly with experimental data.

Slepian and other investigators have made use of a similar method to the second method considered above to plot curves for $U_{r.s} = f(t)$ in the presence of large currents. The only difference was that they obtained the quenching of the arc in the first passage of the current through zero by means of an active shunting resistance. It is characteristic that its value reached 0.1 to 0.3 Ω at currents over 1000 A. It can easily be shown that under these conditions the rate of voltage recovery is low and also aperiodic in character. In order that the voltage on the gap be equal to 160 to 250 V, an amount of time calculated in hundreds of microsec is required in this case. Consequently the strength of the arc column measured by Slepian (160 to 250 V) did not occur at the moment when the current passed through zero, but several hundred microsec later.

Our experiments with the use of a shunting capacitance seem to us more accurate since they enable the value of $U_{r.s}$ to be measured in the first tens of seconds after the current has passed through zero. The values for $U_{r.s}$ obtained by us hundreds of microsec after the arc had been quenched were the same as the experimental data obtained by Slepian (Fig.4).

Whereas we may assume that the " Slepian effect" does not in fact take place, this still does not prevent metallic plates being used in are extinction chambers. The considerable thermal capacitance and heat dissipating capacity of these plates is instrumental in quenching the arc.

The judgements made here relative to the value of $U^0_{r.s}$ must be regarded as preliminary. The difference between our figures and those produced by Slepian only indicates that a serious investigation should be made into the nature of the initial recovery strength of the gap and is quantitative dependence on various factors.

Translated by O.M. Blunn

REFERENCES

1. I.S. Taev: Vest. *Elektroprom.*, No.12, (1958).
2. I.S. Taev and Van Tsi-Pin: *Eletromekh. i avtomat.*, No.2, (1958).
3. O.B. Bron: *The electric arc in control apparatus, (Elektricheskaya duga v apparatakh upravleniia)*, Gosenergoizdat, (1954).
4. I.S. Taev: *Elektrichestvo*, No.10, (1956).

CALCULATING TRANSIENT PROCESSES IN LINEAR CIRCUITS BY RECURRENCE FORMULAE*

N.S. KOCHANOV

(Leningrad)

(Received 14 April 1959)

1960

Transient processes in linear electrical circuits with lumped parameters can be calculated most simply by using the operator method. But if circuits of a high order are calculated, considerable difficulties arise in connexion with the need to solve algebraic equations with high powers. Therefore, the use of the expansion theorem, or, what amounts to the same thing, the summation of deductions, is not acceptable in practice. If use is made of the method of expanding representations into a series arranged according to the negative powers of the operator, quite a lot of time is needed to calculate transient processes.

It can be shown that to determine the transient function of an electrical circuit to the power of n with lumped parameters it is quite sufficient to know $2n$ equally distant values which can easily be calculated by the expansion of a rational fraction into a series arranged according to the negative powers of the operator with subsequent transition into a "Maklorен" series. All the following equally distant values can then be determined by a recurrence formula, provided that the initial values of the transient function were determined with sufficient accuracy.

Methods of calculating transient processes in linear electrical circuits on the basis of recurrence formulae have been published in the U.S.S.R. We can for example point to the work of Khukhrikov [1]. Part I of his book is devoted to the analysis of transient processes in linear circuits. But his method has a number of shortcomings. Firstly, the recurrence formulae are too approximate. Secondly, the initial

* *Elektrichestvo*, No.4, 70-72, 1960.

values of the function for the transient process are determined on the basis of the theorem of substantive conversion of the Laplace transformation which cannot ensure sufficient accuracy. Thirdly, in order to plot the transient process curve it is necessary to calculate discrete values of functions at different intervals. This involves a great deal of calculation. Finally, no criteria of accuracy are given for the approximate method. In this connexion it is impossible to solve the problem of how to select the theoretical interval of time. Similar comments may be made about the method proposed by Ionkin [2]. As regards other methods of calculating transient processes in linear electrical circuits, reference should be made to the approximated operator method [3] and a similar method published abroad [4]. The main shortcomings of these methods are the same as those set out above.

The expansion of certain functions into series in these works entails the use of recurrence formulae. Here it should be mentioned that the appropriate recurrence formulae and the initial equally distant values of the transient functions necessary for these formulae are more accurate than in the first of works under consideration.

The present article sets out a method of calculating transient processes which is free from the above shortcomings. It should however be mentioned that the stated works [1-4] cover a wider range of problems in connexion with the calculation of linear systems with variable parameters and also non-linear systems. A special feature of the proposed method is that the transient functions of linear circuits with lumped parameters are calculated by recurrence formulae from accurate initial values for these functions. Here the error in the calculations is only determined by errors in rounding and the number of correct signs of the numbers. Moreover, the step of the recurrence formulae is doubled. This considerably simplifies the calculation. If use is made of digital computers, this method will enable complex problems to be solved in the calculation of transient processes in linear electrical circuits.

Suppose that as a result of applying the operator method to the determination of the transient process that the time function is represented in the form of a fraction

$$F(p)=\frac{b_0p^{n-1}+b_1p^{n-2}+\ldots+b_{n-2}+b_{n-1}}{p^n+a_1p^{n-1}+a_2p^{n-2}+\ldots+a_{n-1}p+a_n}. \qquad (1)$$

Then, studying the case of simple roots* for the equation

$$p^n+a_1p^{n-1}+a_2p^{n-2}+\ldots+a_{n-1}p+a_n=0, \qquad (2)$$

* The proposed method is also true in the case of multiple roots.

the original can be written in the following form:

$$F(t)=\sum_{k=1}^{n} C_k e^{p_k t}. \tag{3}$$

where P_k are the roots of equation 2.

If we determine the values of the exponential polynomial (3) at equally distant values of variable t, we obtain the following set of equalities:

$$\sum_{k=1}^{n} C_k e^{p_k \nu\tau}=F(\nu\tau);\ \nu=0, 1, 2, 3, \ldots. \tag{4}$$

where τ is the step of the values of function $F(t)$.

1960

Denoting

$$m_k=e^{p_k\tau};\ F(\nu\tau)=F_\nu,$$

the set of equalities (4) can be written

$$\sum_{k=1}^{n} C_k m_k^\nu=F_\nu;\ \nu=0, 1, 2, 3, \ldots$$

It is easy to verify that the equally distant values of the $F(t)$ function (i.e. F_0, F_1, F_2 ....) can be determined like the initial values of the function

$$\Phi(x)=\sum_{k=1}^{n} C_k e^{m_k x} \tag{5}$$

and its subsequent derivatives.

Regard function (5) asthe solution of a uniform linear differential equation with constant coefficients

$$\Phi^{(n)}(x)+A_1\Phi^{(n-1)}(x)+A_2\Phi^{(n-2)}(x)+\ldots+A_n\Phi(x)=0 \tag{6}$$

under the initial conditions

$$\Phi(0)=F_0;\ \Phi^{(1)}(0)=F_1;\ \ldots\ \Phi^{(n-1)}(0)=F_{n-1}.$$

The characteristic equation for equation (6) has the form:

$$m^n + A_1 m^{n-1} + A_2 m^{n-2} + \ldots + A_n = 0, \tag{7}$$

Here

$$\left.\begin{aligned} m &= e^{p\tau}; \\ A_1 &= -[e^{p_1\tau} + e^{p_2\tau} + \ldots + e^{p_n\tau}]; \\ &\ldots\ldots\ldots\ldots\ldots\ldots\ldots \\ A_n &= (-1)^n e^{(p_1+p_2+\ldots+p_n)\tau}. \end{aligned}\right\} \tag{8}$$

If equation(6) is differentiated ν times and x equated to 0, we arrive at the following recurrence or difference equation

$$\left.\begin{aligned} F_{n+\nu} + A_1 F_{n-1+\nu} + A_2 F_{n-2+\nu} + \ldots + \\ + A_{n-1} F_{1+\nu} + A_n F_\nu = 0; \\ \nu = 0, 1, 2, 3 \ldots \end{aligned}\right. \tag{9}$$

Using this recurrence equation and knowing the initial values of the sought for function F_0, F_1, F_2 ..... F_{n-1}, the necessary number of equally distant values can easily be calculated in succession to plot the transient process curve. The problem thus arises of determining the initial values of F_0, F_1, F_2 ....F_{n-1} and the coefficients of recurrence formula(9) without calculating the roots of equation(2).

By dividing the polynomials of the numerator and denominator of the fraction, arranged according to the diminishing powers of the operator p, the fraction can be represented in the form of a series arranged according to the negative powers p, i.e. in the form:

$$F(p) = \frac{S_0}{p} + \frac{S_1}{p^2} + \frac{S_2}{p^3} + \ldots + \frac{S_i}{p^{i+1}} + \ldots$$

Note that the coefficients of the series are also calculated by a recurrence formula:

$$\left.\begin{aligned} S_{n+\nu} = -(a_1 S_{n-1+\nu} + a_2 S_{n-2+\nu} + \ldots + a_n S_\nu), \\ \nu = 0, 1, 2, 3 \ldots, \end{aligned}\right.$$

This is more convenient in practice as the dividing operation is eliminated.

Passing to the original, we have an expansion of the sought for time function in the form of a Makloren series

$$F(t)=s_0+s_1t+s_2\frac{t^2}{2!}+\ldots+s_i\frac{t^i}{i!}+\ldots \qquad (10)$$

Using this series we can calculate the initial values of the sought for time function very simply, in so far as they correspond to low values of the variable t. It is expedient to calculate the even and odd parts of series 10 separately. It is then easily found that $F(\tau)=F_1$ and $F(-\tau)=F_{-1}$, $F(2\tau)=F_2$ and $F(-2\tau)=F_{-2}$ and so on simultaneously, wherefore it is necessary to take the sum or difference of the stated parts of the series.

The values found are first used to calculate the coefficients A_1, A_2 .... A_{n-1} and then to calculate the subsequent values of the sought for time function. Using recurrence formula (9) we can compose the following set of equations to determine coefficients A_1, A_2 ....A_{n-1}:

$$\left.\begin{aligned}
A_1F_{n-2}+A_2F_{n-3}+\ldots+A_{n-1}F_0&=\\
&=-A_nF_{-1}-F_{n-1};\\
A_1F_{n-3}+A_2F_{n-4}+\ldots+A_{n-1}F_{-1}&=\\
&=-A_nF_{-2}-F_{n-2};\\
\ldots\ldots\ldots\ldots\ldots\ldots\ldots\ldots&\\
A_1F_0+A_2F_{-1}+\ldots+A_{n-1}F_{-(n-2)}&=\\
&=-A_nF_{-(n-1)}-F_1.
\end{aligned}\right\} \qquad (11)$$

It should be borne in mind that coefficient A_n is regarded as known in these equations, since it follows from (8) that

$$A_n=(-1)^n e^{-a_1 T}.$$

The set of equations (11) is greatly simplified in a number of cases

$$A_1F_1=A_2F_{-1}-F_2;$$
$$A_2F_{-1}=-A_2F_{-2}-F_1$$

and consequently A_1 is determined from the first equation and A_2 from the second. Here, in so far as the coefficients are calculated both from the values of the sought for function with positive t and from these values with negative t, the calculations are simple and highly accurate.

When the coefficients of the recurrence formula have been determined we can next pass to the calculation of the equally distant values of the sought for function with the constant step.

It is also expedient to consider the method of enlarging the step. Firstly, this method makes it possible to obtain recurrence formulae at a considerable step value. Secondly, it is possible to calculate discrete values of the time function with different intervals. Turn to equation 7, the coefficients of which are expressed by formula 8. If we produce a new equation in which, as in 7, the coefficients are combinations of the squares of its roots, i.e. $e^{2p_1\tau}$, $e^{2p_2\tau}, \ldots, e^{2p_n\tau}$, it is obvious that the transformed equation should correspond to a recurrence formula with a doubled step. This transformation of the equation is performed on the basis of the method of laying of the roots, as used by I.I. Lobachevskii in his method of solving algebraic equations.

The coefficients of the transformed equation $A_1^{(1)}, A_2^{(1)}, \ldots, A_{n-1}^{(1)}, A_n^{(1)}$ are determined as follows according to the coefficients for the old equation:

$$\left.\begin{aligned} -A_1^{(1)} &= A_1^2 - 2A_2; \\ (-1)^{n-1} A_2^{(1)} &= A_2^2 - 2A_1A_3 + 2A_4; \\ &\cdots\cdots\cdots\cdots\cdots\cdots \\ (-1)^n A_{n-1}^{(1)} &= A_{n-1}^2 - 2A_{n-2}A_n; \\ (-1)^n A_n^{(1)} &= A_n^2. \end{aligned}\right\} \qquad (12)$$

We thus have:

$$m^{2n} + A_1^{(1)} m^{2n-2} + A_2^{(1)} m^{2n-4} + \ldots + A_{n-1}^{(1)} m^2 + A_n^{(1)} = 0$$

and consequently, the recurrence formula for the double step assumes the form

$$F_{2n+\nu} + A_1^{(1)} F_{2n-2+\nu} + A_2^{(1)} F_{2n-4+\nu} + \ldots + A_{n-1}^{(1)} F_{2+\nu} + A_n^{(1)} F_\nu = 0.$$

By using this transformation several times it is possible to increase the step 4, 8, 16 and so on times. Note that it is expedient to double the step when the necessary number of initial ordinates of the transient process curveshave been calculated in order to continue the calculation.

Example. Let it be required to calculate the impulse transient function for the low frequency filter shown in Fig. 1.

The transmission function of this filter is written in the following

form:

$$F(p) = \frac{1}{p^3 + 6p^2 + 15p + 15}.$$

The expansion of the F( ) function into a series has the form:

$$F(p) = \frac{1}{p^3} - \frac{6}{p^4} + \frac{21}{p^5} - \frac{51}{p^6} + \frac{81}{p^7} - \ldots$$

Whence we find

$$F(t) = 0.5t^2 - t^3 + 0.875t^4 - 0.425t^5 + 0.112t^6 - \ldots$$

TABLE 1

t	0	0.1	0.2	0.4	0.6	0.8	1.0	1.2	1.4	1.6	1.8	2.0
$F(t)\times10^2$	0	0.408	1.327	3.450	4.938	5.458	5.173	4.396	3.423	2.466	1.646	1.011

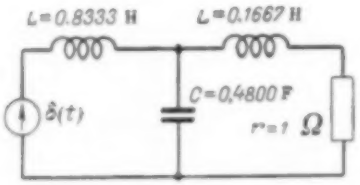

Fig. 1.

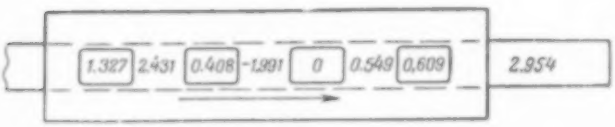

Fig. 2.

With a step $\tau = 0.1$, calculate by this series

$$F_0 = 0;\ F_{-1} = 0.609 \cdot 10^{-2};\ F_1 = 0.408 \cdot 10^{-2};$$
$$F_{-2} = 2.954 \cdot 10^{-2};\ F_2 = 1.327 \cdot 10^{-2}.$$

Using the above method, determine the recurrence formula for the step $\tau = 0.1$:

$$F_{3+\nu} = 2.431F_{2+\nu} - 1.991F_{1+\nu} + 0.549F_{\nu}.$$

If the step is doubled we have

$$F_{6+\nu} = 1.930F_{4+\nu} - 1.296F_{2+\nu} + 0.301F_{\nu}.$$

Using these recurrence formulae we can calculate the discrete values of the impulse transient function shown in Table 1.

$$F(t) = 0.3020e^{-2.322t} + e^{-1.839t}\{0.0832 \sin 1.754t - \\ - 0.3020 \cos 1.754t\}.$$

The analytical solution of the problem has the form:

$$F(1) = 5.14 \cdot 10^{-2}.$$

Using this formula, when $t = 1.0$ we have

$$F(2) = 0.93 \cdot 10^{-2}.$$

and when $t = 2.0$

It has to be acknowledged that the results are comparable.

A special slide rule is particularly helpful for the calculation (Fig. 2). The rule consists of two plates, the top one being made of white celluloid. The plates are secured in such a way that a paper tape can be drawn freely between them. Rectangular windows are provided in the celluloid plate, spaced out at equal distances. The coefficients of the recurrence formulae are inscribed on the sections between the windows (these markings can be erased later), and the discrete values of the exponential polynomials are inscribed in the windows on the paper tape. The result of the calculation by the recurrence formula is inscribed in the extreme window on the left.

When the paper tape is drawn one step along, the values of the exponential polynomials corresponding to the recurrence formula are shown on the right of every coefficient. The result of the new calculation is again written in the left hand window and then the tape moved along one step again and so on.

In Fig. 2 the position of the paper tape corresponds to the calculation of $F(t)$ for the moment of time $t = 0.2$ from the recurrence formula inscribed for step $\tau = 0.1$.

Translated by O. M. Blunn

REFERENCES

1. S. S. Khukhrikov: *Approximate numerical method of calculating transient processes in linear and non-linear systems, (Priblizhennyi chislennyi metod rascheta perekhodnykh protsessov v lineinykh i nelineinykh sistemakh)*, Oborongiz, (1957).

2. P.A. Ionkin; *Elektrichestvo*, No.10, (1958).
3. A.A. Krasovskii and G.S. Pospelov; *Avtomat. i telemekh.*, 14, No.6, (1953).
4. R. Roxer and S. Thaler; *Proc. Inst. Radio Eng.*, No.1, (1956).

ABSTRACTS FROM PAPERS PUBLISHED IN ELEKTRICHESTVO No. 4 1960

Lenin and all-out electrification of the U.S.S.R: I.A. Syromietnikov. (pp 1-6).

The paper relates Lenin's plans for the electrification of the U.S.S.R. and briefly traces the development of electrification in the U.S.S.R. from 1917 to the present time. The long term plans for the next 20 years are also considered. These do not necessarily exclude the development of atomic power stations. The article is in commemoration of Lenin's birthday 90 years ago.

A method for investigating dynamic stability on analogue computers: V.S. Tarasov, A.I. Vaizhnov, Iu.V. Rakitskii, V.V. Popop and L.N. Semenova (pp 7-12).

A method is proposed for using an LPI computer for investigating transient processes in two synchronous machines operating in parallel with a network of infinite power via concentrated resistances. It is assumed that the effect of the active resistance of the stator circuits and the transient processes caused by this resistance can be ignored. The study is made of non-salient pole synchronous machines having a rotor with two symmetrical windings along the d and q axes, a non-saturated magnetic circuit and variable excitation. The author advocates the design of specialized analogue computers.

Electronic excitation for machines in the main drive of reversing rolling mills: M.Ia. Pistrak and L.M. Balabueu. (pp 13-20).

A study is made of the use of ionic converters instead of dynamoelectric amplifiers for the excitation of d.c. machines in connexion with the development of control systems for the drives of blooming and slabbing mills. It is claimed that industrial service has demonstrated the advantages of the ionic converters as described.

A low-inertia motor drive for excavators: M.I. Kraitsberg, D.A. Kaminskaya and V.P. Lomakin. (pp 26-30).

Owing to the frequent shock loads encountered when the bucket strikes an immovable obstacle the authors describe a generator-motor drive system with dynamoelectric control incorporating continuous voltage and current feedbacks with cut-off and a stabilizing transformer. Provision is made for two-stage extinction of the generator magnetic field when the command controller is set in the zero position. A special feature is the additional resistance which is connected in series with the generator excitation winding in order to reduce the electromagnetic time constant of the generator. Stabilization is increased by a ballast resistance connected in parallel with the armature of the amplifier. It is claimed that the proposed scheme prolongs service life, reduces the number of breakdowns, and though costly, more efficient. A smaller transmission ratio is advocated.

Calculating a.c. machine transients using frequency characteristics: E.Ia. Kazovskii. (pp 30-37).

The mathematical relationships underlying the use of frequency methods for the theory of synchronous machines are given. Frequency characteristics are defined as the experimentally determined dependence of the mean stator current on the slip of the rotor for a non-excited 150 MW turbo-generator of 3000 rev/min connected to a power network as a motor. Such relationships have been produced in the All-Union Electrical Engineering Institute. A study is only made of the case of stator symmetry. Only transient processes are considered at a constant speed, no account being taken of machine saturation. Methods are proposed for determining the frequency characteristics according to transient processes and using the frequency characteristic in the event of a three phase short circuit and for the case when the machine is connected to the network.

The differential equations for a synchronous generator in transient stability studies on analogue computers: B.N. Kagan and E.L. Urman. (pp 37-42).

A study is made of the use of automatic digital computers (AT VM type). An improvement is required in the mathematical description of transient processes in synchronous machines and other power system elements as well as the development of new methods of investigation. The results are given of an investigation with a digital computer carried out to elucidate the effect on the theoretical limit to dynamic stability in the first cycle of the swing of various factors (saturation, damper

system, transformer c.m.f.'s induced in the stator windings etc.).

Special performance characteristics of heavily loaded transmission lines: G.M. Sekhniashvili (pp 42-46).

A method is proposed for investigating the conditions of heavily loaded transmission lines which can reveal the physical state of the lines and solve problems connected with the establishment of optimum operating conditions, the discovery of cheap methods of improving conditions and the determination of the requirements as regards automatic equipment. The method takes into account the active resistance of the transmission line conductors.

The error and applicability of formulae for specific permeances: B.K. Bul'. (pp 51-57).

The accuracy with which a magnetic circuit with an air gap can be calculated mainly depends on the accuracy with which the permeance of the field of "swelling" can be determined. This is often impossible as the field is three-dimensional. An investigation has therefore been made into the flux between the side surfaces of the poles with different gaps. The permeance due to field " swelling" is held to be dependent on the ratio of the pole width to the size of the gap. The limits are given within which the Evershed, Roters, Cramp and Colderwood, Finnis and Slivinskii formulae are valid. The " Forb" and Schmidel formulae are not recommended.

Extinction of an open arc. A.S. Maikopar. (pp 64-69).

In order to avoid disconnecting the fault section when an open arc is formed due for instance to mechanical damage to cables, a study is made of the conditions for independent arc extinction. Difficulties arise however due to the tendency for the discharge column to turn into a spiral. After reviewing earlier investigations the author describes the tests carried out and the investigation made into arcs between metallic electrodes corresponding to arcs arising in high voltage equipment.

Theory of current and voltage stabilizers. S.D. Dodik. (pp 73-77).

Current and voltage stabilizers in the presence of small changes in current and voltage are represented as a linear multi-pole for which a set of equations can be produced, this set of equations being rewritable in matrix form. This method of analysis is developed and

relationships produced suitable for investigation into any type of system of current and voltage stabilizer. Examples of the calculation are given.

A new type of small metal-varnish capacitor: V.T. Renne. (pp 77-81).

The widespread use of semiconductor instruments has reduced the voltage at which capacitors operate to the order of tens of volts and below so that the specific volume of capacitors is reduced because of the thinner dielectric. Earlier attempts to use varnished film failed since weak points could not be eliminated. An account is given of new methods used in Western countries where use is made of a coating in the form of very thin layers of metal (less than 0.1 micron thick) which are applied to the surface of the dielectric by vaporization in vacuum. In the event of puncture the layer of metal about the weak point melts and vaporizes.

AN IMPROVED SYSTEM OF ARC EXCITATION IN MERCURY ARC RECTIFIERS*

V.M. MANTROV

(Lenin All-Union Electrical Engineering Institute)

(Received 30 September 1959)

The constantly burning excitation arc is the main consumer of power expended on the valve's own needs. A reduction of this energy and a simplification of the excitation system would cut running costs considerably and to a certain extent reduce the prime cost of the rectifier installation.

Fig. 1(a) shows a modernized system of arc excitation in mercury arc rectifiers**. At positive polarity of the auxiliary anode I, an arc arises between it and the cathode and a half-wave of current passes through the reactor *P*. On diminution of this current in the reactor, an e.m.f. is induced under the effect of which anode 2 is ignited and consequently a second half-period of current passes into the excitation circuit at the expense of the energy stored in the reactor. In subsequent periods the current in the circuit of anode 1 increases at the expense of current in the preceding half-period, through the reactor (Fig. 1c). But the excitation current cannot increase for ever since its value is limited by the power losses in the circuit.

The instantaneous value of the current in the circuit of anode 1 is determined from the equation

$$\sqrt{2}\,U \sin \omega t = \omega L \frac{di_1}{d(\omega t)} + \Delta U,$$

where U is the effective value of voltage on the secondary winding of the excitation transformer T_e;

---

* *Elektrichestvo*, No.5, 13-15, 1960.

** An analogous system of arc excitation has also been proposed by V.M. Kolesnikov.

L the inductance of the reactor P;

ΔU the voltage drop in the excitation arc (its magnitude is practically independent of current).

Having integrated this equation within the limits from the angle of ignition θ_{ig} to ωt and from I_{min} to i_1, we obtain the following formula for determining the current in the circuit of anode 1 in the steady state:

$$i_1 = \frac{\sqrt{2}U}{\omega L}(\cos\theta_{ig} - \cos\omega t) - \frac{\Delta U}{\omega L}(\omega t - \theta_{ig}) + I_{min}. \qquad (1)$$

Expression (1) is true from $\omega t = \theta_{ig}$ to $\omega t = \theta_m$, corresponding to the maximum i_1.

1960

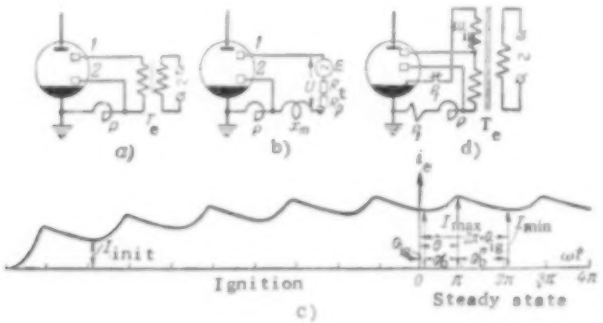

Fig. 1. Main circuit for arc excitation (*a*), approximate equivalent circuit (*b*), diagram of excitation currents (*c*) and ignition – excitation circuit for valves with a semiconductor igniter (*d*).

The ignition angle θ_{ig} is determined from the following equation:

$$\sqrt{2}U\sin\theta_{ig} = U_{ig} \qquad (2)$$

where U_{ig} is the ignition voltage of the excitation anode.

Having differentiated and equated equality 1 to zero, let us find the formula for determining the angle θ_m:

$$\sqrt{2}U\sin\theta_m = \Delta U. \qquad (3)$$

The burning angle of anode 1 equals

$$\theta_b' = \theta_M - \theta_{ig}$$

The instantaneous value of the current in the circuit of anode 2 is determined from the equation

$$\omega L \frac{di_2}{d(\omega t)} = \Delta U,$$

After integration of this equation from θ_m to ωt and from I_{max} to i_2, we have for the steady state

$$i_2 = I_{max} - \frac{\Delta U}{\omega L}(\omega t - \theta_M). \tag{4}$$

The angle of burning for anode 2 equals:

$$\theta_b'' = 2\pi + \theta_{ig} - \theta_M$$

and consequently equation 4 is true from $\omega t = \theta_m$ to $\omega t = 2\pi + \theta_{ig}$. Substituting the value of $\omega t = 2\pi + \theta_{ig}$ into expression 4 we have:

$$I_{min} = I_{max} - \frac{\Delta U}{\omega L}(2\pi + \theta_{ig} - \theta_M).$$

The amplitude of current pulsation is determined from the formula

$$\Delta i = I_{min} - I_{max} = \frac{\Delta U}{\omega L}(2\pi + \theta_{ig} - \theta_M). \tag{5}$$

In order to determine the magnitude of the current in the secondary winding of the transformer T_e and anode 1, use is made of the equivalent circuit shown in Fig. 1(b). According to this circuit the effective value of the voltage appearing in equation 1 will in the steady state equal:

$$U = E - I_{eff}(R_t + R_p),$$

where E is the no load voltage in the secondary winding of the transformer T_e;

I_{eff} – the effective value of the current in the secondary winding of the transformer T_e;

R_t – the resistance in the secondary winding of the transformer T_e;

R_p – the resistance in the winding of reactor P.

In addition, $\omega L + x_t$ should be substituted for ωL in equation 1 in

this case. Bearing the above in mind when $\omega t = \theta_m$ (Fig.1c), we can write:

$$I_{max} = \frac{\sqrt{2}[E - I_{eff}(R_t + R_p)](\cos\theta_{ig} - \cos\theta_m)}{\omega L + x_t} - \frac{\Delta U(\theta_m - \theta_{ig})}{\omega L + x_t} + I_{min}.$$

Calculating I_{min} from this equality we have

$$\Delta i = \frac{\sqrt{2}[E - I_{eff}(R_t + R_p)](\cos\theta_{ig} - \cos\theta_m) - \Delta U(\theta_m - \theta_{ig})}{\omega L + x_t}. \quad (6)$$

Equating expressions 5 and 6 we find

$$I_{eff} = \frac{\sqrt{2}E\omega L(\cos\theta_{ig} - \cos\theta_m) - \Delta U(\theta_m - \theta_{ig})\omega L - \Delta U(2\pi + \theta_{ig} - \theta_m)(\omega L + x_T)}{\sqrt{2}\omega L(R_t + R_p)(\cos\theta_{ig} - \cos\theta_m)}. \quad (7)$$

Assuming this current to be rectangular in shape with a height I_{max} we have

$$I_{max} = I_{eff}\sqrt{\frac{2\pi}{\pi - 2\theta_{ig}}}. \quad (8)$$

The average value of the excitation current approximately equals

$$I_{av} \approx I_{max} - \frac{\Delta i}{2}, \quad (9)$$

whilst the effective value of the excitation current, if pulsations are ignored, can be considered equal to maximum

$$I_{e.eff} = I_{max}. \quad (10)$$

The excitation system under consideration has been tested on valves with two types of igniter, namely, slit and semiconductor. The latter scheme is shown in Fig.1(c). In the scheme in question the ignition current passes through the winding of reactor P, which increases the energy stored in it in the first half period and ensures reliable excitation of the arc. The winding W_{ig} only operates momentarily and therefore need not be made powerful, provided there is a reserve of voltage for reliable ignition. The momentary passage of alternating current through the igniter does no harm to it and the selenium recti-

fier generally used in these cases can therefore be excluded from the circuit (on test, the igniter struck more than 10,000 arcs without any notable changes in its parameters).

In the case of rectifiers with slit igniters it is necessary to ensure that the excitation arc is struck clearly and distinctly besides satisfying condition 7 when choosing the voltage of the excitation transformer. To do this it is necessary for the energy of the reactor to be sufficient to hold until the next period of excitation current commences (equal to or greater than 2 to 3A) after the cathode spot has formed and the first half-wave of current has passed. This condition is approximately characterized mathematically by the following expression:

$$I_{init} \approx \frac{\sqrt{2}E(\cos\theta_{ig} - \cos\theta_{ul}) - 2\pi \cdot \Delta U}{\omega L} > 3. \qquad (11)$$

In low-power transformers used in excitation systems, $x_t \ll R_t$. In addition, when plasma is present in the valve $U_{ig} \approx \Delta U$, the ignition angle $\theta_{ig} \ll \theta_b$, whilst $\theta_{ul} \approx \pi$. On the above assumptions, expression 7 changes into the following formula

$$I_{eff} = \frac{\sqrt{2}E - \Delta U\pi}{\sqrt{2}(R_t + R_p)},$$

which can be used for preliminary calculations.

Fig. 2 shows oscillograms of the excitation current, the currents in the circuits of anodes 1 and 2 and also the voltages on the excitation anodes. They were taken when testing the scheme on a RMV – 250/2 type rectifier which had been in store for several years and had a high inflow of air and voltage drop in the excitation arc greater than 22V.

With 80V on the secondary winding of the excitation transformer and a reactor with a winding of 350 turns, the system of excitation struck the arc quite clearly from slit igniters and, as can be seen from the oscillograms, produced comparatively small current pulsations. With an effective current of 11 A in the secondary winding of the transformer, the average arc excitation current equalled 14 A, minimum 12 A. In the limiting case, the average (and minimum) excitation current can be

times greater than the effective value of the current in the excitation transformer.

It is expedient to combine the excitation scheme for two (or generally an even number of) rectifiers in order that the excitation transformer should operate under conditions of two half-period rectification.

Fig. 2. Oscillograms taken when testing the circuit shown in Fig. 1(a). i_1 – current in circuit of anode 1; i_2 – current in circuit of anode 2; i_e – arc excitation current; u_1 – voltage on anode 1; u_2 – voltage on anode 2.

The reactor should not be saturated in the steady state. Otherwise its large inductance at low currents will worsen the ignition of the arc.

Translated by O.M. Blunn

1960

EXCITATION SYSTEMS FOR VARIABLE FREQUENCY INDUCTION MACHINES*

A.T. GOLOVAN and I.N. KRUGLYANSKII

(Moscow)

(Received 26 October 1959)

There is as yet no method of selecting the system and calculating the parameters of asynchronous self-exciting machines, operating as variable frequency generators**. Neither has the possibility of regulating frequency been elucidated without switching the capacitor. The purpose of the present paper, produced in the faculty of electrical equipment for industrial undertakings at the Moscow Power Institute, is to solve these problems.

No account is taken in the analysis of machine operating conditions of the effect of hysteresis, whilst losses from eddy currents are ignored. Suppose that the currents and fluxes in the machine are sinusoidal and that the leakage reactances only depend on frequency, being practically independent of the saturation of the magnetic circuits in the machine.

The most diverse consumers may be served by the load of an asynchronous self-exciting generator of variable frequency, i.e. induction motors, vibrators, excitation circuits, power amplifiers and so on. All the basic relationships have therefore been obtained for the general case of the load $z_l = r_l + ix_l$.

In order to be definite, an investigation is made below into the performance of an induction motor generator having an impedance z_l which varies in such a way that the generator is under the same conditions as when the motor is supplied.

---

* *Elektrichestvo*, No.5, 31-36, 1960.

** A.T. Golvan and A.A. Dubenskii, *Asynchronous self-exciting generator of variable frequency, (Asinkhronnyi samovozbuzhdaiushchiisia generator peremennoi chastoty), Elektrichestvo*, No.5, 1945.

Suppose that the resistance torque on the shaft of this motor remains unchanged. Consequently, I_1 = const. Since $U_1 = U_{150}F$ torque, then $z_1 = z_{150}F$.

Since the inductance is proportional to frequency, only the active load impedance need be varied.

At low frequencies ($f \leqslant 25$ c/s) it is desirable to observe the relationship

$$\dot{U}_1 = \dot{U}_{150}F + \dot{I}_1 r_{1m}, \tag{1}$$

where r_{1m} is the active resistance of the stator winding in the motor under supply.

The load impedance should in this case vary according to the law

$$r_1 = r_{150}F + r_{1m}$$

and

$$L_1 = \text{const.}$$

A study has been made of the performance of variable frequency generators on the basis of a 1.7 kW AK-51-6 type induction machine with a phase rotor.

The magnetization curve was obtained experimentally for the analysis and used to produce the relationship

$$x_\mu = f'(I_\mu).$$

Since the reactive power of the capacitors is proportional to the capacitance and the square of the voltage, it is necessary to increase the voltage to decrease the capacitance. It is therefore proposed that the voltage on the rings be increased to 380 V by increasing the number of turns on the induction machine's rotor winding.

Consider certain systems of excitation for generators.

Fig. 1 shows the equivalent circuit of an induction machine with capacitors and additional resistances in the rotor circuit together with the corresponding vector diagram of currents and e.m.f.

The following relationships can be obtained from Fig. 1:

$$x_{2C} = x_2(F-\alpha)^2 - (F-\alpha)\sqrt{\frac{R_2(\sigma-F)}{(r_1+r_1)F}z_1^2 - R_2^2} \tag{2}$$

and

$$x_\mu = \frac{z_1^2}{F\left\{-(x_1F + x_1) + \frac{r_1 + r_1}{R_2}\left[x_2(F-a) - \frac{x_{2C}}{F-a}\right]\right\}}, \qquad (3)$$

where

$$z_1 = \sqrt{(r_1 + r_1)^2 + (x_1F + x_1)^2}$$

and

$$z_2 = \sqrt{\left(\frac{R_2}{s}\right)^2 + \left(x_2F - \frac{x_{2C}}{s^2F}\right)^2}.$$

The operating conditions of the generator (frequency, voltage, currents, efficiency and so on) are completely determined by these expressions given the parameters of the system.

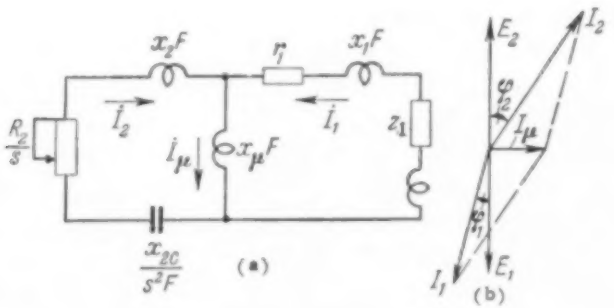

Fig. 1. Equivalent circuit of an asynchronous generator with capacitors and additional resistances in the rotor circuit (a), and the corresponding vector diagram of currents and e.m.f. (b).

Neither the scheme shown in Fig. 1, nor any other system of connecting the capacitors, makes it possible to regulate frequency over a wide range and produce optimum pre-determined operating conditions for the machine by varying just one parameter. It is therefore necessary to vary the capacitance of the capacitors and the resistance of the rotor circuit at the same time.

The corresponding values of R_2 and C_2 at which condition 1 can be

satisfied with a definite range of frequency variation, can be found in the following way.

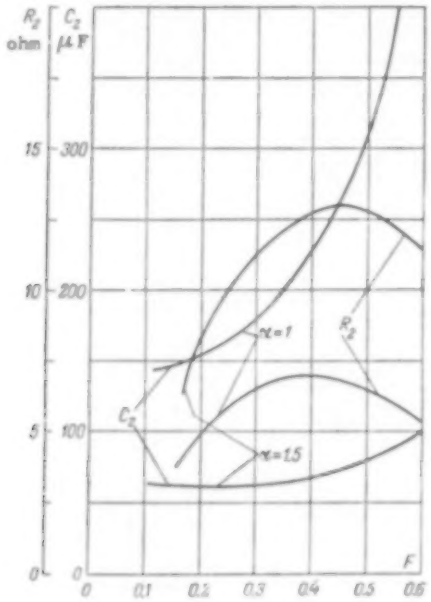

Fig. 2. The relationships of $C_2 = f(F)$ and $R_2 = f(F)$ for the system of connexion given in Fig. 1.

Knowing the value of current I_1 and impedance z_1, we can calculate $I_\mu x_\mu = I_1 z_1 / F$ and then find the value of the magnetization current and the reactance of magnetization from the curves $E = f(I_\mu)$ and $(x_\mu = f''(I_\mu))$. Thus, we can produce the relationship $x_\mu = f'(F)$ starting from the given law of voltage variation.

The value of impedance R can be determined by solving equations 2 and 3 together:

$$R_2 = \frac{z_1^2(-s)}{(r_1 + r_1')\left\{\left[\frac{z_1^2}{x_\mu F} + (x_1 F + x_1')\right]\frac{1}{r_1 + r_1'} + 1\right\}}. \qquad (4)$$

Fig. 2 shows curves for $C_2 = f(F)$ and $R_2 = f(F)$ when $Z_{l\,50} = 70.5 + j\,52.8$; $I_l = 2.5$A; $\alpha = 1.5$ and $\alpha = 1$.

It follows from the curves in Fig. 2 that when $F < 0.35$ regulation is effected by varying the impedance R_2 with practically constant capaci-

tance on the capacitors. It is necessary to increase the capacitance noticeably with increasing F (the more intensively, the higher the frequency), by reducing the value of the impedance R_2 at the same time. This is explained by the need for there to be a sharp increase in the magnetization current at low frequencies. As frequency increases, so the magnetization current should gradually decrease; at $F \gg 0.5$ its value can be assumed fixed.

The intensive increase in capacitance is explained by the decrease in the frequency of the rotor current with increasing F. This increases the reactance of the capacitors and reduces the magnetization current. The need therefore arises for the resistance of the rotor circuit to be reduced.

The efficiency of the generator is very low at low frequencies owing to the increase in losses in the rotor circuit. The losses can be substantially reduced by using a multi-speed induction machine as the drive motor, this machine operating at the lowest speed limit when frequencies are low. However, this measure can cause a certain increase in the requisite capacitance of the capacitors.

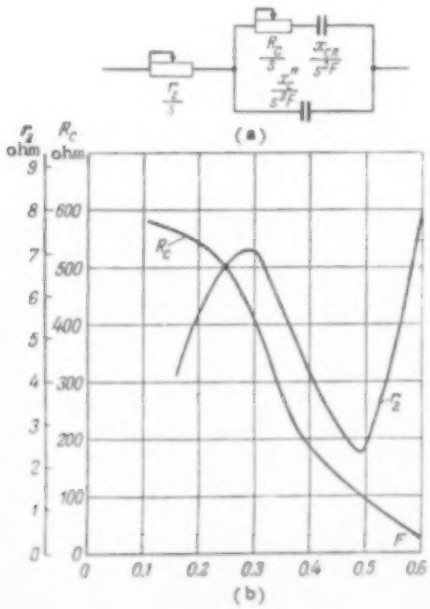

Fig. 3. System of connecting capacitances (a), and regulation characteristics (b) for the low frequency asynchronous generator.

The need to switch the capacitors is a disadvantage of the scheme under consideration.

This disadvantage can be avoided if the capacitors in the machine's rotor are connected as in Fig. 3.

On the basis of the equivalence of the schemes in Figs. 1 and 3 and assuming the capacitances x_{CR} and x_C'' to be constant, we have

$$R_C = \frac{1}{s-F}\sqrt{\frac{x_{2C}(x_{CR}+x_C'')^2-(x_{CR}+x_C'')x_C''x_{CR}}{x_C''-x_{2C}}} \tag{5}$$

and

$$r_2 = R_2 - \frac{1}{s-F}\sqrt{(x_C''-x_{2C})\left(x_{2C}-\frac{x_C''x_{CR}}{x_C''+x_{CR}}\right)}. \tag{6}$$

1960

It follows from equality (6) that the following inequalities should be satisfied at all frequencies within the given range

$$\left.\begin{aligned} C_2 &\geqslant C''; \\ C_2 &\leqslant C_R + C''. \end{aligned}\right\} \tag{7}$$

Since it is desirable to produce the largest possible value of r_2 (in order to decrease the magnitude of capacitance, reduce losses and save copper), it is necessary to try to get the minimum of the radicand

$$\begin{aligned} &(x_C''-x_{2C})\left(x_{2C}-\frac{x_C''x_{CR}}{x_C''+x_{CR}}\right)= \\ &=3\,180^2\left(\frac{1}{C''}-\frac{1}{C_2}\right)\left(\frac{1}{C_2}-\frac{1}{C''+C_R}\right). \end{aligned} \tag{8}$$

It follows from (8) that r_2 is greater, the greater C'' and the smaller the sum of $C''+C_R$.

Bearing all that has been said in mind, it is recommended that the parameters of the scheme in Fig. 3(a) be selected in the following way:

1. The magnitude of C'' should hardly be less than that of capacitance C_2, calculated for the lowest frequency in the scheme in Fig. 1.

2. C_R should be selected from the condition that the sum of C_R and C'' equals capacitance C_2, calculated for the highest frequency in the same scheme.

3. After selecting capacitances C and C_p, the resistances r_C and r_2 should be determined from formulae (5) and (6).

Altogether, we can obtain regulation characteristics $r_C = f(F)$ and $r = f(F)$ (Fig. 3b) in the event of the values of capacitance being constant ($C = 60\ \mu F$ and $C_p = 40\ \mu F$).

In the case of frequencies in the vicinity of nominal or greater than that, when the frequency of the rotor current is small, the connexion of capacitors in the secondary circuit will not ensure that the necessary reactive currents are produced. Capacitors are therefore connected in parallel to the load (Fig. 4a).

After transformation we obtain the equivalent scheme shown in Fig. 4b. The equivalent impedances of the load can be calculated from the formulae:

$$R_e \approx \frac{r_1\left(\frac{x_C}{F}\right)^2}{r_1^2 + \left(\frac{x_C}{F} - x_1\right)^2} \tag{9}$$

and

$$x_e = \frac{\frac{x_C}{F}\left(r_1^2 - \frac{x_C}{F}x_1\right)}{r_1^2 + \left(\frac{x_C}{F} - x_1\right)^2}. \tag{10}$$

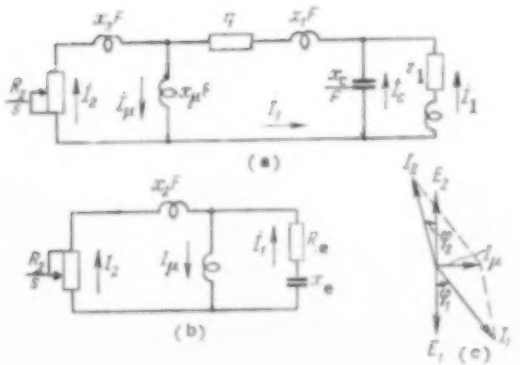

Fig. 4. Equivalent circuit of an asynchronous generator with additional resistances in the rotor circuit and capacitors in parallel to the load (a), the corresponding equivalent network (b) and the vector diagram of currents and e.m.f. (c).

Using Fig.4b and the appropriate vector diagram Fig.4(c), we can obtain the following fundamental dependencies of frequency and magnetization reactance on the parameters of the scheme and the speed of the generator in the same way as before, when capacitors were connected in the rotor circuit:

$$s = \frac{-z_e^2 + \sqrt{z_e^4 - 4R_e^2(x_2F)^2}}{2R_e(x_2F)^2} R_2 \tag{11}$$

and

$$x_\mu = \frac{z_e^2}{F\left(x_e + \frac{R_e}{R_2} x_2 F s\right)}. \tag{12}$$

Ignoring the resistance of the stator winding, the condition for regulating the generator at a constant load torque is $x_\mu = \text{const}$. Therefore, given the frequency, we can find resistance R_2 and

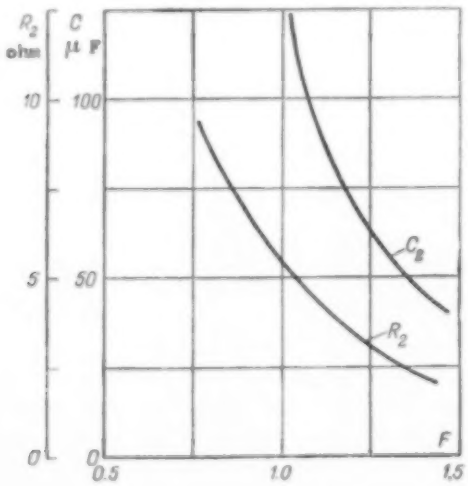

Fig. 5. The relationships of $R_2 = f(F)$ and $C = f(F)$ for the equivalent circuit in Fig.4 (a).

capacitance C from equalities 11 and 12 if we have definite values for the load and x_μ. The connexion of resistance R_2 and capacitance C as in Fig. 4(a) ensures the desired operating conditions. As an example, Fig.5 presents curves for $R_2 = f(F)$ and $C_2 = f(F)$ when $x_\mu = 58\ \Omega$, $\alpha = 1.5$, $I_l = 3.3$ A, $z_{l50} = 58.6 + j\ 44.3$ and $\frac{E}{F} = 235$ V.

An increase in capacitance will lead to an increase in slip (in absolute magnitude) and consequently to a reduction of the frequency of the current under regulation. In its turn the latter circumstance causes an increase in the reactance of the capacitors, thereby reducing the slip. It is therefore necessary to introduce an active resistance into the rotor circuit. This will increase slip. We can try to get a magnetization current of constant value by the appropriate choice of R_2 and C, in so far as the introduction of R_2 causes this current to decrease, and an increase in C causes it to increase.

Although the connexion of a series-connected variable impedance and constant capacitance to the stator terminals enables us to avoid having to switch the capacitors, it brings about a sharp reduction in efficiency and the steady output of the generator is exceeded. It is therefore expedient to make use of the scheme given in Fig. 6 to obtain high frequencies.

From the equations for the balance of active and reactive outputs in the generator-load system we obtain

$$\frac{z_1 R_2}{z_2^2 s} + \frac{z_1 R_1}{z_{R1}^2} + \cos\varphi_1 = 0 \tag{13}$$

and

$$\frac{z_1 F}{x_C} + \frac{z_1 x_{CR1}}{z_{R1}^2 F} = \frac{z_1}{x_\mu F} + \sin\varphi_1, \tag{14}$$

where

$$z_{R1} = \sqrt{R_1^2 + \left(\frac{x_{CR1}}{F}\right)^2}.$$

Equation (14) determines the magnitude of R_1 for the given frequency F, load z_l and reactance x_μ at constant values of the remaining parameters:

$$R_1 = \sqrt{\frac{x_{CR1}}{F\left(\frac{1}{x_\mu F} - \frac{F}{x_C} + \frac{\sin\varphi_1}{z_1}\right)} - \left(\frac{x_{CR1}}{F}\right)^2}. \tag{15}$$

whilst equation 13 determines the magnitude of R_2.

Analysing expression (15) arc can obtain the relationships for selecting the capacitances of the capacitors C and C_{R1}.

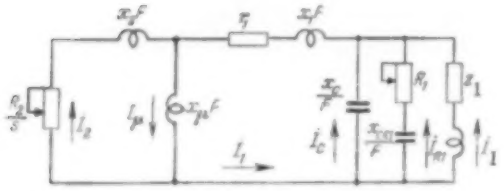

Fig. 6. System of connecting capacitors and resistances for a high frequency asynchronous generator.

Since capacitance C can be expediently selected from the highest limit of the range of frequency regulation, and capacitance C_{B1} from the lowest limit, the theoretical formulae have the form

$$C \leq \frac{3180}{F_1}\left(\frac{1}{x_\mu F_1} + \frac{\sin\varphi_1}{z_{l1}F_1}\right) \tag{16}$$

and

$$C_{B1} = \frac{3180}{F_2}\left(\frac{1}{x_\mu F_2} + \frac{\sin\varphi_1}{z_{l2}} - \frac{F_2}{x_C}\right), \tag{17}$$

where F_1 and F_2 are the upper and lower limits of the range of frequency regulation in the scheme in question;

z_{l1} and z_{l2} are the total load impedances corresponding to frequencies F_1 and F_2.

The dependencies of efficiency, consumable output and current on frequency are shown in Fig.7 for the case when $x_\mu = 58\ \Omega$, $I_\mu = 4$A, $a = 1.5$, $z_l = 58.6 + j44.3$, $C = 35\ \mu$F and $C_{B1} = 35\ \mu$F.

In order to produce medium frequencies ($0.5 < F < 1.1$), it is advisable to connect the capacitors in the stator and rotor circuits. The equivalent circuit for the asynchronous machine and that for this case are both shown in Fig. 8.

Equations can be obtained from the equilibrium state of the active and reactive outputs so as to determine the parameters for this system of connecting the capacitors and those for the impedances as well.

In order to bring about a considerable decrease in the capacitance connected in the rotor circuit and to make it unnecessary to switch the capacitors as well, use may be made of the system shown in Fig.9. The parameters of this scheme are calculated in the same way as that for Fig.8 using the method given above.

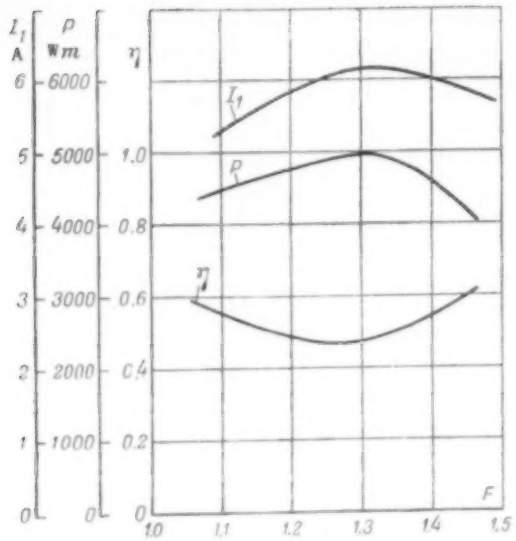

Fig. 7. Characteristics of generator when capacitors and resistances are connected as in Fig. 6.

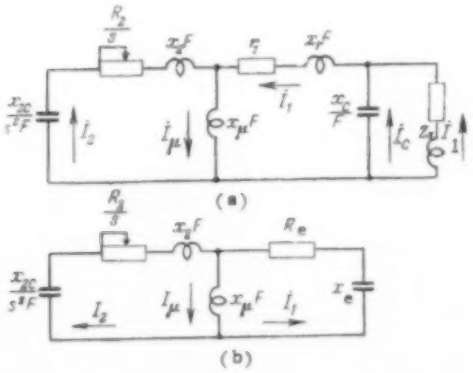

Fig. 8. Substitution circuit (a) and equivalent circuit (b) of a machine when capacitors are connected in the rotor and stator circuits.

Thus the appropriate control system for variable frequency generators should be selected as a function of the required range of frequency regulation. Systems can be combined for large ranges of regulation. Use may thus be made of the system of connecting the capacitors and

additional resistances as shown in Fig. 10.

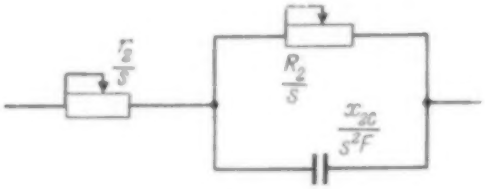

Fig. 9. Equivalent circuit for the secondary circuit of a medium frequency generator.

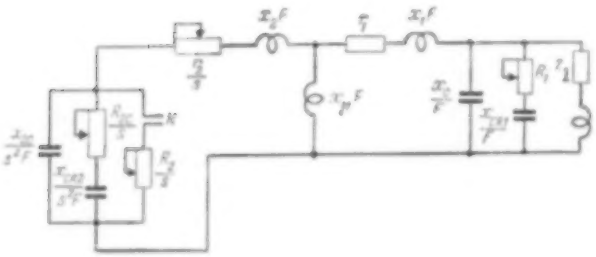

Fig. 10. Typical excitation circuit for a generator with a wide range of frequency regulation.

Contact K is closed when $F = 1.1$ to 1.5 and frequency is regulated by varying resistances R_1 and R_2. At medium frequencies ($F = 0.5$ to 1.1) contact K remains closed, resistances R_1 and R_{2C} are completely withdrawn and the magnitudes of r_2 and R_2 vary. At low frequencies ($F < 0.5$) contact K opens, resistance R_1 is completely withdrawn and regulation is effected by resistances r_2 and R_{2C}.

Conclusions

1. It is necessary to vary two parameters of the system to maintain optimum operating conditions for asynchronous self-exciting generators of variable frequency supplying an electrical motor. Continuous variation of frequency can be produced over a wide range (up to 10 to 15).

2. The efficiency of the generator can be increased at low frequencies by changing down the speed of the drive motor.

3. The capacitance of the capacitors necessary to excite a 1.7 kW machine is 450 to 500 μ F at the maximum range of regulation.

4. It is not advisable to use a machine with a low secondary voltage as a variable frequency generator. The generator should have a slightly smaller resistance in the rotor winding than that in a conventional induction machine.

5. It is necessary to take into account the losses in the active resistances of the machine stators when selecting the output of the generator on operation at low frequencies.

Symbols

$F = \frac{f}{50}$ - relative frequency;

$s = \frac{F - a}{F}$ - relative slip;

$a = \frac{n}{n_c}$ - relative speed of generator;

n_s - synchronous speed at 50 c/s;

r_l, x_l and z_l - resistance, reactance and total impedance of the load;

I_l, U_l, P_l and $\cos\phi_l$ - current, voltage, power and power factor of the load;

z_{l50}, U_{l50} and P_{l50} - impedance, voltage and power of the load at 50 c/s;

x_C - capacitance of capacitors at 50 c/s;

x_μ - reactance of the magnetization in the machine at 50 c/s;

I_μ - magnetization current.

Translated by O.M. Blunn

THE ELECTRICAL AND PHYSICAL PROPERTIES OF ELECTRICAL INSULATING MATERIALS

K.A. VODOP'IANOV, B.I. VOROZHTSOV, G.I. POTAKHOVA and N.I. OL'SHANSKAIA

(Siberian Physico-Technical Institute at the Tomsk State University)

(Received 7 December 1959)

1960

Introduction

There is as yet little published information about the effect of radioactive radiation on the electro-physical properties of industrial electro-insulating materials. The physics of the phenomena taking place in them are still unknown. However, the practical use of atomic energy on a large scale for peaceful purposes requires a physical generalization of the radiation resistance of a number of electrical insulating materials, such as are used in electrical and radio engineering plant and equipment experiencing radioactive radiation.

The present paper introduces experimental data obtained by a study of the effect of gamma-radiation on the electro-physical characteristics of high polymer dielectrics, silicone-organic and phenol-formaldehyde plastics.

Irradiation was effected by a betatron construction at the Tomsk Polytechnical Institute with a gamma ray energy of 15 MeV and a dose rate of 300 to 1200 roentgen per min. Dielectric specimens were exposed at different temperatures (-60, +20 and +60°C) and under conditions of tropical humidity (temperature + 40°C and relative humidity of air 98%).

Measurements were taken of electrical strength, the temperature dependence of electrical conductivity and mainly the temperature and frequency dependencies of the dielectric loss angle and the dielectric permeability of electrical insulating materials before and after irradiation by gamma-rays.

---

* *Elektrichestvo*, No.5, 60-66, 1960.

High molecular substances

The temperature-frequency dependencies of dielectric permeability and the dielectric loss angle in polyethylene, fluoroplast - 4 and product - 10 before and after irradiation by gamma-rays are shown in Fig. 1. It is seen that dielectric permeability and the loss angle are independent of the effect of radiation under normal conditions in all three dielectrics over the measured frequency and temperature ranges. It is apparent that an actual dose of 50,000 roentgen is insufficient to cause a change in dielectric permeability and the loss angle. It can be seen from Fig. 1(c) that the dielectric loss angle is only increased slightly in the case of fluoroplast - 4 even at a dose of 1 million roentgen and above; the variation here in the loss angle of product - 10 was within the limits of error allowed for the measurement. The irradiation of polyethylene under normal conditions at -70°C did not lead to changes in the mechanism of losses, polarization and the absolute values of dielectric permeability, the loss angle (Fig. 2b) and electrical strength. The loss angle and conductance increase (Fig. 2a) after the exposure of polyethylene at low temperatures (t = = -70°C); exposure under tropical conditions (t = 40°C and relative humidity 98%) leads to a reduction of the loss angle in the low frequency region (Fig. 2c) and an increase in volume resistance.

Consequently, the processes taking place in the polyethylene on exposure to gamma-rays are a function of temperature conditions. It may be supposed that the effect of ionization should be at a maximum in exposure under low temperature conditions since a brake is put on the recombination of the radicals; this leads to an increase in the conductance and dielectric loss angle. The variations in the specific volumetrical resistance and loss angle of polyethylene, caused by irradiation under tropical conditions, are apparently produced by the interaction of the products of water radiolysis with the molecules of the polymer.

Independently of irradiation it is of interest to elucidate the character of the dependence of the loss angle on the frequency and temperature of the polymers under investigation.

Polyethylene, fluoroplast-4 and product-10 are usually regarded as non-polar polymers with low values of dielectric permeability and the loss angle. Our experiments have shown (Fig. 1*a* and *b*) that frequency and temperature maxima do exist in polyethylene for the dielectric loss angle, these maxima being caused by the oriented polarization of the polar groups $C = O$.

Fluoroplast-4 can also be regarded as a weakly polar dielectric and the need to increase the loss angle with increasing frequency is there-

fore apparently caused by the orientation of the polar groups appearing in the composition of fluoroplast-4.

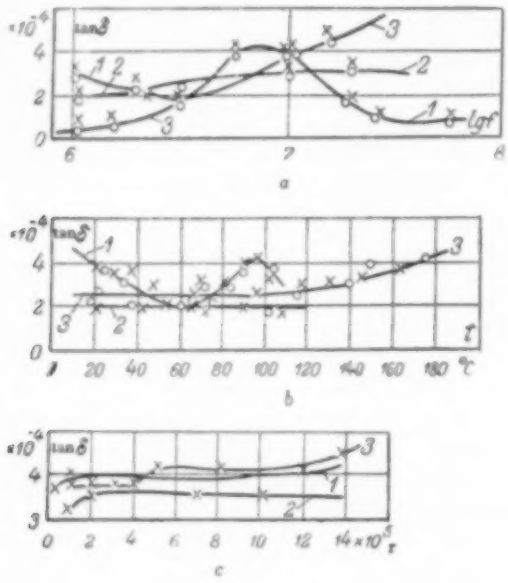

Fig. 1. Dependence of the dielectric loss angle on frequency (a), temperature (b) and dosage (c).
1 – polyethylene; 2 – "product-10"; 3 – "fluoroplast-4".
For (a) and (b) the dosage is 50,000 roentgen; 0 – non-irradiated material; X – irradiated.

Fluoroplast-4 is usually regarded in electrical and radio engineering practice as a good high quality dielectric. It is however necessary to bear in mind that the loss angle of fluoroplast-4 begins to increase noticeably at frequencies higher than 10^7 c/s (Fig. 1a) and that its absolute value becomes considerably greater than that of polyethylene and product-10.

Compared with polyethylene and fluoroplast-4, the loss angle of product-10 is considerably less dependent on frequency and temperature. This is evidence that there are no dielectric losses of a dipole character over the measured temperature and frequency ranges in question.

There was no change in the dielectric permeability of fluoroplast-4 and product-10 before and after exposure as a function of frequency and

temperature. A small decrease in the dielectric permeability of polyethylene occurred with an increase in frequency.

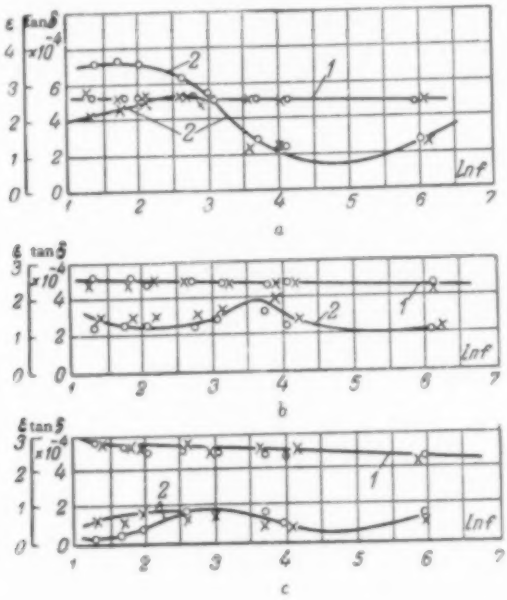

Fig. 2. Dependence of the ϵ and tan δ of polyethylene on frequency.
a – irradiated at $t = -70^{\circ}C$; b – irradiated at $t = -70^{\circ}C$;
c – irradiated under tropical conditions. 1–ϵ; 2–tan δ;
0 – non-irradiated material; X – irradiated

Thus the high polymer dielectrics of the polyethylene, fluoroplast and polystyrene types undergo no noticeable change in their properties on irradiation with gamma rays under normal conditions right up to 1 million roentgen, i.e. they are radioactively stable.

Silicone-organic plastics and rubbers

SKM-1 type glass textolite is made in silicone-organic resin and based on methyl trichlorsilane and phenyl trichlorsilane bonding agent, i.e. it contains polar molecules. Glass textolite will therefore have polarization and dielectric losses of a dipole character over the appropriate temperature and frequency ranges; losses of an ohmic character with a large value of specific conductance are possible in other ranges.

It can be seen from Fig.3 that the dependence of the loss angle on the frequency has a blurred maximum. The maximum loss angle with the corresponding change in dielectric permeability is also discovered in the temperature dependence, despite the fact that the temperature behaviour of the loss angle is mainly due to the change in conductance (Fig.4). The dependence of electrical conductance on temperature is shown in Fig.5.

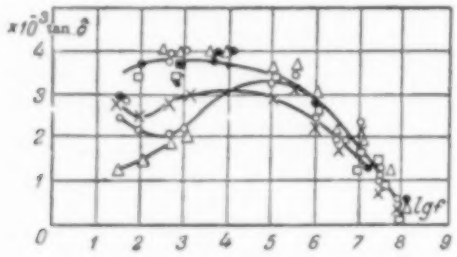

Fig. 3. Dependence of the tan δ of SKM - 1 type glass textolite on frequency under different conditions of gamma-radiation.
Dosage 100,000 roentgen.
0 - non-irradiated; X - irradiated; $t = 20^{\circ}C$; △ - irradiated, $t = 60^{\circ}C$; □ - irradiated, $t = -60^{\circ}C$; ○ - irradiated (tropical conditions).

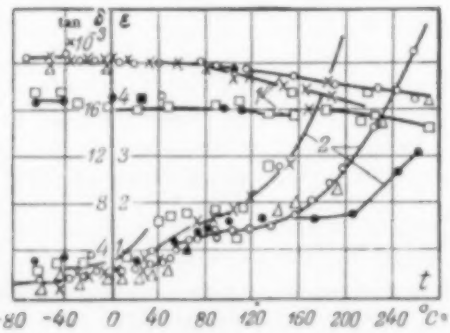

Fig. 4. Dependence of the ϵ and tan δ of SMK-1 glass textolite on temperature at $f = 5 \times 10^2$ c/s and under different conditions of gamma-radiation.
Dosage 100,000 roentgen.
1 - ϵ; 2 - tan δ. Designations as in Fig. 3.

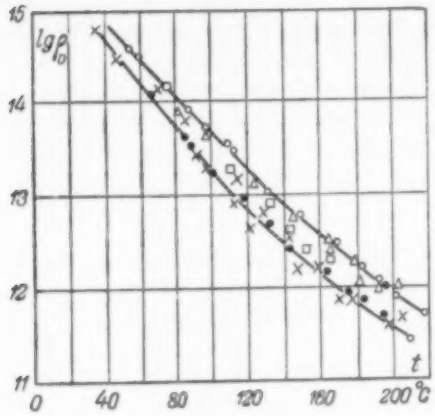

Fig. 5. Dependence of the ρv of SKM - 1 glass textolite on temperature under different conditions of gamma-radiation. Dosage 100,000 roentgen. Designations as in Fig.3.

As the experimental data refer to irradiated and non-irradiated specimens at different temperatures (-60, 20 and +60°C) and under tropical conditions, it is of interest to analyse them as a function of the conditions of exposure to gamma-rays. A notable increase is seen in the dielectric loss angle in the low frequency region as a result of irradiation at room temperature (Fig.3) and at high temperatures (Fig.4). This is apparently caused by the increased electrical conductance of the glass textolite (Fig.5). The electrical strength of glass textolite was practically the same before and after exposure and equalled 28 to 29 kV/mm. As can be seen from the experimental data, exposure at -60°C does not noticeably change the electrical properties of glass textolite. It is possible that annealing of the radiation disorders takes place at high radiation temperatures, i.e. the probability of the ionized fragments re-combining is increased. The probability of recombination is very small at low temperatures and a change is therefore to be seen in the dielectric permeability and loss angle of glass textolite as a result of radiation at low temperatures (-60°C). The loss angle increases considerably over the 50 to 10^5 c/s range. This increase takes place over all the measured range of temperatures (Fig.4). Dielectric permeability falls considerably after irradiation at -60°C. There is no noticeable change in the electrical strength and electrical conductance of glass textolite as a result of irradiation at low temperatures.

The irradiation of glass textolite under tropical conditions leads to

an increase in the dielectric loss angle at low temperatures, but no change occurs in the character of the dependence of the loss angle on frequency. There is a decrease in the loss angle in the temperature behaviour of the dielectric permeability and loss angle, especially at high temperatures. A reduction in dielectric permeability takes place over the whole range of temperatures. Electrical conductance increases, but electrical strength falls after the irradiation of glass textolite under tropical conditions.

Irradiation leads to radiation disorders due to the interaction of the products of water radiolysis absorbed by the glass textolite with the ionized molecules of the polymethyltrichlorsilane.

It can thus be regarded as established that the greatest changes in the dielectric characteristics of SKN-1 type glass textolite take place as a result of irradiation by gamma-rays at a dosage of 100,000 roentgen at low temperatures and under conditions of tropical humidity.

1960

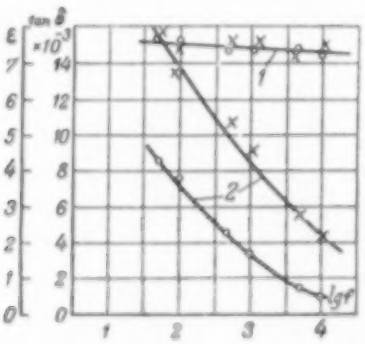

Fig. 6. Dependence of the ϵ and tan δ of 14r - 2 type rubber on frequency.
1 - ϵ; 2 - tan δ. Dosage 50,000 roentgen. 0 - non-irradiated material; X - irradiated.

Widespread use is made of 14r-2, 14r-6 and 14r-15 type silicone-organic rubbers in the electrical engineering industry. They are all based on SKT - type silicone-organic rubber with different fillers, namely, 14r-2 titanium dioxide, 14r-6 powdered silica gel and zinc white (oxide) and 14r-15 powdered silica gel, zinc white and "redoxide".

Figs. 6 and 7 show the dependencies of dielectric permeability and the loss angle on frequency in the case of the 14r-2 and 14r-15 type rubbers.

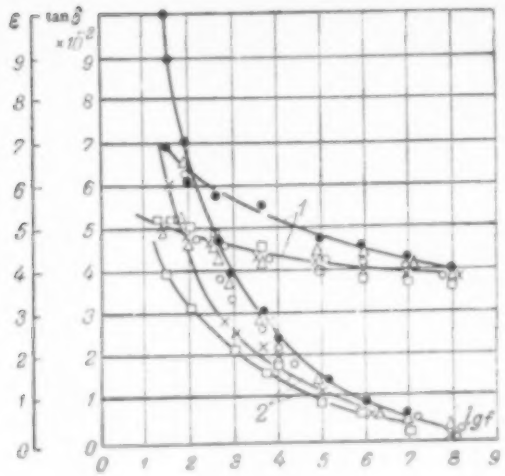

Fig. 7. Dependence of the ϵ and tan δ of 14r – 15 type rubber on frequency under different conditions of gamma-radiation.
1 – ϵ; 2 – tan δ. Dosage 100,000 roentgen. Designations as in Fig. 3.

The dielectric losses are ohmic in character in both cases, i.e. the loss angle diminishes with increasing frequency. There is an increase in the loss angle in the case of 14r-2 rubber on exposure to gamma-rays under room temperature conditions, but it decreases here in the case of 14r-15 rubber. As can be seen from Fig.7, the decrease in the loss angle is greatest during irradiation under low temperature conditions (-60°C).

The dielectric permeability of both rubbers remains unchanged before and after exposure at different temperatures. It only increases under tropical conditions, especially in the low frequency range. The electrical conductance of 14r-2 rubber increases after irradiation, especially at low temperatures (Fig.8).

Analogous qualitative results were produced in the case of 14r-6 type rubber. In this case, when the rubber was completely polymerized, its exposure to gamma-rays brought about an increase in conductance and the loss angle. The reverse picture was produced in the case of incompletely polymerized specimens of rubber. This can be seen particularly from the behaviour of the dielectric permeability and the loss angle in 14r-6 rubber (Fig.9). After irradiation at room temperature, a decrease takes place in the dielectric permeability and loss angle.

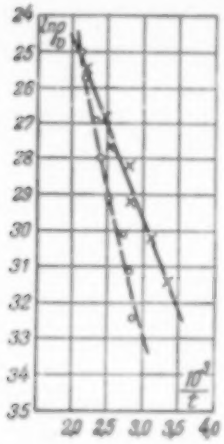

Fig. 8. Dependence of the ρ_v of 14r-2 type rubber on temperature. Dosage 100,000 roentgen. 0 - irradiated material; X - irradiated.

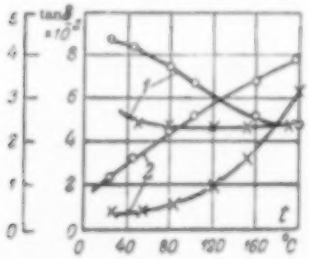

Fig. 9. Dependence of the ϵ and tan δ of 14r-6 type rubber on temperature.

It is characteristic of all kinds of rubber that exposure to gamma-rays brings the process of polymerization in incompletely polymerized rubber to its final stage, whilst the heat treatment of the rubber removes the effects induced by exposure to gamma-rays.

Thus normal rubber, irradiated by gamma-rays, does change its electro-physical properties. The conductance and dielectric loss angle increase. Electrical permeability varies a little. The use of gamma-radiation may be recommended for speeding up the polymerization of raw rubber.

Phenol-formaldehyde plastics

AG-4 type plastic is based on phenol-formaldehyde resin with a filler in the form of glass fibre. Fig. 10 shows the frequency relationships of dielectric permeability and the loss angle of specimens of AG-4 type plastics before and after irradiation under different conditions.

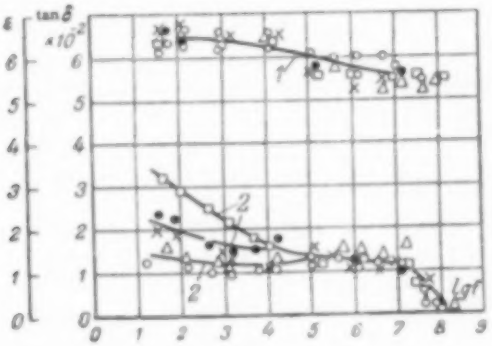

Fig. 10. Dependence of the ϵ and tan δ of AG-4 type plastic on frequency under different conditions of gamma-radiation. 1 – ϵ; 2 – tan δ. Dosage 100,000 roentgen. Designations as in Fig. 3.

As can be seen from the diagram, irradiation of AG-4 type plastic under the stated conditions at a dosage of 100,000 roentgen does not change the character of the dependence of the dielectric losses, but a noticeable difference is apparent in the absolute values of the loss angle in specimens of irradiated and non-irradiated plastic in the low frequency region. Whereas there is only a small increase in the loss angle in the region of the lowest frequencies (from 50 to 10^3 c/s) after irradiation at 20°C, the loss angle increases considerably more under tropical conditions as well as at t = -60°C and differs from the loss angle in non-irradiated specimens over a wide range of frequencies. This difference decreases with increasing frequency. Irradiation at 60°C practically leaves the loss angle unchanged over the whole range of frequencies.

No variations in the dielectric permeability of AG-4 type plastic were detected after irradiation over the measured range of frequencies under all the conditions under consideration.

A study was made of the temperature dependencies of the loss angle and dielectric permeability of irradiated and non-irradiated AG-4 type plastic under different conditions at different frequencies from 50 to

10^6 c/s. Some of these characteristics are given in Figs. 11 and 12. As can be seen from the diagrams, the character of the temperature dependencies of the loss angle are the same in all the investigated specimens, but a difference is again apparent in the absolute values of the loss angle in irradiated and non-irradiated specimens in the region of low frequencies. As in the frequency relationships, the difference is larger for specimens irradiated at -60°C and under tropical conditions. It is lowest in specimens irradiated at +60°C. It can also be seen from the diagrams that the divergence in the absolute values of the loss angle in irradiated and non-irradiated specimens increases with increasing temperature and decreases with increasing frequency. Whereas the absolute values of the loss angle are considerably different at low frequencies in non-irradiated specimens or specimens irradiated under different conditions at high temperatures, all the curves fall within the limits allowed for the error in measurement at a frequency of 10^6 c/s (Fig. 12).

1960

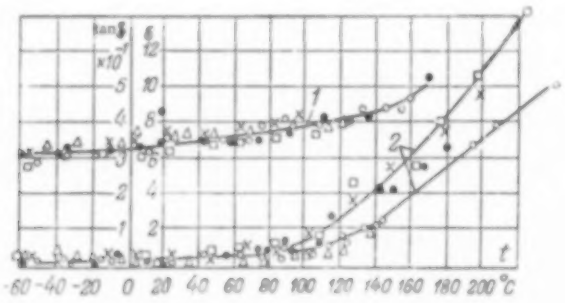

Fig. 11. Dependence of the ϵ and tan δ of AG-4 type plastic on temperature when $f = 10^2$ c/s and under different conditions of gamma-radiation.

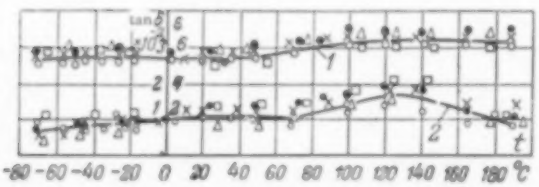

Fig. 12. Dependence of the ϵ and tan δ of AG-4 type plastic on temperature when $f = 10^6$ c/s and under different conditions of gamma-radiation.

Weakly expressed maxima for the loss angle can be seen in the temperature dependencies of the loss angle in all the specimens under investigation at a frequency of 10^6 c/s.

No notable variation is detected in the dielectric permeability of specimens of AG-4 type plastic after irradiation under different conditions and at high temperatures. No variation at all is seen in the value of electrical strength before and after irradiation (E_{ef} = = 15kV/mm).

Fig. 13 shows the frequency dependencies of dielectric permeability and the loss angle of K-114-35 type plastic, whilst Fig. 14 shows the temperature dependence of the loss angle in K-211-3 type plastic. As can be seen from the diagrams, a very small increase obtains in the absolute value of the loss angle in K-114-35 type plastic in the region of the lowest frequencies after exposure; however, in the case of K211-3 type plastic, the difference in the value of the loss angle in irradiated and non-irradiated plastic increases with increasing temperature and decreasing frequency. There is no difference at a high frequency (10^6 c/s).

The loss angle in FKPM-25 type plastic varies along a curve with a maximum as a function of frequency and temperature. The values of the loss angle agree in irradiated and non-irradiated plastic.

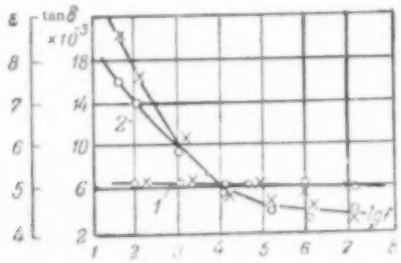

Fig. 13. Dependence of the ϵ and tan δ of K-114-35 type plastic on frequency.
1 – ϵ; 2 – tan δ. Dosage 48,000 roentgen. 0 – non-irradiated material; X – irradiated.

All the plastics under consideration are based on different modifications of phenol-formaldehyde resins. Phenol-formaldehyde resin is a polar resin. This causes a weak degree of polarity in the plastics under investigation. The losses of energy in these plastics when placed in an electrical field will be determined by relaxation processes and conductance. In fact the temperature dependencies of the loss angle

in AG-4 plastic, taken at high frequencies, do have a weakly expressed maximum (Fig. 12). A similar maximum also obtains for FKPM-25 type plastic. The great losses of conductance in the temperature dependencies of the loss angle in AG-4 and K-211-3 type plastics mask the loss angle maximum, typical of relaxation losses (Figs. 11 and 14). Likewise, no maximum obtains in the frequency dependence of the loss angle in AG-4 type plastic taken at room temperature, but it is detected when studying the frequency dependence at -60°C, when the conductance losses are considerably reduced (Fig. 15). Conductance losses prevail in K114-35 and K-211-3 type plastics under the conditions in which the measurements were taken; dependencies of the dielectric loss angle on temperature and frequency which are typical of ohmic losses are therefore produced.

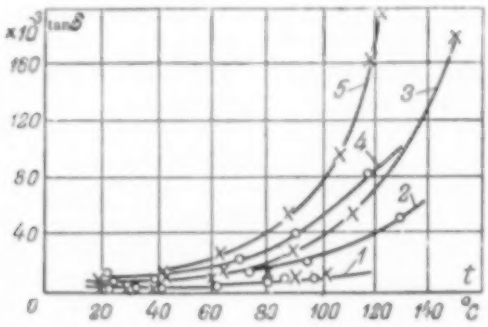

Fig. 14. Temperature – frequency dependence of tan δ for K-211-3 type plastic. Dosage 48,000 roentgen.
0 – non-irradiated material; X – irradiated.
1 – 10^6 c/s; 2 and 3 – 10^2 c/s; 4 and 5 – 50 c/s.

Comparing the temperature and frequency dependencies of the loss angle in non-irradiated and irradiated specimens of the same plastic, the conclusion can be drawn that exposure to gamma-rays under the above conditions (temperature, dosage, power of radiation) does not alter the character of losses in plastics. It can be stated on the basis of experimental data (Figs. 12 and 15) that no change occurs in the absolute magnitude and position of the loss angle maximum. This denotes that the number and degree of fixation of relaxing particles do not change as a result of gamma-radiation. Analysis of Figs. 10, 11, 13 and 14 shows that an increase in conductance losses occurs after the attack of the gamma-rays. This is probably connected with ionization inside the material during irradiation. This change is more marked after the attack of gamma-rays under tropical conditions and at low temperatures (-60°C), an improvement taking place as the temperature at

which the plastic is irradiated rises. This is probably explained by the fact that " heat treatment" of the radiation disorders takes place at high temperatures owing to the further intensification of thermal movement.

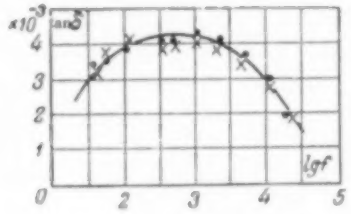

Fig. 15. Dependence of the tan δ of AG-4 plastic on frequency when $t = -60^{\circ}C$. Dosage 100,000 roentgen. 0 – non-irradiated material; X – irradiated.

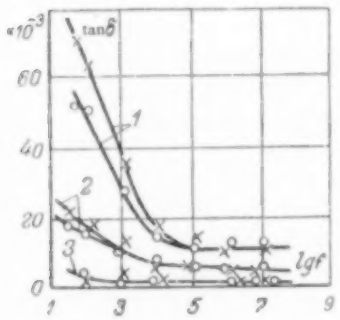

Fig. 16. Dependence of the tan δ of dielectrics on frequency before and after radiation. Dosage 48,000 roentgen. 1 – AG-4 plastic; 2 – K-114-35 plastic; 3 – product 10, 0 – non-irradiated material; X – irradiated.

An increase in conductance losses thus obtains in AG-4 and K-211-3 type plastics after exposure to gamma-rays (under the stated conditions); relaxation losses are practically constant. This causes an increase in the loss angle under those conditions where the conduction losses are large, i.e. at low frequencies and high temperatures. What has been said holds good for many electro-insulating materials. Curves are shown in Fig.16 characterizing the dependence of the loss angle on frequency

for AG-4 and K114-35 type plastics and the high molecular polymer known as product 10. The investigated dielectrics have different values for electrical conductance and the dielectric loss angle. AG-4 type plastic is characterized by large electrical conductance and loss angle values; these values are medium in the case of K-114-35 type plastic and small in the case of product 10. It can be seen from Fig. 16 that with the same dosage of gamma-rays we have a sharper decrease in the loss angle with a high frequency in AG-4 type plastic, and a notable variation in the loss angle in an irradiated specimen in comparison with a non-irradiated specimen. A similar relationship, but more weakly expressed, obtains in the case of K-114-35 type plastic. The weak dependence of the loss angle on frequency and only in the region of low frequencies obtains in the case of product 10, where the loss angle in non-irradiated and irradiated specimens is the same over the whole range of frequencies.

1960

Conclusions

1. High polymer dielectrics of the polyethylene, fluorplast and polystyrene types experience no change in the mechanism of dielectric losses and polarization on exposure to gamma-rays with a dose up to 10^6 roentgen at room temperature. The absolute values of dielectric permeability, loss angle and electrical strength remain unchanged.

2. It has been established that the greatest variations in the dielectric characteristics of SKM-1 type glass textolite take place as a result of irradiation at low temperatures and under conditions of tropical humidity.

Considerable variations in the dielectric loss angle and dielectric permeability take place as a result of irradiation at reduced temperatures and under conditions of tropical humidity.

Considerable variations in the dielectric loss angle and dielectric permeability take place as a result of irradiation over the low frequency range.

3. The electro-conductivity and ohmic part of the dielectric losses in silicone-organic rubber increase after irradiation. The induced conductivity and dielectric losses connected with this are "annealed" with the appropriate heat treatment of the rubber. Gamma-radiation of raw rubber accelerates the process of vulcanization.

4. There is an increase in conduction losses on irradiating phenol-formaldehyde plastics (AG-4, K-114-35, K-211-3 etc) by gamma-rays. The most appreciable change in the loss angle obtains after irradiation at

low temperatures and under tropical conditions.

The dielectric permeability and electrical strength of phenol-formaldehyde plastics do not change after attack by gamma-rays in the conditions under consideration.

The conclusion can be drawn from an analysis of the above experimental data that the radiation resistance of electrical insulating materials depends on the physico-chemical properties of the substances and their structure on the one hand and on the external conditions under which the dielectric is irradiated and investigated on the other. In our opinion, the most important criterion of the radiation resistance of a dielectric is the character of the polarization and dielectric loss in one or another range of temperatures and frequencies. When dielectric losses are ohmic in character there is a notable change in conductivity and the dielectric loss angle when the dielectric is under attack by radioactive radiation. With dielectric losses of relaxation or dipole character there is no notable change in the loss angle and conductivity.

Thus, it is necessary to know the character of the polarization and the dielectric losses before giving a conclusion relative to the resistance of electrical insulating material to gamma-radiation at appropriate dosage and intensity, i.e. it is necessary to have the temperature-frequency characteristics for dielectric permeability and the dielectric loss angle.

The authors express their thanks to V.D. Dedkov, E.A. Zimin, M.D. Lavrov, T.G. Mikhailov, E.S. Nesmelov, T.B. Nedokos, L.A. Prudnikov, G.V. Sitozhevskii and A.I. Tovbin for their active participation in the experiments.

Translated by O.M. Blunn

DESIGNING COOLING SYSTEMS FOR SEMICONDUCTOR TRIODES*

S. I. FEDOROV

(Moscow)

(Received 12 October 1959)

1960

Great value attaches to the cooling of large semiconductor triodes in the development of different kinds of apparatus in view of the fact that full use cannot be made of industrial type triodes without additional heat dissipation.

It is known that the maximum power which a semiconductor triode can dissipate equals

$$P_t = \frac{t_j - t_{amb}}{R_{t\Sigma}}, \tag{1}$$

where t_j is the maximum permissible temperature at the collector junction;

t_{amb} – the ambient temperature;

$R_{t\Sigma}$ – the total thermal resistance of the system.

The equivalent electrical circuit for the thermal process in the system embracing the semiconductor triode and surrounding medium is shown in Fig. 1. The total thermal resistance consists of four thermal resistances in individual sections. In other words:

$$R_{t\Sigma} = R_{t.i} + \frac{(R_{t.j} + R_{t.r})R_{t.b}}{R_{t.j} + R_{t.r} + R_{t.b}}, \tag{2}$$

where $R_{t.i}$ is the internal thermal resistance of the triode;

$R_{t.r}$ – the thermal resistance of the radiator;

$R_{t.j}$ – the thermal resistance of the junction between the body

---

* *Elektrichestvo*, No.5, 73-76, 1960.

of the triode and the radiator;

$R_{t.b}$ - the thermal resistance between the body of the triode and the surrounding medium.

A reduction in total thermal resistance is only possible by reducing $R_{t.j}$ and $R_{t.r}$, since the remaining terms in expression 2 are parameters of the type of triode in question. It follows from equations 1 and 2 that the thermal resistance of the radiator and junction between the body of the triode and the radiator $R'_{t.r}$ equals:

$$R'_{t.r} = R_{t.r} + R_{t.j} = R_{t.b} \frac{t_b - t_{amb}}{P_t R_{t.b} - (t_b - t_{amb})}, \quad (3)$$

where $t_b = t_j - P_t R_{t.j}$ is the temperature of the body of the triode.

When designing cooling systems it is necessary to determine the dimensions of the radiator for the selected difference between the temperatures of the collector junction and the surrounding medium, and the definite dissipated power of the triode.

The value of $R'_{t.r}$ can be calculated from formula 3 if the thermal resistance of the triode body is known, since the remaining parameters are either given or known.

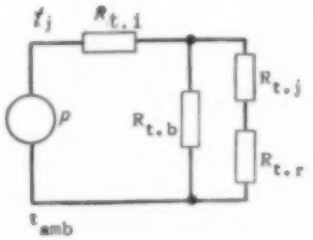

Fig. 1. Equivalent circuit for the thermal processes in triodes with a radiator.

The thermal resistance of the triode body is determined experimentally and from catalogue data in which the maximum dissipated power is given without a radiator at a definite ambient temperature and the largest permissible temperature of the collector junction.

The thermal resistance of the body equals the difference between the total thermal resistance of the triode and its internal thermal resistance, i.e.

$$R_{t.b} = R_{t\Sigma} - R_{t.i} \tag{4}$$

where $R'_{t\Sigma}$ is the total thermal resistance of the triode without a cooling system.

To calculate the value of $R'_{t\Sigma}$, it is necessary to find the temperature of the collector junction at the known dissipated power. Here it is necessary to plot the dependence of the reverse collector current on temperature for several triode models. In practice the temperature of the junction is equal to the ambient temperature when the reverse collector current is passing. As an example, Fig. 2 shows the variation in the reverse collector current $I_{r.c}$ in a P4V type triode as a function of temperature.

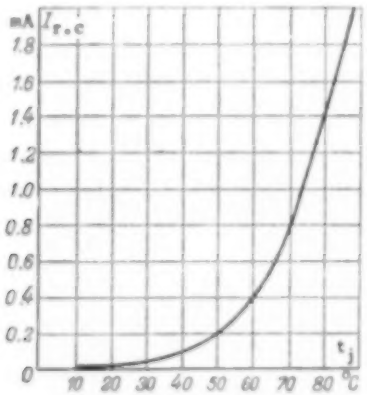

Fig. 2. The dependence $I_{r.c} = f(t_j)$ for a P4V type triode when $U_b = 2$ V.

The temperature of the collector junction in the working state of the triode is determined from the measured value of the reverse collector current and the relationship $I_{r.c} = f(t_j)$. The reverse collector current is measured at the established junction temperature (20 to 30 min after switching on) and in the absence of strong draughts of air. The power evolved in the triode is measured by conventional pointer instruments, but the reverse collector current is measured by an electronic instrument. The disconnexion of the emitter circuit and the measurement of the reverse collector current should take place as quickly as possible, use here being made of a high speed relay. The system of measurement is shown in Fig. 3.

During the measurement, the collector voltage should be between 2

and 5 V so as to have less effect on the amount of reverse current. After determining the temperature of the collector junction, the value of R'_{tE} can be found from expression 1.

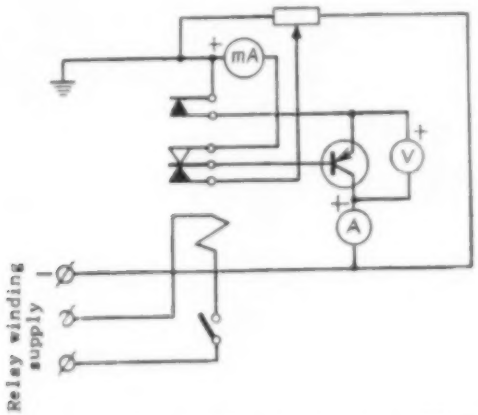

Fig. 3. System of measuring the reverse collector current.

The design of the radiator therefore entails the determination of the area of the radiator as regards its thermal resistance $R_{t.r}$, since in the majority of cases the thermal resistance of the junction between the body and the radiator is many times less than $R_{t.r}$ when the necessary conditions are satisfied and it can be ignored.

The method of calculating the thermal resistance of plates is given in the published literature (1). Unfortunately, it is impossible to use this method to calculate the area of a radiator with a known thermal resistance of the radiator. But it can be determined from the curves given in Fig.4, calculated from the following formulae:

$$t_{av} = \frac{t_b + t_{amb}}{2}; \tag{5}$$

$$\alpha_{rad} = 4.6\varepsilon\left(1 + \frac{t_{av}}{273}\right)^3; \tag{6}$$

$$\alpha_{con} = 1.4\sqrt[4]{\frac{t_{av}}{r_e}}; \tag{7}$$

$$R_{t.r} = \frac{1}{2\pi r_e \lambda b \Psi m}, \tag{8}$$

where

$$r_e = \frac{1}{2}\sqrt{S_r};$$

$$\eta = \frac{I_1(mr_e)K_1(mr_0) - I_1(mr_0)K_1(mr_e)}{I_0(mr_0)K_1(mr_e) + I_1(mr_e)K_0(mr_0)}; \tag{9}$$

$$m = \sqrt{\frac{2a}{\lambda\delta}}; \tag{10}$$

$$a = a_{rad} + a_{con}; \tag{11}$$

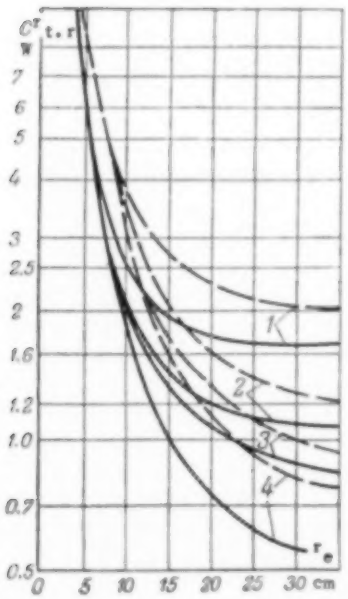

Fig. 4. The dependence $R_{t.r} = f(r_e)$ for "dural" radiators (= 200) in a P4 type triode when $tj - t_{amb} = 40^{\circ}C$. 1 – = 1mm; 2 – = 2mm; 3 – = 3mm; 4 – = 5mm. ——— black radiator; - - - - bright radiator.

a_{rad} – the coefficient of heat transfer by radiation;

a_{con} – the coefficient of heat transfer by convexion;

a – the total heat transfer coefficient;

ϵ – the blackness factor of the body;

r_e – the equivalent radius of the radiator, m;

s_r – the area of the radiator (one side of plate), m^2;

λ – the heat conductance of the material;

δ – the thickness of the material;

$I_0(\pi r_0)$, $I_1(\pi r_0)$, $I_1(\pi r_e)$, $K_0(\pi r_0)$, $K_1(\pi r_0)$, $K_1(\pi r_e)$ – Bessel functions from (πr_0) and (πr_e);

r_0 – radius of the area of contact between triode and radiator, m;

ψ, n – coefficients.

It should be mentioned here that the theoretical thermal resistance of the radiator, the equivalent radius of which is determined from expression 7, has a slightly increased value compared with the actual value in practice. In the event of use being made of the radiators described below with complex shapes, the stated discrepancy between the magnitudes of resistance diminishes. The experimental and theoretical relationships $R_{t.r} = f(r_e)$ given in Fig.5 show that there is fairly exact agreement.

Investigating the coefficient ψ it can be stated that a kink arises in the curve for ψ when $\pi r_e \approx 1$, and a further increase in πr_e does not lead to any appreciable increase in ψ.

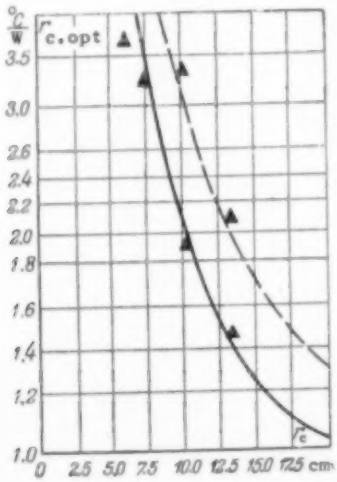

Fig. 5. Theoretical and experimental dependencies of $R_{t.r} = f(r_e)$ for "dural" radiators 3mm thick in P4 type triodes.

The investigations showed that radiators can be conveniently designed according to the optimum equivalent radius

$$r_{c.opt} = \frac{1}{m} = \sqrt{\frac{\lambda\delta}{2a}}. \qquad (12)$$

Besides, the radiator here has the least thermal resistance at the given expenditure of metal (in weight).

If the optimum radius is introduced into equation (9), a simpler expression is obtained for ψ after certain transformations:

$$\psi = \frac{K_1(mr_0) - I_1(mr_0)}{I_0(mr_0) + K_0(mr_0)}. \qquad (13)$$

The dependencies of the optimum equivalent radius on the thickness of the radiator material and of thermal resistance on the optimum equivalent radius are shown in Fig. 6.

1960

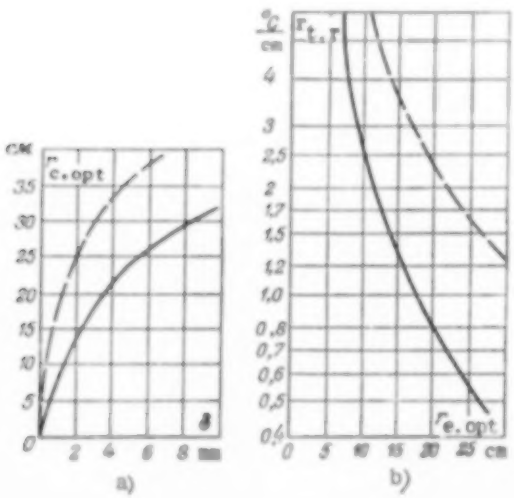

Fig. 6. Theoretical dependencies of the optimum radius on thickness (a) and of thermal resistance on the optimum radius (b), for a radiator made from "dural" at $t_j - t_{amb} = 40^{\circ}C$ in the case of a P 209 type triode.

But in practice it is not always possible to use radiators with an optimum equivalent radius since it is often more important to take up the minimum space by the radiator. Hence the need arises for radiators of more complex shape than plates.

Condry [2] points out that there is no increase in thermal resistance if an arbitrary shape is imparted to vertical plates (without

horizontal sections). In view of this the appropriate experiments were made which showed that the above method is also quite acceptable for designing radiators, consisting of plates of different shapes.

Fig.7 shows one of the types of radiator for which it has proved possible to use the graphical method in its design. The area and theoretical thickness of this type of radiator equal respectively:

$$S_r = H(Bn + 3L - 2l) - 2h(B - 2l_1); \tag{14}$$

$$\delta \approx \frac{\delta_M n}{3}. \tag{15}$$

where n is the number of plates in the plane BH;

δ_M – the thickness of the sheet material from which the components of the radiator are made.

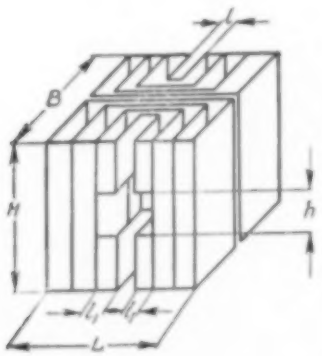

Fig. 7. Drawing of radiator.

As shown by the calculation, the thermal resistance of black radiators is 20 to 40% less than that of white radiators of the same thickness. It is best to produce black radiators by anodizing since the heat transfer factor decreases if use is made of varnishes or paints owing to the bad heat conductance of varnish-paint coatings and the thermal resistance of the radiator is thereby increased.

The place where the radiator comes in contact with the triode and that where individual parts of the radiator come into contact should be left clean and have a smooth surface. To increase the area of contact between the triode and radiator, it is desirable to make use of lead foil 80 to 100 μ thick since the resistance of the junction between the radiator and the body of the triode is considerably reduced in this case.

When designing radiators it is very important to choose the maximum temperature for the collector junction correctly. According to catalogue data, this is allowed to be within 90 to 100°C depending on the type of triode. To increase the reliability of the triode in operation the maximum permissible temperature of the junction at rated supply voltage and maximum dissipated power should be taken as 75 to 80°C.

The maximum temperature of the collector junction must also be reduced on the grounds that the maximum temperature of the surrounding atmosphere inside the gear cannot always be forecast correctly.

Translated by O.M. Blunn

REFERENCES

1. M.A. Mikheev: *Fundamentals of heat transfer, (Osnovy teploperedachi)*, Gosenergoizdat, (1947).
2. R. Condry: *Electronique industrielle*, No.20, (1956).

1960

ABSTRACTS FROM PAPERS PUBLISHED IN ELEKTRICHESTVO No.5, 1960

An analytical method for determining the dynamics of d.c. electro-magnets: A.K. Ter-Akopov (pp. 1-5).

A study is made of the method of finding a formula for the movement time of the armature which would not only take into account the basic parameters the minimum time of movement. Experimental investigation was carried out on an E-shaped magnet made of sheet electrical steel gauge 0.35 mm. The appropriate measures were taken to conform to the theoretical assumptions. Theoretical times were not more than 15 to 18% greater than the test values. The existence of an optimum production force for the minimum time of movement is established.

The effect of corona on voltage surges in transmission lines: G.N. Aleksandrov (pp.6-13).

Formulae are produced illustrating the relationship between the corona discharge effect on overvoltages on the one hand and the parameter of the line and the transient processes in them on the other. Surges under the influence of corona are lower, the greater the amplitude of the voltage compared with the initial corona voltage and the smaller the radius of the conductors and the equivalent frequency of the transient process.

How economic factors affect the parameters of networks with a distributed load: A.A. Derkach and V.M. Sin'kov (pp.15-22).

An attempt is made to find a method which would be free of all assumptions or technical or economic limitations and could be used to solve equations linking the various forms of expenditure on the equipment and operation of electrical networks in order to ascertain the optimum radii at 1 to 3 degrees of voltage, the voltage losses at each degree of voltage, the voltage losses at each degree of voltage and the economic current density.

Electromagnetic pumps for molten metals: A.I. Voldek (pp.22-28)

The paper surveys the method and theory of electromagnetic pump design particularly in view of their growing value for nuclear reactors. Distinguishing conduction and induction pumps the author describes and discusses d.c. pumps, single phase a.c. pumps, cylindrical linear induction pumps, spiral induction pumps with rotating inductors and refers to other types of electromagnetic "pressure pumps" and mixers.

Variable-polarity excitation of synchronous condensers for reactive power consumption performance: N.I. Sokolov (pp. 28-31).

The reactive power of a synchronous machine depends on the excitation current or the e.m.f. proportional to it for a synchronous resistance, the voltage at the terminals and angle of rotor shift (δ) relative to voltage. After considering the operating conditions of compensators when $\delta \neq 0$, the author considers the regulation of a synchronous compensator under angles of rotor shift when $\delta \neq 0$ by a simple regulator under the conditions of reactive power consumption. The utilization of synchronous compensators is increased by 30 to 60%.

Calculation of commutating flux rise for suddenly applied loads: V.A. Iakovenko (pp.36-39).

Simplified methods are proposed for calculating the increases in the commutation flow based on the fact that the load current of a d.c. machine varies very slowly. Good agreement is obtained with experimentally found values.

Grid control of mercury arc rectifiers by means of half-wave magnetic amplifiers: S.S. Roizen (pp. 39-45)

The introduction of such highly productive equipment as reversing rolling mills makes special demands on electrical drives as regards operating speed and control accuracy. The use of a magnetic amplifier with an internal feedback for simultaneously creating a steep front of the network voltage and displacing this front enables a grid control system to be developed with a delay time which does not exceed several periods of the supply voltage. There is however a limited range of variation in the ignition angle and the width of the trigger pulse is variable. The single phase scheme is given special attention.

Calculation of the commutation reaction magneto-motive force in d.c. machines for brush overlapping (sparking) greater than unity: V.V. Fetisov (pp.46-50).

To calculate the transient states in d.c. machines and design dynamo-electric amplifiers (amplidynes) it is necessary to calculate the commutation reaction of the armature. This is considered very complicated owing to the complex physical phenomena of the commutation process. After criticizing various other methods the author proposes a method of calculation for commutation with brush sparking considerably greater than unity which is suitable for usual values of brush sparking in any type of armature winding. Two examples of the method are given.

On electromagnetic calculations on d.c. machines which account for the cooling of their windings: N.A. Panfilov (pp.50-54).

When the electromagnetic parameters of d.c. machines are selected the magnetic flux usually corresponds to the saturated state of the magnetic system and the permissible temperature rise in the windings does not always ensure that the output of the machine is optimum. Here the author considers the determination of the optimum magnetic flux the deciding factor. Criteria are produced for evaluating the output or temperature rise in the windings of d.c. machines in which the magnetic flux corresponding to the saturated state of the magnetic system is optimum.

Derivation of the integral equations for non-linear circuits using operational calculus: M.M. Glinzburg (pp.54-58)

The calculation of steady state and transient processes in circuits containing non-linear elements is facilitated by relating the mathematical operations involved in calculating both the linear and non-linear elements in the scheme under consideration to the non-linear part of the scheme alone. Two examples of the method are given: one example applies to the steady state of a valve generator and the other to the dynamic stability of a system with three generator stations.

Calculation of the current in an R-L circuit with half-wave rectification: A.I. Glukharev, L.A. Foigel and N.B. Gelman (pp 58-60).

In view of the practical difficulties involved in analytically calculating the mean value of the rectified current when an active inductive resistance is present in the circuit for the use of single half-period

rectification, the authors deduce a simpler analytical dependence of the current on the magnitude and relationship between the active resistance and inductance. The method is directly applicable to long distance transmission systems with an inductive converter when the signal is registered by a magneto-electric (moving coil) meter (logometer).

A transistorized d.c. transducer with internal magnetic stabilization: M.E. Poiurovskii (pp.66-70).

An analysis is made of the performance and design of a converter with magnetic stabilization which ensures effective stabilization of the output voltage and frequency. The power losses in the feedback circuits reduce its efficiency but not significantly.

Thermo-resistor KMT-14: A.L. Burkin, O.N. Filippova and I.T. Sheftel (pp.71-73).

An account is given of newly developed Soviet KMT-14 type thermal resistances capable of operating at temperatures up to 300°C.

Non-linear capacitors using Rochelle salt materials: M.M. Nekrasov (pp.76-79)

A tertiary Rochelle salt non-linear electrical system is discussed which is claimed to combine high dielectric permeability, negative capacitive cha change with applied voltage and low dielectric losses.

AN EXPERIMENTAL STUDY OF NEW METHODS OF DETERMINING THE PARAMETERS OF A.C. MACHINES*

M.P. KOSTENKO, E.IA. KAZOVSKII and IA.B. DANILEVICH

(Institute of Electro-mechanics, Academy of Sciences U.S.S.R.)

(Received 12 September 1959)

Using the theoretical research directed by Academician M.P. Kostenko in the Institute of Electro-mechanics of the Academy of Sciences U.S.S.R., E.Ia. Kazovskii Kand.Sc. proposed new methods of experimentally determining the frequency characteristics and other parameters of a.c. machines as well as other methods of calculating transient processes in machines from the frequency characteristics. To check the utility of the new methods, the Institute of Electro-mechanics undertook a detailed experimental study of some of the proposed methods. This paper sets out the method employed and the results obtained from an investigation into a synchronous salient pole GS-1406-6 type machine (320 kW, 400 V, 1,000 rev/min) with magnetic stator wedges.

Method of Investigation

As can be seen from a previous paper [1], there is a definite connexion between the frequency characteristic of a machine in the steady state with constant rotor slip (diagram of stator current for different rotor slips) and the transient processes in the machine. This connexion can not only be used to determine the currents and voltages of the machine in any transient process from the frequency characteristic, but also to determine the frequency characteristic from the curve for the variation in current in the transient process.

The simplest transient processes are those of the increase in stator current when the synchronous machine is connected to a direct voltage

---

* *Elektrichestvo*, 6, 14-16, 1960.

on the stator side and the process of stator current damping when the direct voltage feeding the stator of the machine is disconnected by a short circuit of the stator winding. With a non-moving rotor this particular process was used to determine the frequency characteristic of the machine.

For this purpose oscillgrams were taken of the stator current for the two positions of the rotor corresponding to the longtitudinal and transverse axes of the machine (Fig.1), the d.c. source here being disconnected from the stator circuit simultaneously with a short circuit of the stator winding (with a short circuited rotor winding). The correct position of the rotor was checked by measuring the current induced in the rotor winding when the stator winding was supplied with an alternating current.

One of these oscillograms is shown in Fig. 2.

1960

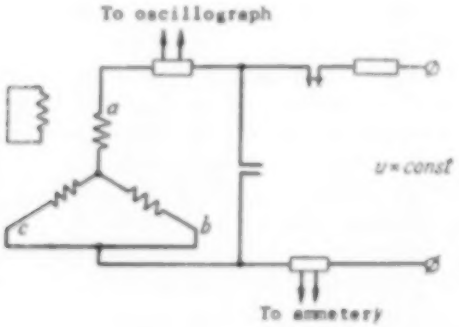

Fig. 1. Principal experimental circuit.

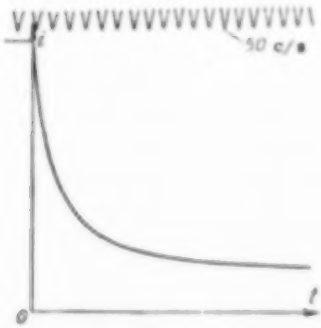

Fig. 2. Oscillogram of variation in stator current when the rotor is on the longtitudinal axis.

After taking the oscillograms the ohmic resistance of the short circuited stator circuit was determined as well as that of the phase winding of the stator.

Treatment of the experimental data

The treatment of the oscillograms consists in isolating the exponential components from the $i = f(t)$ curve and determining the damping coefficient. To do this the curve $i = f(t)$ must be re-plotted on a semi-logarithmic scale. Then a straight line drawn through the points on the curve until it intersects the axis of the ordinates (Fig.3) will give the value of the current i_{t1}, the amplitude of which decreases with the damping coefficient $\lambda'_1 = \frac{1}{T_1}$.

Having plotted the difference $i - i_{t1}\epsilon^{-\lambda'_1 t}$ and drawn a straight line to its intersection with the axis of the ordinates, we obtain a current i_{t2} and so on. In the machine under investigation we in this way successfully distinguished three current components for the position of the rotor along the d axis and two components along the q axis.

Theoretical analysis shows that the following relationship exists between values found for the current components i_{t1}, i_{t2}, ... i_{tn} and the frequency characteristic $\frac{j}{\frac{r}{s}+jx(js)}$ along the axis in question of the rotor:

$$\frac{j}{\frac{r}{s}+jx(js)} = i_{t1}\lambda'_1\frac{js}{js+\lambda'_1} + i_{t2}\lambda'_2\frac{js}{js+\lambda'_2} + \\ + \ldots + i_{tn}\lambda'_n\frac{js}{js+\lambda'_n}. \qquad (1)$$

where $r = r_{s=} + \frac{2}{3}\Delta r$;

$r_{s=}$ is the ohmic resistance of a phase of the stator winding;

Δr is the resistance of the connecting conductors of the short circuited circuit, and

s the rotor slip.

All the quantities in equation (1) are in relative units.

To perform the calculations and plot the curves we have to proceed from the stator current reduced to the rated voltage.

The initial value of the applied stator current from the oscillogram

for the damping of the current equals $1/r$ as a fraction of the rated stator current, if the resistance r is expressed as a fraction of the base resistance of the stator.

The voltage of the direct current $U_{v.d}$ at which the coefficient of application of the stator current equals 1 (according to the first harmonic flux coupling), is as follows:

$$U_{v.d} = 1.5\sqrt{2}U_{p.v}$$

where $U_{p.v}$ is the effective value of the rated phase voltage of the stator.

The value of the direct voltage is only appreciable from the point of view of saturation, since all the calculations and diagrams are based on an initial value of the stator current equal to a fraction of the nominal $1/r$ independently of the actual value of the initial voltage.

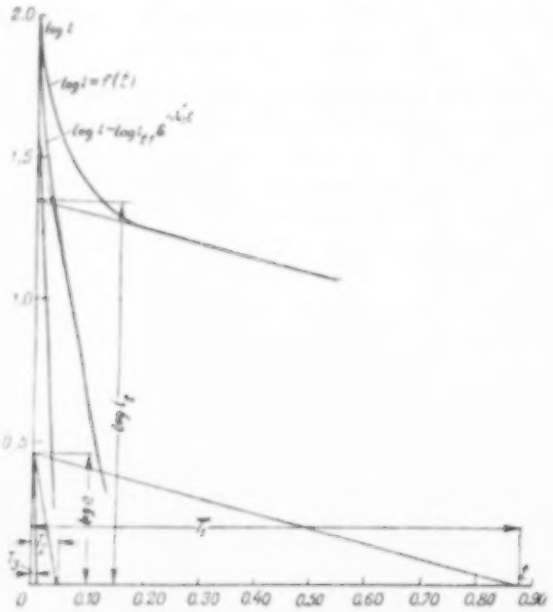

Fig. 3. Isolating the exponential components and determining the time constants when the rotor is on the d axis.

In the machine under investigation, relationship(1)for the position

of the rotor along the d axis has the form:

$$\frac{j}{0.0258/s + jx_d(js)} = 0.031 \times \frac{js}{js + 0.00358} +$$

$$+ 0.952 \times \frac{js}{js + 0.0671} + 4.060 \times \frac{js}{js + 0.255};$$

and for a position along the q axis:

$$\frac{j}{0.0258/s + jx_q(js)} = 0.284 \times \frac{js}{js + 0.0137} +$$

$$+ 3.300 \times \frac{js}{js + 0.182}.$$

If we designate

$$\frac{j}{r/s + jx(js)} = a + jb.$$

we shall obtain for the required frequency characteristic $\frac{1}{x(js)}$

$$\frac{1}{x(js)} = \frac{js}{js - (a + jb)r}(a + jb).$$

The frequency characteristics of the machine in question are shown in Fig. 4.

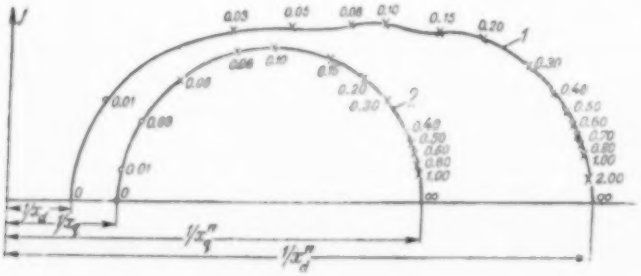

Fig. 4. The frequency characteristics of a GS-1406-6 type machine: 1 – along logtitudinal axis; 2 – along transverse axis.

We can easily obtain expressions for x''_d and x''_q from relationship (1).

In fact,

$$\frac{1}{x''_d} = \lim_{s\to\infty}\left[\frac{j}{\frac{r}{s}+jx_d(js)}\right] = \\ = i_{f1d}\lambda'_{1d} + i_{f2d}\lambda'_{2d} + \ldots + i_{fnd}\lambda'_{nd} \tag{3}$$

or

$$x''_d = \frac{1}{i_{f1d}\lambda'_{1d} + i_{f2d}\lambda'_{2d} + \ldots + i_{fnd}\lambda'_{nd}}.$$

Likewise

$$x''_q = \frac{1}{i_{f1q}\lambda'_{1q} + i_{f2q}\lambda'_{2q} + \ldots + i_{fnq}\lambda'_{nq}}. \tag{4}$$

Using the oscillograms of current damping when the stator winding is short circuited, we can also obtain the values of the synchronous reactances x_d and x_q (1,2):

$$x_d = r\int_0^\infty i\,dt, \tag{5}$$

where i is the current according to the oscillogram as a proportion of the initial current;

t is time in electrical degrees.

Substituting the expressions for current i into equality 5 by the exponential components, we obtain

$$x_d = r^2\left[\frac{i_{f1d}}{\lambda'_{1d}} + \frac{i_{f2d}}{\lambda'_{2d}} + \ldots + \frac{i_{fnd}}{\lambda'_{nd}}\right]; \tag{6}$$

$$x_q = r^2\left[\frac{i_{f1q}}{\lambda'_{1q}} + \frac{i_{f2q}}{\lambda'_{2q}} + \ldots + \frac{i_{fnq}}{\lambda'_{nq}}\right]. \tag{7}$$

Comparison with experimental data obtained by other methods

The high degree of accuracy of the proposed method is borne out if we compare the results of different methods. Thus, in the case of the machine in question, the " super transient reactance" along the longtitudinal axis is 0.198 when calculated from 3, but its value as determined experimentally when two phases were supplied with an alternating current and the rotor was fixed $x''_{d(s=1)}$ equalled 0.231. The values of super transient reactance along the transverse axis were respectively

0.279 and 0.294. Synchronous reactance along the longtitudinal axis, calculated from 6, was almost the same as that found from no load and short circuit experiments.

Kazovskii proposed a method of determining the transient currents with a three phase short circuit for an a.c. rotating machine from the frequency characteristic.

To determine the periodic component of short circuit current we have to re-plot the stator current from the frequency characteristic as a function of rotor slip on a logarithmic scale and replace the curve produced by a stepped curve with sloping sections corresponding to the equality of the increments in the logarithm of current and the logarithm of slip.

Using this stepped curve we can determine the damping coefficients and the amplitude of all the exponential components of the symmetrical short circuit current. The division is arbitrary; here the curve for the transient process is determined with greater accuracy if the complex character of the logarithmic frequency curve increases with an increasing number of steps of the approximating curve. The accuracy of the stepped approximation can be checked by plotting the amplitude-phase characteristic in reverse in accordance with a selected approximation. The method of using stepped approximations is described by Traskel [3].

To make a further check on the utility of the proposed methods, use was made of the frequency characteristic with the rotor positioned on the *d* axis. Curves were then found for the envelope of the periodic component of the stator current in the presence of an external three phase short circuit with the machine on no load. These curves were compared with curves taken direct from a three phase short circuit of a synchronous rotating machine. The experimental frequency characteristic was re-plotted on a logarithmic scale and used to plot on approximating stepped curve. The components and damping coefficients of the symmetrical three phase short circuit current were then found. The experimental and theoretical curves were practically the same.

Conclusions

1. The new methods of experimentally investigating the parameters of machines are quite simple and produce satisfactory results, especially if the transient processes of machines with solid elements are calculated for which the phenomenon of current distortion is of material importance.

2. As we have seen from the experiments, the number of rotor circuits

in a synchronous machine along the longtitudinal axis is greater than two, whilst that along the transverse axis is greater than one. This must be taken into account accordingly. This can be done particularly conveniently by the proposed method regardless of the number of circuits.

3. The use of stepped approximations of the logarithmic frequency characteristic of the machine makes it possible to determine exponential components of the transient current of a.c. rotating machines with sufficient accuracy for practical purposes when the machine is connected in a network with an external short circuit and under other conditions.

Translated by O.M. Blunn

REFERENCES

1. E.Ia. Kazovskii; *Elektrichestvo*, 4, (1960).
2. K.P. Kovaks; *E. i M.*, No.21, (1957).
3. D. Traskel; *Synthesis of automatic control systems, (Sintez sistem avtomaticheskogo regulirovaniia)*, Mashgiz, (1959).

1960

A STUDY OF OUT-OF-STEP CONDITIONS AND THE RE-SYNCHRONIZATION OF A GENERATOR AFTER LOSING TRANSIENT STABILITY*

M.P. CHESHOV

(Power Institute of the Academy of Sciences U.S.S.R.)

(Received 16 November 1959)

It can be seen from operating experience and experimental investigations [1] that there is in many cases a possibility of a generator being restored to synchronous operation after dynamic stability has been disturbed as a result of the action of the generator's voltage regulators and the speed of the prime mover without the service personnel having to interfere. It is therefore worthwhile investigating the conditions under which re-synchronization of the generator will take place. The concept of dynamic stability can be broadened and regarded as assured if a generator which falls out of synchronism due to sharp disturbances is again independently synchronized.**

A quantitative evaluation of the possibility of re-synchronization is reduced by some authors [2,3] to the determination of the average slip and the limits within which the instantaneous slip can vary in the stationary asynchronous state. On this basis re-synchronization is regarded as taking place if the instantaneous slip passes through its zero value. Using this approach to the problem there is of course no need to study the transient process due to the turbine's speed regulator.

In this paper an approximate analytical method is proposed for investigating the motion of the generator rotor with transient conditions taken into account, and the possibility of re-synchronization is established. During our analytical investigations we shall in all cases regard the machine as idealized in the generally accepted sense [4] and make the

---

* *Elektrichestvo*, 6, 21-25, 1960.

** V.A. Venikov uses the concept of resulting stability in this connexion.

following assumptions: (a) the transient electromagnetic processes in machines provided with voltage regulators are taken into account either by the constant E'_d or E'; (b) periodic components of the electromagnetic moment having double frequency are neglected.

These can be regarded as quite acceptable assumptions since modern voltage regulators in asynchronous conditions will maintain the value of E'_d or E' practically constant in practice as shown by output oscillograms [1], whilst the periodic components of the moment with double frequency have very little effect on the motion of the rotor owing to its large mechanical inertia.

The equation of motion for the rotor of a generator connected to finite busbars can be written in the following form* (ignoring the coupling resistance):

$$J\frac{d^2\delta}{dt^2} = M_t - M_e. \tag{1}$$

where

$$M_e = M_{12}\sin\delta + M_{as.av}$$

After transformation of the left hand side of equation 1, we obtain:

$$Js\frac{ds}{d\delta} = M_t - M_{as.av} - M_{12}\sin\delta. \tag{2}$$

where

$$s = \frac{d\delta}{dt}.$$

The values of M_t and $M_{as.av}$ on the right hand side of equation (2) are complex functions of time and slip.

The synchronous moment in asynchronous conditions is due to the periodic deviations of slip of the rotor of the generator from its average value, the amplitude of these deviations here diminishing with increasing speed, since the rotor possesses a great moment of inertia. The speed regulator reacts weakly to the periodic variations in slip owing to its inertia. The synchronous moment during asynchronous operation can therefore be regarded as having no appreciable effect on the law governing the variation in the torque of the turbine. The effect of the asynchronous torque on deviations of slip about its mean value can also be ignored since the amplitude of the variations in slip are not large in asynchronous conditions. Hence the effect of the synchronous torque on the motion of the rotor can be taken into account independently of all the rest of the moments. Integrating equation (2),

* The expression for $M_{as.av}$ is given in other publications [4, 5].

we in this case obtain

$$J\frac{s^2}{2}=\int(M_t-M_{ss.av})\,d\delta+M_{12}\cos\delta+C. \tag{3}$$

The left hand side of this expression represents the value of the rotor stored in a certain interval of variation in angle δ. The right hand side represents the work of forces applied to the rotor on the same section of variation in the angle, the non-periodic terms; here the non-periodic terms produce an average value of work which corresponds

to the average value of the kinetic energy of the rotor, equal to

Consequently, expression 3 can be represented as the sum of two independent terms:

$$J\frac{s^2}{2}=J\frac{s_{av}^2}{2}+M_{12}\cos\delta. \tag{4}$$

where

$$J\frac{s_{cp}^2}{2}=\int(M_t-M_{ss.av})\,d\delta+C. \tag{5}$$

If average slip s_{av} is known (the method of calculating this is given below) the change in the kinetic energy of the rotor and, consequently, in slip can be found from equation (4). The instantaneous slip passes through zero at the instant when the kinetic energy of the rotor is zero during the process of restraining it, i.e. the necessary condition of re-synchronization will be fulfilled. However, the passage of the instantaneous slip through zero still does not mean that the generator is finally synchronized. It is first necessary to bear in mind that the synchronous swings may be " chopped" as a result of the rapid rise of the torque of the motor which has fallen out of step depending on the magnitude of the excess torque on the shaft of the rotor and angle δ when s first equals 0. The problem whether the generator will remain in step after the first passage of the instantaneous slip through zero is a matter dealt with in the usual investigation into dynamic transition and no consideration will be given to its solution in this paper.

The necessary condition for re-synchronization can be represented in the form of an inequality:

$$J\frac{s_{av}^2}{2}+M_{12}\cos\delta\leq 0. \tag{6}$$

During one period of asynchronous operation, we can assume $s_{av.min}$ = = const in the zone of minimum average slip. For this extreme case the

necessary condition for re-synchronization will be:

$$s_{av.min} \leq \sqrt{\frac{2M_{tt}}{J}}. \tag{7}$$

If condition 7 is not fulfilled during the process of asynchronous operation, the instantaneous slip will not pass through zero and, consequently, the generator can remain in the asynchronous state until external conditions alter.

Let us qualitatively analyse the changes in the turbine torque M_t as a function of s_{av}, with the effect of the turbine speed regulator in the transitional asynchronous state taken into account.*

The diagram, besides the relationship $M_t = f(s_{av})$ (curve 1), also shows the static characteristics of the turbine's speed regulator (2) and asynchronous torque of the generator (3). Let the turbine torque be M_{t0} under normal conditions (point a). When the generator falls out of step, a positive excess torque appears on the shaft of the group $M_{t.ex} = M_t - M_{as.av}$, which will accelerate the rotor of the generator. The speed regulator of the turbine begins to affect the closing of the turbine's control (directing) gear when slip increases. Here, however, the change in torque M_t, beginning from point a, does not proceed along the static characteristic of the speed regulator owing to its inertia, but lags behind the change in slip and follows the curve $M_t = f(s_{av})$, shifted up above the static characteristic. The rotor will accelerate until $M_{t.ex} > 0$.

At the moment of time the curve $M_t = f(s_{av})$ intersects the asynchronous torque characteristic (point b), the excess torque is zero. Slip will be maximum at point b and the speed regulator will reduce the admission of the energy carrier as before. This gives rise to a "negative excess torque" which begins to restrain the rotor. Thus, having reached a maximum at the point of equilibrium of the moments, the slip will afterwards decrease until M_t is again positive. The speed regulator will again reduce the admission of energy carrier until the slip exceeds the value defined by the point of intersection of the static characteristic of the speed regulator with the curve $M_t = f(s_{av})$ (points e, e_1 ....).

The turbine torque, continuously decreasing, passes through zero at point c and (if the control gear is open below the no load position) becomes negative. If the control gear is completely closed (point d),

* For the sake of simplicity we shall consider a speed regulator with a rigid feedback.

the restraint moment of the turbine will reach maximum and remain constant on the section over which slip changes from point d to point e, if it is regarded as more or less independent of the speed of the rotor.

The instant the slip is less than the value defined by the point at which the static characteristic of the speed regulator intersects the $M_t = f(s_{av})$ curve (point e), the speed regulator begins to increase the admission of energy carrier in conformity with its static characteristic. But the turbine torque does not vary in conformity with the static characteristic of the speed regulator even in this case owing to its inertia, and will lag behind the change in slip. The turbine torque, increasing here, passes through zero a second time (point f) and then at point k the excess torque is zero and the slip minimum. The equilibrium of the moments is again temporary at this point, since the speed regulator will affect the admission of the energy carrier as before in accordance with its static characteristic and, consequently, a positive excess torque will arise on the shaft of the group and begin to accelerate the rotor.

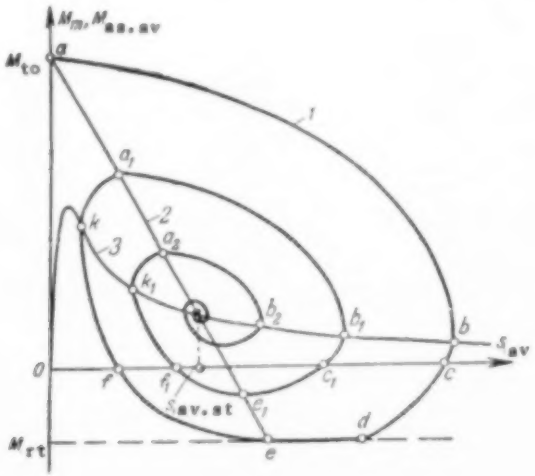

Fig. 1. Variation in turbine torque M_t as a function of average slip s_{av}.

The turbine torque will correspond to the slip according to the static characteristic of the speed regulator at point a_1. This correspondence is however temporary since the positive excess torque acting on the shaft of the group will accelerate the rotor as before. Here further variation in $M_t = f(s_{av})$ will take place along the curve a_1.

b_1, c_1, e_1, f_1, k_1, a_2 analogously to that described above.

Analysis of the relationship $M_t = f(s_{av})$ shows that the slip s_{av} can be considerably smaller in the transitional asynchronous state than the value of the steady state average slip $s_{av.st}$, as defined by the point where the static characteristics of the speed regulator and the asynchronous torque of the generator intersect. When therefore determining the condition for re-synchronization, it is necessary to consider the dynamics of speed regulation and not commence from the asynchronous steady state conditions.

The method of calculating average slip is based on the solution of the differential equation for the motion of the rotor with the effect of the speed regulator taken into account, assuming $M_{12} = 0$.

The equation of motion for the rotor when $M_{12} = 0$ has the form:

$$J\frac{ds}{dt} = M_t - M_{as\,av}. \tag{8}$$

The turbine torque M_t is not constant during the process of asynchronous operation and re-synchronization owing to the effect of the speed regulator on the control gear of the turbine. Using equations for the individual elements of the speed regulator [5,6] and bearing in mind that the dependence of the change in the turbine torque on the opening of the control gear is sually assumed to be linear, we obtain the following equations for the speed regulator:

(a) with the ports of the slide valve partly open ($\sigma < 1$):

$$T_s\frac{dM_{t.av}}{dt} + M_t + \frac{M_{t.nom}}{\delta'_{ip}}s_{av} = M_{to}, \tag{9}$$

where

$$\delta'_{ip} = \delta_{ip}\text{ no load}$$

(b) with the ports of the slide valve completely open ($\sigma = 1$):

$$M_t = M_{t.av} = M_{t.nom}\frac{f}{f_{no\,load}}. \tag{10}$$

In expression (10), the plus sign is used when the control gear of the turbine is open, and the minus sign when it is closed.

Average slip can be found analytically from expressions (8) to (10) if the characteristic for asynchronous torque is represented in the form of a piecewise linear relationship. In this case the equation of

motion for the rotor (8) can be written in the form:

$$J\frac{ds_{av}}{dt}+(a_n+k_n s_{av})=M_t, \tag{11}$$

where $a_n + k_n s_{av}$ is the equation of the nth section of the piecewise linear characteristic for the asynchronous torque of the generator.

Solving equations (11) and (9) jointly and also (11) and (10) with respect to s_{av}, we obtain respectively

$$JT_s\frac{d^2s_{av}}{dt^2}+(J+k_nT_s)\frac{ds_{av}}{dt}+$$
$$+\left(\frac{M_{T.nom}}{s'_{ip}}+k_n\right)s_{av}=M_{to}-a_n; \tag{12}$$

$$J\frac{ds_{av}}{dt}+k_n s_{ip}=M_{t.av}-a_n\pm M_{t.nom}\frac{t}{T_s}. \tag{13}$$
$$\text{no load}$$

Average slip can be found from equations (12) and (13) as a function of time. In the process of calculation, on transition from one linear section of the characteristic for asynchronous torque to the next section, the initial conditions for the latter section will be the final conditions of the preceding section.

Knowing the law governing the variation in the average slip $s_a = f(t)$ when $\sigma < 1$, we can find the law governing the variation in the torque of the turbine M_t with time by using equation (11). When $\sigma = 1$, the torque of the turbine is determined from equation (10).

During the asynchronous state the control gear of the turbine may be completely closed for a certain space of time (see diagram, section d-e). The average slip on this section is then determined from the equation

$$J\frac{ds_{av}}{dt}+k_n s_{av}=(M_{r.t}-a_n). \tag{14}$$

In order to simplify the restraint torque of the turbine when the control gear is completely closed, M_{rt} is assumed to be independent of the speed of the rotor.

We can find the law governing the variation in the extent to which the port of the slide valve is open in the asynchronous state when the relationships $s_{av} = f(t)$ and $M_t = f(t)$ are known by using the equation

for the slide valve of the speed regulator [5,6]:

$$\sigma = \eta - \mu.$$

The calculation of the average slip of the generator rotor is thus based on the solution of linear differential equations (12) to (14), each of which can be used regardless of the state of the group (open slide valve port and control gear).

Having determined the relationships $s_{av} = f(t)$ and $M_t = f(t)$ we can plot the relationship $M_t = f(s_{av})$, which will have the form shown in the diagram.

As an example we have calculated the asynchronous operation and re-synchronization of a hydro-electric generator after dynamic stability has been disturbed. Here we made use of data from certain investigations into the re-synchronization of a hydro-electric generator [1].

1960

The calculation was performed for different servo motor time constants T_s. According to experimental data, the value of T_s for the machines used in those investigations [1] was between 9 and 12 sec, $\mu_{\text{no load}} = 0.75$.

The best agreement between the theoretical and experimental data occurred when $T_s = 10$ sec. The maximum average slip in this case was 24 per cent (28.6 per cent in the experiment). The time of the passage of this maximum from the moment of short circuit was 6.6 sec (7 to 8 sec in the experiment) and duration of asynchronous operation 15.8 sec (15.2 sec in the experiment). Maximum average slip was determined without taking hydraulic shock into account. It's value was therefore less than that obtained experimentally. The effect of hydraulic shock can be taken into account can be obtained by multiplying the quantity obtained by a coefficient of 1 to 1.5 [5].

Symbols•

M_e – electromagnetic moment;

M_{12} – amplitudinal value of the synchronous moment;

$M_{as.av}$ – average value of the asynchronous torque of the generator;

M_t – turbine torque;

$M_{r.t}$ – restraint (counter) torque of the turbine with the valve of the directing gear completely closed;

$M_{t.nom} M_{to}$ – rated and initial values of the turbine torque;

• Angles and times are expressed in electrical radians, the remaining quantities in relative units.

$M_{t.ov}$ – turbine torque when valve completely open;

δ – the angle between the generalized vector of the stator voltage and the transverse axis of the rotor.

σ – extent to which valve open;

η – displacement of the pendulum coupling;

μ no load – extent to which turbine directing gear open on no load;

δ_{ip} – irregularity of pendulum;

T_s – time constant of servo motor;

J – mechanical time constant of the machine.

Translated by O.M. Blunn

REFERENCES

1. L.M. Markovich and S.A. Sovalov; *Elektrichestvo*, No.4, (1955).
2. P.S. Zhdanov; *Elektrichestvo*, No.6, (1934).
3. S.A. Lebedev; *Byull. All Union Electro-Technical Institute*, No.1, (1934).
4. L.G. Mamikoniants; *Currents and torques in synchronous machines when connected by the self-synchronization method, (Toki i momenty vrashcheniia voznikaiushchie v sinkhronnoi mashine pri vkliuchenii ee sposobom samosinkhronizatsii), Trud. Central Scientific Electro-Technical Research Laboratories*, No.4, (1956).
5. V.A. Venikov; *Electromechanical transient processes in electrical systems, (Elektromekhanicheskie perekhodnye protsessy v elektricheskikh sistemakh)*, Gosenergoizdat, (1958).
6. Iu.E. Garkavi and M.S. Smirnov; *The regulation of hydro-electric turbines, (Regulirovanie gidroturbin)*, Mashgiz, (1954).

THE PERFORMANCE OF THREE PHASE DIRECTIONAL IMPEDANCE RELAYS IN THE PRESENCE OF FAULTS AND UNDER UNBALANCED CONDITIONS* (COMPENSATOR DISTANCE RELAYING)

S.B. LOSEV and A.B. CHERNIN

(Moscow)

(Received 6 July 1959)

1960

Widespread use is made of three phase directional impedance relays in the U.S.S.R. for the distance protection of lines from asymmetrical faults. Use has also begun to be made of them abroad.** To appraise this relay it is necessary to examine its performance under abnormal conditions, for example, in the presence of asymmetrical short circuits, under unbalanced conditions accompanied by swings, in the presence of short circuits via intermediate resistances and so on. This problem has been partly elucidated in the papers by Petrov and Feist [1, 2].

This paper proposes a generalized method of investigation three phase directional impedance relays by means of characteristincs in the complex plane for different cases of short circuit and under balanced conditions.

Initial relationships

As is known [3], the electromagnetic moment of a three phase direc-

---

* *Elektrichestvo*, No.6, 29-38, 1960.

** It is incorrectly stated in the article by Sonnemann and Lensner [4] that the three phase directional impedance relay was first proposed in the U.S.A. It is known that this type of relay was first proposed by A.M. Bresler in the U.S.S.R. in 1945 (Auth. Cert. No. 66343). Since then problems connected with the operation of this relay have been elucidated in Soviet technical literature on many occasions.

tional impedance relay can be represented by a scalar product:*

$$M \equiv |\dot{U}_2 - Z_g I_2|^2 - |\dot{U}_1 - Z_g I_1|^2 = \\ = \{\dot{U}_1 + \dot{U}_2 - Z_g (I_1 + I_2)\} \times \\ \times \{\dot{U}_2 - \dot{U}_1 - Z_g (I_2 - I_1)\}. \quad (1)$$

where Z_g – resistance of the compensation corresponding to the setting of the relay;

$\dot{I}_1, \dot{U}_1; \dot{I}_2, \dot{U}_2$ – positive and negative sequence currents and voltages at the point where the relay is installed.

It can be seen from expression (1) that the behaviour of the relay does not depend on the combination of phases corresponding to the given fault or break.

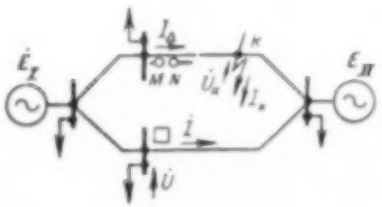

Fig. 1

To calculate short circuits at point K of a complex system (Fig. 1), it is expedient to apply the superposition principle and represent the positive sequence current and voltage in the form of the sum of the currents and voltages of the theoretical load (l) and additional (ad) states:

$$\dot{I}_1 = \dot{I}^{(l)} + \dot{I}_1^{(ad)}; \quad \dot{U}_1 = \dot{U}^{(l)} + \dot{U}_1^{(ad)}.$$

Expression (1) can then be represented in the form:

$$M \equiv \left\{\dot{U}^{(l)} - \dot{U}_K^{(l)} \frac{Z_{AK}}{Z_\Sigma}\right\} \times \\ \times \left\{-\dot{U}^{(l)} + \dot{U}_K^{(l)} \frac{Z_{BK}}{Z_\Sigma}\right\}, \quad (2)$$

where $\dot{U}_K^{(l)}$ is the voltage under load conditions at the point of the

* The co-multipliers of the scalar product will for the moment be enclosed in figured brackets in all expressions for the sake of a more visual exposition.

last short circuit:

$$\dot{U}^{(l)\prime} = \dot{U}^{(l)} - Z_s \dot{I}^{(l)}; \tag{3a}$$

$$Z_{A\kappa} = \left(-\frac{\dot{U}_1^{(ad)}}{I_{1\kappa}} + Z_s \frac{\dot{I}_1^{(ad)}}{I_{1\kappa}}\right) + \tag{3b}$$

$$+ \frac{I_{2\kappa}}{I_{1\kappa}} \left(-\frac{\dot{U}_2^{(ad)}}{I_{2\kappa}} + Z_s \frac{\dot{I}_2^{(ad)}}{I_{2\kappa}}\right);$$

$$Z_{B\kappa} = \left(-\frac{\dot{U}_1^{(ad)}}{I_{1\kappa}} + Z_s \frac{\dot{I}_1^{(ad)}}{I_{1\kappa}}\right) - \tag{3c}$$

$$- \frac{I_{2\kappa}}{I_{1\kappa}} \left(-\frac{\dot{U}_2^{(ad)}}{I_{2\kappa}} + Z_s \frac{\dot{I}_2^{(ad)}}{I_{2\kappa}}\right);$$

Z_s – the resulting impedance of the complex system of sequences for the given type of fault; here

$$Z_\Sigma^{(2)} = Z_{1\Sigma} + Z_{2\Sigma}; \tag{4a}$$

$$Z_\Sigma^{(1,1)} = Z_{1\Sigma} + \frac{Z_{2\Sigma} Z_{0\Sigma}}{Z_{2\Sigma} + Z_{0\Sigma}}; \tag{4b}$$

$$Z_\Sigma^{(1)} = Z_{1\Sigma} + Z_{2\Sigma} + Z_{0\Sigma}. \tag{4c}$$

If a break in phase occurs between points M and N (Fig. 1):

$$M \equiv \{\dot{U}^{(l)\prime} - \dot{K}_{1\Delta} \dot{I}_\Delta^{(l)} \dot{Z}_{A\Delta}\} \times \tag{5}$$

$$\times \{-\dot{U}^{(l)\prime} + \dot{K}_{1\Delta} \dot{I}_\Delta^{(l)} Z_{B\Delta}\},$$

where $I^{(l)}{}_\Delta$ is the current under load conditions at the point of the last break in phase;

$Z_A\Delta$ and $Z_B\Delta$ – the impedances determined by expressions 3b and 3c, if the positive and negative sequence currents at the point of the break $\dot{I}_{1\Delta}$ and $\dot{I}_{2\Delta}$ are substituted there for currents $\dot{I}_{1k}$ and $\dot{I}_{2k}$. (Fig. 1);

$\dot{K}_1\Delta$ – the current distribution factor under load conditions at the point where a positive sequence scheme is broken.

When one and two phases are broken, respectively:

$$\dot{K}_{1\Delta}^{(1)} = -\frac{1}{1 + \frac{Z_{11}}{Z_{22}} + \frac{Z_{11}}{Z_{00}}}; \tag{6a}$$

1960

$$\dot{K}^{(2)}_{1\Delta} = -1. \tag{6b}$$

In expression (6a), Z_{11}, Z_{22} and Z_{oo} are the resultant impedances relative to the point of break.

The values of the ratio $\frac{I_{2k}}{I_{1k}}$ or $\frac{I_{2\Delta}}{I_{1\Delta}}$ are given in Table 1.

TABLE 1

Short circuit			Break	
two phases		one phase	of one phase	two phases
without earth	with earth			
-1	$-\frac{Z_{0\Sigma}}{Z_{2\Sigma}+Z_{0\Sigma}}$	-1	$+\frac{Z_{11}}{Z_{22}}$	-1

Expressions (2) and (5) are the initial ones for investigating three phase directional impedance relays under different operating conditions.

An idea of the behaviour of relays in the presence of various types of short circuit can be obtained from an examination of complex sequence networks (Fig. 2). At extreme values of $Z_{0\Sigma}$ ($Z_{0\Sigma}=0$ and $Z_{0\Sigma}=\infty$) the network in the case of an earth fault of two phases (Fig. 2c) is turned respectively into a network for the case of a fault between two phases (Fig. 2b); also at these values of $Z_{0\Sigma}$ the network for the case of an earth fault of one phase (Fig. 2d) is turned respectively into the network shown in Fig. 2(b) and a symmetrical network for the load state.

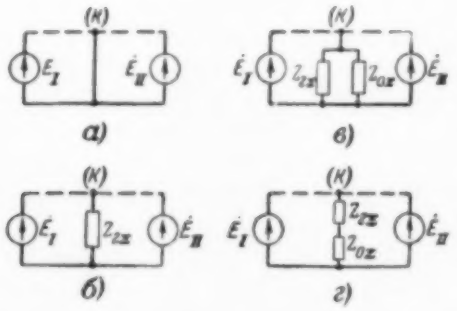

Fig. 2

Since, as follows from expression (1), the relay will not operate in the presence of a three phase short circuit and under load conditions, relays are less sensitive in actual cases of earth faults when $Z_{0\Sigma}$ has a finite value than when there are faults between two phases.

Relay operating characteristics

As is known [3], the operating condition of a three phase directional impedance relay using two currents and two voltages cannot be represented in the complex plane by one characteristic. The following method is therefore proposed for the investigation.

One parameter is isolated which will be denoted by F_{gen} and the behaviour of relays studied when it changes. The initial expressions 2 and 5 are brought to such a form that the moment is an explicit function of this parameter:

$$\begin{aligned} M &\equiv \{\dot{A}\dot{F}_{gen} - \dot{C}\}\{\dot{B}\dot{F}_{gen} - \dot{D}\} \equiv \\ &\equiv \left\{\frac{\dot{A}}{\dot{B}}(\dot{F}_{gen} - \dot{F}_A)\right\}\{\dot{F}_{gen} - \dot{F}_B\} = \\ &= \{\dot{F}_{AB}\dot{F}_I\}\{\dot{F}_{II}\} = F_{AB}F_I F_{II}\cos(\alpha + \varphi_{AB}), \end{aligned} \tag{7}$$

where

$$\dot{F}_A = \frac{\dot{C}}{\dot{A}}; \tag{8a}$$

$$\dot{F}_B = \frac{\dot{D}}{\dot{B}}; \tag{8b}$$

$$\dot{F}_{AB} = \frac{\dot{A}}{\dot{B}}; \tag{8c}$$

$$\dot{F}_I = \dot{F}_{gen} - \dot{F}_A; \tag{8d}$$

$$\dot{F}_{II} = \dot{F}_{gen} - \dot{F}_B; \tag{8e}$$

$$\alpha = \arg \dot{F}_I - \arg F_{II} = \varphi_I - \varphi_{II}; \tag{9a}$$

$$\varphi_{AB} = \arg F_{AB}. \tag{9b}$$

It can be seen from 7 that the relay is on the boundary of operation if

$$\dot{F}_{gen} = \dot{F}_A; \tag{10a}$$

$$\dot{F}_{gen} = \dot{F}_B. \tag{10b}$$

1960

and also

$$\cos(\alpha+\varphi_{AB})=0. \tag{11}$$

The latter condition corresponds to

$$\alpha=\pm 90^{\circ}-\varphi_{AB} \quad (\alpha'=+90^{\circ}-\varphi_{AB},$$
$$\alpha''=-90^{\circ}-\varphi_{AB}). \tag{12}$$

Conditions (12) can be expressed graphically if it is taken into account that the vectors $\dot{F}_{I}$ and $\dot{F}_{II}$ contain the general component $\dot{F}_{gen}$ (see 8d and 8e) which varies with respect to the modulus and argument. Fig. 3 shows the construction of the vectors

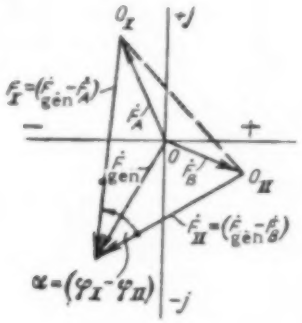

Fig. 3

$\dot{F}_{I}$ and $\dot{F}_{II}$ relative to the origin of the diagram. The tips of the vectors $\dot{F}_{A}$ and $\dot{F}_{B}$ (O_{I} and O_{II}) and peaks of the constant angle α between the variable vectors $\dot{F}_{I}$ and $\dot{F}_{II}$ lie on a line which is the locus of points characterizing the operating condition. It can be shown that the supplementary arcs of the same circle on the chord O_{I} and O_{II} constitute this locus of points (Fig. 4).

The centre of the circle can be determined graphically. When the point O'_{k} is moved in the direction of point O_{II}, the straight line $\dot{F}'_{I}$ within limits occupies a position on the chord $O_{I}O_{II}$, whilst the straight line F_{II} is tangential to the circle at point O_{II}. The angle between these straight lines is $180 - \alpha' = 90^{\circ} + \phi_{AB}$. Consequently, the centre of the circle lies at the point where the perpendicular PQ passing through the middle of the chord $O_{I}O_{II}$ intersects the straight line MN perpendicular to the stated tangent at point O_{II}. Then, to plot the characteristics it is necessary to know the position of the chord $O_{I}O_{II}$, i.e. the position of the tips of the vectors $\dot{F}_{A}$ and $\dot{F}_{B}$ as well as angle ϕ_{AB}.

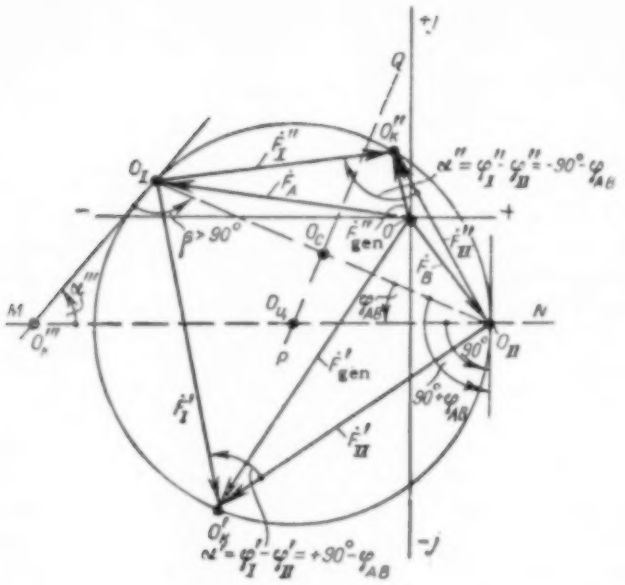

Fig. 4

It can be shown that when

$$+90° > \varphi_{AB} > -90° \tag{13a}$$

the zone of relay operations will lie outside the circle (see triangle $O_I O_{II} O_k$ in Fig.4), but inside it when

$$+90° < \varphi_{AB} < +270° \tag{13b}$$

In both cases the relay will operate when the tip of the vector F_{gen} lies inside the operating zone.

In the special case when A or B are 0 in expression 7

$$M \equiv \{-\dot{C}\}\{\dot{B}\dot{F}_{gen} - \dot{D}\} \equiv \left\{-\frac{\dot{C}}{\dot{B}}\right\}\{\dot{F}_{gen} - \dot{F}_B\} =, \tag{14}$$

$$= -F_{CB} F_{II} \cos(\varphi_{II} - \varphi_{CB}),$$

when

$$\dot{F}_{CB} = \frac{\dot{C}}{\dot{B}}; \tag{15a}$$

(15b)

It can be seen from 14 that when

$$\varphi_{II} = \pm 90^\circ + \varphi_{CB} \tag{16}$$

the relay is on the boundary of operation.

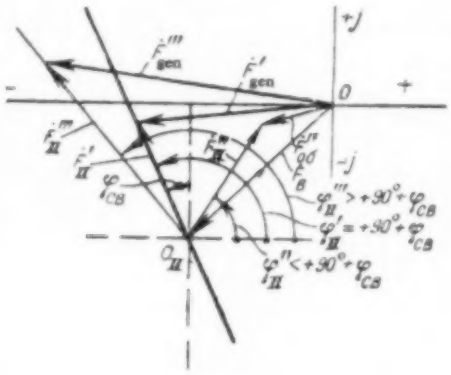

Fig. 5

As can be seen from Fig.5, condition 16 is graphically represented by a straight line which is a continuation of vector $\dot{F}_{II}$ and passes through the tip of the vector $\dot{F}_B$. The straight line with the horizontal forms an angle $\phi'_{II} = +90 + \phi_{CB}$. It can be shown that when

$$-90^\circ < \varphi_{CB} < +90^\circ \tag{17a}$$

the operating zone of the relay will lie to the left of the straight line, but when

$$+270^\circ > \varphi_{CB} > +90^\circ \tag{17b}$$

to the right.

Evaluation of relay sensitivity in the presence of short circuits and breaks in phase on a line fed from two ends

It follows from the above argument that a study must be made of a metallic short circuit between two phases to evaluate the selectivity of relay operation theoretically.

If it is assumed that the resistance of the positive and negative sequences is the same, we shall then obtain in accordance with expres-

sions 3b, 3c and 4a for the network in Fig. 6:

short circuit in the forward direction:

$$Z_{\Sigma}^{(2)} = 2(Z_{1c} + Z_{n}) \frac{I_1^{(ad)}}{I_{1K}}; \quad Z_{AK} = 0;$$
$$Z_{BK} = 2(Z_{1c} + Z_{n}) \frac{I_1^{(ad)}}{I_{1K}}; \tag{18a}$$

short circuit in the reverse direction:

$$Z_{\Sigma}^{(2)} = -2(Z_{11} - Z_{1c} + Z_{n}) \frac{I_1^{(ad)}}{I_{1K}};$$
$$Z_{AK} = 0; \quad Z_{BK} = -2(Z_{11} - \tag{18b}$$
$$- Z_{1c} - Z_{n}) \frac{I_1^{(ad)}}{I_{1K}}.$$

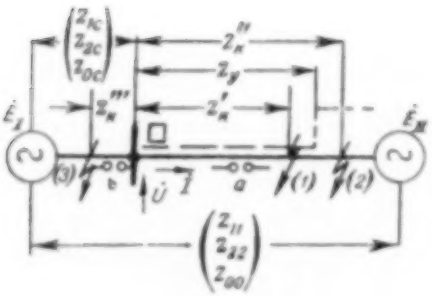

Fig. 6.

Let us consider the behaviour of a relay when there is a change in the angle between the e.m.f.'s $\dot{E}_{I}$ and $\dot{E}_{II}$. Let us represent the moment of the relay as an explicit function of

$$\dot{F}_{\blacksquare} = \frac{\dot{E}_1}{\dot{E}_{II}} = K_{\bullet} e^{j\gamma},$$

where

$$K_{\bullet} = \left| \frac{\dot{E}_1}{\dot{E}_{II}} \right|; \quad \gamma = \arg E_1 - \arg E_{II}. \tag{19}$$

Taking expressions 18 into account and expressing $\dot{U}^{(1)'}$ and $\dot{U}_{\blacksquare}^{(1)'}$ by

e.m.f.'s $\dot{E}_{I}$ and $\dot{E}_{II}$ in accordance with load conditions, let us bring expression 2 into the form of 7 when a two phase short circuit occurs in the forward direction:

$$M = \left\{\left[\left(\frac{1}{1-m_g}\right)\left(\frac{Z_g - Z_c}{Z_{1c} + Z_c}\right)\right] K_e e^{j\pi}\right\} \times \left\{K_e e^{j\pi} + \frac{m_g}{1-m_g}\right\} = \{\dot{F}_{AB}\dot{F}_{gen}\}\{\dot{F}_{gen} - \dot{F}_B\} \quad (20a)$$

and into the form of 14 in the presence of a two phase short circuit in the reverse direction

$$M = \left\{-\left(\frac{1}{1-m_g}\right)\left(\frac{Z_k + Z_g}{Z_{1k} - Z_{1c} + Z_k}\right)\right\} \times \left\{K_e e^{j\pi}\frac{m_g}{1-m_g}\right\} = \{-\dot{F}_{CB}\}\{\dot{F}_{gen} - \dot{F}_B\}. \quad (20b)$$

where

$$m_g = \frac{Z_{1c} + Z_g}{Z_{1k}}. \quad (21)$$

Z_c being the impedance of the system.

The operating characteristic in the presence of a short circuit in the forward direction is a circle passing through the origin, since $\dot{F}_A = 0$ (see expression 7 and Fig.4), but in the presence of a short circuit in the reverse direction, it is a straight line, since $A = 0$ (see expression 14 and Fig.5).

Fig.7 shows the combined characteristics of operation in the presence of short circuits at points 2 and 3 (Fig.6) when the angles of the total impedance of the sections are equal. In the presence of a fault at point 2, angle $\phi_{AB} = 180^{\circ}$ (20a), since $Z_k > Z_g$, but in the presence of a fault at point 3 angle $\phi_{CB} = 0$ (20b). The feature of the combined diagram consists in both characteristics passing through point O_{II} in accordance with expressions (20a) and (20b), point O_{II} here set aside from the origin by $OO_{II} = -\frac{m_g}{1-m_g}$.

In Fig.7 and below the direction of the shading shows the zone of operation.

In accordance with this and expressions (13) and (17), the regions inside the circle and to the left of the straight line are regions of non-

selective protection. To determine the range of angles inside which the relay will operate incorrectly, circles are drawn with their centre at the origin for the given relationship K_e = const, but when γ = var. It can be seen from Fig.7 that for $K_e = K_1$, non-selective operation in the presence of a fault is only possible at point 2 (Fig.6) at angles of $\gamma > \gamma_1$, but for $K_e = K_2$ non-selective operation in the presence of a fault is only possible at point 3 when $\gamma > \gamma_2$. Let us remark that in presence of a fault at point 1 (Fig.6) angle $\phi_{AB} = 0$ (20a), since $Z_k < Z_s$, and the region of correct operation lies outside the shaded circle.

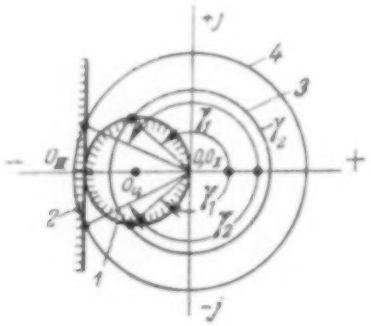

Fig. 7. Combined operating characteristics of relays in the plane of the e.m.f. ratio:
1 – in the presence of a short circuit at point 2 (Fig.6); 2 – short circuit at point 3 (Fig.6); 3 – $K_e = k_1$ = const, = var; 4 – $K_e = K_2$ = const, = var.

Using such approximate combined diagrams, Fig.8 shows the dependencies of the range of angles γ at which relays do not operate selectivity in the presence of a short circuit outside the protected zone and fail in the presence of a short circuit inside the protected zone on the ratio of z_s for the case of a short circuit between two phases (Fig.6) and for different values of K_e (0.6, 1.0 and 1.5). These dependencies show that if the electrical centre of the system characterizing the ratio $\frac{E_I}{E_I + E_{II}}$, is greater than z_s (i.e. lies outside the section $Z_{1c} \div Z_s$), the relay will operate correctly at all angles in the event of short circuits in the forward direction), but may not be selective at certain angles over the range from $-270^0 > \gamma > +90^0$ in the event of short circuits at any point in the reverse direction. If the electrical centre lies on the section ($Z_{1c} \div Z_s$), when $K_e \leq 1$ and if a short circuit is present in the reverse direction the relay

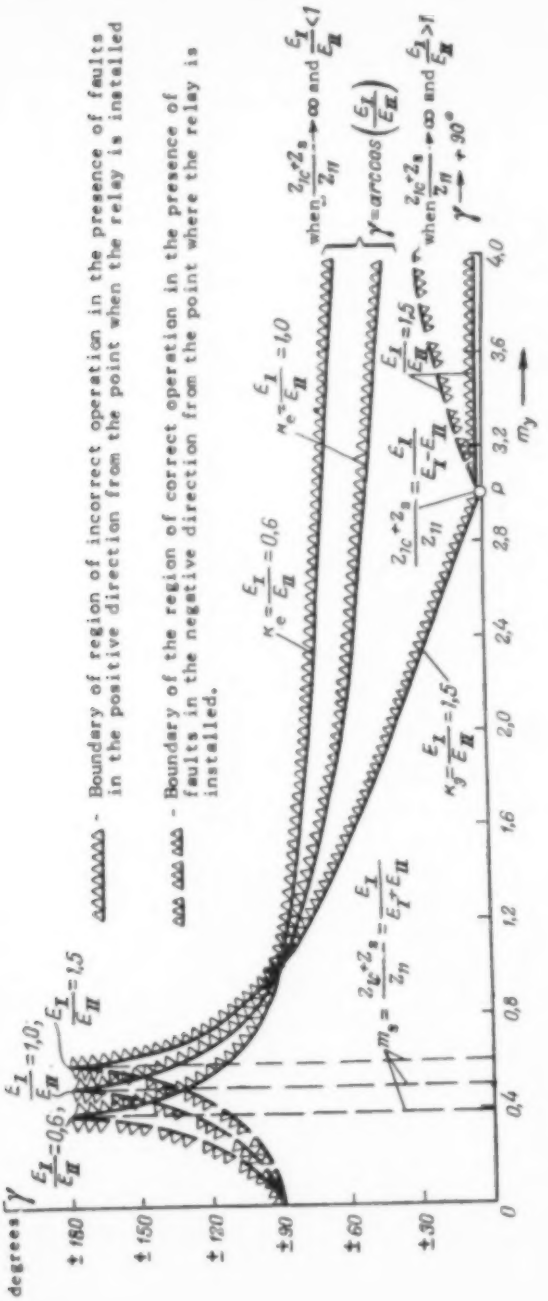
Boundary of region of incorrect operation in the presence of faults in the positive direction from the point when the relay is installed
Boundary of the region of correct operation in the presence of faults in the negative direction from the point where the relay is installed.
degrees
γ
±180
±150
±120
±90
±60
±30
0
0,4
0,8
1,2
1,6
2,0
2,4
2,8
3,2
3,6
4,0
ρ
m_y
$\frac{\dot{E}_I}{\dot{E}_{II}}=0,6;\ \frac{\dot{E}_I}{\dot{E}_{II}}=1,0;\ \frac{\dot{E}_I}{\dot{E}_{II}}=1,5$
$m_s=\frac{z_{sc}+z_s}{z_{II}}=\frac{\dot{E}_I}{\dot{E}_I-\dot{E}_{II}}$
$\kappa_e=\frac{\dot{E}_I}{\dot{E}_{II}}=0,6$
$\kappa_e=\frac{\dot{E}_I}{\dot{E}_{II}}=1,0$
$\frac{z_{sc}+z_s}{z_{II}}=\frac{\dot{E}_I}{\dot{E}_I-\dot{E}_{II}}$
$\kappa_f=\frac{\dot{E}_I}{\dot{E}_{II}}=1,5$
when $\frac{z_{sc}+z_s}{z_{II}}\to\infty$ and $\frac{\dot{E}_I}{\dot{E}_{II}}<1$
$\gamma=\arccos\left(\frac{\dot{E}_I}{\dot{E}_{II}}\right)$
$\frac{\dot{E}_I}{\dot{E}_{II}}=1,5$
when $\frac{z_{sc}+z_s}{z_{II}}\to\infty$ and $\frac{\dot{E}_I}{\dot{E}_{II}}>1$
$\gamma\to\pm 90°$

Fig. 8

will not operate, and can operate incorrectly in the presence of a short circuit at any point in the forward direction (the range of angles at which the relay operates incorrectly here increasing with an increasing m_s ratio). If $K_e > 1$ and $m_s > \frac{E_I}{E_I - E_{II}}$ (point P on Fig.8), the range of angles of incorrect operation begins at $\gamma = 0$ in the event of short circuits in both forward and reverse directions. This circumstance can restrict the use of relays as third stage protection, and as second stage protection also in certain cases.

Using expressions (5) and characteristics similar to those in Fig.7, we have plotted the dependence of the range of angles at which operation is incorrect on the ratio m_s (Fig.9) in the event of a break in phase at point a or b (Fig.6) at given values of $K_e = \frac{E_I}{E_{II}}$ and $\frac{Z_{oo}}{Z_{II}}$. Comparison of the relationships (Figs. 8 and 9) shows that the region of incorrect relay operation is smaller when one phase is broken than when two phases are broken. Therefore, if the correct operation of the relay is assured at the given setting in the event of a short circuit between two phases, then there is no possibility of the relay functioning under line working conditions with two phases at extreme angles of γ.

1960

This analysis is approximate in view of the assumptions that have been made.

Let us appraise the features of relay operation if the angles of the total impedance of the line are not equal $\phi_l = \arg Z_k$ and of a setting $\phi_s = \arg Z_s$, in the event of a short circuit in the vicinity of the end of the zone. To do this we shall alter expression 20(a) to a form in which the moment of the relay is an explicit function of $F_{gen} = Z_k$.

$$M = \left\{\left(m_s - \frac{m_s}{K_e} e^{-j\gamma} - 1\right)(Z_n + Z_{1c})\right\}\{Z_n - Z_s\}. \qquad (22)$$

On the basis of the characteristics plotted from expression 22 for the network shown in Fig.6 and having parameters $Z_{1c} = 15 \angle + 90^\circ$; $Z_s = 32.5 \angle + 65^\circ$, $m_s = 0.77 \angle + 8^\circ$ and $K_e = 1.0$, we have plotted the dependencies (Fig.10) of the lengthening or shortening of the zone $\frac{|Z_k| - |Z_s|}{|Z_s|} = \frac{|\Delta Z_k|}{Z_s}$ on angles γ (19) when $\phi_s - \phi_l = + 20^\circ$ and at certain values of γ possible under load conditions ($\gamma \approx - 40^\circ$ to $- 60^\circ$) there can be a 35 to 60 per cent increase in the relay operating zone. This leads to non-selective operation which would not occur if

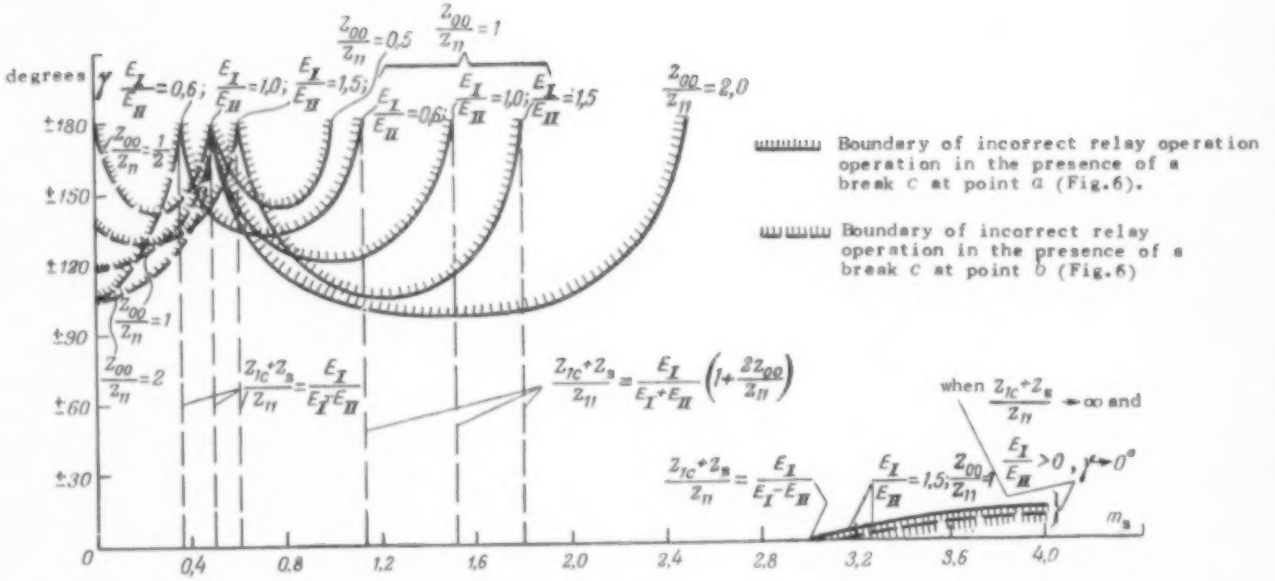
degrees
γ
±180
±150
±120
±90
±60
±30
0
0,4
0,8
1,2
1,6
2,0
2,4
2,8
3,2
3,6
4,0
m_s
$\frac{Z_{00}}{Z_n}=0,5$
$\frac{Z_{00}}{Z_n}=1$
$\frac{Z_{00}}{Z_n}=2,0$
$\frac{E_I}{E_{II}}=0,6;$
$\frac{E_I}{E_{II}}=1,0;$
$\frac{E_I}{E_{II}}=1,5;$
$\frac{Z_{00}}{Z_n}=\frac{1}{2}$
$\frac{Z_{00}}{Z_n}=1$
$\frac{Z_{00}}{Z_n}=2$
$\frac{Z_{1c}+Z_s}{Z_n}=\frac{E_I}{E_I-E_{II}}$
$\frac{Z_{1c}+Z_s}{Z_{11}}=\frac{E_I}{E_I+E_{II}}\left(1+\frac{2Z_{00}}{Z_{11}}\right)$
when $\frac{Z_{1c}+Z_s}{Z_n}\to\infty$ and
$\frac{E_I}{E_{II}}>0$, $\gamma\to 0^\circ$
Boundary of incorrect relay operation operation in the presence of a break c at point a (Fig.6).
Boundary of incorrect relay operation in the presence of a break c at point b (Fig.6)

Fig. 9

$\phi_s = \phi_l$. It is therefore necessary to envisage measures to ensure the requisite setting of the relay as regards both magnitude and angle.

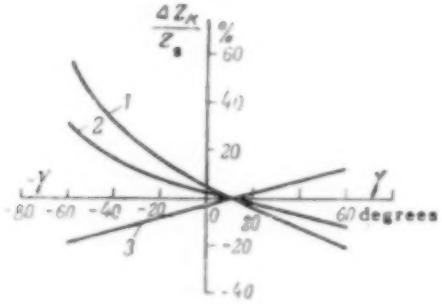

Fig. 10. Dependence of the lengthening or shortening of the operating zone on the angle γ:
1 - $\phi_s - \phi_l = 20^\circ$; 2 - $\phi_s - \phi_l = -10^\circ$; 3 - $\phi_s - \phi_l = -10^\circ$.

To plot the operating characteristics expression 2 can also be latered to a form in which the moment of the relay is an explicit function of

$$F_{gen} = \frac{\dot{U}^{(1)}}{\dot{I}^{(1)}} = Z_p^{(1)}. \tag{23}$$

This shape of the characteristic is expedient for investigating the possibility of preventing the incorrect operation of the relay slowly after the emergence of the short circuit.

Taking equations (18) into account and expressing $\dot{U}^{(1)'}$ and $\dot{U}_k^{(1)}$ by $Z_p^{(1)}$, let us change equation (2) into the form of equation (7): then if a fault occurs between two phases in the positive direction

$$M \equiv \left\{\left(\frac{Z_s - Z_n}{Z_{1c} + Z_n}\right)(Z_p^{(1)} + Z_{1c})\right\}\{Z_p^{(1)} - Z_s\}; \tag{24a}$$

or between two phases in the reverse direction

$$M \equiv \left\{\left(-\frac{Z_n + Z_s}{Z_{11} - Z_{1c} + Z_n}\right)(Z_p^{(1)} - Z_{11} + Z_{1c})\right\} \times \times \{Z_p^{(1)} - Z_s\}. \tag{24b}$$

Fig. 11 shows the combined operating characteristics in the presence of short circuits at points 2 and 3 (Fig. 6). These have been plotted

on the same conditions as those in Fig.7. In plotting the curves account was taken of the fact that $\dot{F}_A = -Z_{1c}$, $\dot{F}_B = +Z_s$ and $\phi_{AB} = 180^0$ in the presence of a short circuit at point 2, since $Z_k > Z_s$ (see 7 and 24a), whilst in the presence of a short circuit at point 3.

$$F_A = +(Z_{11} - Z_{1c}) \geq Z_s;\ F_B = +Z_s \text{ and } \varphi_{AB} = 180^0$$

(see 7 and 24b).

If follows from perusal of Fig.11 that the relay operates selectively if the tip of the vector $Z_p^{(1)}$ lies outside the shaded regions. Let us state that the angle $\phi_{AB} = 0$ in the presence of a short circuit at point 1 since $Z_k < Z_s$ (see 24a). In this case the zone of correct relay operation lies outside the shaded circle with a diameter $0_I 0_{II}$, this being the relay characteristic.

The broken line in Fig.11 shows the characteristics of a single phase directional impedance relay. It can be seen from a comparison of the characteristics that there is a greater probability of a three phase impedance relay acting incorrectly in the presence of faults between two phases than is the case with single phase relays under symmetrical conditions, this probability being the greater the greater the increase in Z_{1c} (Fig.6).

Using the characteristics given in Fig.11 we can judge the behaviour of relays in the event of shorts between two phases when the line is supplied from ond end by an e.m.f. source $\dot{E}_1$ and if the impedance of the positive and negative sequences of all the elements are equal. In this case the relay will act correctly if $Z_p^{(1)} = Z_{11} - Z_{1c}$ lies outside the characteristic for the short circuit in the positive direction (Fig.11), i.e. if

$$Z_s < Z_p^{(1)} = Z_{11} - Z_{1c}. \tag{25}$$

Let us state that the equality of the resistance of the positive and negative sequences is particularly possible if the motors are self-started. More generally, when the resistance of the positive sequence of the load is greater than the resistance of the negative sequence and the angles of total impedance are the same, the correct operation of the relay will be assured in the presence of a short circuit in the forward direction if

$$Z_s < 2\frac{(Z_{11} - Z_{1c} - Z_n)(Z_{22} - Z_{2c} - Z_n)}{(Z_{11} - Z_{1c} - Z_n) + (Z_{22} - Z_{2c} - Z_n)} + Z_n. \tag{26a}$$

and in the presence of a short circuit in the negative direction if [3]:

$$Z_s < \frac{2(Z_{11} - Z_{1c})(Z_{22} - Z_{2c})}{(Z_{11} - Z_{1c}) + (Z_{22} - Z_{2c})}. \qquad (26b)$$

Conditions 25 and 26 can restrict the use of relays as third and possibly second stage protection for lines with supply from two ends but which can be supplied from one end.

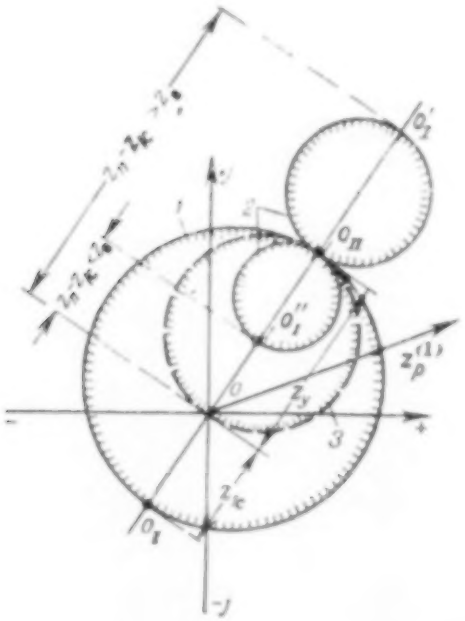

Fig. 11. Combined operating characteristics of relays in the impedance plane.

Evaluation of the sensitivity of relays in the presence of short circuits on a single line with feed from two ends

The curves in Fig.8 and expression 22 can be used not only to evaluate the selectivity of relays but also their sensitivity when metallic short circuits occur between two phases. The necessary relationships are given below to appraise sensitivity in the presence of earth faults and faults via intermediate resistances. As we have seen, a relay is less sensitive in the presence of earth faults than when inter-phase shorts occur. It can be shown that if the resistance

of the positive and negative sequences is the same and the angles of total impedance likewise, the relay will fail if metallic earth faults occur between two phases in the vicinity of the point where it is installed if

$$Z_{dz}^{(1,1)} = Z_s \leq \frac{Z_s - Z_{1c}A^{(1,1)}}{1 + A^{(1,1)}}. \tag{27a}$$

and if metallic earth faults occur in one phase in the vicinity of the end of the zone if

$$Z_{dz}^{(1)} = (Z_s - Z_s) \leq A^{(1)}(Z_{1c} + Z_s). \tag{27b}$$

where $Z_{dz}^{(1.1)}$ and $Z_{dz}^{(1)}$ represent the "dead zone" in which the relay can fail to operate;

$$A^{(1,1)} = \frac{2Z_{0z}}{Z_{1z}}\left[1 + m_s\left(\frac{\cos\gamma}{K_e} - 1\right)\right]; \tag{28a}$$

$$A^{(1)} = \frac{Z_{0z}}{2Z_{1z}}\left[1 - m_s\left(1 - \frac{\frac{m_s}{1-m} + K_e\cos\gamma}{K_e\left(K_e + \frac{m_s}{1-m_s}\cos\gamma\right)}\right)\right]. \tag{28b}$$

Other designations are the same as before.

In view of the complexity of expression (27), a study will be made below for orienting purposes of the case when the e.m.f.'s E_I and E_{II} are equal and the coefficients of current distribution of the positive and zero sequences likewise.* Solving equation (27) for this case we shall obtain:

$$Z_{dz}^{(1,1)} = \frac{Z_s - 2Z_{0c}}{2n+1}; \tag{29a}$$

$$Z_{dz}^{(1)} = \frac{nZ_s + Z_{0c}}{n+2}. \tag{29b}$$

* The coefficients of current distribution are equal for example on a line with supply from one end if the transformers at the receiving substation are unearthed.

where $n = \frac{Z_{0k}}{Z_{1k}}$ represents the ratio of the impedance of the positive and negative sequences up to the point of short circuit.

If follows from expression (29) that the dead zone will only occur when $Z_s > 2\ Z_{0c}$ in the presence of earth faults of two phases, whilst there is always a dead zone if an earth fault occurs on one phase, (here the relays do not generally operate when $Z_s < \frac{Z_{0c}}{2}$, since in this case $Z_{dz}^{(1)} > Z_s$).

Analysis shows that in the presence of earth faults of two phases via an intermediate resistance there is a considerable contraction of the dead zone of a three phase impedance relay. Thus, for example, when $Z_{1c} = Z_{0c} = 5$ ohm and an intermediate resistance is present of roughly 5 to 10 ohm, there is little probability of a dead zone on the line with single sided feed 100 to 200 km long.

1960

If supply is from two ends the additional feed of the arc makes it still less probable. The determination of the dead zone is thus theoretical in the presence of metallic faults.

It is of interest to elucidate whether the dead zone of a three phase directional impedance relay overlaps at the beginning of the line in the presence of metallic earth faults of two phases installed on zero sequence current cut-off lines*. As shown by analysis, the dead zone does not overlap provided that:

$$2Z_{0c} < Z_s < \frac{Z_{1c} - \frac{2Z_{1cM} + Z_{0cM}}{K_r}}{\frac{n+2}{K_r} - 1},$$

If, simultaneously,

$$Z_s > \frac{Z_{1cM} - Z_{0cM}}{n-1} \qquad (30a)$$

or

$$2Z_{0c} < Z_s < \frac{Z_{1c} - \frac{Z_{1cM} + 2Z_{0cM}}{K_r}}{\frac{2n+1}{K_r} - 1},$$

* This question was first considered by V.L. Fabrikant and Iu.A. Gaevenko.

if, simultaneously,

$$Z_s < \frac{Z_{1c\mu} - Z_{0c\mu}}{n-1}, \tag{30b}$$

where K_r is the reliability factor assumed equal to 1.2 to 1.3;

$Z_{1c\mu}$ $Z_{0c\mu}$ represent the positive and zero sequence component of the impedance of the system Z_c (Fig. 6) in the maximum state in which the selection of current cut-off is made.

Conditions (30) are as a rule only fulfilled when the given load conditions under which the short circuit occurs is greatly different from maximum load conditions.

Let us state that in a number of cases overlapping of the dead zone is ensured by a single phase directional impedance relay.

If faults occur between two phases via an intermediate resistance $2R_{int}$ at point 1 (Fig. 6), the moment of the relay can be expediently represented as an explicit function of

$$\dot{F}_{gen} = Z_k + \frac{R_{int}}{K_{1l}} = Z^{(2)}_{prot}, \tag{31}$$

where $K_{1l} = \frac{I_1^{(ad)}}{I_{1k}}$ is the coefficient of positive sequence current distribution.

After altering expression (2) to the form of expression (7) with expressions (31), (18a) and (23) taken into account, we have

$$M \equiv \left\{(-1)\left[\left(Z_k + \frac{R_{int}}{K_{1l}}\right) + Z_{1c}\right]\right\} \times$$

$$\times \left\{\left(Z_k + \frac{R_{int}}{K_{1l}}\right) - \left[Z_s + \frac{(Z_s - Z_k)(Z_{1c} + Z_s)}{Z_p^{(1)} - Z_s}\right]\right\} = \tag{32}$$

$$= \{(\dot{F}_{AB})(\dot{F}_{gen} - \dot{F}_A)\}\{\dot{F}_{gen} - \dot{F}_B\}.$$

Since $\phi_{AB} = 180^\circ$, the zone of relay operation will be inside the circle plotted on the diameter $0_{II}0_{II}$ (Fig. 12). The relay will operate if the tip of the vector $Z^{(2)}_{pro}$ is inside the circle. It can be seen from (32) that the diameter of the circle varies as a function of the point of short circuit and load conditions.

Let us consider the characteristics for the extreme conditions $Z_k = 0$

and $Z_k = Z_s$.

As follows from expression (32), point O_{II} (Fig. 12) will lie on the straight line $O_I' O_{II}''$, (here $\frac{O_{II}\,O_{II}'}{O_{II}''\,O_{II}'} = \frac{Z_k}{Z_s}$). When $Z_k = Z_s$ the relay is on the boundary of operation in the case of a metallic short circuit, whereas when $Z_k = 0$ the relay reacts with the intermediate resistance $R_{int} < OC$ (Fig. 12). Since as a rule $Z_p^{(1)} \gg Z_{lc} + Z_s \quad Z_s,\ Z_k$. We need therefore only consider one characteristic for the case when $Z_k = Z_s$.

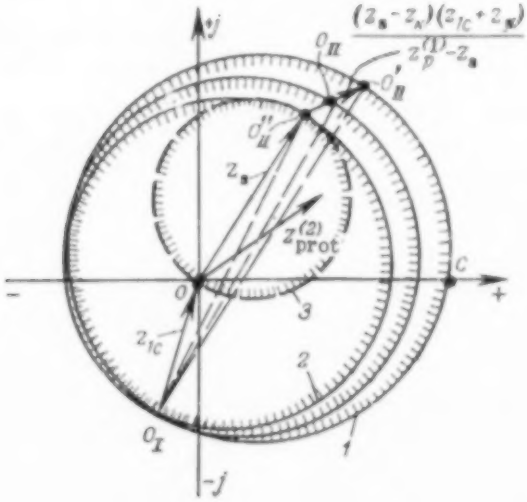

Fig. 12. Combined operating characteristics in the presence of a short circuit via an intermediate resistance under extreme conditions 1 – $Z_k = 0$; 2 – $Z_k = Z_s$; 3 – operating characteristic of a single phase impedance relay.

Comparison of the characteristics of a three phase and single phase relay (Fig. 12, broken line) shows that a three phase impedance relay is more sensitive to the intermediate resistance than a single phase relay, and that this sensitivity is the greater, the greater Z_{lc}.

If an earth fault occurs on one phase via an intermediate resistance $R_{0\,int}^{(1)}$ at point 1 (Fig. 6) we can obtain an expression for the moment agreeing with expression (32) when

$$F_{\text{gen}} = Z_s + \frac{(Z_{1c} + Z_{0s})}{2}\left(\frac{K_{0l}}{K_{1l}}\right) + \frac{3R^{(1)}_{\text{int}}}{2K_{1l}} = Z^{(1)}_{\text{prot}} \qquad (33)$$

In this case, consequently, the operating characteristic has the same form as when there is a fault between two phases. But since $Z^{(1)}_{\text{prot}}$ $Z^{(2)}_{\text{prot}}$, the relay is less sensitive with an earth fault on one phase than when there is a fault between two phases.

If an earth fault occurs at point 1 (Fig.6) on two phases via different phase intermediate resistances R_{int} and the general intermediate earth resistance $R^{(1,1)}_{0\ \text{int}}$ we can obtain an expression for the moment agreeing with expression (32) when

$$F_A = -Z_{1c} + \frac{Z^{(1)}_p - Z_s}{Z^{(1)}_p - Z_s}(Z_{1c} + Z_s)\left(\frac{Z_{1\Sigma}}{Z_{1\Sigma} + 2Z_{0\Sigma}}\right). \qquad (34)$$

where

$$Z_{1\Sigma} = (Z_{1c} + Z_s)K_{1l} + R_{\text{int}} \qquad (35a)$$

$$Z_{0\Sigma} = (Z_{0c} + Z_{0s})K_{01} + R_{\text{int}} + 3R^{(1,1)}_{0\text{int}}. \qquad (35b)$$

The operating characteristic can only be exactly plotted and the maximum value of R_{int} at which the relay reacts exactly determined when

$$R_{\text{int 0.int}}/R^{(1,1)}_{\text{0.int}} = \frac{3m_0}{1 - m_0},$$

where

$$m_0 = \frac{K_{1l}}{K_{0l}}\frac{Z_{1c} + Z_{1s}}{Z_{0c} + Z_{0s}},$$

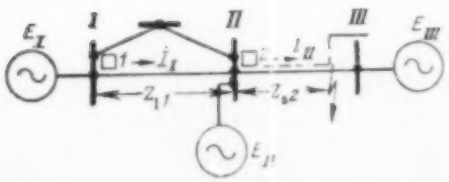

Fig. 13

At other values of the ratio $R_{int}/R_{0\,int}^{(1,1)}$, the characteristic only produces an approximate solution.

It should be borne in mind that an increase in $R_{0\,int}^{(1,1)}$ only increases the sensitivity of a relay and the case when $R_{0\,int}^{(1,1)} = 0$ is therefore only theoretical.

Use may also be of the expressions for evaluating the intermediate resistances to determine the sensitivity of relays in the presence of short circuits on branch lines. Here it is necessary to take the resistance of the branch instead of R_{int} and $R_{0\,int}$.

The behaviour of relays in networks of more couplex configuration

To take into account the feed from an e.m.f. E_{II} (Fig.13), we can select the resistance of the setting Z_{s1} for the second stage of protection from the following formula with a known degree of approximation:

$$Z_{s1} = k_1 Z_{II} + k_2 \frac{Z_{s2}}{S}. \tag{36}$$

where Z_l and Z_s represent the impedances of the protected line and the setting of the protection for the complex section;

$S = \frac{I_I}{I_{II}}$ is the ratio of the three phase short circuit currents calculated for e.m.f.'s E_I and E_{II}, agreeing in phase but different in value, for the maximum ratio of $\frac{E_I}{E_{II}}$

k_1 and k_2 are coefficients of reliability.

To plot the operating characteristic for any type of short circuit in a complex network, let us express the moment as an explicit function of $K_e e^{j\gamma}$ (19) so as to take only two groups of generators with equivalent e.m.f.'s into account:

$$\begin{aligned} M \equiv & \left\{\left(-\frac{\alpha_I Z_\Sigma - \beta_I Z_{Bs}}{\alpha_I Z_\Sigma - \beta_I Z_{As}}\right)\left(K_e e^{j\gamma} + \frac{\alpha_{II} Z_\Sigma - \beta_{II} Z_{Bs}}{\alpha_I Z_\Sigma - \beta_I Z_{Bs}}\right)\right\} \times \\ & \times \left\{K_e e^{j\gamma} + \frac{\alpha_{II} Z_\Sigma - \beta_{II} Z_{As}}{\alpha_I Z_\Sigma - \beta_I Z_{As}}\right\} = \\ & = \left\{\dot{F}_{AB}(\dot{F}_{gen} - F_A)\right\}\left\{\dot{F}_{gen} - F_B\right\}. \end{aligned} \tag{37}$$

where Z_Σ, Z_{As} and Z_{Bs} are determined from expressions (3) and (4), and α and β from the following equations for the theoretical load conditions:

$$\dot{U}^{(l)} = \alpha_{\mathrm{I}}\dot{E}_{\mathrm{I}} + \alpha_{\mathrm{II}}\dot{E}_{\mathrm{II}}; \tag{38a}$$

$$U_{\kappa}^{(l)} = \beta_{\mathrm{I}}\dot{E}_{\mathrm{I}} + \beta_{\mathrm{II}}\dot{E}_{\mathrm{II}}. \tag{38b}$$

We can similarly formulate expressions in the general case for the moment represented as an explicit function of $Z_p^{(l)}$ when the network has any number of supply sources.

Conclusions

The proposed method of investigating a three phase directional impedance relay by means of characteristics represented as explicit functions of one parameter is convenient for appraising the selectivity and sensitivity of relays in the presence of short circuits and breaks in phase in networks of any degree of complexity.

Analysis shows that the stated relay, operating jointly with zero zequence current cut-off, as a rule ensures full protection from all kinds of two phase short circuits. However, the use of this relay at large operating resistances Z_g, for example, in third stage protection, is restricted since it may operate incorrectly even at small angles between the e.m.f.'s of the generators under load conditions preceding an asymmetrical short circuit.

Translated by O.M. Blunn

REFERENCES

1. S.Ia. Petrov; *Elektrichestvo*, No.7, (1954).
2. P.K. Peist; *Elektrichestvo*, No.9, (1957).
3. A.M. Fedoseev; *Relay protection of electrical systems, (Releinaia zoshchita elektricheskikh sistem)*, Gosenergoizdat, (1952).
4. W.K. Sonnemann and N.M. Lensner; *Compensator distance relaying I, Power apparatus and Systems*, No.36, June, (1958).

A HYROTRON WITH CONTROLLED GRIDS (A NEW TYPE OF HIGH FREQUENCY IONIC CONVERTER 0.5 TO 50 KC/S FOR INDUCTION HEATING)*

DAN TEORODESCU

(Roumania)

(Received 18 September 1959)

1960

Introduction

Several types of high output generator have been developed to produce high frequency currents and these are finding ever increasing application in industry. Dynamoelectric, electronic and ionic generators are in greatest demand at the present time.

Dynamoelectric generators are made for frequencies up to 10 k c/s owing to large losses and cooling difficulties. The efficiency of this equipment is about 50 to 60 per cent. This limits their maximum unit output.

Electronic generators will produce frequencies from 0.1 to 100 k c/s, but their efficiency is also about 50 per cent. In addition they are large in volume and quite expensive.

Ionic converters with "exitrons" make it possible to produce currents with a frequency from 0.5 to 1.5 k c/s and an efficiency of almost 1. The great efficiency of these generators, determined by the small losses in the arc, enables us to produce these devices with outputs up to several thousand kW. The top frequency limit of these converters depends on the minimum de-ionization time. In optimum cooling conditions this is roughly 0.5 millisec.

Despite the fact that the frequency of ionic generators is comparatively low, they will in the near future replace dynamoelectric

---

* *Elektrichestvo*, No.6, 68-70, 1960.

converter gear of corresponding frequency on account of their increased efficiency and great output.

To produce higher frequencies the author of this paper has proposed a new type of ionic converter with uncontrolled grids which is called a hyrotron and operates at 0.5 to 50 k c/s.

The operation of the hyrotron is based on the "rotation" of the electric arc in the mercury vapour under the influence of a uniform magnetic field so that it is struck successively on radially disposed anodes in the mercury bath. The mercury cathode is situated in the centre of the bath, a little below the plane of the anodes. The cathode spot is maintained by the central exciting anode. The converter also has an ignition (striking) anode.

An account is given below of the principle underlying the operation of hyrotrons with controlled grids and some of its characteristics are described.

Control and the characteristics of the hyrotron

The molecules inside the bath are in a highly excited state. The majority of them possess somewhat less energy than the energy of ionization (10 eV), but rather more than that of excitation. It is therefore sufficient to impart a small amount of additional energy to the molecules so that they pass from the state of excitation into the state of ionization. The phenomena in the cathode-affected space are the same as in other ionic converters and there is nothing special about the hyrotron in this respect.

However, it is a different matter in the anode-affected space. The entire process of arc transfer from anode to anode is determined by the fact that the molecules in the grid-anode space are in a less excited state than those at other points of the bath. This is explained by large bipolar diffusion. Moreover, the design of the grid plays an important part here.

The molecules in the grid-anode gap thus need additional energy to achieve the state of ionization. In the hyrotron this energy is produced by the electrons which bombard the stated space under the influence of electromagnetic forces and the local increase in current density caused by the controlled grid.

These two factors determine the operation of the hyrotron and by correctly adjusting these factors we can obtain optimum operating conditions.

In the case of the hyrotron with uncontrolled grids, the first factor is the major one in the transition of the arc from anode to anode. The major factor in the hyrotron with controlled grids is the second factor.

Fig. 1 shows a cross-section of the hyrotron with controlled grids and its principal circuit.

The grid of the hyrotron is supplied with a voltage from a load transformer by means of a symmetrical grid transformer and a phase-shifting device. The magnitude of grid bias is regulated by an appropriate change in impedance.

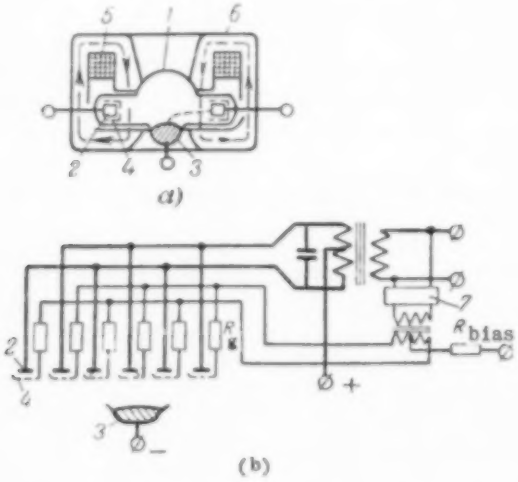

Fig. 1. Section (a) and principal circuit of the anode unit (b) of a hyrotron with controlled grids. 1 - bath; 2 - anodes; 3 - cathode; 4 - grids; 5 - winding; 6 - armature; 7 - shifting device; R_g - grid resistance; R_{bias} - bias resistance.

Let us suppose that the field is so directed that the arc tends to pass from anode A to anode B (Fig. 2). Then the charge carriers will be affected by forces $\bar{F}_l = 2\,[VH]$ and $\bar{F}_E$ determined by the boundary of the arc between two collisions.

When the arc moves from anode A to anode B two cases can occur when the molecules about anode B reach the state of ionization before the grid received the control pulse and when the molecules in the stated space are still in the state of excitation when the grid is fed with the controlling voltage.

This case can occur in a hyrotron with controlled grids if the phase shift of the grid voltage is selected incorrectly, i.e. when the moment of ignition is not regulated exactly.

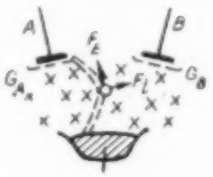

Fig. 2.

The distance between the anodes also has a considerable effect on the operation of the hyrotron. If it is too small it is impossible to regulate the hyrotron. There therefore exists a certain critical distance dependent on the power of the converter. This distance can only be reduced if screens of appropriate size are placed between the anodes.

The second case corresponds to the normal operating conditions of the hyrotron with controlled grids.

If a positive voltage pulse is fed to the grid, the density of the ionization current in its vicinity becomes equal to the critical value and under the action of electromagnetic forces, determined by the presence of an external magnetic field, the arc passes from the preceding anode to that in question.

All this discussion is purely general in nature and is not intended to give a complete explanation of the extraordinarily complicated phenomena which occur in the converter.

The hyrotron can be controlled by means of a sinusoidal voltage. But, as in other converters, this method of control suffers from the disadvantage that the moments of ignition are scattered. The hyrotron is more sensitive to this scatter since the moment of ignition plays the main part in its normal operation. The moment of ignition should therefore be within a rather narrow range and inaccuracy in ignition should not exceed a few degrees.

However, control of the hyrotron by means of a sinusoidal grid voltage is satisfactory in the majority of cases in practice, especially where a small deviation in the phase of the output voltage is permissible, and when there is no danger that a change in the angle of ignition will bring the converter out the controlled state.

The use of peaked or rectangular pulses overcomes the above disadvantage by defining the moment of ignition sufficiently accurately. The pulse control voltage is produced by a special circuit of non-linear elements connected with the secondary winding of the load transformer via a phase-shifting device (here use may be made of R.C. circuits which are fully described in the published technical literature).

It is of interest to note that in the hyrotron with uncontrolled grids there is a considerable variation in the phase of the generated voltage reaching up to about 35 el. degrees. This is explained by the changes in the moment of ignition which depends on the time taken for the grid-anode space to achieve the state of ionization. The phenomenon is easily observed on a screen oscillograph.

Even when a sinusoidal voltage is fed to the grid the screen will show how the "bundle" of sinusoids of the output voltage collects in one sinusoid.

Fig.3 shows curves characterizing the change in frequency as a function of the inductance of the magnetic field in hyrotrons with different numbers of anodes.

The following conclusions can be drawn from these curves.

The hyrotron with controlled grids has fairly non-drooping characteristics $f = \phi(B\delta)$; if considerable changes occur in the inductance of the magnetic control field ($\pm$ 50 per cent) the oscillation frequency of the output voltage varies comparatively little. The characteristic of this same hyrotron without grid control produces rather large variations in frequency with the same change in $B\delta$.

The performance of the hyrotron with controlled grids is only stable over a definite range of values of the field inductance. This means that there are definite critical values of $B\delta$ for the given parameters of the hyrotron. The instability of the hyrotron's performance outside the stated values of $B\delta$ to a large extent depends on the phase of the control voltage.

The frequency of the oscillations under regulation on a hyrotron with six anodes with the same size of the bath is 50 per cent greater than that of a hyrotron with four anodes and, consequently, it is proportional to the number of anodes.

The characteristics $f = \phi(I)$ of a hyrotron with six anodes are given in Fig.4. They are plotted for different values of $B\delta$ at a pressure inside the bath of 1.5×10^{-3} mm Hg. For purposes of comparison, the broken line denotes the characteristic of the same converter with uncontrolled grids for the nominal value of the field. The curves

in Fig.4 show that the oscillation frequency also changes when there is a change in load current and that this change is considerably greater in the hyrotron with uncontrolled grids.

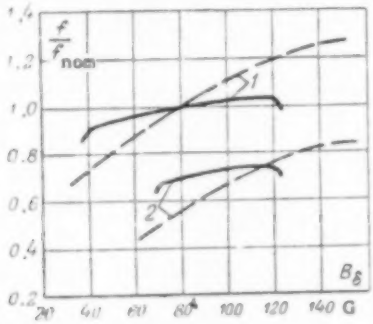

Fig. 3. Dependence of the frequency of the generated oscillations on the inductance of the external magnetic field of a hyrotron with six (1) and four (2) anodes: —— hyrotron with controlled grids; - - - - hyrotron with uncontrolled grids.

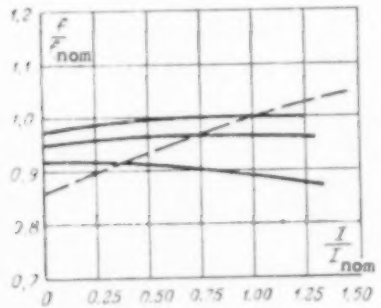

Fig. 4. Dependence of the frequency of the oscillations on the load current of a six-anode hyrotron.

Shape of voltages and currents

The oscillogram of the current of one of the anodes in Fig.5 shows that its shape is practically rectangular.

In the short-circuited state when every other anode is linked by two common feeders and the feed is at a reduced voltage, the shape of the current is practically rectangular in order to determine the parameters

of the hyrotron (Fig.6).

These oscillograms of the anode current indicate the presence of high frequency harmonics. As in ionic converters with "excitrons", these harmonics reduce the total efficiency of the gear. But, efficiency nevertheless remains fairly high thanks to the small losses in the arc.

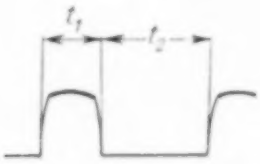

Fig. 5. Oscillogram of the anode current of one of the six anodes of a hyrotron operating under normal conditions.

1960

Fig. 6. Oscillogram of the current of one of the common feeders of a six-anode hyrotron under short-circuited conditions.

The voltage drop in the arc of the hyrotron has two components, i.e. one depends on the inductance of the magnetic field, whilst the other does not. The value of the arc current has practically no effect on the total voltage drop. The voltage at the load terminals is sinusoidal in shape.

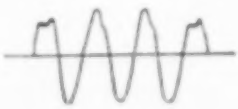

Fig. 7. Shape of hyrotron grid voltage.

Fig.7 shows the shape of the voltage on grids when the hyrotron is controlled by a sinusoidal voltage.

The curve for the grid voltage is distorted in shape owing to losses in the grid impedance at the moment of the grid current pulse.

The oscillogram of the grid current (Fig.8) confirms what we have said. The pulse of current occurs in the first part of the period and its time is equal on average to:

Fig. 8. Grid current curve.

Design of the hyrotron

This hyrotron with six anodes has a bath made from austenitic steel. The bath and cathode are water-cooled. The anodes are radially disposed and provided with cooling vanes. To fix the position of the cathode spot in the mercury bath, provision is made for a molybdenum ring. The ignition anode is on the axis of the bath and an excitation anode of annular shape surrounds it. Rubber sealing is provided, protected with rings from the mercury vapours.

The hyrotron is subjected to evacuation before starting by prolonged operation in the short circuited state at a current greatly in excess of the rated value.

Conclusions

The hyrotron with controlled grids can be used at frequencies from 0.5 to 50 k c/s for both ultrasonic and heat treatment of various materials.

Certain models of this type of converter can be fed direct from a three phase network.

After overcoming the technological difficulties connected with the production of the ionic baths, the hyrotron will make it possible to use methods of heat treatment based on frequency currents in our national industry on a larger scale.

Translated by O.M. Blunn

ABSTRACTS FROM PAPERS PUBLISHED IN ELEKTRICHSTVO No.6, 1960

Why the charge of partial capacitances does not correspond to the resultant field flux: L.R. Neiman and K.S. Demirchian, (pp. 1-6).

The purpose of this paper is to establish that the following inequality generally holds:

$$C_{kp}\, U_{kp} \neq \psi_{kp}$$

where C_{kp} are the changes of the individual capacitances, U_{kp} the potential differences and ψ_{kp} the electrical displacement flux. The method is simply to examine the physical picture of the resulting field and its variation with the variation of one of the bodies. The examination is based on taking into account the mathematical properties and features of the field.

How raising the power factor of a load affects its stability: V.A. Venikov, (pp. 6-10).

As the widespread use of static capacitors to improve the power factor of the load can on occasion reduce the reserve of load stability and lead to a voltage "avalanche", a study is made of the basic relationships characterizing the conditions of a system with a preponderance of asynchronous (induction) motors. A feature of the paper is that certain assumptions are made so that the resistance of the network can be ignored for greater simplicity in the equivalent network as shown. The use of series-connected capacitors is recommended but it is necessary to check self-excitation and self-induced swinging.

A simplified method of appraising the stability criteria of an equivalent load: N.A. Mel'nikov, (pp. 10-14).

As a considerable increase in the total rated power of static capacitors in transverse-capacitive compensation gear can disturb the stability of a system, it is considered useful to investigate the stability of the

system on the basis of a simple circuit with a non-linear element in the form of an equivalent load. To appraise the conditions under which the load is disturbed, use is made of static characteristics of the load plotted with its composition and synchronous motors taken into account, (with automatic regulation of excitation).

On principles and methods of calculating motor drives for a suddenly applied load: D.P. Morozov, (pp.17-21).

A study is made of methods of calculation applicable to the performance of electrical drives under shock loads. Attention is paid to motors with a constant impedance in the rotor circuit, a contactor slip regulator and a fluid slip regulator. Formulae are introduced relative to the energy loss in the secondary circuit, heating of the motor as regards rotor current and losses in the rotor winding, average losses and the equivalent torque of the motor.

The ignition of a sectionalized high voltage valve: N.M. Maslennikov, A.A. Sakovich and V.D. Andreev, (pp.25-29).

Stable high direct voltage transmission is greatly dependent on the clear striking of the arc in each valve in the converter installation, i.e. stable ignition angle and no failures in ignition, particularly in in inverter substations where each failure will produce fault conditions. The author discusses the striking of the arc in a valve with a sectionalized anode and gives the results of an investigation into the process of striking the arc in large sectionalized valves with a mercury cathode which enable the factors affecting clear ignition to be elucidated. A description is given of the valve in question and the striking of the arc on the control electrodes and in the anode.

An electronic computer study of the motor drive in the EVG-15 type excavator; V.G. Vasil'ev, A.I. Kondratenko, V.P. Lomakin and N.Ia. Tarasova, (pp.39-41).

Modern high productivity excavators involve problems which do not lend themselves easily to analytical solution such as the synthesis of the the stabilizing links, the analysis of transient processes, the investigation of the reliability of the main drives, etc. These problems can now be tackled in the design stage by means of computers and the present paper gives the results of such an investigation into the EVG-15 type excavator. After describing the drive, a description is given of the computer study, the purpose of which was to verify the dynamic operating conditions of the electrical equipment and find the

optimum parameters of the stabilizing links and certain static characteristics of the rotary, hoist and thrust drives.

On the signs of the characteristic parameters of symmetrical four-terminal networks: E.V. Zeliakh, (pp.41-46).

Many formulae for determining the characteristic parameters of symmetrical four-poles include radicals and it is necessary to think out the plus or minus sign in front of them before use can be made of the parameters for other problems. These signs must be chosen correctly. However the proper method of choosing them has not as yet been adequately developed and the purpose of this paper is to clarify this problem.

Relative characteristics of asynchronous machines: V.M. Kutsevalov, (pp. 47-50).

The equation for the relative mechanical characteristic of an asynchronous machine at present used in practice is only true for asynchronous machines with constant rotor parameters and does not apply to asynchronous machines with a solid cylindrical rotor where the equivalent applied resistance and reactance of the solid rotor is a function of slip. In the case of an ideal hysteresis asynchronous machine (without eddy currents) the parameters of the rotor circuit in the equivalent network are independent of slip however and other cases are possible. The author therefore proposes new equations relative to the characteristics of asynchronous machines.

Electro-mechanical systems with variable inductance: M. Marinesku, (pp.50-58).

The author reviews and generalizes the results of an investigation into the conversion of electrical energy into mechanical energy in circuits with periodically varying inductance. The investigations began 10 years ago at the Roumanian Academy of Sciences to elucidate the optimum conditions for conversion, to establish to what extent electrical machines can be produced on this basis and to evolve a method of design. he concludes that there is more scope for simple parametric machines with variable inductance, particularly in connexion with parametric resonance (phenomena connected with the periodic variation of inductance observed in synchronous machines). It is expected that parametric generators will be made for the production of currents of ultrasonic frequency and that parametric resonance will be applied in long distance communication and radio engineering.

On a method of cutting off the forcing of a transient: M.N. Fesenko, (pp.58-61).

In order to reduce the length of a transient process and improve its quality in for instance the drive of a reversing rolling mill, use is made of special methods involving the forced variation of the excitation current of the generator. A study has been made of transient processes in a circuit containing a semiconductor triode and inductance with the voltage jump connected at the input to the triode, the purpose being to develop new methods of forcing the transient process in the excitation of a generator. After stating the theoretical considerations he describes a circuit with a d.c. amplifier and semiconductor triode. The advantage claimed for the cut-off method of forcing the transient process in the excitation circuit by the semiconductor triode is that the circuit is simplified and the forcing process is made practically ideal.

The relationship between reactive powers in single phase capacitor motors with three phase stator windings: A.I. Adamenko, (pp.61-68).

Investigations have suggested that single phase capacitor motors with three-phase stator windings are to be preferred to such motors with two-phase stator windings in certain cases. A study is therefore made of single phase motor systems with three-phase stator windings in which the round rotating magnetic air gap can be produced by external reactances for any power factor of the motor phase.

Transients in the windings of multi-layer peak transformers: I.M. Roife, (pp. 71-76).

Pulse transformers with windings having up to 30 layers are now in use for instance for accelerator tubes. It is regarded as very important that a study be made of the transient processes in the windings of these transformers in order to determine the shape of high voltage pulses and ascertain the conditions for the inter-layer insulation. A study is made of certain questions connected with the choice of equivalent circuit of a multilayer winding, the theoretical and experimental investigation of the transients on the leading edge and at the peak of the pulse and the breakdown (puncture) conditions of pulse transformers on load.

A high-speed semiconductor switch and trigger for electronic

computers: Ia.N. Bapat and I.L. Kaganov, (pp.76-82).

Since the counting speed of electronic computers is mainly connected with the rise time of the pulse for the input and output voltages, an investigation has been made into the static conditions of an extra-high-speed semiconductor current switch (key). When based on triggers, switching frequencies of up to 10 M c/s and higher can be achieved.

Overvoltages when switching a germanium diode and its protection: V. Gusa, Ia. Tsigelka and L. Chernyi, (pp. 82-85).

A study is made of a certain method of protecting germanium diodes from the large voltage surges which arise on switching. After a theoretical analysis, the results are given of an investigation into the use of a protective cell consisting of a capacitance and resistance, the magnitude of the capacitance being greater than the natural capacitance of the diode (i.e. > 1000 pF/cm^2 when $U = 0$). Oscillograms are given to illustrate the expediency of the proposed method.

A new scheme for temperature controllers using thermistors: G.K. Nechaev, (pp.85-88).

The Electrical Engineering Institute of the Academy of Sciences U.S.S.R. has developed a temperature controller using thermal resistances which will measure the temperature in machine units etc and produce a signal when overheating occurs. However, they are complicated to use, and the author advocates the use of the "relay effect" for indication purposes. Relay effects are produced in the circuit when the parameters of the surrounding medium and the elements of the circuit vary. The proposed controller is fed from a ferro-resonance voltage stabilizer via a sectional transformer and rectifier. Provision is made for blocking the thermal resistors by a resistance which protects them from prolonged overload.

A model system for studying electronic excitation systems for motor drives: V.V. Rudakov, B.A. Egorov and L.G. Konradi, (pp.88-91).

Only the basic parameters are usually taken into account in the design of generator-motor type variable drives so that there is a great deal of adjustment after installation. Laboratory electro-dynamic models are now in use for investigating excitation and control systems. Difficulties arise here in smoothing the pulsation of the rectified current. The Electro-mechanical Institute of the Academy of Sciences has evolved a system using an auxiliary low power reactor and additional

power amplifiers which is described.

On the reliability of telemechanical devices: N.S. Shabalin, (pp.91-93).

Stressing the need for reliability in such devices, the author urges the formulation of objective criteria to enable the reliability of different devices to be compared. As such criteria he proposes (1) the number of failures over a given period, (2) the average length of time the devices work between failures, (3) the life of the device, these indices to be calculated on the basis of operating statistics. He advocates the use of probability theory to ascertain such criteria. He touches slightly on improvements in the design of devices and the structure of the telemechanical systems. Reference is made to magnetic and semiconductor elements (crystal diodes and triodes).

ABSTRACTS FROM PAPERS PUBLISHED IN ELEKTRICHSTVO No.7, 1960

High quality electrical steels and alloys. A.M. Samarin, (pp.1-4).

The electrification of the U.S.S.R. being the "main core" of the programme of communist construction in the next 15 to 20 years, the author considers means of reducing the cost of material for electrical equipment and ensuring that the right metals and alloys are produced for the electrical industry. He discusses silicon steels, iron, Fe-Al alloys, constructional steel with a low hydrogen content to reduce flaking, semiconductor materials, substitutes for copper and the production of pig iron in electric furnaces.

Electrical equipment at the Bhilai iron and steel works. M.M. Brozgol, (pp.5-10).

An account is given of the integrated iron and steel works built in India with the assistance of the U.S.S.R.

New motor drives for continuous cold rolling mills. F.F. Olefir, (pp.11-15).

A study is made of the system of excitation used for the generators in the control of continuous cold rolling mills. Provision is made for compensation of the ohmic voltage drop in the armature circuit of the motors on the principle of "two-circuit control" which ensures a high degree of control accuracy over the generator voltage at a relatively low amplification factor.

An automatic motor drive for grinding machines with follow-up feed. A.A. Sirotin and V.A. Eliseev, (pp.15-19).

A description is given of "follow up" type electric drives for high output grinders producing better surface finish, as developed in the Moscow Power Institute. The relay-action follow-up drive for the cross feed is used in conjunction with a variable speed drive for the grind-

ing wheel. Formulae are given to determine the transient processes in the drive. A description of the drive is given.

An electronic computer study of an automatic helmsman. I.P. Freidzen, (pp.20-25).

An account is given of the results of an investigation into the control of a ship's steering on an analogue computer. It is claimed that the model simulating the hydrodynamic link can be used to adjust the "automatic helmsman" prior to installation on board ship and so save time.

On power regulation theory of electrical ore-smelting furnaces. V.S. Lerner, (pp.25-30).

A description is given of the automatic system of power control used chiefly in electric ore-smelting furnaces with a deep slag bath. An analysis is made of the link between the basic parameters of the regulator and the object so as to ensure the requisite static and dynamic characteristics. Reference is made to a system comprising a correcting circuit which has passed operational tests.

On control systems for the drives of medium-sized excavators. M.I. Kraitsberg, D.A. Kaminskaia and V.P. Lomakin, (pp.30-35).

A comparison is made between drive systems for excavator shovels (capacity 6 to 8 m^3) using dynamoelectric amplifiers jointly with intermediate magnetic amplifiers (cascade system) and dynamoelectric amplifiers by themselves (KhEMZ system). After studying a series of oscillograms of the performance delivered by these systems it is recommended that external flexible feedbacks be excluded. Lifting and drawing are performed more efficiently on the KhEMZ system. The KhEMZ system is recommended for medium power excavators.

Grapho-numerical methods for calculating transients from structural schemes. A.M. Suchilin, (pp.35-39).

A method is proposed for simplying Basharin's system of calculating transient processes in automated drives. Instead of ascribing a differential equation to each link in the structural scheme, substituting a finite difference equation written in the form of a proportion and then performing the calculations graphically, the author proposes a "programme scheme of calculation" comprising elementary links which are found by recurrence formulae based on the transfer functions of the links.

The d.c. magnetic field in a parallepiped. V.N. Rudakov, (pp.39-41).

Powerful magnetic fields arise in electrolyte baths producing electrodynamic forces causing the metal in the bath to shift. This entails the calculation of the intensity of the magnetic field of the anode current. The present paper proposes a simplified theoretical method of calculating the magnetic field in a rectangular parallepiped.

A synthetic scheme for testing circuit-breakers with long burning arcs. N.M. Chernyshev and Z.A. Abramova, (pp.41-46).

A study is made of methods of testing circuit breakers and an account given of a new synthetic system which is particularly effective in the case of circuit-breakers with long arc combustion time and a relatively large voltage drop in the arc. Use is made of an additional inductance of the order of 0.2 to 0.4 in the circuit.

A combined way of switching in power circuits. N.F. Shishkin and P.Ia. Danilin, (pp.47-50).

The connexion of a constant resistance of practically zero value in parallel to the consumer has not yet been widely used for commutation purposes although it is more quick-acting, (use here being made of a short circuiting device). A new method of commutation which involves no "metallic" short circuit of the supply source is proposed using a combined switching apparatus with tripping and shorting systems of contacts incorporating a spring-magnetic mechanism.

Surge protection of 35-500 kV switchgear today. N.N. Beliakov and A.N. Sherentsis, (pp.51-56).

A study is made of proposals for simplifying the protection of electrical networks from surges. Special attention is paid to direct lightning strikes and the protection of distribution gear from waves of atmospheric overvoltages from the lines.

The electrical characteristics of long insular strings for lines of 500 kV and higher. N.N. Tikhodeev and A.N. Tushnov, (pp.56-61).

A study is made of the electrical characteristics of long chains of suspension insulators in view of their high cost. Tests supported the belief that the type of protective fitting has no marked effect on the

size of the discharge voltage of the chain if the fitting produces the discharge through the air and not along the surface of the insulators. It is argued that with alternating voltage the electrical strength of long chains in the dry state and with a protective fitting is determined by the asymmetrical air gap between the fitting and the tower. Account must be taken of the dry discharge voltage of the chain as well as the wet discharge voltage.

The 500 kV Sverdlovsk substation. L.D. Gustov and others, (pp.61-66).

A description is given of the layour of the Sverdlovsk substation and its 500 kV equipment and apparatus. The substation is intended to receive power from the Lenin hydro-electric station on the Volga, the "Botkinsk" hydro-electric station and large thermal power stations. A special feature of the substation is the reduction in capital and running costs achieved by adding it to the existing 220/110 kV substation and a new high speed 500 kV oil circuit breaker, (arc quenching time 0.015 to 0.004 sec).

On the deficiencies of State Standard GOST-8033-56 "Electrical and Magnetic Units". L.B. Slepian dec'd., (pp.66-67).

The author maintains that the above State Standard is deficient in that two systems for electrical and magnetic units are permitted, namely the MKSA and Gauss systems. He advocates the use of the MKS(G) system, i.e. the practical Gauss system.

Concerning the questions raised by Professor L.B. Slepian in his article "On the deficiences of State Standard GOST 8033-56". L.R. Neiman and E.G. Shramkov, (pp.68-69).

The authors state that Professor Slepian's proposals for the use of the MKS(G) system of units (see previous abstract), though interesting, are less acceptable than the recommended MKSA system because of the need to introduce certain corrections.

The possibilities of detecting ferromagnetic conducting objects in ferromagnetic substances. L.A. Gel'bukh, (pp.69-72).

It is argued that in removing metallic inclusions from powder, it is impossible to detect the metallic inclusions merely by determining the change in the e.m.f. of the signal or frequency. A method of indica-

tion based on changes in phase is described. This is suitable for ore cleaning plant to prevent damage to the crushers in the event of foreign matter falling into the ore.

Condenser paper having a small dielectric loss angle. V.T. Renne, M.N. Morozova and K.I. Karpova, (pp.72-77).

Investigations have shown that Russian sulphate cellulose used for condenser paper has roughly the same pentosane content as that in America. A marked influence of the ash content of the paper on losses has been established. Even though organically equivalent to American paper and superior as regards the adjustment of the ash content, Russian paper is acknowledged to be inferior to the American product and it is recommended that paper with a reduced volumetrical weight, of the order of 0.85 to 0.9 g/cm^3, be produced.

The characteristics of flashover along the layers of paper-oil insulation for direct voltage. M.A. Greisukh, (pp.77-82).

It is considered necessary to take into account the total discharge voltage from the edge of one electrode to another primarily along the layers of paper for condenser-type paper oil insulation in the development of current transformers etc. A study is therefore made of the discharge characteristics of the thickness of the insulation, the construction of the edge and the polarity of the voltage when the discharge voltage is 5 to 6 times lower on d.c. than a.c. and positive polarity is advocated. Temperature changes between 20°C and 75°C and differences in edge thickness from 10 to 85 micron have no effect.

Diagrams for determining the firing angle of a three phase bridge type rectifier. S.R. Glinternik, (pp.82-85).

A simplified diagram is proposed for determining the angle of commutation and the given ignition angle for a three phase bridge converter for current rectification inversion. The diagram can be used to calculate the electromagnetic processes and converter characteristics in all steady state conditions with the exception of a small zone in the vicinity of the short circuit state when three valves are arcing simultaneously.

NEW ELECTRICAL DRIVES FOR CONTINUOUS COLD ROLLING MILLS*

F. F. OLEFIR

(TsKB "Elektroprivod" VNIIEM)

(Received 27 July 1959)

The control of modern continuous cold rolling mills is essentially reduced to controlling the excitation of the generators, since the flux of the drive motors for the stands remains unchanged in the basic operating conditions. Use is only made of regulation for the flux (current) of the drive motors to balance out the load between them and when adjusting the rolling speed to the flux. The requisite operating conditions of a mill are therefore entirely determined by the quality of the control system adopted for the excitation of the generators.

Originally, the drive of mills was controlled by motors which were supplied from common generators, the total voltage of the feeder busbars here being the main means of ensuring the requisite relationship between the speeds of the stands under all the operating conditions of the mill. Control of the excitation of the generators was only involved in obtaining the desired rolling speed and the necessary characteristics for the acceleration and retardation of the mills.

Later, as the technique of cold rolling developed, in order that the maximum amount of strip be produced in accordance with the tolerances, and the thickness of the strip be automatically balanced out at steady rolling speeds, compensation of the ohmic voltage drop Ir was introduced into the armature circuit of the drive motors. This was effected from special booster-generators. In this case the control system of the generators and the system of compensation act independently. Only with independent feed for the motors of each stand did all the basic functions of mill control come under the control of the excitation of the generators (requisite acceleration and retardation states for the mill,

*Elektrichestvo, No. 7, 11-15, 1960.

requisite relationship between the speeds of the stands and automatic compensation Ir).

The excitation of the generators is controlled along two circuits (channels). The voltage from the exciter is set along the first channel. This voltage is common to all the generators of the mill stands. The generator voltage for the stand is brought to a high degree of accuracy along the second channel by comparing it with a standard command voltage. This second circuit is a closed automatic control system.

The electrical link between the generators and the appropriate drives of the mill stands is effected via a standard common command voltage. This link is the greater, the higher the amplification factor of the control system for the excitation of the generators at each individual stand.

The standard voltage and exciter voltage are controlled from a "flat" controller which sets the acceleration, retardation and steady rolling speed of the mill.

The special feature of systems of control for the excitation of the generators consists in the compensation of the ohmic voltage drop Ir in the armature circuit of the motors. It is effected on the principle of two-circuit control. This makes it possible to ensure highly accurate regulation of a generator's voltage with a relatively low amplification factor.

We established the independence of the system of excitation control with stabilization of the generator voltage by TS144-110 type stabilizing transformers during theoretical and experimental investigations in the process of adjusting the drive of the continuous fivestand mill at the Magnitogorsk integrated iron and steel works.

Satisfactory results were obtained at a system amplification factor of the order of 150 to 200 when applying stabilization from a dynamic bridge, one arm of which included the excitation winding of the generator (Fig. 1), and also when use was made of choke stabilization (Fig. 2). In the latter case, use was made of the secondary winding of a TS72-60 type stabilizing transformer (shunted by an ohmic resistance) as the choke and this was connected in the measuring winding IV of the control system.

The use of two cascade connexion of the dynamoelectric amplifier made it possible to improve the static and dynamic characteristics of the system of excitation control, since the residual voltage and non-linear resistance of the armature circuit of the dynamoelectric amplifier A2 is excluded from the circuit for comparing the generator voltage with

the standard, (particularly important when the currents in control winding IV are small).

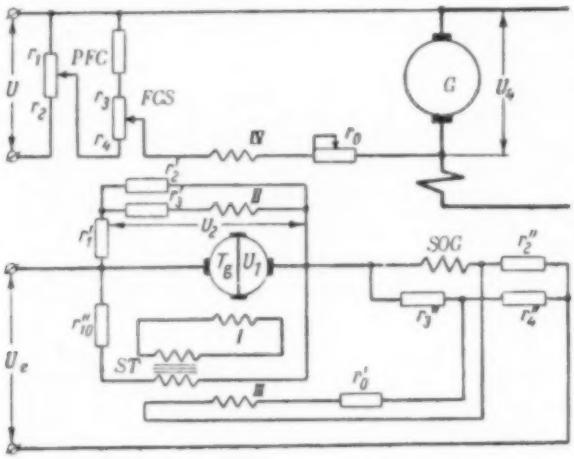

Fig. 1. Excitation control circuit of generator with stabilization by a dynamic bridge: *G* – Generator; *PFC* – principal "flat" controller; *FCS* – flat controller of stand; *ST* – stabilizing transformer.

On the same grounds use was made of a system of excitation control with the dynamoelectric amplifier connected in a two-cascade arrangement and choke stabilization as in Fig. 3* for another continuous five stand mill, (Lenin combine in Poland). Stabilization from a dynamic bridge was not acceptable in this case since it involved impermissible variations in the amplification factor of the system to the extent that the excitation winding of the generator became hot.

It should be pointed out that everything was done in the control system for the mill stand as in Fig. 3 to limit the effect of variations in the parameters of the system on the value of the amplification factor. In particular, we eliminated the effect on the amplification factor of the position of the flat controller *FCS* as in the circuit in Fig. 1, (not shown in Fig. 3). This was done by using two sections of resistance in the circuit of winding IV, the value of which remained constant in any position of the *FCS* traverse.

---

* Polish engineers G. Eigmund, K. Vyshtiga and K. Kromin took part in arranging this system.

The mill using the system shown in Fig.3 operated well at an amplification factor of 275 and above.

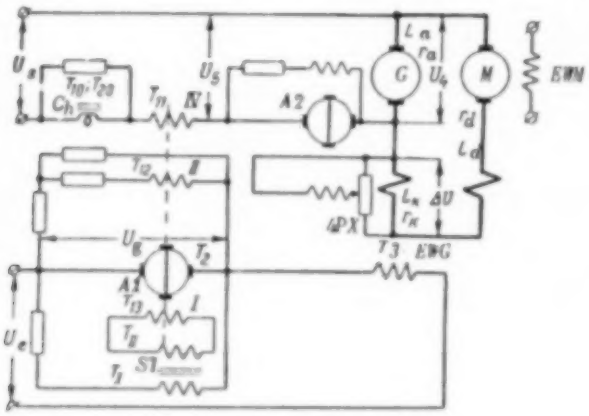

Fig. 2. Excitation control circuit of generator with choke stablization: G – generator; M – motor; $A1$ and $A2$ – dynamoelectric amplifiers; ST – stabilizing transformer; $r_4 = r_a - r_k - r_d$;

$$L = L_a - L_k - L_d; \quad T = T_I - T_{II}.$$

To change over from single cascade systems for the excitation control of generators to two-cascade systems, it was necessary to solve the problem concerning the identical effect of amplifier $A2$ in the circuit as in Fig.2 and winding I in the circuit in Fig.3, intended to compensate the voltage drop Ir. At the same time it was necessary to determine the efficiency of the new means of stabilization and state more precisely the role and value of the compensation Ir in the control system for the stand drive.

Fig.4 represents the system shown in Fig.2, according to which the equations for the individual links can be written as follows (account here being taken of the mutual induction between the amplifier windings):

$$\begin{aligned}
&\frac{1+T_{10}p}{1+T_{20}p}U_{11}+T_{11}pU_1=k_{11}\cdot\Delta U_1;\\
&U_{12}-T_{12}pU_1=k_{21}k_{12}\cdot U_2;\\
&U_{13}-\frac{1+T_1p}{1+Tp}T_{13}pU_1=k_ck_{13}\frac{T_1p}{1+Tp}U_2;
\end{aligned} \tag{1}$$

$$U_1 = U_{11} - U_{12} - U_{13};$$
$$(1 + T_2 p) U_2 = k_2 U_1;$$
$$(1 + T_3 p) E_4 = k_3 U_2;$$
$$(1 + T_m p + T_e T_m p^2) n = k_0 E_4;$$
$$\frac{1}{1 + (1-\varphi) T_m p + (1-\mu) T_e T_m p^2} U_5 = \frac{1}{k_0} n,$$

where $\varphi = \frac{r_a + k_4 r_k}{r_4}$ is the degree of compensation of the ohmic voltage drop in the armature circuit of the motor;

$\mu = \frac{L_a + k_4 L_k}{L}$ the degree of compensation of the inductive voltage drop, and

k_4 the amplification factor of the compensation unit, if the inductance of the amplifier A2 is ignored, this having large negative and rigid feedback.

The equation for the closed automatic control system for the stand drive from equations 1 can assume the form:

$$U_5 = \frac{NU_g}{\left[W(p) \frac{1 + T_m p + T_e T_m p^2}{1 + (1-\varphi) T_m p + (1-\mu) T_e T_m p^2 + N}\right]}, \qquad (2)$$

where $N = k_{11} k_2 k_3$ is the amplification factor, and

$W(p)$ the denominator of the transfer function of the control system for excitation of the generator.

The transfer function of the control system for the excitation of the generator $N/W(p)$ is of the fourth order if stabilization is from a dynamic bridge, but of the fifth order with choke stabilization. Differential equation 2 is therefore of the sixth order in this case and of the seventh in the other case.

All the features of the action of the system of the stand drive derive from analysis of equation 2. Let us consider it in the case of choke stabilization. In the absence of compensation Ir, φ and μ are 0; consequently, the differential equation for the closed automatic control system will be of the fifth order. When $1 > \varphi > 0$ and $1 > \mu > 0$ it will be of the seventh order, but when $\varphi = 1$ and $\mu = 1$ it will be an equation for the transient process in the regulation of the speed of the stand motor.

The speed of the stand motor can also be obtained from Fig.4 in the

following form:

$$n = \frac{NU_s}{\left[W(p)\frac{1+T_m p+T_e T_m p^2}{1+(1-\gamma)T_m p+(1-\mu)T_e T_m p^2}+N\right]} \times \times \frac{k_0}{[1+(1-\gamma)T_m p+(1-\mu)T_e T_m p^2]}. \quad (3)$$

Analysis of this equation shows that the transient processes in the drive of the mill stand are determined on the one hand by the transient processes in the closed automatic control system in accordance with equation (2) (by the first multiplier on the right hand side of the equation), and on the other hand, by the transient processes in the generator-motor system (by the second multiplier on the right hand side of the equation). The extent to which the closed automatic control system is "covered" by the parameters of the generator-motor system depends on the value of the constants ϕ and μ.

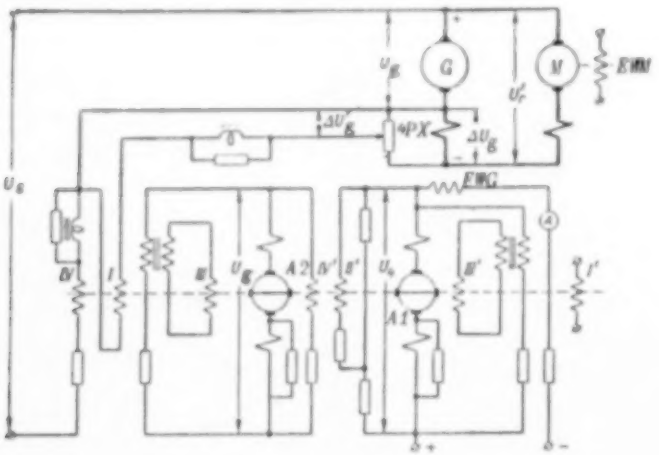

Fig. 3. Excitation control circuit of generators with two cascade connexion of dynamoelectric amplifiers A2 and A1.

The effect of constants ϕ and μ on the value of the constants T_e and T_m of the generator-motor system is used to ensure the requisite relationship between the speeds of the mill stands under all operating conditions.

We can use equations 2 and 3 to produce a very simple link between

the voltage U_5 and the speed of the motor if we assume $T = 0$:

$$n = \frac{k_0}{1 + (1 - \varphi) T_m p} U_s. \tag{4}$$

Equation 4 defines the operating principle of the compensation Ir in the same form as mentioned earlier.

With a linear change in U_5, due to a corresponding change in U_c, the solution of equation 4 can be represented in the following form for a period of time within the limits $t_0 > t > 3(1 - \varphi) T_m$:

$$n = \frac{k_0 U_{5r}}{t_0} [t - (1 - \varphi) T_m], \tag{5}$$

where U_{5r} is the rated value of the voltage at the output of the system, and

t_0 the acceleration time of the mill.

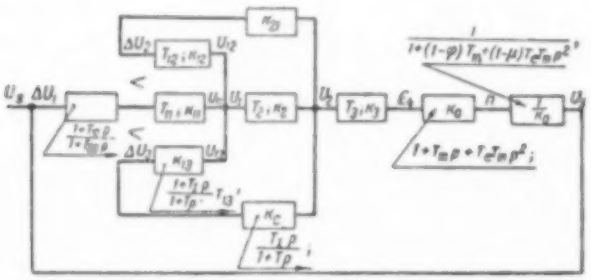

Fig. 4. Control system for the stand of a mill with choke stabilization.

At a large amplification factor N, we can substitute the rated value of the standard voltage $U_{s.r}$ into equation 5 in place of U_{5r} without involving any great error. In the latter case it shows that the compensation Ir essentially consists in being able to establish a different degree of lag in the speeds of the stands relative to the linear variation in the standard voltage during the acceleration and retardation of the mill. As a result, additional tautness is created between the stands whereby the thickness of the strip is equalized.

At steady rolling speeds a change in the extent to which the ohmic voltage drop is compensated in the main circuit will lead to a change in the "rigidity" of the mechanical characteristics of the motors. This also has an effect on the equalization of the thickness of the strip.

Moreover, at different electromechanical constants of the stand drives, as occurs in actual conditions, the requisite degree of correspondence between the speeds of the stands under all operating conditions can be ensured by acting on the value of ϕ.

All the above equations retain their form for the circuit shown in Fig. 3. The only different features are the expression for the coefficient k_4, which characterizes the extent to which the ohmic and inductive voltage drops in the armature winding of the machines are compensated, and the expression for the transfer function $N/W(p)$ of the system for the excitation of the generators.

In its general form the coefficient k_4 is an operator function. As regards the circuits in Figs. 1 and 2, its value can only be assumed constant with a large degree of approximation. It in fact varies with time since the transfer function of the amplifier $A2$ has a time dependence for any magnitude of rigid negative feedback. This can easily be seen by considering the transient processes there with the mutual inductance between the control windings taken into account.

1960

As regards the circuit in Fig. 3, we can always ensure a constant value of k_4 here by the due selection of the transfer functions for the circuits of windings IV and I, independently of the time at any degree of setting of the compensation for the voltage drop. This is very important for improving the dynamic characteristics of the control system of the mill.

Using the transfer function $N/W(p)$ from Fig. 4 we can produce an equation for the closed automatic control system for the excitation of the generators with choke stabilization:

$$(b_0p^5 + b_1p^4 + b_2p^3 + b_3p^2 + b_4p + b_5)U_4 = \\ = k_{11}k_2k_3(1 + Tp)(1 + T_{20}p)U_s. \qquad (6)$$

Coefficients b_0 to b_5 are functions of the parameters given in Fig. 4.

The calculations have shown that for all variants of choke stabilization used in adjustment, the characteristic equation for the excitation system of the PBK215-135 type generator (4250 kW, 750 V, 500 rev/min) has two pairs of complex roots and one real root. Similar results were also obtained for the stabilization of the excitation system of generators from a dynamic bridge, the characteristic equation of which has only two pairs of complex roots for all the variants of stabilization tested during repairs.

The solution of equation 6 for the case of a shock disturbance U_s can in its general form be written as follows for the stated roots.

$$U_4 = [A_0 + A_1 e^{-\sigma_0 t} + A_{23} e^{-\sigma_{23} t} \sin(\omega_1 t + \varphi_1 - \psi_1) + A_{45} e^{-\sigma_{45} t} \sin(\omega_2 t + \varphi_2 - \psi_2)] a U_s, \quad (7)$$

where $a = \frac{k_{11} k_2 k_3}{b_0}$; coefficients A_0, A_1, A_{23}, A_{45} and angles φ_1, ψ_1, φ_2, and ψ_2 are functions of the roots of the characteristic equation and constants T and T_{20}.

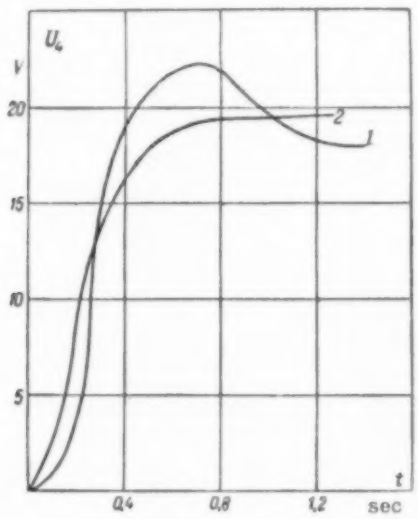

Fig. 5. Theoretical (1) and experimental (2) curves for the transient processes in the generator voltage with choke stabilization.

Fig. 5 shows the experimental (*1*) and theoretical (2) curves for the variation in U_4 at a shock U_s = 20 V. Similar curves are given in Fig. 6 in reference to stabilization from a dynamic bridge. The experimental curves were obtained when the effect of the stabilizing transformer was more marked ($T_1 \approx 0.15$ sec and $T \approx 0.48$ sec) than the theoretical ($T_1 = 0.12$ sec and $T \approx 0.4$ sec).

These theoretical and experimental data confirm the efficiency of the new means of stabilization in systems of excitation for generators used on continuous cold rolling mills which are characterized by a high amplification factor.

Theoretical and experimental investigations into the transient processes in the drive for stands during adjustment have shown that the successful operation of a modern continuous cold rolling mill is mainly

determined by the quality of the control system for the excitation of the generators. The changeover from the dynamoelectric amplifier system of compensation I_r to the system of two-cascade dynamoelectric amplifier connexion has made it possible to increase the amplification factor of the system from 150-200 to 275 and over. By using ionic excitation of the generators or large high frequency magnetic amplifiers there is greater scope for improving the excitation control system of generators and, consequently, for improving the performance of continuous cold rolling mills.

It should be mentioned that the investigation into the transient processes in a separate stand isolated from the whole mill made it possible to evaluate the existing systems of mill control, note further ways of improving them, determine the effect of the parameters of the generators and drive motors on the performance of the control system and formulate the conditions which must be satisfied.

The automatic regulation of the tautness at the reeler end plays a big part in the drive of a modern continuous cold rolling mill. Besides systems with two cascade connexion of the dynamoelectric amplifiers, use is now being made of systems with the diameter of the coil (bundle) "memorized" on the drum of the reeler. A special feature here is the regulation of the current in the armature circuit of the reeler motor by acting on the voltage of the generator and the regulation of the e.m.f. of the motor by acting on its flow. This system, based on a combination of magnetic and dynamoelectric amplifiers, has been developed in TsKB "Elektropivod" VNIIEM in reference to the five-stand mill at the Magnitogorsk integrated iron and steel works.

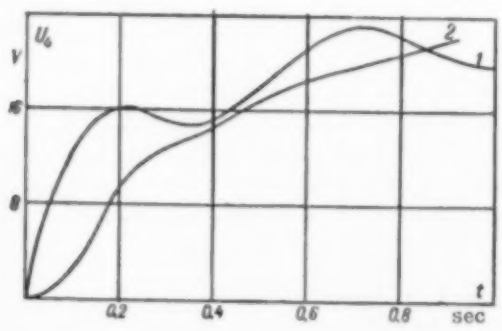

Fig. 6. Theoretical (1) and experimental (2) curves for the transient processes in the generator voltage stabilization from a dynamic bridge.

Good results were produced on the five-stand mill at the Lenin combine

in Poland and on reelers with a two-cascade system of connecting the dynamoelectric amplifiers. This was achieved by selecting the parameters more carefully and applying compensation to the dynamic component of the armature current as regards the current (flow) and voltage of the motor.

Continuous two-stand dressing mills for cold rolling occupy a special position. Such mills are now in operation at the Magnitogorsk integrated iron and steel works and at the Lenin combine in Poland. The rolling speed of the mill is 25 m/sec. The main drive is effected by 17 d.c. motors of special construction. A special feature is the minimum ratio of the external diameter to the diameter of the armature and the ratio of the nominal torque to the fly-wheel torque, (equal to 3.5). In reference to the stands and reeling device, the motors are mechanically connected two on each shaft.

The mill is controlled by seven independent systems of automatic tautness control. Four of these systems act as a function of the armature current at a constant torque and one system is a direct function of the tautness at a constant torque.

The introduction of tautness regulators between the stands (acting as a direct function of the tension of the induction head) was a great success during the process of adjusting the drives of these mills.

Translated by O.M. Blunn

AN AUTOMATIC MOTOR DRIVE FOR GRINDING MACHINES WITH FOLLOW-UP FEED*

A.A. SIROTIN and V.A. ELISEEV

(Moscow Power Institute)

(Received 21 December 1959)

1960

To increase the output of grinding machines and improve the surface finish, the drive should ensure the following cycle of movements by the working parts of the machine: feed of the grinding wheel to the component at a speed of 15 to 20 mm/min, rough grinding with the grinding wheel operating at the maximum permissible feed, grinding at a feed of 0.2 to 0.3 mm/min and rapid removal of the wheel after performing the grinding operation.

Modern machines are provided with an asynchronous drive for the grinding wheel. The wear of the wheel with such a drive brings about a reduction in cutting speed and a considerable deterioration in surface finish. Machines have an imperfect system of transverse feed; they cannot therefore ensure the necessary output or the optimum variation in machining speed, and there is a danger of spoiled components.

The Kuibishev Industrial Institute and Moscow Power Institute have developed electric drives for "follow-up feeds", which increase labour productivity and produce a better quality surface finish. The complicated and expensive feed system effected at the Kuibishev ball bearing works [1] takes no account of the deterioration in the cutting properties of the grinding wheels during the grinding process and provides no control over grinding power.

The laboratory of the faculty of "Electrical equipment for industrial undertakings" at the Moscow Power Institute has after many years research developed a follow-up electric drive for the transverse feed of

* *Elektrichestvo*, No.7, 15-19, 1960.

grinding machines [2, 3]. This drive has been introduced on 72 ball-grinding machines at the First state ball bearing works. The workers there have designed and organized the production of follow-up drives from standard units and components. It is planned to convert all machines in this class to follow-up feed. Follow-up feed will also be used on 3250B and other types of internal grinders.

Thanks to the use of follow-up feed there has been a 20 per cent increase in output from the machines, the number of rejects has been reduced and the operating conditions of the workers have been improved. In all, a considerable saving has been made.

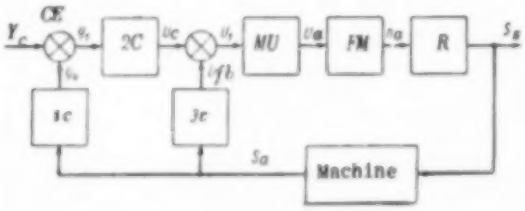

Fig. 1. Electric drive for follow-up feed.

Fig. 1 illustrates the drive for the follow-up feed, (a two circuit relay system). The system is fed with a rough blank having an initial machining allowance (y_c). The allowance to be removed from the workpiece (y_w) is calculated in the *CE*. The remaining allowance of the workpiece (y_1) is converted by the converter *2C* into an electrical signal U_c. The difference between this signal and the feedback signal (proportional to grinding power and obtainable at the output of the converter *3C*), is fed to the input to the measuring unit *MU*. When $U_c - U_{f.b} = U_s$ the measuring unit switches on the feed motor *FM* which effects the transverse feed of the saddle of the grinding machine head via reduction gear *R*. When the grinding power has increased to the desired value ($U_c - U_{f.b} \leqslant U_o$), the measuring unit switches off the feed motor (U_c and $U_{f.b}$ are given during adjustment).

The desired technological grinding characteristics $P_g = f(y_w)$ is ensured by means of two rigid negative feedbacks depending on the machining allowance of the workpiece and the output of the motor for the grinding wheel. During rough grinding the input signal (U_c) is constant and, consequently, grinding power (P_g) is roughly constant. After removing the rough machining allowance from the workpiece, the converter unit reduces U_c, which produces a reduction in grinding power and a changeover to finish grinding. After machining has been completed the measuring unit supplies a signal for the rapid removal of a

grinding wheel from the workpiece.

In the system under consideration grinding power is determined from the power consumed by the grinding wheel motor, which exceeds the grinding power by the value of the losses in the motor, spindel and transmission. It has been established by the investigations that the system, involuntarily maintaining the desired average speed of the grinding wheel motor, also maintains the average value of the effective feed. When the grinding wheel is soiled, the effective feed is automatically reduced and the workpiece protected from damage.

Tests on the follow-up feed have shown that it ensures the prescribed technological grinding cycle. Fig. 2 diagramatically represents the power consumed by the grinding wheel motor. It was recorded by an oscillograph during the grinding process. Curves are also shown for the actual feed S_a and the feed of the saddle S_s.

The electrical circuit of the follow-up drive is shown in Fig. 3.

Use is made of a MUN-1 type general-purpose 100 W motor for the feed. This is used as a motor for independent excitation. The feed motor is switched on and off by the feed relay *IFR*.

Use is made of small scale MKU-48 type relays for the power relays. PKN type telephone relays act as the blocking and time relays. All the rectifier devices are made from germanium diodes. The electrical equipment for the drive of the follow-up feed is mounted in the form of a small detachable block.

It is a complicated matter to calculate the dynamic conditions of grinding machine drives with follow-up feed owing to the presence of elastic deformations and the non-linearity of the individual parts.

It is however necessary to take the elastic deformation of the machine and the wear of the grinding wheel into account because these quantities are commensurate with the radial allowances of the workpiece to be removed and the movement of the saddle.

At any instant during the grinding process the following relationship exists between the movements of the individual devices:

$$y_s = y_w + y_e + y_{wg}, \tag{1}$$

where y_s is the transverse movement of the saddle of the grinding head;

y_w the allowance removed from the workpiece on the side;

y_e the value of the elastic deformation of the machine;

y_{wg} the wear of the grinding wheel on the side.

After differentiation with respect to time we obtain

$$S_s = S_a + S_e + S_{wg}, \tag{2}$$

where $S_s = \frac{dy_s}{dt}$ is the speed of the transverse movement of the saddle or the saddle feed;

$S_a = \frac{dy_w}{dt}$ the rate at which the allowance is removed or the actual feed;

$S_e = \frac{dy_e}{dt}$ the rate of the elastic deformations of the machine-tool-component system;

$S_{w.g} = \frac{dy_{w.g}}{dt}$ the rate at which the grinding wheel wears out.

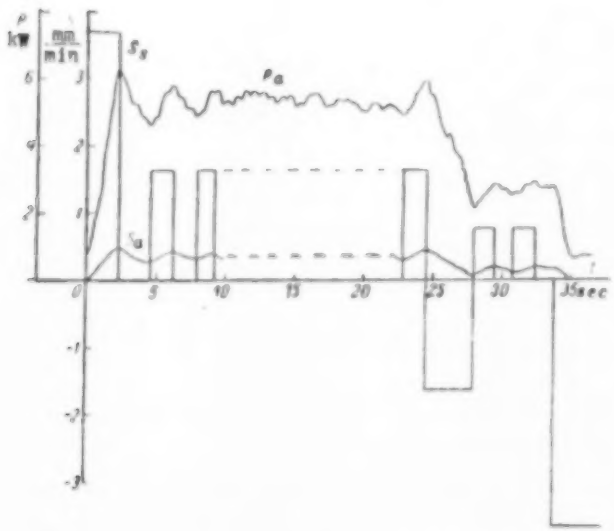

Fig. 2. Variations in the power of the grinding wheel, motor, actual feed and the feed of the saddle during the grinding process.

In Fig. 1 we can represent the machine-tool-component system by a link conventionally called "machine". In the equation for this link (2) the rate of resilient deformations and wear of the grinding wheel depend on the grinding conditions and are functions of the actual feed $S_s = f_1(S_a)$; $S_{wg} = f_2(S_a)$. In order therefore to solve equation 2 we must determine the stated dependencies. As no reliable information has as yet been published on this question, we produced an experimental

rig for measuring and recording the elastic deformations in the process of grinding on a 3250B type internal grinder. The elastic deformations of the forces and moments arising during the grinding process were recorded by means of wire "gauge-transmitters" attached to the shaft of the grinding spindle [3].

The rate of wear of the grinding wheel was defined as the difference:

$$S_{wg} = S_s - (S_a + S_e).$$

The feed of the saddle and the actual feed were determined by differentiation of the curves $y_s = f(t)$ and $y_w = f(t)$. These were taken by a photoelectric indicator and photoelectric gauge whilst grinding.

As a result of the experiments we obtained the relationships $y_e = f_1(S_a)$ and $S_{wg} = f_2(S_a)$, the analytical expression of which has the form:

$$y_e = cS_a^n;$$

$$S_e = cnS_a^{n-1}\frac{dS_a}{dt};$$

$$S_{w.g} = bS_a^m,$$

where $C = 0.157$, $n = 0.75$, $b = 0.414$ and $m = 2.14$.

Substituting these relationships into equation 2, we obtain

$$S_s = S_a + bS_a^m + cnS_a^{n-1}\frac{dS_a}{dt}. \qquad (3)$$

Thus the transient process in the "machine" link can be described by a non-linear differential equation.

As the experiments showed, in the first approximation the non-linear dependencies $y_e = f_1(S_a)$ and $S_{wg} = f_2(S_a)$ can be replaced by linear dependencies with a small degree of error.

Then

$$y_e = \alpha S_a;$$

$$S_e = \alpha\frac{dS_a}{dt}. \qquad (4)$$

$$S_{w.g} = \beta S_a \qquad (5)$$

and the linear equation of the machine corresponds to the equation for

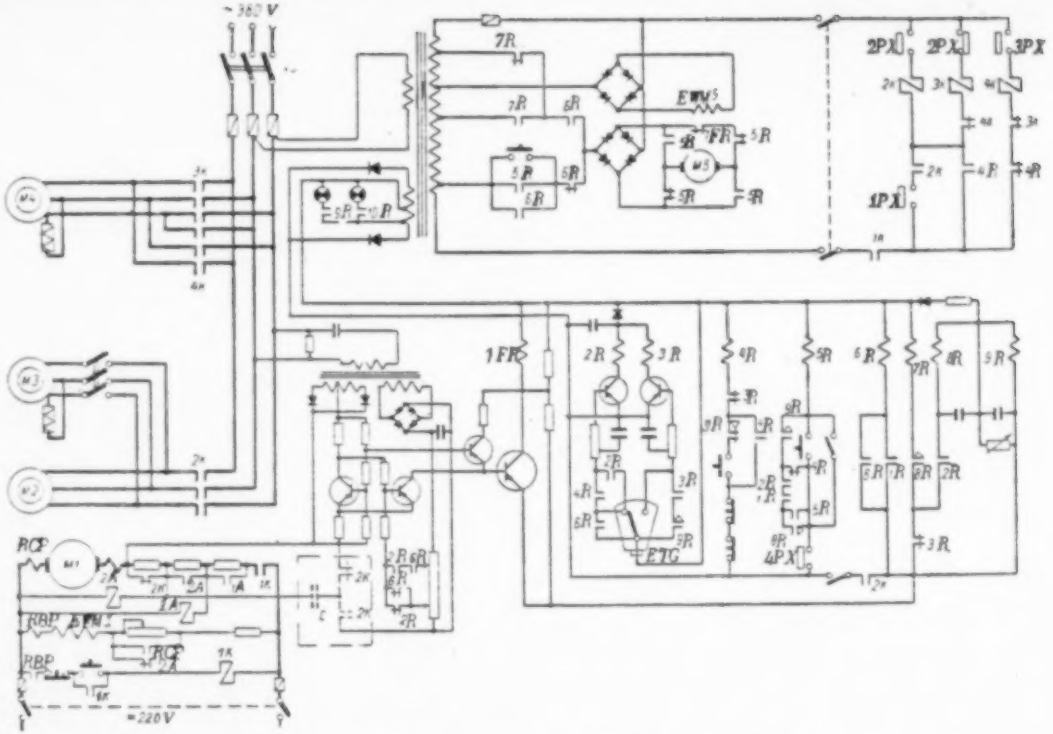

Fig. 3. Main electrical circuit for the control of an L3 type ballgrinding machine;
M1 to *M5* – electrical motors for revolving the grinding wheel, revolving and swinging the workpiece and longtitudinal and transverse feed; *1K* to *4K*-contactors for electrical motors *M1* to *M4*; *1A*, *2A* – acceleration contactors; *RCP* and *RBP* – control relay and break realy for the field of the motor *M1*; *1PX* to *4PX* – path switches; *1FR* – relay maintaining the desired grinding power; *2R* and *3R*, relays for the end of the rough and finishing periods of the cycle; *4R* – intermediate relay; *5R* – relay for rapid removal of the grinding wheel; *6R* and *7R*, relays ensuring different feeds for rough grinding and finishing; *8R* and *9R* – time relays controlling the removal of the elastic deformations of the machine after rough grinding and the time taken for the rapid withdrawal of the saddle; *ETG* – electro-contact "transmitter-gauge" for measuring the workpiece.

an ordinary aperiodic link

$$k_m S_z = S_a + T_m \frac{dS_a}{dt}, \qquad (6)$$

where $k_c = \frac{1}{1+\beta}$ is the amplification factor of the "machine" link;

$T_c = \frac{\alpha}{1+\beta}$ its time constant.

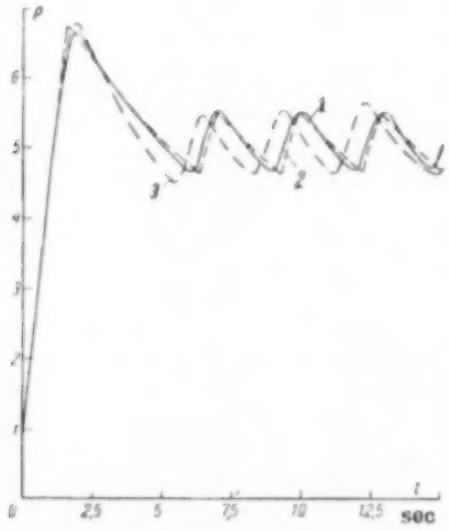

Fig. 4. Theoretical and experimental curves $P_m = f(t)$ in the grinding process: 1 – calculated by displacement theorem; 2 – calculated by the method of phase families; 3 – experiment.

The physical time constant of the "machine" link is the time taken for the elastic deformation of machine to reach its steady value during the grinding process under the effect of continuous saddle feed in the absence of wear to the grinding wheel. The time constant can be obtained by integrating the link equation within the limits from $t = 0$ to $t = 4T_m$, ignoring the wear of the grinding wheel.

The amplification factor of the link takes into account the decrease in the steady value of the actual feed as a result of the wear of the grinding wheel.

The time constant T_m depends on the rigidity of the machine-tool-

component system and the wear of the grinding wheel. In the case of a 3250B type internal grinder, $T_m \approx 10$ sec, but in the case of an L38 type ball-grinding machine, $T_m \approx 3$ sec. If rigidity is reduced owing to the wear of the components of the machine, T_m increases four times over at a maximum, but if soft grinding wheels are used, it is reduced two times over.

The set of differential equations for the drive under consideration has the following form:

$$
\begin{aligned}
&U_3 - U_{Fb}(S_a) = U_1;\\
&k_a U_1 = i_c + T_a \frac{di_c}{dt};\\
&U_{out} = f(i_a);\\
&k_{Pv} U_{out} - k_{Pm} M_s = n + T_c \frac{dn}{dt};\\
&k_r n = S_s;\\
&k_m S_s = S_a + T_m \frac{dS_a}{dt};\\
&U_{Fb} = -U_0 + k_c S_a,
\end{aligned}
\tag{7}
$$

where k_a, k_r, k_m, k_c, k_{fv} and k_{fm} are the amplification factors of the amplifier of the measuring unit, reduction gear, machine, converter 3C and the feed motor (as regards voltage and moment);

T_a, T_f and T_m the time constants of the amplifier of the measuring unit, feed motor and "machine" link;

M_s the static moment on the shaft of the feed motor;

i_c the control current of the measuring unit.

In the feed system of a 3250B type internal grinder

$k_a = 0.8$ mA/V; $k_r = 2.17 \times 10^{-3}$ mm/rev;
$k_m = 0.91$; $k_c = 40$ V x min/mm;
$k_{PV} = 15.4$ rev/V x min; $k_{Pm} = 4880$ rev/min x kg m;
T_a=0.6 sec; T_f=0.02 sec and T_m=11.5 sec.

The dependence U_{fb} (S_a) was obtained from the characteristics of the feedback unit $U_{fb} = f(P_a)$ and the experimental relationship $P_a = f(S_a)$.

The transient process in the system was calculated by a method based on the displacement theorem in operational calculus, it here being supposed that all the links of the system are linear except the relay measuring unit. Use was also made of the method of phase families [4].

As follows from Fig.4 which shows the theoretical and experimental relationships $P_a = f(t)$, good agreement has been obtained between the theoretical and experimental curves. The largest divergence in the curves (10 per cent) obtains at the commencement of the grinding process.

Using this method we can calculate the curves for actual feed and the feed of the saddle, the amount of elastic deformation and the wear of the grinding wheel, the grinding power and that consumed by the grinding wheel motor on various types of grinding machine.

A number of improvements have been made to the system of follow-up drive. A unit has been introduced which enables the value of the actual grinding power to be held constant. The no load losses of the grinding wheel motor can be measured before each cycle and increased by the loss of power by the motor, leaving the grinding power approximately constant. For this purpose a memory capacitor C is provided in the circuit (Fig.3).

The BV-220 type electro-contact "transmitter-gauge' ' for measuring the workpiece works sufficiently stably on machines during operation. This gauge needs to be specially adjusted (after machining 2 to 5 ball bearing races) owing to the wear of the claw which comes into contact with the machining surface. The operator must also check the dimensions of each product by the inspection gauges. In this connexion work is proceeding on the development of a contactless measuring "transmitter-gauge".

The operation of the system shown in Fig.3 is accompanied by a considerable number of contact operations during a cycle and a system using semiconductor contactless switching devices has been designed and installed.

A new electric drive has been developed and produced for the grinding wheel. This maintains grinding speed constant by changing the angular speed of the grinding wheel. To drive the wheel use is made of a d.c. motor with continuously variable speed regulation above basic speed (Fig.3). The field of the motor is weakened by a special circuit rheostat or switch to the extent that the diameter of the grinding wheel is reduced.

The results of tests on this drive were good. It was established that the process of grinding with constant cutting speed proceeded more stably than when grinding with a variable grinding speed. A further increase in productivity was therefore possible.

The amount of metal removed per unit volume of the worked part of the grinding wheel (specific productivity) when grinding at a constant cutting speed was 30 to 40 per cent higher than that when grinding with a variable cutting speed. The durability of the grinding wheels when grinding at a constant cutting speed was 30 per cent higher than when grinding with a variable cutting speed.

A disadvantage of the d.c. motor drive is the need of a greatly stabilized supply source.

Conclusions

1. To increase grinding productivity and improve the surface finish of the workpiece, it is expedient to use a variable drive for the grinding wheel jointly with the follow-up drive for the transverse relay-operated feed.

2. The use of follow-up feeds makes it possible to automate ball-grinding, internal grinding and other types of grinding machine completely and simplify their kinematics.

3. When developing electric drives it is advisable to take the elastic deformations and wear of the grinding wheel into account by representing the machine in the form of an aperiodic link in the system of regulation.

4. On the basis of the derived equations we can calculate the transient processes in these grinding machine drives by methods of solving non-linear problems.

Translated by O.M. Blunn

REFERENCES

1. E.S. Zheleznov; *Electrical follow-up feed for grinding channels in ball bearing races, (Elektricheskaia sledíashchaia podacha dlia shlifovaniia zhelobov kolets podshipnikov)*, Diss. MEI, (1957).
2. A.A. Sirotin, V.A. Eliseev and S.I. Popov; *New electric drive for internal grinders, (Novyi elektroprivod vnutrishlifoval'nykh stanov)*. Trud. MEI, No.30, (1958).
3. V.A. Eliseev; *Follow-up feed for internal grinding machines taking into account the rigidity of the machine and the wear of the grinding wheel,*

(Slediashchaia podacha vnutrishlifoval'noto stanka, uchityvaiushchaia zhestkost' stanka i iznos shlifoval'nogo kruga). Diss. MEI, (1959).

4. A.A. Sirotin; *Automatic control of electric drives, (Avtomaticheskoe upravlenie elektroprivodami).* Gosenergoizdat, (1959).

1960

AN ELECTRONIC COMPUTER STUDY OF AN AUTOMATIC HELMSMAN*

I.R. FREIDZON

(Lenin Electrical Engineering Institute, Leningrad)

(Received 21 January 1960)

One method of developing and investigating automatically controlled steering is to use modelling by means of analogue computers. Here in the first stage of development it is expedient to confine oneself solely to mathematical modelling, i.e. the solution of the mathematical relationships determining the behaviour of the system. The elements of the mathematical model can be replaced by their originals later. Using an electrical model simulating the hydrodynamic link we can adjust real steering systems under laboratory conditions.

To hold the ship on its course it is necessary to turn the rudder periodically to this or that angle. Each turn of the rudder slows the ship down soemwhat and not only compels the ship to return to the desired course but also to deviate the other way.

The following functions must be performed if the ship is to be held on course with sufficient accuracy by the automatic control:

(a) When the ship deviates from the desired course, the system should immediately turn the rudder through a sufficient angle for the ship to begin to return to the desired course. This initial (primary) angle of turn of the rudder depends on the type and conditions of sailing.

(b) As the ship only "obeys" the rudder, the system should begin to turn the rudder and return it to the "forward" position before the ship comes back on course.

(c) When the ship is back on course, the system should ensure that the

---

* *Elektrichestvo*, 7, 20-25, 1960.

rudder is turned a little to the side opposite to the original turn.

(d) It should be possible to widen the zone of insensitivity to the "roaming" of the ship on course as a function of sailing conditions at sea. In good weather the system should react to small angles of deviation of the ship from the set course; in choppy weather the ship should be allowed a certain freedom to roam on course, i.e. the angle of deviation at which the automatic helm will begin to turn the rudder should be increased.

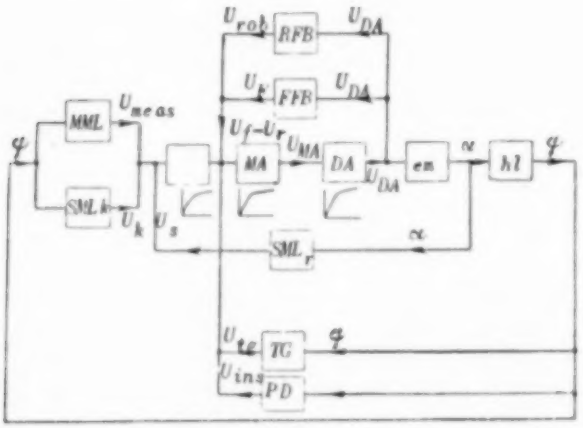

Fig. 1. Block diagram of ship's automatic control system.

In the following the results are given of an investigation into an automatic helm which has already been produced.*

Fig. 1 shows the block diagram for the automatic control of the ship, consisting of a hydrodynamic link *HL* (body of the ship, rudder, mass of the water) and an automatic steering system.

The automatic steering system incorporates an "executive" motor and reduction gear *EM* and a dynamoelectric amplifier *DA*, which is the main power amplifier. The control windings of this amplifier are fed from a magnetic amplifier *MA*, which is the first stage of amplification for the control signal. Diodes are installed at the input to the *MA* to limit the magnitude of the control current (Input to *MA*).

* The automatic steering system was proposed by A.P. Sheffer and G.I. Parfenov. A.V. Mozgalevskii, V.F. Brenev, Iu.A. Lukomskii and V.M. Aleksandrov took part in the experimental investigations.

1960

The measuring unit of the automatic helm circuit is a selsyn-measuring link *(SMLk)*, consisting of a number of linear rotating transformers, a selsyn "transmitter-gauge" and a selsyn-receiver gyrocompas.

The master element in the follow-up rudder control system is like that in the system for automatically controlling the course of the ship, i.e. a control wheel with a master measuring link *MML* connected to it. In the first case the wheel is used for the follow-up control of the rudder, whilst in the other case, changes in the desired course are controlled by the introduction of degree corrections.

Along with the basic feedback (from the object under control) which supplies a signal to the input to the automatic helm proportional to angle of the course ψ, the system also incorporates parallel correcting devices and additional feedbacks.

One of the main parallel correcting devices is that for automatically correcting the desired course under the influence of prolonged external forces *PD* creating a moment around the vertical axis of the ship. A signal is formed at the output of this device proportional to the integral from the angle of the course $\int \psi \, dt$, the introduction of which makes it possible to reduce the static error of the system considerably.

The presence of a tachometer generator *TG* made it possible to introduce the derivative of the deviation $\frac{d\psi}{dt}$ and thereby "suppress" the oscillations which can arise due to the variability of the object and the imperfection of automatic helm itself. The introduction of the derivative into the law governing the regulation to a certain extent compensates the imperfection (non-ideal state) of the automatic helm and makes it possible to force the speed at which the rudder is turned. The automatic helm is also covered by a rigid feedback for the position of the rudder (provided by the selsyn-measuring link of the rudder *SMLr*), which makes it possible to bring about the follow-up state of rudder control. The coefficient of this coupling K_r determines the sensitivity coefficient of the automatic helm.

The automatic helm system comparises two additional negative feedbacks as regards the output voltage of the dynamoelectric amplifier. One is rigid *(RFB)* and produces a signal U_r, whilst the other is flexible *(FFB)* with a signal U_f. The rigid negative feedback is permanently effective and makes it possible to reduce the time constant of the "covered" link, whereas the flexible feedback is only effective in transient conditions, serving to stabilize the system.

It is quite a complicated matter to investigate and perform the necessary calculations for a multi-circuit system in a follow-up drive.

The use of mathematical modelling is therefore most effective.

The following initial equations have been adopted:

$$U_{\psi}(p) = K_{\psi} \cdot \psi(p); \tag{1}$$

$$U_{ma}(p) = K_{ma}(U_k - U_s - U - U_p + U_{int} - U_f \pm U_{tg}); \tag{2}$$

$$(1 + T_{\Sigma a}p)(1 + T_{sk}p) \cdot U_{da}(p) = K_{da} \cdot U_{ma}(p); \tag{3}$$

$$(1 + T_r p) \cdot U_r(p) = K_r \cdot U_{da}(p); \tag{4}$$

$$(1 + T_{em}p)p \cdot \alpha(p) + \frac{57{,}3 r_{\Sigma}}{c_i c_{\omega} i} M_s = \frac{K_m}{i} 57{,}3 U_{da}(p); \tag{5}$$

$$U_f(p) = T_f p \cdot U_{da}(p); \tag{6}$$

$$pU_{int}(p) = K_{int}(\varphi_k - \psi); \tag{7}$$

$$U_{tg}(p) = K_{tg} p\psi; \tag{8}$$

$$U_s(p) = K_s \times \alpha(p); \tag{9}$$

$$p\beta + g_{21}\beta + h_1\beta^2 + r_{21}p\psi + \rho_{21}\alpha = 0; \tag{10}$$

$$p^2\psi + g_{21}\beta + r_{21}p\psi + \rho_{21}\alpha = 0. \tag{11}$$

where U_{ψ}, U_{ma}, U_{da}, U_r, U_f, U_s, U_{int}, U_{tg} and U_k are the output voltages, respectively, of the selsyn-measuring device of the course, magnetic amplifier, dynamoelectric amplifier, rigid feedback, flexible feedback, selsyn-measuring device for the rudder (steering), integrating link, tachometer generator and the master measuring link, proportional to the angle through which the control wheel is turned ϕ_k;

K_{ψ}, K_{ma}, K_{da}, K_r, K_k, K_f, K_s and K_{int} are the coefficients of amplification of the appropriate links;

$T_{\Sigma a}$, $T_{s/c}$, T_{em}, T_f and T_r the time constants of the control windings of the dynamoelectric amplifiers, the electromechanical constant of the executive motor, and of the rigid and flexible feedback circuits;

$c_{\omega} = \frac{(U - r_{\Sigma} I) 30}{\pi n_{nom}}$ and $c_i = 0.102 c_{\omega}$ are coefficients of propor-

1960

tionality calculated from the catalogue (rated) data of the executive motor;

r_{Σ} is the total resistance of the armature circuit of the executive motor;

i is the transmission ratio of the reduction gear from the executive motor to the rudder head;

M_s the moment of resistance on the rudder head, a function of the angle through which the rudder fin is turned;

α the angle of turn of the rudder;

ϕ_k the angle of deviation of the selsyn-measuring device for the course of the ship;

ψ and β angles of the course and drift of the ship;

ε_{21}, r_{21}, ρ_{21}, h_1, ε_{31}, r_{31}, ρ_{31}, coefficients depending on the course of the ship.

These equations describe the behaviour of all the automatic control system of the ship, including the hydrodynamic link and the automatic helm.

Equations 10 and 11 for the hydrodynamic link are adopted in accordance with the equations proposed by L.P. Kuz'minyi, R.Ia. Pershits and E.B. Iudin.

Before turning to the block diagram of the modelling system it is necessary to convert the equations into a suitable form for modelling.

Since the real variables on an analogue computer (speed of rotation, currents etc) are reproduced in the form of voltages, the variations of which with time are governed by a similar law, to convert the quantities into machine units it is necessary to introduce the scale coefficients which take into account the variations in the dimensions of the variable systems. The scale coefficients show how many machine units are necessary per unit of real quantity, i.e.

$$\gamma_{xi} = \frac{X_{i(m)}}{x_i},$$

where $X_{i(m)}$ are the values of the variable quantities in machine units;

x_i the values of the variable quantities in real units.

A "reference" voltage of the model is used for one machine unit. A

new independent variable is also introduced $T_{(m)}$ (machine time):

$$\gamma_t = \frac{T_{(m)}}{t}$$

where γ_t is the scale coefficient of time which takes into account the relationship between the time taken for the processes to take place in nature and the machine. Then

$$\frac{d}{dt} = \gamma_t \frac{d}{dT_{(m)}}$$

or in operator form

$$p = \gamma_t P_{(m)}.$$

Besides introducing the scale coefficients, it is necessary to convert the equations to the form:

$$\frac{dX_{i(m)}}{dT_{(m)}} = F(X_{1(m)}, X_{2(m)}, \ldots, X_{n(m)}t).$$

Thus, the transformed equations in suitable form for modelling will be:

$$u_\varphi(p) = \frac{\gamma_{up}}{\gamma_\varphi} K_\varphi \cdot \varphi(p); \tag{12}$$

$$u_{ma}(p) = \gamma_{ma} k_{ma}\left[\frac{u_k(p)}{\gamma_{u_g}} - \frac{u_g(p)}{\gamma_{u_g}} - \frac{u_\varphi(p)}{\gamma_\varphi} - \right.$$
$$\left. - \frac{u_r(p)}{\gamma_r} + \frac{u_{int}(p)}{\gamma_{int}} - \frac{u_f(p)}{\gamma_f} + \frac{u_{tg}(p)}{\gamma_{tg}}\right]; \tag{13}$$

$$p^q u_{da}(p) = \frac{K_{da}\gamma_{da}}{T_{s/c}T_{\Sigma a}\gamma_t^2\gamma_{ma}} u_{ma}(p) -$$
$$- \frac{T_{s/c} + T_{\Sigma a}}{T_{s/c}T_{\Sigma a}\gamma_t} p u_{da}(p) - \frac{1}{T_{\Sigma a}T_{s/c}\gamma_t^2} u_{da}(p); \tag{14}$$

$$p^2\alpha(p) = \frac{57{,}3 \cdot K\gamma_\alpha}{T_{en}^2\gamma_t^2\gamma_{da}} u_{da}(p) -$$
$$- \frac{57{,}3 r_\Sigma \gamma_\alpha \frac{1}{\gamma_t c}}{\gamma_t^2 c_\omega c_i T_{en}^2} M_s(p) - \frac{1}{\gamma_\omega T_{en}\gamma_t} p\omega(p); \tag{15}$$

1960

$$pu_f(p) = \frac{\gamma_f K_f}{T_f \gamma_{da} \gamma_t} u_{da}(p) - \frac{1}{\gamma_t T_f} u_f(p); \tag{16}$$

$$u_r(p) = \frac{\gamma_r T_r}{\gamma_{da} \gamma_t} pu_{da}(p); \tag{17}$$

$$u_s(p) = \frac{\gamma_{us} K_s}{\gamma_a} \alpha(p); \tag{18}$$

$$pu_{int}(p) = \frac{\gamma_{int} K_{int}}{\gamma_t} \left[\frac{\varphi_k(p)}{\gamma_{\varphi k}} - \frac{\psi(p)}{\gamma_\psi} \right]; \tag{19}$$

$$p \cdot \beta(p) = a_1 \cdot \beta(p) + a_2 \cdot \beta^2(p) + a_3 p \cdot \psi(p) + \\ + a_4 \cdot \alpha(p); \tag{20}$$

$$p^2 \cdot \psi(p) = b_1 \cdot \beta(p) + b_2 p \cdot \psi(p) + b_3 \cdot \alpha(p) \tag{21}$$

A block diagram has been prepared corresponding to these equations, modelling the system (Fig. 2) realized by means of the resolving units of a MN-7 type non-linear electronic model.

The input to the system is the voltage modelling the angle of turn of the control wheel (ϕ_k), whilst the output is the voltage on the amplifier which varies analogously to the variation in the course of the ship (ψ).

The real automatic helm apparatus has made it possible to check how correct the modelling of the system is and establish to what extent the linearization is permissible used in formulating the equations for the automatic helm. For this purpose an investigation was made into the process of turning the fin of the rudder on real apparatus and the model with two values of the master signal.

Fig. 3 shows curves for the variation in the speed of rotation of the drive motor n and the angle of turn of the rudder α, obtained experimentally. With a small input signal the transient processes reproduced on the model (curves 1 and 2) agree quite well with those taking place in the automatic helm (curves 3 and 4), whereas at a large input signal the modelled transient process (curves 5 and 6) is considerably different

from the real thing (curves 7 and 8). At large input signals there is quite satisfactory agreement between the transient processes (the modelled process and that actually taking place in the automatic helm) if account is taken of the non-linearity of the parameters of the system (respectively curves 1, 2 and 3, 4 in Fig. 4).

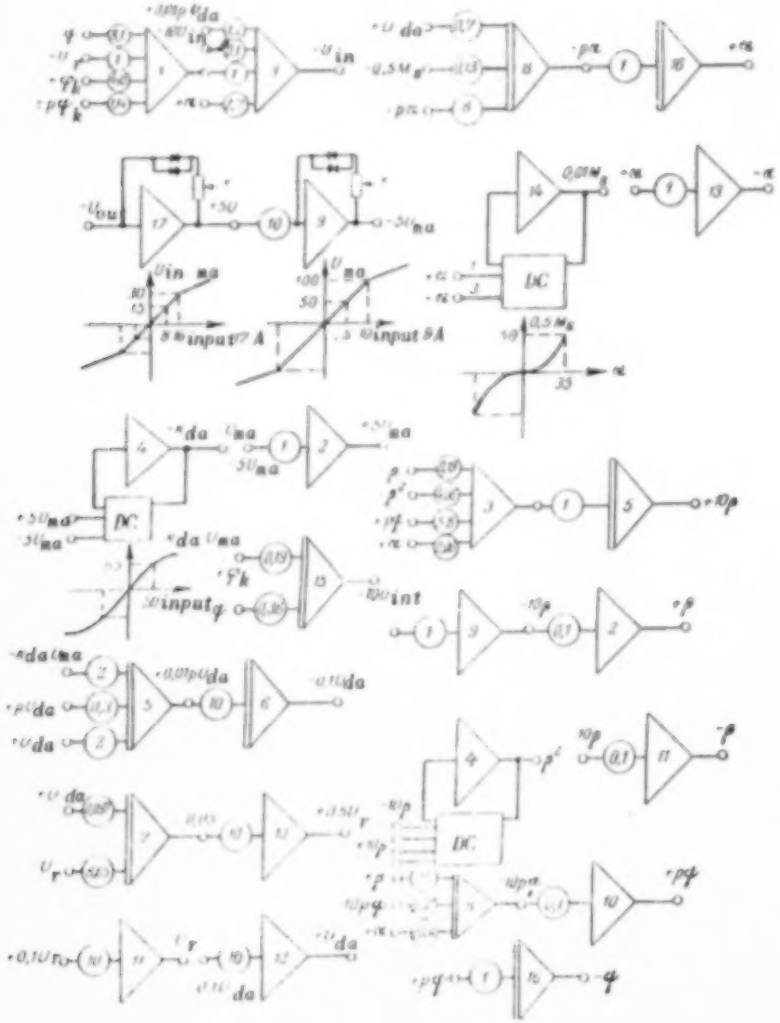

Fig. 2. Block diagram of modelling system.

The greatest effect is had by the non-linearity of the coefficients of amplification *MA* and *DA*, and also the diode limitation at the input

The greatest effect is had by the non-linearity of the coefficients of amplification *MA* and *DA*, and also the diode limitation at the input to the *MA*. Therefore the product of the amplification factor times the input voltage for the corresponding links was adopted in accordance with the curves given in Fig.2. The stated non-linear relationships are realized by means of diode limitation in the feedback of the resolving units 9 and 17, whilst the relationships are realized by means of diode limitation in the feedback of the resolving units 9 and 17, whilst the relationship $K_{da}\ U_{ma} = f(U_{ma})$ is realized by means of a functional diode converter *DC*. Other non-linear relationships ($M_s = f(\alpha);\ \beta^2$) were likewise realized on the model.

The initial propositions of the model thus produce reliable results in practice and can be used as a basis for investigating the automatic helm under all conditions, if account is taken of the non-linear character of the variation in the parameters of the system.

The main problem in the investigation was the choice of the optimum parameters of the system, such as would ensure sufficient stability, and high quality system performance. There was also the problem of investigating the behaviour of the real apparatus jointly with the model.

The stability of the system was evaluated at the same time as the quality of the regulation was determined depending on the type of transient process.

In the first instance an investigation was made into the effect of the parameters which can vary in the finished system during the process of adjustment (e.g. the coefficient of rigid feedback, the sensitivity factor). An investigation was also made into those parameters which may vary during the development stage (amplification factor of the magnetic amplifier, feedback, transmission ratios, coefficient of the integrating link and so on).

The investigation into the effect of the rigid feedback on the operating speed of the automatic helm shows that there is an optimum value for the rigid feedback coefficient at which the transient process is of minimum duration (Fig.5).

The variation in the coefficient of sensitivity K_s notably affects the transient process. The increase in the coefficient of sensitivity within the limits of 0.67 to 1 and above leads to the rise of an oscillation process (Fig.6) and prolongation of the transient process (curves 1 to 3).

The variation in the coefficient of amplification of the system had very little effect on the form of the transient process and the magnitude of regulation (Fig.6, curves 4 to 6).

The character of the transient process had a considerable effect on the integrating link. The presence of an integrating link, due to the need to keep the ship on its course, as a rule leads to the rise of a process of oscillation, as can be seen from the curves in Fig. 7.

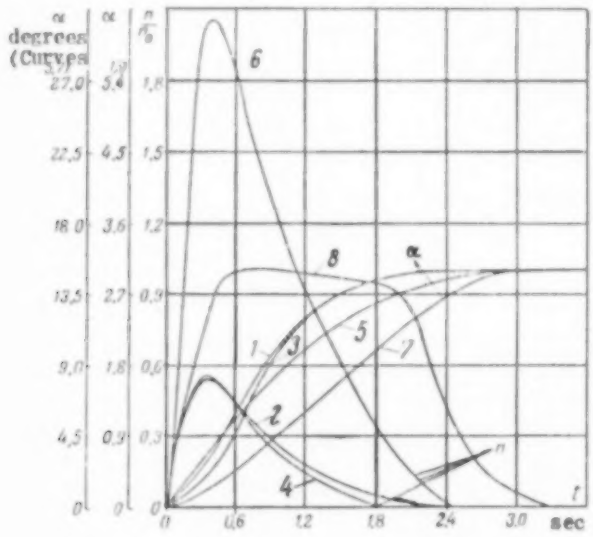

Fig. 3. Curves for the transient process: $\alpha = f(t)$ and $n = f(t)$ (linear state).

The increase in the coefficient of the integrating link, although leading to a certain increase in the "roaming" of the ship, yet sharply reduces the amplitude of the "roaming", and this can be expedient in a number of cases.

It is very important to take into account the effect of the angle of drift on the character of the transient process.

If it is assumed that the rise of the hydrodynamic forces is proportional solely to the angle of drift, the curves for the transient process then bear a pronounced swinging character (Fig. 7, curves 1 to 3).

If it is borne in mind when modelling, as is the case in real conditions, that the hydrodynamic force is proportional to the square of the angle of drift, the transient process will then bear a pronounced aperiodic character (Fig. 7, curves 3 to 5). This again confirms the need to take the non-linear character of the equations into account.

When considering the effect of the tachometer generator on the

operation of the system, it must be mentioned that it is not so much the magnitude of the tachometer generator signal which affects the stability of the system, as its sign (Fig. 8).

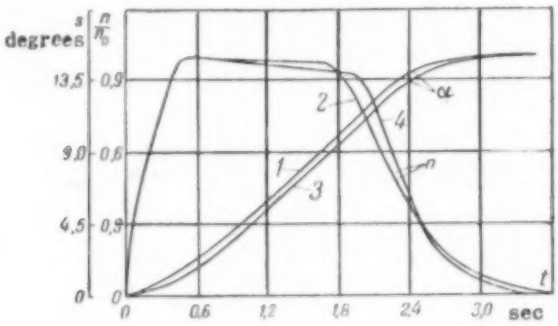

Fig. 4. Curves for the transient process $\alpha = f(t)$ and $n = f(t)$ (non-linear state)

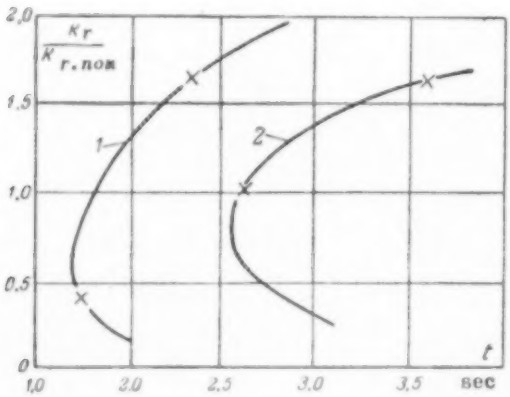

Fig. 5. Dependence of the time of the transient process in the system on the coefficient of rigid feedback:
1 – linear state; 2 – non-linear state. Coefficient of sensitivity 0.67.

Investigation of the real model of the automatic helm jointly with the model of the hydrodynamic link

The electronic mathematical model of the hydrodynamic link, as stated above, makes it possible to adjust the finished apparatus of the auto-

matic helm under automatic operating conditions before installation on board ship.

Since the output of the model of the hydrodynamic link receives a variable voltage governed by a similar law to that governing changes in the course of the ship ψ, whilst the input to the automatic helm system is the angle of turn of the selsyn-receiver, there is a need for a special device to match the output of the model and the input to the automatic helm. In our investigations we in fact used an electrodynamic block *EDB* for this purpose. It converted the voltage into the angle of turn of the selsyn-transmitter.

The angle through which the fin of the rudder turned was proportional to the voltage taken from the selsyn measuring device of the rudder. The rectified voltage of the selsyn measuring device of the rudder is fed to the input to the electronic model of the hydrodynamic link. The helm-hydrodynamic link system is thus closed.

Fig.9 shows curves for $\alpha = f(t)$ and $\psi = f(t)$ when a degree correction is made to the course in the automatic operating conditions of the helm.

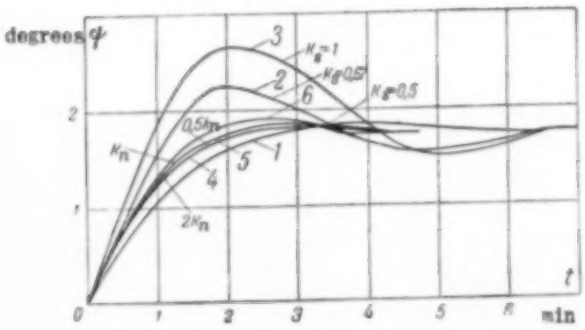

Fig. 6. Curves for the transient process $\psi = f(t)$ at different values of the coefficient of sensitivity K_s = (1-3) and amplification factor of the system K_n (4-6).

The curves for the transient process show that over-regulation occurs when the ship is returned onto its set course, depending on the sensitivity factor of the automatic helm. With a coefficient of sensitivity $K_s = 0.67$, the over-regulation is 125 per cent, but when $K_s = 0.5$, it is 100 per cent. But it takes longer for the ship to return to its set course if K_s is increased.

The use of mathematical modelling by means of analogue computers makes

it possible to investigate the automatic helm under follow-up and automatic operating conditions, the degree of accuracy here being quite adequate for practical purposes.

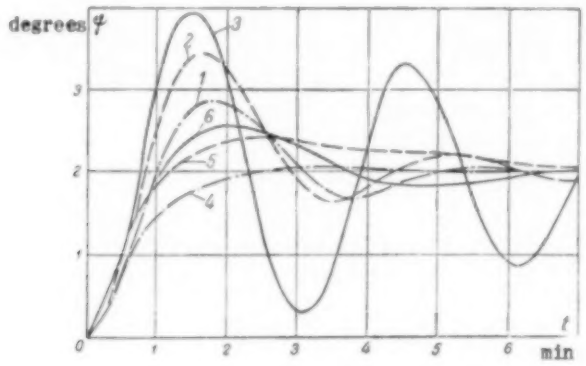

Fig. 7. Curves for the transient process at different values of the coefficient of the integrating device:
–.–.–.–. K_{int} 20 times less than K_{nom};
——— $K_{int} = K_{nom}$; – – – – K_{int} 5 times less than K_{nom}; 1 to 3 – β^2 not accounted for; 4 to 6 – β^2 taken into account.

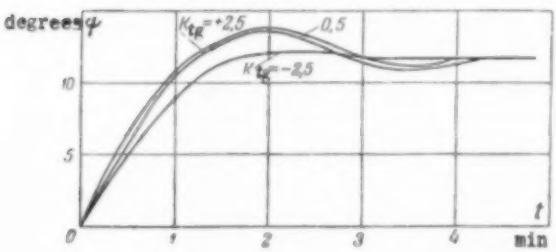

Fig. 8. Curves for the transient process $\psi = f(t)$ for different values of the coefficient of the tachometer generator K_{tg}.

When the deviations are small, the fin of the rudder of the automatic helm can be regarded as a linear system. Its behaviour is described by linear differential equations with constant coefficients. At considerable angles of deviation the fin of the rudder becomes an essentially non-linear system, and its linearization for the investigation leads to an inadmissibly large degree of error.

The appropriate choice of parameters for the automatic helm can ensure the stability of the system in the follow-up state, the return of the ship to its set course here taking the minimum amount of time.

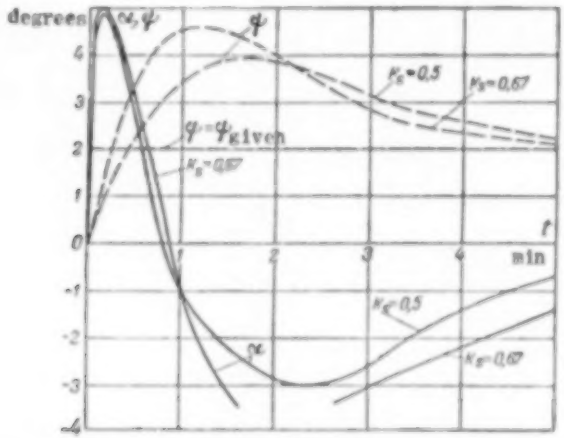

Fig. 9. Curves $\alpha = f(t)$ and $\psi = f(t)$ for combined operation of the real apparatus and the model of the hydrodynamic link.

Using the electrical model simulating the hydrodynamic link, it has proved possible to adjust real automatic helm systems under laboratory conditions. This saves a considerable amount of time on installation work on board ship. The use of mathematical modelling by analogue computers also makes it possible to determine the suitability of existing automatic helms for different types of ship.

Translated by O.M. Blunn

1960

THE 500 KV SUBSTATION AT SVERDLOVSK*

L.D. GUSTOV, M.I. LEVIN, A.ML MARINOV,
L.M. MYZIN and A.P. PETROKOV

Sverdlovsk

(Received 19 January 1960)

The first stage of the substation at Sverdlovsk was begun last year. Provision has been made for equipment and switchgear of 500 kV. The substation is intended to receive power from the Lenin hydro-electric station on the Volga, the "Botkinsk" hydro-electric station and large thermal power stations.

The plan made by the Department of long distance transmission and Teploelektroproekt envisages the connexion of 500 kV lines from Chelyabinsk (transmission system from the Volga hydro-electric station to the Urals) and from the Botkinsk hydro-electric station. In addition, provision is made for the possibility of enlarging the substation in the future by connecting three further 500 kV lines to it. Two groups of single phase auto-transformers (500/242/38.5 kV) will be installed there with booster transformers for prolonged voltage regulation.

In order to reduce the cost of expensive 500 kV apparatus and ensure a high degree of reliability in the 500 kV distribution gear, use is made of the system shown in Fig. 1. The lines are connected to the 500 kV busbars via two circuit breakers and auto-transformers without circuit-breakers.

The Sverdlovsk substation is an extension of the old 220/121/11 kV substation there, with 500 and 35 kV distribution gear added on. The auto-transformers are connected to the 220 kV busbars via two MKP-220 type circuit breakers. The increased amount of 500 kV distribution gear has brought about an increase in the number of 220 and 110 kV lines and

* *Elektrichestvo*, No.7, 61-65, 1960.

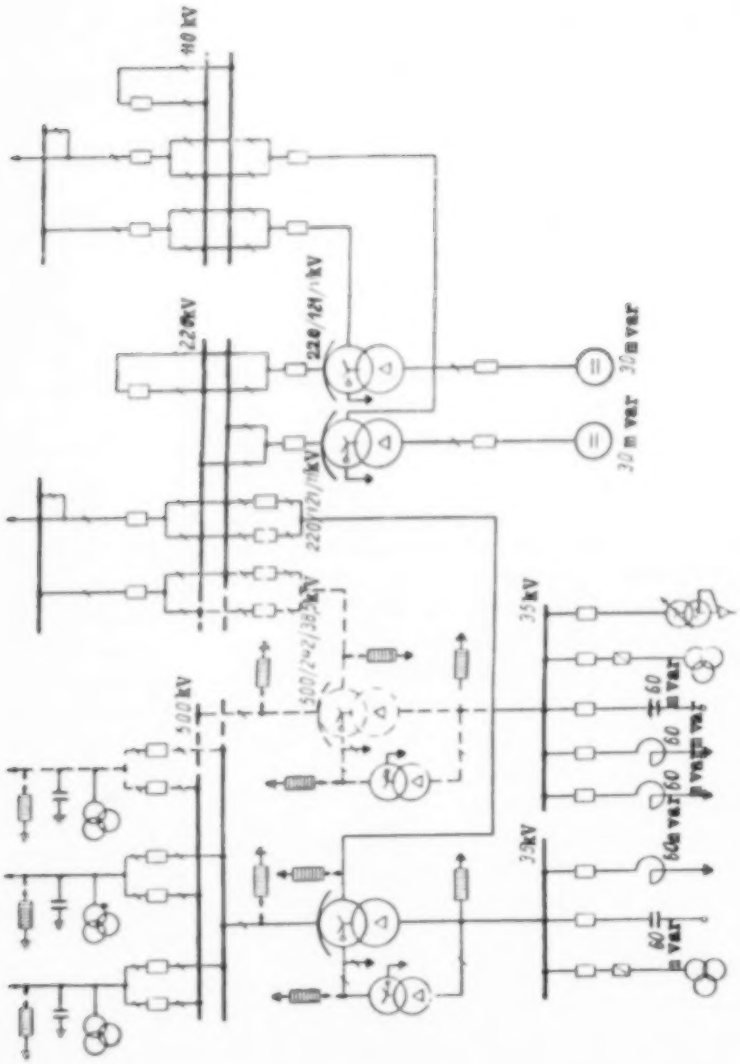

Fig. 1. The electrical connexions of the substation.

the two 220/121/11 kV transformer groups have been replaced by two groups of larger auto-transformers. Provision is made for more 220 and 110 kV oil circuit breakers.

The groups of auto-transformers on the 38.5 kV side operate separately. The 38.5 kV winding of each group is connected to small 35 kV distribution gear.

In the first stage of the substation use has been made of the 500 kV transmission line block system (auto-transformer with one MKP-500 circuit breaker).

To measure the voltage, provision is made for electromagnetic HKF-500 type transformers, connected to the 500 kV lines at the point where they enter the substation. The All-Union Electrical Engineering Institute has carried out tests on the transmission system between the Volga hydro-electric station and Moscow which show that electromagnetic metering transformers are instrumental in reducing internal voltage surges at the ends of the line under transient conditions.

The transmission line between the Volga hydro-electric station and the Urals was originally planned for 400 kV. Later, when construction had already started on the Sverdlovsk substation, it was decided to use 500 kV but with the same insulation levels and, consequently, the same dimensions as had been approved for the 400 kV distribution gear. This was possible owing to the use of special protector "dischargers" which involuntarily limit internal voltage surges of 2.5 U_f. These protectors are installed at the lead-ins to the transmission lines and auto-transformers.

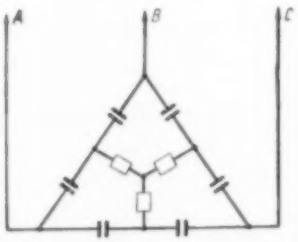

Fig. 2. Principal circuit of the automatically variable bank of static 60 MVA capacitors

On the 220 and 38.5 kV side, RVS-220 and RVS-35 type dischargers have been installed in the immediate vicinity of the lead-ins to the auto-transformers.

To maintain the necessary voltage level under different transmission conditions, provision is made for two banks of 60 MVA static capacitors with an automatic system of forced capacitance (Fig.2) and three three-phase shunting reactors also of 60 MVA each. The capacitor banks and reactors are connected alike to the 35 kV busbars.

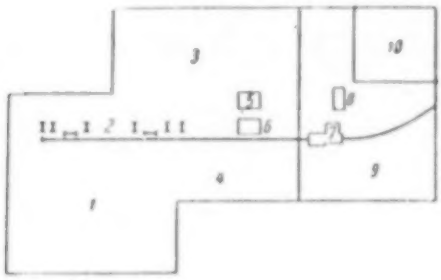

Fig. 3. Layout of substation.
1 – 500 kV distribution gear; 2 – 500/242/38.5 kV auto-transformers; 3 – 220 kV distribution gear; 4 – 110 kV distribution gear; 5 – control panel; 6 – machine room for synchronous compensators; 7 – oil works; 8 – oil store; 9 – auxiliary plant; 10 – living quarters.

The 500 kV oil circuit breakers made by the "Uralelektroapparat" works have been installed.

The advantage of oil circuit breakers over the air-blast kind consists in their greater reliability in operation in the bleak climatic conditions of the Urals. They have built-in current transformers at the inputs, are cheaper and take up less space in the substation. However, until not long ago, oil tank circuit breakers could not compete with air blast circuit breakers as regards operating speed. The "Uralelektroapparat" works has designed an oil tank circuit breaker which ensures the necessary operating speed and rupturing capacity.

A number of measures have been taken so as to reduce the volume of work on the erection of the substation and cut costs, as compared with the substations built on the transmission system between Moscow and the Volga hydro-electric station. At the Sverdlovsk substation all the control panels and relay protection are housed in one building, not two. The busbars of the 500 and 220 kV distribution gear are made from aluminium-steel, coupling devices are simpler, the load lifting devices

in the transformer shop are simpler and they are smaller in size, and so on.

A great saving has been made in construction and erection by adding the 500 kV substation onto the old 220/110 kV substation. Taking into account a certain lengthening of the 500 kV lines, this brought a saving 14 million roubles, much less cable and equipment was used and there was no need to build a number of auxiliary premises and living quarters. The running cost of the combined substation was also less. In particular, the number of employees was the same as that before the 500 kV substation was added on.

The arrangement of the old 220 and 110 kV distribution gear (Fig.3) made it a very simple matter to solve the problems connected with the layout of the 500 kV distribution gear.

The 500/242/38.5 kV auto-transformers were installed in line with the old 220/110 kV transformers along the railway track. The 220 kV busbars were lengthened by a few extra spans. The 35 kV shunting reactors and capacitor banks were arranged between the auto-transformers.

To assemble, erect, inspect and repair the 500/242/38.5 kV auto-transformers, a new large transformer tower with a crane carriage capable of lifting 200 tonnes was added onto the old tower.

Since two circuit breakers had to be installed in the section of each 500 kV line, it seemed advisable to arrange the collector busbars outside (Fig.4). This required far fewer insulators and supports for carrying the busbars.

With multi-sided stress of the conductors in adjacent sections, the axes of the central pylons coincide in all the sections. This has made it possible to reduce the number of pillars on the central pylon considerably, without increasing the weight of each of them. The busbars were suspended 22 m high on the line pylons and 26 m on the central pylon.

The main automobile roads on the distribution gear site were laid between the circuit breakers and the line disconnectors.

So as to be able to transport equipment under the busbars without having to switch them off, the line disconnectors are raised on supports 4 m high. The total width of a 500 kV section is 28 m, length 137 m. The assembled auto-transformers were transported from the tower to the point of insulation along the railway track, which is laid on a reinforced concrete base.

Lighting conductors offer the substation protection from direct

lightning strikes. These are mounted on the pylons, or else stand separately. The individual lightning arresters are used as searchlight poles.

After the installation of the 500 kV distribution gear, the control panel premises and the auxiliary equipment of the old 220/110 kV substation needed no renovations or extensions, with the exception of the open oil store, where three extra tanks of 60m^3 capacity each were installed.

The Sverdlovsk substation is provided with special equipment manufactured by our national electrical engineering industry.

A group of three three-winding single phase AODTG - 135000/500 type auto-transformers was made by the Zaporozhe transformer works. Table 1 shows the main parameters of the single phase transformers.

The group of three single phase auto-transformers is connected on the Y_0 - auto/Δ - 12 - 11 system and has a rated output of 405,000/405,000/180,000 kVA. The auto-transformers are oil-cooled with individual blast.

There are two current transformers at the inputs to all of the high and medium voltage windings and neutral.

The auto-transformers are mounted on a screwed base-plate foundation.

Regulation is maintained over long periods of time by means of a booster transformer (Fig.5). There are 22 degrees of regulation and voltage can be varied within the limits of $\pm$ 6 per cent of rated.

The 500 kV oil circuit breaker installed

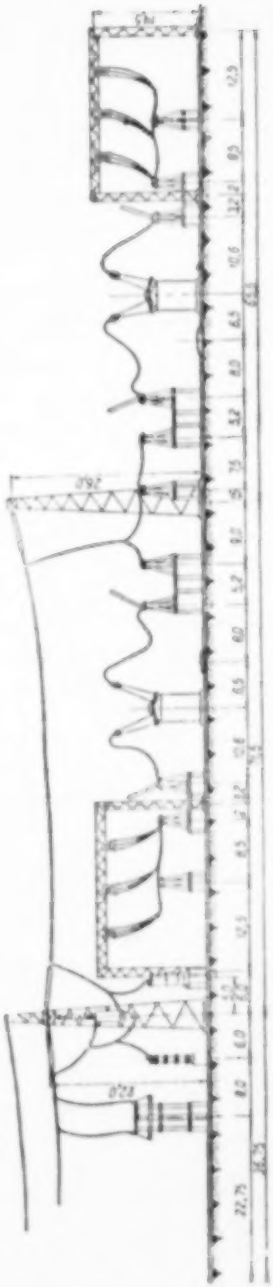

Fig. 4. Section of the 500 kV line.

at the Sverdlovsk substation was the first one ever produced. The breaker consists of three separate phases, each of which is controlled by its electro-magnetic drive and has eight built-in current transformers. The tank of each breaker contains four arc quenching chambers with shunting resistances. The arc quenching chamber has eight breaks, i.e. the total number of breaks per phase is 32. The arc quenching chamber is of the same construction as that of the MKP-220 type breaker. The breaker's contacts have a cermet fusion.

TABLE 1

Rated output with connected blast, MVA	135/135/60
Rated output with disconnected blast, MVA	94.5/94.5/42
No load voltage, kV	$\frac{500}{\sqrt{3}}\Big/\frac{242}{\sqrt{3}}\Big/38.5$
Alternating voltage used to test the insulation at the line end of the winding, kV	700/400/85
No load current, %	3.3–3.6
No load losses, kW	333–348.5
Short circuit losses in the 500/242 kV state at 135 MVA, kW	353–362
Short circuit voltage between 500 and 242 kV windings, in terms of 135 MVA, %	10.6–10.68

Arc quenching time is 0.015 to 0.04 sec when tripping a short circuit, total tripping time is 0.05 sec, it takes 1.5 sec* to connect up the oil breaker and the automatic reclosure cycle is up to 1.65 sec.

The oil filled capacitor MVP-500/1500 type leads were produced for the breaker by the Moscow "Insulator" works. In their assembled form, the leads (from top to bottom contact) stand 8.4 m high, including the extra-tank part 5.1 m high. The leads were designed to operate at ambient temperatures from -45° to + 35°C.

The total height of the 500 kV breaker is 12.2 m, weight of one phase without oil is 35 tonne, with oil 64.4 tonne. The principal character-

* Actual connexion time was 1.2 to 1.3 sec during tests at the substation.

istics of the MKP-500 type breaker are given in Table 2.

To protect the substation's equipment from atmospheric over-voltages, use is made of valve dischargers. The set of RVS-220 type dischargers is mounted on the 220 kV side at a distance of 25 m from the auto-transformer. The same level of insulation is used at the 500 kV substation as for a 400 kV station. In this connexion, provision is made for "combined" dischargers which are to limit the overvoltages occurring in transient processes in 500 kV transmission to 2.5 U_f.

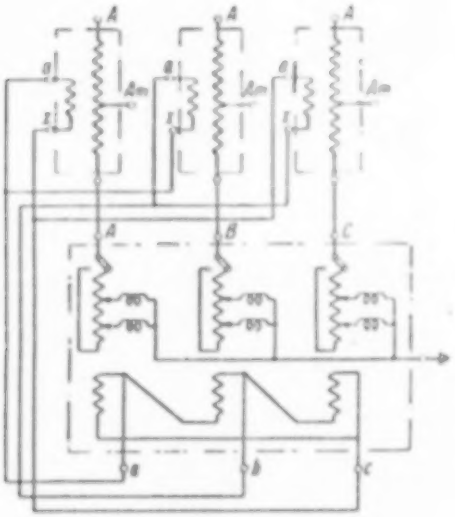

Fig. 5. Connexion of the booster transformer plus a group of auto-transformers.

Precautionary tests were carried out on the insulation of the high voltage equipment during the erection and starting of the substation. Other tests were also made on the auto-transformers, the rupturing capacity of the MKP-500 type circuit breakers and so on.

The insulation of the auto-transformers was tested before drying, whilst drying, at the end of drying and also after final assembly and control heating. Measurements were taken of the insulation's resistance, leakage currents on rectified voltage, dielectric losses, capacitance and the moisture content of the "PKV" instrument's windings. The tests showed that the insulation was up to standard.

The booster transformer was filled with oil at the works and delivered to the substation in this form. As a result of checks made with

1960

the core removed and standard tests, the insulation of the transformer was not subjected to drying.

TABLE 2

Rated operating voltage, kV ..	500
Maximum operating voltage, kV..	525
Rated current, A	1,000
Tripping current, A	13,900
Rupturing capacity, million kVA	12
Maximum possible through current (effective value), A	29,000
Rated voltage of drive, V.. ..	220

TABLE 3

Test voltage-kV	Type of test	Trip current kA	Arc burning time 10^{-2}sec	Maximum voltage recovery speed v/μ sec	Coefficients of voltage increase		Number of tests
					Phase	Between leads of breaker	
220	Tripping short circuit	0.6-5.3	1.9-2.8	200-500	1.25-1.78	1.24-1.58	7
220	Tripping as load line	0.15-0.25	1.6-2.0	–	1.38-1.62	1.25-1.33	6*
475	Tripping as load line	0.15-0.25	0.2-1.4	–	1.15-1.29	1.13-1.31	13**
475	Tripping short circuit	1.0-1.4	2.8-3.7	4,200-4,700	1.23-1.54	1.1-1.37	4

* Accompanied by re-ignitions;

** No re-striking.

Tests were made on the dielectric losses, capacitance, the quality of the oil in the 500 and 220 kV oil-filled leads of the transformer group and the MKP-500 and MKP-220 type oil circuit breakers. The measurements and checks proved satisfactory. The same applies to measurements taken on the oil-filled OMPV-188 type support-suspended insulators for the MKP-500 circuit breaker.

All the 500, 220 and 35 kV dischargers, SMR-133 and OMR-35 type capacitors (of which the 500 kV coupling capacitors were composed), and all the support and suspension insulators of the open 500, 220 and 35 kV

distribution devices were tested in accordance with the supplier's instructions. Before erection the insulation was tested on alternating voltage from a "Foster" test plant (a single phase 10 kVA transformer with continuously variable voltage up to 100 kV). The voltage was applied for 1 min. The insulation was tested after erection by a 2.5 kV megger. About one per cent of the insulators were rejected as a result of the tests.

High voltage, electromechanical and electro-thermal tests were made on the prototype of the MKP-500 circuit breaker at the works 'Uralelektro-apparat" in 1958. The rupturing capacity tests were carried out by the high voltage tests laboratory at the works "Uralelektroapparat" at the point of installation. In order to make the largest possible number of tests, the tests were divided into two stages: before the erection of the auto-transformer was completed and after completion.

In the first stage, the circuit breaker (one phase) was tested at 220 kV, two of the four arc quenching chambers being shunted. The rupturing capacity of the breaker was tested in the presence of a two-pole short circuit at different distances in the cycles of tripping and instantaneous automatic reclosure on the contacts of the 220 kV breaker. In addition, the breaker's rupturing capacity was tested on a no load 220 kV line with a charge current of 150 and 250 A.

In the second stage the same circuit breaker was tested at an actual voltage of 475 kV for tripping the current of a two-pole short circuit without "earth" in the same cycles. The point of short circuit was supplied via an auto-transformer.

The test results are given in Table 3.

Before switching on the operating voltage the auto-transformer was tested by raising the voltage across it from zero. To do this use was made of a 15 MVA synchronous compensator with the acceleration motor, installed at the 110 kV substation, which was connected to the Sverdlovsk substation for the 110 kV lines. The voltage on the 500 kV side was raised to 350 kV, i.e. 70 per cent of rated.

With the opening of the 500 kV substation at Sverdlovsk, a big step forward has been made in the industrial application of the new high level of voltage.

Translated by O. Blunn

ABSTRACTS FROM PAPERS PUBLISHED IN ELEKTRICHESTVO No.7, 1960

High quality electrical steels and alloys. A.M. Samarin, (pp. 1-4).

The electrification of the U.S.S.R. being the "main core" of the programme of communist construction in the next 15 to 20 years the author considers means of reducing the cost of material for electrical equipment and ensuring that the right metals and alloys are produced for the electrical industry. He discusses silicon steels, iron, Fe-Al alloys, constructional steel with a low hydrogen content to reduce flaking, semiconductor materials, substitutes for copper and the production of pig iron in electric furnaces.

Electrical equipment at the Bhilai iron and steel works. M.M. Brozgol, (pp. 5-10).

An account is given of the integrated iron and steel works built in India with the assistance of the U.S.S.R.

On power regulation theory of electrical ore-smelting furnaces. V.S. Lerner, (pp. 25-30).

A description is given of the automatic system of power control used chiefly in electric ore-smelting furnaces with a deep slag bath. An analysis is made of the link between the basic parameters of the regulator and the object so as to ensure the requisite static and dynamic characteristics. Reference is made to "system comprising a correcting circuit which has passed operational" tests.

On control systems for the drives of medium-sized excavators. M.I. Kraitsberg, D.A. Kaminskais and V.P. Lomakin, (pp. 30-35).

A comparison is made between drive systems for excavator shovels (capa-

city 6 to 8 m^3) using dynamoelectric "amplifiers jointly with intermediate magnetic amplifiers (cascade system) and dynamoelectric amplifiers by themselves (KhEMZ system). After studying a series of oscillograms of the performance delivered by these systems it is recommended that external flexible feedbacks be excluded. Lifting and drawing are performed more efficiently on the KEMZ system. The KEMZ system is recommended for medium power excavators.

Grapho-numerical methods for calculating transients from structural schemes. A.M. Suchilin, (pp. 35-39).

A method is proposed for simplying Basharin's system of calculating transient processes in automated drives. Instead of ascribing a differential equation to each link in the structural scheme, substituting a finite difference equation written in the form of a proportion and then performing the calculations graphically, the author proposes a "programme scheme of calculation" comprising elementary links which are found by recurrence formulae based on the transfer functions of the links.

1960

The d.c. magnetic field in a parallepiped. V.N. Rudakov, (pp. 39-41).

Powerful magnetic fields arise in electrolyte baths producing electrodynamic forces causing the metal in the bath to shift. This entails the calculation of the intensity of the magnetic field of the anode current. The present paper proposes a simplified theoretical method of calculating the magnetic field in a rectangular parallepiped.

A synthetic scheme for testing circuit-breakers with long burning arcs. N.M. Chernyshev and Z.A. Abramova, (pp. 41-46).

A study is made of methods of testing circuit breakers and an account given of a new synthetic system which is particularly effective in the case of circuit-breakers with long arc combustion time and a relatively large voltage drop in the arc. Use is made of an additional inductance of the order of 0.2 to 0.4 in the circuit.

A combined way of switching in power circuits. N.F. Shishkin and P.Ia. Danilin, (pp. 47-50).

The connexion of a constant resistance of practically zero value in parallel to the consumer has not yet been widely used for commutation purposes although it is more quick-acting, (use here being made of a

short circuiting device). A new method of commutation which involves no "metallic" short circuit of the supply source is proposed using a combined switching apparatus with tripping and shorting systems of contacts incorporating a spring-magnetic mechanism.

Surge protection of 35-500 kV switchgear today. N.N. Beliakov and A.N. Sherentsis, (pp. 51-56).

A study is made of proposals for simplifying the protection of electrical networks from surges. Special attention is paid to direct lightning strikes and the protection of distribution gear from waves of atmospheric overvoltages from the lines.

The electrical characteristics of long insular strings for lines of 500 kV and higher. N.N. Tikhodeev and A.N. Tushnov, (pp. 56-61).

A study is made of the electrical characteristics of long chains of suspension insulators in view of their high cost. Tests supported the belief that the type of protective fitting has no marked effect on the size of the discharge voltage of the chain if the fitting produces the discharge through the air and not along the surface of the insulators. It is argued that with alternating voltage the electrical strength of long chains in the dry state and with a protective fitting is determined by the asymmetrical air gap between the fitting and the tower. Account must be taken of the dry discharge voltage of the chain as well as the wet discharge voltage.

On the deficiences of State Standard GOST - 8033 - 56 "Electrical and Magnetic Units" L.B. Slepian dec'd., (pp. 66-67).

The author maintains that the above State Standard is deficient in that two systems of electrical and magnetic units are permitted, namely the MKSA and Gauss systems. He advocates the use of the MKS(G) system, i.e. the practical Gauss system.

Concerning the question raised by Professor L.B. Slepian in his article "On the deficiencies of State Standard GOST 8033 - 56". L.R. Neiman and E.G. Shramkov, (pp. 68-69).

The authors state that Professor Slepian's proposals for the use of the MKS(G) system of units (see previous abstract), though interesting, are less acceptable than the recommended MKSA system because of the need to introduce certain corrections.

The possibilities of detecting ferromagnetic conducting objects in ferromagnetic substances. L.A. Gel'bukh, (pp. 69-72).

It is argued that in removing metallic inclusions from powder, it is impossible to detect the metallic inclusions merely by determining the change in the e.m.f. of the signal or frequency. A method of indication based on changes in phase is described. This is suitable for ore cleaning plant to prevent damage to the crushers in the event of foreign matter falling into the ore.

Condenser paper having a small dielectric loss angle. V.T. Renne, M.N. Morozova and K.I. Karpova, (pp. 72-77).

Investigations have shown that Russian sulphate cellulose used for condenser paper has roughly the same pentosane content as that in America. A marked influence of the ash content of the paper on losses has been established. Even though organically equivalent to American paper and superior as regards the adjustment of the ash content, Russian paper is acknowledged to be inferior to the American product and it is recommended that paper with a reduced volumetrical weight, of the order of 0.85 to 0.9 g/cm^3, be produced.

The characteristics of flashover along the layers of paper-oil insulation for direct voltage. M.A. Greisukh, (pp. 77-82).

It is considered necessary to take into account the total discharge voltage from the edge of one electrode to another primarily along the layers of paper for condenser-type paper oil insulation in the development of current transformers etc. A study is therefore made of the discharge characteristics of the thickness of the insulation, the construction of the edge and the polarity of the voltage when the discharge distances vary within wide limits. The discharge voltage is 5 to 6 times lower on d.c. than a.c. and positive polarity is advocated. Temperature changes between 20°C and 75°C and differences in edge thickness from 10 to 85 micron have no effect.

Diagrams for determining the firing angle of a three phase bridge type rectifier. S.R. Glinternik, (pp. 82-85).

A simplified diagram is proposed for determining the angle of commutation and the given ignition angle for a three phase bridge converter for current rectification inversion. The diagram can be used to calculate the electromagnetic processes and converter characteristics in all

steady state conditions with the exception of a small zone in the vicinity of the short circuit state when three valves are arcing simultaneously.

AN ELECTRICAL CURRENT STABILIZER*

V.S. POPOV, M.N. SOLOV'EVA and Iu.A. MAL'TSEV

(Leningrad)

(Received 28 January 1960)

1960

The existing types of static direct current and voltage stabilizers usually have a marked temperature error and little stability over long periods of time [1].

These shortcomings are to a large extent eliminated in the stabilizer with a thermistor [2]. This stabilizer consists of a bridge which contains a resistance R_3 in one arm directly heated by a thermistor heater R_h which is connected via an amplifier in the diagonal of the bridge (Fig. 1). We thus have negative feedback, which automatically ensures the balancing of the bridge. The load is connected to the output of the amplifier, in series with the heater R_5 or parallel to it R_6.

The bridge is not completely balanced during the process of operation. But if the amplication factor of the system is large enough, it is then practically in the equilibrium state.

Since the resistances R_1, R_2 and R_4 in the three arms of the bridge are constant, the quality of the stabilizer is in fact determined by the stability of the thermistor s characteristics. Metallic thermistors are the most suitable for use in stabilizers. The stability of semiconductor thermistors is considerably less and, in view of this, there is limited scope for using them in stabilizers.

The thermistor-stabilizer is suitable for stabilizing direct and alternating current and voltage. If alternating voltage is in the first case first rectified at the output of the amplifier, a stable direct current will flow across the load. Here negative feedback will

* *Elektrichestvo*, 8, pp. 36-39, 1960.

cover both rectifier and amplifier. To increase operating reliability, a magnetic amplifier can be substituted for the electronic amplifier.

Let us analyse the stabilizer error as a function of variations in the amplification factor of the analyser, the load impedance, the bridge supply current I, and also in the presence of amplifier drift.

It follows from Fig. 1 that the current I_s passing through the heater is directly proportional to the voltage U_d in the diagonal of the bridge and the amplification factor k of the amplifier. It also follows that I_s is inversely proportional to the impedance z. Impedance z depends on the parameters of the output circuit of amplifier

$$I_s = \frac{kU_d}{z}. \tag{1}$$

In turn

$$z = \frac{(R_5 + R_6 + R_h) z_i + R_6 (R_h + R_5)}{R_6}, \tag{2}$$

where z_i is the internal impedance at the output of the amplifier.

The voltage in the diagonal of the bridge is

$$U_d = \frac{(R_1 R_4 - R_2 R_3) R_{in} I}{R_{in} (R_1 + R_2 + R_3 + R_4) + (R_1 + R_3)(R_2 + R_4)},$$

where U_{in} is the input impedance of the amplifier.

Let us introduce the following designations:

$$R_1 R_4 - R_2 R_3 = b;$$
$$R_{in} (R_1 + R_2 + R_3 + R_4) + (R_1 + R_3)(R_2 + R_4) = a.$$

Hence

$$I_s = \frac{kIR_{in}b}{za}. \tag{3}$$

The temperature of resistance R_3 is a function of currents I and I_s:

$$R_3 = f(I_s; I).$$

To compensate for variations in ambient temperature, a similar type of resistance without a heater circuit is connected in the arm of the bridge AB. The resistance R_1 therefore generally depends on the current I.

$$R_1 = f(I).$$

We have to determine how the current I_s varies when the amplification factor of the amplifier changes.

Differentiating expression 3, we find

$$\frac{dI_s}{dk} = \frac{R_{in} Ib}{za} + \frac{klR_{in}\left(a\frac{db}{dI_s} - b\frac{da}{dI_s}\right)}{za^2}\frac{dI_s}{dk}.$$

Hence, taking into account the facts that the bridge is practically in the equilibrium state during operation (i.e. $R_1 R_4 \approx R_2 R_3$) and that b is very small and, consequently, $R_2 \gg \frac{b}{a}(R_{in} + R_2 + R_4)$, we get, after a number of transformations,

$$\frac{dI_s}{I_s} \approx \frac{1}{1 + \frac{klR_{in}R_1}{za}\frac{df(I_s; I)}{dI_s}}\frac{dk}{k}.$$

The expression $\frac{klR_{in}R_1}{za}\frac{df(I_s; I)}{dI_s}$ is the amplification factor of the system K.

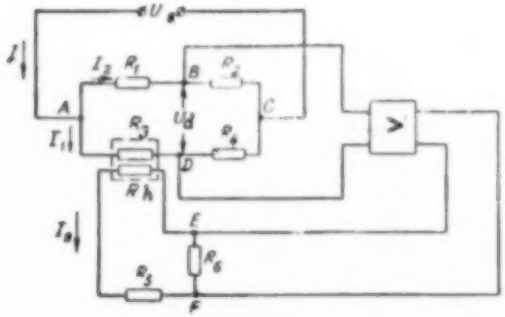

Fig. 1. Fundamental circuit of the stabilizer.

Thus,

$$\frac{dI_s}{I_s} \approx \frac{1}{1+K}\frac{dk}{k}. \qquad (4)$$

Likewise, we find that if the impedance z varies, the change in the

1960

stabilized current amounts to

$$\frac{dI_s}{I_s} \approx -\frac{1}{1+K}\frac{dz}{z}.$$

Taking 2 into account, we have

$$\frac{dI_s}{I_s} = \frac{1}{1+K}\left\{\frac{(R_s+R_h)z_i}{(R_s+R_s+R_h)z_i+R_s(R_h+R_s)}\frac{dR_s}{R_s} - \right.$$

$$\left. - \frac{d(R_h+R_s)}{R_h+R_s+\frac{z_iR_s}{z_i+R_s}} - \frac{dz_i}{z_i+\frac{(R_h+R_s)R_s}{R_s+R_s+R_h}}\right\}. \qquad (5)$$

Thus the error of the stabilizer due to variations in the amplification factor of the amplifier and load impedance is inversely proportional to the amplification factor of the system.

Fig. 2 shows the variation in amplifier output voltage with signal voltage U_d without drift (1) and with it (2).

If drift occurs and the voltage of the signal is constant (direct), a change will occur in the output voltage of the amplifier. Since the amplification factor of the amplifier is the ratio of the output voltage of amplifier to the voltage of the signal, the increment in the amplification factor due to "drift" amounts to:

$$\Delta k = k\frac{U_0}{U_d},$$

where U_0 is the "drift" voltage.

Consequently, according to expression 4, we have

$$\frac{\Delta I_s}{I_s} \approx \frac{1}{1+K}\frac{U_0}{U_d}. \qquad (6)$$

Expression 6 can assume the form

$$\frac{\Delta I_s}{I_s} \approx \frac{kU_0}{(1+K)I_sz} \approx \frac{aU_0}{1\cdot I_sR_{in}R_s\frac{df(I_s;\ I)}{dI_s}}.$$

Hence it follows that the instability due to the "drift" of the amplifier is independent of the amplification factor of the amplifier. It can be reduced by using thermistors if the slope of the characteris-

tic is thereby increased and if there is an increase in current I, the output impedance of the amplifier and the resistance R_2.

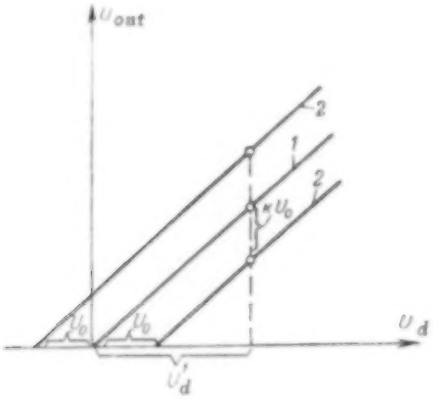

Fig. 2. The effect of "drift" on the characteristic of the amplifier.

Let us consider how the current I_s varies with a change in current I.

Differentiating equation 3 and taking it into account that $R_4 \gg \frac{b}{a}(R_{in} + R_2 + R_4)$ and $R_2 \gg \frac{b}{a}(R_{in} + R_2 + R_4)$, we get

$$\frac{dI_s}{I_s} \approx \left\{1 + \frac{I}{b}\left[R_4 \frac{df_1(I)}{dI} - R_2 \frac{df(I_s; I)}{dI}\right]\right\} \frac{dI}{I}. \quad (7)$$

In certain types of thermistor, the dependence of the resistance on the combined effect of currents I_s and I equals

$$\frac{dI_s}{I_s} = \frac{1 + \frac{kR_{in}I^2}{azI_s}\left[R_4 \frac{df_1(I)}{dI} - R_2 \frac{df(I)}{dI}\right]}{1 + K} \frac{dI}{I}. \quad (8)$$

It follows that the amplifier amplification factor in the expressions right can under definite conditions be considerably less than one. A variation in current I will then have rather less effect on the magnitude of the current I_s than variations in the load and the amplification factor of the amplifier.

Fig. 3 shows the fundamental circuit of a d.c. stabilizer with a metallic thermistor and a magnetic amplifier. The thermistor used in the stabilizer is a platinum spiral, wound on a "nichrome" heater which is enclosed in a glass insulating tube. The thermistors are mounted on

the base of radio valves and placed in pairs in brass cylinders for protection from mechanical damage.

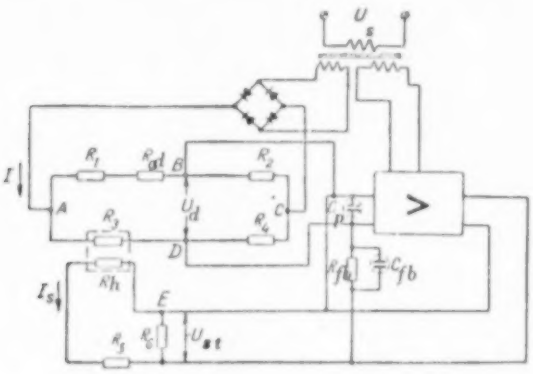

Fig. 3. Circuit of the direct current and voltage stabilizer.

The time constants of the thermistors are between 0.1 and 0.6 sec depending on their size.

The maximum working temperature of the thermistors is between 400 and 450°C since the glass insulating tube melts at temperatures over 550°C.

The relative variation in the characteristics of the thermistors $R = f(I_s; I)$ does not exceed $\pm$ 0.2 per cent after 4000 hr continuous use at about 250°C.

From test results, the dependence of the resistance R of the spiral on the combined effects of currents I_s and I can be expressed by the following formula

$$R = R_0 + cI_s^{\alpha} + c_1 I^{\beta}, \tag{9}$$

where R_0 is the initial resistance of the spiral.

Equation 9 holds for temperature rise of the spiral from 20 to 250°C. At higher temperatures the non-linearity indices α and β (equal respectively to 1.7 and 2) and the constants c and c_1 will vary, but the form of the equation is unaltered.

If use is made of metallic thermistors in the system shown in Fig. 3, the change in resistance R_3, if current I_s changes, and the total amplification factor are respectively equal to

$$\frac{dR_3}{dI_g} = \alpha c I_g^{\alpha-1};$$

$$K = \frac{\alpha c k I_g^{\alpha-1} I R_{in} R_2}{2a}.$$

Considering that the components of current I in resistances R_3 and R_1, are respectively

$$I_1 = \frac{R_2}{R_2 + R_4} I, \quad I_2 = \frac{R_4}{R_2 + R_4} I,$$

and that

$$f(I) = c_1 \left(\frac{R_2}{R_2 + R_4}\right)^{\beta} I^{\beta};$$

$$f_1(I) = c_1 \left(\frac{R_4}{R_2 + R_4}\right)^{\beta} I^{\beta},$$

and

$$\beta \approx 2,$$

equation 8 can be re-written in the form

$$\frac{dI_g}{I_g} = \frac{1 - \frac{2c_1 k R_{in} I^2 (R_2^2 - R_4^2)}{a z I_g (R_2 + R_4)^2}}{1 + K} \frac{dI}{I}.$$

The amplification factor of a magnetic amplifier is independent of "drift" and the amplification factors of the stages. In the main it only varies when the supply voltage varies:

$$\frac{dk}{k} = h \frac{dU_g}{U_g},$$

where h is a constant and U_g the supply voltage.

Since $I \equiv U_g$, the relative change in I_g as a function of a change in the supply voltage, with expression 4 taken into account, amounts to

$$\frac{dI_g}{I_g} = \frac{1 + h - \frac{2c_1 k R_{in} I^2 (R_2^2 - R_4^2)}{a z I_g (R_2 + R_4)^2}}{1 + K} \frac{dU_g}{U_g}. \qquad (10)$$

If the resistances in the arms of the bridge are such that $R_2 > R_4$, then with an optimum value of current I equal to

$$I' = \sqrt[3]{\frac{azI_s\,(R_2 + R_4)^2\,(1+h)}{2\varepsilon_1 k R_{in}\,(R_2^3 - R_4^3)}}, \tag{11}$$

the current I_s is practically independent of the current I and the stabilization coefficient is theoretically equal to infinity.

The expression 10, when considered with equation 11, is transformed into the following equation:

$$\frac{dI_s}{I_s} = \frac{(1+h)\left[1 - \left(\frac{I}{I'}\right)^3\right]}{1+K} \frac{dU_s}{U_s}. \tag{12}$$

It follows from formula 12 that the current I_s always decreases if any deviation of current I from its optimum value occurs. It should be mentioned that a similar phenomenon occurs in simple bridge stabilizers with a non-linear element.

To increase the stability of the amplifier's amplification factor, the amplifier is provided with an external negative feedback (Fig.3). The capacitor C_{fb}, which shunts the feedback resistance R_{fb}, serves to eliminate auto-oscillations.

The temperature of the thermistor under working conditions is approximately 120 to 160°C. This ensures that the parameters of the thermistor are highly stable. The amplification factor of the system is about 40.

In view of the reduction in the temperature coefficient as the temperature of the thermistor increases, an additional resistance R_{ad} is connected in series with the compensation resistance R_1 in order to compensate the temperature error. (Fig.3). To satisfy the inequality $R_2 > R_4$, the sum of the resistances $R_1 + R_{ad}$ should be slightly greater than the resistance R_3 during the operation of the stabilizer.

The appropriate choice of additional resistance R_{ad} can completely compensate the temperature error of the stabilizer. But, in practice, this resistance only serves to produce a rough compensation of the error. A greater reduction can be achieved by the use of copper wire as a small fraction of the resistance R_2 and R_1. The advantage of this latter method is that the resistances of all the arms of the bridge remain constant.

The stabilized current I_s can be regulated by shunting the heater by a variable resistance. The stabilized voltage U_{st} can be varied by the variable resistance R_5.

As an illustration of the properties of the stabilizer, the following table shows the variation in voltage U_{st} for a load impedance R_g = 220 at various ambient temperatures.

TABLE 1

Voltage U_s, V	Voltage U_{st}, V ct		
	t_{amb} = 20°C	t_{amb} = 35°C	t_{amb} = 50°C
100	1,976	1,969	1,964
110	1,980	1,978	1,977
120	1,980	1,980	1,980
130	1,980	1,980	1,980
138	1,976	1,978	1,979

It will be seen from the Table that the stabilizer's coefficient of stabilization is roughly 100 for variations in the supply voltage of ± 10 per cent. The average temperature error is 0.07 per cent for a change in temperature. With increasing temperature, the zone of stabilization is shifted towards higher voltages, since the resistances in the arms of the bridge increase and a slight change occurs in the parameters of the magnetic amplifier. Hence, according to expression [11], the optimum value of the current I varies.

If a sudden and large change occurs in the supply voltage, there is a sudden and large change in the load voltage, but this change rapidly decays along a practically exponential curve. The maximum relative change in the load voltage is about 70 per cent of the relative change in the supply voltage. The load voltage returns to its original value after 0.1 sec, having first completed one or two oscillations about the equilibrium position.

A real merit of the stabilizer under consideration is the highly stable nature of the indications. Even after a considerable idle period, it will reproduce previous stabilized current or voltage values with a high degree of accuracy.

As shown by test results, the stabilized voltage varies by less than 0.2 per cent from the original value after the stabilizer has worked for six months. The accuracy of measurement is of the same order.

The main advantages of the stabilizer are the absence of electronic valves and moving parts, the considerable stabilization coefficient and the negligible temperature error.

Translated by O.M. Blunn

1960

REFERENCES

1. I.G. Gol'dreer; *Voltage stabilizers, (Stabilizatory napriazheniia).* Gosenergoizdat, (1957).
2. V.S. Popov; *A stabilizer with a thermistor, (Stabilizator s podogrevnym soprotivleniem). Sborn. po voprosam e'lektromekhaniki, No.2,* Gosenergoizdat, (1958).

CONDITIONS FOR THE SYMMETRICAL PERFORMANCE OF A CAPACITOR MOTOR*

G.G. REKUS

(Moscow Higher Technical College)

(Received 23 February 1960)

1960

To ensure the necessary starting properties of a capacitor motor with squirrel cage rotor, especially when the supply voltage is subject to considerable variations, use must be made of special circuits which require complex starting equipment [1].

Unlike other known schemes, that considered in this article with a capacitance shunted by a resistance (Fig. 1) is simple and requires no complicated starting apparatus (the shunting resistance can be disconnected simultaneously with the starting capacitance by the same contactor). This system makes it possible in a number of cases to reduce the size of the additional starting capacitance of the motor.

Experimental investigations show that under favourable conditions the use of this system can reduce the starting capacitance by a factor of 2 to 3, or alternatively increase the starting torque by 1.5 to 2.5 [2]. It is also possible to use this system not only for two phase capacitor motors but also for three phase asynchronous (induction) motors connected as in the capacitor motor system.

But, as shown by experiments, preference must be given to the two phase motors with equal phase zones of the stator winding (equal to or approximately 90°) which possess the best starting properties [2]. The phenomena occurring when the capacitor motor is operating on this system (Fig. 1) can be understood by studying the circle diagram shown in Fig. 2.

The line OK at an angle of $\beta =$ arc tan k to the axis of the abscissa

* *Elektrichestvo*, 8, pp. 51-54, 1960.

(where $k = \frac{w_a}{w_b}$ is the transformation ratio of the motor's stator winding) is equal to the ratio of the effective turns of the main phase to the effective turns of the capacitor phase.

If the capacitor motor is only operating with a capacitance $C(r_{sh} = \infty)$, the position of the tip of the vector $jkY'_C \dot{U} = \overline{AC}$ on the circle diagram is determined by the value of motor's transformation ratio k. C should be on the straight line OK. This is the locus of the tips of the vectors $jkY'_C \dot{U}$, where $Y'_C = \frac{1}{k^2 x_C}$ and x_C the reactance of the capacitor.

In the case of the capacitor motor under consideration (Fig. 2), at a given k there are only two points on the circle diagram corresponding to slips s' and s'' at which strictly symmetrical motor operating conditions are possible for a definite value of the capacitance.

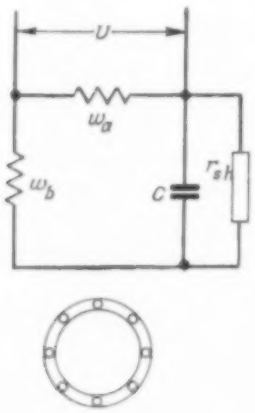

Fig. 1

On starting ($s = 1$), the operating conditions of the motor whose circle diagram is shown in Fig. 2 cannot possibly be symmetrical for any capacitance value. If, however, for the same value of the capacitance C, a resistance r_{sh} is connected in parallel to the capacitor, then as a result of constructions performed in accordance with Nekrasov's proposals [2], it can be established that the tip of the vector $jkY'_C \dot{U}$ (AC) is shifted to the right of the line OK (point C') and occupies the position of the vector $AC' = jkY'_{Cr} \dot{U}$, the modulus of the vector here remaining unchanged. The deflexion of the vector will be the greater,

the smaller the value of the resistance. The shift of the tip of vector $jkY'_C \dot{U}$ to the right denotes its approximation in this case to the point corresponding to $s = 1$, i.e. the operating conditions of the motor on starting are more symmetrical and, consequently, the starting torque is greater.

Like systems which ensure the symmetrical performance of capacitor motors under any load solely by the use of reactances [3], this system also makes it possible under definite conditions to obtain symmetrical performance over the whole range of slip.

Thus, for the given value of k = const, it is possible to obtain a strictly symmetrical performance from a capacitor motor at any point on the circle diagram, provided that it lies to the right of OK. A strictly symmetrical performance at a given value of slip implies that there are definite unique values of capacitance and shunting resistance.

1960

It follows from the analysis of the circle diagram in Fig. 2 that a strictly symmetrical performance of the capacitor motor on starting is only possible when the capacitance is shunted by a resistance if

$$\arctan k > \frac{\pi}{2} - \varphi_k,$$

where $\phi_k = \arccos \frac{r_k}{z_k}$ is the angle defined by the short circuit power coefficient of the appropriate two-phase symmetrical motor, whilst

r_k and z_k are the short circuit resistance and total impedance in the main phase of the motor.

The performance can only be symmetrical over the whole range of slip if

$$\arctan k > \frac{\pi}{2} - \varphi_{max},$$

where ϕ_{max} is the angle defined by the maximum value of the power factor of the corresponding two phase symmetrical motor.

Besides establishing criteria for the expediency of using a capacitor motor with a circuit having a shunted capacitance, it is important to determine the values of the circuit parameters (C and r_{sh}) necessary to obtain symmetrical performance from the motor at the given value of k and slip. In the majority of cases the choice of the circuit parameters merely involves the examination of the most important operating conditions of the capacitor motor, namely, the starting conditions ($s = 1$) and the working load conditions ($s = s_\omega$).

However, symmetrical operating conditions may also be necessary over the entire range of slip or over only part of this range. This can be achieved by the appropriate adjustment of the parameters C and r_{sh}. Although such adjustment is complicated in practice, it is practicable in individual cases by using special circuits. We shall therefore consider the method of selecting the parameters of the circuit as regards the general case.

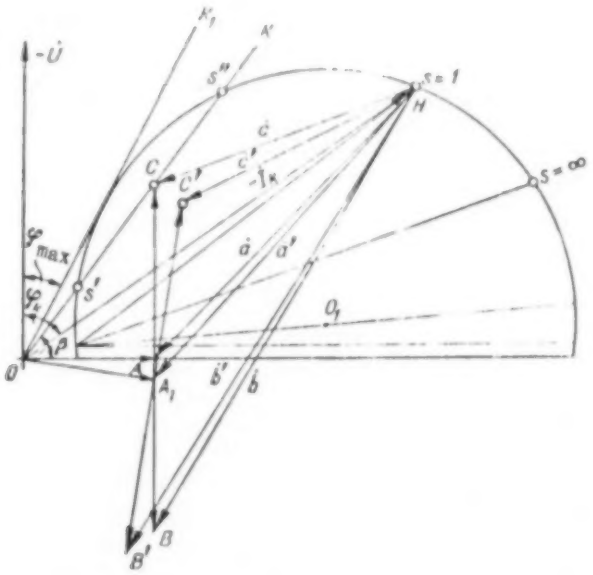

Fig. 2.

It is known that the condition for the symmetrical performance of a capacitor motor is fulfilled if the vector c on the circle diagram (Fig. 2) and, consequently, the negative sequence current is zero.

In this case the following equation [2] holds for the negative sequence current as regards the system in question

$$I_{2-s} = \frac{-Y_{2-s}\,[Y_s + (1 + j3)(Y'_C + Y'_r)]\,\dot{U}}{2(Y'_C + Y'_r) + Y_s + Y_{2-s}} = 0. \qquad (1)$$

Substituting the appropriate resistances for the conductances in equation 1, we obtain, after simple conversions:

$$r'Z'_C + (1 + jk)(r' + Z'_r)Z_{2-s} = 0. \qquad (2)$$

where $Z'_C = jk^2 x_C$ is the impedance of the capacitor referred to the turns of the main phase;

$r' = k^2 r_{sh}$ is the shunting resistance referred to the turns of the main phase, and

$Z_s = r_s + jx_s$ is the total positive sequence impedance for the slip in question obtained by an exact or equivalent network for the positive sequence of the phases of a two phase symmetrical motor.

Substituting the values of the total and applied "resistances" into 2, we obtain

$$\begin{aligned}(r_s r_{sh} - kx_s r_{sh} + x_s x_C + kr_s x_C) + j(-k^2 x_C r_{sh} + \\ + x_s r_{sh} + kr_s r_{sh} - r_s x_C + kx_s x_C) = 0.\end{aligned} \tag{3}$$

Equating the real and imaginary parts of 3 to zero, we have

$$\left.\begin{aligned} r_{sh}(r_s - kx_s) + x_C(x_s + kr_s) = 0; \\ x_C(-k^2 r_{sh} - r_s + kx_s) + \\ + r_{sh}(x_s + kr_s) = 0. \end{aligned}\right\} \tag{4}$$

Using equation 4 and since $x_C = \dfrac{1}{2\pi fC}$ it is easy for the parameters of the circuit for the symmetrical operating condition of the motor to be fulfilled at any value of slip:

$$r_{sh} = \frac{(1+k^2)z_s^2}{k^2(kx_s - r_s)} \ [\Omega]; \tag{5}$$

$$C = \frac{k^2(kr_s + x_s)}{2\pi f(1+k^2)z_s^2 \cdot 10^{-6}} \ [\mu F]. \tag{6}$$

where

$$z_s^2 = r_s^2 + x_s^2 .$$

In the case of fully symmetrical motors with equal numbers of effective turns in the stator phases, formulae 5 and 6 simplify to:

$$r_{sh} = \frac{2z_s^2}{(x_s - r_s)} \ [\Omega]; \tag{7}$$

$$C = \frac{r_s + x_s}{4\pi f z_s^2 \cdot 10^{-6}} \ [\mu F]. \tag{8}$$

There is another method of determining the parameters (C and r_{sh}) of

the system necessary for ensuring the symmetrical performance of the capacitor motor. Let us now consider this geometrical method.

The symmetry condition postulates the equality of the vector of the positive sequence current ($\dot{I}_s$) and the sum of the vectors $\overline{OA}_1$ and $\overline{A_1C}$ (Fig. 3). The angle between the vectors $\overline{OA}_1$ and $\overline{A_1C}$ should always be $\frac{\pi}{2}$, and that between $\overline{OA}_1$ and $\overline{OC} = \dot{I}_s$ (for the symmetry condition) should be β = arc tan k; the modulus of the vector $\overline{A_1C}$ is always k times greater than the modulus of the vector $\overline{OA}_1$ (1,2). Bearing in mind that the angle $< \overline{OA}_1C$, equal to $\frac{\pi}{2}$ rests on the corresponding current vector $\dot{I}_s$ under symmetrical motor operating conditions, then to determine the parameters C and r_{sh} at the given slip by the geometrical method, it is necessary to plot a circle with a centre O_2 and then to draw a straight line from the origin at an angle β = arc tan k to the current vector $\dot{I}_s$ until it intersects the newly plotted circle (point A_1).

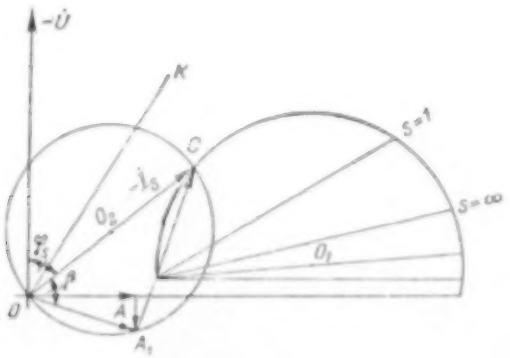

Fig. 3.

If a perpendicular is now erected from point A_1 to the axis of the abscissa until it intersects it at point A, we then obtain the vectors $\overline{OA} = Y'_C$ and $U\,\overline{AA}_1 = Y'_r\,U$. After measuring these on the current scale and dividing them by U, we obtain the conductances Y_r and Y_C referred to the voltage of the main phase. Since $Y_r = \frac{1}{k^2 r_{sh}}$ and $Y_C = -\frac{1}{k^2 x_C}$, we can determine those values of C and r_{sh} which ensure the symmetrical performance of the motor for the given slip.

This is illustrated by an example in Fig.3 for $s \neq 1$. For the sake of clarity, the circle diagram is plotted with an increased no load motor current.

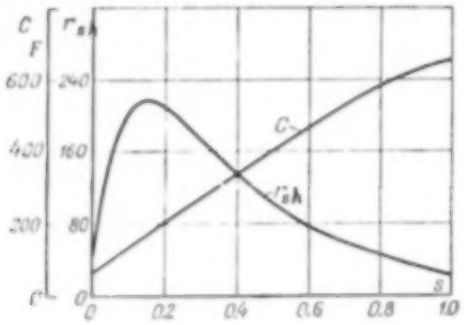

Fig. 4.

Fig.4 shows curves plotted by the proposed method which illustrate the variation of the capacitance and shunting resistance necessary to obtain symmetrical performance from a two-phase AOS42-2 type motor with a transformation ratio of $k = 3$ over the range from $s = 1$ to $s = 0$ at 380 V.

It should be mentioned that the use of a shunting resistance can lead to a reduction in efficiency if the motor is in operation for long periods owing to the inevitable power losses in the shunting resistance. However, this circumstance may not play the decisive role in a number of cases.

Translated by O.M. Blunn

REFERENCES

1. R. Rikhter: *Electrical machines, (Elektricheskie mashiny).* GONTI, Vol.4, (1939).
2. O.A. Nekrasov and G.G. Rekus: *Elekt. i avtomat.*, No.1, (1958).
3. V.S. Kulebankin: *Elektrichestvo*, No.7, (1956).

STEP MOTORS*

B.A. IVOBOTENKO

(Moscow Power Institute)

(Received 18 March 1960)

Step motors (electrical pulse motors) serve to convert electrical pulses into discrete angular or linear motions ("steps"). Step motors are now widely used in programme control systems for electrical drives. By converting digital information in the form of electrical pulses into a corresponding motion, i.e. performing the function of an output decoding link, step motors make it possible to design automatic control systems of the successively discrete type which have no need of feedback since the motion is made to correspond unambiguously to the digit.

The following types of step motor are in existence: (a), indicator (servo-step) motors and power motors; (b), reversing and non-reversing motors; (c), motors with a rigid mechanical or flexible electromagnetic shaft coupling; (d), d.c. and a.c. motors**; (e), motors with disconnexion of the control winding or with polarity reversal of the control winding (on arrival of the controlling pulse); (f), motors with a react ·e or active rotor and (h), single-or multistator motors of the cylindrical or "face" designs.

Other distinctive characteristics of step motors are the size of the step, the number of separately switchable control windings, the method of damping the free oscillations of the rotor which arise when the

---

* *Elektrichestvo*, No.8, 54-61, 1960.

** In the following we consider step motors supplied from a d.c. source. By taking the appropriate measures to compensate the variable component of the synchronizing moment, we can feed the control winding of the step motor with a.c. Here the mains frequency is the carrier and the frequency at which the controlling pulses follow is the modulator.

step is produced and so on.

Review of existing step motor systems

Step motors with rigid shaft coupling. The first step motor which appeared in the last century and is still widely used is a combination of a magnet with a ratchet and reduction gear. This type of step motor cannot be reversed. The reversing step motor has two magnets and two ratchets. The steps are produced by connecting the magnet winding to a direct voltage source. The ratchet retaining device ensures that the shaft is stopped exactly after the step has been made. Thanks to the rigid shaft coupling, the step motor does not itself produce errors in the system, but the presence of a cam, "anchor" or ratchet device complicates the design, reduces its reliability and imposes limitations on the rate at which pulses can be passed. Step motors of this type operate reliably with pulses up to 50 c/s. They develop a torque on the output shaft of the order of several hundred gram-centimetres. They are used in "counters", step selectors and various indicator devices.

One of the modern designs [1] has been produced for aero-navigation instruments. The axle of the step motor is turned in steps of $\alpha = 36^{\circ}$ from a solenoid drive. Location is by means of a perforated divider disk, cam and dog. In the reversing design two solenoids are used.

Step motors with unequal numbers of stator and rotor poles. Step motors with an electromagnetic clutch include the broad class of motors with unequal but approximately the same numbers of salient poles on the stator and rotor. These enable a considerable number of steps to be made per revolution with a comparatively small number of poles, i.e. these motors use the principle of electro-mechanical reduction.

In the case of SCh type step motors [2] there are 6 stator poles and 4 rotor poles. There are 24 steps of $\alpha = 15^{\circ}$ per rev.

Only some of the concentrated control windings on the stator are connected to a direct voltage source at any time. The step is produced by the excitation of another combination of windings and stator poles (the previously connected windings being disconnected). Static synchronizing moments on the shaft do not exceed several thousand g.cm. The dynamic torque of step motors falls very sharply with the frequency of the pulses (with a fixed supply source voltage). The pulse rate (without forcing may be at a frequency of $f = 70$ to 100 c/s.

Step motors with distributed stator windings. Use may be made of a synchronous reactive motor (for example, an ST type motor or a three phase selsyn) as a step motor. Here the phase windings are star-connected without bringing out the neutral point. At each instant two

of the phases in parallel and in series with the third phase are connected to a direct voltage source. The steps are produced by successive polarity reversal of the windings. Each reversal corresponds to the revolution in space of the vector of the resulting m.m.f. through 60 el deg. ST-type step motors develop a static synchronizing torque up to several thousand g.cm. Their dynamic properties and value in use are considerably higher than those of salient pole step motors, but the large step, the distorting influence of tooth harmonics (reducing the exactness with which the step is produced) and the low specific synchronizing torque due to the distributed field in the air gap often detract from their stated merits.

Power step motors. The development of programme-controlled machines has led to a demand for power step motors which will develop a torque of up to 1 kg.m or more on the shaft. The way in which power step motors are being developed is by combining servo-type step motors with torsion amplifiers. Another way is to create power step motors proper.

The Machine Institute of the Academy of Sciences U.S.S.R. and the Scientific Research Institute POLYGRAFMASH in 1950 jointly produced a step motor with a mechanical torsion amplifier [3]. The power source in this gear was a built-in induction motor from which rotation was transmitted to half-sleeves freely mounted on the shaft. The steps were produced by a brake device with an electromagnetic drive. The direction of the steps was determined by the connexion of one of the half-sleeves. Further research is continuing in the Machine Institute of the Academy of Sciences U.S.S.R. on the improvement of step motors with mechanical torsion amplifiers.

A system has been developed in ENIMS which uses a servo-type step motor with a hydraulic torsion amplifier thereby ensuring an output torque of M = 5 kg. m. A description has been given elsewhere [4] of two modified three-stator step motors, i.e. with an external rotor and with an intermediate hollow rotor. Without dwelling on the operating principle of three-stator step motors which will be elucidated below, let us confine ourselves here to the basic data of the ShDE-01 type step motors made at ENIMS.

Depending on the system of control (based on semiconductor triodes), this type of step motor has steps of $\alpha = 1.5^\circ/0.75^\circ$, $3^\circ/1.5^\circ$ and $6^\circ/3^\circ$. The maximum static synchronizing torque of the ShDE-01 ($1.5^\circ/0.75^\circ$) type motor is $M_{max} = 30$ kg. cm; the torque on the production of single pulses is $M_{f=0}$ 17.5 kg. cm. The motor will start with an instantaneous increase in the pulse rate (pick-up frequency) of $f_p = 200$ c/s with a load torque of $M_l = 6$ kg. cm (with forcing $r_{ext} = r_{\omega} = 5.5$).

Multi-stator step motors. A three-stator step motor [5,6] was pro-

duced in the U.S.A. in 1952. This was a modified version of the step motor proposed by the Russian engineer S.A. Nozdrevskii in 1925. The step motor consists of three indentical stators and three rotors. The control windings are laid in open slots in each stator. The number of control poles is usually the same as the number of teeth on the stator and rotor, which can either be active or reactive. The rotor "packets" are offset 1/3 tooth pitch relative to one another, whereas the axes of the stator teeth coincide. When voltage pulses are fed to the stator control windings in a certain cycle (1 – 2 – 3 – 1), the rotor is turned producing a step equal to 1/3 tooth pitch for each pulse. Reversing is effected by changing the sequence in which the pulses are fed (1 – 3 – – 2 – 1). Stopping is brought about by a long passage of current through the winding of one of the stators. The control system for the three-stator step motor shown in Fig.1 is quite simple.

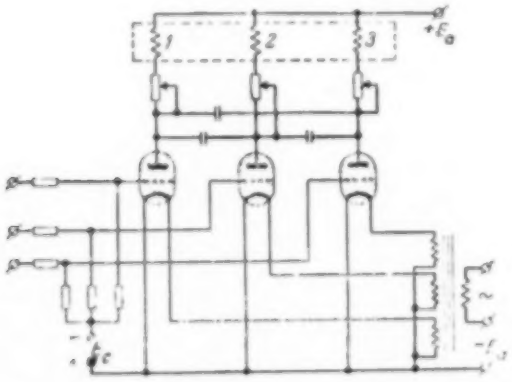

Fig. 1. Basic circuit of a three phase trigger: 1 – 3 – control windings of a three-stator step motor.

The Industrial Controls Corporation has produced a trial batch of three-stator power step motors [7]. The largest motor in this series has a maximum static torque of 34.5 kg. m. The greatest pulse rate at which the step motor in this series can be started without loss of step (pick-up) varies between 70 and 100 c/s.

The dimensions and moment of inertia of a three-stator step motor can be reduced one third by changing over to the two-stator design [8] shown in Fig.2(a). The packets of the two rotors are shifted a half of a tooth division relative to one another. A two-stator rotor can only work if a "ratchet" type of sleeve is fitted which ensures free rotation in one direction but which wedges the shaft during movement in the opposite direction.

Fig. 2(b) shows a reversing two-position "ratchet" retainer, which in its simplest form consists of a pulley, a band with two rollers and a wedging shoe with an oblique-angled slot milled in it. The steps are produced by the successive energization of the stator control winding. The two-position retainer is thrown over into another position to obtain reverse.

The Electrical Engineering Institute of the Academy of Sciences U.S.S.R. (E.E.I.), the Moscow Power Institute (M.P.I) and the All-Union Scientific Research Institute METMASH have jointly developed and in conjunction with a number of other project organizations constructed various types of three-stator power step motors.

The E.E.I. motor [9] has the following characteristics: number of steps per rev $i = 108$; a four-pole control winding is arranged on each stator in 36 slots; the maximum static moment is 1 kg. m; pick-up with sevenfold forcing $f_p = 150$ c/s; the pulse pass band is up to 350 c/s.

The M.P.I. and METMASH step motors (Fig. 3) make 72 steps per rev; a single-layer 24-pole control winding is arranged on each stator in 24 slots; the maximum static moment is 1.5 kg. m. In order to reduce the moment of inertia, the rotor is made hollow; pick-up with 1½ times forcing $f_p = 110$ c/s; the pulse pass band is up to 550 c/s.

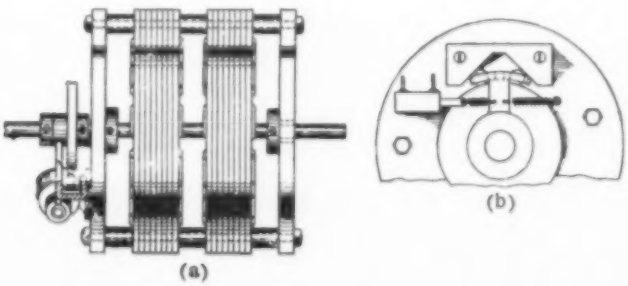

Fig. 2. General view of a two-stator step motor with a ratchet retainer (a) and of a two-position reversing retainer (b).

To eliminate labour consuming operations involved in packing the multi-pole control winding in the stator slots and to reduce the magnetic leakage, METMASH has developed a type of three-stator step motor with a toroidal control winding on each stator (Fig. 4). The magnetic circuit of the stators comprises radially-oriented π-shaped packets of sheet steel which are secured by non-magnetic separators. The

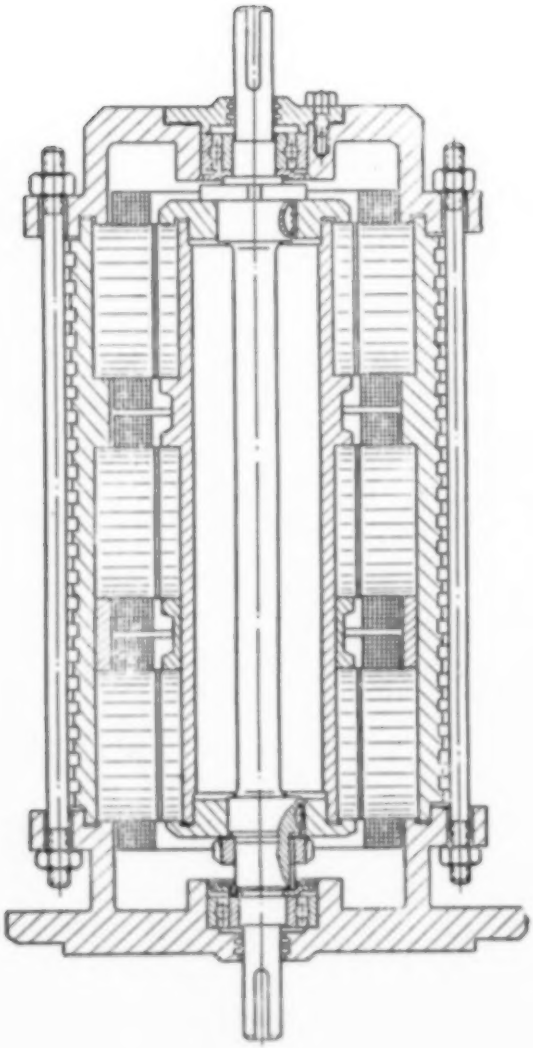

Fig. 3. MPI-METMASH – type three-stator step motor.

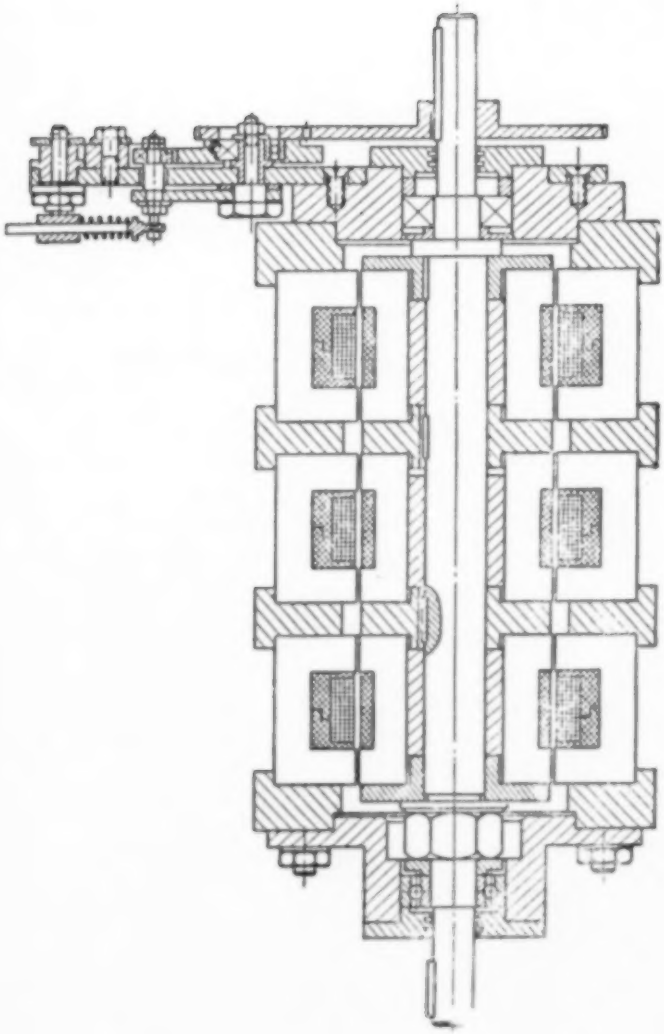

Fig. 4. METMASH-type three-stator step motor with ratchet retainer.

design of the windings is simple and yet a considerable increase in their time constants has been achieved.

Basic operating conditions and the requirements step motors have to satisfy

The basic quantities which fully characterize step motors are:

1. The step in degrees α or the number of steps per rev $i = \frac{360^\circ}{\alpha}$.

2. The maximum static synchronizing moment M_{max}.

3. The specific synchronizing moment $\frac{dM}{d\theta}$, where θ is the mis-match of the longtitudinal axes of the stator and rotor in geometric degrees.

4. The multiple of the starting moment $\frac{M_{st}}{M_{max}}$

5. The static quality factor, defined as the ratio of the maximum static moment to the weight of the step motor: $D_S = \frac{M_{max}}{G}$.

6. The electromagnetic time constant of the control winding T.

7. The dynamic quality factor, defined as the ratio of the maximum static moment to the mouent of inertia of the rotor $D_d = \frac{M_{max}}{J}$.

8. Pick-up (i.e. the greatest frequency of pulse rate f_p at which the step motor can be suddenly started or stopped without loss of step) depends on the dynamic quality factor of the step motor.

9. The pulse pass band. Its upper limit corresponds to the pulse rate f_o at which the average dynamic moment on the shaft of the step motor, without forcing the pulses, falls practically to zero (it depends on the electromagnetic time constant of the control winding).

The dynamic quality factor and electromagnetic time constant, pick-up and pulse pass band define the dynamic properties of step motors (their operating speed).

10. The internal damping C, by which is meant the size of the coefficient for the time derivative of the angle in the rotor control winding in the production of a step, is caused by the internal properties of the step motor itself, and not by the properties of the load or starting device.

11. Efficiency. This is a function of the pulse rate. The efficiencies of two step motors can be compared when the electromagnetic time constants of their control windings are "equated" by means of addition-

al resistances taken into account.

We can call the following items "characteristic states". Altogether these constitute the performance of the motor when control pulses governed by any arbitrary law are supplied:

1. Fixed stopping under current.

2. The production of single pulses. Depending on the nature of the load, the design of the damping device and the magnitude of the internal damping, the damping of the free oscillations of the rotor occupies an interval of time which considerably exceeds the time taken to produce the step, or the production of the step is aperiodic.

3. Starting, stopping and reversing. The step motor can perform the listed commands in the range of frequencies up to the pick-up frequency. Given identical external conditions, the starting frequency is always slightly lower than the stopping frequency of the step motor. In the process of starting with the pick-up frequency, the step motor, in overcoming the inert masses, produces an incomplete step after each pulse during the first few pulses, but it remains within the limits of the zone of stability after each subsequent pulse. The wider the zone of stability (relative to the amount of step), the higher is the frequency with which the motor is started without loss of step (and only with time delay of the rotor in the process of acceleration).

4. The quasi-stationary stepping state with a pulse rate up to the pick-up frequency. Depending on the dynamic properties of the step motor, the nature of the load and the pulse rate, the production of the step may bear an oscillatory or aperiodic character. The free oscillations of the rotor are expressed most significantly at low frequencies of the pulse rate and at the resonance frequency of the drive in question. In this case the ratchet retainer really improves the performance of the step motor or is sometimes necessary for normal performance.

5. The state of synchronous rotation corresponding to a pulse rate higher than the pick-up frequency. Step motors need a change of state, cannot be stopped suddenly and cease to be "stepping" motors in the true sense of the word.

Let us state certain general requirements which modern step motors must satisfy:

1. Maximum operating speed.

2. The production of steps of the order of several degrees of fractions of a degree.

3. The simultaneous use of all the active materials of the machine in the creation of the synchronizing moment on the shaft.

4. The possibility of internally damping the free oscillations of the rotor in the process of producing the step.

5. Sufficiently wide range of stability with regard to step size.

6. The minimum angular error in the performance of the system due to the step motor, i.e. a considerable specific synchronizing moment is required.

7. No accumulation of errors should occur when the number of steps is increased.

8. The minimum number of control windings which can be separately switched.

9. Reliable operation.

1960

Comparative characteristics of various step motor systems

The step motors considered above satisfy the enumerated requirements to varying extents.

Step motors with a rigid shaft coupling do not themselves bring errors into the performance of the system, but they have the slowest performance. The theoretical maximum efficiency cannot be more than 50 per cent since the energy of the magnetic field accumulated in the control winding circuit when the step is produced is dissipated in the form of heat in the switching device and has to be accumulated again when the next pulse is fed.

The same shortcoming is inherent in salient-pole motors with different numbers of stator and rotor poles and in multi-stator step motors. The production of a small step in these mcahines leaves some of the active materials unused. Hence greater weight, dimensions and moment of inertia of the rotor. Consequently, pick-up is inadequate.

The excitation and quenching of the field in the air gap cyclically with the pulse rate bring about considerable pulsations in torque on the shaft of the step motor. If there is no "overlapping" in the periods of successive excitation of the control windings, the instantaneous values of the synchronizing moment pass through zero. This is instrumental in causing vibration in the production of the step and renders it difficult to operate on active load. It is impossible to

fit a damping "cage" on the rotor since the contours of the damping cage slow down the increase in flux or current and create a negative asynchronous moment in the process of producing the step. The magnetic circuits of both rotor and stator should be laminated for the same reasons. The oscillations of the rotor are damped either by the moment of friction of the load or by the ratchet retainer.

The possibility of producing a very small step, the considerable specific synchronizing moment and the comparative simplicity of the control system are the main merits of step motors with salient poles on the stator and rotor.

Step motors with distributed windings on the stator are characterized by considerably greater operating speed, usage of the active materials, effeciency, uniformity of the synchronizing moment and there is greater scope for damping the free oscillations of the rotor. They cannot however produce a sufficiently small step; they possess a low specific synchronizing moment, cannot ensure the same degree of accuracy in the production of the step and require more complicated systems of control.

Let us consider the Stovbunenko step motor with its intermediate swinging (pendulum) rotor.

In the excitation of a two-pole stator the intermediate rotor completes oscillations and during forward operation engages the internal rotor which is connected direct to the output shaft. From the point of view of the requirements which step motors have to satisfy, this is not a successful design and possesses the following real disadvantages: (a) the useful forward movement of the shaft corresponds to the double (forward and back) movement of the intermediate rotor, i.e. other things being equal, twice as much time is taken to produce a step; (b) the intermediate rotor brings about a large (considerably larger than in the internal rotor) parasitic moment of inertia which sharply reduces the dynamic quality factor of the step motor; (c) an electromagnetic or mechanical retainer is required to hold the internal rotor during the pause between two pulses.

Regardless of the type of design, servo step motors possess a considerably better dynamic quality factor than do power step motors. This is explained by the fact that the moment of inertia of the rotor increases in proportion to the fourth power of the motor's diameter, whilst the synchronizing moment only increases in proportion to the third power.

With an increase in the number of poles, given the same dimensions of the step motor, there is a sinultaneous reduction in the synchronizing moment and the electromagnetic time constant of the control windings,

but magnetic leakage increases.

Step motors with an active rotor have a zone of stability which is twice that of step motors with a reactive rotor.

Reversing step motors require a larger number of control windings and more complicated control systems than do non-reversing step motors.

New step motor systems

Research has been going on in the electro-mechanical problem laboratory of the Moscow Power Institute into the design of step motors combining the satisfactory features of salient pole step motors and step motors with distributed stator windings. The possibility is opening up for step motors with two, three or several control windings which in their entirety on the stator form a two-phase, three-phase or m-phase winding respectively with a number of slots per pole and phase of $q = 1$. All the control windings are simultaneously connected to a direct voltage source and participate in the creation of the synchronizing moment. The control windings are transformer - connected between themselves and with the damping cage which must be provided on the rotor. The rotor can be either reactive or active (with an excitation winding, magnetization on the stator side, permanent magnets or hysteresis "sleeve"). There should be the same number of rotor poles as there are stator teeth divided by the number of control windings.

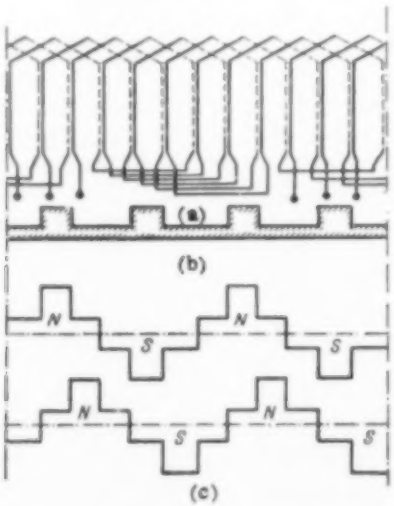

Fig. 5. Three phase step motor with a step equal to one stater tooth pitch.
a - control windings; b - schematic representation of stator;
c - curves for the resulting m.m.f. displaced on step.

All the control windings jointly create the resulting m.m.f. in the air gap. When the controlling pulse is applied the polarity of one of the winding connexions is reversed, (the resulting m.m.f. and rotor are then displaced by one tooth pitch of the stator in the clockwise or anti-clockwise direction as a function of the sequence in which and two control windings respectively, the orientation of the rotor poles and the steady state diagram of the m.m.f. in the air gap.

The controlling pulses create no additional flux in the air gap. The field only deformed and shifted one step. As a result, (a) the electromagnetic time constants of the control windings are strictly dependent on the size of the step and the number of control windings which can be separately switched; (b) efficiency increases sharply, the theoretical maximum value of which reaches 100 per cent; (c) a continuous torque is ensured on the shaft of the step motor.

The increase in the number of separately switchable control windings complicates the switching system of the step motor, but the zone of stability is extended and pick-up is appreciably improved.

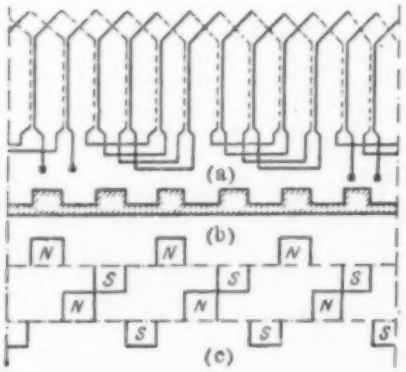

Fig. 6. Two phase step motor with a step equal to one stater tooth pitch:
a – control windings; b – schematic representation of rotor; c – curves for the resulting m.m.f.

The greatest practical interest is attached to step motors with two control windings (Fig. 6) and a reactive rotor with a large damping cage (stability zone $\pm \frac{1}{2} \alpha$) or an active rotor with permanent magnets or hysterisis (stability zone $\pm \alpha$) [10].

A step of the order of one degree, or a fraction of a degree, may be produced with a small number of slots on the stator if teeth are cut

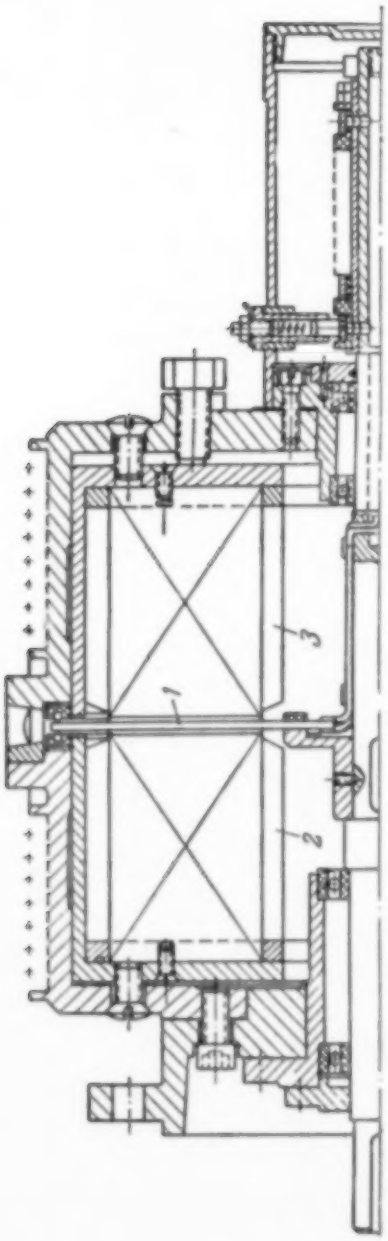

Fig. 7. Step motor with printed windings on a disk rotor:
1 – rotor; 2 and 3 – stators.

1960

in the stator poles of the step motor and the rotor made in multi-pole (toothed) form. The step motor is similar in design to an inductor generator. The teeth of the rotor are co-axial with the teeth of any pair of stator poles and are displaced by a fraction ($^1/_3$, $^1/_4$, $^1/_6$) of a tooth division relative to the teeth of the remaining stator poles. The rotor may be active or reactive; if active, use is made of the "hysteresis" material vikalloy.

The radical improvement in the pick-up of the step motor is achieved by a flat rotor in the form of a thin disk 1 to 2 mm thick, the faces of this disk carry the control winding circuits (two or three) in printed form. Due to the large cooling surface and the absence of insulation on the conductors, the current density of the windings can be made of the order of 30 to 40 A/mm^2 during prolonged operation and 100 A/mm^2 momentarily. This high current density makes it possible to develop a high electromagnetic moment when the rotor interacts with the stator field, and yet the weight, dimensions and moment of inertia of the rotor are negligible.

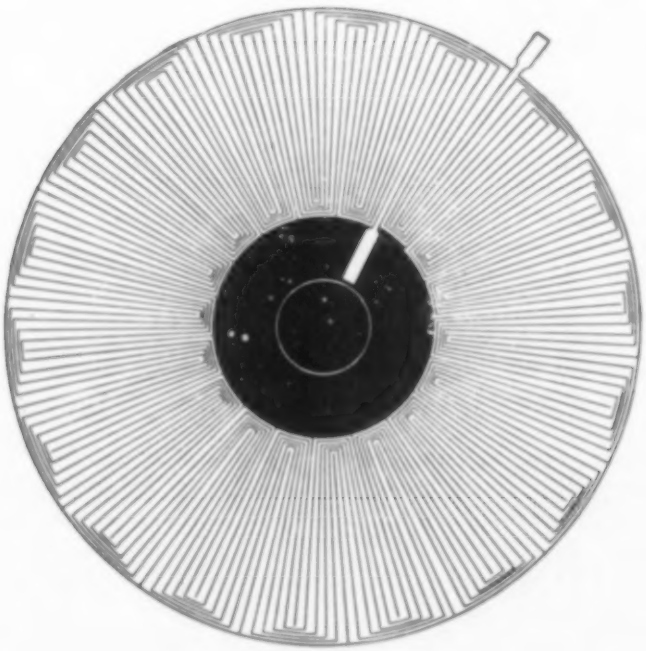

Fig. 8. A wave-type 36-pole printed rotor control winding.

Fig. 7 shows the design of these step motors as developed in the

electromechanical problem laboratory of the Moscow Power Institute [11]. The face-type stator consists of two symmetrical halves with radially oriented excitation poles in the form of sectors of a circle. The stator poles are made from permanent magnets or are provided with a single-layer winding along which direct current passes. The pole system of the stator creates a flat-parallel field in the air gap of the machine. The lines of this field are oriented along the axis of the step motor shaft. The disk rotor can be mounted on a non-magnetic or ferromagnetic base; in the latter case, supports are provided around the periphery of the air gap on the stator which protect the rotor from "sticking" as a result of unilateral magnetic stresses of distortion. The rotor consists of one or several layers stuck together. The number layers can be equal to, or a multiple of, the number of control windings. Wave windings are applied photochemically on both sides of the layer (Fig.8). These form a multilayer system similar to the stator pole system. Provision is made for a shift equal to the size of the step between the windings. The beginnings and ends of the windings are connected to slip rings. The controlling pulses are fed to these rings via brushes. The presence of sliding contacts is a shortcoming in step motors with printed control windings on the rotor.

1960

Translated by O.M. Blunn

REFERENCES

1. Patent No.2752513 (U.S.A.). Express information, No.47, (1957).
2. Iu.S. Chechet; *Micro machines for automatic devices, (Elektricheskie mikromashiny avtomaticheskikh ustroistv)*. Gosenergoizdat (1957).
3. M.G. Breido, A.E. Kobrinskii and V.K. Besstrashnov; *Stanki i instr.*, No.12 (1958).
4. V.G. Zusman and V.A. Ratmirov; *Stanki i instr.*, No.12 (1958).
5. A.G. Thomas; Motor, 2,782,354. d/d 19 February 1957, United States Patent Office, No.2.
6. A.G. Thomas; *Elec. Mfg.*, 56, No.6, 152-153, 318-322 (1955).
7. A.G. Thomas and F.J. Pleischauer; *Cont. eng.*, 74-81, Jan. (1957).
8. A.G. Thomas; 2,808,556 d/d 1 October 1957, United States Patent Office.
9. B.O. Sigov; *Avtomatika, Akad. Nauk Ukr.S.S.R.*, No.4, (1957).
10. B.A. Ivobotenko and V.K. Tsatsenkin; Auth. Cert. No.126768, *Byull. izobretenii*, No.5, (1960).
11. A.A. Sirotin, B.A. Ivobotenko, L.A. Sadooskii, N.G. Sokolov and V.K. Tsatsenkin; Auth. Cert. No.126394. *Byull. izobretenii*, No.4 (1960).

AUTOMATIC ELECTRICAL OPTIMIZERS*

L.N. FITSNER

(Institute of Automatics and Telemechanics of the Academy of Sciences, U.S.S.R.)

(Received 29 October 1959)

During recent years a number of works have been published dealing with extremal systems of regulation [1-6]. In these systems the value of one or several input quantities (x_1, x_2 .... x_n) of the object of search is found for which the output quantity of the object, depending on the input quantities $y\ (x_1, x_2, \ldots . x_n)$, will assume its maximum or minimum value. If y is a differentiable function, then at the extreme point

$$\frac{\partial y}{\partial x_i} = 0, \tag{1}$$

where $i = 1, 2, \ldots, n$.

An analysis of the state of the extremal systems at a certain instant is not enough to determine the requisite direction of change in that parameter x_i which will bring the system into a state that satisfies the given conditions. To define this direction, it is necessary to measure the changes in x_i when they occur in the system, or even to introduce them specially (here it is necessary to analyse the changes in the value of y due to changes in x_i).

This process is called "trial". Only by comparing the quantities or, in the extreme case, just the signs of the increments or decrements in x_i and y, can we determine the direction of change in x_i and then bring the system into the state such that equation (1) is satisfied.

The entire process of automatic searching consists of a series of

* *Elektrichestvo*, 8, pp. 61-67, 1960.

trials and operational movements. External systems, like other automatic control systems, can be represented in the form of the connexion between the object on which the search is made and the controlling part which we shall call the automatic optimizer.

Automatic optimizers make it possible to find and maintain automatically the relationship between the quantities of fuel and air at which the greatest amount of heat is generated in the process of combustion. They make it possible to find the most economic relationship between the amount of mazut ("DERG") and gaseous fuel fed to an open-hearth furnace fired on mixed fuel. They make it possible to tune oscillatory circuits in the large cascades of radio transmitters to the frequency of the master generator and so on.

In the following, a description is given of two automatic electrical optimizers developed in the Institute of Automatics and Telemechanics of the Academy of Sciences U. S. S. R. These optimizers make it possible to find the extremal values of functions y for one variable x if one point in the given region corresponds to the value $dy/dx = 0$.

1960

The automatic relay-type optimizer

The block diagram of this optimizer is shown in Fig. 1. The optimizer comprises a differentiating block *DB*, intended to determine the sign of the variation in the value of y to be optimized during a period of time T given by the pulse generator *PG*.

When determining the minimum of y, the executive device *ED* will vary input quantity of the object *O* towards the extreme point if

$$y(t+T) < y(t). \tag{2}$$

If the sign in inequality 2 is changed, it is necessary for the input quantity x to change in the opposite direction. This operation is performed by the "direction-of-movement unit" *DM* which gives the command "reverse" to the executive device.

The relay optimizer (Fig. 2) consists of a polarized relay P_1, three non-polarized moving-coil relays P_2, P_3 and P_4 and a resistance r. On closure of the contact $2P_2$, the input voltage of the optimizer is fed at the input to a cell consisting of a capacitor C_1 and the polarized relay P_1, which are connected in series. In this case the direction of the current through the coil of the polarized relay P_1 at the moment of closure of the contact $2P_2$ depends on the sign of the variation in y during the interval of time given by the pulse generator *PG*.

If the optimizer has to find the minimum value of the voltage y, then the input quantity of the object should vary under the action of the

executive device if the changes in y are negative.

If the changes in y are positive, it is necessary to reverse the direction of movement *DM*. This operation is performed by the contacts $2P_3$ and $3P_4$. Relay P_1 is tuned in such a way that if there is no current or, if it is in the negative direction, in its winding, the contact $1P_1$, acting on the relay trigger (Relay P_3 and P_4) is in the position indicated in the circuit. If the variations in y are positive, the contact opens for a small interval of time.

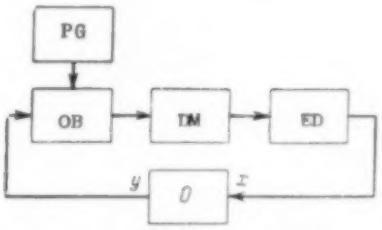

Fig. 1. Block diagram of automatic relay-type optimizer.

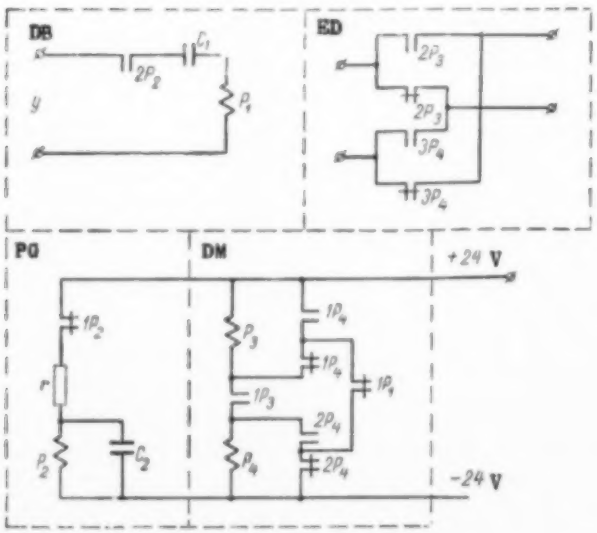

Fig. 2. Electrical circuit of relay-type optimizer.

Current passes through one of the windings of relay P_3 or P_4. The position of the contacts shown in the circuit corresponds to the passage of current through winding P_3. There is no current through

winding P_4 since it is shunted by contacts $1P_1$ and $2P_4$. If the contact $1P_1$ breaks the shunting circuit, relay P_4 will operate and this switches the contacts $1P_4$ and $2P_4$ to a new position in which the winding of relay P_3 is shunted. The passage of current through the relay winding P_3 ceases and its contacts are switched. Thus, with positive changes in y, contact $1P_1$ breaks the circuit shunting one of the windings of relays P_3 or P_4. As a result, the position of the contacts of these relays and the direction of motion of the executive device controlled by the contacts $2P_3$ and $3P_4$ change.

Fig. 3. Block diagram of extremal system.

The periodic connexion of the voltage y by contact $2P_2$ is carried out by the pulse generator *PG*. In order to increase the sensitivity of the differentiating block, provision is made to include a two-stage semiconductor triode amplifier. If use is made of a polystyrene capacitor as the capacitance C_1, the interval of time between measurements of the changes can be increased to several hours.

Let us consider the process of finding the extremal point in a system comprising an automatic optimizer *AO* (Fig.3) and an inert object *O* which can be represented in the form of two series-connected parts: a linear inert part (*LI*) and a non-linear "non-inert" part (*N*).

Suppose that the linear part of the object can be represented in the form of a chain of n series-connected inert links with a transfer function $\eta(t)$ and an integrating link.

Three main types of search process are possible in this system. The top of Fig.4 shows the static characteristic of the object. The bottom shows the variation in the input quantity of the non-linear part of the object over the course of time. The horizontal lines correspond to pulses fed to the winding of the optimizer's input relay P_1 (see Fig.2). The space of time between these pulses is T.

Let the parameter x at the start of the search move at maximum speed from x_0 to x_a and pass successively through points 1, 2 and 3. At point 4 the optimizer will not detect changes in the sign of the variations since points 3 and 4 refer to identical values of y. It is only at point 5 that the optimizer will detect the incorrect direction of movement and by means of relays $2P_3$ and $3P_4$ (see Fig.2) change the polarity of the voltage at the input to the object. The nature of

further movement in the system depends on the relationship between the parameters of the inert part of the object and the time intervals T.

The next measurement of the variation in y can be taken at points lying close to (6′) and further than (6) from the extremal point compared with point 5. In the first case the system will continue movement in the correct direction to the extremal point and begin to "roam" about the latter (curve 1). In the second case the variation in the output quantity of the object y will be positive in sign. The optimizer will change the polarity of the voltage at the input to the object and the variation will begin to change in the incorrect direction. The optimizer will detect the positive variation and change the polarity of the voltage at the input to the object only at point 8 or 8″.

Further movement of the system is only possible in two directions. If during the interval of time between points 7 and 8 the output quantity of the "little chain of inert links" (μ) should fail to reach maximum and is sufficiently small, then x will drop from point 8″ to point 9″. In this case the variation in y will be negative and x will vary in the direction of the extremal point (curve 2). Finally, if the value of μ at point 8 is large enough, x will drop from point 8 to point 9, which is further removed from the extremal point. The optimizer will change the polarity of the voltage at the input to the object and x will pass through points 10, 11, 12 and 13 successively, moving further away from the extreme (curve 3). In this case the search process is unstable.

Let us determine the relationships between the parameters of the optimizer and those of the object O corresponding to the cases of system movement that we have considered.

Fig. 5 shows the behaviour of the output quantity of the chain of inert links μ on receipt at their input of a command to move in the positive direction (section 5-6 or 5 – 6′ in Fig. 4).

The equation of this curve has the form

$$\mu = \mu_{max}[2\eta(t) - 1]. \tag{3}$$

The area of the shaded section S_1 in Fig. 5 is proportional to the distance between x and the extremal point after the sign of the input quantity of the object has been changed. The area of the shaded section S_2 is proportional to the change in x on the section 5-6 towards the extreme.

The movement of the system along the curve 1 (see Fig. 4) is only possible if point 6 is nearer point 5 than to the value of x_m, i.e. if

$$S_2 > S_1. \tag{4}$$

When the sign of this inequality is positive, parameter x will be moved further from the extreme point (curves 2 and 3).

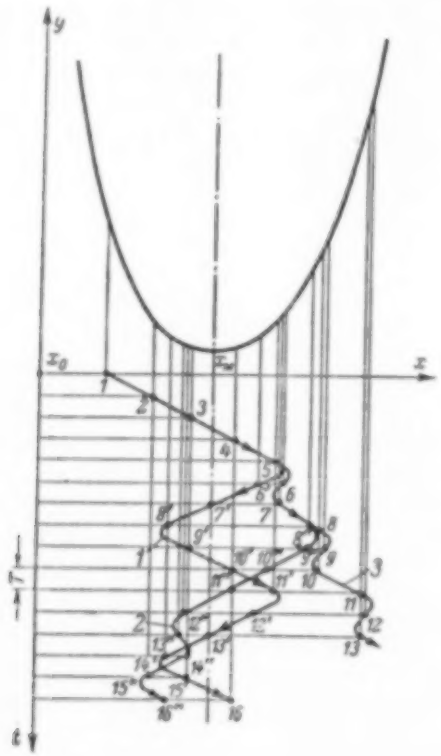

Fig. 4. Various trajectories of the automatic search for the extremal point.

The following equation holds for the boundaries between these two types of movement

$$S_1 = S_2 \tag{5}$$

or

$$\mu_{max} \int_0^T [2\eta_1(t) - 1]\, dt = 0. \tag{6}$$

Using equations (5) and (6), we can define the regions of the parameters and the initial states of the automatic search system for a given T or the values of T for given regions of parameters or initial

states at which the system would "roam" about the extremal point after it has been defined (curve 1).

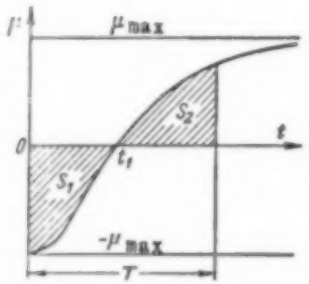

Fig. 5. The behaviour of the output quantity from a chain of inert links after the command to change the direction of the search.

Assume that the inert part consists of one inert link with a time constant τ and an integrating link. After substituting the transfer function of the inert link in equation (6) we get $T = 1.59\tau$. Consequently, such a system is capable of operating when $T > 1.59\ \tau$. Likewise for an object whose linear part consists of a delay link with a delay time τ_d and an integrating link, we get: $T > 2\ \tau_d$.

The automatic search relay system has been investigated on an electronic model. Oscillograms of the search process corresponding to the three types of trajectory of motion under consideration are shown in Fig. 6.

The interference-resistant proportionality optimizer

As a rule the determination of the quantity $z = dy/dx$ in extremal systems is connected with great difficulties. Only the sign of z can be defined comparatively easily. This is not always acceptable since auto-oscillations arise in the system at the extremal points of the functions. The amplitude of the auto-oscillations in inert systems can be considerable and the error caused by them impermissible.

Methods of devising extremal systems have been studied by Draper [2] in which, to determine the extremal point, the input signal contains a component of triangular or sinusoidal shape with a constant amplitude and frequency in addition to the basic slowly varying component. In the majority of cases such a system makes it possible to find the deviation of the input quantity from the points at which y assumes extreme values and to use it to form the controlling signal.

But this method of determining the extremal values of functions is unacceptable because the system is constantly under the effect of disturbances, sometimes of considerable magnitude.

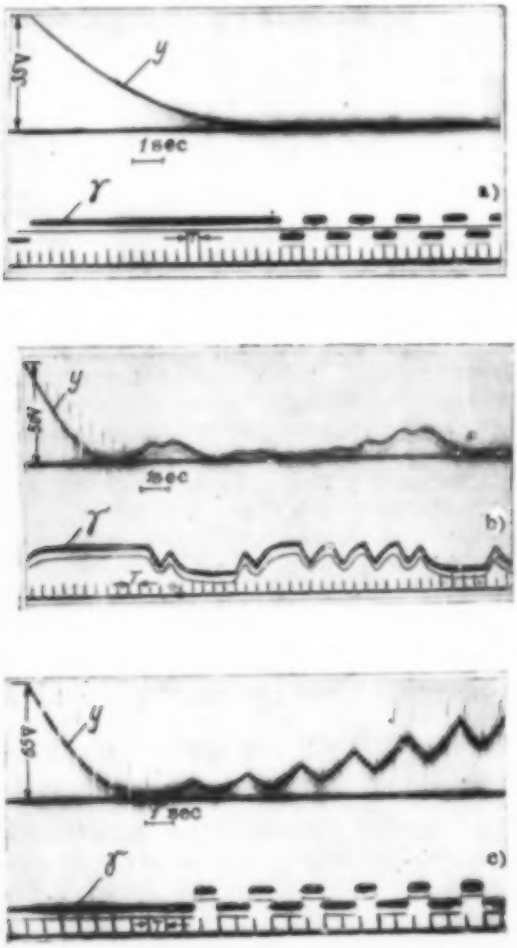

Fig. 6. Oscillograms of the search process: a – search in an inert system; b – search in a system with $\tau_1 = 0.3$ sec and $\tau_2 = 0.03$ sec; c – search in a system with $\tau_3 = 0.85$ sec; y is the output quantity of the object of the search and γ the input quantity of the object of search.

The automatic optimizer under consideration below is to a consider-

able extent free from the stated shortcoming.

A memory device *MD* is installed at the input to the optimizer. This determines the difference between the current (contemporaneous) value of y and the value of y at the moments of time taken as zero (y_o) which the memory device *MD* has stored.

The difference $y-y_o$ is fed to the input to the integrating link IL. The output quantity of this link is

$$V = c\int_0^t (y - y_0)\,dt. \tag{7}$$

If during the process of integration the value of V reaches the threshold P, equal to $\pm P_o$, commands are then fed into the memory device in order to store the new value of the output quantity y_o, into the integrating link in order to return it to the original zero state and into the unit for forming the controlling signal (*UFCS*). The latter gives an order for the adjustment of the executive device (*ED*) to one or the other side depending on the sign of P. In the event of minimum being determined on movement of *ED* in the correct direction, the values of V should be negative. Therefore, if V are positive, a command is given from the *UFCS* for the *ED* to reverse, so that the direction of the last step is opposite to the direction of the previous step.

In this method of determining minimum, the executive device receives orders after intervals of time T which are connected with the output quantities of the object by the equation

$$P = c\int_0^T (y - y_0)\,dt, \tag{8}$$

which is obtained from 7 by substituting P for V and T for t. It follows from the latter equation that the value of P will reach one of the values $\pm P_0$ the more rapidly, the greater the difference $y-y_0$. Consequently, on increasing this difference, the intervals of time will be reduced between pulses fed to the *ED* and the speed of the latter will be increased.

If there were no interference in the object *O* or the optimizer, the executive device would then stop at the minimum point if the command pulses were of short duration. In fact, the system varies about the minimum point; but the period of these variations is large and, consequently, the additional disturbances introduced into the system are relatively small.

The electrical circuit of the optimizer is shown in Fig.8. The input quantity y is fed to the memory device *MD*, which consists of two cathode

followers (F_1).

A capacitance C is connected to the first cathode follower. On operation of relay P_1, this capacitance is connected for short intervals of time to a point with zero potential. For the larger part of the period T the capacitance is connected to the grid of the second cathode follower. The output of this follower in this case receives a voltage which is proportional to the difference $y_o - y$. Here y_o stands for the voltage stored in capacitor C.

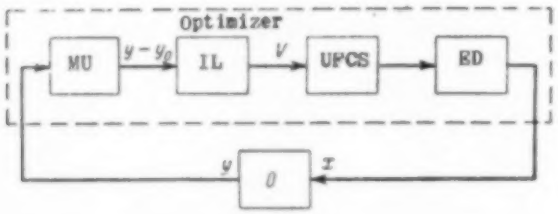

Fig. 7. Block diagram of interference-resistant proportionality optimizer.

The voltage is fed from the output of the *MD* to the integrating link which incorporates amplifiers with a large amplification factor (A_2 or A_3) operating under deep negative feedback conditions. The striking anode of the thyratron with a cold cathode T_1 is connected at the output from the integrating link (*IL*).

If the voltage at the output of the *IL* exceeds the striking voltage of the thyratron T_1, the latter is ignited. Relay P_1 operates here. This switches the capacitance in the *MD*, discharges the capacitor of the integrating link, feeds a voltage to the coil of relay P_3 and breaks the the supply circuit of the thyratron T_1.

When relay P_3 operates, a voltage is fed to the executive device *ED*, which in this case is a two phase induction motor.

The positive voltage at the output of the *IL* testifies to the incorrect direction of the movement of the system. If this voltage exceeds that of the ignition voltage of the neon tube N in value, the latter is ignited. The voltage pulse arising in this case is fed to the input to the thyratron triggers T_2 and T_3. Under the action of the pulse, the trigger changes state and by means of the two-winding polarized relay P_2 switches the motor winding in order to change the direction of rotation of the executive device.

The neon tube N is ignited at a lower voltage than that igniting the

1960

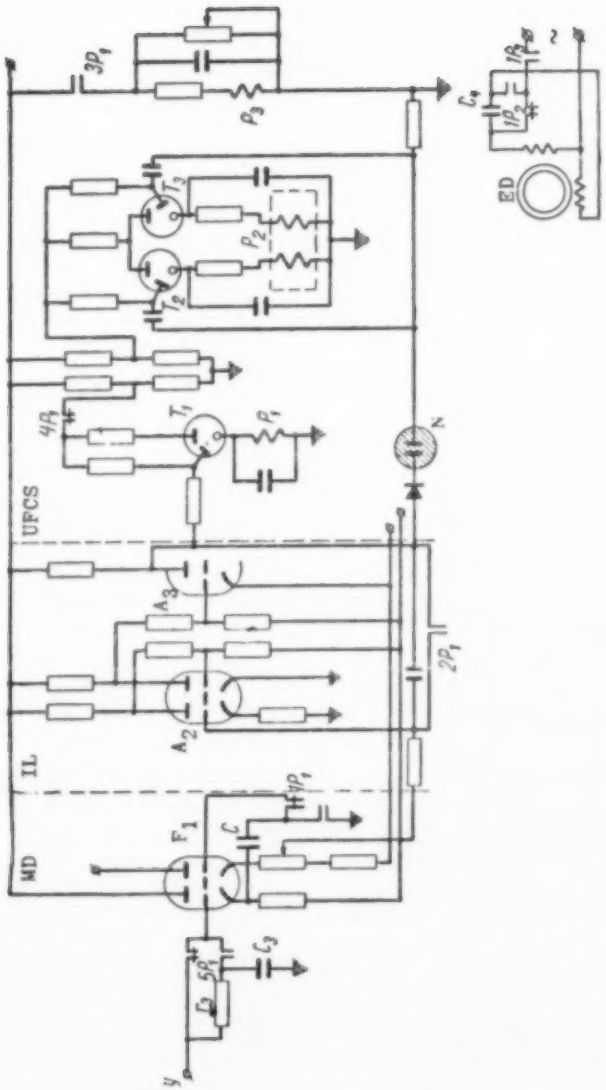

Fig. 8. Electrical circuit of optimizer.

thyratron T_1. Therefore, if the voltage at the output of the *IL* is positive, the winding of the motor is first of all switched by contact IP_2. A voltage is then fed to the motor, which in this case rotates in the opposite direction.

In order to reduce the effect of interference on the memorized quantity without appreciably affecting the time taken for the search, the input quantity of the *MD* is fed from the output of an inert link (r_3 and C_3) for storage.

This type of optimizer can also find the values of x for which the derivative dy/dx equals any desired value other than zero. To do this, a direct voltage source is connected at the input to the *IL*.

This type of optimizer can also find the values of x for which the derivative dy/dx equals any desired value other than zero. To do this, a direct voltage source is connected at the input to the *IL*.

1960

The optimizer has been tested on an electronic model and in a real system of automatic anode-circuit tuning in the power cascade of a radio transmitter in resonance with the frequency of the master generator.

The anode circuit was tuned by a motor controlled automatic optimizer. Since the tuning of the circuit in resonance with the master generator corresponds to the minimum value of the constant component of the anode current, a drop in voltage proportional to this component was fed to the input to the optimizer.

At the same time as the anode circuit was tuned in resonance, use was made of a second motor to regulate the link with the aerial whilst keeping the anode current at a definite value. The link was increased or decreased by means of a regulator with the aerial. In this case the automatic search system and regulation system worked together. This made it possible to maintain the minimum value of the anode current with a high degree of accuracy. The existance of a considerable variable frequency component of 50 c/s in the anode current had practically no effect on the search process.

The combined operation of the regulation and search systems did not introduce any appreciable mutual interference. The tuning of the transmitter lasted for 10 to 20 sec. Tuning time depended on the value of the established integration constant and the amount of preliminary tuning of the transmitter. The error in maintaining the minimum anode current did not exceed 0.5 per cent. After completing the search process, the optimizer "roamed" about the extreme point on account of the interference. The "roaming" period depended on the magnitude of the integration constant and did not take more than 10 to 25 sec. An

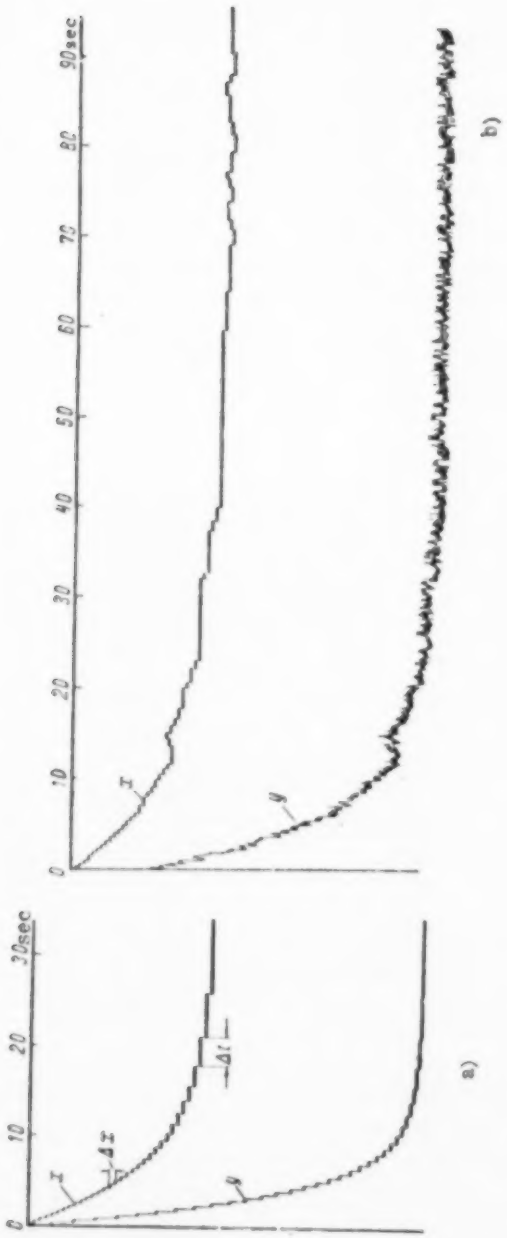

Fig. 9. Oscillograms of the search process:
a – without interference; b – with interference.

optimizer is installed at a radio transmitter which is now in commission.

Fig.9 shows the process of finding the extremal point in a system consisting of an automatic optimizer, and an electronic model of the object of the search. The oscillograms describe the behaviour of the parameters x and y over the course of time. The search process in Fig.9(a) took place without random noise. The size of the step $\triangle x$ is independent of the distance to the extremal point, whilst the intervals of time $\triangle t$ between steps increase in so far as the system approaches the extremal point.

Fig.9(b) shows the search process in a similar system but with random noise at the output of the object. The values of x, y and t are on the same scale in Fig.9. The optimizer will find the extremal point even if interference is present, although in this case it takes slightly longer to complete the search.

1960

Fig. 10. General view of the 1A01 - 1 type optimizer.

A photograph of the 1A01-1 type optimizer is shown in Fig.10.

Conclusion

Experimental investigations into an automatic relay-type optimizer

have shown that the performance of the optimizer will be reliable and the search process stable if the intervals of time between variations in y are chosen correctly by the stated formula.

The performance of the interference-resistant proportionality optimizer has been checked in two extremal systems. The first system enabled us to find the minimum value of the anode current in the output cascade of a radio transmitter in order to tune its oscillatory circuit automatically. The other system was a carriage whose movement was controlled by an automatic optimizer. The carriage automatically found the plane of the region with maximum or minimum values of illumination. Substantial interference had no appreciable effect on the search process. The proportionality optimizer is now installed on an existing radio transmitter.

It is proposed that use be made of such optimizers to determine automatically the best relationship between fuel and air in open-hearth furnaces and soaking pits, to determine the best disposition of workpieces in machining processes and to automate certain objects in the chemical industry.

Translated by O.M. Blunn

REFERENCES

1. V.V. Kazakevich; *On extremal regulation, (Ob ekstremel'nom regulirovanii)*, Diss. MVTU, (1945).
2. C.S. Draper and Y.T. Li; *ASME*, No.1, (1951).
3. A.A. Fel'dbaum; *Avtomat. i telemekh.*, No.8 (1958).
4. B. White; *Instruments and automation*, No.11 (1956).
5. L.N. Fitsner; Auth. Cert. No.598259, 25 April (1958).
6. L.N. Fitsner; Auth. Cert. No.589657, 8 January (1958).

ABSTRACTS FROM PAPERS PUBLISHED IN ELEKTRICHESTVO No.8 1960

Mathematical modelling of a power system with "strong-acting" field regulation of its generator. B.M. Kagan and E.L. Urman, (1-9).

In view of the scope for computers in the analysis of dynamic and static stability of synchronous generators in power transmission systems, an investigation has been made to develop a mathematical description and methods of simulating transient processes for transmission systems incorporating synchronous generators with high response type excitation regulators. The authors also elucidate the extent to which the results of mathematical simulation by the proposed method agree with the results of experiments in the same system. The high response type regulator is illustrated by a diagram.

A computer distributing real power flow for a given fuel consumption. V.M. Sin'kov, V.L. Zasenko, V.P. Kovalenko and K.Iu. Fol'kman, (pp. 9-16).

After referring to the various computing devices developed in the U.S.S.R. for power distribution, the authors consider the main criteria of economic distribution. An account is given of EKRAN-3 and EKRAN-4 computing devices. They comprise a device for reviewing the load graphs of the power stations, load distribution units at the stations and total system and line distribution units. The devices are now in production for the Bashkir, Donbas, Sverdlovsk and Chelyabinsk grid systems.

Accounting for the inter-system effect in designing large power transmission systems. V.V. Bolotov, G.E. Burtseva and E.P. Zakharova, (pp.16-22).

A description is given of a method of taking into account the savings made by combining power systems in the national grid with different types of power station and different load conditions. The article

discusses the systems existing in Central Siberia and Kazakhstan using the abundant open cast coal available there.

The basis for the development of the consolidated Siberian power pool system. V.I. Veits, (pp. 22-28).

Referring to the priority given in the U.S.S.R. to the development of electricity and the unique untapped power resources of Siberia in cheap open cast coal and its mineral resources, an account is given of the plans for the development of this region and the role the electrical industry is to play. Reference is made to plans for power transmission from Siberia to the Urals. The Siberian grid system is to be based on hydro-electric power stations and conventional fuel fired stations. An account is given of the main features of the system.

Zero sequence circuit diagram for several closely running lines. N.G. Geinin, (pp. 28-32).

When transmission lines are running parallel with each other a few metres apart, the zero sequence impedance of each line depends on the currents in the adjacent lines owing to mutual inductance. As this should be taken into account for relay protection against earth faults, the author proposes certain zero sequence equivalent networks.

Transforming a quasi-stationary magnetic field to the potential field of its sources. V.M. Greshniakov, (pp. 33-36).

The author considers the magneto-static problem of the field of vector H. In the presence of currents this field does not possess the solenoid character of the physical field of the vector B nor the potential nature of the simple field of the sources. He proposes a method of eliminating these difficulties by introducing a generalized intensity vector.

Analysis of a transistorized stabilizer circuit. A.N. Ananas'ev, (pp. 39-42).

A description is given of the physical aspect of the performance of transistorized stabilizers and the factors affecting the stability of the output voltage are elucidated. The purpose is to facilitate work on transistorized voltage stabilizers in the project stage.

The analysis of transistors in multivibrators. I. Kalish, (pp. 43-47).

Reference is made to the Konev modulator used to generate rectangular

voltage control pulses and a study is then made of the effect on the discharge time of the controlling voltage applied to the discharge circuits of the condensers.

The torque and speed characteristics of d.c. micromotors. L.I. Stolov, (pp. 47-51).

After reviewing the factors affecting the torque speed curves of fractional horse power motors, the author proposes new design equations for f.h.p. motors with various excitation systems, but series excitation in particular. The case of reversing is considered. Good agreement between theoretical and experimental results is obtained.

The electrical properties and application of VK-2, VK-3 and VK-4 type piezoelectric crystals and variable condensers. T.N. Verbitskaia, (pp. 68-75).

1960

The author is specially interested in the use of non-linear properties of piezo-electric crystals (Rochelle-salt-ceramics) and the development of apparatus using variable condensers. He lists the positive and negative aspects of V.K.-1 type piezo-electric crystals and gives an account of the research undertaken to develop new grades type VK-2, VK-3 and VK-4. VK-2 can now be used for technical purposes and VK-3 and VK-4 have been used to produce specimen laboratory variable condensers. The new materials have good technological properties. Further research is being undertaken to improve their coefficients of non-linearity, increase their stability characteristics and reduce dielectric losses.

Compensation of the temperature error in induction meters and wattmeters by means of semiconductor thermistors. A.M. Iliukovich, (pp. 76-79).

To remedy the great temperature error in induction meters and wattmeters and so improve accuracy the author refers to the various methods which have been proposed on the basis of thermo-magnetic alloys. He advocates the use of semiconductor thermal resistors instead such as the Russian MMT-8 and MMT-9. He proposes a scheme whereby this can be done so that the shift in phase between the flows remains constant under different temperature conditions. A quantitative analysis is made by means of a vector diagram and equivalent network.

A current diagram and a universal equivalent circuit for

salient synchronous and parametric machines. I.M. Postnikov, (pp. 79-81).

The theory of parametric (or "reactive") synchronous machines has been worked out in detail by Iu.S. Chetet and the author confines himself to deriving the locus of the current hodograph (circle diagram) with stator resistance and losses in the steel taken into account and to obtaining an accurate equivalent network which is applicable to machines having poles which are excited by direct current or permanent magnets besides parametric synchronous machines.

FIRST FUNDAMENTALS OF AN ANALYTICAL THEORY FOR DISCONTINUOUS FUNCTIONS IN THE DESIGN OF NON-LINEAR ELECTRICAL CIRCUITS*

L. L. IVANOV

Bauman Technical College, Moscow

(Received 9 May 1960)

1960

Widespread use is made of discontinuous functions or functions having discontinuous derivatives in the study of non-linear circuits for modern automatic systems cybernetics, electronics and current rectification. The known methods of calculating processes in such circuits require solutions for the individual intervals of time bounded by the points of discontinuity and the subsequent conjugation (assignment) of these solutions to the points of discontinuity.

This paper expounds a method developed by the author which enables the processes in such circuits to be described by analytical expressions covering the entire region of variation of the unknowns. The solutions referring to the individual regions bounded by the points of discontinuity are automatically assigned. The method is based on the use of modulus-functions and "anti" functions. Its application to the solution of practical electrical engineering and mechanical problems has been expounded in a previous article by the author "Collected Scientific Works of the MVTU"**.

---

* *Elektrichestvo*, 9, 23-29, 1960.

** L. L. Ivanov, Contribution to the solution of problems with discontinuous functions or functions with discontinuous derivatives), (K resheniiu zadach s funtsiiami imeiushchimi razryvnye proizvodnye ili razryvy nepreryvnosti), Sborn. nauchnyth trud, MVTU (Bauman Technical College Moscow), 87, 1958.

There it was shown that, in order to remove the necessary reservations imposed on the use of the method, an analytical theory of discontinuous functions based on special hyper-complex numbers generalizing (normalizing) both real and complex numbers had to be developed. There have been many attempts to produce such a theory, the first being in 1913, but it was a hopeless situation and the attempts were cut short. The author renewed his attempts in 1937 and only in 1947 did he obtain a first acceptable result. The start of this theory is formulated in this article. But first we shall deal with the elements of the theory and consider a number of examples. It will be seen that the theory is of practical value even though further elaboration is required. The elements of the theory and the examples have been studied in greater detail in the article previously referred to.

Elements of the theory. In the design of non-linear electrical circuits that can be characterized by discontinuous functions, use may conveniently be made of the modulus – function (Fig. 1):

$$y=|x|=\begin{cases} x & \text{if } x>0; \\ -x & \text{if } x<0; \end{cases} \tag{1}$$

the "anti"-function (the nearest whole function contained in x, Fig. 2):

$$y=\overleftarrow{E}_1(x) \tag{2}$$

and the periodic-function with a period of one (Fig. 3):

$$\overleftarrow{\theta}_1(x)=x \quad \overleftarrow{E}_1(x). \tag{3}$$

Fig. 1.

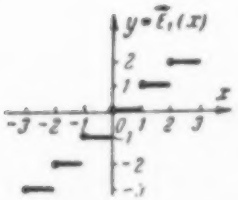

Fig. 2.

Fig. 3.

A function with a period $|L|$ can also be considered:

$$\overleftarrow{\theta}_L(x)=L\theta_1\left(\frac{x}{L}\right)=x-L\overleftarrow{E}_1\left(\frac{x}{L}\right)= \\ =x-\overleftarrow{E}_L(x). \tag{4}$$

The following function

$$y = f[\overleftarrow{\theta}_L(x)] \tag{5}$$

will be periodic with a period no greater than $|L|$.

If $L > 0$, the values of $f(x)$ will be periodically repeated when $0 < x < L$; if $L < 0$, when $L < x < 0$.

In order to produce discontinuous functions or functions with discontinuous derivatives, we have to introduce discontinuities (Figs. 4 to 7):

$$\overset{b}{1}_a(x) = \frac{1}{2}\left(\frac{|x-a|}{x-a} - \frac{|x-b|}{x-b}\right), \tag{6}$$

$$1_a(x) = \overset{+\infty}{1}_a(x) = \frac{1}{2}\left(1 + \frac{|x-a|}{x-a}\right), \tag{7}$$

$$\overset{b}{1}_{-\infty}(x) = \overset{b}{1} = \frac{1}{2}\left(1 - \frac{|x-b|}{x-b}\right) = \overset{0}{1}(x-b) = 1 - \overset{b}{1}_b(x). \tag{8}$$

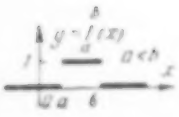

Fig. 4.

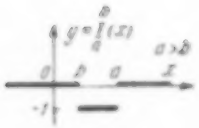

Fig. 5.

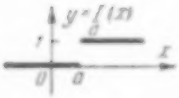

Fig. 6.

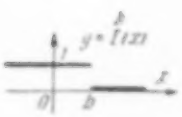

Fig. 7.

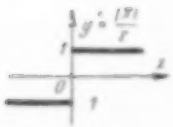

Fig. 8.

In transformations with discontinuities it is convenient to use identities of the following type:

$$\frac{|x-y|}{x-y} f(x, t) = 2f\left(\frac{x+y+|x-y|}{2}, t\right) - f(x, t) - f(y, t) + \frac{|x-y|}{x-y} f(y, t), \tag{9}$$

where $t = \phi(x)$ is any arbitrary function of x.

One inequality or equality can be substituted for several inequalities. Thus, for example, $A \geqslant 0$ is equivalent to

$$A - |A| = 0, \tag{10}$$

whilst $A > 0$ corresponds to

$$1 - \frac{|A|}{A} = 0. \tag{11}$$

If there are n inequalities

$$F_1 > 0;\ F_2 > 0, \ldots,\ F_n > 0$$

we have to write the corresponding n equalities

$$F_1 - |F_1| = 0; \quad F_2 - |F_2| = 0, \ldots, \quad F_n - |F_n| = 0$$

and then one equality equivalent to all the inequalities:

$$\sum_{i=1}^{n} F_i - \sum_{i=1}^{n} |F_i| = 0. \tag{12}$$

The two inequalities $A > 0$ and $B > 0$ are equivalent to one inequality

$$A + B - |A - B| > 0. \tag{13}$$

In the same way, n inequalities are reduced to one inequality and the latter to one equality.

The derivative of $y = |x|$ is obviously (Fig. 8):

$$y' = \frac{d|x|}{dx} = \frac{|x|}{x} = \frac{x}{|x|}. \tag{14}$$

Consequently,

$$\frac{d|f(x)|}{dx} = \frac{|f(x)|}{f(x)} \cdot \frac{df(x)}{dx}. \tag{15}$$

In the case of higher order derivatives when $x \neq 0$, we get:

$$\frac{d^n|x|}{dx^n} = 0.$$

Generally speaking

$$\frac{d^n|x|}{dx^n} = (-1)^{n-2}(n-2)!\frac{2\delta(x)}{x^{n-2}}. \tag{16}$$

if $n \geqslant 2$ $(0! = 1)$

Here $\delta(x)$ is the Dirac delta function:

$$\delta(x) = -\frac{1}{2}\frac{d^2|x|}{dx^2}, \tag{17}$$

since

$$-\frac{1}{2}\int_{-\infty}^{+\infty} d\frac{|x|}{x} = 1,$$

if the integral is considered in the Stieltjes sense.

Quite general formulae can be produced for integrals such as

$$\int f[x, |\varphi(x)|]dx \quad \text{and} \quad \int f[x, E(x)]dx$$

In the simplest case

$$\int |x|^n dx = \frac{x|x|^n}{n+1} + C \quad (n \neq -1). \tag{18}$$

We can also produce the formula:

$$\frac{dE_1(x)}{dx} = \pi\delta(\sin \pi x). \tag{19}$$

Example 1.

Imagine the following function (Fig. 9):

if $x < a$

$$y = b,$$

if $x \geqslant a$

$$y = b\cos(x - a).$$

Applying discontinuities (7) and (8), the function becomes one equality:

$$y = \overset{a}{1}(x)\, b\cos(x-a) + \overset{a}{1}(x)\, b =$$
$$= \frac{1}{2}\left(1 + \frac{|x-a|}{x-a}\right) b\cos(x-a) +$$
$$+ \frac{1}{2}\left(1 - \frac{|x-a|}{x-a}\right) b.$$

Applying identity (9), we get:

$$\frac{|x-a|}{x-a}\cos(x-a) =$$
$$= 2\cos\left(\frac{x+a+|x-a|}{2} - a\right) - \cos(x-a) -$$
$$- \cos 0 + \frac{|x-a|}{x-a}\cos 0.$$

Therefore the function can be expressed by one equation

$$y = b\cos\left(\frac{x-a+|x-a|}{2}\right).$$

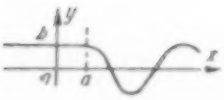

Fig. 9.

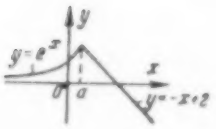

Fig. 10.

Fig. 11.

Fig. 12.

Fig. 13.

Example 2.
The equation of the line in Fig.10 is

$$y = \frac{1}{2}(e^x - x + 2 - |e^x + x - 2|).$$

N.B. There is no need to know the co-ordinate a of the point of con-

jugation. Neither need the co-ordinates of many points of conjugation be calculated.

Example 3.

It is supposed that $y = f_1(x)$ with increasing x and that $y = f_2(x)$ with decreasing x (Fig. 11).

Both relationships can be described by one equation:

$$y = \frac{1}{2}[f_1(x) + f_2(x)] + \frac{1}{2}\frac{|dx|}{dx}[f_1(x) - f_2(x)].$$

Such functions frequently occur in practice and are usually regarded as multiple-valued. The method in question is suitable for phase diagrams ("portraits").

If $x = \text{const}$, we can study the limits on the right or left to remove the indeterminacy.

1960

Example 4. Suppose that an electrical circuit includes a rectifier valve (Fig. 12) having resistances r_1 and r_2 in the conducting and reverse directions respectively ($r_2 \gg r_1$). It is assumed that the valve current is

$$i = \overset{1}{\underset{0}{}}(u)\frac{u}{r_1} + \overset{0}{\underset{}{1}}(u)\frac{u}{r_2},$$

Hence

$$i = au + b|u|,$$

where

$$a = \frac{1}{2}\left(\frac{1}{r_1} + \frac{1}{r_2}\right) > 0; \quad b = \frac{1}{2}\left(\frac{1}{r_1} - \frac{1}{r_2}\right) > 0.$$

Likewise, the voltage is

$$u = mi - n|i|,$$

where

$$m = \frac{1}{2}(r_2 + r_1) > 0; \quad n = \frac{1}{2}(r_2 - r_1) > 0.$$

If the valve is ideal, i.e. $r_1 = 0$ and $\frac{1}{r_2} = 0$, the voltampere characteristic is shaped like that in Fig. 13. The points within, and on the sides of, the second co-ordinate angle correspond to

$$-u \geqslant 0,\ ki \geqslant 0,$$

where k is any positive quantity (in Ω).

Substituting one equivalent inequality (see 13) for these inequalities, and casting away the inequality sign, the equation of the volt-ampere characteristic is:

$$u - ki + |u + ki| = 0.$$

Example 5.

Using the formulae produced in example (4), we can produce a formula for the output voltage u_2 of the two-sided valve-amplitude-limiter shown in Fig. 14, namely,

$$u_2 = \frac{u_1}{A} + \frac{B}{2AC}(|u_1 + CE| - |u_1 - CE|),$$

where

$$A = 1 + r_0\left(\frac{1}{r_1} + \frac{1}{r_2} + \frac{1}{r}\right) > 0;$$

$$B = r_0\left(\frac{1}{r_1} - \frac{1}{r_2}\right) > 0;$$

$$C = A - B > 0,$$

Here r_1 and r_2 are the resistances in the conducting and reverse directions respectively.

If $r_1 = 0$ and $\frac{1}{r_2} = 0$, we get

$$u_2 = \frac{1}{2C}(|u_1 + CE| - |u_1 - CE|),$$

where

$$C = 1 + \frac{r_0}{r}.$$

Example 6.

Suppose that the formula for the steady state current in a diode coil (Fig. 15) is

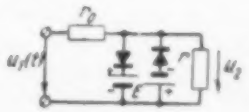

Fig. 14.

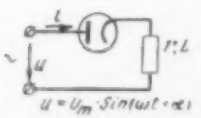

Fig. 15.

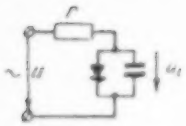

Fig. 16.

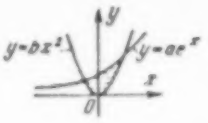

Fig. 17.

$$i=\frac{U_m}{2z}\left\{\sin(\omega t+\alpha-\varphi)+\right.$$

$$+(\sin\varphi)\,e^{-\frac{r}{\omega L}\theta_{2\pi}(\omega t+\alpha)}\Big|+\sin(\omega t+\alpha-\varphi)+$$

$$\left.+(\sin\varphi)\,e^{-\frac{r}{\omega L}\theta_{2\pi}(\omega t+\alpha)}\right\}.$$

The differential equation for current i is

$$\left|u-L\frac{di}{dt}\right|+u-L\frac{di}{dt}=2ri.$$

However, such an equation satisfies the voltage u_C of a capacitor to which an ideal valve is connected in parallel (Fig.16):

$$\left|v-rC\frac{dx}{dt}\right|+v-rC\frac{dx}{dt}=2x,$$

where

$$x=-u_C;\quad v=-u=U_m\sin(\omega t+\alpha+\pi).$$

Fundamentals of an analytical theory for discontinuous functions

It can be seen from these examples that use may expediently be made of modulus-functions and "anti" functions in the solution of non-linear problems. The proposed method ensures the automatic conjugation of the solutions at the points of discontinuity in functions and their derivatives. This at times eliminates the numerous and laborious conditions (usually inequalities) which divide up the region of variation of the variables. This method also reduces the number of equalities required to obtain the solution, thereby making it a clearer and more convenient method of analysis.

Various n - dimensional loci can be represented by one equation. The character of the variation of the variables can be taken into account at the same time (in the sense of example 3). For example, the co-ordinates of the points of the shaded area in Fig.17 are

$$ae^x - y \geq 0 \quad \text{and} \quad y - bx^3 \geq 0.$$

Substituting one equivalent inequality for these two (see 13), we get:

$$F = ae^x - bx^3 - |ae^x + bx^3 - 2y| \geq 0.$$

Disregarding the inequality sign we obtain the equation of the perimeter of the shaded area

$$F = 0. \tag{20}$$

The co-ordinates of the shaded area are obviously satisfied by the equation

$$F - |F| = 0$$

and all the points of the shaded area with the exception of those round the perimeter correspond to

$$1 - \frac{|F|}{F} = 0$$

But, when using modulus functions, there will be ensuing reservations determining the sub-region of variation of the variables in which one or another dependence is significant. Circumstances therefore arise which "partly contradict the purpose" of modulus - functions as functions instrumental in eliminating the reservations on the regions of variation of the variables, which reduces flexibility in operations with modulus-functions.

Thus, for example, solving equation (20) with respect to y, we get:

$$y = \frac{1}{2}[ae^x + bx^3 \pm (ae^x - bx^3)] \tag{21}$$

on condition that

$$ae^x - bx^3 \geq 0.$$

Otherwise, equation (20) is meaningless and there is no value for y.

Some equalities, for example, are senseless for all x:

$$|x| = -1; \quad |x| = 3 + 2j; \quad E(x) = 0{,}5;$$

$$E(x) = 0.5 + 3j \quad \text{and so on}$$

The first one, like $x^2 = -1$, is a senseless expression. The reason is this. The concept of numbers is too narrow in modern mathematics. The aim of an analytical theory of discontinuous functions is to eliminate this shortcoming by widening the concept of numbers. The conventional theory of analytical functions is a special case of theory based on the algebra of hyper-complex numbers (called "polinions"). Polinions are based on "real units"

$$1_0 = 1;\ 1_1;\ 1_2;\ 1_3 \ldots 1_n,$$

where n is the order of a real "one" 1_n.

The general form of an n-th order polinion is

$$z = a_0 + a_1 \cdot 1_1 + a_2 \cdot 1_2 + \ldots + a_n \cdot 1_n \ (a_n \neq 0),$$

where a_k ($k = 0, 1, 2, \ldots, n$) are conventional complex numbers.

1960

If all the a_k are real, the polinion z is also called real. Otherwise it is called complex. The equality of two polinions and the main operations on them are defined in the same way as in operation on complex numbers.

Suppose that the real numbers a and b are in a binary set:

$$a = 2^{\alpha_1} + 2^{\alpha_2} + \ldots + 2^{\alpha_p};$$
$$b = 2^{\beta_1} + 2^{\beta_2} + \ldots + 2^{\beta_q}.$$

The "partial" sum of a and b is

$$a \bullet b = 2^{\gamma_1} + 2^{\gamma_2} \ldots + 2^{\gamma_r},$$

where the terms (addends) consist of all the binary terms (addends) taken just the once. For example,

$$17 \bullet 20 = (2^4 + 1) \bullet (2^4 + 2^2) = 2^4 + 2^2 + 1 = 21.$$

The product of the real units is defined by the equality:

$$1_m 1_n = 1 - 1_m - 1_n + 2 \cdot 1_{m \bullet n}, \tag{22}$$

in particular, by

$$\begin{gathered} 1_0 1_0 = 1 - 1_0 - 1_0 + 2 \cdot 1_0 = 1 = 1 \cdot 1; \\ 1_m 1_0 = 1 - 1_m - 1_0 + 2 \cdot 1_m = 1_m = 1_m \cdot 1; \\ 1_m 1_m = 1_m^2 = 1; \end{gathered} \tag{23}$$

for example,

$$1_{17}1_{20}=1-1_{17}-1_{20}+2\cdot 1_{21}.$$

It can easily be seen that the "associative" and "commutation" laws are valid in polinion algebra, i.e.

$$(1_m1_n)1_p=1_m(1_n1_p)=(1_m1_p)1_n$$

and

$$1_m1_n=1_n1_m,$$

and, consequently, there are zero devisors (invariants), the general form of which is

$$\sum_{k=1}^{n} a_k(1\pm 1_k). \tag{24}$$

A modulus-function with a polinion variable is defined by the fundamental formula:

$$\begin{aligned}|x+1_ky|=\frac{1}{2}\Big[&(1-1_k1_{k-1})\frac{|x+y|}{x+y}+\\&+(1+1_k1_{k-1})\frac{|x-y|}{x-y}\Big](x+1_ky).\end{aligned} \tag{25}$$

Here x and y can be arbitrary polinions in their turn. This formula will always give the same result regardless of the type of transformation with polinions x and y and their coefficients a_k only if the polinion $x+1_ky$ is other than zero or the zero devisor (invariant).

From formula (25) we get

if $y=0$

$$|x|=\frac{|x|}{x}x;$$

if $x=0$

$$|1_ky|=-1_{k-1}\frac{|y|}{y}y. \tag{26}$$

Consequently,

$$\begin{aligned}|1_1y|&=-1_0|y|=-|y|;\\|1_0y|&=-1_{-1}|y|.\end{aligned} \tag{27}$$

Thus,

$$1_{-1} = -1, \ \ldots, \ 1_{-k} = -1 \tag{28}$$

when $k > 0$, if k is a whole number.

The following relations are also true:

$$|-z| = |z|, \tag{29}$$

$$|z_1 z_2| = |z_1| \cdot |z_2|, \tag{30}$$

whilst, for real polinions,

$$|z|^2 = |z^2| = z^2. \tag{31}$$

If t is a conventional complex variable quantity and $f(t)$ can be expanded in a Laurent series, the following identity will exist

$$\begin{aligned} f(x + 1_k y) = \frac{1}{2}[f(x+y) + f(x-y)] + \\ + 1_k \frac{1}{2}[f(x+y) - f(x-y)] = u(x, y) + \\ + 1_k v(x, y). \end{aligned} \tag{32}$$

For example,

$$e^{x+1_k y} = e^x \left[\frac{1}{2}(e^y + e^{-y}) + 1_k \frac{1}{2}(e^y - e^{-y})\right],$$

i.e.

$$e^{x+1_k y} = e^x [\cosh y + 1_k \sinh y].$$

Here x and y are any polinions.

The necessary and sufficient conditions for the existence of a derivative of the function

$$f(z) = u(x, y) + 1_k v(x, y), \tag{33}$$

where

$$z = x + 1_k y,$$

are

$$\left.\begin{aligned} \frac{\partial u}{\partial x} &= \frac{\partial v}{\partial y}; \\ \frac{\partial u}{\partial y} &= \frac{\partial v}{\partial x}. \end{aligned}\right\} \tag{34}$$

Here

$$\frac{df(z)}{dz}=\frac{\partial u}{\partial x}+1_k\frac{\partial v}{\partial x}=\frac{\partial v}{\partial y}+1_k\frac{\partial u}{\partial y}. \tag{35}$$

For example, we find from relations (32) to (35) that

$$(\cos z)'=-\sin z,$$

i.e. we get the same function as when differentiating functions of real variables. It is a very important property of polinion algebra that the rest of the known differentiation formulae retain their form.

We can put

$$\int_{z_0}^{z}F(z)\,dz=\int_{z_0}^{z}(u+1_k v)\,d(x+1_k y)=$$
$$=\int_{x_0,y_0}^{x,y}(u\,dx+v\,dy)+1_k\int_{x_0,y_0}^{x,y}(v\,dx+u\,dy). \tag{36}$$

If condition (34) is satisfied, the integrands in (36) are full differentials.

The following, for example, can easily be got from (36):

$$\int\sin(x+1_k y)\,d(x+1_k y)=$$
$$=-\cos(x+1_k y)+C.$$

If z is a real polinion, then, using a formula similar to (18), we get:

$$\int|z|\,dz=\frac{z|z|}{2}+C.$$

Suppose that $|x|=a$, where a is a real number. It can then easily be seen that the function, the reverse modulus-function (antimodulus), is

$$x=|a|_{-1}=\pm\frac{1}{2}[(a+|a|)+1_1(a-|a|)]=$$
$$=\pm\frac{|(a+1)+1_1(a-1)|}{(a+1)+1_1(a-1)}\cdot a.$$

We can also produce a formula for the anti-modulus of any polinion. Repeating the operation k times we get $|z|_{-k}$.

It can be seen that many expressions hitherto regarded as senseless now acquire a definite meaning. In this connexion we can draw the following analogy. Until use was made of complex numbers, the expression $x^2-y^2=1$ (Fig. 18) was meaningless if $x^2<1$. Similarly, $|x|-|y|=1$ (Fig. 19) is senseless when $|x|<1$ unless polinions are used. On the other hand, by using polinions we get for any real x:

$$y=\big||x|-1\big|_{-1}=\pm\frac{1}{2}[(|x|-1+\big||x|-1\big|)+$$
$$+1_1(|x|-1-\big||x|-1\big|)]$$

or

$$y=\pm\frac{1}{2}\Big[(1+1_1)(|x|-1)+(1-1_1)\big||x|-1\big|\Big].$$

Thus

if $|x|\geqslant 1$

$$y=\pm(|x|-1);$$

if $|x|<1$

$$y=\pm 1_1(|x|-1).$$

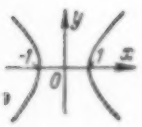

Fig. 18.

Fig. 19.

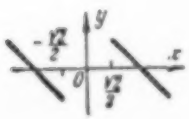

Fig. 20.

Polinions enable us to substitute variables (convert co-ordinates) unreservedly even in the case of the stated type of discontinuous functions.

For example, suppose that

$$v=\frac{|u|}{u}.$$

Putting

$$u=\frac{\sqrt{2}}{2}(x-y) \quad \text{and} \quad v=\frac{\sqrt{2}}{2}(x+y),$$

we get (Fig. 20):

$$x+y=\sqrt{2}\,\frac{|x-y|}{x-y}.$$

Previously this equation was meaningless if $|x|\leqslant \frac{\sqrt{2}}{2}$. Using polinions for any $|x|\neq \frac{\sqrt{2}}{2}$ we get:

$$y=-x+\sqrt{2}\,\frac{|2x\pm 1_k\sqrt{2}|}{2x\pm 1_k\sqrt{2}}.$$

This theory can be further extended if it is desired to impart meaning to $|x|=j$. Putting

$$\begin{aligned} j_k&=\frac{1}{2}(j-1)+1_k\frac{1}{2}(j+1)= \\ &=\frac{1}{2}(1+1_k)j-\frac{1}{2}(1-1_k), \end{aligned} \tag{37}$$

we find:

$$j_k^2=-1_k;\ j_0=j;\ j_{-1}=-1, \tag{38}$$

and also

$$j1_k=1-j-1_k+2\,j_k; \tag{39}$$

$$jj_k=j_k-j-1_k; \tag{40}$$

$$1_m j_n=1-1_m-j_n+2\cdot j_{m\cdot n}; \tag{41}$$

$$\begin{aligned} j_m j_n&=-1_{m\cdot n}-1_m-1_n+2\cdot j_{m\cdot n}= \\ &=j-j_m-j_n+(1+j)j_{m\cdot n}. \end{aligned} \tag{42}$$

N.B. Equality 42 is similar to 22, which can be written in the form

$$1_m 1_n=1_0-1_m-1_n+(1+1_0)1_{m\cdot n}.$$

On the usual assumption that $|j|=|j_0|=1$, we can obtain the recurrence formula:

$$|1_k j_k|=1_{k\cdot(k-1)}j_{k-1}, \tag{43}$$

which can also be represented as:

$$|j_k|=-1_{k-1}\cdot 1_{k\cdot(k-1)}j_{k-1}. \tag{44}$$

For example,

$$|1_1 j_1| = 1_{1\cdot 0} j_0 = 1_1 j,$$

i.e.

$$|1_2 j_1| = j$$

or

$$|j_1| = -1_1 j.$$

Likewise,

$$|1_2 j_2| = 1_{2\cdot 1} j_1 = 1_2 j_1,$$

i.e.

$$|1_1 1_2 1_4 j_2| = j_1$$

or

$$|j_2| = -1_1 1_2 j_1$$

and so on.

1960

There is a formula for the modulus $|x + j_k y|$ similar to the fundamental formula (25). Relations (29) and (30) also hold good. Instead of the Cauchy-Riemann conditions we have

$$\left.\begin{aligned} \frac{\partial u}{\partial x} &= \frac{\partial v}{\partial y}; \\ \frac{\partial u}{\partial y} &= -1_k \frac{\partial v}{\partial x}. \end{aligned}\right\} \tag{45}$$

We get Cauchy-Riemann conditions ($1_0 = 1$) if $k = 0$.

If $k = -1$, we get conditions (34) for the existence of a derivative of a real polinion function ($1_{-1} = -1$). Thus the fundamental formulae of the theory of analytical functions acquire a more general form.

In conclusion, imagine the function:

$$e^z = e^{x + j_k y}.$$

Putting

$$\cos_k y = \frac{1}{2}[(1 - 1_k)\cosh y + (1 + 1_k)\cos y];$$

$$\sin_k y = \frac{1}{2}[(1 - 1_k)\sinh y + (1 + 1_k)\sin y],$$

we get

$$e^z = e^{x + j_k y} = e^x [\cos_k y + j_k \sin_k y].$$

Using the adopted designations, we obtain the following formulae

$$\frac{de^z}{dz} = \frac{\partial u}{\partial x} + j_k \frac{\partial v}{\partial x} = e^z;$$

$$\cos_k^2 y + 1_k \sin_k^2 y = 1;$$

$$\cos_k^2 y - 1_k \sin^2 y = \cos_k 2y;$$

$$2 \sin_k y \cos_k y = \sin_k 2y \text{ etc}$$

If $k = 0$ ($1_0 = 1$) we obtain known trigonometrical formulae, but if $k = -1$ ($1_{-1} = -1$), hyperbolic formulae.

Translated by O.M. Blunn

MODELLING THE LEAKAGE LOSSES OF LARGE POWER TRANSFORMERS*

N.V. BORIV

Zaporozhe Transformer Works

(Received 22 May 1960)

1960

The rapid development of our electrical power, constantly requires the design of new power transformers with an ever increasing unit-output.

A major problem in the development of large transformers is the study of the distribution of the magnetic leakage fluxes and the additional losses and heating of the transformer components caused by them.

These problems are all the more important in the case of auto-transformers which have comparatively greater leakage fluxes than transformers proper, since the maximum permissible power that auto-transformers can transmit is in many cases determined by the very heating that the leakage fluxes cause.

It is a very difficult matter to investigate the heating of the magnetic circuit, yoke beams, rings, plates, bars and so on in a finished transformer and, in any case, this only defines the actual value of local temperatures. It is often necessary to impose special conditions, even a reduction in rated output.

This article describes a method of studying electromagnetic processes, in particular, local losses in transformers, by means of specially scaled down models.

Investigation of such models not only allows the study of the losses in the components before the transformer is actually made, but provides

---

* *Elektrichestvo*, 9, 38-41, 1960.

the possibility of modifying the design at the project stage by helping in the elaboration and verification of special measures which can be taken to reduce the local losses and heating due to leakage fields.

It is implied in the similarity criteria that the leakage losses be the same in both model and original.

The expressions for electromagnetic processes in a conducting medium, ignoring bias currents, are [1]

$$\text{rot}\, H = \delta = \gamma E; \tag{1}$$

$$\text{rot}\, E = -\frac{dB}{dt} = -\mu \frac{dH}{dt}. \tag{2}$$

Permeability is a function of the intensity of the magnetic field calculated at the surface of the material. Neiman [2] has shown that practical use can be made of formulae (1) and (2) assuming that μ = const. The electromagnetic processes for the original and model should described by similar equations:

original

$$\text{rot}\, \dot{H}_{or} = \dot{\delta}_{or} = \gamma_{or} \dot{E}_{or}; \tag{3}$$

$$\text{rot}\, \dot{E}_{or} = -\frac{d\dot{B}_{or}}{dt_{or}} = -\mu_{or} \frac{d\dot{H}_{or}}{dt_{or}}; \tag{4}$$

model

$$\text{rot}\, \dot{H}_{m} = \dot{\delta}_{m} = \gamma_{m} \dot{E}_{m}; \tag{5}$$

$$\text{rot}\, \dot{E}_{m} = -\frac{d\dot{B}_{m}}{dt_{m}} = -\mu_{m} \frac{d\dot{H}_{m}}{dt_{m}}; \tag{6}$$

Comparing these equations and adding scale coefficients, the similarity criteria for electromagnetic process in a conducting medium are:

$$\frac{m_H}{m_l} = m_\delta = m_\gamma m_E \tag{7}$$

$$\frac{m_E}{m_l} = m_\mu \frac{m_H}{m_l} \tag{8}$$

where $m_H = \frac{\dot{H}_m}{\dot{H}_{or}}$ is the ratio (scale) of the intensity of the electro-

magnetic field;

$m_l = \frac{l_m}{l_{or}}$ the ratio of the linear dimensions;

$m_f = \frac{f_m}{f_{or}} = \frac{f_{or}}{f_m}$ the ratio of the supply frequency;

$m_E = \frac{\dot{E}_m}{\dot{E}_{or}}$ the ratio of the intensity of the electrical field;

$m_\delta = \frac{\delta_m}{\delta_{or}}$ the current density ratio;

$m_\gamma = \frac{\gamma_m}{\gamma_{or}}$ the ratio of the electrical conductance;

$m_\mu = \frac{\mu_m}{\mu_{or}}$ the ratio of the magnetic permeability.

1960

The local losses due to leakage fields can be equal at corresponding points of the original and model if the current density due to the leakage fluxes is the same, i.e.

$$m_\delta = 1 \tag{9}$$

when

and

$$\left.\begin{aligned} m_\gamma &= 1 \\ m_\mu &= 1. \end{aligned}\right\} \tag{10}$$

The joint solution of (7) and (8), when considered with (9) and (10), produces the fundamental criterion for modelling the additional losses at the point in question:

$$m_t = \frac{1}{m_f} = m_l^2 , \tag{11}$$

i.e. scaling down the transformer's geometric dimensions m_l times requires a $\frac{1}{m_l^2}$ times increase in the frequency of supply to the model. Conditions (9) and (10) are satisfied if the model and original are both made of the same material.

These criteria were first checked on L-62 type brass and grade 3 steel testpieces.

The losses in the testpieces were investigated in a uniform homogeneous field as produced by Helmholz coils. The scale and dimensions of the original and model were determined by the dimensions of the coils and the frequencies of the supply source, 50 and 100 c/s.

The scale of the linear dimensions was

$$m_l = \sqrt{m_l} = \sqrt{\frac{f_{or}}{f_m}} = 0{,}707.$$

The current in the coils and, consequently, the field inductance, were established from condition (7):

for the original

$$H_{or} l_{or} = I_{or} w_{or},$$

for the models (12)

$$H_{or} m_l l_{or} = I_{or} m_I w_{or}.$$

Since the field was produced by the same coils, w_{or} = const and l_{or} = = const, whilst $m_I = m_l$.

Losses were measured by thermocouples. Their arrangement is shown in Fig. 1. They were soldered or embedded on the surface of the testpiece. A recording millivoltmeter measured the rise in temperature after switching on for 50 to 60 sec and the fall in temperature immediately after switching off.

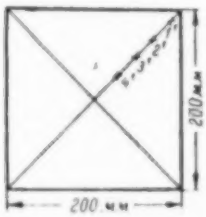

Fig. 1. Arrangement of thermocouples on brass and steel testpieces. Figures represent the number of the thermocouple.

The conclusion drawn from laboratory tests and heat balance theory is that the algebraic difference between the rates at which the temperature rose and fell during the time $\Delta t \to 0$ is directly proportional to the local losses at the point in question:

$$P_{sp} = \frac{ck}{0,24} \Sigma \frac{\Delta\theta}{\Delta t}, \qquad (13)$$

where P_{sp} is the local losses in w/kg, C the specific heat consumption of the material in cal/g. deg, k the instrument constant, deg/division, θ°C the temperature of the testpiece at the point in question, and

$\Sigma \frac{\Delta\theta}{\Delta t} = \frac{\Delta\theta}{\Delta t} - \left(\pm \frac{\Delta\theta}{\Delta t}_{\text{cooling}}\right)$ the algebraic difference of the temperature change in divisions of the meter per second.

The local losses as measured on the model and original are given in Table 1. For purposes of comparison the losses, as measured in brass without observing the scale criteria, are also shown.

It can be seen that there is good agreement between the losses in the model and those in the original if the scale criteria are observed.

The results confirm that μ can be regarded as constant in equations 1 and 2 in the case of ferromagnetic bodies in leakage fields with an inductance $B_{\blacksquare} \approx 700$ G, and that $\blacksquare\mu = 1$ in the scale criteria equations.

Using the scale criteria, the laboratory at the Zaporozhe transformer works produced and investigated a 1 : 10 scale model of a 400 kV step-up auto-transformer with a bar or ring ("through") output of 167 MVA and a generator winding output of 82.5 MVA.

The supply frequency to the model was 5000 c/s to match the linear scale. All the linear dimensions of the original auto-transformer were reduced to a tenth. The design of the individual parts was slightly simplified to assist in their production. The m.m.f. distribution in the windings over the height of the model was strictly in accordance with that in the original. The scale factor as regards the m.m.f. was $\blacksquare_{IW} = \blacksquare_l^2 = \frac{1}{100}$. The model was supplied from a specially designed power amplifier using electron valves. A bank of capacitors was connected in series with the model at the output of the amplifier.

The method of measuring the local losses was similar to that previously described with the exception that the instrument for measuring temperature on the model had to be highly sensitive (of the order of 4 to 6 x 10^{-3} deg/div). The local losses on the model were measured automatically. A single measurement cycle lasted 10 sec. The rig used for these measurements is illustrated in Fig. 2.

Losses from the leakage fields on the model were measured on the bars, ring and in the magnetic circuit. The arrangement of the thermo-

couples on the model and original is shown in Fig. 3.

Table 2 compares the local losses on the model and original, as measured under similar conditions at similar points, (average values of three to four measurements are given).

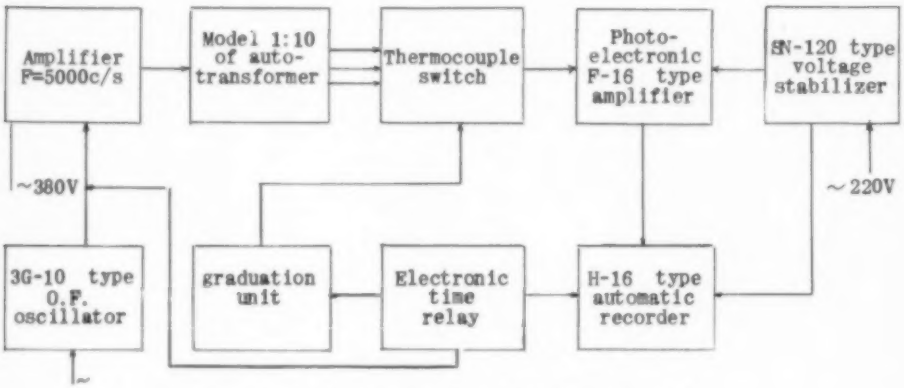

Fig. 2. Block diagram of system for measuring local losses on the model.

It can be seen that there is good agreement between the local losses in the model and those in the original as regards both magnitude and spatial distribution. The lack of correspondence between certain values of P_{sp} is to a large extent explained by small errors in the production of the model and the mounting of the thermocouples.

By way of example, tests were made to determine how effectively the yoke beams were screened from leakage fields by copper, aluminium or brass screens. Losses with and without screens are compared in Table 3.

A slot was made in the lower yoke beam to reduce overheating and local losses were thus reduced 20%.

All the measurements showed that the distribution and magnitude of local leakage losses can in practice be measured on models to within ± 10 per cent.

In addition to the study of leakage losses, this electromagnetic model permits the reactance to be checked and the inductance in the windings due to leakage above and below the yoke beams to be measured. The resistances, reactance voltage and the leakage inductance as measured on the model are related to the real transformer by the formulae

$$x_t = x_m \frac{1}{m_l m_w^2 m_l} \quad [\Omega]; \tag{14}$$

TABLE 1

Local losses W/kg, as measured on original and model

No. of thermocouple	Scale criteria observed				Scale criteria not observed	
	Grade 3 Steel		L-62 Brass			
	Original 200X200X6.25 mm	model 141X141X4.4 mm	Original 200X200X1.5 mm	model 141X141X1.06 mm	Original 141X141X1.06 mm	model 141X141X1.06 mm
	B = 650 G f = 50 c/s	B = 460 G f = 100 c/s	B = 650 G f = 50 c/s	B = 460 G f = 100 c/s	B = 460 G f = 50 c/s	B = 650 G f = 50 c/s
1	79	83.5	592	594	141	280
2	72.5	74	510	523	145	290
3	61	59	450	475	124	248
4	26	28.9	142	144	-	-

TABLE 2

Local losses W/kg, as measured on model and original

Object	Lower yoke beam (Fig.3a)					Upper yoke beam (Fig.3b)			Stamped ring (Fig.3d)			Magnetic circuit cover (Fig.3c)	
	No. of thermocouple												
	1	2	3	4	5	6	7	8	9	10	11	12	13
Model	4.9	6.4	11.4	14	7.7	7.3	5.45	1.3	3.1	1.75	3.16	7.85	29.4
Transformer..	5.7	8.0	13.2	15.3	7.1	7.7	6.7	2.5	3.2	1.33	3.77	10.8	25.4

$$u_{sk\,t} = u_{sk\,m}\frac{m_t}{m_{tw}m_t m_l} \quad [\%]; \tag{15}$$

$$B_t = B_m\frac{1}{m_t} \quad [G]. \tag{16}$$

Under the test conditions, the inductance, resistance and reactance voltage of the model were accurate to within 15% of the original transformer.

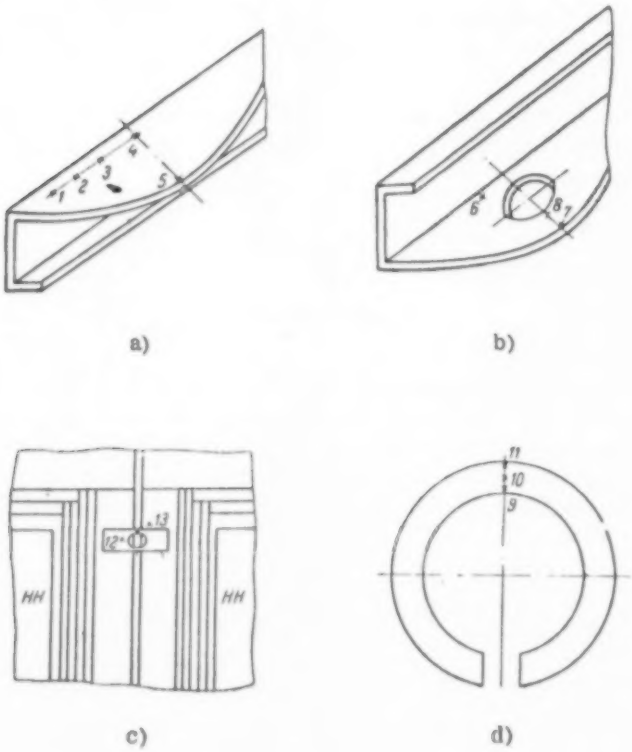

a) b)

c) d)

Fig. 3. Arrangement of thermocouples on model and transformer. a – on lower yoke beam; b – on upper yoke beam; c – on magnetic circuit cover; d – on stamped ring. Figures denote number of thermocouple.

Investigations into leakage inductance on models is also valuable for studying the mechanical forces in the windings.

TABLE 3

Local losses W/kg as measured on a model with various screens

Screen	No. of thermocouple			
	14	15	16	17
Copper, 0.75 mm thick ..	2.57	3.6	2.9	4.1
Aluminium, 1 mm thick ..	3.15	1.48	0.77	2.34
Brass, 1 mm thick	2.56	3.36	3.0	4.92
Aluminium, 1 mm thick ..	10.6	9.75	7.2	7.2

These scale criteria for power transformers as regards leakage losses ought to be used extensively in the design of large new transformers and auto-transformers.

Translated by O.M. Blunn

REFERENCES

1. L.R. Neiman and P.L. Kalantarov; *Theoretical bases of electrical engineering, (Teoreticheskie osnovy elektrotekhniki).* Gosenergoizdat, (1956).
2. L.R. Neiman; *The surface effect in ferromagnetic bodies, (Poverkhnostnyi e'ffekt v ferromagnitnykh telakh).* Gosenergoizdat, (1949).
3. V.A. Venikov and A.V. Ivanov-Smolenskii; *Physical modelling of electrical systems, (Fizicheskoe modelirovanie elektricheskikh sistem),* Gosenergoizdat, *(1956).*

FULL WAVE RECTIFICATION WITH "ZERO" ANODES AND ITS USE FOR EXCITING EXCITRONS*

V.M. KOLESNIKOV

Moscow

(Received 11 September 1959)

Widespread use is now made of excitron valves on electrified railways and in industry, i.e. mercury arc rectifiers with a constantly burning excitation arc. It is known that the extinction of the arc even for 0.001 sec, or a reduction in the cathode spot current below the critical value, leads to failures in the rectifiers. The existing methods of eliminating these undesirable phenomena are unreliable and cause great power losses.

Unlike known systems of single phase current rectification, these shortcomings are eliminated in the full wave rectification system with zero (neutral?) anodes as proposed by the author of this article. Moreover, this system improves the power factor and efficiency of the converter plant. The proposed systems are now in use at converter substations on electrified railways for the excitation of excitrons.** This makes a considerable saving in electricity and at the same time improves the performance of the rectifiers.

The parallel system with zero anodes

When feeding one (Fig. 1) (sic) or two (Fig. 2) (sic) consumers, the system generally comprises a transformer with two secondary windings, valves V and a cathode reactor L_d with two windings.

---

* *Elektrichestvo*, 9, 42-45, 1960.

** V.M. Kolesnikov; *Device for exciting and igniting excitrons, (Ustroistvo dlia vozbuzhdeniia i zazhiganiia ekzitronov)*. Auth. Cert. No. 115627, 23 October, 1957.

The circuits operate as follows. Suppose that the anode V_2 has the greatest positive potential relative to the cathode after connecting the transformer. A current i_2 will then pass through it; this current begins to fall after attaining a maximum and induces an e.m.f. in the winding L_d of the cathode reactor. Under the effect of this e.m.f. a current i_1 appears in the circuit of anode V_1. Yet another current i_3 appears almost simultaneously, also under the action of the e.m.f. in the secondary winding of the transformer (shifted 180° relative to the first), but this time in the circuit of anode V_3. After the current i_2 has dropped to zero, two currents will pass via the load, namely, i_1 and i_3. These will be equalized by the mutual inductance between the reactor windings and will be the same in shape and magnitude, given definite circuit parameters (Fig. 3). Current i_4 appears during the decrease in current i_3 and so on. There will thus be currents in all the valves in the intervals of commutation (switching), but during the rest of the time there will only be current in V_1 and V_3 or V_2 and V_4. Here a current I_d passes along the windings of the cathode reactor and via the load. The pulsation of this current is negligible, a very important factor in the stability of the cathode spot.

The theoretical (typical) output of cathode reactors, as required for producing equal pulsation in the circuits shown in Figs. 1 and 2, is roughly the same as that of a system with the neutral point brought out if $\frac{x_d}{r_d} > 0.2$ and the link coefficient between the windings is 0.2, i.e.

$$S_{\text{к}} \approx 0{,}17 P_d.$$

The fundamental analytical relationships between the circuit parameters are given below for finite magnitudes of the cathode reactor. The expressions for the maximum and minimum of the rectified current i_d in the circuits considered above and the (overlap) angles between the anode currents enable us to find the rest of the required quantities comparatively easily:

$$i_{d(0)} = a_1 + a_2 - a_3 + a_4 - a_5;$$

$$i_{d(\beta)} = a_1\beta + \frac{a_2}{\beta} + a_3 + a_4 - a_5;$$

$$\cos\gamma_1 = 1 - \frac{x_1 + x_{\text{к}}}{E_m}(a_1 + a_2 - a_3 + a_4 - a_5),$$

where

$$\beta = \frac{e^{p_2\pi} - e^{p_1\pi} + 2}{e^{p_1\pi} + e^{p_2\pi}};$$

$$a_1 = \frac{E_t \sqrt{r^2(r^2 + x^2 + x_M^2)^2 + x^2(r^2 + x^2 - x_M^2)^2}}{(r^2 + x^2 + x_M^2)^2 - 2x^2x_M^2} \times$$

$$\times \frac{(e^{p_1\pi} + e^{p_2\pi}) \sin \varphi_1}{2(1 - e^{p_1\pi})(1 + e^{p_2\pi})};$$

$$a_2 = \frac{E_t x_M (e^{p_2\pi} - e^{p_1\pi} + 2) \sin \varphi_1}{2\sqrt{(r^2 - x^2 + x_M^2)^2 + 4x^2r^2}(1 + e^{p_2\pi})(1 - e^{p_1\pi})};$$

$$a_3 = \frac{E_t e^{p_1\pi} \sin \varphi_2}{2\sqrt{r^2 + (x + x_M)^2}(1 + e^{p_2\pi})};$$

$$a_4 = \frac{E_t e^{p_2\pi} \sin \varphi_3}{2\sqrt{r^2 + (x - x_M)^2}(1 - e^{p_1\pi})};$$

$$a_5 = \frac{\Delta U(1 - e^{p_1\pi})}{r(1 - e^{p_2\pi})};$$

$$\varphi_1 = \arctan \frac{x(x^2 + r^2 - x_M^2)}{r(x^2 + r^2 + x_M^2)};$$

$$\varphi_2 = \arctan \frac{x + x_M}{r};$$

$$\varphi_3 = \arctan \frac{x - x_M}{r};$$

$$\varphi_4 = \arctan \frac{2rx}{r^2 - x^2 + x_M^2};$$

$$p_1 = -\frac{r}{x + x_M};$$

$$p_2 = -\frac{r}{x - x_M};$$

$$x = x_\kappa + x_d;$$

$$x_1 = \frac{x_{\kappa 12} + x_{\kappa 13} - x_{\kappa 23}}{2},$$

where E_t is the amplitude of the secondary voltage of the transformer;

ΔU the voltage drop in the rectifier arc;

r the load impedance;

x_d the inductive reactance of the cathode reactor;

x_M the mutual-inductive reactance of the reactor;

x_{k12} and x_{k13} the leakage inductive reactance between the primary and appropriate secondary windings as defined by short circuit tests (in our case $x_{k12} = x_{k13} = x_k$);

x_{k23} the leakage inductive reactance between the secondary windings.

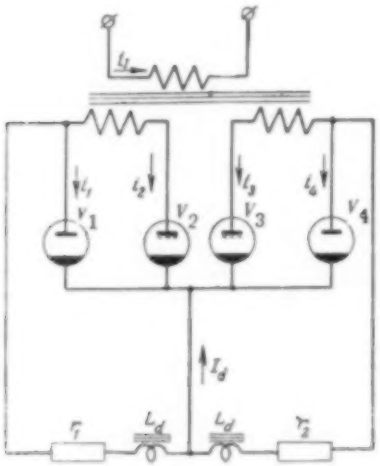

Fig. 1.

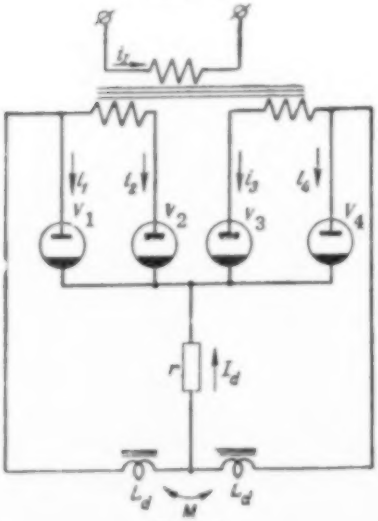

Fig. 2.

1960

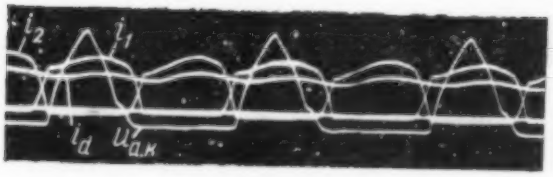

Fig. 3.

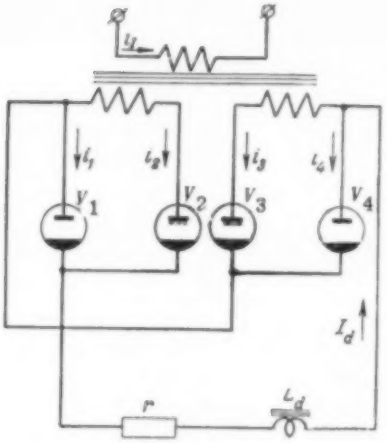

Fig. 4.

The overlap angle γ_2 can be approximated quite well in practice:

$$\gamma_2 = \gamma_1 \frac{i_{d(P)}}{i_{d(0)}}.$$

The series system with zero anodes

Fig. 4 shows the series system of full wave rectification. It has two zero and two potential anodes. The sequence in which they operate can be seen from the diagram. The series and parallel systems are both of special interest when control valves are incorporated (see below).

Comparative evaluation

The principal comparative data are given in the table. Each circuit has two isolated secondary windings. This to some extent gives them

an advantage over systems with the neutral point brought out where the voltage between the windings is twice as big. This advantage still stands despite the presence of four anodes as in the bridge system, because the cathodes are in common and the anodes can be contained in one rectifier. Moreover, the average anode currents, voltage drops, maximum reverse voltages and their sudden fluctuations (jumps) in these circuits are no more and may even be less.

Grid control makes these circuits even better.

For purposes of illustration, Figs. 5(a) and (c) show current and voltage oscillograms for a circuit with the neutral point brought out with mutual inductance between the secondary windings of the transformer and with or without grid control respectively. Figs. 5(b) and (d) show similar oscillograms in respect of the series system with zero anodes. Fig. 6 shows similar oscillograms when there is no mutual inductance between the transformer windings.

1960

The oscillograms are directly comparable as the elements of the systems are substantially identical and also the transformer voltage and curve scales.

In the new circuits there are practically no sudden fluctuations in the reverse voltage between cathode and anode after "extinguishing" the rectifier valve, and this reverse voltage is also halved. This, together with the presence of common cathodes, is the real merit of the proposed systems, particularly when semiconductor rectifiers are used. The power factor of the converter is also improved considerably.

Excitation system

Fig. 7 shows the circuit for firing and exciting RMNV-type excitrons, as based on the above parallel system of rectification with zero anodes.

The circuit includes ignition transformers *TI*, excitation transformers *TE*, a cathode (balancing) reactor *CR*, rectifier-exciter contactors *K*, jet coils *C* and a pulse contactor *PK*.

The firing process is as follows. On connecting the transformer, the current excites the jet coils and a jet of mercury instantly makes the anode ignition-cathode circuit. When this circuit is broken an arc is struck which then passes to one of the anodes, i.e. if a firing arc appears at the moment when the voltage on anode 2 is positive, it will in fact be picked up by anode 2, otherwise the arc will be picked up by anode 1 under the influence of the e.m.f. induced in the winding of the cathode reactor when the ignition current disappears. The sequence of currents in the anodes proceeds as above.

Parameter	System				
	Bridge	Neutral brought out	Fig. 1.	Fig. 2.	Fig. 4.
I_a	$\frac{I_d}{2}$	$\frac{I_d}{2}$	$\frac{I_d}{4}$	$\frac{I_d}{4}$	$\frac{I_d}{2}$
$I_{a.max}$	I_d	I_d	$\frac{I_d}{2}$	$\frac{I_d}{2}$	I_d
U_{rev}	$\sqrt{2}E_2 \sin\gamma$	$2\sqrt{2}E_2 \sin\gamma$	$\sqrt{2}E_2 \sin\gamma$	$<2\sqrt{2}E_2 \sin\gamma$	$\sqrt{2}E_2 \sin\gamma$
$U_{rev.max}$	$\sqrt{2}E_2$	$2\sqrt{2}E_2$	$\sqrt{2}E_2$	$<2\sqrt{2}E_2$	$\sqrt{2}E_2$
ΔU	$2\Delta U$	ΔU	ΔU	ΔU	$2\Delta U$

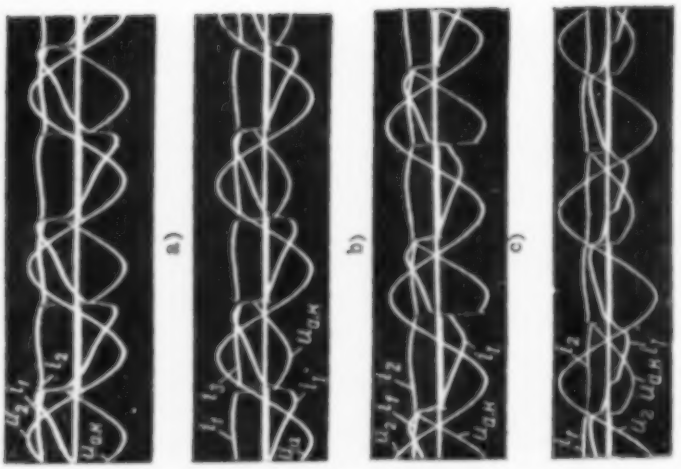

Fig. 6.

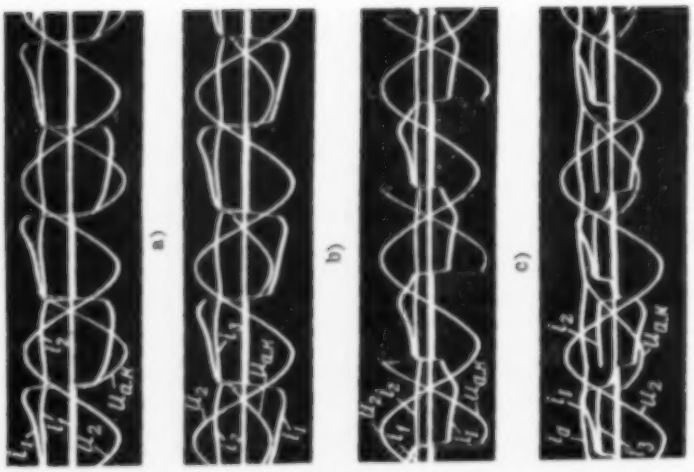

Fig. 5.

1960

The successive passage of the anode firing current through the reactor ensures that the emergence of the firing arc is properly timed with the discharge of the energy stored in the reactor through anode 1. This ensures that there is no failure in the excitation of the exitron regardless of variations in the mains voltage and the state of the rectifier.

It can be seen from the oscillograms in Fig. 3 that the current through the cathode spot is practically constant in magnitude despite the fact that the excitation circuit of each rectifier valve is fed from the transformer for half periods. It has been shown theoretically and by prolonged tests that the requisite steady output of the balancing reactor is roughly the same as that of the reactor in the full wave system.

The shape of the rectified current and stability of the cathode spot for the same average current values vary as a function of changes in the mutual inductance factor.

In order to utilize the existing equipment contained in ShRV-20 type cubicles on conversion to the excitation system in question, use has been made of the reactors installed there without the mutual inductance link. This made it necessary to increase the average current through the cathode spot. The inter-anode voltage required is 80 V. Any industrial mercury arc rectifier can be similarly excited at very little cost.

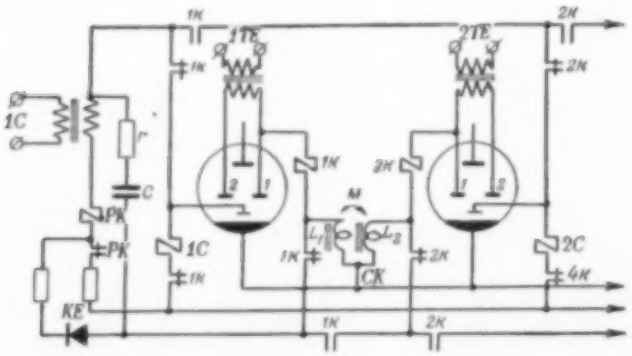

Fig. 7.

Compared with ShRV-20 and ShRV-30 type excitation systems, the advantages of the proposed system are: increased firing reliability and excitation stability, no false tripping of the protection subsequent

to installation, unfailing firing and excitation when the RMNV (excitron?) is connected even after a week's shutdown, power consumption of RMNV cut by a factor of 2 to 3.

Finally, these systems can be used in inverter stations and the governing laws stated here can be used as a basis for evaluation their utility in actual conditions.

Translated by O.M. Blunn

THE IMPULSE CHARACTERISTICS OF TURBINE GENERATORS*

V.A. LIUL'KO

Leningrad branch of the All-Union Scientific Research Institute of Electro-mechanics

The impulse characteristics of electrical machine windings to a large extent determine the maximum voltage that the winding insulation can withstand during surges. This not only applies to small machines, but also to large turbo generators, including those unit-connected with a transformer. A theoretical method has been specially proposed for such generators. This makes it possible to measure the voltage at the winding terminals due to the reduction in the surge in the transformer and so to establish whether or not special protective devices are necessary [1].

The surge impedance of the generator is one of the items required in this method. The impulse characteristic have been measured on turbo-generators made by "Elektrosila". This paper gives the results of these measurements, studies how these measurements can be taken and re-states the term "surge impedance" more precisely as applied to electrical machine windings.

Surge impedance and the method of measurement

Practical experience has shown that machine windings can be satisfactorily characterized by a conventional value of impedance in surge calculations. But different methods of measuring sink impedance give different results for the same winding, and the dependence of the surge impedance itself on such factors as time wave shape and the parameters of the measuring scheme even makes quantities measured by the same method indefinite. This is inconvenient for design and research purposes and makes it difficult to obtain comparable results. It is

* *Elektrichestvo*, 9, 49-52, 1960.

therefore desirable to standardize the method of measurement and to establish what quantity ought in fact to be adopted as the surge impedance of the winding.

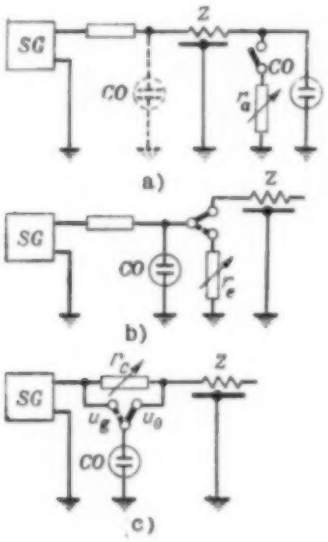

Fig. 1. Various methods of measuring surge impedance. *SG* - surge generator; *CO*- cathode ray oscillograph.

There are three main methods of measurement:

1. A voltage surge is applied to the start of the winding. The end is earthed through a resistance r_a. This resistance is such that there is no end reflection to the start of the winding, or alternatively the voltage at the end of the winding is halved when the resistance is connected (Fig. 1a). If this condition is satisfied, it is assumed that the surge impedance $Z = r_a$.

2. An equivalent resistance r_e is substituted for the winding in the measuring circuit. The magnitude of r_e is such that the oscillograms of the voltage across this resistance and winding coincide at definite points (Fig. 1b). In this case it is assumed that $Z = r_e$.

3. An oscillogram is taken of the surge voltage u_0 at the start of the winding and u_g at the output of the generator, as applied to the winding via resistance r_b (Fig. 1c). It is assumed that the surge impedance equals the ratio of the surge voltage to the surge current at any given time:

$$Z = \frac{u_a}{u_g - u_a} r_b.$$

The first method requires a lead from the end of the winding which every machine does not have. Z can only be measured at the end of the winding, which is generally different from that at the start, whereas the latter is the decisive quantity in determining the extent of the surge at the terminals of the machine. Reflections are not always noticeable on the oscillograms and this can result in r_a being rather inaccurate. The measurements are taken direct from the oscillograph screen and not from the oscillogram. This causes more errors. Finally, variations in surge impedance with time cannot be traced.

The last two drawbacks apply equally to the second method, but this has an advantage in that the surge impedance is measured at the input part of the winding. This is a useful method if a unit scheme is under investigation, comprising both machine and associated equipment.

The third method is the most universal, the most convenient experimentally and also the most accurate, as the initial data for calculating Z are taken from the oscillogram. If analysed carefully, the error can be made very small. The surge impedance can be measured at the start of the winding and variations with time can be traced.

But in giving preference to the third method, reference must be made to a number of conditions affecting the measuring circuit and the way the data are handled.

It can be seen from Fig. 2 that there can be a considerable variation in the magnitude of Z with time.

All values of Z must be such that the winding is characterized as correctly as possible and that the reading can be conveniently obtained. The latter requirement is best satisfied by the value of Z corresponding to the maximum voltage at the machine terminals. This instant must be before the arrival of the end-reflected wave at the start of the winding (Fig. 3a). This is more often than not the maximum value of Z for the winding in question, depending on the type of winding. But since it defines the maximum, i.e. the most dangerous voltage at the terminals of the winding due to the incident wave, and since it is usually the ultimate aim of the calculation to find that maximum, it is this maximum that ought to be adopted as the characteristic of the winding. Another reason why this value is convenient is that the time at which Z is measured can easily be fixed on the oscillogram.

The surge impedance depends on wave shape. But Fig. 2 suggests that this dependence is negligible and that the surge impedance is even less

important for surge with a longer wave front. Similar conclusions are reached from comparable curves for other turbogenerators. Since the appearance of a surge at the machine terminals with a wave front less than 1 to 1.5 μ sec is very improbable, and bearing in mind that the standard surge in impulse testing is 1.5/40 μ sec, the impulse characteristics should be measured with this wave shape. The impedance for surges with longer fronts will be determined with some margin.

Reading accuracy is at a maximum in analysing the oscillograms (Fig. 3a) if $u_g - u_o$ and u_o are equal. Therefore r_b in Fig. 1(c) should be approximately equal to the surge impedance of the winding. The accuracy of r_b is of no special importance as is obvious from Fig. 4. The curves for $Z = f(t)$ in this diagram are in close agreement although r_b differed from Z by a factor of as much as 2 and 3. These curves also show that the values obtained for surge impedance by this method can be used in the design of any circuit.

1960

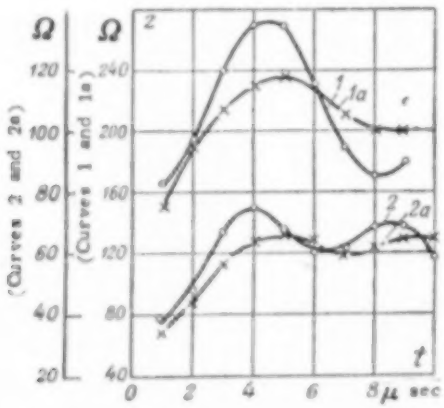

Fig. 2. The surge resistance of T2-6-2 (1 and 1a) and TV2-100-2 (2 and 2a) type generators as a function of time for one phase. 1 and 2 – length of wave front, $\tau_0 = 1.5\,\Omega$ sec; 1a and 2a – $\tau_0 = 7\,\Omega$ sec.

A marked dependence of Z on the magnitude of r_b as obtained elsewhere [1] is not confirmed, notwithstanding repeated tests on different machine windings. This could be explained by the (surge impedance) in the cited paper being measured after too long a period of time when end-reflected waves had appeared at the staff of the windings. The conventional methods of measuring Z cannot be used under these conditions.

The surge impedance is thus the ratio of the surge voltage with a front of 1.5 μ sec to the surge current at the input to the winding at the instant corresponding to the maximum surge voltage timed so as to occur after the start of the pulse but before the arrival of the end-reflected wave at the start of the winding. The current has to be measured from the voltage drop on r_b connected in front of the winding and close in magnitude to the surge impedance.

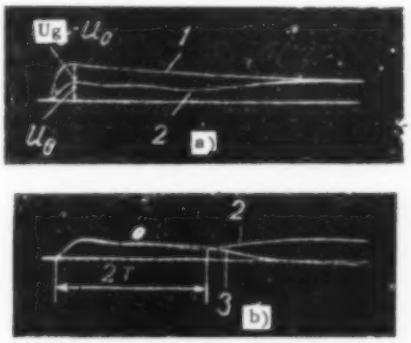

Fig. 3. Oscillograms for determining the surge impedance (a) and average wave propagation rates (b). 1 – surge at output of wave generator; 2 – surge at start of winding with other end isolated; 3 – the same, but other end earthed; timing frequency 1 Mc/s.

The measuring apparatus

The impulse characteristics were measured on a surge analyser, a special apparatus developed for investigating surge propagation in machine windings [3]. Waves of various shapes were applied to the winding. The voltages arising at different points along the winding were recorded on an oscillograph. Since it had been established [4] that the impulse characteristics of electrical machine windings, and especially turbo generator windings having semiconductor coatings, are practically independent of the amplitude of the incident wave, an additional low voltage surge-generator was used to supply the voltage pulses. This generator, made with a TGI1/50/5 type thyraton, had an output voltage of about 80V and a discharge circuit capacitance of 20 μ F. The output impedance was so small that a wave shape could be produced that was independent of the load even when windings with a very low surge impedance were under investigation.

Special measures were taken to reduce the inductance of the discharge circuit of the generator. The output wave had no superposed oscillations, despite the extremely small output impedance.

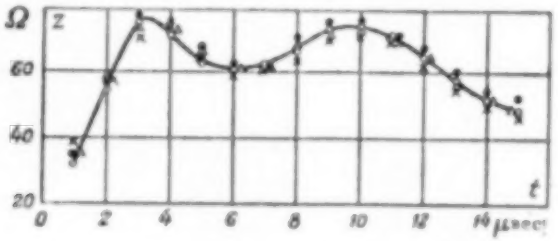

Fig. 4. The effect of impedance r_b on the magnitude of surge impedance for one phase of a TV2-150-2 type turbine generator.
× r_b = 200 Ω; △ r_b = 140 Ω; ○ r_b = 70 Ω; ● rb = 35 Ω.

The simplicity of design, reliability in performance and the undistorted wave shape of the generator enables us to recommend the apparatus for surge investigations in the windings of large machines.

Test results

The impulse characteristic of turbo generators were measured on one and three phases using the arrangement shown in Fig. 1(c). The start and end of the other phases were earthed when measuring one phase.

The results are given in Table 1. The surge impedances correspond to the instant when the voltage at the winding terminals was a maximum. The time from the start of the surge is shown in the appropriate column.

Table 1 also shows the time taken for the wave to travel along the winding and the average rate of propagation. Travelling time T was defined as half the time 2T necessary for the wave to travel from the start to the end and back again as determined from oscillograms of the voltage at the start of the winding with the other end first isolated and then "dead earthed" (Fig. 3b). The average propagation rate was assumed equal to the quotient of the length of one path of the phase winding divided by time T.

The majority of the characteristic values in the Table are averages for several machines. Deviations from average on the individual machines were not large, usually no more than 2-6%. Deviations of 10%

TABLE 1

Surge impedance of turbogenerators for waves of 1.5/40 μ sec

Type	Output kVA	Voltage kV	No. of phases along which surge propagated simultaneously	Surge impedance	Reading time of surge impedance μ sec	Travelling of surge along working μ sec	Average propagation speed, m/μ sec
TVF-200-2*	200	11.0	1 (one winding)	39	3.0	3.3	33
TVF-200-2	200	11.0	1 (two windings)	39	6.0	7.2	15
TVF-200-2	200	11.0	3 (one winding)	14	2.0	3.0	36
TVF-200-2	200	11.0	3 (two windings)	13	1.0	6.0	18
TV2-150-2	150	18.0	1	74	3.0	8.6	20
			3	23	3.0	6.1	28
TV2-100-2	100	13.8	1	72	4.0	7.8	19
			3	20	4.0	5.5	27
TVF-100-2	100	10.5	1	62	7.0	6.7	19
			3	16	3.5	5.0	25
TV-60-2..	60	10.5	1	73	3.0	6.5	21
			3	21	1.5	4.5	31
T2-6-2	6	6.3	1	280	4.5	4.8	31
			3	67	4.0	3.7	40
TF-6-2	6	6.3	1	230	4.0	5.7	25
			3	57	4.0	4.0	37
T2-4-2	4	6.3	1	290	5.0	5.5	32
			3	65	4.0	4.0	44
T2-1, 5.2	1.5	6.3	1	620	7.0	6.6	40
			3	140	6.0	5.1	52

* Turbogenerator with two independent windings; separate connexion permissible.

were very rare. The differences in the impulse characteristics of the various phases are also within permissible limits.

Thus, the tabulated values are quite exact and can be recommended for calculating surges in turbo generator windings.

The results show that the surge impedances for three phases of a winding in parallel on average 3.9 times smaller than for one phase. On different types of machine the surge impedance ratio for one and three phases varies between 3.2 and 4.4, but sometimes it does not reach the conventionally used figure of 3.

The analogous ratio of average propagation rates is 1.3 to 1.6 with a mean of 1.4.

The TVF-200-2 type generator was not studied when comparing the surge impedance for one and three phases as it has two windings with a particularly complicated link between them.

Translated by O.M. Blunn

1960

REFERENCES

1. A.P. Hayward, J.K. Dillard and A.R. Hileman; *Lighting protection of unit-connected turbine generators – field and laboratory studies, Power apparatus and Systems*, Feb, (1957).
2. P.A. Abetti, I.B. Johnson and A.J. Sohultz; *Surge phenomena in large unit-connected steam turbine generators, Trans. AIEE*, 71, pt.3, (1952).
3. V.A. Liul'ko; *Equipment for investigating the wave parameters of electrical machines, (Ustanovka dlia issledovania volnovykh parametrov elektricheskikh mashin)*. Sborn. "Elektrosila", 16, (1959).
4. V.A. Liul'ko; *The effect of the voltage on the wave parameters of electrical machines, (Vliianie napriazheniia na volnovye parametry elektrocheskikh mashin)*. Sborn. "Elektrosila", 17, (1959).

ABSTRACTS FROM PAPERS PUBLISHED IN ELEKTRICHESTVO No.9. 1960

The first international congress on automatic control, (pp.1-4).

A first international congress on automatic control was held in Moscow from 27 June to 7 July 1960 attended by 1190 delegates from 29 countries, members of IFAC. A short account is given of the work of the sections at which 140 reports were read. The theme of the congress was the practical application of theory, the reliability of equipment and the efficiency of systems.

A method of accounting for power system operating conditions for planning purposes. V.M. Gornshtein, (pp.4-11).

Attention is focussed on determining fuel consumption and the outlay connected with it. The major errors often committed in cost analysis are discussed. Formulae are proposed for calculating variations in fuel consumption and variations in cost when the power station(s') load changes. Power station graphs are plotted for various types of turbine. Use is made of equivalent curves for the case when some of the generators at a station are shut down.

Computations for d.c. power systems on network analysers. A.I. Kazachkov, V.A. Klimov and G.I. Poliak, (pp. 11-14).

The static models currently used for calculations on a.c. transmission systems are adapted for use on d.c. systems.

Regulation of a d.c. transmission line working in parallel with an a.c. transmission line. S.R. Buachidze, (pp. 14-18).

The author extends a previous paper published in 1955 by studying certain moments of the combined automatic regulation of active and reactive loads on a d.c. line when operating in parallel with an a.c. line.

Attention is concentrated on reversible transmission. A method of eliminating asynchronous swings between systems is described.

Accounting for the service life of equipment in power system engineering cost calculations. V.N. Livshits, (pp. 18-23).

A method is proposed for dealing with estimated repair costs under changing price level conditions.

A powerful unit converting a.c. into d.c. N.S. Klimov, (pp. 29-34).

The difficulties associated with converters for high direct voltage transmission have been partly overcome in a new design where the air gaps do not experience ionization at pressures of 5 to 10 atm.

A voltage regulator with booster transformers. V.A. Somov, (pp. 34-38).

It is supposed that voltage regulators with booster transformers can be used in high powered equipment of several megawatt. To fill a gap in the published literature, the author gives details of such regulators.

Determining the initial conditions for transient calculations when the circuit structure changes. S.I. Kurenev and M.I. Pines (pp. 45-49).

Further to other published papers dealing with the transient processes arising when a knife-switch closes in a circuit, the author establishes a general method of determining the independent initial values of currents in inductance coils and voltages in capacitors in the case of transient processes arising when the structure of live circuits changes. The method is suitable for use on computers.

A method of calculating the amortisseur winding currents in synchronous machines. Iu.A. Kulik, (pp. 53-59).

On the grounds that the currents in the damping windings of synchronous machines ought to be calculated in the design stage, the author proposes a relatively simple mathematical method which covers the majority of cases. Very close approximation is claimed.

Transient stability of synchronous and asynchronous-

synchronous motors with compound excitation for suddenly applied loads. N.R. Ipatenko, (pp. 59-63).

To establish performance ratings and the maximum load despite the non-linearity of the moments' equations and the presence of compound excitation, the author applies the "Lenar" graphical-analytical method to estimate the dynamic stability of synchronous and asynchronous-synchronous motors with compound excitation in drive systems under suddenly applied loads.

A method of calculating the characteristics of solid-rotor induction motors. V.M. Kutsevalov, (pp. 63-67).

A graphical method is proposed for calculating the characteristics of induction motors with solid rotors. It takes into account the variation in magnetic permeability and hysteresis losses. Good agreement with experimental data has been obtained.

A survey of foreign design calculations for electrical ore-smelting furnaces. L.I. Moroz, (pp. 67-73).

A table of the output and current of 15 furnaces made in Russia, France, Germany and Roumania is given to illustrate the different ideas prevalent on the most economic relationship between output, current and voltage. The various electrode and bath dimensions are also considered. Interest is roused most by F.V. Andreae's and W.M. Kelly's work in this field. 15 references.

Nature of the electrical strength of mica insulation. K.A. Andrianov, V.A. Volkov and A.V. Khval'kovskii, (pp. 73-80).

An experimentally-based physical study is made of the electrical strength of impregnated and non-impregnated mica paper and the effect of the distribution of the splittings on electrical strength. The breakdown process is analysed. Thinner splittings of increased size are advocated. The production process should preserve a "continuous anisotropic structure".

A static modulator using a controlled semiconductor resistor O.M. Kudriavtsev, (pp. 80-83).

A study is made of a static modulator in which the resistance of the semiconductor is periodically varied by a changing electrical field (as in Auth. Cert. No. 468904, 5 July 1958). When fitted at the input to

d.c. amplifiers, stability is improved and the amplifiers are suitable for measuring the value of constant or slowly varying voltages and currents in automatic systems etc.

A method of approximation for wire-wound resistors with frequency modulus compensation. Iu.A. Skripnik, (pp.83-85).

A mathematical study is made of wire-resistors for use in phase-insensitive circuits, e.g. in voltmeters. Attempts to reduce reactance increase the frequency error in the "resistance modulus" and thereby reduce accuracy. The use of double-strand windings and high-ohmic resistances is advocated.

SELF-ADJUSTING DECENTRALIZED SYSTEM AUTOMATICALLY CONTROLLING POWER SYSTEM FREQUENCY AND REAL POWER FLOW*

A.G. MOSKALEV

(All-Union Research Institute for Electrical Engineering)

(Received 1 July 1960)

The main purpose of automatically regulating the real power flow and frequency of a power system is to ensure the most economic operation of the system whilst maintaining the frequency at the desired level. This task can only be performed if account is taken of economic and technical characteristics and if the necessary reliability can be ensured under normal and fault conditions.

From the broadest point of view, automatic control of the most economic state of the power system implies that the operating costs are a minimum in monetary terms over a given period of time (e.g. a year, a day) for given thermal and electrical load curves. This is achieved by correctly choosing the equipment and rationally distributing the load between the power stations and generating units.

Fuel-fired power equipment is at present started or stopped by hand because the problems involved in the automation of these operations have yet to be fully solved. We shall therefore consider the matter from a narrower point of view. Automatic control of the most economic state of the power system is here understood to mean that the optimum composition of the units at hydro-electric stations is determined and maintained for the given equipment at fuel-fired powered stations and that the load is distributed in the most economical way between the power stations and their units.

Power systems differ from other forms of industry in that they are

---

* *Elektrichestvo*, 10, 1-7, 1960.

continuously in operation, electrical and thermal energy is constantly being transmitted and consumed, the stations, substations and consumers are spread over vast territories, and the demand for electrical and thermal energy is arbitrarily variable. It is therefore impossible to apply the principles of automatic control developed for individual factories and plant to power systems without further consideration. The principle underlying the automatic control of power systems should be such that the best possible use is made of the physical characteristics of the process of generation, and that the fundamental technical and economic characteristics of the power system be observed.

The following factors must be considered in a solution of this problem: (a) the economic characteristics of the individual units and stations; (b) the technically permissible range over which each unit can be regulated; (c) the given head of water at hydro-electric stations; (d) transmission losses as a function of the load; (e) changes in the units operating and in the configuration of the network during the process of operation etc. Moreover, the system of regulation should not only operate correctly when all the stations in the system are in step, but also when parts of the system are out of step. Some of these factors have to be taken into account all the time, others have to be taken into account as soon as they come into play, whilst others need only be considered periodically. The latter factors can be taken into account automatically or else dealt with manually.

The main characteristics for distributing the load in the most economic way between parallel-operating units and power stations are marginal cost curves (financial expenditure, conventional fuel). As is well known, these curves relate small changes in cost to small changes in output:

$$b = \frac{\partial G}{\partial P}, \tag{1}$$

where G is the conventional consumption of fuel, steam, water of monetary means; and

P is the power of the load.

The loading of parallel-operating boilers and parallel-operating hydro-electric units is most economic when the marginal costs are equal

$$b_1 = \ldots = b_i = \ldots = b_n. \tag{2}$$

The loading of parallel-operating steam turbines is most economic when the units with the smallest values of marginal cost are loaded

first and then those with the largest.* The distribution of the load between boiler-turbine-generator units on the one hand and power stations (fuel-fired and hydro-electric) on the other is most economic when their marginal costs are equal**

$$b_1 = \ldots = b_i = \ldots = b_n = b_0, \tag{3}$$

where b_0 is the marginal cost of the power system.

The load distribution in power systems, especially large combined systems, having long transmission lines where the load losses must be considered will be most economic if the marginal costs of the stations are equal provided the losses in the network relative to a single point in the power system are included:

$$b_1 \frac{1}{1-\sigma} = \ldots = b_i \frac{1}{1-\sigma_i} = \ldots b_n \frac{1}{1-\sigma_n} = b_0 \tag{4}$$

or, alternatively,

$$b_1 b_{1\,\text{net}} = \ldots = b_i b_{i\,\text{net}} = \ldots = b_n b_{n\,\text{net}} = b_0, \tag{4a}$$

where $b_1 \ldots b_n$ are the marginal costs of the stations relative to the bus bars (i.e. network losses ignored);

$b_{1.\text{net}} \ldots b_{n.\text{net}}$ the marginal costs of the individual stations due to the losses in the network when their output is transmitted; and

$\sigma_1 \cdot \ldots \sigma_n$ the marginal costs of the real power flow in the network when the output of the stations is transmitted.

Owing to the energy stored in boiler units, the marginal cost curves of these units (for short transient fluctuations) are very different from the curves obtained if there is a slow secular change, such as occurs in normal operation. The same applies to turbine units, but to a less extent. This prevents the use of the "trial and error" method for finding the optimum state of the power system by varying the control object. The system of automatic control should therefore be such that the marginal cost curves of the boilers and turbines are included. If there is a considerable divergence between these curves and the

---

* The relative increments of generators and transformers have practically no effect on load distribution economics.

** Marginal cost curves for water consumption at hydro-electric stations are different. Equivalent marginal cost curves (in terms of conventional fuel) are obtained by multiplying by a coefficient λ [1,2].

actual curves, they should be changed. At the present time this operation is performed manually in all known systems of power syster regulation.

As regards the marginal cost curve of the network, this can be determined from instantaneous changes in the parameters of the network since the stored energy is comparatively small.

It has been proved [3, 4] that the marginal cost of losses in real power in the network due to the output of the i-th station can be defined quite accurately by the formula:

$$\sigma = \frac{2}{U_i} \cdot \frac{\Delta U_i' + \tau \Delta U_i''}{1 + \tau^2}, \tag{5}$$

where $\Delta U_i'$ and $\Delta U_i''$ are the direct axis and quadrature axis components of the voltage drop between station i with a voltage U_i' and the conventional centre of the power system O with the voltage $\dot{U}_0$; and

τ is the ratio of the inductive reactance of the line to its resistance.

1960

If lines with considerably different values of τ are connected in series (i.e. lines of different rated voltages), then information concerning the voltage in the conventional centre of the power system received at a boundary point of the network I (to define the voltage drop $\Delta \dot{U}_i$) is transmitted to network II (of another rated voltage) in "distorted" form (Fig. 1):

$$\dot{U}_{0II} = (\dot{U}_{0I} - \dot{U}_b)\frac{\tau'}{\tau} + U_b = \Delta \dot{U}_{0II} + \dot{U}_b, \tag{6}$$

where τ refers to the stage at which the information is received;

τ' refers to the stage at which the information is continued, and

U_b is the voltage at the boundary point of the network.

With certain additional assumptions, the marginal cost of the losses in the network can be defined from the formula [1-4]:

$$\sigma = \frac{2\sqrt{3}}{U_r} \sum_1^n I_{a\,k} r_k = \frac{2}{U_r} \sum_1^n \frac{P_k r_k}{U_i} = \sum_1^n \sigma_k, \tag{7}$$

where I_{ak} and P_k are the real current and real power flow of the k-th line respectively;

r_k the resistance of the k-th line;

σ_k – the marginal increase in losses on the k-th line;

U_r – the rated voltage, and

U_j – the voltage at the point where P_k is measured.

The marginal increase in losses for a given station equals the algebraic sum of the marginal increases in loss on the sections of the network between the station and the conventional centre of the power system, calculated along any of the connected parallel branches.

There are two ways of solving this problem at the present time. The first, which is also the first chronologically, consists in the provision of a centralized system of automatic control. The second requires a decentralized system of automatic control.

By "centralized" is meant a system in which the output of each station is determined at a central (e.g. despatcher) point in the system and from which control is transmitted to the power stations.

By "decentralized" is meant a system in which each station determines its own output from the marginal increase.

A decentralized system can include a centralized system for part of the power grid, whereas the reverse is not true. Consequently, the principle of decentralization is the more general.

The individual power stations have to receive representative information about the power system conditions if the load is to be distributed in the most economical way. In a centralized system of regulation a very large number of items of external information are required. Thus, in a combined power system the following data are necessary besides the frequency, which is available,

(a) at the central point – output of the stations, output of the substations in the main network, the state of the transmission lines (whether each given line is connected or not), the composition of the units and the control range of every unit in the system;

(b) at the stations – the required output .

The provision of this information requires at least the following telemetering channels: (a) from each station to the central point; (b) from each substation in the main network to the centre; (c) from the centre to every station. It is therefore impossible to create a reliable centralized system of automatic control in large combined power systems, not to mention the great cost in terms of material and labour involved in installing such a system and maintaining it.

Moreover, the whole system is deprived of automatic control if the

centre is out of order. A centralized system of control does not allot the correct output to stations in parts of a power system operating separated from the main system and does not automatically adjust for changes in the configuration of the network or the composition of the units at the power stations. If the composition of the power system is changed, or if power systems are combined, the existing resolving devices have to be replaced and, in the latter case, a whole new network of telemetering channels has to be created. A centralized system cannot therefore be recommended for combined power systems, or for a single national grid.

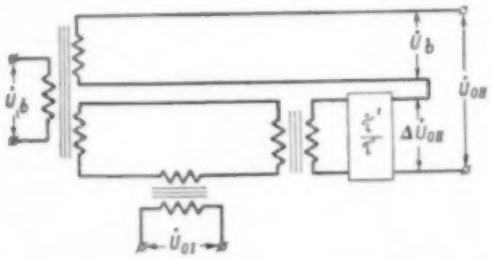

Fig. 1. Conversion of the voltage of the conventional centre on transition to a network with a considerably different value of τ.

In 1951, in the All-Union Research Institute of Electrical Engineering, the author proposed a method of control based on the balanced e.m.f. principle and a decentralized automatic control system was subsequently developed that satisfied all the stated requirements. This system of control is effected by three criteria, namely, (1) deviations from the desired value of the basic quantity defining the output or "product" (i.e. frequency, voltage, pressure etc); (2) the actual output or "product" per sec; (c) a certain integral function of the deviation of the basic variable criterion from the desired value.

As regards the regulation of frequency and real power flow with network losses ignored, the control equation is:

$$\Delta f - s_i(P_i - \varphi_i \int_0^t k\,\Delta f\,dt) = 0,\ (i = 1, 2, \ldots, n), \qquad (8)$$

where Δf is the frequency deviation;

P – the output of a unit;

ϕ – a function defining the economic characteristic of a unit

over the range of control and the limiting function for the limits of the control range;

s – the coefficient of "statism", ("statism" is defined as the deviation of the regulated quantity at rated load from its no load value expressed as a percentage of the latter *Translator*).

k – a constant coefficient;

t – time.

The integral function of the frequency deviation is a measure for comparing the marginal increments of the power stations. Quantitatively, it equals the marginal increment in a closed automatic control system:

$$\int_0^t k\,\Delta f\,dt = b_0. \tag{9}$$

The function ϕ is the marginal cost curve of the unit $P = \xi(b)$.

Thus, the product of the integral function times the function ϕ gives the desired output of the unit. This output corresponds to the equivalence of the marginal costs. On the other hand, the integral function (9) is no other than the deviation of synchronous time T_{synch} from astronometric time T_{ast}:

$$\int_0^t k\,\Delta f\,dt = \int_0^t kf_{\text{ast}}\,dt - \int_0^t kf_{\text{synch}}\,dt = \\ = b \equiv T_{\text{ast}} - T_{\text{synch}} = \Delta T. \tag{10}$$

This is a permissible system of control since the variation in the functions $\int k\,\Delta f\,dt$ и $b = \psi(P)$ is qualititatively the same if the power balance in the system is disturbed and, consequently, when the frequency deviates from its rated (standard) value. These qualities are compared quantitatively during the process of automatic control in closed systems.

A load distribution device URAN is used in the control system of a fuel-fired power station with a common steam main. This device allots the load to the various units in the most economical way.

For a combined power system when the marginal increment of the network $\frac{1}{1-\sigma}$ is taken into account, the control equation after certain conversions is

(a) for boiler-turbine-generator-type stations and hydro-electric stations:

$$\Delta f - s_i\left[P_i - \varphi_i(1-\varepsilon_i)\int_0^t k\,\Delta f\,dt\right]=0; \tag{11}$$

(b) for fuel-fired stations with a common steam main

$$\Delta f - s_i\left\{P_i - \varphi_i\int_0^t [\Delta f - b_0 + (b_{st\,i} b_{i\,net})]\,dt\right\}=0. \tag{12}$$

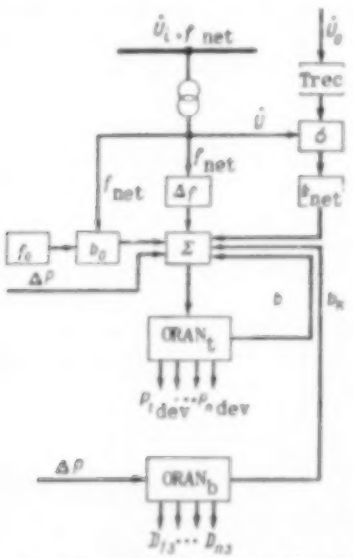

Fig. 2. The decentralized self-adjusting system for controlling the operating load of a fuel-fired power station with a common steam main.

To simplify the design of the control system, all the marginal cost curves (of the units, stations and the network) are produced on a semi-logarithmic basis so that the marginal increments are added instead of multiplied. The semi-logarithmic basis also makes it easier to change automaticaly the marginal cost curve of the station, if the given head of water, head of steam or number of units operating at hydro-electric stations is changed, as well as in other cases.

Fig. 2 shows the system employed in the self-adjusting decentralized system for regulating the performance of a fuel-fired power station with a common steam main. The components of the logarithm of the marginal increment of the station relative to the conventional centre of the power system are fed to the integrator " Σ " from the right:

$$\lg b_{st} = \lg b_b + \lg b_t + \lg b_c,$$

where b_b is the marginal increment of the boiler house;

b_t – the marginal increment of the generating plant;

b_n – the marginal increment of the network.

The logarithm of the marginal increment of the power system, $\log b_0$, is fed in from the left.

The system of regulation is in a state of equilibrium when the frequency in the system equals its rated value and when the marginal cost of the station equals the marginal cost of the power system. If the composition of the running units is changed at the station, the heat balance is upset, the instruction from the device for controlling the load distribution between the boiler units ($URAN_b$) is altered and likewise the marginal cost of the boiler house. In the process of regulation, a new station loading is established for different values of b_b, b_t and b_n. A change in the configuration of the network, or in the operating conditions of the stations, leads in the same way to an automatic change in the operating loading of the station in question if it is accompanied by a change in b_n at this station.

Thus, the system automatically adjusts changes in the power system, or at the station to the most economic conditions.

The functions ϕ take into account the economic characteristic and restricts the control range of each unit (boiler, turbine) separately. The power developed by the station is automatically restricted by the introduction of the pressure deviation criterion Δ_p not only when the control ranges of the generating plant and boiler house are not matched, but also when the limit of the control range is approached. This feature is also used to curtail output under other conditions e.g. if the heat balance is disturbed at the same time.

For boiler-turbine-generator stations, the system is more simple (Fig.3). The marginal increments are also supplied in logarithmic form.

The system of automatic control in hydro-electric stations includes an auto-operator which maintains the composition of the units in the most economic state (Fig.4). The auto-operator also starts the standby units if a drop in frequency occurs. Under this system there is complete automatic control over the real power flow of the hydro-electric station, including the determination of the most economic load, the most economic composition of the units and maintenance of these conditions.

It follows from equations (8), (11) and (12) that the load allocated to each unit is not a function of the overall load of the station, but of the integral of the deviation in frequency. Therefore an arbitrary function of the load can be specified for each unit separately, including a function which will only change the load of the unit in question within the defined range (from P_{min} to P_{max}) for all possible marginal increments of the power system. This is very important for controlling the operation of units in fuel-fired power stations.

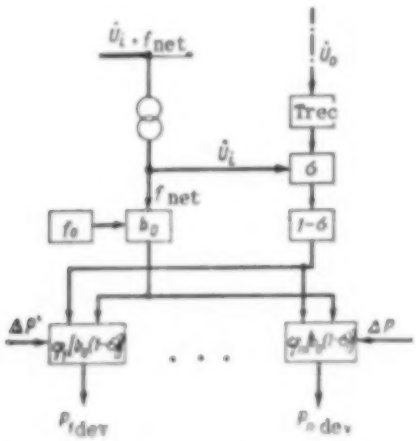

Fig. 3. The decentralized self-adjusting system for controlling the operating load of a unit-type power station.

All the necessary information is available at the power stations for automatic control in accordance with equation (8). In point of fact, the actual output is measured at the station and there is a single frequency in the power system. Therefore, if the frequency "transmitter-gauges" are sufficiently accurate, the functions

$$\int_0^t k\,\Delta f\,dt$$

are the same at all the stations. Control in accordance with equations (11) and (12) requires additional information about the marginal increment in the network losses with respect to the load of the station in question. This information is generally obtained at the station through telemetering channels. The number of channels depends on the method used to determine the marginal increment in losses. Methods

have been developed to send this information to every station along one channel.

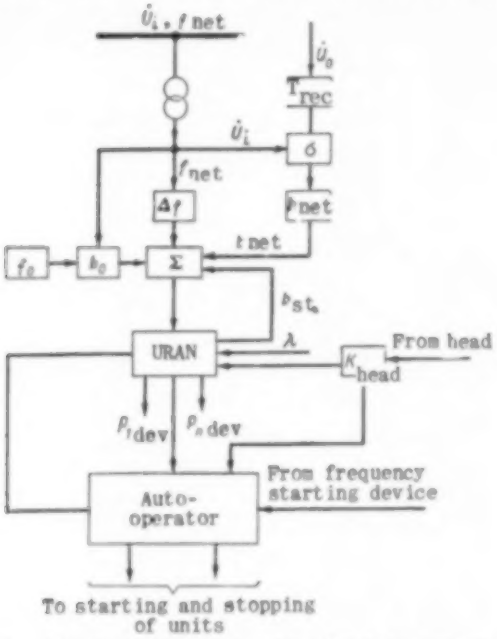

Fig. 4. The decentralized self-adjusting system for controlling the operating load of a hydro-electric power station with a low head of water.

The block diagram in Fig.5 refers to a self-adjusting decentralized system of control for a part of a power system having five stations and two rated voltages in the main network. In this case the marginal increment in network losses is determined from formula 5. The conventional centre of the power system is assumed to be the bus bars of substation *O*. On transition from a network of one rated voltage to the next network of a different rated voltage, the voltage vector of the conventional centre O is converted in the device *CV* in accordance with formula 6.

The system of regulation illustrated in Fig.5 will operate correctly if the power system is divided up into separate parts provided the voltage vector $\dot{U}_0$ is transmitted through the nodal stations (substations). Loss of synchronism of various parts of the power system can be detected from the angle of the voltage vectors $\dot{U}_0$, and the sense at the point $\dot{U}_i$ in question. Using an automatic device at the input to the tele-transmitter *Ttr*, we can supply the voltage of the point in question instead of the received voltage $\dot{U}_0$. The latter point becomes the new conventional centre for the separated part of the power system. When

synchronizm is restored the automatic device will again supply at the input to the tele-transmitter the voltage $\dot{U}_0$ received along the tele-channel.

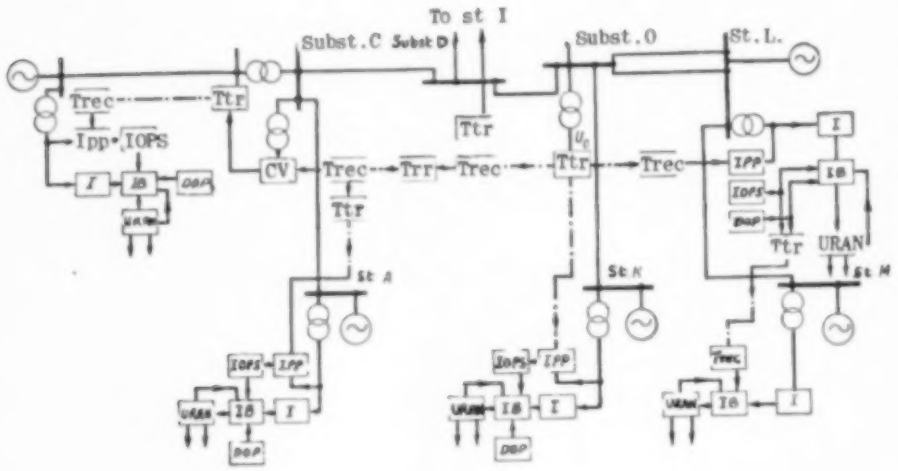

Fig. 5. A second type of decentralized self-adjusting system of regulation for a combined power system.

If the marginal increment in losses is determined in accordance with formula (7), the system of regulation is that shown in Fig.6. Both principles of accounting for network losses can be combined, for example, up to a certain point the increment σ may be defined by the voltage vector, and beyond that point by formula (7).

Regulation in accordance with equations (11) and (12) prevents disturbance to parallel operation by overloading of individual stations and lines, since the station stops load build-up before the maximum transmitting capacity of the line is reached.

The necessary apparatus for this type of control has been developed and is largely in batch production.

The above system of control can ensure the most economic conditions within a given power system, and guarantee the observance of contracts between power systems and nations for the exchange of power and electrical energy. For this purpose a correction is made to the foregoing law of regulation so that the following equations hold:

(a) If in the regulation of the power system the losses in the network are neglected

$$b_1 = \ldots = b_i = \ldots = b_n = \alpha b_0; \tag{3a}$$

(b) if the losses in the network are considered

$$b_1 b_{1\,\text{net}} = \ldots = b_i b_{i\,\text{net}} = \ldots = b_n b_{n\,\text{net}} = \alpha b_0, \tag{4b}$$

where α is a coefficient taking into account the contractual relationships.

It is expedient to consider the following three types of co-operation for the exchange of electricity between power systems (nations).

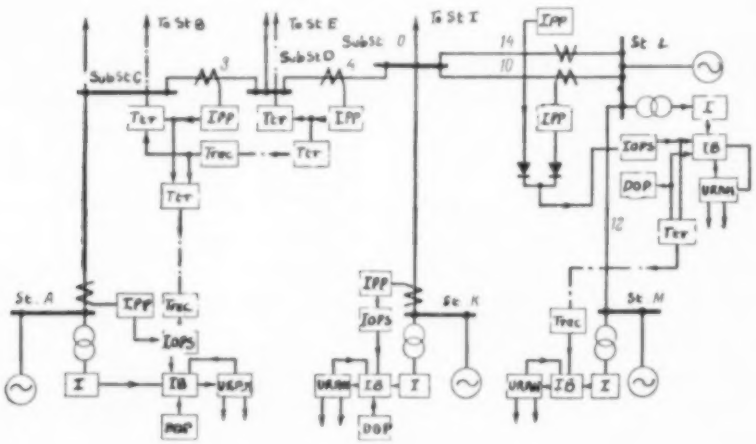

Fig. 6. The first decentralized self-adjusting system of regulation for a combined power system.

1. The load is distributed between the power stations of given power system (nation) in the most economic way, whilst the output is exchanged between power systems in conformity with defined values (daily load charts). The load can be distributed between the stations of the power system in question with or without network losses taken into account. Under this system, coefficient α is a function of the deviation from the desired value of the power flow between the system ΔP:

$$\alpha = \alpha_0 + \psi(\Delta P). \tag{13}$$

2. The load is distributed between the power stations of the power system (nation) in question in the most economical way, whilst the electrical energy is exchanged between the power systems (nations)

within the limits fixed by the plans or bilateral negotiations without strictly fixing the power exchanged. Here the coefficient is a function of the given value of the power exchanged. It varies discretely over a cyclical period of time (a day, week) during which it remains constant. To prevent over-generation of electricity in individual power systems (countries), to transmit it to other power systems in off-peak periods and to stimulate the production of extra power during peak load periods, it is expedient to introduce a two- or three-part tariff for energy transmitted to or received from another power system in accordance with actual average production costs. This tariff is fixed as a function of the actual value of the marginal increment of the power system.

3. The load is distributed between power systems in the most economic way on condition that the consumption of conventional fuel or the financial outlay is a minimum. In this case the coefficient α should be equal to unity or some other constant quantity as a function of the equivalent adopted for b_0.

The system of regulation described with local "transmitter-gauges" for the marginal increment was first installed on the Kharkov power system in 1957. It has produced good results in operation. The control process has been stable and of good quality and the most economic conditions have been maintained.

In 1959 the system of regulation was tested on the combined southern power system involving five power stations and its good qualities were shown again.

Translated by O.M. Blunn

REFERENCES

1. V.M. Gornshtein: *The most economic load distribution between parallel-operating power stations, (Naivygodneishee raspredelenie nagruzok mezhdu parallel'no rabotaiushchimi elektrostantsiiami).* Gosenergoizdat. (1949).
2. V.M. Gornshtein: *The most economic distribution of the active load between power stations, (Naivygodneishee raspredelenie aktivnoi nagruzki mezhdu elektrostantsiiami).* Trud. TsNIE'L. No. VI. Gosenergoizdat. (1957).
3. N.A. Mel'nikov: *Elektrichestvo,* No.2, (1960).

4. A.G. Moskalev; *Automatic regulation of the frequency and real power flow in power systems, (Avtomaticheskoe regulirovanie rezhima energeticheskoi sistemy po chastote i aktivnoi moshchnosti).* Gosenergoizdat, (1960).

TRANSIENTS IN MAGNETIC AMPLIFIERS WITH AN RL (ACTIVE INDUCTIVE) LOAD IN THE RECTIFIED CURRENT CIRCUIT*

KHU-TSZIA-IAO and V.A. SHUBENKO

(Received 9 April 1960)

1960

There is a dynamic redistribution of voltage in the transient states of magnetic amplifiers with an RL load in the rectified current circuit which in a number of cases has a considerable effect on the course of the transient. This phenomenon has still to be fully studied.

Bessonov [1] has suggested a graphical-analytical method of determining transient phenomena in magnetic amplifiers which takes this dynamic voltage redistribution into account. This method is based on the method of "successive intervals" and is therefore extremely complicated.

Safris [2] has studied a more convenient method which uses a simple equivalent network, but the author confines himself to the study of magnetic amplifiers without feedback operating in the presence of weak signals when all the parameters can be regarded as constant. If this method is used, the equivalent time constant of the load circuit may often be low.

Our investigations show that dynamic voltage redistribution is a feature of any rectifier circuit with an RL load and that it is caused by a pre-connected resistance. A previous paper has dealt with this phenomenon in the stated circuits [3].

In this paper a description is given of a more general method determining transient phenomena in magnetic amplifiers, which allows the effect of dynamic voltage redistribution, feedback and also circuit non-linearity to be taken into account.

---

* *Elektrichestvo*, 10, 38-41, 1960.

Suppose we begin with the simplest case. It is assumed that it is required to find the law governing the variation in the transient currents in magnetic amplifiers without feedback but with an RL load in the rectified circuit when the control voltage is connected (Fig. 1a).

To simplify the analysis, it is assumed that the rectifiers are ideal.*

In the following we shall use average half period values of the electrical and magnetic quantities.

The equations of the arrangement in Fig. 1(a) are:

$$\Delta u_r = L_l \frac{d\Delta i_l}{dt} + \Delta i_l r_l; \tag{1}$$

$$\Delta u_c = w_c \frac{d\Delta\Phi_0}{dt} 10^{-8} + \Delta i_c r_c; \tag{2}$$

$$\Delta u_b = w_b \frac{d\Delta\Phi_0}{dt} 10^{-8} + \Delta i_b r_b, \tag{3}$$

where i_l, i_c and i_b are the average currents in the load, control and bias circuits respectively, *a*;

u_r and u_c – the rectified voltage and control circuit voltage, *V*;

L_l – load inductance, *H*;

r_l, r_c and r_b – the resistances in the load, control and bias circuits, Ω;

w_c and w_b – the number of turns in the control and bias windings; and

Φ_0 – the constant component of the magnetic flux, *M*.

From an analysis of the magnetic characteristics, we get

$$\Delta u_r = k'_w \Delta\Sigma i_0 w_0 - \Delta i_{\sim av} r_l; \tag{4}$$

$$\Delta\Phi_0 10^{-8} = k'_\Phi \Delta\Sigma i_0 w + a_1 \Delta u_r; \tag{5}$$

$$\Delta\Sigma i_0 w_0 = \Delta i_c w_c + \Delta i_b w_b, \tag{6}$$

where i_{av} is the average alternating current, and

* Germanium rectifiers were used in the experiments.

$$k'_w = \frac{\partial u_r}{\partial \Sigma i_0 w_0}, \qquad r'_i = \frac{du_{\sim av}}{\partial i_{\sim av}} = -\frac{\partial u}{\partial i_{\sim av}},$$

$$k'_\Phi = \frac{\partial \Phi_0}{\partial \Sigma i_0 w_0} 10^{-8}, \quad \alpha_1 = \frac{\partial \Phi_0}{\partial u_r} 10^{-8}$$

are coefficients dependent on the properties and design of the magnetic amplifier and parameters of the circuits.

Putting $\varepsilon = \frac{\Delta i_{\sim av}}{\Delta i_l}$, equation (4) becomes

$$\Delta u_r = k'_w \Delta \Sigma i_0 w_0 - \Delta i \, r'_i , \tag{7}$$

where $r'_i = \varepsilon r_l$.

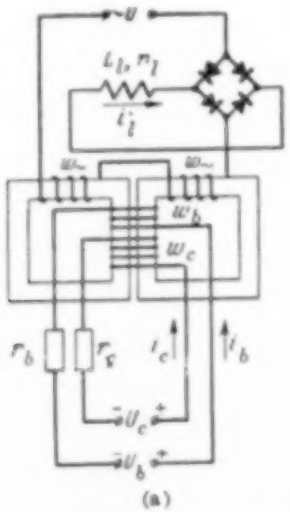

(a)

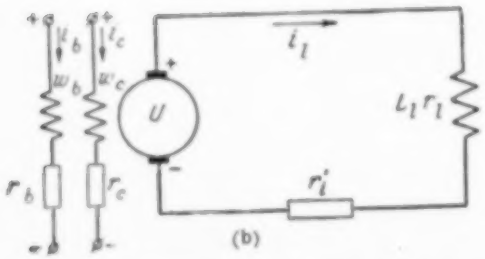

(b)

Fig. 1. Main circuit (a) and equivalent network (b) of a magnetic amplifier without feedback with an RL load in the rectified current circuit.

Hence, the main circuit of the magnetic amplifier without feedback can be replaced by the equivalent network shown in Fig. 1(b) where u_e and r_i' are the voltage and internal impedance of the equivalent generator.

The voltage u_e varies during the transient as a function of the instantaneous values i_c and i_b. At the end of the transient u_e is equal to the average half-period value of the main voltage.

The impedance r_i' depends on both the steady state and instantaneous values of the m.m.f. The dependence of r_i' on the instantaneous value is not significant and it can therefore be regarded as constant during the transient.

It is pre-supposed that r_i' corresponds to the steady state value of the inductive reactance of the operating windings of the magnetic amplifier and so r_i' can be readily defined by steady state parameters.

The steady state equations for the arrangement in Fig. 1(b) are

$$U_e = U_{ek} = k_w' \Delta I_c w_c = U_{av} = I_l (r_l + r_i'), \tag{8}$$

whence

$$k_w' = \frac{\Delta I_l}{\Delta I_c w_c} (r_l + r_i') = k_w \frac{r_e}{r_l} = k_l \frac{r_e}{w_c} \tag{9}$$

and

$$r_e = r_i' + r_l = \frac{U_{av}}{I_l}, \tag{10}$$

where

$$k_w = \frac{\Delta U_l}{\Delta I_c w_c} = \frac{\Delta I_l r_l}{\Delta I_c w_c}; \quad k_l = \frac{\Delta I_l}{\Delta I_c}.$$

Formula (10) usually produces a slightly reduced value of r_e since the variation in σ and r_i' during the transient is ignored. It is therefore recommended that the following experimentally determined formula be used:

$$r_e = r_l + r_i' = m \frac{U_{av}}{I_l}, \tag{10a}$$

where m takes into account the fact that the average value of r_e during

the transient will be greater than its steady state value owing to the variation in σ and r_i.

It has been established that $n = 1.05$ to 1.15 for magnetic amplifiers having an E-shaped transformer steel core.

In general the coefficients k_ψ', k_Φ' and $\alpha\gamma$ are not constant. But these values can be assumed constant for a weak signal, when operating on the linear part of the magnetic characteristics. Equations (1) to (7) can then be solved by the operator (transform?) method.

The initial conditions (if $t = 0$) are:

$$\Delta\Phi_0(0) = 0; \tag{11}$$

$$\Delta\Sigma i_0 w_0(0) = 0; \tag{11a}$$

$$\Delta i_l(0) = 0. \tag{11b}$$

Solving equations (2), (3) and (11a), the value of the initial control current is

$$\Delta i_c(0) = \frac{\beta_b}{1+\beta_b}\Delta I_c \tag{11c}$$

where

$$\beta_b = \frac{w_b^2}{r_b}\cdot\frac{r_c}{w_c^2}.$$

Hence the control current is subject to sudden fluctuations at the beginning of the transient owing to the transformer "link" between the control and bias current circuits.

Solving equations (1) to (7) with the initial conditions taken into account, we get

$$\Delta i_c(p) = \frac{\Delta I_c}{p}\times$$
$$\times\frac{(\tau_l'\tau_{b(s)} + \tau_l\tau_{b(T)})p^2 + (\tau_l' + \tau_{b(s)} + \tau_{b(T)})p + 1}{(\tau_l'\tau_{0(s)} + \tau_l\tau_{0(T)})p^2 + (\tau_l' + \tau_{0(s)} + \tau_{0(T)})p + 1} \tag{12}$$

$$\Delta i_l(p) = \frac{\Delta I_l}{p}\times$$
$$\times\frac{1}{(\tau_l'\tau_{0(s)} + \tau_l\tau_{0(T)})p^2 + (\tau_l' + \tau_{0(s)} + \tau_{0(T)})p + 1}. \tag{13}$$

1960

Equations (12) and (13) correspond to the following differential equations:

$$\Delta I_c = (\tau_l' \tau_{0(s)} + \tau_l \tau_{0(\gamma)}) \frac{d^2 \Delta i_c}{dt^2} + \\ + (\tau_l' + \tau_{0(s)} + \tau_{0(\gamma)}) \frac{d\Delta i_c}{dt} + \Delta i_c; \tag{12a}$$

$$\Delta I_l = k_{lw} \Delta I_c w_c = (\tau_l' \tau_{0(s)} + \tau_l \tau_{0(\gamma)}) \frac{d^2 \Delta i_l'}{dt^2} + \\ + (\tau_l + \tau_{0(s)} + \tau_{0(\gamma)}) \frac{d\Delta i_l}{dt} + \Delta i_l, \tag{13a}$$

where

$$\tau_l = \frac{L_l}{r_l}; \quad \tau_l' = \frac{L_l}{r_e} = \tau_l \frac{r_l}{r_e};$$

$$\tau_{0(s)} = \left(\frac{w_c^2}{r_c} + \frac{w_b^2}{r_b} \right) k_\Phi' = (1 + \beta_b) \frac{w_c^2}{r_c} k_\Phi';$$

$$\tau_{0(\gamma)} = \left(\frac{w_c^2}{r_c} + \frac{w_b^2}{r_b} \right) \alpha_\gamma k_w = (1 + \beta_b) \frac{w_c^2}{r_c} \alpha_\gamma k_w;$$

$$\tau_{(s)} = \frac{w_b^2}{r_b} k_\Phi'; \quad \tau_{b(\gamma)} = \frac{w_b^2}{r_b} \alpha_\gamma k_w.$$

Hence dynamic voltage redistribution leads to a lower equivalent time constant of the load circuit. The relative decrease in the time constant is defined by the expression:

$$\frac{\tau_l'}{\tau_l} = \frac{r_l}{r_e} = \frac{I_{l'}}{mI_{l.\max}} = f\left(\frac{\Sigma I_0 w_0}{\Sigma I_0 w_{0\max}} \right). \tag{14}$$

Fig. 2 shows $\frac{\tau_l'}{\tau_l}$ as a function $f\left(\frac{\Sigma I_0 w_0}{\Sigma I_0 w_{0\max}}\right)$, UM-51-65/46 type amplifier. The value of τ_l' is considerably less than τ_l for slight magnetization, but it approaches τ_l as $\Sigma I_0 w_0$ approaches maximum. Therefore, the weaker the magnetization, the greater is the magnetic amplifier. Conversely, this effect is negligible if there is great magnetization.

The effect of dynamic voltage redistribution on the transient also

depends on the ratio $\frac{\tau_0}{\tau_l'}$. The greater $\frac{\tau_0}{\tau_l'}$, the more slowly does the voltage in the operating circuit vary. At a certain high value of $\frac{\tau_0}{\tau_l'}$ the effect of dynamic voltage redistribution on the transient can be ignored [4].

Owing to the existence of an electromagnetic link between the primary and secondary circuits of the magnetic amplifier, the dynamic voltage redistribution also affects the secondary circuits. Consequently, the transient in the control circuit cannot strictly speaking be defined by one time constant. But, as we shall see, this phenomenon is often unimportant and can therefore be ignored in practical calculations.

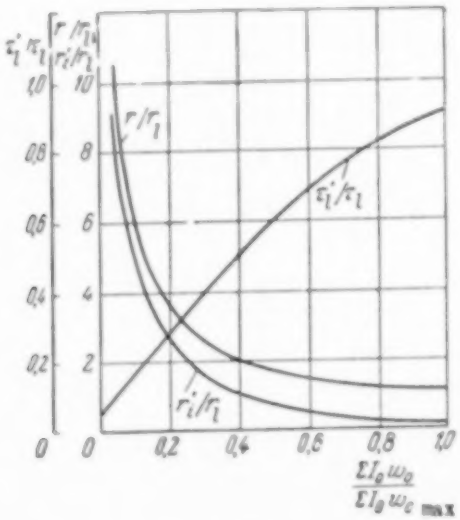

Fig. 2. The values of r_i'/r_l, r_e/r_l and τ_l'/τ_l as a function of $\Sigma I_0 w_0$.

Transients in magnetic amplifiers with external feedback (Fig. 3). In this case, instead of equations (1), (6) and (7) we have:

$$\Delta u_r = L_l \frac{d\Delta i_l}{dt} + \Delta i_l r_l + w_{fb} \frac{d\Delta\Phi_0}{dt} 10^{-8}; \qquad (15)$$

$$\Delta\Sigma i_0 w_0 = \Delta i_c w_c + \Delta i_b w_b + \Delta i_l w_{fb}; \qquad (16)$$

$$\Delta u_r = k'_{w\,fb} (\Delta i_c w_c + \Delta i_b w_b) - \Delta i_l r_i', \qquad (17)$$

where w_{fb} is the number of turns in the feedback winding; and

$$k'_{w\,fb} = k'_w\left(1 + k_{I\,fb}\,\frac{w_{fb}}{w_c}\right); \quad k_{I\,fb} = \frac{\Delta I_l}{\Delta I_c}.$$

(N.B. "fb" stands for feedback).

Solving equations (2), (3), (5) and (15) to (17), we get:

$$\Delta i_c(p) = \frac{\Delta I_c}{p} \times \times \frac{\left[\tau_{b(s)}\tau'_l + \tau_l \tau_{b(T)}\left(1 + k_{I\,fb}\,\frac{w_{fb}}{w_c}\right)\right]p^2 + \tau_{e.b}\,p + 1}{\left[\tau_{0(s)}\tau'_l + \tau_l \tau_{(T)}\left(1 + k_{I\,fb}\,\frac{w_{fb}}{w_y}\right)\right]p^2 + \tau_{e.o}\,p + 1}, \tag{18}$$

$$\Delta i_l(p) = \frac{1}{p} \times \times \frac{\Delta I_l - \frac{w_c}{w_{fb}}\left[\tau'_{fb(s)} + \tau_{fb(T)}\left(1 + k_{I\,fb}\,\frac{w_{fb}}{w}\right)\right]p\Delta I_c}{\left[\tau_{0(s)}\tau'_l + \tau_l \tau_{0(T)}\left(1 + k_{I\,fb}\,\frac{w_{fb}}{w_c}\right)\right]p^2 + \tau_{e.o}\,p + 1}, \tag{19}$$

where

$$\tau = \tau'_l + \tau'_{fb(s)} + \tau_{b'}\left(1 + k_{I\,fb}\frac{w_{fb}}{w_c}\right) - \frac{\alpha_1 w_{fb} r'_i}{r_e}; \tag{20}$$

$$\tau_{e.o} = \tau'_l + \tau'_{fb(s)} + \tau_0\left(1 + k_{I\,fb}\,\frac{w_{fb}}{w_c}\right) - \frac{\alpha_1 w_{fb} r'_i}{r_e}; \tag{21}$$

$$\tau'_{fb(s)} = \frac{w^2_{fb}}{r_e}\,k'_\Phi; \quad \tau_{fb(T)} = -\frac{w^2_{fb}}{r_l}\,\alpha_1 k_w;$$

$$\tau_b = \tau_{b(s)} + \tau_{b(T)}; \quad \tau_0 = \tau_{0(s)} + \tau_{0(T)}.$$

Equations (18) and (19) correspond to the following differential equations

$$\Delta I_c = \left[\tau_{0(s)}\tau'_l + \tau_l \tau_{0(1)}\left(1 + k_{l\,fb}\frac{w_{fb}}{w_c}\right)\right]\frac{d^2\Delta i_c}{dt^2} + \\ + \tau_{e.o}\frac{d\Delta i_c}{dt} + \Delta i_c; \tag{18a}$$

$$\Delta I_l = k_{l\,fb}\Delta I_c w_c = \\ = \left[\tau_{0(s)}\tau'_l + \tau_l \tau_{0(1)}\left(1 + k_{l\,fb}\frac{w_{fb}}{w_c}\right)\right]\frac{d^2\Delta i_l}{dt^2} + \\ + \tau_{e.o}\frac{d\Delta i_l}{dt} + \Delta i_l \tag{19a}$$

If $\omega_{fb} = 0$, equations (18) and (19) are converted into (12) and (13).

These results agree well with the data given by Safris [2] and Rozenblat [5]. For proof of this, consider the following cases.

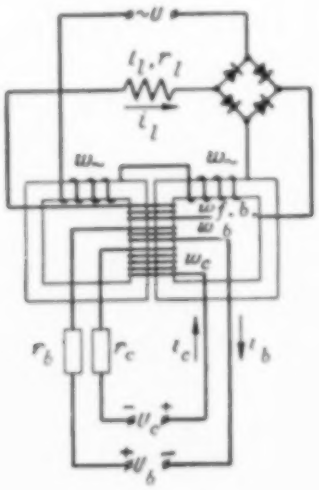

Fig. 3. A magnetic amplifier with external feedback and an RL load in the rectified current circuit with control voltage connected.

Case 1. In the absense of bias ($w_b = 0$ and $r_b = 0$), equations (12)

1960

and (13) simplify to

$$\Delta i_c(p) = \frac{\Delta I_c}{p} \times$$

$$\times \frac{1 + \tau'_l p}{(\tau'_l \tau_{0(s)} + \tau_l \tau_{0(T)}) p^2 + (\tau'_l + \tau_{0(s)} + \tau_{0(T)}) p + 1}; \quad (22)$$

$$\Delta i_l(p) = \frac{\Delta I_l}{p} \times$$

$$\times \frac{1}{(\tau'_l \tau_{0(s)} + \tau_l \tau_{0(T)}) p^2 + (\tau'_l + \tau_{0(s)} + \tau_{0(T)}) p + 1}. \quad (23)$$

Equations (22) and (23) have been produced by Safris for magnetic amplifiers without feedback or bias and with a weak signal [2].

Case 2. In the absense of dynamic voltage redistribution ($r_i = 0$ and $\tau_l = \tau_l$) the equations from (12a) and (13a) are:

$$\Delta I_c = \tau_0 \tau_l \frac{d^2 \Delta i_c}{dt^2} + (\tau_l + \tau_0) \frac{d \Delta i_c}{dt} + \Delta i_c. \quad (24)$$

$$\Delta I_l = \tau_0 \tau_l \frac{d^2 \Delta i_l}{dt^2} + (\tau_l + \tau_0) \frac{d \Delta i_l}{dt} + \Delta i_l, \quad (25)$$

where

$$\tau_0 = \tau_{0(s)} + \tau_{0(T)}.$$

Equations (24) and (25) agree with those produced by Rozenblat [5] if dynamic voltage redistribution is ignored.

In this case, equations (12), (13) and (18) to (21) also agree with those produced in an earlier paper [4]*.

Case 3. In the event of a purely active load ($\tau_l = \tau_l = 0$), equations (12a) and (13a) become

$$\Delta I_c = \tau_0 \frac{d \Delta i_c}{dt} + \Delta i_c; \quad (26)$$

* An error was committed in the deduction of the formulae in [4]. Equation (6), instead of $u_r = u_x + k_u i_c w_c$, should be: $u_r = u_x + k_u (i_c w_c + i_b w_b)$. Consequently, equation (11) in [4] should contain τ_0 and not τ_c.

$$\Delta I_l = \tau_0 \frac{d\Delta i_l}{dt} + \Delta i_l. \tag{27}$$

These results also agree with the theoretical data obtained for transients in magnetic amplifiers with an active load when the lag of the load current behind the control current is ignored [5].

If equations (12), (13) and (18) to (21) are to be used for practical calculations, it is first necessary to define the characteristic values of k'_Φ, a_T and k_w. This is rather complicated.

Our analysis of theoretical and experimental data has shown that simplified equations can be used for practical purposes with a sufficient degree of accuracy. This, for magnetic amplifiers with E-shaped transformer steel cores we usually find that $(\tau_{0(s)} \gg \tau_{0(\gamma)}$. In this case, if there is no feedback, we can assume that $\tau_{0(\gamma)} = 0$ and $\tau_{0(s)} = \tau_0$. Then equations (12a) and (13a) are:

$$\Delta I_y = \tau'_l \tau_0 \frac{d^2\Delta i_c}{dt^2} + (\tau'_l + \tau_0)\frac{d\Delta i_y}{dt} + \Delta i_c; \tag{28}$$

$$\Delta I_l = \tau'_l \tau_0 \frac{d^2\Delta i_l}{dt^2} + (\tau'_l + \tau_0)\frac{d\Delta i_l}{dt} + \Delta i_l. \tag{29}$$

If there is external feedback, equations (18a) and (19a) in the first approximation become

$$\Delta I_c = \tau'_l \tau_{0(\mathrm{fb})} \frac{d^2\Delta i_c}{dt^2} + (\tau'_l + \tau_{0(\mathrm{fb})})\frac{d\Delta i_c}{dt} + \Delta i_c; \tag{30}$$

$$\Delta I_l = \tau'_l \tau_{0(\mathrm{fb})} \frac{d^2\Delta i_l}{dt^2} + (\tau'_l + \tau_{0(\mathrm{fb})})\frac{d\Delta i_l}{dt} + \Delta i_l, \tag{31}$$

where

$$\tau_{0(\mathrm{fb})} = \tau_0\left(1 + k_{l\,\mathrm{fb}}\frac{w_{\mathrm{fb}}}{w_c}\right) = \tau_0 \frac{k_{l\,\mathrm{fb}}}{k_l}. \tag{32}$$

These equations are based on the assumption that the magnetic amplifier is operating with a weak signal and that all the circuit parameters are constant. But magnetic amplifiers usually operate on the non-linear parts of the characteristics and τ_0 and k_l are usually variable during the transient. Under these conditions linear sections can be substituted for the non-linear characteristics. The equations of each section can be solved separately.

1960

To solve this problem we have to substitute the following equations for (30) and (31):

$$I_c = \tau_l' \tau_{0(\mathrm{fb})} \frac{d^2 i_{ck}}{dt^2} + (\tau_l' + \tau_{0(\mathrm{fb})}) \frac{di_{ck}}{dt} + i \quad ; \tag{30a}$$

$$I_{1k} = I_{1xk} + k_{Iw\,\mathrm{fb}} \, I_c w_c = \tau_l' \tau_{0(\mathrm{fb})} \frac{d^2 i_{lk}}{dt^2} +$$

$$+ (\tau_l' + \tau_{0(\mathrm{fb})k}) \frac{di_{1k}}{dt} + i_{1k} \tag{31a}$$

where k refers to the length of the k-th section.

We can find τ_{ok} from the curves for $\Phi_0 = f(\Sigma I_0 w_0 E_{\sim \mathrm{av}})$ and $E_{\sim \mathrm{av}} = f(\Sigma I_0 w_0)$ by a graphical method described by Rozenblat [5]. We can find $k_{Iw(fb)k}$ from the load curve $I_l = f(I_c w_c + I_b w_b)$.

The solutions of equations (30a) and (31a) are:

$$i_{ck} = I_c + A_k e^{p_{1k} \Delta t_k} + B_k e^{p_{2k} \Delta t_k}, \tag{33}$$

$$i_{lk} = I_{lk} + C_k e^{p_{1k} \Delta t_k} + D_k e^{p_{2k} \Delta t_k}, \tag{34}$$

where

$$p_{1k} = -\frac{1}{\tau_{0(\mathrm{fb})k}}; \quad p_{2k} = -\frac{1}{\tau_l'}; \tag{35}$$

and A_k, B_k, C_k and D_k are constants of the k-th section defined by the initial or boundary conditions.

The initial conditions of the transient in the magnetic amplifier with external feedback and a control voltage connected are defined by the following formulae:

$$i_{l\,(t=0)} = I_{1x}; \tag{36}$$

$$i_{c\,(t=0)} = \frac{\beta_b}{1 + \beta_b} I_c; \tag{37}$$

$$\frac{di_l}{dt}_{(t=0)} = -\frac{w_{\mathrm{fb}}}{w_c} \cdot \frac{U_c}{L_l (1 + \beta_b)}; \tag{38}$$

$$\frac{di_c}{dt_{(t=0)}} = \frac{I_c}{1+\beta_b} \cdot \frac{\tau' + \tau'_{fb}}{\tau'_l \tau_{0\,(fb)}}. \tag{39}$$

The boundary conditions on transition from the k-th to the $k+1$ section are:

$$(i_{l\,(k+1)})_{t_k} = (i_{l\,(k)})_{t_k}; \tag{40}$$

$$(i_{c\,(k+1)})_{t_k} = (i_{c\,(k)})_{t_k}; \tag{41}$$

$$\left(\frac{di_{l\,(k+1)}}{dt}\right)_{t_k} = \left(\frac{di_{l\,(k)}}{dt}\right)_{t_k}; \tag{42}$$

$$\left(\frac{di_{l\,(k+1)}}{dt}\right)_{t_k} = \frac{\tau_{0(k)}}{\tau_{0\,(k+1)}} \left(\frac{di_{c(k)}}{dt}\right)_{t_k} +$$

$$+ \frac{\tau_{0(k)} - \tau_{0\,(k+1)}}{\tau_{0(fb)k+1}(1+\beta_b)} \frac{w_{fb}}{w_c} \left(\frac{di_{l\,(k)}}{dt}\right)_{t_k}. \tag{43}$$

Conditions (36), (37), (40) and (41) are based on the assumption that sudden fluctuations cannot occur in electrical and magnetic energy. Conditions (38), (39), (40) and (43) are obtained from equations (2) to (5) and (15) to (17).

Corresponding conditions for magnetic amplifiers without feedback can be obtained on the assumption that $w_{fb} = 0$ and $\tau_{fb} = 0$ for the above expressions.

We have considered transients in magnetic amplifiers with a control circuit connected. The results are also applicable if a sudden increase occurs in the control voltage, or if the impedance of the control circuit is suddenly decreased.

But it is quite a different picture if the control circuit is disconnected. Let us consider this situation for a magnetic amplifier without feedback if there is no bias circuit.

The alternating current will instantaneously drop to a value corresponding to the no load condition, whilst the load current will be maintained by the inductive e.m.f. and decrease in accordance with an exponential law defined by the time constant of the load circuit:

$$i_l = I_{(t=0)} e^{\frac{-t}{\tau_l}}. \tag{44}$$

1960

The decrease in the load current as in equation (44) will continue until its instantaneous value is equal to the instantaneous value of the alternating current (the moment of coincidence depends on the initial moment of the transient). The transient phenomenon in the load circuit is then again governed by the law obtained earlier.

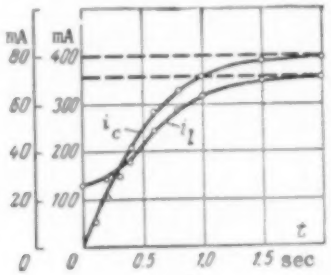

(a)

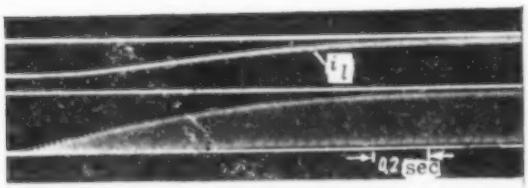

(b)

Fig. 4. The transient currents in a magnetic amplifier without feedback having an RL load in the rectified current circuit with control voltage connected.

The decrease in the load current as in equation (44) will continue until its instantaneous value is equal to the instantaneous value of the alternating current (the moment of coincidence depends on the initial moment of the transient). The transient phenomenon in the load circuit is then again governed by the law obtained earlier.

Hence, the transient in a magnetic amplifier without feedback or bias with an RL load in the rectified current circuit when the control circuit is disconnected takes place in two stages. Since the value of the load current in the second stage is very close to the steady state value, whilst the start of this stage is indeterminate, being dependent on the moment of disconnexion, it can be ignored in practical calculations for the sake of simplicity. The transient load current from its

original value to the steady state value can then be approximation by equation (44).

The accuracy of this approximation has been checked by comparing theoretical and experimental data (Figs. 4 to 6).

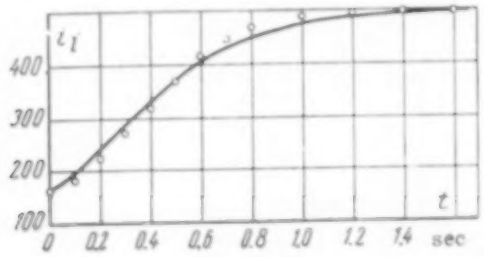

(a)

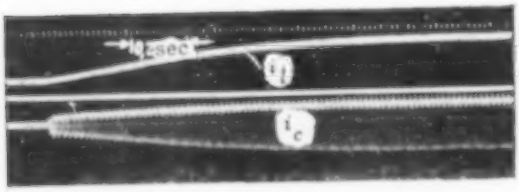

(b)

Fig. 5. The transient currents in a magnetic amplifier with external feedback and an RL load in the rectified current circuit with control voltage connected:
—— experimental; 0000 theoretical.

Figs. 4 and 5 show theoretical and experimental curves for the transient currents if a control voltage is suddenly connected. The curves in Fig.4 refer to magnetic amplifiers without feedback having an RL load in the rectified current circuit. Fig. 5 refers to a magnetic amplifier with external feedback.

Fig.6 shows theoretical and experimental curves for the transient load current of a magnetic amplifier without feedback or bias and the control circuit disconnected.

Comparison of the theoretical and experimental curves shows that the proposed method is sufficiently accurate for practical purposes for all transient phenomena under consideration.

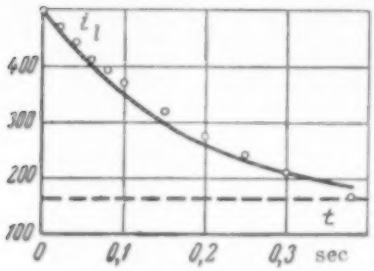

(a).

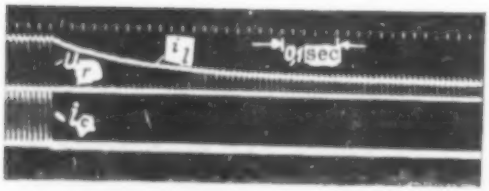

(b)

Fig. 6. The transient currents in a magnetic amplifier without feedback having an RL load in in the rectified current circuit with disconnected control voltage.

Conclusions

The fundamental results produced in this paper can be extended to magnetic amplifiers when used in more involved circuits if the particular features of the amplifiers are taken into account.

Translated by O.M. Blunn

REFERENCES

1. L.A. Bessonov: *Auto-oscillations in electrical circuits with steel, (Avtokolebaniia v elektricheskikh tsepiakh so stal'iu).*
2. L.V. Shfris; *Avtomat. i Telemekh.*, No.3, (1958).
3. Khu Tsia-iao and V.A. Shubenko; *Elektromekh.*, No.5, (1960).

4. Khu Tsia-iao and V.A. Shubenko; *Elektrotekh.*, No.4, (1959).
5. M.A. Rosenblat; *Magnetic amplifiers. (Magnitnye usiliteli).* "Sov. Radio", (1956).

1960

A NEW INSTRUMENT FOR INVESTIGATING SURGE PHENOMENA IN WINDINGS*

S.A. SOKOLOVSKII and P.P. SNOVGENOV

(Zaporozhe Transformer Works)

(Received 9 April 1960)

The development and improvement of high voltage transformers of great power requires further penetrating research into the propogation of surge in windings. A study of these phenomena, which arise during overvoltages of atmospheric origin will allow the "longtitudinal" (interturn?) insulation of the windings to be selected more correctly and the performance and reliability of transformers thus improved.

These phenomena are now studied by instruments called gradientographs which consist of a cathode-ray oscillograph and a low voltage standard surge generator. The generator produces periodic surges at intervals of time sufficient to allow the disappearance of all the effects of the previous surge in the winding. The sweep of the oscillograph is synchronized with the generator so that there is a constant picture of the surge phenomena on the screen.

The advantage of this method of investigating transient overvoltages in windings compared with other methods is that the phenomena can be studied quite accurately and all the overvoltage conditions on the section of the winding under consideration can be measured. It is also the most economical in time. Gradientographs are simple to use, and there is no high voltage.

Until recently the VEI model of the IPG-3 gradientograph has been employed for this purpose. But the IPG-3 no longer meets all the requirements of research.

Research into surge phenomena requires the gradientograph to produce not only standard impulses of 40μ sec and a wavefront of

---

* *Elektrichestvo*, 10, 56-59, 1960.

1.5 μ sec, but also those with a short wavefront of about 0.03 μ sec. A scanning speed of about 0.5 to 400 μ sec on the screen is required. But the IPG -3-type gradientograph only provides a wavefront of about 0.15 μ sec, and the scanning need on the screen does not exceed 2.5 μ sec.

The IPG-3 also has other disadvantages. There is no standardized inductance and neither is there any damping resistance in the "cut-off" loop so that conditions equivalent to impulse tests on transformers cannot be reproduced. The "front" capacitances and impedances are such that standard impulse cannot be guaranteed. It is difficult to determine time intervals by a calibrated sine curve since they have to be photographed on tracing cloth.

An amplifier is used in the IPG-3 for measuring small gradients. Its pass band is narrow and therefore unsuitable for taking measurements.

It has been necessary to develop a new and better gradientograph for investigating surge phenomena in transformer windings.

The IPT-1 type gradientograph shown in Fig.1 was accordingly developed by P.P. Shovgenev and D.V. Minutinyi. It has been used at the Zaporozhe Transformer Works with success.

The circuit and performance of the IPT-1 type gradientograph.

The main circuit of the apparatus is shown in Fig.2. The apparatus consists of a synchronizing unit, a surge generator, a wave cut-off unit, a time scanning unit, a time marker unit and a supply tube unit.

The apparatus works as follows. On switching on, heating voltages are supplied to all the valves and the synchronizing unit comes into operation, the purpose of which is to synchronize the scanning, time marker and surge generator units (in order to produce a steady picture on the screen). An intermediate relay (IR), which pre-heats the radio valves and tubes prior to switching on the high voltage, is incorporated in the high voltage circuits of the supply tube, scanning generator and surge generator units.

The thyratron syncrhonizing unit T_3 emits 100 c/s synchronizing impulse in each half period of the mains voltage. These impulses start the surge and scanning generators.

The surge generator (thyratron T_5) operates at 50 c/s. This is achieved by leaving capacitor C_{30} uncharged in the negative half-period

of the mains voltage (a half-period system of charging). The thyratron is fired the instant the synchronizing impulse arrives and capacitor C_{30} is discharged via resistances r_{48} and r_{49} from which the output surge is taken. The discharge time constant of the capacitor C_{30} is regulated by varying the resistance r_{49}, which affects the length of the wave tail. To regulate the wave front, use is made of the rC circuit consisting of resistances r_{45} and r_{46}, and capacitors C_{18}-C_{28}.

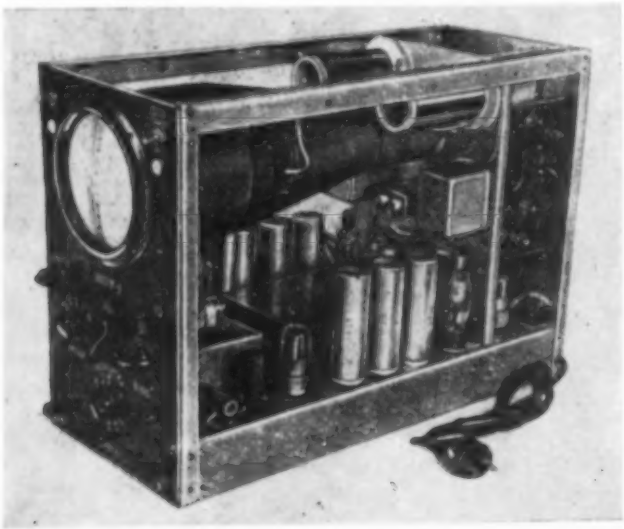

Fig. 1. General view of the IPT-1 gradientograph.

Resistances r_{45}, r_{46}, r_{48} and r_{49}, and capacitances C_{18}-C_{28} and C_{30} are so adjusted that surge of the required characteristics can be produced at the output of the apparatus regardless of the type of high voltage transformer on test.

To obtain the oscillatory wave necessary for transformer tests, an inductance coil L_2 is connected inside the apparatus between the surge generator and wave cut-off unit. The inductance of the coil is varied to suit test requirements.

The wave cut-off unit (thyratron T_4) makes it possible to produce chopped waves of any required length, i.e. to ensure that the surges from the generator are cut-off at the specified time. This is done by regulating (by means of rheostat r_{44}) the rate of voltage increase across capacitor C_{17} up to the trigger voltage of the thyratron T_4.

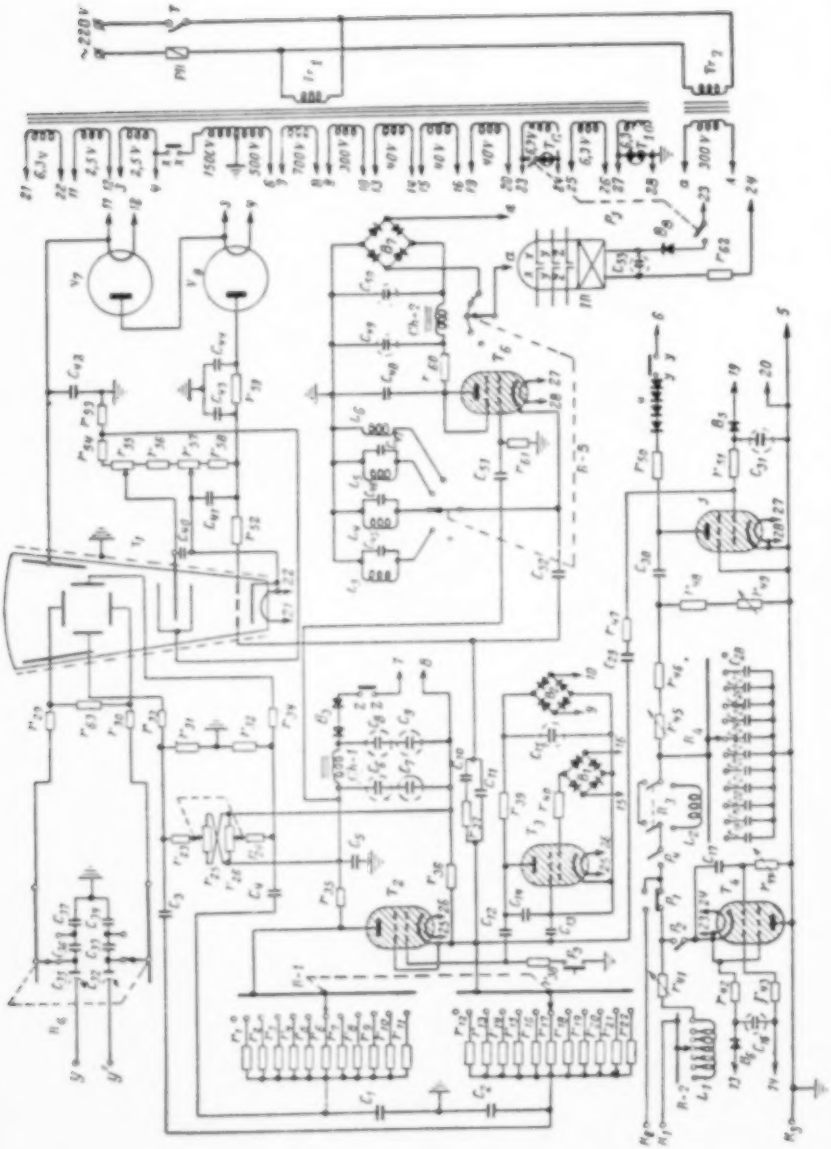

Fig. 2. Main circuit of the IPT-1 gradientograph.

To regulate the first oscillation peak after the cut-off, the cut-off loop may contain an inductance L_1 and resistance r_{41}. The inclusion of these items creates conditions equivalent ot impulse test conditions, which makes it much easier to investigate transformers.

If it is required to simulate the breakdown of the main insulation at any point of the transformer (i.e. to cut off the potential at this point), the wave is taken from terminal K_2, and terminal K_1 of the cut-off unit with its adjusting elements L_1 and r_{41} is connected to the necessary point of the transformer.

The scanning unit (T_2) operates in the "slave" state. On arrival of the synchronizing impulse the thyratron fires and capacitors C_1 and C_2 discharge via one of the pairs of resistances r_1-r_{22}. During this discharge the beam completes its forward movement and the return movement is completed whilst charging. This scanning circuit produces a voltage that is symmetrical relative to earth and ensures high scanning speeds with a relatively low rectifier voltage. The scanning unit operates on 100 c/s, and the pulse generator unit on 50 c/s, so that there is always a zero line on the screen of the cathode-ray tube. This facilitates observation and measurement of the surge phenomena. The speed of the scanning unit can be varied in eleven steps. This is useful since the scanning speed can be selected quickly if an overvoltage has to be re-measured, or the results of measurements have to be checked.

The scanning impulse is also supplied to the cathode-ray tube modulator so that the beam appears during the forward scanning move. No separate unit is therefore required for "brightening" the beam.

To shift the beam along the horizontal axis the voltage from the rectifier of the scanning unit is used. No separate d.c. voltage source is therefore required.

The scanning unit also emits a negative impulse to the time marker unit (thyratron T_6). Valve T_6 is "on" until this impulse arrives and direct current is passing through the connected oscillating circuit (one of the circuits, L_3-C_{45}, L_4-C_{46}, L_5-C_{47} or L_6-C_{wiring}). When the pulse arrives valve T_6 is turned "off", giving rise to sinusoidal damping oscillations in the connected circuit ("ringing" circuit). These oscillations are fed to the tube modulator and the brightness of the beam is modulated; time "marks" are then formed on the screen. The use of these marks allows exact and rapid determination of time intervals.

To weaken a signal to the required value, a capacitive voltage divider is connected to the input to the apparatus. This divider has

two positions giving a ratio of $K_1/K_2 = 1/2$. The arms of the divider are balanced by trimmers C_{32} and C_{35}.

The apparatus allows the measurement of gradients of 5% of wave amplitude. Surge gradients can therefore be investigated in channels between winding coils without additional amplification.

The use of a capacitive voltage divider is essential to accurate measurement of the amplitude of a square voltage surge with a time lag of up to 400 μ sec.

A full-wave system of rectification with voltage doubling using kenotrons V_7 and V_8 is used in the supply tube unit (13 LO-37).

The minimum number of units is used so that all the voltages and even the anode voltage of the time marker unit may be obtained from the same transformer. The rational unification of the supply circuits has reduced the number of secondary windings and eliminated the stray (parasitic) phenomena associated with the presence of steep-fronted surges of large amplitude. The time marker unit requires a considerable amount of power (30W for a total power of 100 W of the apparatus). The connexion and disconnexion of a winding of such power affects the general operating conditions of the transformer. A separate transformer is therefore used to supply the anode circuit of the unit.

These features of the system together with the elimination of the amplifier have made it possible to reduce the size of the IPT-1 considerably.

Main technical characteristics

1. The apparatus allows the investigation of surge phenomena in windings of any power and voltage;

2. The apparatus produces:

a. full wave surges with a continuously variable wavefront of 0.03 to 25 μ sec and a wave tail of 16 to 130 μ sec;

b. oscillatory waves of the shape and duration used in impulse tests on windings;

c. chopped full and oscillatory waves. The "chop" can be varied at any point of the surge. The peak valve of the first oscillation after the chop is continuously variable. The inductance in the cut-off loop can be varied in steps.

3. The shape of an overvoltage of 0.02 to 400 μ sec can be studied.

1960

4. The potential can be cut-off at any point of the transformer. The same parameters can be varied in the cut-off loop as for chopped waves.

5. Scanning can be adjusted to eleven speeds from 0.5 to 400 μ sec on the screen.

6. The duration of the phenomena can be measured by four types of time marker (0.25, 1, 4.1 and 8.2 μ sec) to within 5% accuracy.

7. The vertical deflection divider will change the voltage to be measured in the ratio $K_1/K_2 = 1/2$.

8. The input capacitance of the apparatus and the capacitance of the divider relative to earth are 7 and 10 pF respectively when the divider is in position K_1, and 9 and 11 pF respectively when the divider is in position K_2.

9. The dimensions of the apparatus are 555 x 400 x 235 mm.

Conclusion

The new apparatus for investigating surge phenomena in windings fully satisfies research requirements. It generates surges of all the types required for investigating any high voltage winding. The scanning speed is such that transients can be studied with the required care.

The IPT-1 type gradientograph is simple in design and easy to use. It has considerably widened the scope for impulse testing of windings of transformers, electrical machines and other equipment.

Operating experience of the IPT-1 in the high voltage laboratory at the Zaporozhe Transformer Works has shown that it possesses high operating qualities.

Translated by O.M. Blunn

A NOVEL EXCITATION SYSTEM FOR THE COMPOLES OF D.C. MACHINES*

O.G. VEGNER

(Leningrad Branch of the VNIIE'M)

(Received 11 April 1960)

The usual system of excitation for the compoles of d.c. machines has the following disadvantages:

1. The proportionality factor between the commutating field and the armature current is regulated by varying the air gap under the shoes of the compoles, or by varying the thickness of non-magnetic shims between their cores and the magnet yoke. In both cases it is difficult to maintain the symmetry of the compoles, especially in large machines. It is also a rather complicated operation to vary the air gap.

2. The constant ratio between the armature current and commutating field m.m.f. is not always adequate, especially in motors with a wide range of speeds and if considerable current overloads occur, when the saturation of the magnetic circuit of the compoles has an adverse effect.

3. In the event of a sudden fluctuation in the load, changes in the commutation field lag behind changes in the armature current owing to the effect of eddy currents in the solid parts of the magnetic circuit. To eliminate this requires a more rapid increase in the m.m.f. of the excitation winding of the compoles than can be provided by the usual system of series excitation.

Let us examine the practical importance of these shortcomings and the known methods of combatting them.

It is quite often necessary to vary the gaps under the compoles of large d.c. machines. One reason for this is the difficulty in making a final adjustment of the poles in the factory prior to despatch owing to the short duration of the tests or the time allowed for finishing prototype machines. Another reason is the difference between condi-

* *Elektrichestvo*, 10, 59-62, 1960.

tions on the test bed and in actual operation. Very large special machines are usually tested under short circuit conditions when it is even more difficult to adjust the compoles correctly. On the other hand, if it is a question of a machine that has been in operation for a long period of time, it is sometimes necessary to adjust the compoles when the brushes are replaced or operating conditions are changed.

Preliminary tests have to be carried out to determine the region of sparkless operation before the necessary gap under the compoles can be established. This requires special equipment and wastes a considerable amount of time since the machine has to be shut down. This often leads to the machines being run for long periods with unsatisfactory commutation, badly worn collectors and brushes etc.

Certain foreign firms insert non-magnetic shims between the shoes of the main and the compoles and will even tolerate a complicated design in order to make it simpler to regulate the gaps under the compoles and maintain their symmetry.

This is illustrated by Fig.1 which shows the design of a compole of a d.c. machine of 7000 h.p. The magnetic gap is adjusted by replacing the shims between the core of the pole and the yoke. These shims are set in a special "pocket" and can be replaced without disturbing the system of securing the compoles. The commutation flux passes along a magnetic circuit of small cross section and not along the main solid magnet yoke. This magnetic circuit connects the cores of the main and auxiliary poles.

For variable speed machines the compoles have a relatively greater effect at higher than at lower speeds. This is due to the change in the inductance of the armature windings owing to the damping effect of the eddy currents in the conductors, and the lower saturation of the magnetic circuit when the speed is changed by varying the excitation current of the main poles. This circumstance requires reliable commutation, and its injurious effect cannot be eliminated in the usual system of series excitation for the compoles.

In the event of a sudden and considerable fluctuation in the load there are two unfavourable factors at work, namely, the log in the change in the commutating field behind the variation of armature current owing to the damping effect of eddy currents in the magnetic circuit, and saturation of the individual parts of the magnetic circuit.

The first factor can be eliminated by using magnetic shunts, but it is difficult to set them correctly. Tests on certain machines have shown that the magnetic shunts do not always operate as required. To

function correctly, it is necessary that the time constant of the magnetic shunt winding is considerably greater than the time constant of the compole circuits. The use of magnetic shunts for adjusting the compole involves great inconvenience, even though it is an improvement on the method of adjusting the air gap.

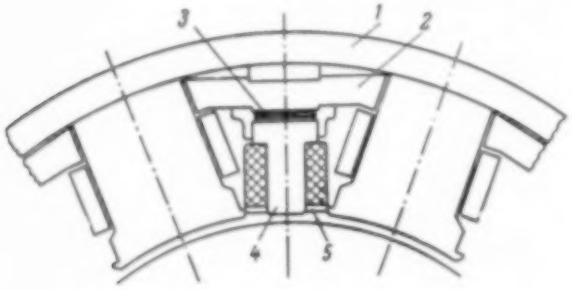

Fig. 1. The design of a compole of a 7000 h.p. motor made by Allis-Chalmers.
1 – solid yoke; 2 – magnetic circuit for conducting the flux of the auxiliary pole; 3 – "pocket" for the shims; 4 – core of compole; 5 – non-magnetic spacers between the shoes of the main and auxiliary poles.

Therefore it is proposed to improve the excitation system for compoles by using an additional excitation winding on the cores of the compoles. This is supplied from an a.c. network via a magnetic amplifier and a semiconductor rectifier bridge (Fig. 2).

In the event of sudden changes in the load current, a transformer e.m.f. is induced in the additional excitation winding. The latter can be designed for relatively low currents and should have a considerable number of turns. This e.m.f. opposes the increase in current in the additional winding. But this constraint cannot be allowed. To compensate the transformer e.m.f. and force the change in the current in the additional winding, use is made of a compensating transformer with an "opened" magnetic system. The dynamic properties of the compensating transformer should correspond to the dynamic properties of the magnetic circuit of the compoles. This is ensured by means of the variable damper winding in the compensating transformer.

The magnetic amplifier has two control windings. One is series-

connected in the load current circuit of the machine whilst the other is in parallel with the series winding via a variable semiconductor resistance. The circuit of the additional excitation winding of the compoles includes a control rheostat. Alternatively, both control windings can be connected in parallel with the series windings of the machine. The main control winding is then connected via the control rheostat whilst the auxiliary control winding is connected via the variable semiconductor resistance. If only the main control winding of the magnetic amplifier is used, a linear relationship can be produced between the load current and the current in the additional winding with a variable coefficient of proportionality between them. The effect of this is equivalent to altering the air gap under the compoles.

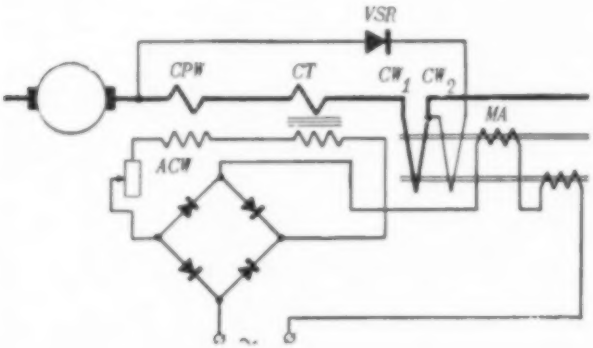

Fig. 2. Automatic supply system for compoles. *CPW* - compole winding; *ACW* - additional compole winding; *CT* - compensating transformer; *MA* - magnetic amplifier; CW_1 and CW_2 - control windings of the magnetic amplifier; *VSR* - variable semiconductor resistance.

If both control windings are used, the current in the additional winding can be made to vary non-linearly. The desired shape can be imparted to this variation by means of the variable semiconductor resistance.

Fig. 3 shows the current in the additional excitation winding of the compoles as a function of the load current of a 130 kW generator. By varying the parameters of the compensating transformer we can vary the extent of forcing in the additional winding under transient conditions.

Fig. 4 shows oscillograms of the currents in the armature of the additional winding for different air gaps in the magnetic circuit of

the compensating transformer. With sufficient "forcing" we can considerably reduce the lag in the commutating flux behind the load current in machines with a solid magnet yoke.

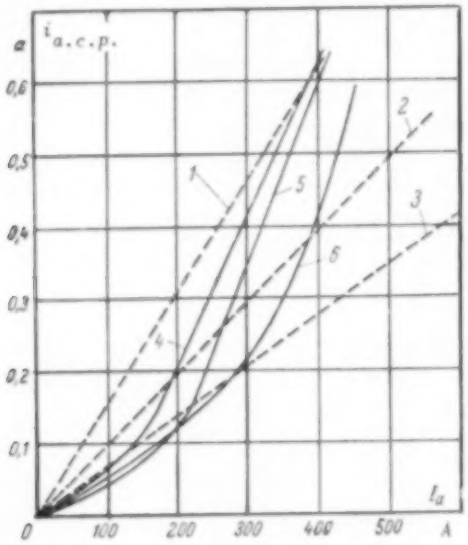

Fig. 3. The current in the additional compole winding $i_{a.c.p.}$ as a function of armature current i_a:
1 to 3 – when using one control winding of the magnetic amplifier CW_1 with different values of the variable resistance in the ACW circuit;
4 to 6 – when using both control windings of the magnetic amplifier with different values of the semiconductor resistance in the CW_2 circuit.

The compoles are supplied automatically under this system. The variation of the equivalent supply current is governed by the law

$$\Delta I_e = k I_a^n,$$

where k and n are quantities which can be regulated.

The proposed system may be further improved since it is possible to regulate k and n automatically by connecting the control winding of the magnetic amplifier to a brush spark detector, or by using the variation in the relationship between the transient voltages under the leading

and trailing edges of the brushes when the commutation deteriorates.

Automatic control for machines operating as generators and motors can be made with two magnetic amplifiers in a push-pull system. If necessary, the auxiliary current can be automatically corrected as a function of armature voltage or speed.

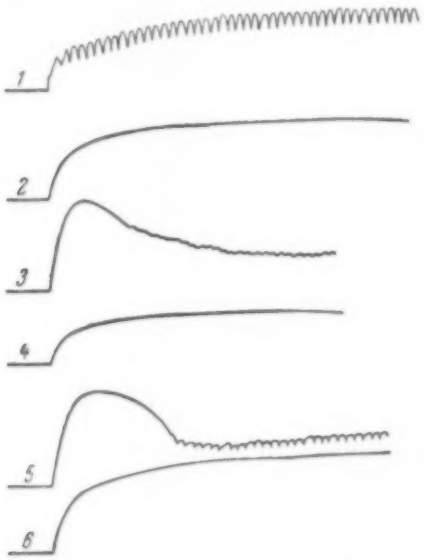

Fig. 4. Oscillograms of the variation in the current in the armature of a generator under short circuit conditions (2, 4 and 6), and the variation of the current in the additional compole winding (1-5) with different airgaps in the magnetic circuit of the compensating transformer (curve 5 refers to the smallest gap).

The automatic control can also be produced using dynamoelectric amplifiers for the supply and directly connecting them to the main excitation winding of the compoles. The control can finally be produced in its simplest form, but with more restricted possibilities, by supplying the additional winding of the compoles via a variable resistance in parallel with the series windings of the machine, or in parallel with a small ballast resistance.

If it is borne in mind that the width of the sparkless black band measured by variation in compole excitation constitutes not more than

5% of the m.m.f. of the main excitation winding of the poles. There are no special difficulties involved in fitting such a winding on a machine. Neither should any difficulties arise in connexion with the assurance of a reliable a.c. network, since any fluctuation is not very serious as this is equivalent to a variation of the supply device, and not to a removal of all the excitation from the compoles.

The proposed system has the specially important advantage that the compoles of a machine can be adjusted by a sparking detector whilst running.

The system of automatic supply for compoles can be used for:

1. Prototypes of large d.c. machines, especially with high armature voltages. The use of the improved system of excitation for the compoles considerably speeds up the adjustment of the commutation of machines and makes it unnecessary to use a supply machine with insulation of great electrical strength. It is known that even modern electrical machine manufacturers avoid supplying the compoles on test at the rated voltage of the machine, if over 500 to 600 V. At the same time, the main field can sometimes have a considerable effect on commutation. The use of the proposed system of excitation allows commutation to be adjusted at any rated armature voltage.

2. Large d.c. machines, where it is difficult to make the final adjustment to commutation in the works' test owing to the impossibility of reproducing actual operating conditions, or because the amount of time allowed for testing is limited.

3. Large d.c. machines that are in operation under rapidly fluctuating loads.

Translated by O.M. Blunn

1960

ABSTRACTS FROM PAPERS PUBLISHED IN ELEKTRICHESTVO No. 10, 1960

Cables

Calculating the Cooling of a Cable after being overheated by a Fault Current. S.M. Bragin, (pp. 65-67).

The dissipation of heat from the cable after heating by a short circuit current is taken into account to define the temperature rise of the sheath and the temperature of the core shortly after cooling starts.

Control Systems

The Type of Current for Remote and Automatic Control Systems for Underground Mechanisms. B.M. Stolbov, (pp. 23-27).

The use of rectified current instead of a.c. is advocated for remote control systems in collieries and other mining work.

Poles and Zeros Analysis

Analysis and Synthesis of Ladder Networks from the Zeros and Poles of their Input Impedances. Z.G. Kaganov, (pp. 41-47).

The input impedance of networks is expressed by continuous fractions so as to define the resonant frequencies from the number of links and their parameters and vica versa.

Power Systems

Some Prospects for the Use of Computers in Power Systems. V.M. Sin'kov, (pp. 7-12).

Possible types of device for calculating the most economic

operating conditions in power systems are discussed. This excludes devices for the primary control of the generating units.

Fault Currents in Networks containing Autotransformers with voltage regulation Boosters. A.B. Chernin, (pp. 13-19).

Symmetrical component analysis for various faults with different connexions of the autotransformer and booster transformer and booster transformer for voltage regulation.

Determining the Optimum Power Factor for Industrial Installations, P.G. Grudinskii and L.V. Litvak, (pp. 20-22).

A technical-economic method is proposed for defining the optimum power factor for industry.

1960

Rolling Mills

The Physical Principles of a Multi-motor Drive for continuous sheet rolling Mills. N.N. Druzhinin, (pp. 27-31).

Results of an experimental investigation into the drive of a new Russian five-stand mill are given. The resilience of the sheet and the stand-roll system is considered from the point of view of voltage compensation.

Synchronous Drives for Rolling Mills. V.I. Pleskov and G.G. Magazinnik, (pp. 31-34).

Synchronous drives for rolling mills can be safely designed on a cheaper basis with automatic forced excitation.

Switchgear

A Measuring Device for the Residual Current in Circuit Breakers. L.Z. E'idel', (pp. 48-52).

The errors occurring in measuring the residual current are studied together with the limiter circuit and measures for suppressing interference. Oscillograms taken by the proposed measuring device are shown.

Thermistors

Correction of Thermistor Temperature Characteristics. G.K. Nechev, (pp. 62-65).

Special systems of applying correcting resistors are mathematically analysed with a view to equating sensitivity.

Transformers

The Mechanical Work and Energy of the Armature Reaction of a Magneto. G.N. Senilov, (pp. 52-55).

The mechanical work of a magneto is shown to be equivalent to the electromagnetic energy by a graphical-analytical method. The proof is based on constant transformer flux. Losses to be considered later.

Transmission Lines

Hardened Glass Line Suspension Insulators for Areas with Conducting Precipitations. N.A. Nikolaev et al., (p. 68).

New PSG-45-type line suspension insulators with a leakage path of 340 mm.

CALCULATING COMPLICATED FAULTS USING THE RESULTS OF COMPUTATIONS OF SIMPLER SYSTEM CONDITIONS*

G. G. KOSTANIAN

(Tbilisi Research Institute for
Equipment and Hydro-electric Power)

(Received 21 March 1960)

General considerations

Complex faults can be represented as the result of several successive asymmetrical faults. Using this approach, we can calculate more complex asymmetrical conditions from several simple asymmetrical ones. This considerably simplifies the investigation.

In this paper a general method of calculation is proposed which is applicable to every possible combination of complex asymmetrical faults arising as a result of two asymmetrical faults with maximum asymmetry in branches k and n of a power system**. Branches k and n can be any combination of single phase or two phase earth faults, or any combination of open circuits in one or two phases if the other branches of the power system contain no sources of asymmetry.

We use the following subscripts: k and n refer to branches k and n respectively, 1, 2 and 0 refer to the positive, negative and zero se-

---

* *Elektrichestvo*, 11, 20-28, 1960.

** The method can be extended to more complicated conditions with maximum asymmetry in three or more branches of the system.

quences individually, i refers to the sequences together, and A, B and C refer to phases A, B and C respectively.

Our analysis is based on the following propositions:

1. Any combination of asymmetrical conditions in any branch (e.g. branch k or n) can be represented as the result of the short circuit or open circuit of a single phase in the previous symmetrical condition (with three phases open or short circuited as shown in Fig.1). In fact, by short circuiting one phase in circuits a and b (Fig. 1), we can obtain any combination of single phase short circuits or combinations of open circuits in two phases (the first kind of fault), whilst by opening one phase in circuits c and d (Fig.1), we can obtain any combination of two phase short circuits and any combination of open circuits in one phase (the second kind of fault).

These two types of fault exhaust all the possible combinations of asymmetrical faults in power systems.

Using symmetrical component analysis, the point of the first type of fault can be represented by the arrangement in Fig.2(a), and the point of the second by that in Fig.2(b). U' in Fig.2(a) is numerically equal to the voltage between the ends of the short circuited phase, and I' in Fig.2(b) to the current of the open phase. The arrangement in Fig.2(b) differs from that normally used to determine symmetrical components of the second type of fault in that the networks of the individual sequences are connected in parallel whilst a current source is substituted for the e.m.f. source. As a result of these changes, the network in Fig. 2(b) is converted into the dual network in Fig. 2(a), i.e. the laws governing the current variation in Fig. 2(a). The symmetrical components at the point of every possible combination of individual asymmetrical fault can therefore be studied in two mutually-dual circuits.

2. The original condition P_1 with one asymmetrical fault in branch k and all three phases in branch n either short circuited or open defines the initial conditions for a subsequent complex fault conditions.

Every possible combination of these initial conditions can be represented as four complex networks (Fig.3). The networks in Fig.3(a) and (b) are the initial conditions of the first type of fault in branch k, whilst those in Fig.3(c) and (d) refer to the second type of fault in branch k. The networks in Fig.3(a) and (c) represent conditions with three phases open in branch n, and those in (b) and (d) refer to conditions with three phases short circuited in branch n. The short

circuited or open circuit conditions of branch n in Fig.3 represents the normal conditions corresponding to that shown in Fig. 1(a) and (d) , or a condition with three phases open (Fig. 1b), or short circuited (Fig. 1c).

The complex positive sequence networks in Fig.(3) should correspond to the moment when an asymmetrical fault occurs in branch n, i.e. they take into account changes* that take place between the occurrence of the fault in branch k and its occurrence in branch n.

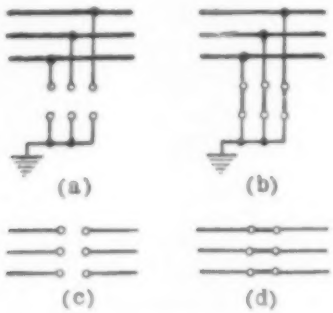

Fig. 1. The branches permitting the representation of every possible combination of asymmetrical faults as a short circuit (a, b) or as an open circuit in one phase (c, d).

The networks in Fig.3 only contain one asymmetrical fault. The methods of determining these changes and the currents and voltages in branches k and n are generally known and require no explanation.

3. The combinations of complex faults which can occur in the complex condition P_2 can be regarded as the result of a short circuit or open circuit of one phase in branch n in the networks of the initial condition P_1.

The transition from P_1 to P_2 via an intermediate-condition D is shown in Fig. 4(a) and (b) for a network with the same phase sequence; Fig. 4(a) shows the changes due to a short circuit on one phase, and Fig. 4(b) to an open circuit on one phase. The fourpoles for condition D in Fig.4 contain no internal e.m.f.'s and are passive in all three

* In approximate calculations these variations in the impedance of the positive sequence networks can be determined by theoretical curves, as proposed by Lek'nikov and Satarov [1] for instance.

1960

sequences, whilst the fourpoles in condition P_1 and P_2 are active in the positive sequence network and only passive in the negative and zero sequences.

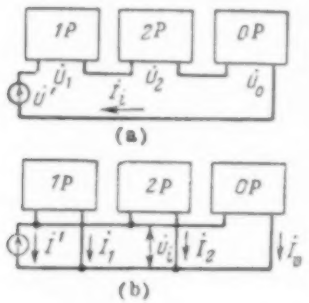

Fig. 2. Dual complex networks representing every possible individual asymmetrical fault.

The passive fourpole elements of condition D in each phase sequence are no different than those of condition P_1 in the calculation of condition D.

Using the principles laid down in previous papers [2,3], we can establish the relationships between the currents and e.m.f.'s in the branches of the passive fourpoles of condition D. These relationships are valid for any combination of faults in branches k and n. They can be represented in two main forms for each phase sequence:

first form Z'

$$\Delta\dot{E}_n = \dot{E}_n - \dot{U}' = Z'_n(\dot{I}' - \dot{I}_n) - \dot{\alpha}Z'_k\Delta\dot{I}_k; \tag{1}$$

$$\Delta\dot{E}_k = \dot{\beta}Z'_n(\dot{I}' - \dot{I}_n) - Z'_k\Delta\dot{I}_k; \tag{2}$$

second form Y'

$$\Delta\dot{I}_n = \dot{I}_n - \dot{I}' = \dot{\beta}Y_k\Delta\dot{E}_k - Y_n(\dot{E}_n - \dot{U}'); \tag{3}$$

$$\Delta\dot{I}_k = \dot{\alpha}Y_n(\dot{E}_n - \dot{U}') - Y_k\Delta\dot{E}_k, \tag{4}$$

where $\dot{U}'$ and $\dot{I}'$ are the voltage and current respectively in in branch n in condition P_1 (for the network in Fig.4 (a) $I' = 0$, and for that in Fig. 4(b) $U' = 0$).

$\dot{E}_n$ and $\dot{I}_n$ the e.m.f. and currents in branches n in the required condition P_2;

$\Delta\dot{E}_n$, $\Delta\dot{I}_n$, $\Delta\dot{E}_k$, $\Delta\dot{I}_k$ changes in the e.m.f. and currents in branches n and k represented by condition D;

Z'_n, Z'_k the input impedances of branches n and k in the condition when branches n and k are open;

Y_n and Y_k the input conductivities in branches n and k (branches n and k short circuited);

$\dot{\alpha} = \frac{Y_{kn}}{Y_n}$ and $\dot{\beta} = \frac{Y_{nk}}{Y_k}$. coefficients establishing the link between the mutual and input conductivities of branches k and n ($Y_{kn} = Y_{nk}$).

1960

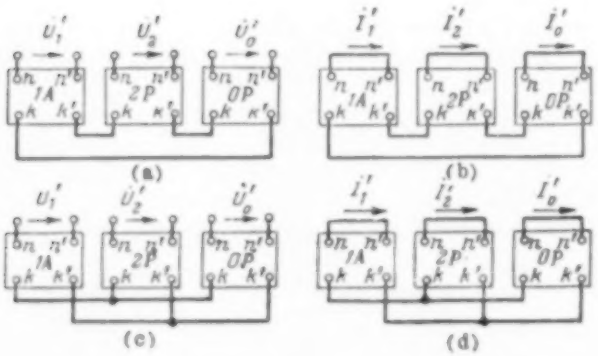

Fig. 3. Complex networks defining the currents and voltages in condition P_1.

The equations of forms Z' and Y are reciprocals and their coefficients are linked as follows [3]:

$$\dot{\alpha}Y_n = \dot{\beta}Y_k;\ \dot{\alpha}Z'_k = \dot{\beta}Z'_n;$$
$$Y_n Z'_n (1 - \dot{\alpha}\dot{\beta}) = Y_k Z'_k (1 - \dot{\alpha}\dot{\beta}) = 1. \qquad (5)$$

4. The relationships between the various current and voltage components at the fault point are established by well known boundary

conditions* as a function of the type of fault in branches k and n. These conditions also govern the components I_n and E_n shown in Fig. 4 and also

$$\Delta \dot{I}_k = \dot{I}_k - \dot{I}'_k; \tag{6}$$

$$\Delta \dot{E}_k = \dot{E}_k - \dot{E}'_k, \tag{7}$$

i.e. the components of condition D in branch k and state P_2 in branch n.

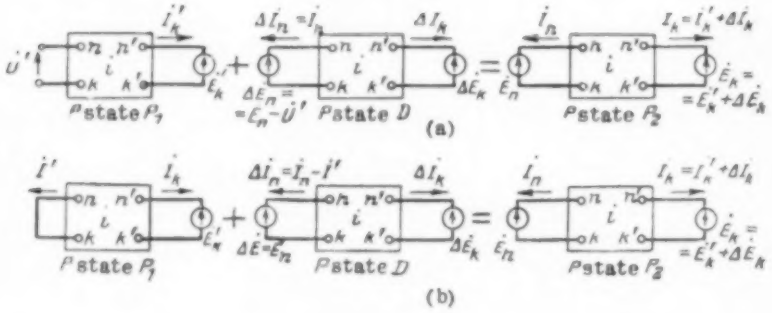

Fig. 4. Transition from P_1 to P_2 for each phase sequence in the presence of type 1 faults (a) and type 2 faults (b) in branch n.

5. To restrict the number of combinations with different faulted phases in branches k and n, we assume that all the faults are caused by a short circuit or interruption in phase A of branch k and any phase A, B, or C of branch n. The short-circuited or open phase of a branch is known as the *special* phase**.

6. Having defined the components of each sequence in condition D with the known components of the initial conditions, we can find*** the components in the complex condition, P_2.

---

* See, for example, the equations on page 10 in [4].

** Even though the two other phases of the faulted branch are rarely under identical conditions, which distinguishes a complex fault from a simple fault.

***This was proposed by Chernin [5] for special combination of a complex fault. It allows a considerable amount of calculation to be carried out on a d.c. model.

Such a method makes it possible to take into account the changes brought about by each successive fault in the passive networks of each sequence in state *D*. This allows the continued calculations of conditions P_1 regardless of simultaneous asymmetry at two points in the system, as recommended elsewhere [4, 6, 7, 8].

The current and e.m.f. components of branches *k* and *n*

Using the foregoing initial condition, we obtain twelve equations for any combination of faults in branches *k* and *n* with twelve unknowns, and determine the six required current components and six required voltage components (three in each branch). An example of a combination representing an earth fault in phase A in branch *k* and in phase B in branch *n* will show this. For this combination we have from the boundary conditions of the fault:

$$\left.\begin{aligned} \Delta \dot{I}_{k1} &= \Delta \dot{I}_{k2} = \Delta \dot{I}_{k0}; \\ \Delta \dot{E}_{k1} + \Delta \dot{E}_{k2} + \Delta \dot{E}_{k0} &= 0; \\ a^2 \dot{I}_{n1} &= a \dot{I}_{n2} = \dot{I}_{n0}; \\ a^2 \dot{E}_{n1} + a \dot{E}_{n2} + \dot{E}_{n0} &= 0. \end{aligned}\right\} \qquad (8)$$

Solving 8 jointly with 1 and 2, we get:

$$\Delta \dot{I}_{k0} Z'_{k\Sigma} + \dot{I}_{n0} \dot{c} = 0;$$

$$\Delta \dot{I}_{k0} \dot{b} + \dot{I}_{n0} Z'_{n\Sigma} = a^2 \dot{U}_1 + a \dot{U}_2 + \dot{U}_0 = \dot{U}_B,$$

where

$$Z'_{k\Sigma} = Z'_{k1} + Z'_{k2} + Z'_{k0}; \quad Z'_{n\Sigma} = Z'_{n1} + Z'_{n2} + Z'_{n0};$$

$$\dot{c} = a \dot{\beta}_1 Z'_{n1} + a^2 \dot{\beta}_2 Z'_{n2} + \dot{\beta}_0 Z'_{n0};$$

$$\dot{b} = a^2 \dot{\alpha}_1 Z'_{k1} + a \dot{\alpha}_2 Z'_{k2} + \dot{\alpha}_0 Z'_{k0}.$$

Since $\dot{\beta}_i Z'_{ni} = \dot{\alpha}_i Z'_{ki}$, in each phase sequence, we find that

$$\dot{c}\dot{b} = (\dot{\beta}_1 Z'_{n1} + \dot{\beta}_2 Z'_{n2} + \dot{\beta}_0 Z'_{n0})^2 -$$

$$- 3(\dot{\beta}_1 \dot{\beta}_2 Z'_{n1} Z'_{n2} + \dot{\beta}_1 \dot{\beta}_0 Z'_{n1} Z'_{n0} + \dot{\beta}_2 \dot{\beta}_0 Z'_{n2} Z'_{n0}).$$

1960

Putting

$$\frac{\dot{b}\dot{b}}{Z'_{n2}} = \dot{m}\dot{b} = \dot{\Delta},$$

we get:

$$a^{\circ}\dot{I}_{n1} = a\dot{I}_{n2} = \dot{I}_{n0} = \frac{\dot{U}_B}{Z'_{n2} + \dot{\Delta}}\ ; \tag{9}$$

$$\Delta\dot{I}_{ki} = -\dot{m}\dot{I}_{n0}\ . \tag{10}$$

Components ΔE_k and E_n can be found by substituting 9 and 10 into 1 and 2. This defines the twelve unknowns.

The final values of the components of branch k in state P_2 are determined for each sequence network in accordance with 6 and 7. Likewise we can solve the corresponding equations for every other combination of asymmetrical faults in two branches. Table 1 shows the results of these equations for every possible combination of asymmetrical faults in two branches determining the zero current or e.m.f. components in branch n. Using Table 1 and the boundary conditions defined by the type of fault in branch n we can pass on to the corresponding components of any phase sequence. This makes it possible to find the current in the short circuited phase and the voltage in the open phase.

The foregoing method can also be extended to the transition from an asymmetrical fault in two branches to an asymmetrical fault in several branches. It is possible to pass successively from a condition defined by two faults to one defined by three faults and so on. With n faults the fourpoles (Figs. 3 and 4) become $2n$-poles in the last $(n-1)$ transition. In accordance with the principles laid down by Adonts (8), we can derive $3n$ equations similar to equations 1 to 4 for these $2n$-poles; in addition, the boundary conditions of the n faults produce $3n$ equations. Thus, for any number of faults n, we can derive $6n$ equations which define the $6n$ required components ($3n$ current components and $3n$ voltage components).

All the combinations in Table 1 are subdivided into four groups. The solutions for groups I and III are dual to the solutions for groups II and IV.

Each group in Table 1 contains four different combinations as a function of the type of fault in branches k and n (two combinations for short circuits and two combinations for interruptions). Each of the sixteen combinations contains three different combinations as a function

TABLE 1

Zero sequence components for various combinations of faults in branches k and n

Type of fault in branch n / Type of fault in branch k	First type of asaymetrical fault in branch n (combinations of an earth fault in one phase or an open circuit in two phases)	Second type of asaymetrical fault in branch n (combinations of an earth fault in two phases or an open circuit in one phase)
Earth fault in phase A or open in phases B and C	Group I $\dot{I}_{n0} = \dfrac{\dot{U}'}{Z'_{n\Sigma} + \dot{\Delta}^{(1)}}$	Group II $\dot{E}_{n0} = \dfrac{\dot{I}'}{Y'_{n\Sigma} + \dot{\delta}^{(1)}}$
Earth fault in phase B and C or open phase A	Group III $\dot{I}_{n0} = \dfrac{\dot{U}'}{Z_{n\Sigma} + \dot{\Delta}^{(1,1)}}$	Group IV $\dot{E}_{n0} = \dfrac{\dot{I}'}{Y_{n\Sigma} + \dot{\delta}^{(1,1)}}$

$\dot{U}'$ voltage between the ends of the short circuited phase in branch n in state P_1;

$\dot{I}'_1$ current in broken phase of branch n in state P_1;

$Z'_{n\Sigma}$, $Z_{n\Sigma}$, $Y'_{n\Sigma}$, $Y_{n\Sigma}$ impedances and conductivities of complex network as regards the point of the fault in branch n ($Z'_{n\Sigma}$, $Y'_{n\Sigma}$) with an open branch k ($Z_{n\Sigma}$, $Y_{n\Sigma}$) and short circuited branch k;

$\dot{\Delta}^{(1)}$, $\dot{\Delta}^{(1,1)}$, $\dot{\delta}^{(1)}$, $\dot{\delta}^{(1,1)}$ coefficients defined by the fault combinations.

1960

of whether A, B or C is the *special* phase in branch n if A is the *special* phase in branch k. Thus, the solutions in Table 1 for groups I to IV relate to 48 combinations with simultaneous limiting asymmetry in branches k and n.

In the general case of a complex fault, the values of $\dot{I}'_{n0}$ and $\dot{E}'_{n0}$ appearing in Table 1 are defined by the following three parameters:

1. The voltage $\dot{U}'$ and current $\dot{I}'$, depending on the effective e.m.f. in the network, as defined by condition P_1. Here $\dot{U}'$ is the voltage between the ends of the short circuited phase in branch n (it can be measured in the networks in Fig. 1a and b, or Fig. 3 a and c), whilst $\dot{I}'$ is the current in the broken phase n which can be measured in the networks in Fig. 1(c) and (d) or Fig. 3(b) and (d).

2. The impedances and conductivities $Z'_{n\Sigma}$, $Z_{n\Sigma}$, $Y'_{n\Sigma}$, and $Y_{n\Sigma}$, (independent of the e.m.f.) can be defined on the assumption that there is no asymmetrical fault in branch k: $Z'_{n\Sigma}$, $Y'_{n\Sigma}$ refer to three open phases in branch k; $Z_{n\Sigma}$ and $Y_{n\Sigma}$ to three short circuited phases in branch k.

3. Coefficients (independent of the e.m.f.) having the dimension of impedance $\dot{\Delta}^{(1)}$ and $\dot{\Delta}^{(1,1)}$ or conductance $\dot{\delta}^{(1)}$ and $\dot{\delta}^{(1,1)}$, depending on the combinations of complex faults.

If $\dot{\Delta} = 0$ and $\dot{\delta} = 0$, the expressions in Table 1 become the familiar expressions generally used for calculating individual asymmetrical faults.

The values of the coefficients in Table 1 are shown in Table 2.

By investigating the physical sense of coefficients that are independent of the e.m.f., we see that $\dot{\Delta}$ and $\dot{\delta}$ correct the quantities $Z'_{n\Sigma}$, $Z_{n\Sigma}$, $Y'_{n\Sigma}$, and $Y_{n\Sigma}$ and take into account changes due to the various combinations of asymmetrical faults in branch k. The short circuit of one phase in branch k alters the impedance or conductance in branch n by $\dot{\Delta}^{(1)}$ or $\dot{\delta}^{(1)}$, whereas an open phase causes a change of $\dot{\Delta}^{(1,1)}$ or $\dot{\delta}^{(1,1)}$. Therefore

$$(Z_{n\Sigma}+\dot{\Delta}^{(1)}),\quad (Z_{n\Sigma}+\dot{\Delta}^{(1,1)}),\quad (Y'_{n\Sigma}+\dot{\delta}^{(1)}),\quad (Y_{n\Sigma}+\dot{\delta}^{(1,1)})$$

represent the impedance or conductance of branch n in a single phase-sequence network with a simultaneous asymmetrical fault in branches n and k. In the general case they contain components of all three sequences and thus take into account the mutual link between networks of individual sequences for the various combinations of asymmetrical faults in branches n and k.

It is characteristic that the expressions determining the coefficients

$\dot{\Delta}$ and $\dot{\delta}$ contain no operator $a = e^{j120}$ or $a^2 = e^{j240}$ as is typical of other methods of calculating combinations of complex faults with different *special* phases in branches k and n. Consequently, if only the inductive reactance is taken into account (as is frequently the case when calculating short circuits), phases $\dot{I}_{n0}$ and $\dot{E}_{n0}$ are independent of the coefficients $Z'_{n\Sigma}$, $Z_{n\Sigma}$, $Y'_{n\Sigma}$, $Y_{n\Sigma}$, $\dot{\Delta}$ and $\dot{\delta}$ are solely defined by the phases $\dot{U}'$ and $\dot{I}'$.

It is obvious that the coefficients $Z'_{n\Sigma}$, $Z_{n\Sigma}$, $Y'_{n\Sigma}$ and $Y_{n\Sigma}$ can either be measured on single phase a.c. network analysers or on d.c. analysers, either for individual sequence networks, or for complex networks at the point of fault in branch n (e.g. in the networks shown in Fig.5 for $\dot{\Delta} = 0$ and $\dot{\delta} = 0$). The coefficients $\dot{\Delta}$ and $\dot{\delta}$ can be determined on the same analysers. It is then more convenient to use the complex networks shown in Fig.3, with the exception of the positive sequence network for the generator e.m.f., provided an e.m.f. or current source is included at the point of fault as shown in Fig.6. Measuring the currents and voltages in Fig.6, and using the expressions in column 5 in Table 3 we can determine the coefficients $\dot{\Delta}$ and $\dot{\delta}$ for any complex fault combination.

The data of Tables 1 to 3 in conjunction with complex equivalent networks considerably simplify the calculation of complex faults.

Complex equivalent networks

The solutions contained in Table 1 can be represented by the complex networks for individual asymmetrical faults, but they differ in that they contain additional impedances $\dot{\Delta}$ and conductances $\dot{\delta}$ and are only suitable for calculating the components of one phase sequence in a branch with only one fault. They are unsuitable for directly calculating the components of all the branches in the system.

In these networks the branch k can be either open or short circuited, i.e. with three open or short circuited phases. In fact one phase in branch k is in special conditions (short circuited with two open phases, or open with two short circuited phases). This is a source of asymmetry. Its effect is taken into account in Fig.5 by impedance $\dot{\Delta}$ or conductance $\dot{\delta}$.

In conformity with the subdivision of the combinations into four groups in Table 1, the complex network representing group I is shown in Fig. 5(a), group II in (b), III in (c) and IV in (d). Fig. 5(a) and (c) contain e.m.f. sources U', and (b) and (d) current sources I'. These are the same values of U' and I' as in Tables 1 and 2.

TABLE 2

Coefficients in Table 1

None of faulted phase in branch n	Short circuit	A	B	C
	Open phase	BC	AC	BA
Coefficients $\dot{U}'$ and $\dot{I}'$ defined by the e.m.f. in state P_1		$\dot{U}' = \dot{U}'_A = \dot{U}'_1 + \dot{U}'_2 + \dot{U}'_0$ $\dot{I}' = \dot{I}'_A = \dot{I}'_1 + \dot{I}'_2 + \dot{I}'_0$	$\dot{U}' = \dot{U}'_B$ $\dot{I}' = \dot{I}'_B$	$\dot{U}' = \dot{U}'_C$ $\dot{I}' = \dot{I}'_C$
Coefficients $\dot{\Delta}$ and $\dot{\delta}$, defined by the combinations of complex asymmetrical faults	Group I	$\dot{\Delta}^{(1)} = \dot{\Delta}_A = -\frac{\dot{n}_A^2}{Z'_{k\Sigma}}$ $\dot{n}_A = \dot{n}_1 + \dot{n}_2 + n_0$	$\dot{\Delta}^{(1)} = \dot{\Delta}_n = \dot{\Delta}_A + \frac{3\dot{n}_n}{Z'_{k\Sigma}}$ $\dot{n}_n = \dot{n}_1 n_2 + \dot{n}_1 n_0 + n_2 n_0$	
	Group II	$\dot{\delta}^{(1)} = \dot{\delta}_A = \frac{\dot{P}_A^2}{Z_{k\Sigma}}$ $\dot{P}_A = \dot{P}_1 + \dot{P}_2 + \dot{P}_0$	$\dot{\delta}^{(1)} = \dot{\delta}_n = \dot{\delta}_A - \frac{3\dot{P}_n}{Z_{k\Sigma}}$ $\dot{P}_n = \dot{P}_1 \dot{P}_2 + \dot{P}_1 \dot{P}_0 + \dot{P}_2 \dot{P}_0$	
	Group III	$\dot{\Delta}^{(1,1)} = \dot{\Delta}_A = \frac{\dot{\alpha}_A^2}{Y'_{k\Sigma}}$ $\dot{\alpha}_A = \dot{\alpha}_1 + \dot{\alpha}_2 + \dot{\alpha}_0$	$\dot{\Delta}^{(1,1)} = \dot{\Delta}_n = \dot{\Delta}_A - \frac{3\dot{\alpha}_n}{Y_{k\Sigma}}$ $\dot{\alpha}_n = \dot{\alpha}_1 \dot{\alpha}_2 + \dot{\alpha}_1 \dot{\alpha}_0 + \dot{\alpha}_2 \dot{\alpha}_0$	
	Group IV	$\dot{\delta}^{(1,1)} = \dot{\delta}_A = -\frac{P_A^2}{Y_{k\Sigma}}$ $\dot{P}_A = \dot{P}_1 + \dot{P}_2 + P_0$	$\dot{\delta}^{(1,1)} = \dot{\delta}_n = \dot{\delta}_A + \frac{3\dot{P}_n}{Y_{k\Sigma}}$ $\dot{P}_n = \dot{P}_1 \dot{P}_2 + \dot{P}_1 P_0 + \dot{P}_2 P_0$	

Table 2 continued

None of faulted phase in branch n	Short circuit	A	B	C
	Open phase	BC	AC	BA
Coefficients $Z'_{n\Sigma}, Z_{n\Sigma}, Y'_{n\Sigma}$, and $Y_{n\Sigma}$, defined by the state with no asymmetrical fault in branch k_0:		Impedance at the point of fault in branch n with 3 open ($Z'_{n\Sigma}$) or short circuited ($Z_{n\Sigma}$) phases in branch k	Conductance at the point of fault in branch n with 3 open ($Y'_{n\Sigma}$) and short circuited ($Y'_{n\Sigma}$) phases in branch k	
		$Z'_{n\Sigma} = Z'_{n1} + Z'_{n2} + Z'_{n0}$ $Z_{n\Sigma} = Z_{n1} + Z_{n2} + Z_{n0}$ $Z'_{n\Sigma} = Z_{n\Sigma} + \dot{\alpha}_1^2 Z'_{k1} + \dot{\alpha}_2^2 Z'_{k2} + \dot{\alpha}_0^2 Z'_{k0}$	$Y'_{n\Sigma} = Y'_{n1} + Y'_{n2} + Y'_{n0}$ $Y_{n\Sigma} = Y_{n1} + Y_{n2} + Y_{n0}$ $Y_{n\Sigma} = Y_{n\Sigma} - \dot{\beta}_1^2 Y_{k1} - \dot{\beta}_2^2 Y_{k2} + \dot{\beta}_0^2 Y_{k0}$	

N. B. Coefficients with subscripts B and C are defined by the symmetrical components of coefficients with subscripts A for example: $\dot{U}'_B = a^2\dot{U}'_1 + a\dot{U}'_2 + \dot{U}'_0$; $\dot{Y}'_C = a\dot{Y}'_1 + a^2\dot{Y}'_2 + \dot{Y}'_0$.

2. The values $Z'_{k\Sigma}, Z_{k\Sigma}, Y'_{k\Sigma}, Y_{k\Sigma}$ are defined by the corresponding sequence components as follows: $Z'_{n\Sigma}, Z_{n\Sigma}, Y'_{n\Sigma}, Y_{n\Sigma}$.

3. The coefficients in Table 2 for the circuit of each phase sequence are related as follows: $n_i = \beta_i Z'_{ni} = a_i Z'_{ki}$; $P_i Z_{ki} Z_{ni} = \beta_i Z_{ni} = a_i Z_{ki}$.

The circuits in Fig. 5 can be represented as complex circuits of individual asymmetrical faults (if $\Delta = 0$ and $\delta = 0$), but we must substitute the voltage U'' for $\dot{U}'$ in Figs. 5(a) and (c), and I'' for $\dot{I}'$ in Figs. 5(b) and (d). The values of U'' and I'' are shown in column 3 Table (3). This substitution of $\dot{U}''$ for $\dot{U}'$ and I'' for I'' maintains the current I' constant in Fig. 5(a) and (c) and the voltage E_{n0} constant in (b) and (d).

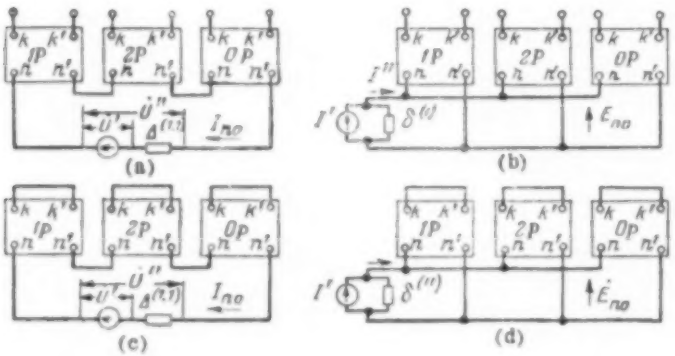

Fig. 5. Complex networks for the current or e.m.f. components at the point of a No. 2 type asymmetrical fault in branch n.

The complex networks in Fig. 5 make it possible to find $\dot{I}_{n0}$ or $\dot{E}_{n0}$ for any of the 48 combinations of faults in any two branches of a three phase system. At the same time, the relationships defined by the boundary conditions of the faults in branch n make it possible to pass from values of $\dot{I}_{n0}$ or $\dot{E}_{n0}$ to values of $\dot{I}_{n1}$, $\dot{I}_{n2}$ or $\dot{E}_{n1}$, $\dot{E}_{n2}$ via operator a or a^2 without having to make any calculations. This defines all the current or e.m.f. components at the point of the second fault in branch n.

The current or e.m.f. components at the point of the first fault in branch k can be defined in a similar way on the assumption that the fault occurred first in branch n and subsequently in branch k, i.e. if we substitute the values relating to branch k for the quantities relating to branch n in the circuits and foregoing expressions. But this method of defining the components in branch k involves unnecessary work since no use is made of the values of $\dot{I}_{ni}$ or $(\dot{E}_{ni})$ as already calculated. Instead, by using these values of $\dot{I}_{ni}$ (or $\dot{E}_{ni}$), we can find ΔI_{ki} or $\Delta \dot{E}_{ki}$ from the networks in Fig. 6 if $E_e = 0$ and $I_e = 0$,

TABLE 3

Determination of the coefficients in Table 1 on a single phase a.c. model or a d.c. model

Type of fault in branch n	Combination group	Voltage U'' and current I'' for circuits in Fig. 5	Complex network for measuring $\dot{\Delta}$ and $\dot{\delta}$ and the applied power	Expressions defining the coefficients in Table 1 and 2
First type	I	$\dot{U}'' = \dot{U}' \dfrac{Z'_{n\Sigma}}{Z'_{n\Sigma} + \dot{\Delta}^{(i)}}$	$\dot{P} = \dot{E}_e I_i$ (Fig. 6a)	$\dot{U}_\Sigma = \dot{U}_1 + \dot{U}_2 + \dot{U}_0$ $U_n^2 = \dot{U}_1^2 + \dot{U}_2^2 + \dot{U}_0^2$ $\dot{\Delta}_A = \dfrac{\dot{U}_\Sigma^2}{\dot{P}}$ $\dot{\Delta}_n = \dfrac{3\dot{U}_n^2 - \dot{U}_\Sigma^2}{2\dot{P}}$
	III	$\dot{U}'' = \dot{U}' \dfrac{Z_{n\Sigma}}{Z_{n\Sigma} + \dot{\Delta}^{(1,1)}}$	$\dot{P} = \dot{E}_i I_e$ (Fig. 6c)	
Second type	II	$I'' = I' \dfrac{Y'_{n\Sigma}}{Y'_{n\Sigma} + \dot{\delta}^{(i)}}$	$\dot{P} = \dot{E}_e I_i$ (Fig. 6b)	$I_\Sigma = I_1 + I_2 + I_0$ $I_n^2 = I_1^2 + I_2^2 + I_0^2$ $\dot{\delta}_A = \dfrac{I_\Sigma^2}{\dot{P}}$ $\dot{\delta}_n = \dfrac{3I_n^2 - I_\Sigma^2}{2\dot{P}}$
	IV	$I'' = I' \dfrac{Y_{n\Sigma}}{Y_{n\Sigma} + \dot{\delta}^{(1,1)}}$	$\dot{P} = \dot{E}_i I_e$ (Fig. 6d)	

N.B. The value of P can be measured by a volt ammeter on the a.c. model, and by a current-wattmeter on the d.c. model.

since $\Delta \dot{I}_{ki} = \Delta \dot{I}_{k1} = \Delta \dot{I}_{k2} = \Delta \dot{I}_{k0} = \Delta \dot{I}'_{k1} + \Delta \dot{I}'_{k2} + \Delta \dot{I}_{k0}$, in the first type of fault in branch k, and

$$\Delta \dot{E}_{ki} = \Delta \dot{E}_{k1} = \Delta \dot{E}_{k2} = \Delta \dot{E}_{k0} = \Delta \dot{E}'_{k1} + \Delta \dot{E}'_{k2} + \Delta \dot{E}'_{k0}$$

for the second type of fault in branch k. Each component marked with an apostrophe originates from the corresponding component $\dot{I}_n$ or $\dot{E}_n$ and either coincides in phase with the other components ("special" phases the same in branches k and n), or else is shifted by a or a^2 relative to them ("special" phases different in branches k and n). Therefore, if we put the components $\dot{I}_n$ or $\dot{E}_n$ alternately in branch n in the circuits of Fig. 6, and alternately measure $\Delta \dot{I}'_{k1}$, $\Delta \dot{I}'_{k2}$, $\Delta \dot{I}'_{k0}$ or $\Delta \dot{E}'_{k1}$, $\Delta \dot{E}'_{k2}$, $\Delta \dot{E}'_{k0}$, in three ways in these networks, we can find their sums $\Delta \dot{I}_{ki}$ or $\Delta \dot{E}_{ki}$, and then $\dot{I}_{ki} = \dot{I}'_{ki} + \Delta \dot{I}_{ki}$ or $\dot{E}_{ki} = \dot{E}'_{ki} + \Delta \dot{E}_{ki}$ (as shown in the example in Fig. 7).

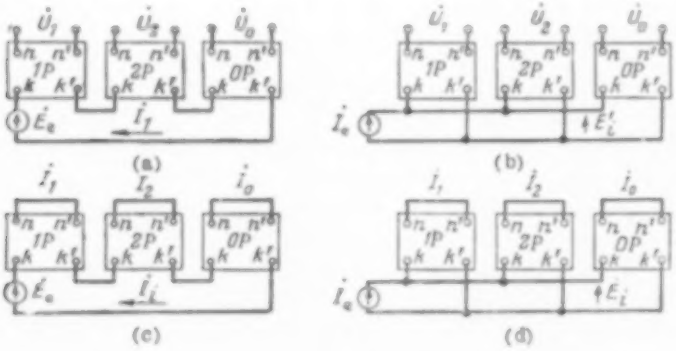

Fig. 6. Complex networks for calculating the coefficients Δ and δ in accordance with the expressions in Table 3.

Knowing the values of $\dot{I}_{ni}$ (or $\dot{E}_{ni}$) and $\Delta \dot{I}_{ki}$ (or $\Delta \dot{E}_{ki}$), we can also find the current distribution in conditions D in the branches of a network with any phase sequence. The currents thus found, if superposed on the currents of condition P_1, define the final currents of the required condition P_2 for any phase sequence network.

The currents in the branches of the circuit in condition D are determined by introducing each phase sequence of the corresponding sources into the branches n and k, these sources establishing the vector values $\dot{I}_n$ (or $\dot{E}_n$) and $\Delta \dot{I}_k$ (or $\Delta \dot{E}_k$). Each of these vector values can be represented in the form of two components, namely,

components, containing no operator a (coinciding in phase with $\dot{I}'_k$ or $\dot{E}'_k$), and components that do contain operator a.

The currents in the branches of the network can be calculated from either of these components. This makes it possible to measure them on a single phase a.c. or d.c. analyser. This method of calculation thus enables us to analyse not only the components in the fault branches k and n, but also those in any branch of the system. Compared with other simple analogue methods of calculation, e.g. that proposed in an earlier paper [2], this new method saves the time involved in dividing complex numbers and solving sets of equations in order to convert the networks so as to substitute current sources for e.m.f. sources.

Example

Let us consider an example of the claculation of a special combination of a complex fault with different *"special"* phases in branches k and n on a d.c. analyser and without it.

It is pre-supposed that it is required to calculate an earth fault in phase B of branch k and in phase C of branch n. Instead of this combination it is convenient to perform the calculation by conventionally orienting the calculations to the special phase A in branch k, in other words, perform the calculation as for a combination of an earth fault in phase A of branch k and in phase B of branch n. The changeover from this calculation to the original calculation is made by shifting the positive sequence components by a^2 and the negative sequence components by a. To simplify the calculation and its notation, it is presupposed that the fault in branch k occurs at the same time as that in branch n and that only reactances are taken into account, whilst these are conventionally replaced by resistances in order to ignore the 90^0 shift between the e.m.f. and the current of this e.m.f.

Calculation on a d.c. analyser

Fig. 7 (a, b, c and d) illustrates the calculations performed on a d.c. analyser. The complex analyser network in Fig. 7(a) represents the initial condition P_1. From this we can find the voltage in phase B for branch n:

$$\dot{U}' = \dot{U}_B = a^2\dot{U}'_1 + a\dot{U}'_2 + \dot{U}'_0 = 2{,}185a^2$$

whilst the current in branch k is $I'_k = 0{,}5\ a$.

By omitting the generator e.m.f. from the network in Fig. 7(a), and maintaining the current I_k' by means of the e.m.f. source U, we get a network in Fig. 7(b) which makes it possible to measure U_1, U_2 and U_0 and calculate the coefficient $\Delta_n^{(1)}$ in accordance with the expressions in column 5 of Table 3. In fact, using the measurements in the network in Fig. 5(b), we get: $U_\Sigma = 0.3125$; $U_\Sigma^2 = 0.0975$ and $U_n^2 = 0.0351$. Hence $\Delta_n^{(1)} = -0.0075$.

By converting the network in Fig. 7(b) into that in Fig. 7(c), we are able to measure $z'_{n\Sigma} = \frac{U_p}{I_p} = 1.4\,\Omega$ and determine $U'' = \frac{U z'_{n\Sigma}}{z'_{n\Sigma} + \Delta_n^{(1)}} =$ $= 2.2\ a^2$. Changing U_p in the network in Fig. 7(c) by U'', we can measure $I_{n0} = 1.56\ a^2$ and, using the boundary conditions of the fault under consideration, we come to the values $I_{n1} = 1.56$ and $I_{n2} = 1.56\ a$.

Putting I_{n1}, I_{n2} and I_{n0} into the network in Fig. 7(d) (which coincides with that in Fig. 7b, if $U = 0$), we can measure all three components ΔI, namely, $I'_{k1} = 0.098$, $\Delta I'_{k2} = 0.196\ a$, $\Delta I'_{k0} = 0.196\ a^2$. Hence $\Delta I_k = 0.098$ and $I_{ki} = 0.598$.

This defines the current components in the faulted branches k and n. The components in the other branches of each phase sequence can be found from the network in Fig. 7(d) by superposition of the currents I_k (with a break in the circuit 1 - 1′ and the introduction of a current source I_k at the point of break) or the currents I_{ni}, I_{n2} and I_{n0} (with a break in circuit 1 - 1′). It then only remains to pass from the values thus found to the corresponding original values of the components in the combination in question and to take into account the 90° shift in the current relative to the e.m.f., i.e. to shift the e.m.f. 120° and the current 30°. All the vectors will then be oriented relative to the e.m.f. of phase A.

Similarly we can measure the currents or voltages for any other two combinations of the complex fault under consideration.

The calculation without a network analyser

We shall give the solution of the same problem using the results obtained from the simplest type of asymmetrical fault. These results can either be taken from calculations already performed in power systems, or those performed by ordinary methods which require no explanation.

The necessary data are obtained from (1) the quantities shown in Fig. 7(a), (2) $Z'_{n1} = 0.343$, $Z'_{n2} = 0.686$ and $Z'_{n0} = 0.375$ as in Fig. 7(c),

(3) the voltage of phase A $U_{nA}^{(3)} = 1.875$ in branch n in the presence of a three phase short circuit in branch k and three open phases in branch n.

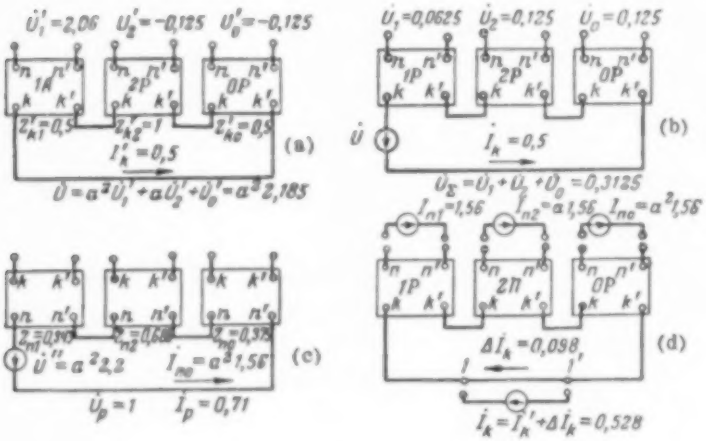

Fig. 7. Example of the calculation of an asymmetrical fault combination on a d.c. network analyser.

The calculation is performed in the following order.

Using the data in Fig. 7(a) and the values $U_{nA}^{(3)}$, we find all the coefficients* in Table 1 in accordance with Table 2:

$$\alpha_1 = \frac{2,06 - 1,875}{0,75} = 0,25;\ \alpha_2 = 0,25;\ \alpha_0 = 0,5;$$

$$n_A = 0,625;\ n_n = 0,185;\ Z_{k\Sigma} = 2;\ \dot{U}' = 2,185 \cdot a^2;$$

$$\Delta = -0,0075.$$

By further calculations, we find

(1) the current components in branch n:

$$a^2 I_{n1} = a I_{n2} = I_{n0} = \frac{2,185\ a^2}{1,404 - 0,0075} = 1,56\ a^2;$$

(2) the change in the current components of branch k in accordance

* The e.m.f. of the generators has to be omitted from the positive sequence network in Fig. 6(a) to find α_1.

with (10):

$$\Delta I_{k1} = \Delta I_{k2} = \Delta I_{k0} = \frac{0,125 \cdot 1,56}{2} = 0,098;$$

(3) the change in the voltage components of branch k in accordance with (2):

$$\Delta E_{k1} = -0,24;\ \Delta E_{k2} = -0,39a - 0,098;$$
$$\Delta E_{k0} = -0,39a^2 - 0,049;$$

(4) the total current and voltage components of branch k in accordance with (6) and (7):

$$I_{k1} = I_{k2} = I_{k0} = 0,5 + 0,098 = 0,598;$$
$$E_{k1} = 0,51;\ E_{k2} = -0,6 - 0,39a;\ E_{k0} = -0,3 - 0,39a^2.$$

This completes the calculation of the current and voltage components of branches k and n.

This method of calculation involves no conversions and is therefore independent of the complexity of the network.

Conclusions

1. Complex asymmetrical faults can be calculated by the successive transition from simple to more complex asymmetrical conditions. This paper shows that such a transition is possible from individual asymmetrical faults to a complex fault when asymmetry is simultaneously present in two branches of a three phase circuit.

2. The current (or e.m.f. components can be determined in accordance with the expressions given in Table 1 for any possible combination of faults in two branches of a three phase circuit by the conditions of a single asymmetrical fault.

3. The complex networks described in this paper can be produced for any possible combination of faults with maximum asymmetry in two branches of a three phase circuit. These networks contain no phase-rotating transformers. Practically all the computations involved in the calculation of a complex fault can be carried out on a single phase network analyser (and on a d.c. analyser if the inductive reactances are taken into account).

Translated by O.M. Blunn

REFERENCES

1. N.A. Mel'nikov and V.A. Satarov; *The calculation of the conditions of an asymmetrical short circuit in asymmetrical electrical systems by the superposition method, (Raschet rezhimov nesimmetrichnogo korotkogo zamykaniia v nesimmetrichnykh elektricheskikh sistemakh metodom nalozheniia).* Trud. VZÉI, No. 6, (1955).
2. G.G. Kostanian; *Elektrichestvo*, No.2, (1958).
3. G.G. Kostanian; *Izvest. Akad. Nauk Arm. S.S.R.*, XII, No.2, (1959).
4. A.B. Chernin; *Short circuits in unbalanced power system conditions, (Korotkie zamykaniia pri nepolnofaznykh rezhimakh elektricheskikh sistem).* Gosenergoizdat, (1952).
5. A.B. Chernin; *Elektrichestvo*, No.3, (1955).
6. N.N. Shchedrin and S.A. Ul'ianov; *Problems in the calculation of short circuits, (Zadachi po raschetu korotkikh zamykanii).* TÉI, (1955).
7. G.I. Atabekov; *The relay protection of high voltage networks, (Teoreticheskie osnovy releinoi zashchity vysokovol'tnykh setei).* Gosenergoizdat, (1957).
8. G.T. Adonts; *Elektrichestvo*, No.9, (1951).

1960

A CORELESS TOROIDAL REACTOR FOR POWER SYSTEMS*

L. V. LEITES

(Kuibishev Electrical Works, Moscow)

(Received 25 January 1960)

High voltage power reactors are acquiring ever increasing importance owing to the greater voltage and output of power systems. Use is made of shunting reactors in long distance transmission lines of 220 kV and above in order to compensate the changing MVA power of the lines. They usually incorporate a steel core. High-power transmission systems often require the installation of current-limiting reactors. Such reactors do not as a rule have a ferro-magnetic core. Widespread use is made of dry concrete current-limiting reactors. But their field of application is restricted to comparatively low voltages. At large outputs and high voltages use is made of oil-tank current-limiting reactors with a cylindrical coreless winding (Fig.1). To reduce losses due to eddy currents in the tank and its component parts, use has to be made of copper or aluminium electromagnetic screens in these reactors.

The main disadvantages of such reactors are the extra cost of copper or aluminium for the screens and the comparatively high additional losses.

The relationships between the winding dimensions of oil-tank reactors are rarely the same as the optimum relationships between the dimensions of unscreened coreless coils. A coil of optimum size should be comparatively large in diameter and have a small radial dimension. In this case the weight of the coil and its losses will be at a minimum. But the additional losses in the winding, the weight of the screens, the losses in the screens, the size of the tank, and the reduction in inductance owing to the effect of the screens will be

* *Elektrichestvo*, 11, 76-81, 1960.

extremely large. Therefore the diameter and axial dimension of the winding are usually increased and the radial dimension reduced. This involves using considerable quantities of copper, and the losses in reactors are greater than with coils of optimum size.

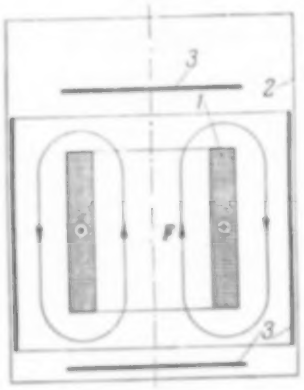

Fig. 1. The coreless oil-tank reactor:
1 - winding; 2 - tank; 3 - electromagnetic screens.

The extra losses in the winding conductors limit the maximum output of such reactors.

The development of power systems requires an increase in the power of reactors, including current-limiting reactors. This can be achieved by installing several comparatively low-powered units. But this is not justified economically since it considerably increases costs. It is more economic to install as few reactors as possible with the same total output and thus save material and reduce losses. We shall study the dimensions, weight and losses of a coreless reactor as a function of its power.

Dimensions

If the dimensions of a reactor winding are reduced by a factor of l, whilst the current density and content (space factor) of the winding section are constant, the m.m.f. of the reactor varies by a factor of l^2, inductance by l, and the section for the magnetic flux by l^2. Consequently, the magnetic flux is proportional to l^3 and the output of the reactor to l^5. Since volume and weight are only proportional to the cube of the linear dimensions, the weight of copper varies in

proportion to output by a factor of $\frac{3}{5}$. For example, if the increase in output per unit is doubled, the consumption of materials is only increased by 52 per cent. The losses of the reactor also vary similarly. Fig. 2 shows the specific consumption of conductor material and the losses of the proposed toroidal reactor as a function of output. In conventional steel-core transformers, the consumption of copper and the losses are 75 per cent proportional to output.

With fixed dimensions, the output of a reactor is proportional to the square of the current density, but not "primarily" as in transformers. At a given output and a similar change in dimensions, the losses are proportional to l^{-2}; i.e. they are $-\frac{2}{3}$ proportional to weight, and not $-\frac{1}{3}$ as in transformers.

At a given output and losses, a change in the conductivity of the winding material by a factor γ and in density by a factor d causes a $\gamma - \frac{1}{2}$ change of l and a $\gamma\frac{3}{2}$ d change of weight. Consequently, a changeover from copper to aluminium reduces the weight of the conductors by a factor of 1.58.

As can be seen, the advantage of using coreless reactors increase with increasing output. But the output of a reactor of the coil type with screens is limited. It is therefore advisable to use the toroidal coreless reactor shown in Fig.3, which is free of the stated shortcomings. Owing to circular symmetry, it has practically no external magnetic field and therefore requires no screening; the reactor winding can be developed on any number of coil groups, connected in parallel or in series. This makes it possible to design the reactor for large currents and voltages without increasing the number of parallel conductors in the disk coils. The coreless toroidal reactor involves no technological problems such as occur in the manufacture of windings for toroidal transformers and reactors with a closed annular magnetic circuit.

The question of additional losses is very important, more particularly with increasing output of the reactor. If the dimensions of the conductor strip were increased in proportion to the rest of the dimensions of the conductor, the specific additional losses would vary in proportion to the square of the induction and the square of the conductor dimensions, i.e. they would be proportional to l^4, and the total additional losses would vary in proportion to l^7. But a smaller conductor strip can be used in the toroidal reactor without increasing the number of parallel conductors in the coil. A considerable role is played in other types of reactor by the additional losses and mechanical forces of the transverse component of the magnetic field.

The winding of a toroidal reactor consists of a large number of single or double disk coils (Fig. 3) of circular, rectangular or oval shape. They are secured by wedges, spacers and other insulating components of special shape.

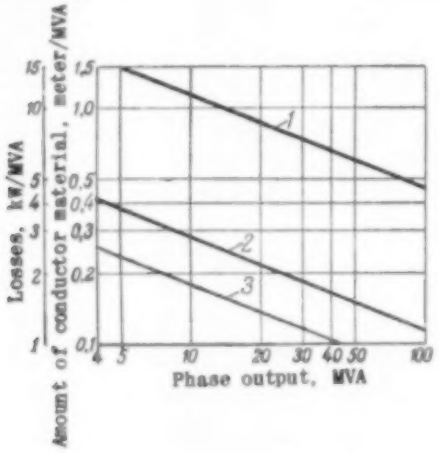

Fig. 2. Losses (1), weight of copper (2) and aluminium (3) as a function of the output of a toroidal reactor: 1 – losses; 2 – winding of copper conductor; 3 – winding of aluminium conductor.

To ensure that the voltage between adjacent coils nowhere exceeds the value across the single or double disk coils, it is necessary for one half of the reactor winding to be wound "left-handed", and the other half "right-handed". The two halves must be connected together in parallel (Fig. 4).

Design of the toroidal reactor

The preliminary approximate calculations involved in designing a toroidal reactor are more or less the same as for high-power transformers and reactors. The final electromagnetic calculation is slightly more complicated. It is however difficult to regulate the inductance of a finished toroidal reactor and it is therefore necessary to design it with the greatest possible accuracy.

If there are a large number of coils we can ignore the non-uniformity of the magnetic field around the circumference due to the reactor being composed of discrete disk coils. We can therefore assume that the m.m.f. is uniformly distributed round the circumference of the

toroid. We also ignore the distortion of the magnetic field due to eddy currents in the winding conductors. All the lines of force of the magnetic field are then concentric circles, whilst the induction of the magnetic field only has a tangential component*:

$$B = \frac{\mu_0 i w}{2\pi r} = B_{av} \frac{R_{av}}{r} \cdot \frac{I}{I\sqrt{2}} \cdot \frac{w}{w_r}. \tag{1}$$

The distribution of the induction across the width of the reactor winding is shown in Fig. 5(a).

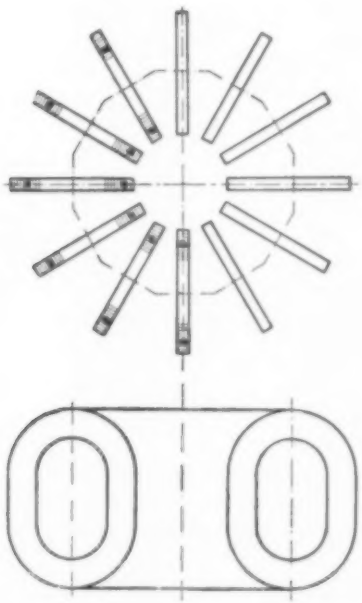

Fig. 3. Arrangement of the toroidal reactor.

Given the induction we can calculate the additional losses due to eddy currents in the conductors of the winding and the electrodynamic forces at any point [1]:

$$p_r = \frac{\omega^2 b^2 B^2 \gamma}{24 d} \tag{2}$$

and

$$dF = Bi\, dl. \tag{3}$$

* Symbols listed at the end of the paper. See also Fig. 5(b).

Formulae are derived below for the case of oval coils. The shape of coil is shown in Fig. 5(b). The inductance of the reactor in terms of the energy of the magnetic field is:

$$L = \frac{1}{\mu_0 I^2} \int_V B^2 \, dV.$$

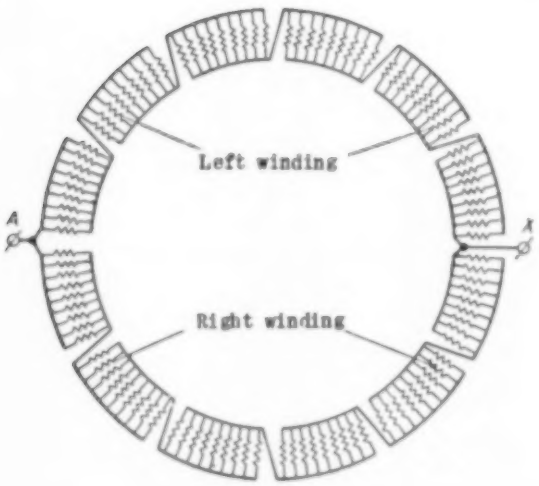

Fig. 4. Arrangement of the winding coils of a current-limiting toroidal reactor (rated current 1350A, voltage 110 kV, inductance 15%).

Using equation 1, and since $dV = 2\pi r dS$, we get:

$$L = \frac{\mu_0 w_r^2}{2\pi} \int_S \frac{1}{r} \left(\frac{w}{w_r} \right)^2 dS. \tag{4}$$

The reactor winding has to be divided into several parts. (Fig. 5b). Performing integration by parts, we get,

$$L = L_1 + L_2 + L_3 + L_4 + L_5. \tag{5}$$

The formulae are known [2] for parts 1 and 2 where $w/w_r = 1$:

$$L_1 = \frac{\mu_0 w_r^2}{2\pi} h \ln \frac{R_{av} + R_1}{R_{av} - R_1} \tag{6}$$

and

$$L_2 = \mu_0 w_r^2 \left(R_{av} - \sqrt{R_{av}^2 - R_1^2} \right). \tag{7}$$

In part 3 .

$$\frac{w}{w_r} = \frac{r - (R_{av} - R_2)}{a};$$

$$dS = h\,dr;$$

$$L_3 = \frac{\mu_0 w_r^2}{2\pi} \cdot \frac{h}{a^2} \int_{R_{av}-R_2}^{R_{av}-R_1} \frac{(r - R_{av} + R_2)^2}{r}\, dr.$$

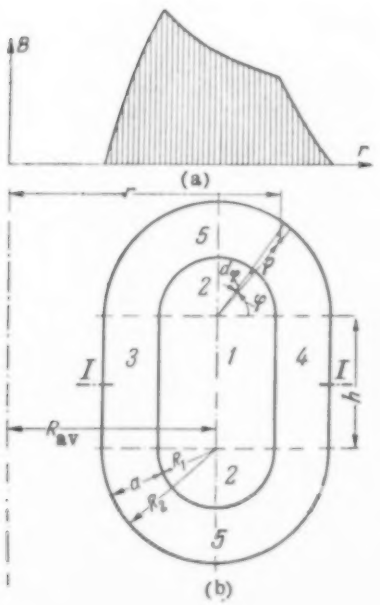

Fig. 5. Reactor design:
a – induction across section $l - l$; b – division into parts.

After integration and substitution of the limits, we get:

$$L_3 = \frac{\mu_0 w_r^2}{2\pi} h \left[0{,}5 - \frac{R_{av} - R_2}{a} + \left(\frac{R_{av} - R_2}{a} \right)^2 \ln \frac{R_{av} - R_1}{R_{av} - R_2} \right]. \tag{8}$$

Likewise,

$$L_4 = \frac{\mu_0 w_r^2}{2\pi} h \left[-0{,}5 - \frac{R_{av} - R_2}{a} + \right.$$
$$\left. + \left(\frac{R_{av} + R_2}{a} \right)^2 \ln \frac{R_{av} - R_2}{R_{av} + R_1} \right]. \qquad (9)$$

To calculate L_5 it is convenient to introduce the polar co-ordinates (Fig. 5b):

$$r = R_{av} + \rho \cos \varphi;$$

$$\frac{w}{w_r} = \frac{R_2 - \rho}{a};$$

$$dS = \rho d\varphi \, d\rho;$$

$$L_5 = \frac{\mu_0 w_r^2}{2\pi} 2 \int_{R_1}^{R_2} \int_0^{\pi} \left(\frac{R_2 - \rho}{a} \right)^2 \frac{\rho \, d\rho \, d\varphi}{R_{av} + \rho \cos \varphi} =$$

$$= \frac{\mu_0 w_r^2}{a^2} \int_{R_1}^{R_2} \frac{(R_2 - \rho)^2}{\sqrt{R_{av}^2 - \rho^2}} \rho \, d\rho =$$

$$= \mu_0 w_r^2 \frac{R_{cp}}{a^2} \left[(R_{av}^2 + R_2^2)(A_1 - A_2) + \right.$$
$$+ R_2 (R_2 A_2 - R_1 A_1) - R_2 R_{av} A_3 -$$
$$\left. - \frac{1}{3} R_{av}^2 (A_1^3 - A_2^3) \right], \qquad (10)$$

where

$$A_1 = \sqrt{1 - \left(\frac{R_1}{R_{av}} \right)^2};$$

$$A_2 = \sqrt{1 - \left(\frac{R_2}{R_{av}} \right)^2};$$

$$A_3 = \arcsin \frac{R_2}{R_{av}} - \arcsin \frac{R_1}{R_{av}}.$$

Formula (10) is quite cumbersome. It is therefore convenient for preliminary calculations to use a simplified formula, derived on the assumption that the induction varies linearly as a function of $(R_2 - \rho)$

with a constant co-ordinate ϕ:

$$L_5 \approx \frac{\mu_0 w_r^2}{2\pi} 2 \int_{R_1}^{R_2} \int_0^{\pi} \frac{(R_2-\rho)^2}{a^2} \cdot \frac{\rho\, d\varphi\, d\rho}{R_{av} + \left(R_1 + \frac{a}{3}\right)\cos\varphi} = \tag{11}$$

$$= \mu_0 w_r \frac{a}{3}\left(R_1 + \frac{a}{4}\right)\left[R_{av}^2 - \left(R_1 + \frac{a}{3}\right)^2\right]^{-\frac{1}{2}}$$

Likewise we obtain simplified formulae for L_3 and L_4:

$$L_{3,4} \approx \frac{\mu_0 w_r^2}{2\pi} \cdot \frac{a}{3} \cdot \frac{h}{R_{av} \mp R_1 \mp \frac{a}{3}}. \tag{12}$$

When calculating the mean additional losses, we replace the total losses within the limits of the conductors (turns) by integration over the width of the coil, since the width of the coil is many times greater than the thickness of the conductor. Parts 3 and 4 can be calculated by quite exact formulae similar to those used in transformer design:

$$P_{\phi 1\,3,4\,av} \approx \frac{\omega^2 b^2 \gamma}{24 d} B_{cp}^2 \frac{1}{3}\left(\frac{R_{av}}{R_{av} \mp R_1 \mp \frac{a}{3}}\right)^2. \tag{13}$$

For part 5, on the same assumptions as for the derivation of formula 11, we get:

$$P_{\phi 1\,5\,av} \approx \frac{\omega^2 b^2 \gamma}{24 d} B_{av}^2 \frac{2}{a(R_1+R_2)\pi} \int_{R_1}^{R_2} \int_0^{\pi} \left(\frac{R_2-\rho}{a}\right)^2 \times$$

$$\times \left[\frac{R_{av}}{R_{av} + \left(R_1 + \frac{a}{3}\right)\cos\varphi}\right]^2 \rho\, d\varphi\, d\rho = \tag{14}$$

$$= \frac{\omega^2 b^2 \gamma}{24 d} B_{av}^2 \frac{l}{3}\left[1 - \left(\frac{R_1}{R_{av}} + \frac{a}{3R_{av}}\right)^2\right]^{-3/2} \times$$

$$\times \left[1 - \frac{a}{2(2R_1 + a)}\right].$$

The total electrodynamic forces acting upon parts 3 and 4 of the winding can be estimated by formulae similar to those used in trans-

former design:

$$F_{3,4} \approx \left(\frac{i}{I}\right)^2 \frac{B_{av}}{\sqrt{2}} I w_r h \frac{1}{2} \cdot \frac{R_{av}}{R_{av} \mp R_1 \mp \frac{a}{3}}. \tag{15}$$

The load on a single section $d\phi$ of part 5 is:

$$dF_5 \approx \left(\frac{i}{I}\right)^2 \frac{B_{av}}{\sqrt{2}} \cdot \frac{R_{av}}{R_{av} + \left(R_1 + \frac{a}{3}\right)\cos\varphi} \times$$

$$\times I w_r \int_{R_1}^{R_2} \frac{R_2 - \rho}{a} \cdot \frac{d\rho}{a} \rho \, d\varphi = \left(\frac{i}{I}\right)^2 \frac{B_{av}}{\sqrt{2}} \times \tag{16}$$

$$\times \frac{R_{av}}{R_{av} + \left(R_1 + \frac{a}{3}\right)\cos\varphi} I w_r \frac{1}{2} \left(R_1 + \frac{a}{3}\right) d\varphi.$$

The shape of the curved (face) parts of the coils

The load of the electrodynamic forces on the curved parts of the coils is not at all uniformly distributed. Consequently, if their curvature is constant (Fig. 5b), then not only tensile but also bending stresses will occur. But the curved parts can be made in such a way that there are no bending stresses.

The specific load q on a given middle turn normal to it is inversely proportional at each point to the distance between this point and the axis of the toroid. For zero bending stress, the tensile force F_{tens} should be constant over the length of the turn and related to the radius of curvature ρ as follows: $F_{tens} = q\rho = \text{const}$. Consequently, the radius of curvature should vary in proportion to the distance from the axis of the toroid (Fig. 6):

$$\rho = \rho_1 \frac{r}{r_1} = \frac{F_{tens} r}{q_1 r_1}. \tag{17}$$

Analytically, the shape of the curved parts of the turn is defined in Cartesian co-ordinates by the equation:

$$\frac{d^2y}{dr^2} = \frac{q_1 r_1}{F_{tens}} \cdot \frac{1}{r} \left[1 + \left(\frac{dy}{dr}\right)^2\right]^{3/2} \tag{18}$$

with the boundary conditions $\frac{dy}{dr} = \infty$ if $r = r_1$ and $r = r_2$.

There is a simple "step by step" graphical solution for this equation, using a pair of compasses, in which the required curve is plotted in accordance with 17. The value of ρ_1 is made such that the end of the curve coincides with the external straight line section of the curve ($\frac{dy}{dr} = -\infty$ if $r = r_2$). This value is found comparatively easily by two or three successive approximations.

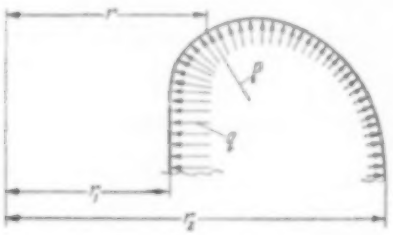

Fig. 6. Optimum shape of the curved parts of the reactor coils.

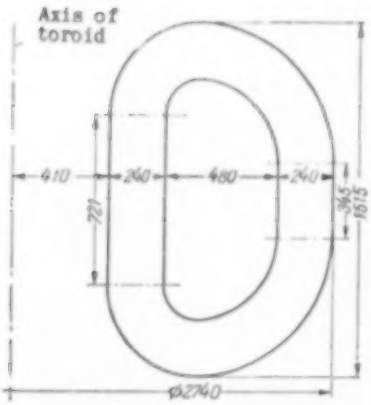

Fig. 7. The winding of a 110 kV current-limiting reactor for 1350A with 15% reactance. Dimensions in mm.

Fig. 7 shows the optimum shape of a coil for current-limiting reactors (see example). The tensile stresses in the winding conductors are 140 kg/cm^2 or less. This permits aluminium conductors to be used.

This shape cannot be rigorously maintained for all the curved parts

simultaneously on all turns of the coil, since the radii of curvature of the various turns are different by a constant quantity. Slight bending stresses are therefore set up in the winding. Such stresses are at a minimum if the turns conform to equation (17) at a distance of 0.3 to 0.4 a from the internal edge of the coil.

A coil having curved parts of variable curvature has a relatively shorter straight external section. The clamping of the windings is therefore facilitated. One drawback of this design is the slightly more complicated shape of the winding. In addition the electromagnetic calculation has to be performed by numerical integration.

Conclusion

For high output current-limiting reactors, the use of a toroidal design instead of a coil type design with screens results in a considerable saving in capital outlay, reduces losses and the consumption of non-ferrous metal. Thus, a 12.9 MVA toroidal reactor requires no copper for the winding (a saving of 4.5 tonnes of copper) and reduces losses by 20 per cent (35 kW) for a slightly larger consumption of aluminium.

Example

The characteristics of an oil-tank current-limiting reactor are: voltage 110 kV, rated current 1350 A, "reactance" 15%, frequency 50 c/s, peak short circuit current in a system of unlimited power 1350 x $\times \frac{100}{15}\sqrt{2} \times 1.95 = 24.8$ kA. The voltage across the reactor under rated conditions is $110 \times 0{,}15/\sqrt{3} = 9{,}54$ kV; output is 8.54 x 1350 = 12,900 kVA. The inductance of the reactor L = 22.5 mH.

We have performed these calculations on several models. Using these we can select the current density, the dimensions of the winding and conductor, and the number of turns. The penultimate approximation is determined by exact formulae. The theoretical inductance can be adjusted to the required value by a small change in the dimension h. Only the final calculation is given below.

We first have to consider a reactor having coils of the shape shown in Fig. 5(b). Use is made of an APB-type conductor 2.44 x 14.5/3.79 x x 15.85 mm and 34.9 mm^2 in section. The coil consists of 61 turns. The radial dimension of the coil a = 240 mm. The arrangement of the single disk coils is shown in Fig. 4. Six groups of nine parallel-connected coils are connected in series in each turn. The total number

of turns $w = 366$. There are 18 parallel conductors and $n = 108$ coils.

The minimum distance between adjacent coils (at the opening of the toroid $r = R_{av} - R_2$) to 6 mm, whilst that between group is 24 mm. The control opening is 820 mm in diameter.

Winding dimensions: $R_1 = 240$ mm; $R_2 = 480$ mm; $R_{av} = 890$ mm, and $h = 553$ mm. Average length of a turn is 3.46 m. The weight of aluminium in the winding is 2140 kg.

Inductance from formulae 6 to 9 and 11: $L_1 = 8.85$ mH, $L_2 = 5.53$ mH, $L_3 = 2.18$ mH, $L_4 = 1.12$ mH, $L_5 = 4.82$ and $L = 22.5$ mH.

Induction $B_{av} = 1570$ G. Maximum induction (on part 3 at the point $r = R_{av} - R_1$) is 2150 G.

Current density is 2.15 A/mm^2, and specific basic losses 60 W/kg.

The greatest additional losses from formula 2 are 12.2 W/kg.

Mean specific additional losses from formulae (13) and (14): $p_{ed.3\ av} = 5.21$ W/kg, $p_{ed.4\ av} = 1.16$ W/kg, and $p_{ed.5\ av} = 2.2$ W/kg. Mean additional losses over the winding are 2.52 W/kg, i.e. 42% of basic losses. Total reactor losses are 134 kW.

The electrodynamic loads from formulae (15) and (16)

$$F_3 = 900\ T;\quad F_4 = 420\ T;\quad \frac{dF_3}{n\left(R_3 + \frac{a}{3}\right)d\varphi}$$

vary from 65.5 kg/cm if $\phi = 0$ to 139 kg/cm if $\phi = \pi$.

Owing to the large load on the curved parts, these should be shaped as in Fig. 6. The appropriate winding is shown in Fig. 7. The following results have been calculated: with the original inductance (22.5 mH) the weight of aluminium was practically constant (2120 kg); losses were 135 kW; $F_3 = 1150\ T$; $F_4 = 275\ T$; the maximum load on the curved parts of the coil was 139.5 kg/cm, and at this point the radius of curvature $\rho_1 = 21.5$ cm whilst the tensile stresses in the conductor according to formula (17) were 140 kg/cm^2.

For purposes of comparison we should point out that two parallel-connected oil tank reactors of the coil-type with screens for a voltage of 110 kV and a current of 675A each requires 4.5 tonne of copper for the windings and 1.9 tonne of aluminium for the screens with losses of 170 kW. Aluminium cannot be used for the windings of these reactors owing to the large mechanical loads on the conductor in the event of short circuits.

Symbols

B – induction of the magnetic field, instantaneous value;

B_{av} – amplitude of the induction half way across the coil of the reactor ($r = R_{av}$) at a current I;

$$B_{av} = \frac{\mu_0 W \sqrt{2} I \omega_r}{2\pi R_{av}};$$

i – instantaneous value of the reactor current;

I – effective value of the current;

W_r – number of turns in reactor winding;

W – number of turns coupled with a line of force passing through the point in question;

P_{ed} – specific losses due to eddy currents;

ω – angular velocity;

b – thickness of conductor;

d – density (specific gravity) of the conductor material;

γ – specific electrical conductance;

F – electrodynamic force;

L – inductance;

V – volume of the magnetic field;

S – section of the magnetic flux;

r – distance between a point and the axis of the toroid.

The geometric dimensions of the winding are shown in Fig. 5(b).

Translated by O.M. Blunn

REFERENCES

1. G.N. Petrov; *Electrical machines, pt.I, Transformers, (Elektricheskie mashiny, ch. 1, Transformatory).* Gosenergoizdat, (1956).
2. P.L. Karantarov and L.A. Tseitlin; *The calculation of inductance, (Raschet induktivnostei)* Reference manual, Gosenergoizdat, (1955).

1960

THE USE OF TRANSISTORS FOR CONTROLLING MERCURY ARC RECTIFIERS*

L.M. TVERDIN and Iu.M. KURZANOV

Moscow

(Received 12 December 1959)

In automatic drive systems using controlled mercury arc rectifiers, e.g. mar-motor systems and mar-machine excitation winding systems, the mean rectified voltage is usually regulated by a phase shift of the positive trigger voltage impulses across the grids of mercury arc rectifiers. To form the pulses and shift them in phase, widespread use is made of systems incorporating pulse generators, pulse-chokes, static phase-regulators, half-wave magnetic amplifiers and controlled pulse-chokes etc.

The development and introduction of such devices was a step forward in the improvement of automatic control systems. These systems, based on variations in the magnetic state of the core, have high inertia and require a large power consumption for control purposes and particularly to achieve high operating speeds. In addition, they are large and require non-ferrous metals and special steels.

Semiconductor devices make it possible to produce equipment which forms the control pulses and shifts them on a different principle.

A number of semiconductor grid control systems have recently been developed in the Leningrad and Kharkov departments of the GPI "Tiazhpromelektropoekt". These systems still work on the same basis as before. The number of pulse forming and shifting units is a half of, or equal to, the total number of grids in the mercury arc rectifier. Thus, for example, a three phase mercury arc rectifier has three pulse forming and three phase shifting devices (Fig. 1). The presence of

* *Elektrichestvo*, 11, 82-84, 1960.

separate pulse generators means that special steps have to be taken to ensure the regular production of identical impulses relative to the anode voltage.

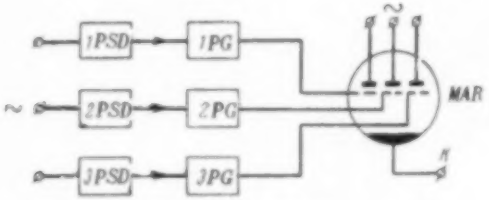

Fig. 1. Block diagram of the grid control of a controlled mercury arc rectifier with magnetic apparatus:
1 *PSD* to 3 *PSD* – phase shifting devices;
1 *PG* to 3 *PG* – generators for positive trigger pulses.

1960

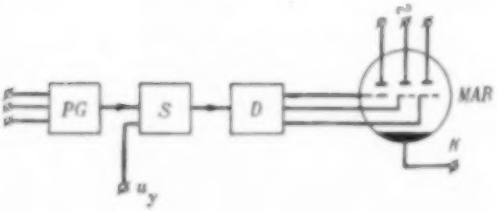

Fig. 2. Block diagram of the grid control of a controlled mercury arc rectifier using transistors:
PG – generator for triangular pulses; *S* – shaper for π-shaped pulses; *D* – device for distributing pulses between the grids; u_y – control voltage.

Since the anode firing time of a three phase mercury arc rectifier is $\frac{1}{3}$ of a period, it is quite practicable to adopt a system in which the generator forms three successive impulses of 112 to 117 el. deg. in width during one a.c. period and then for these pulses to be distributed between the converter grids by the "logical" part of the system (Fig. 2).

The main circuit of such a system is shown in Fig.3. It consists of three main units, namely, a relaxation oscillator, a pulse forming device and a distributer.

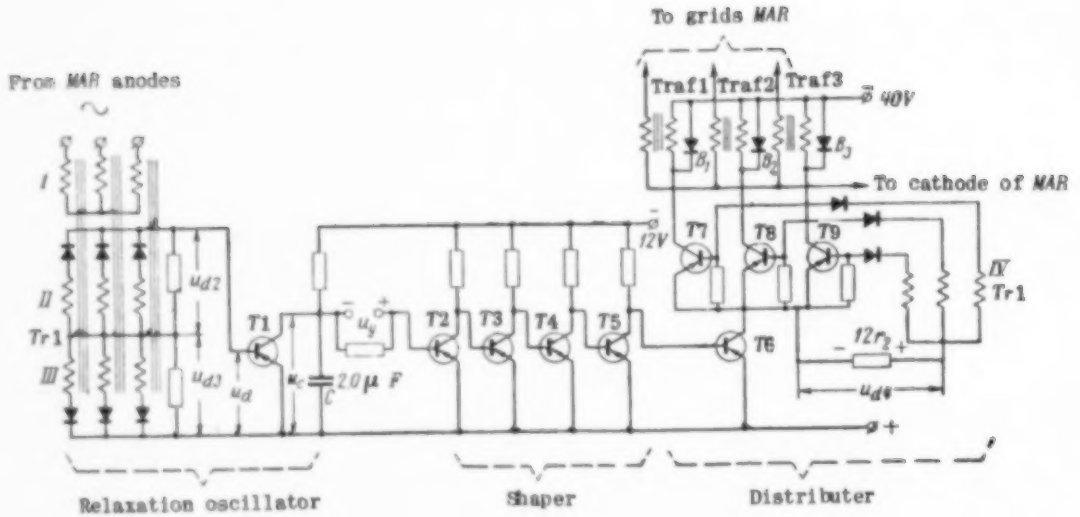

Fig. 3. Arrangement of transistor grid device for controlling a three phase mercury arc rectifier.

The difference between the instaneous values of the rectified voltages u_d is received at triode T1. Triode T1 is "off" on section 1-2 (Fig. 4a) and capacitor C is charged. When the polarity of voltage u_d is changed (interval 2-3) triode T1 is "on" and shunts capacitor C, which is discharged during 2 to 4 el. deg. Then the process is repeated and during one period three voltage pulses 112 to 117 el. deg. in width are formed.

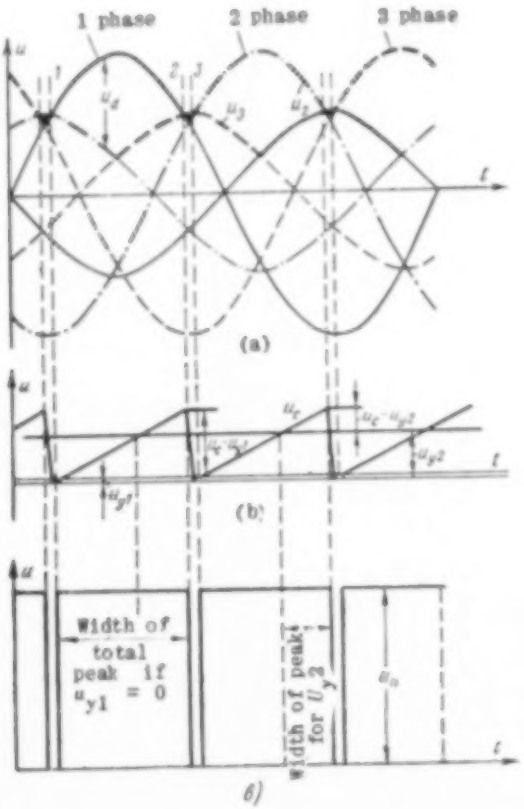

Fig. 4. The variation in u_d, u_c and pulse width for the arrangement in Fig. 3.

The triangular shaped voltage u_c from capacitance C is compared with the control voltage u_y (Fig. 4b). When the voltage u_c equals u_y, triode T2 of the shaper becomes "on" and shorts the input to the amplifier (triodes T3-T5). Triode T6 is then "on" and a positive trigger pulse is formed on the secondary windings of the transformers

Traf 1 and Traf 2. At point 2 the capacitor C begins to discharge. The polarity of the voltage at the input to the shaper is reversed. Triode $T2$ and then $T6$ become "off" and the pulse is stopped. The wavetail of the pulses is fixed in time and defined by the moment at which the capacitor C begins to discharge. The wavefront is defined by the moment triode $T2$ becomes "on".

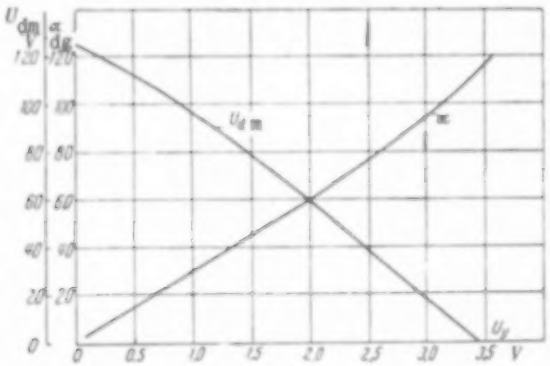

(a)

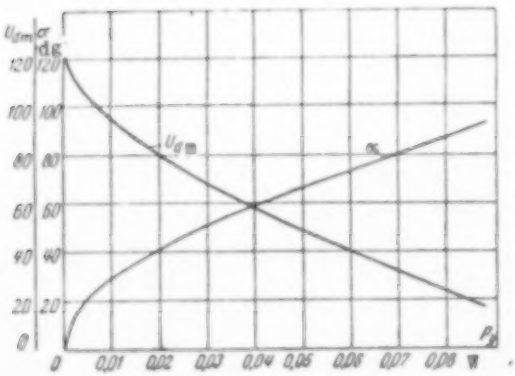

(b)

Fig. 5. Angle $\alpha = f(P_y, u_y)$ and the mean rectified voltage $u_{dm} = \phi(P_y, u_y)$.

The pulses are distributed between the grids of the controlled mercury arc rectifier (*MAR*) by triodes $T7$ to $T9$, which together with winding IV of the transformer Tr 1, constitute a three phase rectifier loaded across impedance r_2. Each triode is "on" for one third of a period and passes the voltage peak to the next grid of the anode to be

fired. The triodes T7 to T9 are synchronized with the anodes of the mercury arc rectifier by matching the performance of Tr 1 with the power transformer of the MAR.

The trigger voltage pulses are formed on the grids of the MAR in the following way. When triode T6 becomes "on", a current passes through the primary winding of one of the transformers Traf 1, 2 or 3. A distributer triode (T7, T8 or T9) is live in the circuit of this transformer at that particular moment. A square voltage pulse of the required amplitude is formed in the secondary winding. The width of the pulse is defined by the period of time that triode T6 is "on". Its amplitude depends on the transformation ratio of Traf 1 - Traf 3.

The main power losses in the formation of the pulses occur in triode T6, since triodes T7 to T9 are switched without current and only prepare the appropriate circuits for the passage of the pulses.

1960

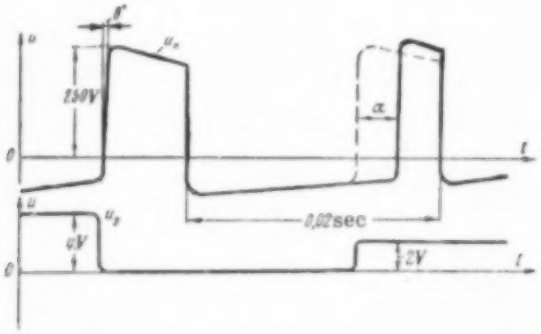

Fig. 6. Oscillogram of the voltage peaks u_p across the grid of a controlled mercury arc rectifier for $u_y = 4$ V and $u_y = 2$ V.

The mean rectified voltage is regulated by a continuous or pulsating variation in the absolute magnitude of the control voltage u_y (Fig. 4b). The beginning of peak formation is displaced in time and, consequently, the instant when the anodes are fired is likewise displaced (Fig. 4c). Fig. 5 shows the angle of firing delay α and the magnitude of the mean rectified voltage $u_{d\alpha}$ as a function of control output P_y and control voltage u_y, as ascertained from tests on an RM - 200 type mercury arc rectifier.

Fig. 6 shows an oscillogram of the voltage trigger peaks across the grid of the controlled mercury arc rectifier for various firing delay angles.

The main merits of this system are its high operating speed (below 0.001 sec), low control power consumption (less than 0.1 W required to change α from 0 to 90°), small size, low weight, simplicity in production and adjustment, reliability, constant peak amplitudes and very steep wavefronts (at least 80 to 100° for 1 V). Its performance is not notably affected by swings in a.c. mains voltage of ± 20 per cent, or by changes in temperature within the permissible limits of the triodes, since the latter operate solely on the relay system.

These arrangements are applicable to all gear using controlled mercury arc rectifiers in which the range of the firing delay angle is 90 el deg or less. It allows continuous electronic, pulsatory or combined control over the mean rectified voltage of mercury arc rectifiers in irreversible automatic electric drive systems in which a controlled mercury arc rectifier is used in conjunction with a motor or the excitation winding of an electrical machine.

The lack of inert links in the *MAR* grid control system improves the dynamic characteristics of the control system and creates favourable conditions for the design of simple single-circuit systems. The amplification factor of the system depends on the number of triodes in the pulse shaper. Practically any number can be used. If several control signals arrive at the input to the gear, they are added by a potentiometer or low-inertia magnetic amplifier. To maintain normal performance, the control voltage should be confined within the limits $0 < u_y \leqslant u_c$.

The proposed system was developed and tested in the laboratory of the department of electrical equipment for industry at the Moscow Power Institute.

P-15 type triodes were used for triodes *T*1 to *T*3, P-203 type for *T*4 and *T*5, and P4-B type for *T*6-*T*9.

Translated by O.M. Blunn

THE SCREENING OF RAILWAY COMMUNICATION CABLES - A NEW APPLICATION FOR 3% SILICON STEEL*

Ia. S. SHVARTSBART

(Received 14 July 1960)

1960

The original electrical application of silicon steel was in transformers and electrical machines. Its known electromagnetic properties (high specific electrical resistance and magnetic permeability compared with iron, low coercive force, high saturation, high wear resistance and so on) were used for producing the magnetic circuits of transformers and electrical machines etc. Use has been made of cold-rolled 3 per cent silicon steel for over twenty years to produce top quality magnetic circuits.

But, during the past five years, railway electrification with alternating current at power frequency has made it necessary to protect trunk communication cables from induced currents. A search was made for materials to screen the sheaths of railway cables. New properties of cold-rolled 3 per cent silicon steel were found, namely, high magnetic permeability ($> 4 \times 10^3$ G oerst in a field of 1.0 oerst) when in a state of pliable - resilient bending (i.e. wrapped round the core of the cable), and high ductility, which provides a satisfactory "armour" for the cable.

It has been shown [1] that high magnetic permeability in silicon steel strip when wrapped round the core of a cable is created by the same technological methods as are used for cold-rolled transformer steel, namely, the production of a high quality alloy by an electrometallurigcal process, "raffination" of the annealed strip (a special form of refinement), double-cold rolling and final high temperature annealing

* *Elektrichestvo*, 11, 84-86, 1960.

in order to correct the grain structure of the steel orientation .

But the experience of the first batches of such strip showed that it is a difficult matter to combine high magnetic permeability and satisfactory ductility in this steel. It can only be done if certain specific production conditions are satisfied.

This production procedure thus deserves special consideration. A number of papers [2,3,4] dealing with the structure of industrial silicon-iron alloys state that an 0.01% carbon content in silicon-iron alloys (with 3% silicon) leads to the formation of a structurally free carbide in the structure of the steel after high temperature annealing and that this free carbide is in the form of boundary segregations fringing the ferrite grains of the steel. These boundary carbide segregations in the microstructure of the alloy reduce its ductility, and all the characteristics of a brittle silicon steel obtain if there are large amounts of carbide.

The high temperature annealing of such silicon strip is a necessary part of the production process (the best magnetic properties are produced at annealing temperatures of 1100 to 1150°C). On the other hand, the present day methods of producing cold-rolled transformer steel in the U.S.S.R. only reduce the carbon content to 0.01% minimum. The various factories do not have the necessary equipment to reduce the carbon content of silicon steels below 0.01% (decarbonization under a layer of scale, or "black" annealing and vacuum annealing).

These two circumstances together, i.e. the need for high temperature annealing and the unavoidable carbon-content of at least 0.01%, result in the appearance of boundary segregations of carbide in the structure of the steel and, consequently, in lower ductility, even to the extent of brittleness, which prevents the normal process of armouring being used to clad cable cores with such strip.

The problem is to find a means of eliminating the structurally free boundary segregations of carbide from the steel.

One method has been found [4]. Here the boundary carbide segregations are removed after high temperature annealing by heat treatment. The steel is heated after high temperature annealing to 800°C. It is held for a short while at this temperature (2 min for strip 0.5 mm thick) and is then cooled in hydrogen. The structurally free carbides are dissolved in the main mass of grains and, owing to the comparatively rapid cooling, they set in the solution. The ductility of the steel (as defined by the standard brittleness test) is increased several times over, compared with its state immediately after high temperature annealing, and its magnetic properties are not reduced.

TABLE 1

Method of production	Magnetic permeability in a field of 1 oerst in the pliable - elastic bent state	Ductility
Double cold rolling with final high temperature annealing at 1100°C in dome-type furnace in dry hydrogen.	High, over 4000 G/oerst	Large variation in ductility in the length of the strip. Partial brittleness. Unsuitable for armouring purposes.
Double cold rolling with high temperature annealing of strip in final thickness at 1100°C in dome-type furnace followed by quenching in a transfer-type furnace at 800°C in dry hydrogen.	High, over 400° G/oerst	Satisfactory. Armouring possible without special difficulty.
Double cold rolling with short (5 min) period of high temperature annealing of strip in final thickness at 1100°C in transfer-type furnace in dry hydrogen.	Satisfactory, over 2700 G/oerst	High. No difficulties involved in armouring.
Double cold rolling with high temperature annealing of strip in final thickness at 950°C in dissociated ammonia.	Non-uniform permeability with "fall-outs" in the regions of low permeability.	Non-uniform ductile properties with brittle parts, strip unsuitable for armouring.

A sample batch of strips has also been drawn through a furnace and quenched in hydrogen.

This quenching of cold-rolled silicon steel is not the only possible procedure. Ductility can be improved without reducing its magnetic properties by a technological process that reduces the carbon content

1960

to 0.005% or less. This can be done by special heat treatment in a transfer-type furnace using wet hydrogen (according to dew point) at + 30°C.

It has been planned to produce silicon steel with a very low carbon content in transfer-type furnaces at the Novolipets iron and steel works. It may also be started at a number of works engaged on the production of cold-rolled transformer steel.

Table 1 shows the methods at present used for the production of silicon strip for armouring cables and makes an attempt to assess the quality of this necessary material.

Table 1 also shows that the second method of production is the best. Still better results are to be expected from the planned production of cold-rolled 3% silicon steel by decarbonization in wet hydrogen. The magnetic and ductile properties of the steel will undoubtedly be improved.

Translated by O.M. Blunn

REFERENCES

1. Liubimov, Ukstin and Shvartsbart; *Railway communication cables with magnetic armouring, (Zheleznorozhnye kabeli aviazi s magnitnoi bronei).* Trud. NIIKP, No. IV.
2. Carbon in silicon-iron alloys, *J. Iron and Steel Inst.*, 167, (1951).
3. Shteinberg; *Fiz. met. i metalloved.*, I, No. 1, (1955).
4. Shvartsbart; *Metalloved. i termich. obrabot.*, No. 2, (1960).

ABSTRACTS FROM PAPERS PUBLISHED IN ELEKTRICHESVO No. 11, 1960

Control engineering

Determining the parameters of linearized models of control systems from experimental frequency characteristics. A.A. Kardashov and others, (pp. 51-56).

A simple and accurate method is proposed for finding the parameters of control and drive systems and in solving problems of synthesizing circuits. Linear "models" of these systems are described by differential equations. The method is based on the approximation of the experimental amplitude-phase characteristic by the method of least squares.

Induction furnaces

The electrical design of an induction furnace without a steel core. I.A. Toropov, (pp. 72-76).

The author brings the mathematical methods used to design induction furnaces up to date by making provision to take the "edge effect" into account.

Insulation

Recording the ionization characteristics of insulation. G.S. Kuchinskii and others, (pp. 42-48).

A comparative study is made of systems in use for registering corona and creep discharges etc on dielectrics. The sensitivity of the test rig as regards the apparent intensity of ionization is considered to be of the order of 10^{13}k.

Measurement of capacitance

A method of estimating electrical capacitance. Iu.S. Rusin, (pp. 48-50).

A new qualitative formula is proposed which enables electrical

capacitance to be estimated satisfactorily for one conductor, two conductors and a two-dimensional system, (even if the conductors are close together). The method can also be used for determining the normal component of the vector of field intensity for electrodes at different potentials. Examples are given.

Power systems

The application of computer techniques in power system operation and design today. I.M. Markovich and others, (pp. 1-8).

The authors review the ways in which network analysers and computers are now being used in the world at large for operating and planning power systems, (34 references).

A method of calculating changes in the head of water after erecting or developing hydro-electro stations. V.M. Gornshtein, (pp. 13-19).

Marginal analysis is applied to the rate of water flow and operating costs of hydro-electric power stations to define their optimum economic efficiency.

Calculating complicated faults using the results of computations of simpler system conditions. G.G. Kostanian, (pp. 20-28).

The author distinguishes two broad classes of asymmetrical fault which can occur in a power system and then uses symmetrical component analysis to study all the possible combinations of symmetrical conditions. These "complex" faults are regarded as the result of several successive asymmetrical faults.

Propagation of electromagnetic waves

The propagation of electromagnetic waves on multi-conductor lines. M.V. Kostenko, (pp. 8-12).

Simplified "telegraph" equations are proposed for a practical solution of the problem of electromagnetic wave propagation along multi-conductor lines. The simplifying assumptions are: no "end effect" along the line, no "wave effect" across the line, no "proximity effect", no discontinuities, no longtitudinal components of the bias currents in the air, no transverse components of the intensity of the electrical field in the earth and conductors, and a number of other minor assumptions.

Rectifiers

The use of transistors for controlling mercury-arc rectifiers. L.M. Tverdin, (pp. 82-84).

A description is given of a transistorized system in which a pulse generator forms three successive pulses 112 to 117 el. deg. in width during an a.c. cycle. These pulses are then distributed by the "logical" part of the system to the grids of the converter. The system consists of a relaxation generator, a pulse forming device and a distributer.

Relays

An impedance relay with a pre-magnetized choke coil. A.F. Berezovskii, (pp. 28-33).

The author describes his patented device for "controlling" the total impedance of transmission lines. The Author's certificate (patent) was granted in December 1958. The relay makes use of chokes with weakly pre-magnetized cores. The chokes are connected in parallel with an electromechanical relay. The advantage of the system is that fewer contacts and relays are required. The device is used when an exact measurement of total impedance is not required and when voltmeter blocking or voltage cut-off with current blocking is not satisfactory.

Rotating machines

Starting an induction motor from a synchronous generator of similar capacity. Ia.B. Kadymov, (pp. 56-61).

The assumption of a constant speed of the prime mover is discarded. The starting of an induction motor from a synchronous generator of similar output is analysed on the supposition that the electromagneto moment produced by the transient currents averages out to zero. Use is then made of expressions for the steady state.

Calculating the mechanical characteristics of an induction motor in a closed regulation system for a dissymmetry in in the stator circuit. M.M. Sokolov and others, (pp. 66-72).

A graphical-analytical method is proposed for calculating the mechanical characteristics of induction motors in closed and open

systems of control, e.g. in hoist-conveyance equipment, when the supply of the stator circuit is asymmetrical. The parameters of the elements of the system to define the static mechanical characteristics of the motor can also be found.

Special steel

The screening of trunk communication lines - a new application for grain oriented 3% silicon steels. Ia.S. Shvartsbart, (pp. 84-87).

Details are given of a special heat treatment and a method of reducing the carbon content to 0.005% which has made it possible to produce a highly ductile cold-rolled 3% silicon steel with a high magnetic permeability (over 4×10^3 G/oested in a field of 1.0 oest). This steel has been developed for protecting communication lines from induced currents along electrical railway lines and for screening railway cables.

Traction motors

A method of calculating the continuous rating and efficiency of electrical traction machines for diesel engine and gas turbine locomotives. N.A. Boldov, (pp. 62-66).

A study is made of the criteria for the efficiency of traction motors for diesel and gas-turbine locomotives. A simple method of estimating the sustained standard output of traction motors and d.c. generators is given.

Transmission lines.

The surge protection of transmission lines today. N.N. Beliakov and others, (pp. 33-41).

The author studies the measures which can be taken for the lightnin protection of transmission lines of 110 to 500 kV. The new State regulations (PUE) on this matter are described.

A coreless toroidal reactor for power systems. L.V. Leites, (pp. 76-82).

Owing to the shortcomings of high voltage power reactors and

current-limiting reactors for long distance transmissions lines of 220 V and above, the author studies the design of a coreless toroidal current-limiting reactor and analyses the relationships between dimensions, weight, and losses. The proposed design will save about 4.5 times tonnes of copper on a 12.9 MVA reactor and reduce losses by 35 kW.

THE APPLICATION OF COMPUTER TECHNIQUES IN POWER SYSTEM OPERATION AND DESIGN*

I.M. MARKOVICH, V.A. TAFT, S.A. SOVALOV,
V.A. VENIKOV and L.V. TSUKERNIK

(Received 16 August 1960)

The use of computer techniques and particularly digital machines to solve the problems connected with the operation and design of power systems is still in its initial stage. It is of very great importance from the national economic point of view that these techniques are used in the operation of power systems and to establish the correct ways of developing them. It is therefore expedient to study the most important problems and the scope for computer techniques.

Problems in the operation of power systems

These can be divided into three groups, namely, (1) operational calculations, (2) the formulation of daily plans, and (3) the formulation of long term plans.

The first group of problems is mainly concerned with the operational distribution of the real and reactive (wattless) power flow, the choice of system, the regulation of the voltage, determination of the margin of reserve, and the distribution of this power reserve on the basis of actual information about the total load and the state of the equipment etc. The second type of problem deals with similar matters except that the initial data are forecasts of total loads and planned repairs etc.

Suppose we list these problems in order of complexity:

(a) calculation of the daily distribution of the real loads between

* *Elektrichestvo*, 12, 9-15, 1960.

fuel-fired power stations, given the state of the equipment, and taking the network losses into account;

(b) calculation of the daily distribution of the real load between fuel-fired and hydro-electric power stations, given the state of the equipment, the rate of water flow and network losses, but ignoring changes in the head of water at hydro-electric stations;

(c) the same as in (b), but with changes in the head of water at hydro-electric stations taken into account, as well as the interaction between these factors when operating in tandem.

(d) calculation of the optimum daily margin of real power using a defined reliability coefficient.

(e) calculation of the optimum daily distribution of the margin of real power, i.e. calculation of the optimum use of the units at the fuel-fired and hydro-electric power stations, but neglecting transient processes in such equipment;

(g) calculation of the daily distribution of the reactive loads, or of the daily chart for the optimum voltages in the network with the optimum tapping of the transformers taken into account;

(h) calculation of the complex daily distribution of the real and reactive loads, or of the real loads and voltages in the networks, provided that the conditions stated in items (a) to (e) are satisfied.

The problems listed under (a), (b), (c) and (g) can be solved by computers using either analogue or digital techniques. The problems listed under (d), (e), (f) and (h) require high speed electronic digital computers using programme control or special digital-type machines. The computing devices used for solving these problems may also be a part of control computers.

The most important problems in the third group (long term plans) are:

(a) estimation of the economic distribution of power generation between fuel-fired power stations (with network losses taken into account) for monthly and annual plans;

(b) Estimation of the economic distribution of power generation between hydro-electric and fuel-fired power stations for monthly and annual plans;

(c) Calculation of the optimum long term distribution of the water flow at hydro-electric stations, e.g. for each month over six months;

(d) The same as (c) over a month, for each week separately,

(e) The same as (c) and (d) over a week, for each day separately.

The formulation of such long term plans requires the use of high speed electronic digital computers, or special digital type machines.

In combined power systems, all the enumerated problems should be solved with the transmission capacity of the links with other systems taken into account, or else the output should be distributed between the systems separately with the links taken into account.

One of the important problems connected with the use of computer techniques in power systems is the development of control machines which automatically regulate the conditions of the power system (automatic dispatchers), or the conditions of individual parts of such systems (e.g. boiler-turbine units, inter-system communication lines etc).

Bearing in mind the complexity of power supply systems, the need to obtain a continuous inflow of information about the numerous characteristics of thermal, hydraulic, mechanical and electrical processes, and the need of numerous devices to exercise control, we cannot afford to underestimate the practical difficulties involved in the solution of these problems. New "pickups" and servo-mechanisms have to be designed. These must be reliable and quite exact. These same requirements must also be satisfied by the devices necessary for converting continuous into discrete quantities and vice versa if digital techniques are used. The same also applies to the telemetering and remote-control devices if an "automatic dispatcher" is used, and to the computing equipment itself.

The development of computer-type control machines for power systems, or indeed any other object of comparable complexity and importance, must be divided into the following phases:

I. Study of the production technology, development of the mathematical apparatus for producing analogues and programming the work of the computers, the compilation of standard programmes, and the accumulation of experience in the performance of these calculations on computers.

II. The creation of semi-automatic control systems with a continuous inflow of data and a trial period of service to test these devices under real conditions.

III. The creation of an economically and technically closed system in the light of the computing devices available in phases I and II.

We must warn the reader against that abstraction of the problem in

which the automatic control of combined power systems is considered without regard to economics, operating reliability or the necessary phases of development, e.g. Bruk's paper [2], which has already attracted criticism [1].

At this stage we should pay our main attention to the automation of large fuel-fired power stations, and boiler-turbine-generator units in particular. This is being done, for example, by the Kharkov power station in collaboration with the Central research institute for complex automation [3,4] and the Kharkov polytechnical institute.

In Kharkov they have estimated that a central control panel with a computer for a 150 MW boiler-turbine unit saves about three million rubles per annum in capital outlay; roughly the same saving is made in running costs by automatically ensuring operation under conditions that are practically optimum. The Kharkov power system is now finishing a trial control arrangement for a 50 MW boiler-turbine unit.

1960

A control computer for a 300 MW unit is now being developed in the U.S.S.R.

The use of computer techniques for solving operating problems will enable radical changes to be made in measuring, control and costing systems at power stations and substations. The conventional indicators and recorders will be replaced by digital measuring devices, i.e. pick-ups which are not only capable of digital reading of the various physical phenonomena, but which also feed the data automatically into a computer which records, makes a primary statistical analysis, and if necessary uses the results for automatic control purposes.

A good example is the computer at the fuel-fired power station in Louisiana (U.S.A.). This digital computer takes a continuous record of 100 items and replaces all the registering devices at the station. The computer "covers" 250 control points at a rate of five per sec and automatically controls the temperature. It is planned to produce a machine to "cover" 300 points per second.

Problems in the planned development of power systems

Here the problem is to find the optimum arrangement of the network and generating capacity. In view of the complexity of this problem we can in some cases divide it into two separate problems, namely,

1. Determination of the optimum generating capacity (i.e. the timing

and siting of the new units to cover the load and the necessary safety margin) and the design of the units. We ignore expenditure on transmission and distribution. The optimum generating capacity is calculated from the cost of this generating capacity. The periods of time over which the investment is to be spread is taken into account.

2. Determination of the optimum network corresponding to the selected system of generation, i.e. determination, on the basis, minimum estimated outlay, of the carrying capacity, type and completion date of the lines and substations to transmit and distribute the power generated by the new units.

Alternative versions of problems 1 and 2 are then compared and that version which requires the minimum total estimated outlay on generating plant and network is then selected.

Instead of providing new generating units, we sometimes have to consider linking the system to a grid with optimum carrying capacity and increasing the carrying capacity of the grid up to its optimum value in the new conditions, since the demand for new generating capacity can thereby be reduced by the "inter-system effect".

The problems in order of complexity are:

1. Determination of the periods of time over which new real power will be supplied to cover the developing load on the power system, given the reduction in the reliability factor.

2. Determination of total financial outlay (i.e. the annular expenditure and the defined proportion of capital outlay on the various methods of installing the new generating capacity) and selection of the optimum scheme.

3. Determination of the periods of time over which the new network equipment will be supplied in the development of the load;

4. Determination of total estimated outlay on the various alternative schemes with network losses taken into account. Selection of the optimum scheme;

5. Determination of the periods of time over which the new reactive power flows will be supplied to cover the developing loads on the power system, given the minimum voltage level of the optimum schemes for the network and generator plant;

6. Determination of the total estimated outlay on the alternative means of introducing the reactive power flows and selection of the optimum scheme.

High speed electronic digital computers are required to solve all these problems.

But there are also other problems which concern, for example, the determination of the regions in which it is expedient to use particular voltages of particular types of current etc. These problems often entail a very large number of laborious technical and economic calculations. It also appears that computers are essential here.

Computer techniques should be particularly effective in a planned economy. However, in the socialist system, the calculations involved in the long term planning of the power supply have to satisfy more stringent requirements than is the case in the capitalist system. This is connected with the need to maximize the efficiency of the economy as a whole and the need to consider the relationships between the main branches of the economy. No definite criteria have as yet been fully worked out which satisfy these requirements and permit and development of a practical method of technical-economic calculation on the basis of modern computer techniques.

The application of computer techniques also implies that the initial data satisfy certain special requirements. In long term planning the initial data should be based on the large scale treatment of statistical material and other kinds of general and specific information. Here we can distinguish a separate problem concerning the definition of the required type of information, its sources and the methods of transmitting and processing it before feeding it into the computer.

It is urgently necessary to study methods of calculation for the long term planning of the electricity supply and to work out criteria of optimum schemes in connexion with the plans being elaborated for the development of the economy in the next twenty years.

The main types of mathematical problem and the scope for the various types of computer

We can divide the problems connected with the calculations involved in power system operation and design into three groups, namely, (1) those connected with dynamic processes (electromagnetic and electromechanical), (2) those connected with selection of optimum conditions, and (3) those connected with determining the effects of fault conditions.

The first group of problems involves the solution or investigation of sets of differential equations (usually non-linear) or algebraic equations, i.e. for the calculation of

1. stationary conditions (current-distribution of output etc);

2. electromagnetic transient processes (surges, transient short circuit currents etc);

3. the stability of parallel operation and the electromechanical transient processes connected with changes in the position of the generator;

4. the electromechanical transient processes in power systems with the action of the automatic control system taken into account (frequency regulation etc).

The second group of problems requires the comparison of alternative arrangements and the determination of the maxima or minima of functions with many variables which are inter-connected by definite relationships. In particular, this includes load distribution between generating units and between fuel-fired- and hydro-electric stations with network losses, the characteristics of the equipment, transient processes etc all taken into account.

The third group of problems can be mathematically formulated on the basis of "logical" algebra. The solution of these problems requires the use of relay-contact or digital techniques. This group includes the operational problems arising in determining the action of the service personnel under different fault conditions and elucidating the consequences of the various courses of action. It is well known that a control panel capable of solving such logical problems was installed at the Kashir hydro-electric station in the early 1930's.

Combinations of these three types of problem can also occur, for example, selection of the optimum form of a dynamic process.

Either analogue or digital computers can be used with success for the first group of problems which involve the solution or investigation of sets of differential equations; some of these investigations, more particularly with the new type of elements, can be made by dynamic (physical) simulation. Many such power problems, though involving large numbers of equations, do not need a mathematically exact solution. Use may also be made of a.c. network analysers to investigate many electromagnetic and electromechanical processes. Each of the stated methods has its own field of application and its own special features.

Thus, for example, dynamic simulators are very useful for obtaining those fundamental results which pre-determine the course of other more detailed quantitative investigations. If these are used there is no need to investigate the effects of simplifying the mathematical des-

criptions of phenomena or discarding parts of the physical phenomena which is unavoidable in mathematical analogues, but which has less effect on physical simulation, which directly reflects the nature of the phenomena under consideration. Dynamic simulators make it possible to carry out complicated tests with equipment actually used in practice. This is their advantage. But if dynamic simulators are used to investigate complex systems, difficulties arise in the creation of large "models" and the substitution of a simple (equivalent) system for the system being investigated. Dynamic simulators are therefore best used for studying fundamental problems which can be elucidated in comparatively simply networks.

Under certain conditions use may be made of a.c. and d.c. network analysers to investigate quite complicated systems. A.c. network analysers can be used for steady state and for transient conditions. Transients are investigated by numerical integration.

Problems that can be made linear may successfully be solved by frequency methods. The field of application of a.c. network analysers can be extended by the recent improvement in their design (automation and the addition of amplifiers and various converters etc). But if a more careful analysis of the processes is required, fewer assumptions can be made in the description of dynamic processes in power systems and it is then necessary to change over to digital computers.

Dynamic equations are solved on digital computers by means of a programme devized in a certain way (e.g. the "Runge-Kutt" method, the "Adams-Shtermer" method). In principle, digital computers allow investigation of processes of any degree of complexity but the more complex the problem, the longer it takes to prepare it and the more difficult it is to devize the programme and check the results. Further investigation must be made to find out whether it is advisable to use digital computers for such calculations, whether it is feasible to combine elements of digital techniques with network analyser and analogue techniques, and what are the advantages and disadvantages of digital techniques compared with network analysers.

Analogue computers can be used to investigate and solve sets of dynamic equations also.

The second group of problems can be solved by digital or analogue computers. These problems are usually solved by trial and error. Digital computers are superior in this respect in that they are more exact and flexible and can be applied to a wider range of problems. The determination of optima can in principle be carried out on analogue computers, but the result may not always be accurate enough to solve

technical-economic problems. Accuracy is particularly necessary in finding the optimum conditions of a power system which will only increase total efficiency by 1 to 2 per cent.

The question of network losses arises in determining optimum conditions. In order to find the coefficients of distribution necessary for calculating network losses, use may be made of digital computers or network analysers. But the latter do not provide sufficient accuracy. There has therefore been a tendency to solve these problems on digital computers. This applies all the more to complex investigations involving all three types of problem.

In spite of the improvements in digital techniques, the greater number of digital computers, their improved performance (larger storage capacity, higher operating speeds, reliability), and the greater number of standard programmes that have been devized, the field of application of digital computers and other means of computation in the last analysis depends on economic expediency, i.e. the comparative cost of solving these problems in terms of manpower and real resources.

But digital computers do have a number of advantages over other means of computation. In the first place, digital computers are not only capable of solving individual problems, but with the appropriate programme they can also make intermediate calculations and draw logical deductions like a planning engineer. Improvements in the design of computers and in programming technique will make it possible to solve even more complex problems. As more programmes are accumulated, so digital computers will be used for a still wider range of problems.

This indicates the need for a collective effort to widen the scope of digital computers in power supply problems.

The third group of problems ("logical" algebra), has not yet been developed. In the early stages use may be made of relay-contact techniques to solve these problems. But digital techniques will probably be applied in due course.

Summarizing the foregoing remarks, we can draw the following conclusions:

1. Digital computers will soon be extensively used for complex and more particularly for non-operational calculations in large combined power systems, pwer systems consisting of fuel-fired and hydro-electric power stations and to solve logical problems.

2. Special computing devices using analogue and digital techniques will be used extensively for operational calculations and as controlling

machines.

3. D.c. and a.c. network analysers will still be used for the same purposes, i.e. mainly for calculating stability, short circuit currents, current distribution in normal and fault conditions etc.

4. Dynamic simulators will still be just as important for fundamental investigations, analysing the qualitative aspect of conditions, investigating stability and "piloting" control devices, especially the new makes.

5. Analogue computers will also still be used for the same purposes. They will chiefly be used for investigating transient processes, dynamic regulations and stability in simple networks.

Different types of computing device may in the future be combined to solve a number of problems.

1960

Conclusion

Certain recommendations can already be made on the basis of accumulated experience of computing techniques in power system operation and design.

Large power research organizations, higher educational establishments, planning institutes and combined dispatcher control centres must have their own computer departments. These computer departments should be equipped with modern high speed electronic digital computers now in batch production, electronic analogue computers, and modern a.c. and d.c. network analysers. Calculations for which special types of computer are required can be sent to these large computer departments in the research organizations. There should be continued and increasing callaboration between the research organizations which have electrodynamic analogues of power systems at their disposal, and organizations which directly operate power systems, and can undertake tests in real conditions. The most effective approach is a flexible one in which different computer techniques are used for different kinds of tests. Calculations which have to be very exact, e.g. those connected with losses in complex networks with many nodal points and closed circuits, or those undertaken to find the most economic load distribution in systems with fuel-fired and hydro-electric power stations with losses in complex networks taken into account, and those connected with long term planning (if there are many alternative arrangements and quite adequate technical and economic criteria) are all problems in which digital computers have doubtful advantages. However, owing to their wide range

of application and their ability to carry out complex logical programmes automatically, digital computers can produce more effective results than network analysers and analogue computers, particularly if standard programmes are available to solve the respective problems.

It is not advisable to replace all other types of computer by digital computers, as sometimes advocated in the published literature. In this respect, the experience of the French power system is quite convincing [6]. Reference should also be made to the satisfactory results achieved in the U.S.S.R. by the joint use of digital and analogue computers [7], and the joint use of a.c. network analysers and analogue computers [8].

Bearing in mind the great cost of electronic general purpose digital computers and their complexity, we do not suppose that the dispatcher control points of small and medium regional power systems will have these computers for some years. They will have to rely on network analysers and analogue computers.

The recent discussion [9] of the long term prospects for the use of electrodynamic power system analogues has shown that the use of physical simulation is not only far from being excluded by the development of computing techniques, but on the contrary, is acquiring still greater importance. In certain cases, physical simulation makes it possible to imitate actual experiments (especially in the development of new automatic devices). It aids the elucidation and precise statement of mathematical descriptions and, consequently, the efficient use of computing techniques.

The application of computing techniques to automatic control depends on rapid completion of the research going on into the design of trial control equipment for large units at fuel-fired power stations and the changeover to the production of this equipment in industry.

Heavy demands have to be made on the electrical industry to produce digital-type measuring apparatus and pickups for the physical characteristics of the conditions of thermal-mechanical equipment which are required to feed the information into computers automatically in digital and analogue form. The most serious attention needs to be paid to attempts to determine directly the value of the relative increment in fuel consumption (or its marginal cost) at fuel-fired power stations. The solution of this problem will bring us considerably nearer to the actually optimum load distribution in power systems that can be found by computers. In this connexion it is again pertinent to stress the importance of correct initial data in the use of computers. The problem is not only to obtain the necessary amount of information and to speed

up the process of obtaining it and processing it, but also to ensure that this information accurately reflects the variety of possible changes in conditions.

The widely held opinion that the application of computers will bring a reduction in staff and simplify the operation and design of power systems etc is not therefore generally speaking correct. In a number of cases the increase in national income from optimalizing operating conditions and real investment, and improving the reliability of the power supply obtained as a result of using computers will outweigh the cost of employing more personnel and will fully justify the greater complexity involved in operation and design, both of which will be raised to a higher technical level.

Organizations engaged on the application of computing techniques to the solution of power system problems and, particularly, computer centres, should calculate typical problems and formulate the results in such a form that after extensive discussion they can be used to build up a library of typical operating programmes.

Regional power authorities, or their commercial organizations, should initiate or expand the existing punch card systems for preparing subscribers' accounts, mechanizing the accounting system and preparing routine statistical returns.

• • •

This paper does not touch upon the more long term prospects of computing techniques, or the development of power systems on the basis of cybernetic control.

Further development should lead to the design of extremal and self-adjusting control devices which will find the optimum conditions in steady state and in transient processes. The discovery of the minimum necessary information for automatic super high speed calculation of conditions and processes and the means of optimalizing them are topics which are already within the field of vision of research engineers, who should have in view the even more distant prospects of cybernetics in electrical systems.

Naturally, neither cybernetics, nor any other form of automation should be an end in itself. Its development and introduction has to be justified by technical-economic analysis which reveals the real gain in national income.

Translated by O. Blunn

REFERENCES

1. E.D. Zeilidzon; *Elektrichestvo*, No.1, (1959).
2. I.S. Bruk; *Elektrichestvo*, No.12, (1957).
3. B.Ia. Nechaev; *A control computer for boiler-turbine units, (Upravliaiushchaia vychislitel'naia mashina dlia bloka kotelturbina). Sborn. dokl. na Nauchno-tekh coveshchanii po primenenii vychislitel'noi tekhniki pri proektirovanii i ekspluatatskii energosistem*, No.III. Kiev, (1960).
4. M.A. Due' l'; *The use of a control computer with the 67-2SP type straight-flow boiler and VK-50 type turbogenerator unit, (Avtomatizatsiia bloka priamotochnyi kotel 67-2SP - turbogenerator VK-50 s primeneniem upravliaiushchei vychislitel'noi mashiny)*. Reference as in 3.
5. D.T. Taylor; *ISA Journal*, No.10, (1958).
6. V.A. Venikov; *Elektrichestvo*, No.1, (1959).
7. V.M. Kagan and E.L. Urman; *Selection of the differential equations of transient processes in synchronous machines to calculate dynamic stability, (K voprosu o vybore differentsial'nykh uravnenii perekhodnykh protsessov sinkhronnoi mashiny dlia reschetov dinamicheskoi ustoichivosti). Trud. nauchno-issled. inst. elektroprom., 4*, (1959).
8. Ia.N. Luginskii and M.G. Portnoi; *The use of mathematical analogues for the investigation of transient electromechanical processes in electrical systems, (Primenenie matematicheskikh modelei dlia issledovaniia elektromekhanicheskikh perekhodnykh protessov v elektricheskikh sistemakh)*. Trud. VNIIE, IX, (1959).
9. Discussion of I.S. Bruk's article; *Elektrichestvo*, 2, 4, 5, 7, 9 and 10 (1958) and No.1 (1959).

A STUDY OF RADIO INTERFERENCE FROM CORONA ON TRANSMISSION LINES*

K. Ia. KAFIEVA

(Moscow)

(Received 11 March 1960)

1960

An intensive study has been made of radio interference from corona on transmission lines in pursuance of the decisions of the XXI congress of the C.P.S.U. concerning the electrification of our country and the opening of new 330-500 kV transmission lines and the conversion of existing lines to higher voltages.

The Electro-energy Institute (VNIIE) has accordingly studied the radio interference of transmission lines with aerial radio receivers, and the carrier interference (i.e. that propagated along the wires of transmission lines) which interferes with the performance of high frequency carrier communication channels. This paper contains the results of these investigations at the VNIIE into interference from corona on the wires of transmission lines in the U.S.S.R.

Standards for the level of maximum interference and measuring apparatus

The starting point for estimating the maximum level of interference is the signal to noise ratio at the output of the receiver. The quality of reception is very good if the signal is 40 db greater than the level of interference (a hundred times greater in voltage), and satisfactory if it is 26 db higher (twenty times greater in voltage).

The standards for radio interference from industrial plant, published

* *Elektrichestvo*, 12, 28-34, 1960.

by the State Inspectorate of Electrocommunications of the Ministry of Communications U.S.S.R. [1] provide for a zone 50 m. wide on both sides of transmission lines in which it is not recommended to set up radio receiver aerials. Outside this zone satisfactory reception is ensured if the level of interference does not exceed 100 μ V for frequencies of 0.15 to 0.5 Mc/s, 50 for 0.5 to 2.5 Mc/s, 20 for 2.5 to 20 Mc/s and 50 for frequencies up to 400 Mc/s. In estimating the carrier interference of transmission lines, we were guided by the standard for telephone channels, according to which the useful signal should exceed the interference by at least 3 nep, or 26 db, i.e. by a factor of 20 as regards voltage.

Radio interference from lines in the frequency range 0.15 to 150 Mc/s is usually measured by IP-12-2 M or IP-14-type resonant aerial devices which record the quasi-peak values [2]. Interference in the 30 to 300 kc/s range is measured by IUU-LEP-type selective level-indicators which are connected to the feeder of the communication channel under investigation along the line and show the average interference in the 2 kc/s band. It has been our practice in the overwhelming majority of cases to take measurements by the same apparatus, or different sets of the same type of apparatus, after careful and repeated adjustment.

The study of radio and high frequency interference from corona

Under normal operating conditions there is usually no undue interference from 35, 110, 220 and 400 kV lines. Nevertheless, we have studied the effect on interference of a number of factors, particularly atmospheric conditions and design features of the lines. The measurements are given in Table 1. We shall briefly consider the effect of various factors in the light of these figures.

Precipitations. Rain and sleet have roughly the same effect on interference. At the beginning of the precipitation there is a gradual increase in the level of radio interference by a factor of 3 to 20 and of carrier interference by 0.5 to 1.5 nep (on 110 and 220 kV lines). When the surface of the conductor is thoroughly wet there is a slight variation in the level of interference. When the precipitation stops, the level of interference falls and owing to the removal of dust and foreign matter the level of interference may be below that normal in fine weather. There is sometimes a reduction in interference on 35 kV lines during rain. On some lines we detected irregularities in the coupling components and insulators and these factors mainly defined the level of interference in such cases the spark gaps were covered with

TABLE

Levels of radio and

No. of line	Rated voltage kV	Type of conductor	Diameter of conductor, mm	Length of line km	Attitude above sea level, m	Type of region	Operating voltage, kV
1	110	MG-70	9.6	28.1	40	Rural	115
2	110	MG-70	10.6	21.2	372	Industrial	109
3	110	MG-70	10.6	18.8	40	Rural	115
3	110	MG-70	10.6	18.8	40	"	114.5
4	110	MG-70	10.6	47.5	6	"	109
5	110	AS-120	15.3	56	50	"	112
5	110	AS-120	15.3	56	50	"	121
6	110	AS-120	15.3	27	6	"	109
7	110	AS-150	17.0	28	1,300	Industrial	110
8	110	AS-150	17.0	28	1,300	"	110
9	110	AS-150	17.0	40	1,500	Rural	110
9	110	AS-150	17.0	40	1,800	"	110
10	110	AS-150	17.0	59.2	21,000	"	112
11	110	AS-150	17.0	66	1,800	"	118
12	110	AS-150	17.0	66	2,300	"	110
13	110	AS-185	19.1	21.8	372	Industrial	112
14	220	AS-300	24.4	250	50	Rural	231
14	220	AS-300	24.4	117	50	"	246
14	220	AS-300	24.4	250	50	"	246
15	220	AS-300	25.2	275.3	23.7	"	230
15	220	ASO-300	25.2	275.3	23.7	"	246
15	220	MP-240	30r0	275.3	15	Industrial	230
16	220	AS-341	28.0	278.2	23.7	Rural	230
16	220	AS-341	28.0	278.2	23.7	"	230
16	220	AS-341	28.0	278.2	23.7	"	230
17	220	ASO-480	30.2	234.4	23.7	"	230
17	220	ASO-480	30.2	234.4	23.7	"	230
17	220	ASO-480	30/2	234.4	23.7	Industrial	220
18	400	3xASO-330	3x25.2	80	180	"	354
18	400	3xASO-330	3x25.2	80	180	"	417
19	400	3xASO-480	3x30.2	125	180	"	405
19	400	3xASO-480	3x30.2	125	180	"	422
19	400	3xASO-480	3x30.2	125	180	"	410
19	400	3xASO-480	3x30.2	126	180	"	421

1960

1

carrier interference*

Weather	Air temperature	Relative air density	Theoretical gradient of middle phase kV/cm(amplitude value)	Radio interference at 50m from the line at 1 Mc/s, μV	Average high frequency interference in 2kc/s frequency band, nep
Cloudless	19.0	1.02	21.5	6	-5.0
"	26.0	0.95	20.4	10	-4.0
"	21.2	1.03	21.5	12	-4.5
"	19.0	1.02	21.4	8	-4.5
Slight rain	20.0	1.01	20.5	Not measured	-5.0
Cloudless	22.6	1.0	19.2	5	-5.5
Dull	0.5	1.08	20.8	20	-4.3
Slight rain	20.0	1.01	17.5	1	-6.5
Cloudless	20.0	0.86	17.6	Not measured	-3.5
"	20.0	0.86	17.6	20	-3.5
Bright periods	15.0	0.64	17.6	Not measured	-4.5
Dull	12.0	0.84	17.6	25	-4.0
Bright	12.0	0.70	17.8	10	-4.0
Rain	10.0	0.83	17.4	15	-4.0
Stormy	14.0	0.80	14.9	20	Not measured
Bright	25.0	0.95	12.9	2	" "
"	26.9	0.97	24.9	60	-3.5
"	24.5	0.98	26.5	60	-3.0
Dull	-1.8	1.08	26.5	10	Not measured
"	21.0	0.99	23.9	10	" "
Bright	18.0	1.0	25.9	15	-3.43
"	22.4	0.99	19.2	30	Not measured
Bright	21.1	0.99	22.2	20	" "
Bright	22.0	1.0	22.2	Not measured	-3
"	18.0	0.99	22.2	5	Not measured
Dull	24.0	0.998	20.6	10	-3.1
"	22.0	1.0	20.6	5	-3.2
Bright	26.0	0.95	19.7	2	-3.5
Dull	-7.0	1.1	20.0	10	-3.5
"	-7.0	1.1	23.6	15	-3.5
Bright	-15.0	1.14	19.7	12	-3.8
Snow	-10.0	1.11	20.8	22	-3.5
Bright	-12.0	1.01	20.0	15	-3.5
Sleet	-0.5	1.04	20.5	20	-3.4

moisture and discharges were suppressed.

There was a far more marked variation in interference levels during snow and hail. The use of a split phase (on 400 kV LEP lines) greatly reduced the effect of precipitations on the level of interference.

Relative humidity of the air. Radio interference voltage increases by a factor of 1.5 to 2 on 110 kV lines in coastal districts for an increase in air humidity from 52 to 71 per cent.

Air density. A number of lines were studied in mountainous regions 1300 to 2300 m. above sea level.

At potential gradients of 15 to 17 kV/cm on the surface of the conductors*, the interference is comparable with that on lines operating at gradients of 20 to 22 kV/cm, but at 50 m above sea level. Measurements on 220 kV lines shows that in wintertime during dry weather the level of radio and carrier interference was below that in bright weather during the Summer. This is undoubtedly due to the increase in air density in winter.

The article [3] by Bartenstein and others gives a straightforward relationship between the level of interference and air density. It is well known that corona voltage is proportional to air density. If the initial corona voltage is changed 1 kV, the level of radio interference increases by approximately 0.125 db. Consequently, a 20 per cent change in air density should entail an 0.2 x 240 x 0.125 = 6 db change in the level of radio interference on 220 kV lines with an initial corona voltage of 240 kV. Our observations agreed with this figure quite well.

The state of conductor surfaces. This factor has been repeatedly studied in foreign investigations [4]. Its effect has also been confirmed by our measurements on 220 kV lines (Table 1, No.17) using ASO-480 type conductors 30.2 mm in diameter. At the same voltages, the interference was greater from this line than from other lines in the system (Table 1, Nos. 15 and 16) using AS-341 type conductors 28.0 mm in diameter. The explanation is that the No.17 line had only been in use for 5-6 months, whereas the other two (Nos.15 and 16) had been in use for much longer periods and had undergone the process of "ageing".

Design of the line. The most important point is the diameter of the wires. At the same maximum gradients,** interference is lower from

---

* The amplitude value of the potential gradient on the middle phase appears throughout.

** The potential gradient of non-split conductors was found by the formula

$$E_{max} = \frac{80{,}65 \cdot I_c}{r_0} \text{ (kV/cm)},$$ where I_c is the capacitive current of the wire and r_0 its radius (cm).

split conductors and, moreover, these are more stable under variable atmospheric conditions.

If earthing cables are used or the line is suspended at a lower height, the field of interference beneath the line is amplified, but it is weakened more rapidly as you go away from the line.

Measurements on 110 kV lines showed that the level of radio interference from vertically-suspended two-circuit lines is roughly 1.2 times greater than that from horizontally-suspended single circuit lines. The level of radio interference from horizontally-suspended two-circuit lines is roughly 1.5 times greater than that of single circuit lines. The level of carrier interference is hardly affected by a second circuit or the arrangement of the phase conductors.

The practicability of converting lines to higher voltages. This investigation was carried out in stages. In the first stage we used an experimental line section and in 1958-1959 we did the tests on 110, 220 and 400 kV lines.

Lines 110 kV. We studied corona interference on two mountain lines 1500 to 2300 *m* above sea level and on coastal lines of 140-145 kV in regions of high air humidity (Table 2, Nos.6, 9 and 11).

We drew the conclusion from these measurements that there is a large margin of radio and carrier interference on 110 kV lines equipped with AS-120 and AS-150 type conductors under normal conditions. The conversion of these lines to 140 kV will have no notable effect on radio reception or the performance of communication channels.

Lines 220 kV. In August and December 1958 we tested line No.14, and in May 1959 lines Nos. 15, 16 and 17 (Table 2). Line No. 14 produced maximum radio interference under normal conditions (220-230 kV) in bright weather in summer (Fig.1). At voltages of the order of 246 kV (gradient 26.5 kV/cm) radio interference was in excess of maximum by a factor of 1.5 to 2. At 316 kV (gradient 34.1 kV/cm) interference at a distance of 50 *m* from the wire at a frequency of 1 Mc/s exceeded maximum 12 times over. At higher voltages the rate of increase in radio interference is slower, and during general corona (voltage 350 kV, gradient 37.8 kV/cm) a slight drop occurs in the curves for radio interference (Fig. 2).

There is a fairly regular increase in carrier interference with increasing voltage from 175 to 350 kV (Fig.3), reaching maximum at approximately 270 kV. In winter during dry weather the level of interference is slightly less than in summer at voltages up to 310 kV owing to higher air density (radio frequency is approximately 1.5 times less,

TABLE

Radio and carrier interference on

No. of line	Rated voltage, kV	Type of conductor	Line voltage, kV	Weather
6	110	AS-120	140	Rain
9(altitude 1,500 m)	110	AS-150	145	Storm, Hail
9(altitude 1,800 m)	110	AS-150	145	Storms
11(altitude 1,800 m)	110	AS-150	145	Rain
11(altitude 2,300 m)	110	AS-150	145	Storms
14	220	AS-300	246	Bright
14	220	AS-300	290	"
14	220	AS-300	316	"
14	220	AS-300	290	Rain
14	220	AS-300	300	Dull
14	220	AS-300	330	"
14	220	AS-300	350	"
15	220	ASU-300	230	"
15	220	ASU-300	246	Bright
15	220	ASU-300	280	"
15	220	ASU-300	295	"
15	220	ASU-300	304	Bright periods
15	220	ASU-300	333	Bright
15	220	MP-240	230	"
15	220	MP-240	280	"
15	220	MP-240	295	"
15	220	MP-240	333	"
16	220	AS-341	230	Dull
16	220	AS-341	230	Bright
16	220	AS-341	230	"
16	220	AS-341	270	Dull
16	220	AS-341	297	"
16	220	AS-341	325	"
17	220	ASO-480	230	"
17	220	ASO-480	230	Bright periods
17	220	ASO-480	300	"
17	220	ASO-480	327	"
18	400	3xASO-330	435	Dull
18	400	3xASO-330	444	"
18	400	3xASO-330	378	Sleet
18	400	3xASO-330	453	"
18	400	3xASO-330	480	"

1960

2
lines operating under extra-high voltages

Air temperature °C	Relative air density	Theoretical gradient of middle phase kV/cm (amplitude value)	Radio interference 50 m from line at a frequency of 1 Mc/s, μV	Mean h.f. interference in 2 k/cs band, nep
23.0	1.0	22.5	10	-4.3
15.0	0.86	23.2	350-700	-4.0
12.0	0.84	23.2	17-70	-3.5
10.0	0.80	21.3	18	-3.2
14.0	0.80	19.6	50	Not measured
24.5	0.98	26.5	80	-3.2
24.5	0.98	31.2	120	-1.8
24.5	0.98	31.1	600	-1.5
2.1	1.06	31.2	180	-1.8
0.5	1.076	32.4	150	-1.5
0.5	1.077	35.6	300	-0.8
0.6	1.077	37.8	300	-0.76
21.0	0.99	23.9	10	Not measured
18.0	1.0	26.9	15	-3.43
18.0	1.0	29.4	20	-2.2
22.0	0.99	31.0	40	-1.5
18.0	0.97	31.9	65	Not measured
18.0	0.98	31.7	120	-1.0
22.4	0.99	19.2	30	Not measured
22.4	0.98	24.2	35	" "
22.4	0.98	25.5	40	" "
22.4	0.98	28.5	120	" "
21.0	0.99	22.2	20	" "
22.0	1.0	22.2	–	-3.4
18.0	0.98	22.2	5	Not measured
21.0	0.99	24.3	15	-2.6
21.0	0.99	28.8	25	-1.5
21.0	0.99	31.35	60	-0.8
24.0	0.99	20.6	10	Not measured
22.0	1.0	20.6	5	-3.2
22.9	1.0	26.8	50	-1.2
22.0	1.0	29.2	150	-0.5
-7.0	1.1	24.6	30	-3.25
-7.0	1.1	25.1	70	-2.5
-1.0	1.07	21.4	25	-2.5
-1.0	1.07	25.6	50	-1.7
-1.0	1.07	27.6	70	-1.5

carrier interference 0.2 to 0.5 nep less). The levels of interference are higher in rainy weather during winter than in Summer at voltages up to 300 kV (radio interference 2 to 3 times greater, carrier interference 1 to 1.5 nep greater).

It was noticed that the difference between interference levels caused by the weather decreases with increasing line voltage, becoming insignificant in the region of general corona (Figs. 2 and 3).

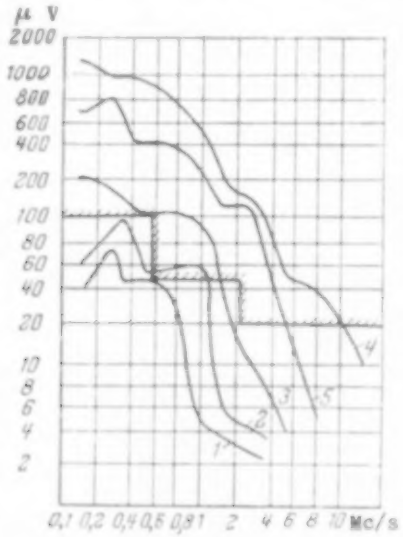

Fig. 1. Frequency characteristics of radio interference at different voltages 50 m away from a 220 kV line (line No. 14 in Table 2, fine weather).
1 – voltage of 175 kV; 2 – 231 kV; 3 – 246 kV;
4 – 316 kV; 5 – 350 kV.

The radio interference on line No.16 (330 kV) is roughly twice the standard level. Carrier interference affects normal performance of communication channels even at 297 kV (-1.5 nep).

The supply end of line No.15 had been fitted with an ASU-300 type conductor 25.2 mm in diameter but the rest with an MP-240 conductor 30 mm in diameter. Measurements taken on the thinner supply end showed that radio interference begins to become excessive at voltages of 300 kV, and carrier interference at 290 kV. Carrier interference was not measured on the other part of the line. Radio interference was roughly doubled at voltages up to 290 kV and was practically the same as that at the supply end in the region of general corona. At the same gradients (up to 30 kV/cm) the rise is 2 to 6 times greater.

1960

Apparently, this difference is due to the contamination of the surface of the thicker MP-240 conductor since the section of the line with this type of conductor passed through an industrial region with a considerably polluted atmosphere.

Line No. 17 (ASO-480 conductor, 30.2 mm in diameter) created excessive radio and carrier interference even at voltages of roughly 270 kV. At gradients of 31 kV/cm radio interference was approximately double the permitted value; the level of carrier interference reached - 0.8 nep, which makes it difficult to use the channels. Such a high level of interference on lines with comparatively large diameters can be explained by the ageing of the line.

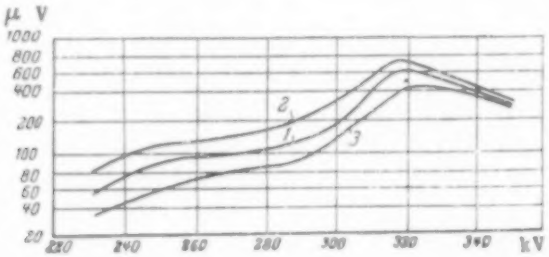

Fig. 2. Radio interference as a function of line voltage (line No. 14 in Table 2, 220 kV).
1 - Bright weather; 2 - rain; 3 - dull without precipitations.

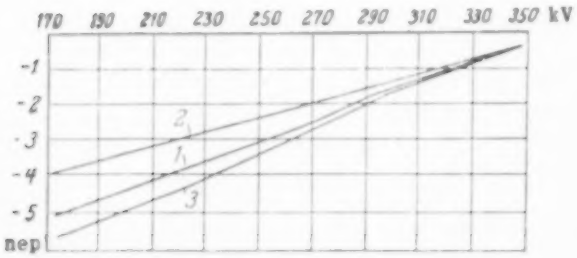

Fig. 3. Carrier interference as a function of line voltage (line No.14 in Table 2, 220 kV).
1 - Bright weather; 2 - rain; 3 - dull without precipitation.

From tests on 220 kV lines with AS-300, ASU-300, AS-341, MP-240 and ASO-480 type conductors we can conclude that:

1. The levels of radio and carrier interference from corona on lines with non-split conductors are in the maximum range at gradients of 26 kV/cm or less. Conductors not less than 33 mm in diameter (ASO-580) should therefore be used for future 330 kV lines.

2. At gradients over 26 kV/cm, communication channels must be provided with large output amplifiers and nearby radio receivers with extensible aerials on converting existing 220 kV lines to 330 kV.

3. Radio interference rapidly diminishes with frequency as you go further away from the line. If the line passes through sparsely populated areas, operation can be allowed at gradients up to 28 kV/cm without taking special anti-interference measures (if prior approval of the State Inspectorate of Electro-communications is obtained).

Lines 400 kV. In March 1959 we measured the interference from a 400 kV line 80 km in length with a three-wire split phase (ASO - 332 type 25.2 mm in diameter) at voltages up to 550 kV and in single phase conditions. The voltage was supplied on one phase, but the measurements give an idea of the line's performance under three phase conditions at the respective voltages (up to 480 kV).

In dry weather radio interference is within the permissible limits at gradients up to 26 kV/cm, but exceeds the maximum values roughly by a factor of 1.2 to 1.5 at higher gradients up to 27 kV/cm.

It was established that radio interference diminishes more quickly as you go away from the line in damp weather, and the increase in interference directly underneath the wires has little effect on levels measured 50 m away.

In dry weather carrier interference on a 100 Ω feeder was roughly -2.5 nep on average at voltages of about 450 kV. At 488 kV in sleet conditions carrier interference reached -1.5 nep. It is therefore possible that radio and carrier interference will be excessive on lines such as those investigated if converted to 50 (sic). But the majority of 400 kV lines in the U.S.S.R. are fitted with 3 x ASO-480 type conductors and there is therefore good reason to suppose that these can be converted to 500 kV (gradient 24.5 kV/cm) without resorting to special measures.

Other investigations

Frequency characteristics. The characteristics of the interference field in the range of interest to us (0.16 to 150 Mc/s) have an almost

horizontal section on long and medium wavelengths (up to 1.5 Mc/s) and a sloping section at frequencies over 1.5 Mc/s. At frequencies over 10 to 20 Mc/s, the radio interference of even the most "noisy" lines (if the insulators and coupling components are in good order) is seldom excessive, and it is frequently enough to measure the middle part of the range, which is much simpler. In the first approximation we can regard the interference voltage as inversely proportional to the frequency at frequencies over 1.5 Mc/s.

Our study of carrier interference at frequencies of 30 to 300 kc/s has shown that the frequency characteristic of the interference in this range is roughly parallel to the X-axis in the absence of extraneous signals.

The reduction in interference away from the line. The intensity of the field of radio interference diminishes as you move away from the line. Elsewhere [4,5] it has been shown that at distances up to 100 *m* along a perpendicular from the projection of the extreme conductor to the ground, the weakening of the field is governed by the law

$$u = u_0 \frac{H^2}{H^2+d^2}, \tag{1}$$

where u_0 is the interference voltage under the extreme conductor, H the height of the conductor in metres, and d the distance from the projection of the extreme conductor in metres.

We do not however think that radio interference is so markedly dependent on distance. According to our investigations, in bright weather this relationship is

$$u = u_0 \left(\frac{H^2}{H^2+d^2}\right)^{0.7}. \tag{2}$$

Fig.4 shows radio interference voltage as a function of distance from the line as calculated by formula (2) and as found experimentally. These curves confirm the opinion of many authors that radio interference voltage diminishes more quickly with distance during precipitations than in dry weather.

The inter-relationship between radio and carrier interference. This relationship is of considerable interest since there is as yet no means of calculating one type of interference from the other. Radio and carrier interference has been measured in various frequency bands. At this stage of the investigations there is no point in comparing other values than those in the 0.16-0.3 Mc/s band, which are common to both

types of measurement. From many measurements on an experimental section, in which attenuation of the signal in the test apparatus was taken into account [3], it can be said that the ratio of carrier to radio interference is 50 under the conductor and 350 to 450 at a distance of 50 m. for a conductor 13 m. high. According to formula 2, this ratio at 50 m. from the line is 350 for a conductor 13 m. high and 400 for one 12 m. high.

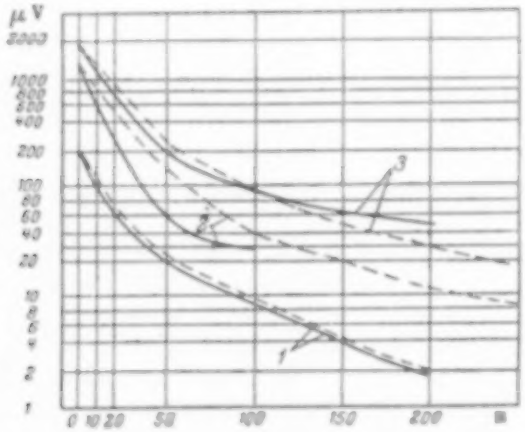

Fig. 4. Radio interference voltage as a function of distance from the extreme phase of the line. Theoretical values (broken lines) and measured values. Height of conductor 12 m, frequency f = = 1.5 Mc/s (line No. 14 in Table 2). 1 – line voltage 231 kV (gradient 2.49 kV/cm), bright weather in summer; 2 – 290 kV (gradient 31.2 kV/cm), rain in winter; 3 – 350 kV (gradient 37.8 kV/cm) dull, winter.

Carrier frequency and polarity of the voltage. Fig. 5 shows the test circuit for studying carrier interference as a function of the polarity of the voltage at power frequency. The cathode-ray oscilloscope simultaneously receives a small voltage of 50 c/s, which roughly coincides in phase with the line voltage, and the interference voltage from the carrier feeder in a narrow frequency band (in our case in the 130 ± 2.5 kc/s band of a filter at the output of the feeder).

Fig. 6 shows the curves on the screen of an oscilloscope for the different conditions of the experimental section and a real 220 kV line. It can be seen that slight interference appears on both half-waves of

voltage of 50 c/s at gradients of the order of 20 kV/cm. At gradients over 25 kV/cm there are distinct flashes of interference near the maxima of the positive half-wave: interference on the negative half-wave is practically constant and can be ignored. The other two weaker flashes on the oscillograms of the real line are the effect of adjacent phases (the flashes are shifted 120° relative to each other).

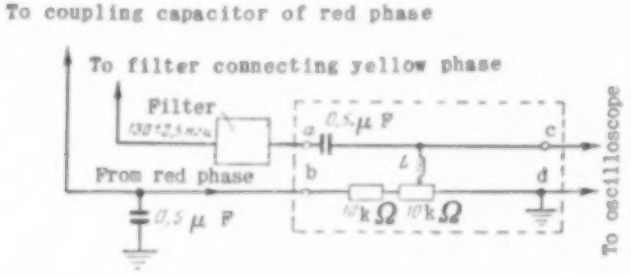

Fig. 5. Test circuit for investigating the relationship between carrier interference and voltage polarity on an experimental line (voltage of power frequency is only supplied to the yellow phase and is taken from the red phase by a divider consisting of inter-phase capacitances, a coupling capacitor and a capacitance of 0.5μF).

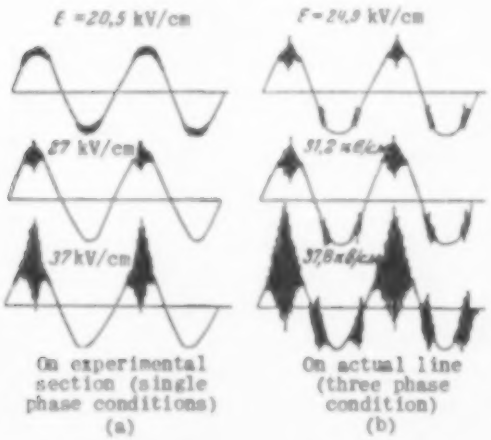

Fig. 6. Carrier frequency as obtained on oscilloscope screen.
a – experimental section, single phase conditions;
b – actual line, three phase conditions.

The results of our investigation do not allow us to agree with the the opinion of Chevallier [6] that interference on transmission lines is in the nature of "white noise" and that pulse interference only appears during precipitations. According to our observations, interference from corona on lines is of the "smooth" type with a continuous frequency spectrum and it differs from white noise in being distributed irregularly in time and pulsating cyclically with voltage at 50 c/s [2]. The flashes at the maxima of positive polarity are connected with the potential gradient on the line conductors (of the order of 24 kV/cm). On lines with much lower theoretical potential gradients, this value may increase during precipitation owing to the formation of numerous small "projections" on the conductor, e.g. drops of water.

Translated by O. Blunn

1960

REFERENCES

1. *Standards for maximum industrial radio interference, (Normy predel'no dopustimykh industrial'nykh radiopomekh).* Sviaz'dat, Moscow, (1956).
2. M.A. Fatoskii and I.M. Furmanov; *Apparatus for measuring industrial radio interference, (Tipovye pribory dlia izmereniia industrial'nykh radiopomekh).* Sudpromgiz, (1959).
3. R. Bartenstein and Meyer J. de Stadelhofen; CIGRE, Report No. 408, (1958).
4. K.Ia. Kafieva; *Radio interference from corona on transmission lines. Review of foreign literature, (Radiopomekhi ot korony na liniiakh elektroperedachi, obzor zarubezhnykh materialov.*
5. Ia.L. Vykhovskii; *Carrier interference on an experimental section of a 400 kV line, (Issledovanie vysokochastotnykh pomekh na opytnom uchastke linii 400 kv).* Trud. TsNIEL, No. 1, Gosenergoizdat, (1953).
6. A. Chevallier; CIGRE, No. 341, (1958).
7. Ia.L. Rykhovskii; *Telephone communications along high voltage transmission lines, (Telefonnaia sviaz' po provodam linnii vysokogo napriazheniia).* Gosenergoizdat, (1953).

THE EFFECT OF TRANSIENT STARTING CURRENTS IN INDUCTION MOTORS ON THE STARTING LOSSES*

A. T. GOLOVAN and IIUI-IAN'

(Moscow Power Institute)

(Received 4 July 1960)

The following formula is usually used to calculate the losses in the windings of induction motors due to operating currents:

$$\Delta A_0 = A_{k0}\left(1 + \frac{r_1}{r_{2r}} B_r\right), \tag{1}$$

where $\Delta_{k0} = 9{,}81 \frac{J\omega_0^2}{2}$ is the kinetic energy of the moving parts at synchronous speed;

J the total moment of inertia of the moving parts referred to the rotor of the motor;

ω_0 the synchronous speed of the motor;

r_1 the resistance of the stator phase;

r_{2r} the resistance of the rotor at rated load referred to the stator;

B_r a coefficient of the reduction in losses in the stator winding due to skin effect in the rotor slots.

For motors with circular slots in which the skin effect is weak, $B_r = 1$. For motors with deep slots in which the skin effect is more

---

* *Elektrichestvo*, 12, 58-61, 1960.

marked, $B_r < 1$. This coefficient depends on the depth of the rotor slots, the type of material used for the rotor cage and other factors.

Fig. 1 shows the effective resistance of the rotor as a function of slip on the basis of Field's formula [1] in respect of AO-type motors. Fig. 2 shows B_r as a function of P_r for AO-type motors (rotor slots 17.5 to 35 mm deep).

To check the validity of the formula, we made appropriate tests on squirrel-cage motors of the A062-6 and A042-6 types.

The currents and power input of the motor on starting was recorded on an oscillograph. There was good agreement between the stator losses as defined by the current and output oscillograms.

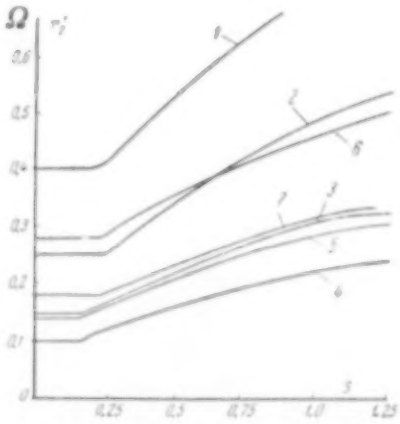

Fig. 1. The effective resistance of the rotor as a function of slip.
1 – for A062-6 type motors; 2 – A063-6; 3 – A092-6; 4 – A073-6; 5 – A082-6; 6 – A062-4; 7 – A063-4.

The following Table shows the calculated and experimentally-determined starting time and starting losses in the stator winding of an A062-6 type motor during no load starting ($GD^2 = 0.6$ kg.m^2). The experimental losses are an average figure taken from several oscillograms.

This Table shows that the discrepancy between calculated and experimentally-determined losses and starting times is quite large.

	Starting time, sec	Stator losses on starting kW.sec
Experimental	0.196	1.37
Theoretical	0.12	0.885
Error, %	-63.4	-54.8

Since actual starting times and losses are greater than the calculated figures on no load starting, this indicates the existence of an additional restraining moment during starting. This torque apparently must be a function of time since it has relatively less effect if starting time is increased. This can be deduced from the tests which showed that the error in starting time decreases as the moment of intertia increases.

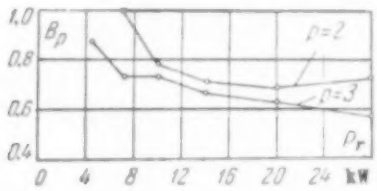

Fig. 2. B_r as a function of P_r for AO-type motors.

Test results also indicate that the discrepancies between calculated and actual starting time and losses are roughly of the same magnitude. It can therefore be supposed that an increase in losses due to the effect of free (transient) currents is a consequence of the increased starting time which they cause. In point of fact, the free currents have very little effect on total starting current.

Thus, we can assume that changes in losses due to the effect of free currents are proportional to changes in starting time. Actual losses can therefore be found from the following relation:

$$\Delta A_{o.a} = \Delta A_{o.t}\, k_t; \tag{2}$$

$$k_t = \frac{t_{o.a}}{t_{o.t}}, \tag{3}$$

where $\Delta A_{0.a}$ are the actual power losses in the transient process, and

$\Delta A_{0.t}$ the calculated power losses in the transient process neglecting the free currents;

$t_{0.a}$ the actual time of the transient process;

$t_{0.t}$ the calculated time of the transient process as calculated from the static characteristic.

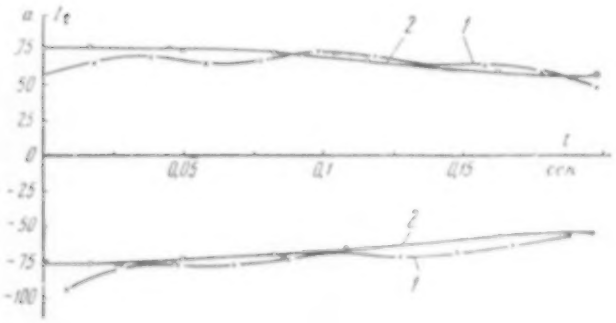

Fig. 3. Envelopes of starting currents.
1 – experimental; 2 – calculated (free currents ignored).

It is easy to check the validity of this relationship by substituting the calculated and actual losses and corresponding starting times from the Table. The error is only –4.85 per cent for starting.

It is well known that the torque developed by a motor on starting can be represented as the sum of six components [2]. The first is the torque defined by the static mechanical characteristic which is dependent on slip. The second, third, fifth and sixth components are variable in sign and vary with fading amplitude. These components, now accelerating the process, and now retarding it, on average only create a small torque and therefore have little effect on the duration of the starting process. The fourth component, which is continuous (aperiodic), exerts a restraining effect.

We can therefore calculate the losses and starting time from this particular restraining moment, which can be found from the formula:

$$M_s = kI_2' I_\mu' \sin(\varphi_\mu' - \varphi_2') e^{2\alpha_1 t}, \qquad (4)$$

1960

where $$k = \frac{C_M}{k_\Phi} \frac{1}{4,44 k_0 f_1 w_1} x_\mu,$$

C_M is the coefficient of proportionality between the torque and the product of the secondary current times the fundamental "flux";

x_μ the magnetic reactance corresponding to the state of the motor;

k_Φ a correction for the saturation of the magnetic circuit;

I'_2 a component of the free current of the rotor with the smallest damping factor;

I'_μ the free component of the magnetizing current;

ϕ'_μ the angle between the vectors of the voltage and current I'_μ;

ϕ'_2 the angle between the vectors of the voltage and current I'_2.

The factors in 4 are as follows:

(See page 618)

where T_1 and T_2 are the time constants of the stator and rotor windings;

M the mutual inductance of the windings;

L_1 and L_2 the leakage inductance of stator and rotor windings;

α_1 and β_1 the real and imaginary parts respectively of one of the roots of the characteristic equation*;

ω_r the angular speed of the rotor;

σ a leakage factor.

To avail ourselves of expressions (5), (6) and (7), we need to know the relationship between speed and time and the instantaneous values of the motor's characteristics. This is an extremely complicated problem and to simplify it we make the following assumptions;

1. The motor is stationary during the effect of the continuous component of the torque (M_4);

---

* The characteristic equation of an induction motor is

$$s_r^2 + \left[\left(\frac{1}{T_1} + \frac{1}{T_2}\right) - j\omega_r\sigma\right] p + \left(\frac{1}{T_1 T_2} - j\frac{\omega_r}{T_1}\right) = 0.$$

$$I_2' I_\mu' = \frac{U^2 M (p_1 - j\omega_r)\left[M(p_1 - j\omega_r) - \left(\frac{1}{T_2} + p_1 - j\omega_r\right) L_2\right]}{(p_1 - j\omega_0)^2 \left(2p_1 a + \frac{1}{T_1} + \frac{1}{T_2} - j\omega_r a\right)(L_1 L_2)^2}; \tag{5}$$

$$\varphi_2 = \operatorname{arc\,tan} \frac{2a\alpha_1^2(\omega_r - \omega_0) - \alpha_1^2\left(\beta_1 - \frac{\omega_r}{2}\right) - (\beta_1 - \omega_0)(\beta_1 - \omega_r)\left(\beta_1 - \frac{\omega_r}{2}\right)}{2a\alpha_1^3 + 2a\alpha_1(\beta_1 - \omega_0)(\beta_1 - \omega_r) + 2(\beta_1 - \omega_r)\left(\beta_1 - \frac{\omega_r}{2}\right) - a\left(\beta_1 - \frac{\omega_r}{2}\right)(\beta_1 - \omega_0)}; \tag{6}$$

$$\varphi_\mu' = \operatorname{arc\,tan} \frac{\left[\alpha_1(2\beta_1 - \omega_r)a - (\beta_1 - \omega_0)\left(\frac{2}{T} - 2a\alpha_1\right)\right]\left[\frac{L}{T} - a_1(L+M)\right] - \left[2\alpha_1\left(\frac{1}{T} + \alpha_1 a\right) + (\beta_1 - \omega_0)(2\beta_1 - \omega_0)a\right][(L+M)(\beta_1 - \omega_0)]}{\left[2\alpha_1\left(\frac{1}{T} + \alpha_1 a\right) - (\beta_1 - \omega_0)(2\beta_1 - \omega_0)a\right]\left[\frac{L}{T} - a(L+M)\right] + \left[\alpha_1 a(2\beta_1 - \omega_r) - (\beta_1 \omega_0)\left(\frac{2}{T} - 2a\alpha_1\right)\right]}. \tag{7}$$

2. The motor windings are symmetrical ($r_1 = r_2 = r$ and $L_1 = L_2 = L$);

3. The mains frequency is much greater than the equivalent frequency of the free moment:

$$2\pi f_1 \gg \frac{1}{2T},$$

where $T = \frac{L}{r}$.

Formula 4 then takes the form

$$M_4 = -M_{max} e^{-\frac{t}{T}} \sin\theta, \tag{8}$$

where $M_{max} = k \frac{U^2 M^2 \left(1 + \frac{L}{M}\right)}{L^4 \omega_0^2 (2-\sigma)^2}$ is the maximum value of the moment M_4,

which solely depends on the characteristics and design of the motor in question, and

θ the difference between angles ϕ_2' and ϕ_μ'.

To simplify the calculation, we assume that

$$\sin\theta = \sin\frac{\pi}{\tau} t, \tag{9}$$

where τ is the time when $e^{-\frac{t}{T}} = 0.05$, i.e. when $\tau = 3T$.

Thus, we can estimate the restraining moment by the formula:

$$M_4 = -M_{max} e^{-\frac{t}{T}} \sin\frac{\pi}{\tau} t. \tag{10}$$

This simplification is quite permissible as can be seen by comparing the curves of exact formula (4) with those of the approximate formula (10) (Fig.4).

We can take the continuous restraining component of the torque during starting into account if we know its "impulse" a. The latter is defined as follows:

$$a = \int_0^{t_i} M_q dt, \tag{11}$$

where t_i is the period of time that component M_q is effective.

Real starting time can be found from the formula

$$t_{o.a} = \frac{J\omega_0 + a}{M_{e.t}}, \tag{12}$$

where $M_{e.t}$ is the calculated effective starting torque found from the static mechanical characteristic.

Since starting time equals $\frac{J\omega_0}{M_{e.t}}$ if we ignore the free moments, we can define k_t (which is the ratio of the actual starting time to that found from the static characteristic) as follows:

$$k_t = 1 + \frac{a}{J\omega_0}. \tag{13}$$

For practical estimates and calculations, it is useful to introduce the notion of a relative value α for the impulse of the continuous moment and relate its value to the moment of the rotor's momentum at synchronous speed:

$$\alpha = \frac{a}{J_n\omega_0}. \tag{14}$$

This is a constant for the motor in question.

Fig. 5 shows α as a function of P_r for AO-type four- and six-pole machines. Knowing the value of α, it is easy to find k_t for any moment of inertia J referred to the motor shaft.

Fig. 5 also shows k_t and the average torque $\frac{M_{c4}}{M_r}$ caused by the continuous component of the current as a function of P_r. It is apparent that the equivalent average torque $\frac{M_{c4}}{M_r}$ has less effect on starting time, the greater the flywheel mass of the system. With increasing flywheel torque, there is a corresponding decrease in the

difference between the effective moments with or without the free currents taken into account.

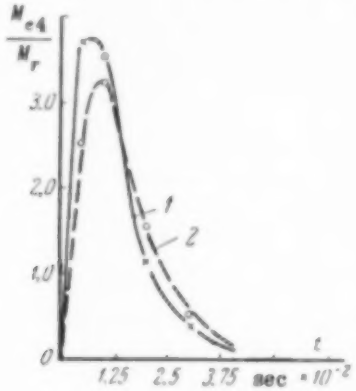

Fig. 4. The "continuous" restraining component as a function of time.
1 – calculated by formula 4; 2 – calculated by formula 10.

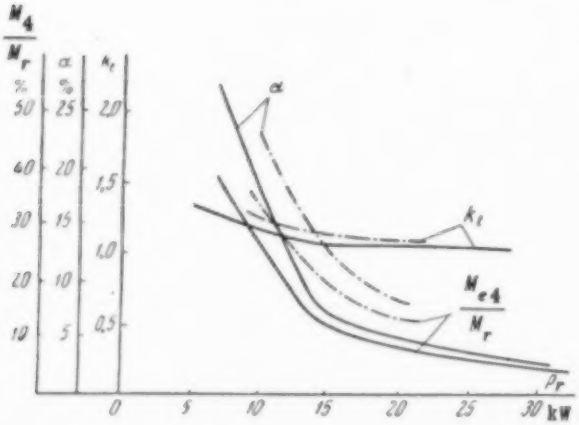

Fig. 5. Coefficients α, k_t and the relative "continuous" restraining component $\frac{M_{e4}}{M_r}$ as a function of motor power.
——— – $r = 3$; –.–.–.– – $r = 2$.

Coefficient k_t decreases with increasing flywheel torque.

Conclusions

1. The continuous (aperiodic) restraining moment has greatest effect on the starting time and losses of small motors.

2. The effective starting moment with free currents taken into account tends to be the same as that without the free currents taken into account as the power of the motor is increased.

3. The coefficient k_f tends to unity as the power of the motor is increased. Assuming a permissible error of 0.05, we can ignore these processes in motors of 30 kW or more.

4. The time constant T is small in motors where there is considerable slip. The continuous (aperiodic) restraining component M_4 is quickly damped and it has little effect on transient conditions.

The effect of free currents on time and losses in braking by counter-current can also be studied in a similar way.

Translated by O. Blunn

1960

REFERENCES

1. P. Rikhter; *Electrical machines, (Elektricheskie mashiny)*, (1939).
2. N.A. Sazonov; *Elektrichestvo*, No. 12, (1949).

THE COMMUTATION OF WIDE-RANGE VARIABLE-SPEED MACHINES*

I.Z. AGEEV

(Moscow)

(Received 29 July 1960)

It is a difficult matter to arrange good commutation in d.c. machines with a large range of speeds $\left(\frac{n_{max}}{n_{min}} \geqslant 3\right)$ (particularly heavy duty machines) for not only does the load and speed vary, but also the saturation of the magnetic system and the distortion of the main field.

Moreover, in special-purpose machines, e.g. aircraft generators, the air gap is made as small as possible and the relatively large load is linearized, in order to save space and weight and for this reason the resulting field under the leading edge of the pole is negative at maximum speed, i.e. it changes sign under the pole and not between the poles. The physical neutral is shifted 60 to 65 electrical degrees relative to the geometric neutral in generators without compoles, and 70 to 80 electrical degrees in generators with compoles.

The commutation of machines without compoles

Under the foregoing conditions it is impossible to shift the brushes to improve commutation. In this case the brushes are set at the geometric neutral and the magnitude of the reactive e.m.f. is determined not only by the leakage fields ($B_p + B_l$), but also by the external field of the interpole space (in this case the armature field)

---

* *Elektrichestvo*, 12, 61-69, 1960.

$$e_{ra} = 2wlv(B_p + B_b + B_q)10^{-8} = \\ = 2wlv(\lambda A + B_q)10^{-8}, \tag{1}$$

where λ is the equivalent specific conductance, which also takes the effect of mutual inductance between the sections in the same slot into account.

Since the armature field increases abruptly as it approaches the edge of the pole, the average value of B_q in the zone of commutation of heavy duty machines ought to take the difference in width between the inter-pole space b_{ips} and the commutation zone b_{cz} into account:

$$B_q = \frac{(0.5\tau - 0.25b_{ips})A}{0.8\delta_c}; \tag{2}$$

where

$$\delta_c = \sqrt{\left(\frac{b_{ips}}{2} - \frac{b_{cz}}{2}\right)^2 + (\delta')^2}; \tag{3}$$

A the linear load;

τ the pole pitch;

δ' the gap under the edge of the pole.

Thus, if the brushes are arranged at the geometric neutral, the commutation of machines without compoles, and the main factors appearing in formula 1, depend to a considerable extent on the size of the gap between the edges of the poles and boundaries of the commutation zone $\dfrac{\delta_n = b_{ips} - b_{cz}}{2}$.

If gap δ_n is small and linear load A large, the sections at the beginning and end of the period of commutation at maximum speed fall into a powerful (unfavourable) field, and the current there even increases (Figs. 1). The voltage drop under the leading edge of the brush is negative, but that under the trailing edge large.

A large additional current i_{add} appears in the sections at the beginning and end of the period of commutation (Fig. 1). The trailing edge of the brush is overloaded and the brushes begin to spark. Moreover, low frequency (1 to 2 c/s) variations of the current, the speed of the motor, the excitation current and the voltage of the generator

may arise in variable machines operating in a weakened field owing to the powerful effect of the m.m.f. of the commutating sections and unstable commutation. These variations are not as a rule smoothed out by the system of regulation and they are undesirable.

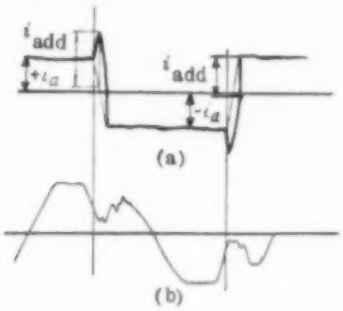

Fig. 1. Current variation in the section (a) and field (b) at maximum speed.

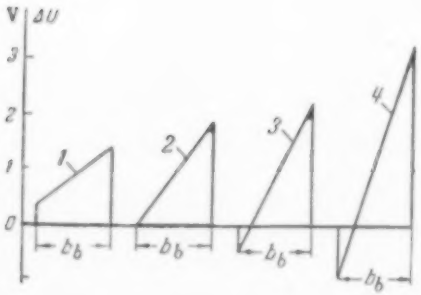

Fig. 2. Voltage drop in brush contact of a generator without compoles at various speeds: 1 – n = 3000 rev/min, degree of commutation k = 1¼; 2 – n = 4000 rev/min, k = 1½; 3 – n = 5000 rev/min, k = 2; n = 6000 rev/min, k = 3.

In order that the component of the reactive e.m.f. of the armature field B_q should not be significantly greater than the component of the "leakage" field λA, the gap δ_n should be quite large in machines without compoles with a large range of speeds:

$$\delta_n \geq 1 + 0{,}04\tau \ [\text{mm}]. \tag{4}$$

In machines with a narrow range of speeds, e.g. in converter motors, in which the field is not weakened more than 1.5 times, it is advisable to ensure a ratio $\frac{F_\delta}{0.5 b_p A} = 1$, where F_δ is the m.m.f. of the air gap and b_p the pole-arc. In this case the gap δ_n may be minimum (1 to 1.5 mm) and the brushes can be mounted at the physical neutral.

If the brushes are mounted at the physical neutral, the reactive e.m.f. is defined by the formula

$$e_r = 2wlv\lambda A 10^{-8}. \tag{5}$$

The m.m.f. of the commutating sections diminishes owing to the absence of the external field B_q from the commutation zone. For greater stability, it is also necessary that $\delta' \geqslant 2\delta$.

Operating experience has shown that the maximum reactive e.m.f. should be at most 1.3 to 1.5 V for EG-type brushes and 0.5 to 0.7 V for MGS-7 and MGS-8 type brushes to ensure that the degree of commutation k in high speed machines should equal 1.5 (owing to the great vibration and heating of the brushes).

Commutation of machines with compoles and a wide range of speeds

In these machines changes in the saturation of the main magnetic system and distortion of the main field make it difficult to compensate the "leakage" fields $B_p - B_l$ by the commutating field B_k over the entire range of speeds and loads.

The chief difficulties arise in adjusting the commutation to maximum speed when the difference $e_r - e_k$ becomes critical

$$e_r - e_k = 2wlv(\lambda A - B_k) 10^{-8}, \tag{6}$$

where e_k is the commutating e.m.f.

An increase in speed from v_{min} to v_{max} at U = const entails a corresponding decrease in the main field, and in heavy-duty machines running at maximum speed the armature field is so distorted that it affects the commutating field by reducing its width at the base (Fig. 3).

On the other hand, an increase in speed (with a decrease in saturation) entails a reduction in the m.m.f. which is expended on conducting

the flux Φ_d on the sections of the main system, which leads to an increase in the commutating field (Fig. 3), particularly in machines with half as many compoles as there are main poles [2]. Sparking as a rule only arises in these machines at minimum speed because the commutating field B_k is inadequate, but at maximum speed it can be a consequence of the commutating field B_k being too large or too small.

To oscillograph the field (Fig. 3), we put a small conductor at the bottom of the slot and its ends were taken out to two insulated rings. In this case the cathode-ray oscilloscope during commutation displays not only the true field of the main poles, but also the slot field B_p, which in machines with half the number of compoles is superimposed with the same sign on the field of the inter-pole space in one commutation zone, but with the opposite sign on the compole field in the other commutation zone.

Depending upon the type of slot field and its arrangement in the zone without the compole, and also upon the distortion of the compole field by the slot fields with the commutating sections, we can judge when and in what field the commutation begins and ends, and we can also judge the nature of the commutation (retarded, rectilinear, or accelerated).

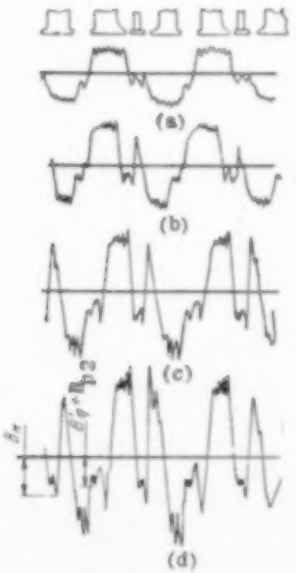

Fig. 3. The field of a 9 kW generator with 6 main poles and 3 compoles ($2p = 6.3$) at various speeds. a – n = 3600 rev/min; b – n = 4000 rev/min; c – n = 6000 rev/min; d – n = 9000 rev/min.

As can be seen from Fig. 3 at n equal to 3600 and 4000 rev/min the compole field B_k is reduced practically to zero by the slot field, whereas at n = 6000 rev/min and, especially at n = 9000 rev/min, the compole field is still sufficient to compensate the field of the second commutation zone ($B'_q + B_{p2}$) even after reduction by the slot field.

Consequently, the commutation of machines with half the number of compoles (if F_d = const) is relatively slower at minimum speed than at maximum and medium speeds.

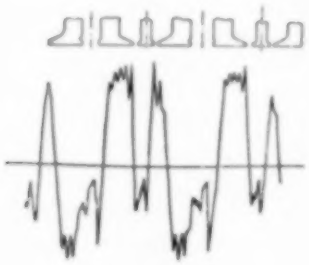

(a)

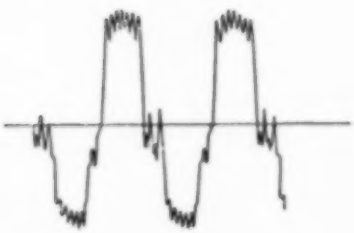

(b)

Fig. 4. The field of a 9 kW generator with $2p$ = 6/3 at maximum speed (n_{max} = 9000 rev/min). a – load 150%, U = 28.5 V, i_e = 2.5 A; b – load 100%, U = 90 V, i_e = 2.5 A.

On overload at maximum speed the increase in B_k is retarded in comparison with current I by the saturation of the compole, but with half the number of compoles the increase in B_k is also retarded by the saturation of the teeth and the greater difference $p'-p''$ between the displacement of the neutral zones of the armature field.

Moreover, an increase in the load as well as in the armature field

in the commutation field without the compole entails a decrease in the width of the resulting field B_k owing to the increase in B'_q, since $B'_k = B_k - B'_q$ [2]

Satisfactory commutation at maximum speed can therefore even be obtained in heavy duty generators with half the number of compoles, for which A = 350 to 400 A/cm at rated load, if there is a temporary 50 per cent overload, provided that the compoles are correctly designed over the width of the commutation zone ($b_d \approx b_k$) and slightly saturated ($B_{d.s}$ = 18,000 G).

It can be seen by comparing the oscillograms in Fig. 4 that the total saturation of the main system in machines with half the number of compoles has a considerably greater effect on the proportionality of B_k to I than does a change in the ampere-turns of the armature in consequence of an increase in the saturation of the teeth by the flux Φ_d on overload at maximum speed, which confirms that it is advisable to use machines with half the number of compoles in the stated conditions.

Thus, more powerful compoles are required if the magnetic system is saturated and the generator is operating at low speed under overload conditions, whilst at maximum speed under 30 and 100 per cent load, weaker compoles are required to ensure rectilinear commutation, i.e. to prevent magnetization by the commutating sections $F_{k.d}$. This is an even more complicated situation in that the zone of dark (sparkless) commutation is very narrow in heavy duty machines at maximum speed, which allows no considerable variation in the m.m.f. of the compole without impairing the commutation.

If the rate of current variation is high (at maximum speed), eddy currents affect the commutation and reduce the leakage field of the slots in the vicinity of the small conductor.

In this case the slot conductance is defined by the formula:

$$\lambda_s = \frac{h}{3h_s k_r} + \frac{h_0}{b_s} + \frac{h_k}{b_{sl}}, \qquad (7)$$

where h is the height of the conductors in the slot

h_0 the depth of the slot occupied by the wedge;

h_k the height of the "crown";

b_s and b_{sl} the width of the slot and "cut".

The conductance of the crowns and front parts is defined by the

usual formulae.

Bearing in mind that only a part of the conductance λ_s is reduced by the effect of the eddy currents and that $k_c \leq 1.15$ to reduce losses in the copper, changes in commutation due to the effect in question can be ignored. The value of k_c is defined by equation 283 in Arnold and La Cour's book [3].

The zone of sparkless commutation

The zone of sparkless commutation in machines with a large range of speeds is defined by the distance between the curves

$$+\frac{\Delta I_d}{I}\,\%=f(I) \text{ and } -\frac{\Delta I_d}{I}\,\%=f(I),$$

or between the curves

$$+\frac{\Delta I_d}{I}\,\%=f(n) \text{ and } -\frac{\Delta I_d}{I}\,\%=f(n).$$

Since sparking (for the given type of brush) arises at a given difference between the e.m.f.'s e_r-e_k, the zone of sparkless commutation defines the permissible variance between the compole field and the leakage field. The more exact the coincidence between the shape of the field B_c and that of the leakage field λA, the wider is the zone of sparkless commutation at a given speed.

The difference e_r-$e_k = 2wlv\,(\lambda A - B_c)\,10^{-8}$ is relatively small at low speeds on variable machines and the zone of sparkless commutation is of maximum width. Other things being equal, an increase in speed causes the difference e_r-e_k to attain the critical value more quickly and the zone of sparkless commutation is reduced.

Fig. 5 shows typical curves for the zones of sparkless commutation in machines operating at a wide range of speeds with the full number of compoles. In machines with half the number of compoles, owing to the considerable effect of the saturation of the main magnetic system on the flux Φ_d (which is magnified when the load is increased by the increase in the fundamental flux and the flux Φ_d), the upper boundary of the sparkless zone at low and medium speeds even moves further away from the X axis when the load is increased, and the sparkless zone is considerably wider than with the full number of compoles (Fig. 6). Thus, on a 9 kW generator with $2p = 6/3$ and $A = 340$ A/cm at 6000 rev/min and 100 per cent load, the width of sparkless commutation $b_{s.c} = 68$ per cent, whereas

$b_{s.c}$ = 10 per cent on 6 kW generator with 2p = 4/4 and A = 370 A/cm. At maximum speed the fundamental magnetic system is unsaturated and B_k varies approximately in proportion to F_d, i.e. the same as with the full number of compoles (if the compoles are not saturated). The difference is solely due to a change in the field in the zone without the compole.

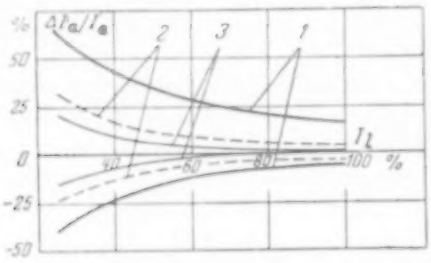

Fig. 5. Sparkless zones of commutation of a 6 kW generator with 2p = 4/4 at various speeds: 1 – n = 4000 rev/min; 2 – n = 6000 rev/min; 3 – n = 9000 rev/min.

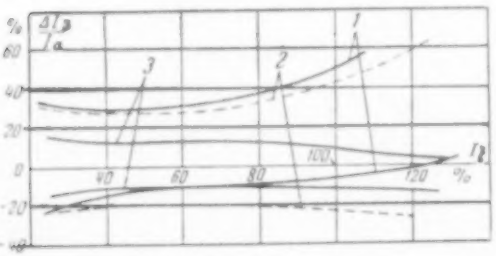

Fig. 6. Sparkless zones of commutation of a 9 kW generator with 2p = 6/3 at various speeds: 1 – n = 4000 rev/min; 2 – n = 6000 rev/min; 3 – n = 9000 rev/min.

We can find the approximate maximum difference $\Delta e = e_r - e_k$ with the full number of compoles from the supply current at no load.

If $I = 0$, then $e_r = 0$ and $e_k = \Delta e - 2wlv B_k 10^{-8}$, where

$B_k = \dfrac{I_s w_d}{0.8\, k_1 \delta_d}$, I_s the supply current and ω_d the number of turns in the compole windings and δ_d and k_1 the gap under the compole and the coefficient of the air gap respectively. This method is unsuitable for

half the number of compoles since the armature reaction and saturation of the fundamental magnetic system are neglected.

Adjustment of commutation

In heavy duty machines, and more particularly in machines with copper-graphite brushes, when the maximum difference $e_r - e_k$ should be no more than 0.6 to 0.7 V, the shape of the commutating field must be favourable (i.e. coincident with the slot field) when operating at maximum speed U_{max} = 55 to 70 m/sec. From this point of view, the winding has to be designed so that the slot field is rectangular in shape since this is the easiest to compensate. If the shape of the compole field B_k is significantly different from that of the leakage field $B_p + B_l$, there is generally speaking no zone of sparkless commutation at maximum speed. This may be the result of an incorrectly shaped tip of the compole, or the inexact positioning of the commutator relative to the slot in machines with a non-rotary traverse. This is illustrated by a 150 kW generator with 2_p = 8/8 and n = 6000 rev/min.

1960

Here a shift of 1.1 to 1.4 mm of the commutator in one machine relative to the position of the commutator in another machine produced a change in commutation from 1¼-1½ to 2-3 relative to that in the former machine.

Commutation was improved by shifting the tip of the compole in the direction of rotation, but the degree of commutation deteriorated with increasing voltage at the terminals (saturation of the fundamental magnetic system) and attained 2 at U = 120 V and I = 1400 A. The degree of commutation was therefore improved to 1¼ by reducing the gap δ_d by 0.2 mm with a steel shim.

It is more difficult to make the fields of machines with half the number of compoles coincide in shape because the compole not only compensates the slot leakage fields B_{p1} and B_{p2}, but also the field of the commutation zone without the compole ($B'_q = B_q + B_0$), the shape of which varies as a function of the load and speed [2].

In this case, if the compoles are not carefully adjusted, a machine which has a wide zone of sparkless commutation at medium speeds and otherwise good commutation at higher speeds under a 50 per cent overload, will still spark considerably at maximum speed under a 100 or 50 per cent load (owing to the excess field B_k) (see Table).

Commutation is a complicated process associated with thermal and chemical phenomena. The fundamental propositions (r_b = const and T =

$= \frac{b_b}{U}$) of the classical theory of commutation are only valid if commutation is practically rectilinear and the degree of sparking does not exceed 1¼-1½. If the degree of sparking reaches 2 on account of unfavourable conditions, an active ionic process is set up in the brush contact and, owing to a sudden reduction in the impedance of the "transfer" contact, sparking continues for a long period (if n = max) even if the load is reduced by a half or two thirds, (the supply of the compoles here having no significant effect).

In such a case it is necessary to begin commutation at a lower speed when the machine is in the cold state. First it is necessary to determine whether positive or negative supply has the better effect on commutation and then to verify the commutation at maximum speed by varying the gap under the compoles on the appropriate side.

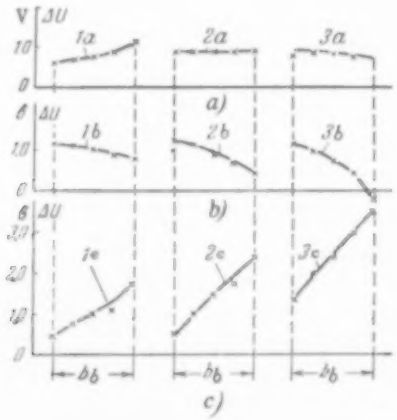

Fig. 7. Voltage drop in the brush contact of a 21 kW generator with $2p$ = 8/4 under rated load at various speeds:
a – no supply to compoles; b – supply to compoles (+0.25 I_d); c – the same, but (0.15 I_d);
1a to 1c – n = 3530 rev/min;
2a to 2c – n = 6000 rev/min; 3a to 3c – n = = 9000 rev/min.

We can establish the sparking due to the different types of commutation from potential diagrams (Fig. 7) and the time when brushes of different polarity begin to spark. With moderately retarded commutation, the first to commence sparking are brushes of negative

polarity as these have a transfer contact of lower impedance, but with notably accelerated commutation the first to spark are brushes of positive polarity, since in this case the current in the section at the end of commutation is much greater than i_a and on the trailing edge this current passes from the brush to the segment (plate) and not the other way.

It can be seen from Fig. 7 that the F_d of commutation varies considerably with changes in speed in machines with a wide range of speeds at a constant m.m.f.

With greatly accelerated commutation, the voltage drop under the trailing edge of the brush is opposite in sign, whilst at greatly retarded commutation, this drop is extremely large at n = 9000 rev/min (Fig.7, curves 3b and 3c).

Commutation of a 20 kW generator, $2p$ = 8/4

n, rev/min ..	4,000	6,000	8,200	9,000	9,300	9,300	δ_n = 0.85 mm
I, %	100	100	100	100	100	80	
Degree of commutation	1	1	1¼	1½–2	2	> 1½	
The same ..	1	1	1	1¼	1½	1	δ_n = 0.95

In adjusting commutation, the problem "boils down to" ensuring sufficient width of the sparkless zone and stability of the characteristics at maximum speed. To provide the sparkless zone and ensure that F_d is proportional to I, the magnetic system should not be saturated. The commutation of finished machines should first of all be improved by selecting the necessary shape of the pole extremity and varying the gaps δ_n and δ_d, since the magnitude and shape of the commutating field B_k are then both changed. An increase in the gap between the tips of the compoles and the main poles of either polarity reduces the effect of the main field on the compole field, but in machines with half the number of compoles there is also a reduction in the armature field in the second commutation zone and the shape of the resulting commutating field B_k is wider and more sloping. A small gap δ_n requires a large m.m.f. F_d.

It is usually sufficient for the gap in compole machines to be

$$\delta_r = \frac{b_r - b_s}{2} = (4-5)\delta_d \qquad (8)$$

If the gap δ_d is small, the field B_k is sharper (more acute), but if large, B_k is more sloping and stable. But an increase in δ_d will increase leakage and, consequently, the gap δ_d in machines with closely spaced poles is confined within small limits $[\delta_d \approx (1{,}1 - 1{,}4)\delta]$

With large compoles, in order to preserve the size of the gap δ_d, i.e. to avoid the increase in the leakage factor with larger δ_d use may be made of a diamagnetic spacer between the compole and the armature. The diamagnetic spacer increases the reluctance not only for the useful flux Φ_d, but also for the leakage flux of the compole and, consequently, the proportionality between Φ_d and I on the one hand and the stability of the commutating field on the other are both increased especially during overloads. But if the compoles have no large margin, the spacer can cause considerable distortion.

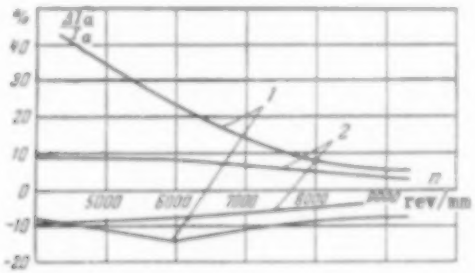

Fig. 8. The zone of sparkless commutation of a 21 kW generator:
1 - 2p = 8/4; 2 - 2p = 6/6.

It is relatively easier to produce favourable commutation over the whole range of speeds in machines with the full number of compoles given the electromagnetic load and reactive e.m.f. and provided the compoles are correctly designed.

But it should be borne in mind that the current density, A and ϵ_r are always 15 to 20 per cent greater in machines with the full number of compoles, given the weight and size of machine.

This is illustrated in Fig. 8 which shows curves for the zones of sparkless commutation in two 21 kW machines of equal size and weight, one of which has the full number of compoles and the other half the number. For machines with the full number of compoles the linear load A = 460 A/cm and the current density is 19.2 A/mm^2, whereas for machines with half the number of compoles A = 350 A/cm and the current density is 15.4 A/mm^2. The machine with the full number of compoles was not put

into production owing to the rise in temperature without any contingent advantage as regards commutation.

Practical experience in the design of special machines with a wide range of speeds has shown that machines with half as many compoles as there are main poles can be produced with a linear load A = 350 to 400 A/cm and a reactive e.m.f. $e_r \leqslant 3.5$ V.

The adjustment of commutation from oscillograms of the fields and current in the sections

In high speed multi-pole machines ($2p$ = 8 and 10, and n = 9000 to 9500 rev/min) the period of commutation is 0.00013 to 0.00015 sec. In this case it is convenient to adjust the commutation by oscillograms of the fields displayed on the screen of a cathode-ray oscillograph.

1960

With accelerated commutation the changes of the current in the sections and of the slot field mainly take place at the beginning of the process and, consequently, the compole field has a greater distorting effect on the slot field along the leading edge (Fig. 9 d-h), whereas with retarded commutation the effect is more marked on the trailing edge (Fig.9, i-l). In the first case, the first peak of the slot field is

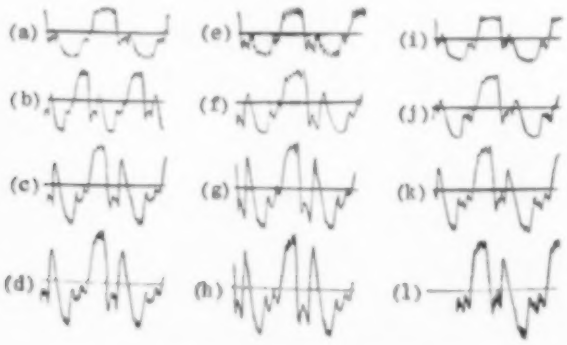

Fig. 9. The field of a 21 kW generator with $2p$ = = 8/4 under 100% load at various speeds:
a to d – no supply to compoles; e – $I_p = 0.35\ I_d$; f – $I_p = 0.22\ I_d$; g – $I_p = 0.12\ I_d$; h – I_p = = 0.085 I_d; i, j – $I_p = -0.14\ I_d$; k, l – $I_p = -0.11\ I_d$; a, e, i – n = 4300 rev/min; b, f, j – n = 6000 rev/min; c, k – n = 8200 rev/min; d, h, l – n = 9300 rev/min.

greater than the second, and in the second case, the first peak is smaller than the second (Fig. 9, e and Fig. 5 - 5c in Karasev's book [4]).

Tests on high speed machines with a large range of speeds have shown that the horizontal section (more exactly, the inflexion of the curve) is only pronounced at low speeds during relatively slow commutation, i.e. if e_k is too small (Fig. 10a).

With accelerated commutation, the variation in current is usually continuous and therefore the degree of equilibrium in the intermediate phase of commutation must be regarded as a negative factor, and not positive [5].

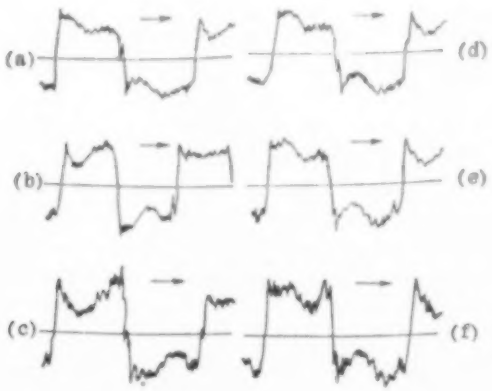

Fig. 10. The current in the section of a 9 kW generator with $2p = 6/3$ under 100% load at various speeds:
a – $n = 4000$ rev/min, $I_p = -0.23\ I_d$, $k = 1¼$;
b – $n = 6000$ rev/min, $I_p = -0.23\ I_d$, $k = 1$;
c – $n = 9000$ rev/min, $I_p = -0.1\ I_d$, $k = 1¼$;
d – 4000 rev/min, $k = 1$; e – $n = 6000$ rev/min $k = 1$; f – $n = 9000$ rev/min, $k = 1$. The arrow indicates the direction of the generator armature.

With accelerated commutation the actual period of commutation is less than the theoretical period. This can be seen by comparing the ratio $\frac{\delta_b}{\tau}$ in Fig. 10 with the theoretical value 8.4/62.8, but the oscillograms of the slot fields do not confirm this. With retarded commutation, the

period of commutation agrees with the theoretical value by the current oscillograms in Fig. 10(a) also.

The effect on commutation of brush heating and other factors

Commutation, especially its stability, depends not only on the magnitude and shape of the commutating field, but also on the "transfer" impedance of the brushes, mechanical factors and so forth. The oscillograms in Fig. 11 illustrate the variation in commutation due to heating. These show that the slot field varies as a function of temperature and that the peak is shifted from the trailing edge to the leading edge.

This phenomenon occurs at both maximum (9000 rev/min) and at minimum speed and it is quite regular.

1960

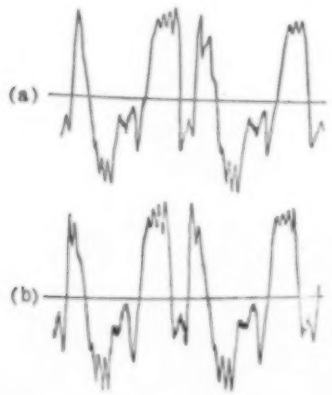

Fig. 11. The field of a 9 kW generator with $2p = 6/3$ under 100% load at $n = 9000$ rev/min. a – non-heated machine (2 to 3 min after starting); b – hot machine (30 min after starting).

It can be explained by the change in the transfer impedance of the brush contact due to heating and a slight displacement of the brush. In the cold state the coefficient of friction is larger and the brush is shifted in the direction of rotation by a toppling moment so that a better contact is obtained, a small impedance is obtained on the leading edge, and a larger impedance on the trailing edge.

The heating of MGS-type brushes results in a larger voltage drop ΔU_b, a smaller coefficient of friction and a different brush contact conductance. The change in commutation and the state of the magnetic system due to heating can de-stabilize the output characteristics of the machine so that a slow self-produced change in speed takes place in motors and in excitation current in generators (if U = const).

This phenomenon is particularly noticeable in machines operating with a weakened field, and it is amplified by the longtitudinal reaction of the armature. With greatly retarded commutation, there is a greater variation in the current of motors without compoles if the brushes are shifted in the direction of rotation by the longtitudinal reaction of the armature and the deterioration in commutation. The same phenomenon occurs with accelerated commutation in machines with compoles, but the brushes are shifted in the opposite direction to rotation. In such cases it is expedient to increase the rated value of r_b and improve the stability of the brush contact (e.g. by using sectional brushes).

Conclusions

1. For variable speed machines without compoles it is expedient to mount the brushes at the geometric neutral to avoid commutation in an unfavourable field.

2. The zone of sparkless commutation at minimum and medium speeds is considerably wider in machines with half the number of compoles than with the full number of compoles, owing to the great effect of saturation of the main magnetic system on the flux Φ_d (which in its turn increases saturation).

At maximum speed under the same electromagnetic loads, the zone of of sparkless commutation must be narrower than with the full number of compoles owing to the changed shape of the field in the commutation zone without compoles.

But, given machines of the same weight and dimensions, those with the full number of compoles always have a 15 to 20 per cent larger electromagnetic load and a larger e_r.

3. Tests have shown that fundamental difficulties only arise in the production of re-designed machines with a large range of speeds in the adjustment of commutation at maximum speed when e_r, or the difference $e_r - e_k$, is at a maximum. In this connexion, Karasev's conclusion that "the relationship $e_r = f(n)$ is a straight line parallel to the X-axis" (see his book [4], page 48) does not agree with practice.

4. There may be no zone of sparkless commutation in variable heavy duty machines if the shape of the field B_k is unfavourable. It is therefore necessary to prevent the brushes being displaced from neutral by more than 1.0 mm due to production tolerances, and the tip of the compole must be of the correct shape [2].

5. The commutation of re-designed machines should be adjusted by changing the gaps δ_n and δ_d, since this varies both the magnitude and the shape of the commutating field.

6. The oscillograms show that the variation in current during commutation is only in the form of two separate process with retarded commutation.

With accelerated commutation the variation in current is usually continuous. In the latter case, the actual period of commutation is less than the theoretical period. With retarded commutation the theoretical and actual figures agree.

The commutation, the magnitude of e_r and the shape of the field depend to a large extent on the type and design of the winding. This topic needs to be studied separately. But (in order to facilitate the commutation of heavy duty machines of 18 kW or more with a large range of speeds) we recommend the use of a winding with $u_k = 1$ and a shortened pitch "by a unit interval". It is desirable to use a combined frog-leg winding having 100 per cent equalizers.

8. Practical experience has shown that machines with half the number of compoles can be produced with satisfactory commutation if $A \leqslant 350$ to 400 A/cm and $e_r \leqslant 3.5$ V.

Translated by O. Blunn

REFERENCES

1. I.Z. Ageev; *Elektrichestvo*, No.11, (1959).
2. I.Z. Ageev; *Elektrichestvo*, No.3, (1960).
3. E'. Arnol'd and La-Kur; *D.c. machines, (Mashiny postoiannogo toka)*. Gostekhizdat, (1931).
4. M.P. Karasev; *The commutation of d.c. machines, (Kommutatsiia mashin postoiannogo toka)*. Gosenergoizdat, (1955).
5. O.G. Vegner; *Elektrichestvo*, No.7, (1956).

1960

ABSTRACTS FROM PAPERS PUBLISHED IN ELEKTRICHESTVO No. 12 1960

Electric Drives

The design of variable drives with magnetic amplifiers. Ia.B. Rozman, (pp. 75-78).

An account is given of the development of electric drives using magnetic amplifiers. The author considers the choice of selenium rectifiers, the rectification of the magnetic amplifier characteristics, the relationship between the currents and power circuits and means of adjusting the speed of standard PMU-type drives.

Electrification

The 40-th anniversary of Lenin's plan on electrification. (pp. 1-8).

Past achievements are reviewed and means of ensuring the fulfulment of the current seven year plan are considered.

Ferroresonant voltage stabilizers.

Calculating the inductance of a coil with an open ferromagnetic core and the leakage inductance of a ferroresonant stabilizer. V.M. Greshniakov, (pp. 69-75).

The inductance of a coil with a core such as is used in ferroresonant voltage stabilizers is determined. An infinitely thin coil is substituted for the real coil. The author reduces the problem to the magnetostatic problem. The formulae of a ferroresonant stabilizer is considered briefly.

Power system regionalizing in the Chinese Peoples' Republic Republic. Siui Shou-Bo, (pp. 15-20).

In this paper China is itself only used as an example to illustrate a novel method of classifying the power resources of economic

regions. Information about the electricity supply system and fuel resources of China is given indirectly.

The method and algorithm for calculating power loss partial derivatives of complex networks on digital computers. V.S. Shakhanov, (pp. 21-28).

A novel method of calculating the partial derivatives of power losses in power systems of complex configuration is proposed. The proposed algorithm for this method and the programme realizing this algorithm for computer use are described in detail. The results of a practical calculation are given. The method is intended to replace the "grid coefficients" method as described by Early and Watson.

Current flow from elements of the reinforced concrete foundations of transmission line towers. A.L. Vainer, (pp. 34-40).

It is established that the capillary suction of moisture from the surrounding earth by the external layer round concrete piles makes this layer highly conducting. It is established that the flow of line frequency currents and impulse currents is governed by the laws relating to ordinary earths. A theoretical analysis is made and experimental results are given.

Relays and Protection

Analysis of pilot-wire differential line relaying by circle diagrams in the complex plane. V.L. Fabrikant, (pp. 40-47).

The method used in the planning of protection for long distance transmission lines whereby the various conditions are represented by impedance diagrams in the complex plane is adapted for use in the development of pilot-wire differential line relaying.

On distance relaying for all types of line faults. S.B. Losev, (pp. 47-58).

A comparison is made between the Westinghouse distance relay and the Russian mhometer. A method of improving the mhometer is suggested.